POLYMERIC NANO-BIOMATERIALS FOR MEDICAL APPLICATIONS: ADVANCEMENTS IN DEVELOPING AND IMPLEMENTATION CONSIDERING SAFETY-BY-DESIGN CONCEPTS

EDITED BY: Gerrit Borchard, Olga Borges, Vasile Ostafe, Giuseppe Perale, Claudia Som, Peter Wick and Manfred Zinn

PUBLISHED IN: Frontiers in Bioengineering and Biotechnology

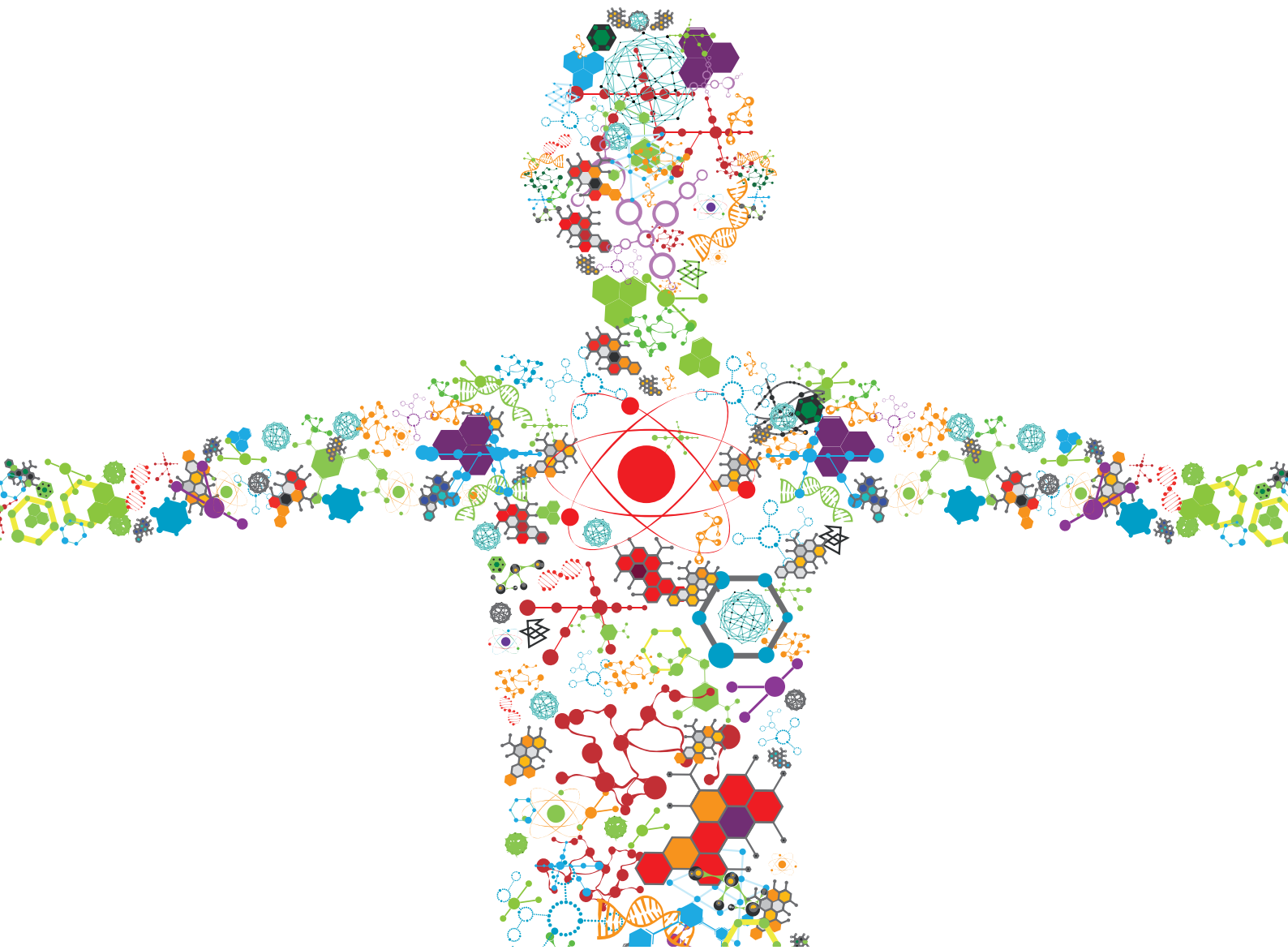

frontiers Research Topics

frontiers

ISSN 1664-8714
ISBN 978-2-88966-256-2
DOI 10.3389/978-2-88966-256-2

About Frontiers

Frontiers is more than just an open-access publisher of scholarly articles: it is a pioneering approach to the world of academia, radically improving the way scholarly research is managed. The grand vision of Frontiers is a world where all people have an equal opportunity to seek, share and generate knowledge. Frontiers provides immediate and permanent online open access to all its publications, but this alone is not enough to realize our grand goals.

Frontiers Journal Series

The Frontiers Journal Series is a multi-tier and interdisciplinary set of open-access, online journals, promising a paradigm shift from the current review, selection and dissemination processes in academic publishing. All Frontiers journals are driven by researchers for researchers; therefore, they constitute a service to the scholarly community. At the same time, the Frontiers Journal Series operates on a revolutionary invention, the tiered publishing system, initially addressing specific communities of scholars, and gradually climbing up to broader public understanding, thus serving the interests of the lay society, too.

Dedication to Quality

Each Frontiers article is a landmark of the highest quality, thanks to genuinely collaborative interactions between authors and review editors, who include some of the world's best academicians. Research must be certified by peers before entering a stream of knowledge that may eventually reach the public - and shape society; therefore, Frontiers only applies the most rigorous and unbiased reviews.
Frontiers revolutionizes research publishing by freely delivering the most outstanding research, evaluated with no bias from both the academic and social point of view. By applying the most advanced information technologies, Frontiers is catapulting scholarly publishing into a new generation.

What are Frontiers Research Topics?

Frontiers Research Topics are very popular trademarks of the Frontiers Journals Series: they are collections of at least ten articles, all centered on a particular subject. With their unique mix of varied contributions from Original Research to Review Articles, Frontiers Research Topics unify the most influential researchers, the latest key findings and historical advances in a hot research area! Find out more on how to host your own Frontiers Research Topic or contribute to one as an author by contacting the Frontiers Editorial Office: researchtopics@frontiersin.org

POLYMERIC NANO-BIOMATERIALS FOR MEDICAL APPLICATIONS: ADVANCEMENTS IN DEVELOPING AND IMPLEMENTATION CONSIDERING SAFETY-BY-DESIGN CONCEPTS

Topic Editors:
Gerrit Borchard, Université de Genève, Switzerland
Olga Borges, University of Coimbra, Portugal
Vasile Ostafe, West University of Timișoara, Romania
Giuseppe Perale, University of Applied Sciences and Arts of Western Switzerland, Switzerland
Claudia Som, Swiss Federal Laboratories for Materials Science and Technology, Switzerland
Peter Wick, Swiss Federal Laboratories for Materials Science and Technology, Switzerland
Manfred Zinn, HES-SO Valais-Wallis, Switzerland

Citation: Borchard, G., Borges, O., Ostafe, V., Perale, G., Som, C., Wick, P., Zinn, M., eds. (2020). Polymeric Nano-Biomaterials for Medical Applications: Advancements in Developing and Implementation Considering Safety-By-Design Concepts. Lausanne: Frontiers Media SA.
doi: 10.3389/978-2-88966-256-2

Table of Contents

frontiers in Bioengineering and Biotechnology

EDITORIAL
published: 19 October 2020
doi: 10.3389/fbioe.2020.599950

Editorial: Polymeric Nano-Biomaterials for Medical Applications: Advancements in Developing and Implementation Considering Safety-by-Design Concepts

Gerrit Borchard[1]*, *Claudia Som*[2], *Manfred Zinn*[3], *Vasile Ostafe*[4], *Olga Borges*[5], *Giuseppe Perale*[6] *and Peter Wick*[2]

[1] School of Pharmaceutical Sciences, Université de Genève, Geneva, Switzerland, [2] Swiss Federal Laboratories for Materials Science and Technology, Dübendorf, Switzerland, [3] Institute of Life Technologies, University of Applied Sciences and Arts Western Switzerland (HES-SO Valais-Wallis), Sion, Switzerland, [4] Advanced Environmental Research Laboratories, Department of Biology-Chemistry, Faculty of Chemistry, Biology, Geography, West University of Timisoara, Timisoara, Romania, [5] Centre for Neuroscience and Cell Biology, University of Coimbra, Coimbra, Portugal, [6] Department of Innovative Technologies, University of Applied Sciences and Arts of Southern Switzerland (SUPSI), Manno, Switzerland

Keywords: nano-biomaterials, safe-by-design, nanotechnology, nanomedicines, drug carriers

Editorial on the Research Topic

Polymeric Nano-Biomaterials for Medical Applications: Advancements in Developing and Implementation Considering Safety-by-Design Concepts

The aging population represents an enormous social, structural, and financial burden on society. To address the potential problems of supporting an elderly population, it is important to consider ways of enabling individuals to maintain independence and quality-of-life (QoL) for as long as possible. To achieve this, we need to develop new solutions and novel concepts through technologies, and researchers have been exploring how disease and aging are mediated by molecular processes at the nanoscale. The subsequent nanotechnology-enabled approaches that have emerged in recent years include innovative nano-materials and nano-devices, which could enable interventions at the molecular length scale and are, therefore, an important cornerstone in building solutions.

As for every novel technology or material, a careful safety assessment is needed early in its development to avoid social and economic drawbacks. While guidelines and legislation have been put in place for therapeutics of low molecular weight along with much more complex biologics as well as their follow-on products (generics and biosimilars, respectively), the regulatory approach for advanced therapeutics including polymeric biomaterials is still in its infancy. The rise of so-called "nanomedicines" or complex therapeutics along with follow-on products such as "nanosimilars" or "complex generics" have provided advantageous attributes on the nanoscale, but the lack of guidance is a difficult challenge that needs to be addressed in the development of such products in future.

This issue describes some of the different nano-biomaterials that are currently being studied for the preparation of nanoscale drug carriers. These include: chitosan (see Jesus, Marques et al.; Marques et al.), a chitin derivative biopolymer obtained mostly from crustaceans; the family of poly(lactide-*co*-glycolide) (PLGA) polymers (Essa et al.); poly(D,L-lactic acid) (Casalini, Rossi et al.; Da Silva et al.); polyhydroxyalkanoates (Casalini, Rosolen et al.), a polyester produced by bacteria; and hydrogel systems made up of hyaluronic acid and alginate (Lynch et al.). As indicated

OPEN ACCESS

Edited and reviewed by:
Gianni Ciofani,
Italian Institute of Technology (IIT), Italy

***Correspondence:**
Gerrit Borchard
gerrit.borchard@unige.ch

Specialty section:
This article was submitted to Nanobiotechnology, a section of the journal Frontiers in Bioengineering and Biotechnology

Received: *28 August 2020*
Accepted: *04 September 2020*
Published: *19 October 2020*

Citation:
Borchard G, Som C, Zinn M, Ostafe V, Borges O, Perale G and Wick P (2020) Editorial: Polymeric Nano-Biomaterials for Medical Applications: Advancements in Developing and Implementation Considering Safety-by-Design Concepts. Front. Bioeng. Biotechnol. 8:599950. doi: 10.3389/fbioe.2020.599950

in this issue, some studies have found that for some materials [e.g., chitosan (Marques et al.)], the description of the specifications of the nano-biomaterial is often incomplete. The preparation of nano-vectors using these materials is also complex that needs to be better understood, in particular when self-assembly processes are used to implement therapeutic drug delivery (Yadav et al.). These issues render comparative efficacy studies difficult and preclude the introduction of a "safe-by-design" concept, as developed in the framework of the European project "GoNanoBioMat" (https://gonanobiomat.eu/). As a concept, safe-by-design is currently being adapted for use in research on nano-biomaterials, based on the processes used in drug discovery and development, which adopt safety aspects early in the process (Schmutz et al.). It is intended that this concept in combination with other existing regulatory frameworks, will guide small and medium-sized companies during the development process of nanomedicines, span stages from material selection and design, characterization, assessment of human, and environmental health risks, to manufacturing and control, as well as storage and transport of the final product.

This special issue also focuses on the hazard assessment of polymeric biomaterials for medical use [see the literature study (Jesus, Schmutz et al.)], and the determination of the impact of certain properties of nanoscale drug vectors on their safety (cytotoxicity, immunotoxicity) (Jesus, Marques et al.), which discuss membrane diffusion characteristics and pharmacokinetics. Some of these parameters, including nanomaterial interactions with their biological environment (Casalini, Rosolen et al.) and the evaluation of the risks of their degradation products (Roman et al.) can be assessed by computational simulation (Casalini, Limongelli et al.) or systematic evaluation of animal studies (Hauser and Nowack), resulting in concrete suggestions for nano-biomaterial design to achieve optimized efficacy and enhanced safety. Finally, the different options of targeted anti-schistosomal therapy using nanotechnology are reviewed (Adekiya et al.).

The diversity of the different papers presented in this special issue are indicative of the significant interplay between life and the material sciences with computational approaches. We believe that this exchange of ideas is one of the best approaches to tackling the increasingly complex challenges of an aging society.

AUTHOR CONTRIBUTIONS

GB has drafted the manuscript and submitted in final form. CS, MZ, VO, OB, GP, and PW have revised the manuscript draft. All authors contributed to the article and approved the submitted version.

FUNDING

This work was supported by Romanian Ministry of National education UEFISCDI - grant PN3-P3-285.

ACKNOWLEDGMENTS

This work was financed by the European Regional Development Fund (ERDF), through the Centro 2020 Regional Operational Programme under project CENTRO-01-0145-FEDER-00008: BrainHealth 2020, and through the COMPETE 2020—Operational Programme for Competitiveness and Internationalization and Portuguese national funds via FCT—Fundação para a Ciência e a Tecnologia, I.P., under project PROSAFE/0001/2016, and the strategic projects POCI-01-0145-FEDER-030331 and POCI-01-0145-FEDER-007440 (UID/NEU/04539/2019). This work is part of the GoNanoBioMat project and has received funding from the Horizon 2020 framework program of the European Union, ProSafe Joint Transnational Call 2016, and from the CTI (1.1.2018 Innosuisse) under grant agreement number 19267.1 PFNM-NM.

Conflict of Interest: The authors declare that the research was conducted in the absence of any commercial or financial relationships that could be construed as a potential conflict of interest.

frontiers in Bioengineering and Biotechnology

BRIEF RESEARCH REPORT
published: 06 June 2019
doi: 10.3389/fbioe.2019.00137

Poly(D,L-Lactic Acid) Nanoparticle Size Reduction Increases Its Immunotoxicity

Jessica Da Silva[1,2], *Sandra Jesus*[1], *Natália Bernardi*[1,2], *Mariana Colaço*[1,2] *and Olga Borges*[1,2]*

[1] Center for Neuroscience and Cell Biology, University of Coimbra, Coimbra, Portugal, [2] Faculty of Pharmacy, University of Coimbra, Azinhaga de Santa Comba, Coimbra, Portugal

Polylactic acid (PLA), a biodegradable and biocompatible polymer produced from renewable resources, has been widely used as a nanoparticulate platform for antigen and drug delivery. Despite generally regarded as safe, its immunotoxicological profile, when used as a polymeric nanoparticle (NP), is not well-documented. Thus, this study intends to address this gap, by evaluating the toxicity of two different sized PLA NPs (PLA_A NPs and PLA_B NPs), produced by two nanoprecipitation methods and extensively characterized regarding their physicochemical properties in *in vitro* experimental conditions. After production, PLA_A NPs mean diameter (187.9 ± 36.9 nm) was superior to PLA_B NPs (109.1 ± 10.4 nm). Interestingly, when in RPMI medium, both presented similar mean size (around 100 nm) and neutral zeta potential, possibly explaining the similarity between their cytotoxicity profile in PBMCs. On the other hand, in DMEM medium, PLA_A NPs presented smaller mean diameter (75.3 ± 9.8 nm) when compared to PLA_B NPs (161.9 ± 8.2 nm), which may explain its higher toxicity in RAW 264.7. Likewise, PLA_A NPs induced a higher dose-dependent ROS production. Irrespective of size differences, none of the PLA NPs presented an inflammatory potential (NO production) or a hemolytic activity in human blood. The results herein presented suggest the hypothesis, to be tested in the future, that PLA NPs presenting a smaller sized population possess increased cytotoxicity. Furthermore, this study emphasizes the importance of interpreting results based on adequate physicochemical characterization of nanoformulations in biological medium. As observed, small differences in size triggered by the dispersion in cell culture medium can have repercussions on toxicity, and if not correctly evaluated can lead to misinterpretations, and subsequent ambiguous conclusions.

Keywords: polylactic acid, poly(D,L-lactic acid), polymeric nanoparticles, drug delivery systems, immunotoxicity, size-dependent cytotoxicity, hemocompatibility, cell culture medium

OPEN ACCESS

Edited by:
Michele Iafisco,
Italian National Research Council (CNR), Italy

Reviewed by:
Vuk Uskokovic,
University of California, San Francisco, United States
Daniele Catalucci,
Institute for Genetic and Biomedical Research (IRGB), Italy
Michele Chiappi,
Imperial College London, United Kingdom

***Correspondence:**
Olga Borges
olga@ci.uc.pt

Specialty section:
This article was submitted to Nanobiotechnology, a section of the journal Frontiers in Bioengineering and Biotechnology

Received: *27 March 2019*
Accepted: *21 May 2019*
Published: *06 June 2019*

Citation:
Da Silva J, Jesus S, Bernardi N, Colaço M and Borges O (2019) Poly(D,L-Lactic Acid) Nanoparticle Size Reduction Increases Its Immunotoxicity. Front. Bioeng. Biotechnol. 7:137. doi: 10.3389/fbioe.2019.00137

INTRODUCTION

Polylactic acid (PLA) is a Food and Drug Administration approved polymer that has proven to be a very versatile material, with interesting properties such as biocompatibility and biodegradability (Essa et al., 2012; Legaz et al., 2016). Thus, PLA has been explored regarding many therapeutic applications, including as a nanoparticulate antigen and drug delivery vehicle (Essa et al., 2012; Legaz et al., 2016).

The great interest in using nanoparticles (NPs) for biomedical applications (Jiao et al., 2014) is transversal to various polymeric materials, despite the poorly understood correlation between their physicochemical properties and their effects on the immune system. This knowledge gap partially results from the fact that NPs physicochemical properties, particularly its reduced size, hinder the application of traditional toxicity assays and further contribute to the misinterpretation of results and ambiguous conclusions among research groups (Dobrovolskaia et al., 2009). Additionally, the mandatory use of biological medium during toxicological assays can modify the NPs characteristics such as size, surface charge and morphology, through phenomenon's like protein corona formation and particle agglomeration, which will therefore influence the immunotoxicity profile of the NPs (Kendall et al., 2014). Therefore, a detailed characterization of the NPs in the experimental assay conditions is crucial to discuss the results, but is commonly absent from the scientific published reports. Biodegradable polymers such as PLA are generally regarded as safe, but their immunotoxicological profile when used as NPs, is not well documented (Singh and Ramarao, 2013). Previously, da Luz et al. has published an interesting paper assessing the toxicity and biocompatibility of PLA NPs in A549 cells (da Luz et al., 2017). Similarly, Legaz et al. conducted toxicity studies in Schneider's D. melanogaster line 2 (S2) cells (Legaz et al., 2016).

In this study, we described the production method of two different sized PLA NPs (PLA_A NPs and PLA_B NPs), in order to evaluate how the NP size affects their toxicological profile using cells from the immune system. *In vitro* immunotoxicity studies comprised hemocompatibility assays, cell viability experiments with peripheral blood mononuclear cells (PBMCs) and RAW 264.7 macrophage cell line, and nitric oxide (NO) and reactive oxygen species (ROS) production assays in RAW 264.7 cells. Furthermore, for the discussion of these results we have included the characterization of both PLA NPs regarding its size, polydispersity index (PDI) and zeta potential in the different cell culture media used in *in vitro* studies. In contrast to other published reports evaluating the toxicity of PLA NPs, this report aims to highlight the importance of the NPs characterization under *in vitro* experimental conditions for the establishment of relationships between the NPs properties and their effect in cells of the immune system. Not being an exhaustive study of immunotoxicology, it nevertheless intends to emphasize the importance of these studies in the development of nanomedicines.

MATERIALS AND METHODS

Poly(D,L-Lactide) Polymer

Poly(D,L-lactide) (PDLLA) polymer with an average molecular weight (MW) of 1,01,782 g/mol [analyzed by gel permeation chromatography/size exclusion chromatography (GPC/SEC)] and an inherent viscosity of 0.68 dL/g was obtained from Sigma-Aldrich Corporation (St. Louis, MO, USA).

PLA NP Production

For PLA_A NPs production, PDLLA was dissolved at 2 mg/mL in acetone. NPs formed spontaneously upon dropwise addition of 4.5 mL of PDLLA solution to 13.5 mL of an aqueous solution (pyrogen-free water) with 1% of Pluronic® F68 Prill (Basf Corporation, Ludwigshafen, Germany) using a high-speed homogenizer at 13,000 rpm. The homogenization was maintained for another 2 min, after total addition of the PDLLA solution. The PLA_A NPs were concentrated by centrifugation at 13,000 g for 20 min at 10°C, resuspended in pyrogen-free water and concentrated again. This procedure was repeated 2 more times, and finally each batch was concentrated in a final volume of 2 mL. On the other hand, for the production of PLA_B NPs, PDLLA was dissolved at 0.75 mg/mL in acetone. NPs formed spontaneously upon dropwise addition of 1 mL of PDLLA solution to 2.5 mL of an aqueous solution with 0.1% of Pluronic F68 using a vortex homogenizer and the agitation was maintained for another 2 min, after the total addition of the PDLLA solution. In order to concentrate and wash the NPs, 8 batches of PLA_B NPs (20 mL) were centrifuged with Vivaspin 20 centrifugal concentrator (MWCO 300 KD, ThermoFisher Scientific Inc., Waltham, MA, USA) at 3,000 g at 10°C until <1 mL was recovered in the centrifuge tube. The NPs were then resuspended in 10 mL pyrogen-free water, the centrifugation procedure was repeated, and the NPs were resuspended in a final volume of 1 mL pyrogen-free water. *In vitro* experiments and the respective characterization in *in vitro* conditions, were performed by diluting these concentrated NP suspensions in serum supplemented cell culture media as described below.

PLA NP Characterization

Zetasizer Nano ZS (Malvern Instruments, Ltd., Worcestershire, UK) was used to measure particle size, and the respective polydispersity index (PDI), by dynamic light scattering (DLS) and particle zeta potential through electrophoretic light scattering (ELS). The samples were characterized dispersed in pyrogen-free water and in supplemented culture media (RPMI and DMEM). In the second case, the size and zeta potential assessment was done immediately after dilution in the culture medium, and after 24 h of incubation at 37°C. The NP size when dispersed in pyrogen-free water was also confirmed by transmission electron microscopy (TEM). Samples were placed on a microscopy grid and observed under a FEI-Tecnai G2 Spirit Biotwin, a 20–120 kV TEM (FEI Company, OR, USA).

Immunotoxicity and Hemocompatibility Assays

In vitro Studies With Human Blood

Hemolysis assay

Hemolysis assay was performed according to published protocols with minor modifications (Pattani et al., 2009; Villiers et al., 2009). Whole blood was collected from healthy donors after formal acceptance with a written informed consent. Blood was diluted with PBS to adjust total blood hemoglobin (TBH) concentration to 10 ± 2 mg/mL (TBHd). A volume of 100 μL of PLA NPs suspensions, PBS (negative control), or Triton-X-100 (positive control) were added to 700 μL PBS in different

tubes. Then, 100 μL of TBHd was added to each tube, followed by incubation at 37°C for 3 h ± 15 min. NPs were also incubated with PBS without blood to evaluate the possible NP interference. After the incubation time, the tubes were centrifuged at 800 g for 15 min. One hundred microliter of each supernatant and 100 μL cyanmethemoglobin (CMH) reagent were added to a 96-well-plate. The CMH reagent was prepared by mixing 1000 mL Drabkin's reagent and 0.5 mL of 30% Brij 35 solution (Sigma-Aldrich, St. Louis, MO, USA). The absorbance (OD) at 540 nm was determined and the percentage of hemolysis was calculated by Equation 1:

$$Hemolysis\ (\%) = \frac{(OD\ sample\ (540\ nm) - OD\ PBS\ (540\ nm))}{(OD\ TBHd\ (540\ nm) - OD\ PBS\ (540\ nm))} x\ 100 \quad (1)$$

In vitro Studies With PBMCs

PBMCs isolation

Buffy coats obtained from normal donors (heparinized syringes) were kindly given by IPST, IP (Coimbra, PT). PMBCs were isolated on a density gradient with Lymphoprep (Axis-Shield, Dundee, Scotland) according to the provider's guidance protocol and as published by our group (Jesus et al., 2017). Isolated PBMCs were cultured in Roswell Park Memorial Institute medium (RPMI) with 10% heat inactivated fetal bovine serum (FBS), supplemented with 2 mM L-glutamine, 1% penicillin/streptomycin and 20 mM HEPES.

Nanoparticle toxicity

PLA NPs cytotoxicity was evaluated on human PBMCs using 3-(4,5-dimethylthiazol-2-yl)-2,5-diphenyltetrazolium bromide (MTT) assay. Cells were plated in a 96-well plate at a density of 5 x 10^5 monocytes/well. Serial dilutions of NPs and controls were incubated with the cells for 24 h, at 37°C and 5% CO_2. After this period, 20 μL of MTT solution (5 mg/mL) in PBS were added to each well-followed by additional 4 h incubation. To ensure dissolution of the formazan crystals, cell culture plates were centrifuged (800 g, 25 min, 20°C) and the culture medium was replaced by DMSO and the OD of the resultant colored solution was measured at 540 and 630 nm. Cell viability (%) was calculated by Equation 2:

$$Cell\ viability\ (\%) = \frac{(OD\ sample\ (540\ nm) - OD\ sample\ (630\ nm))}{(OD\ control\ (540\ nm) - OD\ control\ (630\ nm))} \times 100 \quad (2)$$

The inhibitory concentration for 50% of cell viability (IC_{50}) was calculated by plotting the log concentration of the NPs vs. inhibition percentage of cell viability and extrapolating the value from a non-linear regression using Prism 6.0 (GraphPad Software, San Diego, CA, USA).

Cytotoxicity results obtained with MTT assay were confirmed with propidium iodide (PI) assay. Briefly, cells incubated with 4 nanoparticle concentrations previously used in MTT assay were centrifuged (800 g, 25 min, 20°C), resuspended in PBS and collected for analysis in a BD FACSCalibur Flow Cytometer (BD Biosciences, Bedford, MA, USA) using PI solution (0.5 μg/mL).

In vitro Studies With RAW 264.7 Macrophage Cell Line

RAW 264.7 (ATCC® TIB-71™) were acquired to ATCC (Manassas, VA, USA), cultured in Dulbecco's Modified Eagle Medium (DMEM) supplemented with 10% heat inactivated FBS, 1% Penicillin/Streptomycin, 10 mM HEPES and 3.7 g/L Sodium Bicarbonate, and used until passage 18.

Nanoparticle cytotoxicity

PLA NP toxicity in RAW 264.7 was assessed as described previously for PBMCs with some modifications. Briefly, for MTT assay, macrophages were plated at a concentration of 2 × 10^4 cells/well and the incubation with MTT solution was performed for 1 h 30 min.

For the assay with PI, the cells were collected using the dissociation medium (PBS-EDTA 5 mM) followed by centrifugation (250 g, 10 min, 20°C) to replace the medium with PBS.

Nanoparticle effect on production of the reactive oxygen species

The ROS production was assessed using the dichlorofluorescein diacetate probe (DCFH-DA) (Thermo Fisher Scientific Inc., Waltham, MA, USA). The RAW 264.7 cells were incubated in a black 96-well plate for 24 h at 37°C and 5% CO_2, at density of 0.5 × 10^5 cells/well. After that period, serial dilutions of PLA NPs were incubated with the cells, to evaluate ROS stimulation. LPS was used as a positive control (1 μg/mL).

After 24 h, cell culture medium was replaced by DCFH-DA (50 μM) in serum free DMEM and the cells were incubated for another 2 h at 37°C and 5% CO_2. The resulting fluorescence was read at 485/20 nm and 528/20 nm (excitation/emission wavelengths).

To calculate the stimulation of ROS production, Equation (3) was applied:

$$ROS\ production\ \left(mean\ fluorescence\ increase\right) = \frac{Fluorescence_{SAMPLE}}{Fluorescence_{NEGATIVE\ CONTROL}} \quad (3)$$

Nanoparticle effect on nitric oxide production

The NO production by RAW 264.7 was evaluated based on nitrite quantification using the Griess reagent. RAW 264.7 cells were incubated in a 48-well-plate at a density of 2.25 × 10^5 cells/well for 24 h at 37°C and 5% CO_2. After that period, cell culture medium was replaced by serial dilutions of PLA NPs diluted in cell culture medium without phenol red. LPS was used as a positive control (1 μg/mL). To test if the NPs were able to inhibit LPS stimulated NO production, the same NP concentrations were incubated together with cells in the presence of the LPS (1 μg/mL).

The Cell supernatants were collected 24 h after incubation, and 100 μL of each test sample was plated in a 96-well-plate and combined with 100 μL of Griess reagent. A calibration curve performed with sodium nitrite (0–80 μg/mL) was also plated in duplicate. The optical density of the samples was measured

at 550 nm and NO quantification was extrapolated from the calibration curve.

To calculate the inhibition of NO production upon stimulation with LPS (Equation 4) was applied:

$$Inhibition\ of\ NO\ production\ (\%) = \frac{NO(\mu g/mL)_{\ SAMPLE}}{NO\ (\mu g/mL)_{\ POSITIVE\ CONTROL}} \times 100 \quad (4)$$

Statistical Analysis

Data were analyzed using GraphPad Prim 6 (GraphPad Software, Inc., La Jolla, CA, USA), in which significant differences were obtained from one-way ANOVA, and values were considered statistically different when $p < 0.05$. *In vitro* data were expressed as means ± standard error of the mean (SEM).

RESULTS

PLA_A NPs Are the Largest in Water but the Smallest in Culture Medium

Although PLA polymer has been approved by FDA for human use in an extensive range of applications (Tyler et al., 2016). The information about its toxicological profile when used as a NP is scarce (Singh and Ramarao, 2013). In order to give new insights on the relationship between NP physicochemical properties and their immunotoxicity, two different sized PLA NPs were produced and characterized regarding their mean size, PDI and zeta potential (**Figure 1**). PLA_A NPs presented a mean diameter of 187.9 ± 36.9 nm and a zeta potential of −24.0 ± 4.7 mV in pyrogen-free water, while PLA_B NPs presented a mean diameter of 109.1 ± 10.4 nm and a zeta potential of −6.6 ± 11.2 mV, both presenting a low PDI compatible with only one narrow-size population of particles (see graphics on **Figure 1**). The more negative charge of PLA_A NPs could be explained by the higher concentration of Pluronic F68 used in the NP production method, since increased surface layer of surfactant may decreases the NPs zeta potential (Santander-Ortega et al., 2006). Sizes were also analyzed after dispersion in cell culture media, in order to evaluate the stability of the NPs in the experimental assay conditions. These tests were performed right after dispersion in DMEM and RPMI, and 24 h after incubation at 37°C. Results from initial dispersion and after 24 h incubation were comparable (**Figure 1**), so the 24 h-incubation period did not altered the characteristics of the particles. However, great differences, when compared with the initial size (pyrogen-free water), were observed when the particles were suspended in RPMI, but especially in DMEM. In case of PLA_A NPs, the size decreased and in case of PLA_B NPs the size increase. To better understand the differences, representative graphs of differential and cumulative intensities of size distribution were obtained for both particles, suspended in pyrogen-free water and after 24 h incubation in RPMI and DMEM. When comparing the PLA_A graphs from cell culture media with the ones obtained in the original medium (pyrogen-free water), we observed the appearance of 3 size-populations, compatible with a higher PDI. To highlight, the appearance of a small size population of particles explaining the decrease of the mean size diameter. The same phenomenon was not observed with PLA_B NPs. On the contrary, in RPMI the size remained unaltered and in DMEM the size increased as a result of some aggregation of the particles. In order to confirm the initial differences in size between PLA_A NPs and PLA_B NPs, TEM images were obtained with particles dispersed in pyrogen free water (**Figure 2**). As illustrated, both NPs are round shaped and sizes confirmed the DLS measurements.

Both PLA NPs Present a Good Hemocompatibility Profile

Hemolysis is the breakdown of red blood cells with subsequent release of intracellular contents. *In vivo*, this can lead to anemia or other pathological conditions (Dobrovolskaia et al., 2008). It is important to assess the NP effect on these blood elements not only when the intravenous route of administration is considered but also when addressing other administration routes, in order to establish their hemocompatibility (Dobrovolskaia et al., 2008). For that reason, PLA NP hemocompatibility was assessed in human whole blood and hemolytic values were considered above 5%, as recommended by American Society for Testing and Materials International (ASTM, 2013).

The results from **Figure 3** showed that both PLA NPs (A and B) have a good hemocompatibility profile, since none induced hemolysis above 5%, considering the concentration range tested (38–250 μg/mL for PLA_A NPs and 75–400 μg/mL for PLA_B NPs).

PLA_A NPs Show a Pronounced Cytotoxicity Profile in Comparison to PLA_B NPs in RAW 264.7

The colorimetric MTT assay for measuring cell metabolic activity is based on the cellular conversion of a tetrazolium salt (MTT) into an insoluble formazan, that can be dissolved in DMSO generating a purple signal (Altmeyer et al., 2016). Therefore, through an indirect way, MTT assay was used to evaluate the cytotoxicity of PLA NPs after 24 h incubation with PBMCs and RAW 264.7.

Results presented in **Figure 4A** show that neither PLA_A NPs nor PLA_B NPs induced cytotoxicity in PBMCs, since the incubation with both resulted in cell viabilities above 70% under the concentration range tested (0.55–562.5 μg/mL for PLA_A NPs and 1.05–536 μg/mL for PLA_B NPs). Importantly, the similarity in the cytotoxicity profile in this primary culture could be explained by the similar mean diameter and zeta potential of PLA NPs when dispersed in RPMI medium. In fact, the differences in size previously seen in water were masked in RPMI.

Concerning cytotoxicity in RAW 264.7, we can observe in **Figure 4B** that PLA_A NPs presented a higher cytotoxicity than PLA_B NPs, since they presented an estimated IC_{50} of 540.6 μg/mL, while with PLA_B NPs cell viabilities below 70% were never observed, and therefore the estimation of IC_{50} was not possible under the concentration range tested (1.05–536 μg/mL). These results are probably correlated with the size of the both PLA NPs in DMEM (RAW 264.7) medium. In case of the PLA_A

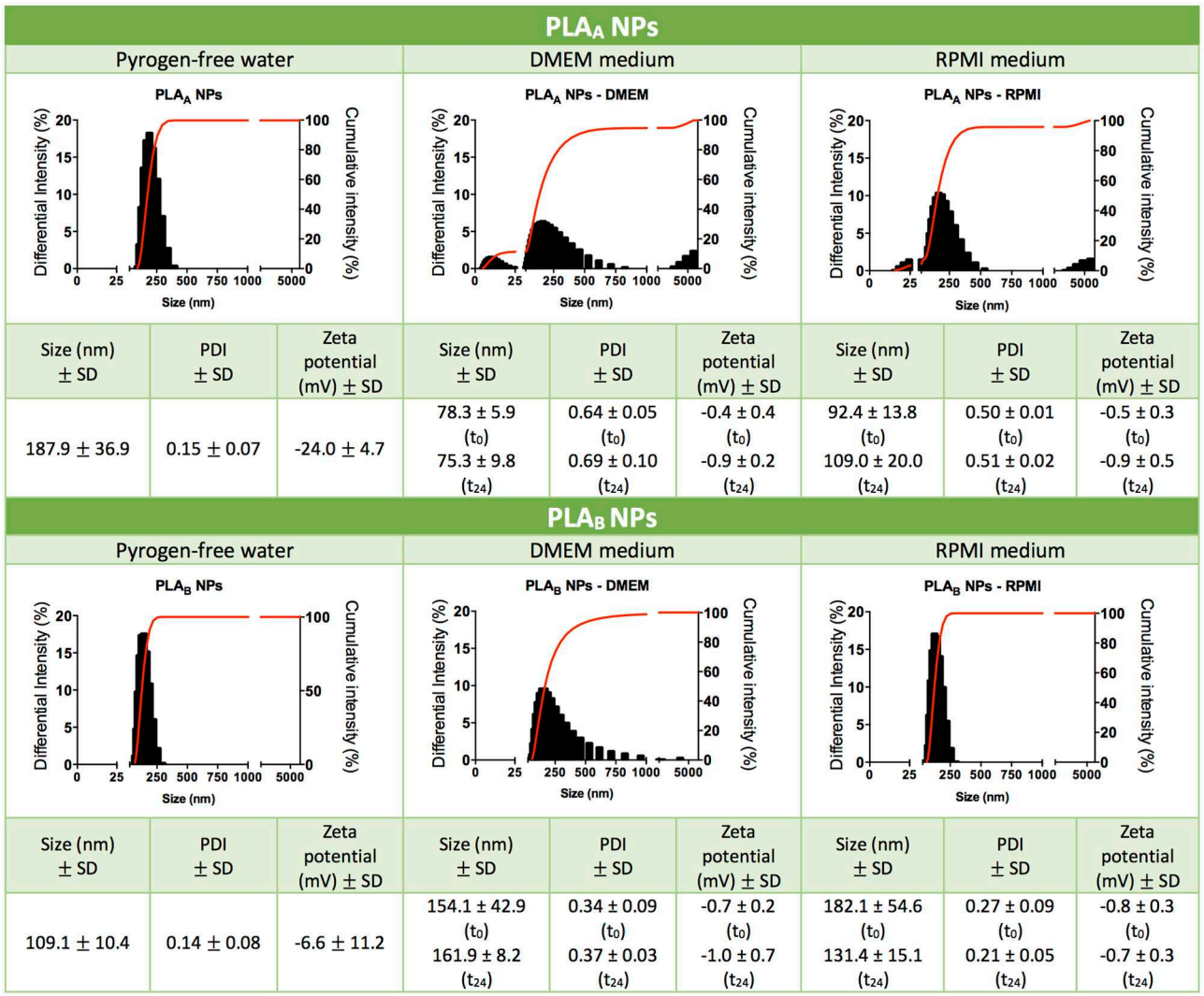

Size (nm) ± SD	PDI ± SD	Zeta potential (mV) ± SD	Size (nm) ± SD	PDI ± SD	Zeta potential (mV) ± SD	Size (nm) ± SD	PDI ± SD	Zeta potential (mV) ± SD
187.9 ± 36.9	0.15 ± 0.07	-24.0 ± 4.7	78.3 ± 5.9 (t_0) 75.3 ± 9.8 (t_{24})	0.64 ± 0.05 (t_0) 0.69 ± 0.10 (t_{24})	-0.4 ± 0.4 (t_0) -0.9 ± 0.2 (t_{24})	92.4 ± 13.8 (t_0) 109.0 ± 20.0 (t_{24})	0.50 ± 0.01 (t_0) 0.51 ± 0.02 (t_{24})	-0.5 ± 0.3 (t_0) -0.9 ± 0.5 (t_{24})

Size (nm) ± SD	PDI ± SD	Zeta potential (mV) ± SD	Size (nm) ± SD	PDI ± SD	Zeta potential (mV) ± SD	Size (nm) ± SD	PDI ± SD	Zeta potential (mV) ± SD
109.1 ± 10.4	0.14 ± 0.08	-6.6 ± 11.2	154.1 ± 42.9 (t_0) 161.9 ± 8.2 (t_{24})	0.34 ± 0.09 (t_0) 0.37 ± 0.03 (t_{24})	-0.7 ± 0.2 (t_0) -1.0 ± 0.7 (t_{24})	182.1 ± 54.6 (t_0) 131.4 ± 15.1 (t_{24})	0.27 ± 0.09 (t_0) 0.21 ± 0.05 (t_{24})	-0.8 ± 0.3 (t_0) -0.7 ± 0.3 (t_{24})

FIGURE 1 | Characterization of PLA NPs. Particle mean size distribution (nm), polydispersity index (PDI), zeta potential (mV) and illustrative graphics of differential and cumulative intensities, after concentration and resuspension in pyrogen-free water, or after 24 h of incubation in cell culture media (DMEM medium or RPMI medium). Data are presented as mean ± standard deviation (SD), $n \geq 3$ (three or more independent experiments, each in triplicate).

NPs, the presence of great NP population with a size below 25 nm might explain their higher cytotoxicity.

In these experiments, the control with the stock solution vehicle (mainly pyrogen-free water from the last NP wash), was tested in the volume correspondent to the highest NP concentration and no decrease in cell viability was verified. These controls ensured that the decrease in cell viability is from the NPs in suspension and not the vehicle of the NP suspension.

In order to avoid possible excessive assumption regarding cytotoxicity when using only a metabolic assay, these results were confirmed with PI assay, which evaluates the integrity of the cell membrane. Results for PLA_A NPs and PLA_B NPs in both cellular models were similar to the ones obtained with MTT (**Figure 4**) and confirmed the higher toxicity of PLA_A NPs in RAW 264.7 cells.

PLA_A NPs but Not PLA_B NPs Induce a Significant Concentration-Dependent ROS Production

The ROS, such as superoxide or hydrogen peroxide, are continually produced during metabolic processes (Brüne et al., 2013; Kwon et al., 2017). ROS generation is normally counterbalanced by the action of antioxidant enzymes and other redox molecules (Brüne et al., 2013; Kwon et al., 2017). However, when overproduced by activated macrophages, ROS can lead to cellular injury (Circu and Aw, 2010; Brüne et al., 2013; Kwon et al., 2017). It has been proven by Saini and co-workers that NPs may promote apoptotic cell death, through the induction of oxidative stress by accumulating ROS (Saini et al., 2016). Therefore, it is important to evaluate the potential effect of PLA NPs in ROS production. This assay was performed using

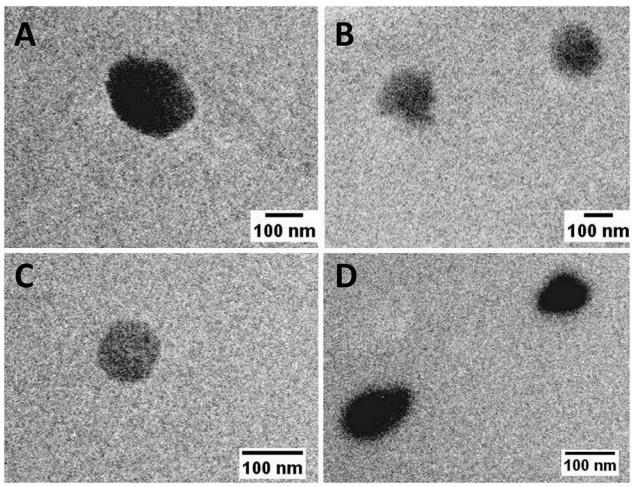

FIGURE 2 | TEM images of PLA NPs dispersed in pyrogen-free water (scale bar: 100 nm). **(A,B)** PLA_A NPs; **(C,D)** PLA_B NPs.

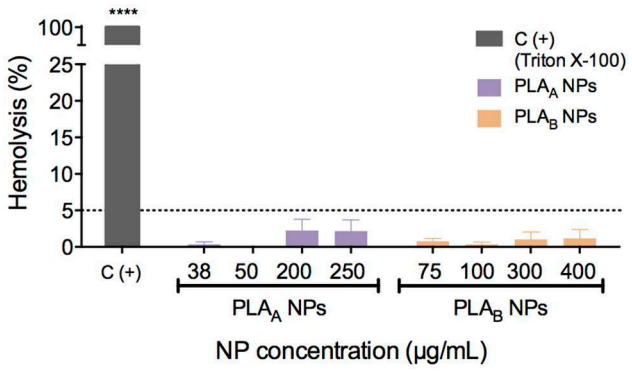

FIGURE 3 | Hemolytic activity of PLA NPs in human blood after 3 h of incubation at 37°C. Triton X-100 was used as a positive control. Hemolytic values were considered above 5%, as recommended by American Society for Testing and Materials International (ASTM, 2013). Data are presented as mean ± SEM, $n \geq 3$ (three or more independent experiments, each in duplicate). ****$p < 0.0001$ indicates values that differ significantly from negative control (PBS).

the cell-permeable fluorogenic probe DCFH-DA, which can be detected on a standard fluorometric plate reader (Zolnik et al., 2011). ROS production assay in RAW 264.7 was performed after 24 h of incubation and as demonstrated in **Figure 5A**, there was a concentration-dependent ROS production for PLA_A NPs. The same effect was not observed for the PLA_B NPs, even considering that a lower PLA_A NP concentrations were tested, when compared with PLA_B NPs (4.3–340 µg/mL for PLA_A NPs and 8.6–690 µg/mL for PLA_B NPs). We could hypothesize that this concentration-dependent ROS production is an indication of cellular toxicity, as demonstrated by the cell viability assay in the **Figure 5B**, where for the higher PLA_A NP concentration the resultant cellular viability was near 70%. For PLA_B NPs it was observed an increased trend of ROS production. However, the values observed were not statistically different from the unstimulated cells. Furthermore, in opposition to the results of PLA_A NPs, no trend for decrease in cell viability was shown for PLA_B NPs (**Figure 5B**).

PLA NPs Do Not Have an Inflammatory Potential in RAW 264.7

The NO is a reactive nitrogen specie, produced by nitric oxide synthase enzymes (Boscá et al., 2005; Caruso et al., 2017). It is an important inflammatory mediator released by macrophages during inflammation, and is one of the main cytostatic, cytotoxic, and pro-apoptotic mechanisms of the immune response (Boscá et al., 2005; Caruso et al., 2017). In order to assess the inflammatory or anti-inflammatory properties of PLA NPs, NO production by RAW 264.7 cells was measured using the Griess reaction method after 24 h of incubation with different test samples.

The pro-inflammatory effect of PLA NPs was evaluated by measuring the NO release upon stimulation with NPs, and the anti-inflammatory effect was evaluated by measuring the ability of the NPs to inhibit NO release induced by LPS. In the first approach, none of the PLA NPs induced NO production under the concentration range tested (0.5–50 µg/mL for PLA_A NPs and 1–100 µg/mL for PLA_B NPs) (**Figure 5C**). Importantly, these concentrations were chosen because they did not induce significant cellular death under the assay conditions, and higher concentrations would result in cellular death above 30%, which could compromise NO production (**Figure 5D**).

The second approach, using the same concentration ranges, revealed that both PLA NPs did not inhibited the NO production stimulated with LPS (**Figure 5E**) and test conditions did not significantly reduce cell viability (**Figure 5F**).

DISCUSSION

According to our results, PLA NPs did not present hemolytic activity in concentrations up to 250 and 400 µg/mL for PLA_A and PLA_B NPs, respectively. Importantly, these are very high concentrations, far from the reality of *in vivo* administrations. In fact, apart from the fact that the experiment is performed with diluted blood (>10 times diluted), 250 µg/mL would correspond to a intravenously injected human dose of 1400 mg of NP and 400 µg/mL to a dose of 2240 mg [in a 70 kg person, with 5.6 L of blood (Dobrovolskaia and McNeil, 2013)]. Results confirm therefore the hemocompatibility of PLA NPs and are accordant with Altmeyer and co-workers, who described that no erythrocyte damage is caused by blank PLA NPs produced by an emulsion/solvent evaporation method with polyvinyl alcohol (PVA) (Altmeyer et al., 2016).

One of the most important conclusions herein presented is that even small changes in the physicochemical characteristics of similar NPs can originate different cytotoxicity profiles. In detail, results from RAW 264.7 suggested that PLA_A NPs induced the higher toxicity, and data from the NP characterization in the experiment conditions revealed these NPs presented the smaller mean diameter, resultant from a higher heterogeneity of the NP population, with emphasize for a population presenting a

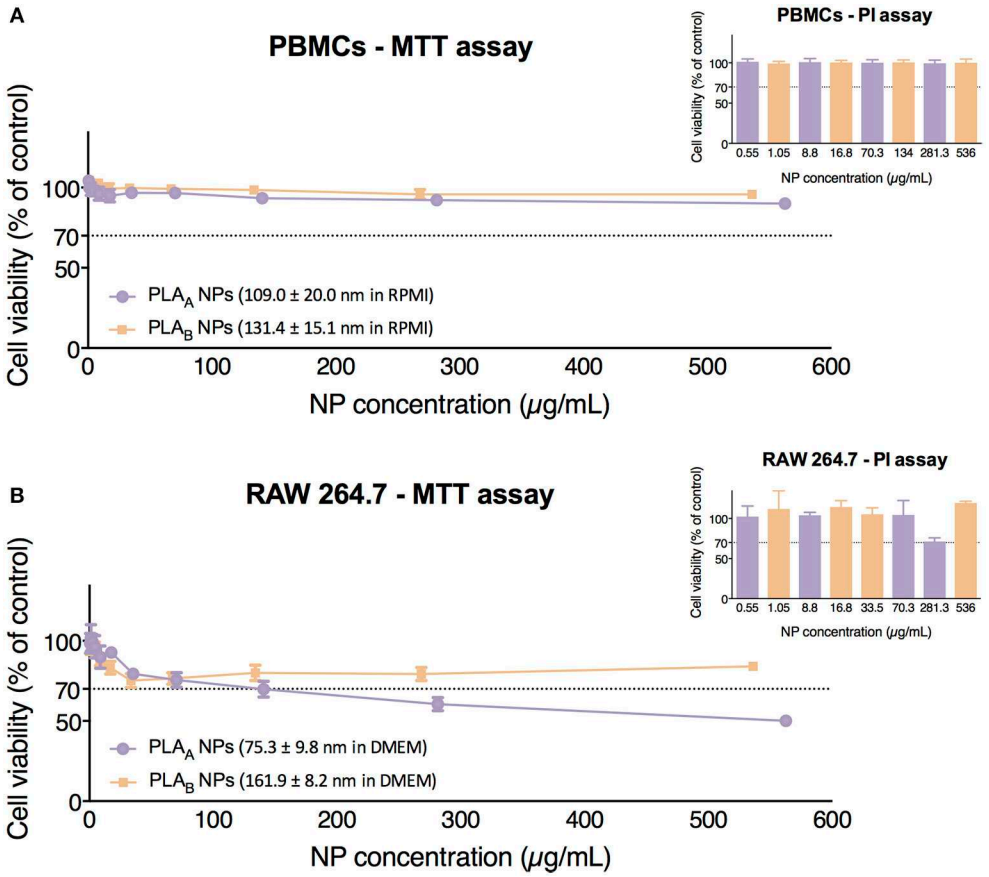

FIGURE 4 | Cytotoxicity assays (MTT and PI) performed in PBMCs **(A)** and in RAW 264.7 cell line **(B)** after 24 h of incubation with PLA NPs. Data are presented as mean ± SEM, $n \geq 4$ (four or more independent experiments, each in triplicate).

mean diameter of 10 nm. However, in PBMCs, both PLA NPs presented a similar cytotoxicity profile. Interestingly, in RPMI medium, used for PBMCs experiments, PLA_A NPs and PLA_B NPs presented a similar mean size and a more similar size-distribution profile than in DMEM medium. Considering these results, we can hypothesize that the smaller NP population in PLA_A NPs, resultant from a modification after dispersion in cell culture medium, is contributing to the increased toxicity of PLA_A NPs. These results are concordant with the concept that smaller NP can induce more cellular damages, due to increased ability to enter the cells, and particularly, sizes <10 nm can even reach the cell nucleus (Sukhanova et al., 2018). For instance, in a recent study (da Luz et al., 2017) it was proposed that small sized PLA NPs were mainly internalized in A549 cells through clathrin-coated pits in detriment of other endocytic pathways. In the future, the assessment of the mechanisms involved in the uptake of PLA_A NPs and PLA_B NPs could help clarify the cause of increased toxicity observed in PLA_A NPs.

The evaluation of the ROS production confirmed the correlation of the different toxicity profile of PLA NPs with the NP physicochemical differences and highlighted the importance of performing case-by-case evaluations. In fact, we demonstrated that PLA_A NPs induced a concentration-dependent ROS production, whereas PLA_B NPs did not stimulate statistically significant ROS production even with higher concentrations. A published report from Singh and co-workers (Singh and Ramarao, 2013) suggested that PLA NPs (emulsion-diffusion-evaporation method using PVA) induced no effect on ROS production up to 100 μg/mL concentration, whereas 300 μg/mL showed 1.5- to 2-fold stimulation of ROS production. Their results are in agreement with ours for PLA_A NPs, however, they are not aligned with the results from PLA_B NPs. This stresses the importance of an adequate evaluation when testing distinct polymeric nanomaterials rather than excessively extrapolating conclusions.

According to literature, PLA may induce inflammatory responses, due to its hydrophobicity, lack of bioactivity, and release of acidic degradation by-products (Li and Chang, 2004; Farah et al., 2016; Yoon et al., 2017). Nevertheless, this study showed that PLA polymer properties are not fully exchangeable with nanosized PLA particles. Actually, we showed that both PLA NPs produced within this study did not present effects on NO production under the concentration range tested, suggesting it does not induce an inflammatory response in RAW 264.7.

Importantly, during the execution of these studies we also hypothesized that the accentuated toxicity profile presented by PLA_A NPs could be related to the use of a higher concentration of Pluronic F68 during the production. Despite

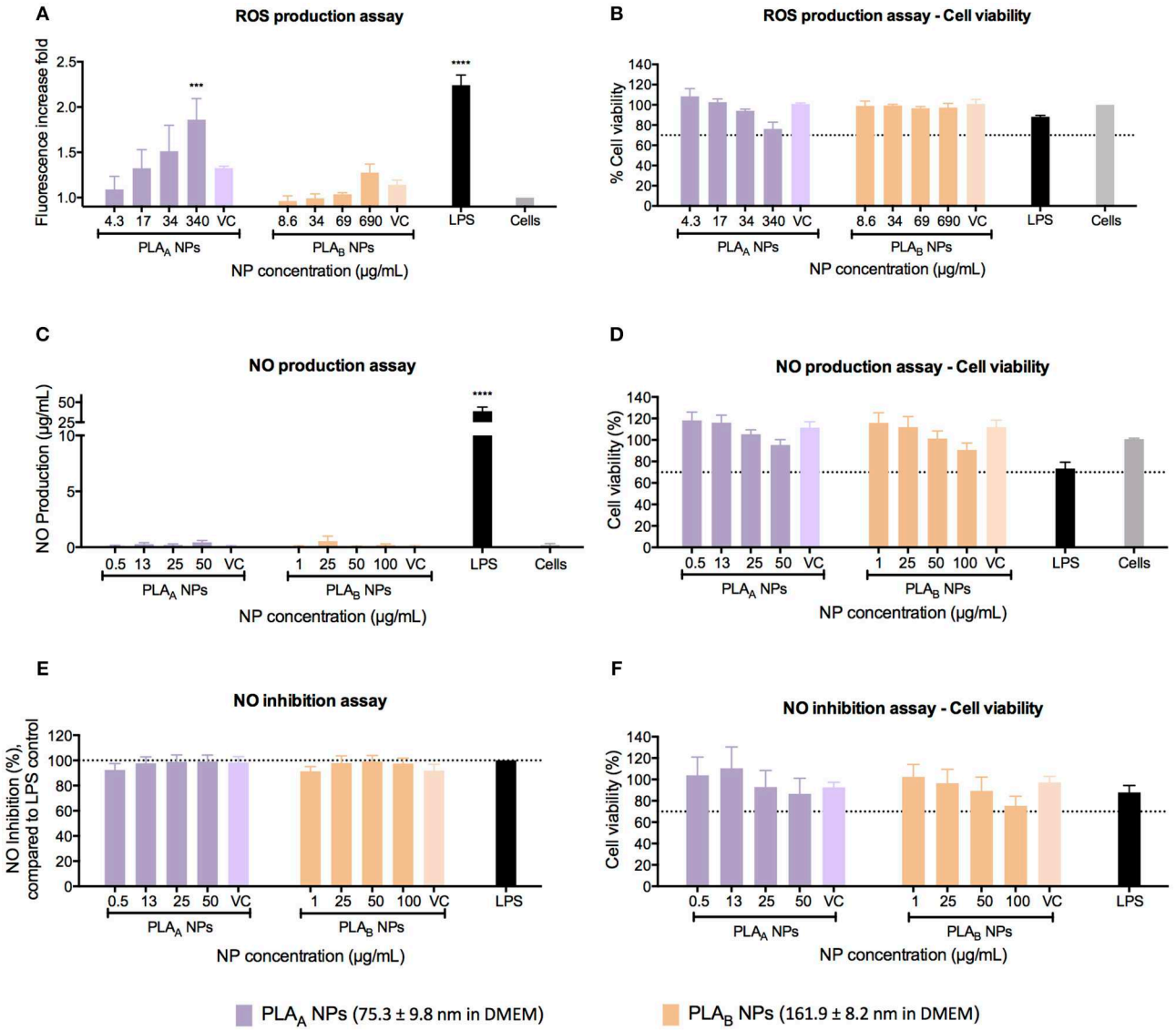

FIGURE 5 | Immunotoxicity assays, performed in RAW 264.7 macrophage cell line after 24 h of incubation with PLA NPs and PLA NPs dispersion media (VC). **(A)** ROS production assay using LPS as a positive control and unstimulated cells as a negative control. Results are presented in fluorescence increase fold compared to the negative control. **(B)** Cell viability assay (MTT) after the performance of ROS production assay. **(C)** NO production assay using LPS as a positive control and unstimulated cells as a negative control. **(D)** Cell viability assay (MTT) after the performance of NO production assay. **(E)** NO inhibition assay. For the estimation of PLA NPs inhibitory effect on NO production, PLA NPs were incubated simultaneously with LPS. The percentage of NO inhibition was calculated considering 100% the NO production induced by LPS without PLA NPs **(F)**. Cell viability assay (MTT) after the performance of NO inhibition assay. Data are presented as mean ± SEM, $n \geq 3$ (three or more independent experiments, each in triplicate). ***$p < 0.001$ and ****$p < 0.0001$.

we have washed the PLA_A NPs more exhaustively than PLA_B NPs to remove the surfactant, the negative zeta potential in pyrogen-free water gave an indication that PLA_A NPs could have more surfactant on its surface. To better understand whether PLA_A NPs accentuated effect on ROS production could result from Pluronic F68, the assay was repeated using a range of surfactant dilutions in water (0.00025–0.25%) and no pro-oxidative effect was verified and also no decrease in cell viability.

Lastly, polymeric NPs application into clinical research is dependent on more accurate knowledge of the NP interactions with the human body (Hoshyar et al., 2016). To address this issue, well-executed *in vitro* studies are needed to establish relationships between their biological activity and their physicochemical properties, such as the NP size (Hoshyar et al., 2016). In this sense, exploiting PLA NPs properties correlation with toxicity in a rigorous way represented an interesting challenge for our research group. Accordingly, important

recommendations were considered for the development of this work, such as the detailed characterization of the NP physicochemical properties in the original medium (pyrogen-free water) and in *in vitro* assay conditions, the inclusion of positive and negative controls, as well as the assessment of the NP interference before implementing testing protocols. To highlight, in every experiment, the NPs solvent (vehicle control) were also evaluated, in order to ensure that the observed effects were specific from PLA NPs. Also, for cytotoxicity assessment, more than one cell type was used to estimate the same endpoint, and two different methodologies (MTT and PI) were employed to confirm the results. These details shall increase the results reliability and relevance, as extensively discussed by (Drasler et al., 2017).

CONCLUSION

In this study, we observed that size highly influences PLA NPs toxicity profile. A new hypothesis to be confirmed in future arose in the course of this work. The smaller NPs are able to induce higher cellular toxicity, particularly mediated by ROS production. Nevertheless, the effect of size was only accurately addressed after characterization in *in vitro* assay conditions. Indeed, we exposed the influence of cell culture media on these polymeric NPs physicochemical characteristics and the respective repercussions on their toxicity. This report illustrates how an adequate NP characterization is crucial, in order to avoid misinterpretations, and consequent ambiguous conclusions. This remark can be further transposable to *in vivo* conditions, since the contact of NP with biological solutions, such as blood, saliva, nasal or gastric fluids can change the NP physicochemical properties, and those are known to be essential for the generation of a biological effect (Oh and Park, 2014).

We strongly believe that this study will help other research groups to achieve better understanding of their results and to obtain improved conclusions supporting the current scientific evidence.

DATA AVAILABILITY

All datasets generated for this study are included in the manuscript and/or the supplementary files.

AUTHOR CONTRIBUTIONS

JD carried out the experimental work. JD, SJ, and OB conceived and planned the experiments. All authors discussed the results and contributed to the final manuscript, reading, and approving the submitted version.

FUNDING

This work was financed by the European Regional Development Fund (ERDF), through the Centro 2020 Regional Operational Programme under project CENTRO-01-0145-FEDER-000008:BrainHealth 2020, and through the COMPETE 2020 - Operational Programme for Competitiveness and Internationalization and Portuguese national funds via FCT – Fundação para a Ciência e a Tecnologia, I.P., under project PROSAFE/0001/2016, and the strategic projects POCI-01-0145-FEDER-030331 and POCI-01-0145-FEDER-007440 (UID/NEU/04539/2019).

ACKNOWLEDGMENTS

The authors thank Dr. Ana Donato for expertise and assistance in hemocompatibility studies in the Clinical Analysis Laboratory of the Faculty of Pharmacy of Coimbra University (Portugal), Prof. Dr. Manfred Zinn for the determination of the exact MW of PDLLA by gel permeation chromatography/ size exclusion chromatography in the University of Applied Sciences and Arts Western Switzerland (HES-SO//Valais – Wallis) and Dr. Mónica Zuzart for the TEM microscopy analyses that were performed at iLAB—Bioimaging Laboratory of the Faculty of Medicine of the University of Coimbra.

REFERENCES

Altmeyer, C., Karam, T. K., Khalil, N. M., and Mainardes, R. M. (2016). Tamoxifen-loaded poly(L-lactide) nanoparticles: development, characterization and *in vitro* evaluation of cytotoxicity. *Mater. Sci. Eng. C* 60, 135–142. doi: 10.1016/j.msec.2015.11.019

ASTM (2013). ASTM E2524-08(2013) - *Standard Test Method for Analysis of Hemolytic Properties of Nanoparticles.* West Conshohocken, PA: ASTM International. Available online at: https://www.astm.org/Standards/E2524.htm (accessed September 26, 2018).

Boscá, L., Zeini, M., Través, P. G., and Hortelano, S. (2005). Nitric oxide and cell viability in inflammatory cells: a role for NO in macrophage function and fate. *Toxicology* 208, 249–258. doi: 10.1016/j.tox.2004.11.035

Brüne, B., Dehne, N., Grossmann, N., Jung, M., Namgaladze, D., Schmid, T., et al. (2013). Redox control of inflammation in macrophages. *Antioxid. Redox Signal.* 19, 595–637. doi: 10.1089/ars.2012.4785

Caruso, G., Fresta, C. G., Martinez-Becerra, F., Antonio, L., Johnson, R. T., de Campos, R. P. S., et al. (2017). Carnosine modulates nitric oxide in stimulated murine RAW 264.7 macrophages. *Mole. Cell. Biochem.* 431, 197–210. doi: 10.1007/s11010-017-2991-3

Circu, M. L., and Aw, T. Y. (2010). Reactive oxygen species, cellular redox systems, and apoptosis. *Free Radical Biol. Med.* 48, 749–762. doi: 10.1016/j.freeradbiomed.2009.12.022

da Luz, C. M., Boyles, M. S., Falagan-Lotsch, P., Pereira, M. R., Tutumi, H. R., de Oliveira Santos, E., et al. (2017). Poly-lactic acid nanoparticles (PLA-NP) promote physiological modifications in lung epithelial cells and are internalized by clathrin-coated pits and lipid rafts. *J. Nanobiotechnol.* 15, 11. doi: 10.1186/s12951-016-0238-1

Dobrovolskaia, M. A., Clogston, J. D., Neun, B. W., Hall, J. B., Patri, A. K., and McNeil, S. E. (2008). Method for analysis of nanoparticle hemolytic properties *in vitro*. *Nano Lett.* 8, 2180–2187. doi: 10.1021/nl0805615

Dobrovolskaia, M. A., Germolec, D. R., and Weaver, J. L. (2009). Evaluation of nanoparticle immunotoxicity. *Nature Nanotechnol.* 4, 411–414. doi: 10.1038/nnano.2009.175

Dobrovolskaia, M. A., and McNeil, S. E. (2013). Understanding the correlation between *in vitro* and *in vivo* immunotoxicity tests for nanomedicines. *J. Controll. Release* 172, 456–466. doi: 10.1016/j.jconrel.2013.05.025

Drasler, B., Sayre, P., Steinhäuser, K. G., Petri-Fink, A., and Rothen-Rutishauser, B. (2017). *In vitro* approaches to assess the hazard of nanomaterials. *NanoImpact* 8, 99–116. doi: 10.1016/j.impact.2017.08.002

Essa, S., Louhichi, F., Raymond, M., and Hildgen, P. (2012). Improved antifungal activity of itraconazole-loaded PEG/PLA nanoparticles. *J. Microencapsul.* 30, 205–217. doi: 10.3109/02652048.2012.714410

Farah, S., Anderson, D. G., and Langer, R. (2016). Physical and mechanical properties of PLA, and their functions in widespread applications—a comprehensive review. *Adv. Drug Deliv. Rev.* 107, 367–392. doi: 10.1016/j.addr.2016.06.012

Hoshyar, N., Gray, S., Han, H., and Bao, G. (2016). The effect of nanoparticle size on *in vivo* pharmacokinetics and cellular interaction. *Nanomedicine* 11, 673–692. doi: 10.2217/nnm.16.5

Jesus, S., Soares, E., Borchard, G., and Borges, O. (2017). Adjuvant activity of poly-ε-caprolactone/chitosan nanoparticles characterized by mast cell activation and IFN-γ and IL-17 production. *Mol. Pharma.* 15, 72–82. doi: 10.1021/acs.molpharmaceut.7b00730

Jiao, Q., Li, L., Mu, Q., and Zhang, Q. (2014). Immunomodulation of nanoparticles in nanomedicine applications. *BioMed Res. Int.* 2014, 1–19. doi: 10.1155/2014/426028

Kendall, M., Hodges, N. J., Whitwell, H., Tyrrell, J., and Cangul, H. (2014). Nanoparticle growth and surface chemistry changes in cell-conditioned culture medium. *Philos. Trans. R. Soc. B. Biol. Sci.* 370:20140100. doi: 10.1098/rstb.2014.0100

Kwon, D. H., Jeong, J. W., Choi, E. O., Lee, H. W., Lee, K. W., Kim, K. Y., et al. (2017). Inhibitory effects on the production of inflammatory mediators and reactive oxygen species by *Mori folium* in lipopolysaccharide-stimulated macrophages and zebrafish. *An. Acad. Bras. Ciênc.* 89, 661–674. doi: 10.1590/0001-3765201720160836

Legaz, S., Exposito, J.Y., Lethias, C., Viginier, B., Terzian, C., and Verrier, B. (2016). Evaluation of polylactic acid nanoparticles safety using drosophila model. *Nanotoxicology* 10, 1136–1143. doi: 10.1080/17435390.2016.1181806

Li, H., and Chang, J. (2004). Preparation and characterization of bioactive and biodegradable wollastonite/poly(D,L-lactic acid) composite scaffolds. *J. Mat. Sci. Mat. Med.* 15, 1089–1095. doi: 10.1023/B:JMSM.0000046390.09540.c2

Oh, N., Park, J. H. (2014). Endocytosis and exocytosis of nanoparticles in mammalian cells. *Int. J. Nanomed.* 9(Suppl. 1), 51–63. doi: 10.2147/ijn.s26592

Pattani, A., Patravale, V. B., Panicker, L., and Potdar, P. D. (2009). Immunological Effects and Membrane interactions of chitosan nanoparticles. *Mol. Pharma.* 6, 345–352. doi: 10.1021/mp900004b

Saini, P., Saha, S. K., Roy, P., Chowdhury, P., and Sinha Babu, S. P. (2016). Evidence of reactive oxygen species (ROS) mediated apoptosis in *Setaria cervi* induced by green silver nanoparticles from *Acacia auriculiformis* at a very low dose. *Experiment. Parasitol.* 160, 39–48. doi: 10.1016/j.exppara.2015.11.004

Santander-Ortega, M. J., Jódar-Reyes, A. B., Csaba, N., Bastos-González, D., and Ortega-Vinuesa, J. L. (2006). Colloidal stability of Pluronic F68-coated PLGA nanoparticles: a variety of stabilisation mechanisms. *J. Colloid Interface Sci.* 302, 522–529. doi: 10.1016/j.jcis.2006.07.031

Singh, R. P., and Ramarao, P. (2013). Accumulated polymer degradation products as effector molecules in cytotoxicity of polymeric nanoparticles. *Toxicol. Sci.* 136, 131–143. doi: 10.1093/toxsci/kft179

Sukhanova, A., Bozrova, S., Sokolov, P., Berestovoy, M., Karaulov, A., and Nabiev, I. (2018). Dependence of nanoparticle toxicity on their physical and chemical properties. *Nanoscale Res. Lett.* 13:44. doi: 10.1186/s11671-018-2457-x

Tyler, B., Gullotti, D., Mangraviti, A., Utsuki, T., and Brem, H. (2016). Polylactic acid (PLA) controlled delivery carriers for biomedical applications. *Adv. Drug. Deliv. Rev.* 107, 163–175. doi: 10.1016/j.addr.2016.06.018

Villiers, C., Chevallet, M., Diemer, H., Couderc, R., Freitas, H., Van Dorsselaer, A., et al. (2009). From secretome analysis to immunology. *Mole. Cell. Proteomics* 8, 1252–1264. doi: 10.1074/mcp.M800589-MCP200

Yoon, S.D., Kwon, Y.S., and Lee, K.S. (2017). Biodegradation and biocompatibility of poly L-lactic acid implantable mesh. *Int. Neurourol. J.* 21, 48–54. doi: 10.5213/inj.1734882.441

Zolnik, B., Potter, T. M., and Stern, S. T. (2011). "Detecting reactive oxygen species in primary hepatocytes treated with nanoparticles," in *Characterization of Nanoparticles Intended for Drug Delivery; Methods in Molecular Biology Series*, ed S. E. McNeil (New York, NY: Humana Press), 173–179.

Conflict of Interest Statement: The authors declare that the research was conducted in the absence of any commercial or financial relationships that could be construed as a potential conflict of interest.

frontiers in Bioengineering and Biotechnology

ORIGINAL RESEARCH
published: 06 September 2019
doi: 10.3389/fbioe.2019.00214

Computational Assessment of the Pharmacological Profiles of Degradation Products of Chitosan

*Diana Larisa Roman[1], Marin Roman[1], Claudia Som[2], Mélanie Schmutz[2], Edgar Hernandez[2], Peter Wick[3], Tommaso Casalini[4], Giuseppe Perale[4], Vasile Ostafe[1] and Adriana Isvoran[1]**

[1] Advanced Environmental Research Laboratories, Department of Biology-Chemistry, Faculty of Chemistry, Biology, Geography, West University of Timisoara, Timisoara, Romania, [2] Empa, Swiss Federal Laboratories for Materials Science and Technology, Technology and Society Laboratory, St. Gallen, Switzerland, [3] Empa, Swiss Federal Laboratories for Materials Science and Technology, Particles-Biology Interactions Laboratory, St. Gallen, Switzerland, [4] Department of Innovative Technologies, University of Applied Sciences and Arts of Southern Switzerland (SUPSI), Manno, Switzerland

Chitosan is a natural polymer revealing an increased potential to be used in different biomedical applications, including drug delivery systems, and tissue engineering. It implies the evaluation of the organism response to the biomaterial implantation. Low-molecular degradation products, the chito-oligomers, are resulting mainly from the influence of enzymes, which are found in the organism fluids. Within this study, we have performed the computational assessment of pharmacological profiles and toxicological effects on human health of small chito-oligomers with distinct molecular weights, deacetylation degrees, and acetylation patterns. Our approach is based on the fact that regulatory agencies and researchers in the drug development field rely on the use of modeling to predict biological effects and to guide decision making. To be considered as valid for regulatory purposes, every model that is used for predictions should be associated with a defined toxicological endpoint and has appropriate robustness and predictivity. Within this context, we have used FAF-Drugs4, SwissADME, and PreADMET tools to predict the oral bioavailability of chito-oligomers and SwissADME, PreADMET, and admetSAR2.0 tools to predict their pharmacokinetic profiles. The organs and genomic toxicities have been assessed using admetSAR2.0 and PreADMET tools but specific computational facilities have been also used for predicting different toxicological endpoints: Pred-Skin for skin sensitization, CarcinoPred-EL for carcinogenicity, Pred-hERG for cardiotoxicity, ENDOCRINE DISRUPTOME for endocrine disruption potential and Toxtree for carcinogenicity and mutagenicity. Our computational assessment showed that investigated chito-oligomers reflect promising pharmacological profiles and limited toxicological effects on humans, regardless of molecular weight, deacetylation degree, and acetylation pattern. According to our results, there is a possible inhibition of the organic anion transporting peptides OATP1B1 and/or OATP1B3, a weak potential of cardiotoxicity, a minor probability of affecting the androgen receptor, and phospholipidosis. Consequently, these results may be used to guide or to complement the existing *in vitro* and *in vivo* toxicity tests, to optimize biomaterials properties and to contribute to the selection of prototypes for nanocarriers.

Keywords: chito-oligomers, ADME-Tox, pharmacokinetics, toxicity endpoints, biological effects

OPEN ACCESS

Edited by:
Michele Iafisco, Italian National Research Council (CNR), Italy

Reviewed by:
Sinosh Skariyachan, Dayananda Sagar Institutions, India
Naveed Muhammad, Nanjing Medical University, China

***Correspondence:**
Adriana Isvoran
adriana.isvoran@e-uvt.ro

Specialty section:
This article was submitted to Nanobiotechnology, a section of the journal Frontiers in Bioengineering and Biotechnology

Received: *10 June 2019*
Accepted: *22 August 2019*
Published: *06 September 2019*

Citation:
Roman DL, Roman M, Som C, Schmutz M, Hernandez E, Wick P, Casalini T, Perale G, Ostafe V and Isvoran A (2019) Computational Assessment of the Pharmacological Profiles of Degradation Products of Chitosan. Front. Bioeng. Biotechnol. 7:214. doi: 10.3389/fbioe.2019.00214

INTRODUCTION

Chitin is a polysaccharide abundantly found in nature, especially in crustaceans, but also in insects and fungi. Chitosan is obtained from chitin by chemical or enzymatic deacetylation (Rinaudo, 2006). The difference between chitin and chitosan consists of the acetyl content, chitin contains mostly N-acetyl-D-glucosamine (GlcNAc, A) units and chitosan contains especially D-glucosamine (GlcN, D). Chitin and chitosan reveal biocompatibility, biodegradability, and non-toxicity for humans and the environment (Rinaudo, 2006). These characteristics, added to the anti-fungal, anti-bacterial, anti-microbial, and anti-oxidant properties of chitosan conducted to numerous applications in different fields: food industry, cosmetic and personal care products, wastewater management, pharmacological products, and implantable materials (Enescu and Olteanu, 2008; Raafat and Sahl, 2009; Cheung et al., 2015). Chitosan nanoparticles are approved by the Food and Drug Administration (FDA) for tissue engineering and drug delivery and by FDA and EU for dietary use and wound dressing applications (Mohammed et al., 2017).

There are many different ways in which humans have exposure to chito-oligomers (COs): by the degradation of implanted materials based on chitosan, the use of pharmaceutical products containing COs and/or occupational exposure. The low-molecular degradation products of chitosan, the chito-oligomers, occur as a result of the influence of enzymes which are present in bodily fluids (Saikia et al., 2015). Due to the limitations concerning the applications of chitosan polymer related to its higher viscosity and insolubility in neutral and basic environments (Giri et al., 2012; Ways et al., 2018), COs with an increased solubility and lower viscosity have been obtained by chemical or enzymatic hydrolysis of chitosan and are largely used in the pharmaceutical field (Enescu and Olteanu, 2008; Patrulea et al., 2015; Ways et al., 2018). As an example, food supplements containing COs and their derivatives are used by many people for treating osteoarthritis (Jerosch, 2011) but their clinical importance is unclear (Liu et al., 2018). Occupational exposure to these compounds may also occur.

The chitosan oligomers that result from the hydrolysis processes may be classified in two types: (i) homo-chito-oligosaccharides containing only GlcN or GlcNAc units and (ii) hetero-chito-oligosaccharides, containing both GlcN and GlcNAc with varying degrees of deacetylation (the percent of glucosamine units in the oligomer, DDA) and a varying position of glucosamine residues in the oligomer chain (acetylation pattern, AP). GlcN unit carries an amino group that is protonated at physiological pH (Cheung et al., 2015). Both homo- and hetero-oligomers may differ in the degree of polymerization (the number the monomeric units within an oligomer, DP). Hetero-chito-oligomers with DP<10 are considered as water soluble (Liaqat and Eltem, 2018).

Taking into account the possible ways of exposure of humans to COs, the concept of Safe-by-design (SbD) must be considered when producing and using chitosan and its oligomers. Safe-by-design is a relatively new concept planned to be used in the research and development (R&D) field and industry, and include safe design, safe production, safe use and waste management for new materials and technologies (van de Poel and Robaey, 2017). Safe design addresses safety early in the R&D and design phases, such as in the design of safe products for professionals, consumers and the environment, and is usually based on prediction and experimental testing (*in vitro* and *in vivo* short term assays) tools. Safe production considers the use of environmentally friendly technologies and the potential risk for professionals involved in R&D and industrial processes. Safe use and waste management reflect safe handling (by both consumers and professionals) of products and wastes. Safety profiles of COs should depend on their structure and physicochemical properties (van de Poel and Robaey, 2017). Computational studies may have a valuable contribution to assess the safe designing of compounds by predicting the biological effects and toxicity profiles and by correlating them with the physicochemical and structural properties.

COs have numerous pharmaceutical properties and medical applications: anti-microbial, anti-oxidant, anti-tumoral, anti-inflammatory, immunostimulatory, anti-obesity, anti-hypertension, and anti-Alzheimer (Mourya et al., 2011; Cheung et al., 2015; Muanprasat and Chatsudthipong, 2017). COs having DP<20 are soluble in water and reveal antimicrobial, antioxidant, antitumoral, antiviral, antiangiogenic, and prebiotic properties (Sánchez et al., 2017; Long et al., 2018; Lu et al., 2019). COs with a molecular weight lower than 2000 Da and DDA>90% revealed a moderate neuroprotective activity and no toxicity against neurons (Santos-Moriano et al., 2018) and COs with molecular weight lower than 1000 Da showed high antioxidant activity (El-Sayed et al., 2017). Literature data reveal that COs having DP>6 possess enhanced anti-tumor, antimicrobial and immunopotentiation properties, favorable biological activities of smaller COs being also reported (Liaqat and Eltem, 2018). These activities of COs are dependent on their physicochemical properties: molecular weight (MW), the degree of deacetylation (DDA), the degree of polymerization (DP), and charge distribution (acetylation pattern, AP) (Park et al., 2011), but their structure–activity relationships are rather unknown (Santos-Moriano et al., 2018).

Specific literature contains little or no information about the biological effects of every possible variant of COs (Liaqat and Eltem, 2018). A chito-oligomer with specific physicochemical properties (MW, DDA, AP) may display all, some or none of all considered bioactivities of COs (Sánchez et al., 2017). The low reproducibility of results and sometimes the opposite reported effects concerning the COs biological activities could mainly be due to relatively poorly characterized oligomer mixtures that have been used in experimental studies and/or to inconstant reporting of the properties of COs (Mourya et al., 2011; Park et al., 2011; Li et al., 2016). Furthermore, available information concerning the effects of COs is mainly derived from *in vitro* and *in vivo* studies with animal models and there are limited human experimental data concerning the absorption, distribution, metabolism, excretion, and toxicity of these compounds (Cheung et al., 2015; Phil et al., 2018). It reflects the insufficiency of safety data concerning their use by humans.

The number of used chemicals is increasing constantly and there is a need to assess their safety for humans and environment. Considering the costs of the laboratory studies and the ethical concerns on using animals for testing, the role of bioinformatics in hazard assessment is well-recognized. The explosive growth in the magnitude and diversity of data from physics, chemistry, and biology conducted to the creation of specific databases and computational packages for data manipulation (Luechtefeld and Hartung, 2017). The easy access to these data allowed scientists to build accurate computational models for toxicology assessment. These models are used in drug discovery and development and for assessment of the effects of xenobiotics on humans and environment. Computational tools that were developed for hazard assessment include (quantitative) structure-activity relationships [(Q)SARs], read-across methods, expert rule-based (structural alerts) methods, and molecular modeling techniques (Alves et al., 2018a; Myatt et al., 2018; Yang et al., 2018). The Organization of Economic and Co-operation Development (OECD) created QSAR guidelines already in 2004 and the principles for the construction of (Q)SAR models, computational methods, and model validation methods are described in detail since 2007 (Fjodorova et al., 2008; Lo Piparo and Worth, 2010). Furthermore, REACH (Registration, Evaluation and Authorization of CHemicals) regulation mentions the QSAR techniques for studying the toxicological profile of chemicals (Kleandrova and Speck-Planche, 2013). Consequently, QSAR has been a reliable computational tool used for decades for connecting the properties and biological activity. Taking into consideration the limitations, the number of improvements has been recorded and various descriptors have been explored: molecular properties (0D-QSAR), fragment counts (1D-QSAR), topological descriptors (2D-QSAR), spatial coordinates (3D-QSAR), a combination of atomic coordinates and sampling of conformations (4D-QSAR), multiple expression of ligand topology (5D-QSAR), considering the solvation function (6D-QSAR) and receptor or target-based receptor model data (7D-QSR) (Kar and Leszczynski, 2019). Nowadays, many software and web servers are available for predicting chemical toxicity before synthesis, as it is recognized that computational techniques provide high-quality predictions for chemical hazard assessment (Yang et al., 2018), meaning 2D-QSAR and 3D-QSAR methods are frequently used.

Besides the large applicability of these modern tools for human and environment hazard assessment, there also are some limitations, mostly related to the robustness and predictability of the used models and to the fact that they do not provide a clean mechanistic interpretation of the outcomes (Luechtefeld and Hartung, 2017). The methods mentioned above are not applicable for assessing the pharmacokinetics of nanoparticles, especially due to the fact that fundamental mechanisms that support drug-handling within the human organism are not understood for nanoparticles (Nel et al., 2009; Beddoes et al., 2015). Also, as most QSAR models are based on *in vivo* or *in vitro* data from specific experimental conditions, the applicability domain of the QSAR model is more limited for nanomaterials (Choi et al., 2018). Furthermore, data concerning the effects of the oligomer components cannot be transferred to nanoscale polymers since in the case of nanoparticles, not only the dose and their elemental composition, but their shape, size, and surface characteristics determine the biological activities and therapeutic effects and it increases the difficulty of modeling the biological effects of nanomaterials (Nel et al., 2009; Beddoes et al., 2015). Consequently, within this study we focus on the chito-oligomers both as degradation products of chitosan nanoparticles and as independent food supplements.

The objectives of this study are: (1) prediction of the pharmacological profiles and toxicological endpoints (skin sensitization potential, endocrine disruption potential, cardiotoxicity, hERG channel blocking potential, carcinogenicity, and mutagenicity) of COs containing up to 8 monomeric units (water soluble chito-oligomers) and (2) assessment of the influence of the MW, DDA, and AP on the toxicological and pharmacological profiles of investigated COs by using computational approaches.

MATERIALS AND METHODS

Among the numerous available computational tools for predicting the pharmacological properties and toxicological effects of chemical compounds on human health, we have selected those with an accuracy of a prediction usually higher than 70% and with friendly interfaces and tutorials that are available for free (online or open-source). The chito-oligomers that we have considered in this study are presented in **Table 1** together with the computed values of their molecular weights using admetSAR2.0 tool (see further). We specify that each amino group of the deacetylated units is protonated. Furthermore, **Table 1** shortly reviews known information concerning medical and side/toxicological effects of small COs. Some of these compounds are approved by FDA only as food supplements and/or for use in wound dressings (Wedmore et al., 2000). In Europe, GlcN and GlcNAc are approved as drugs in the form of glucosamine sulfate (Jordan et al., 2003).

The simplified molecular-input line-entry system (SMILES) formulas of the considered COs are built using ACD/ChemSketch software (https://chemicalize.com). This software also generates structural files in *mol* format to be used for further predictions We have obtained 3D sdf files using OpenBabel (O'Boyle et al., 2011) on the online server http://www.cheminfo.org/Chemistry/Cheminformatics/FormatConverter/index.html, starting from their structural files in *mol* format generated by ACD/ChemSketch software. Structure minimization has been done using Chimera software (Pettersen et al., 2004) using 1000 steepest descent steps, step size 0.02 Å, 10 conjugate gradient steps, conjugate gradient step size 0.02 Å.

FAF-Drugs4 (Lagorce et al., 2017) tool has been considered for assessing the oral bioavailability as a part of the pharmacokinetic profile and the overall toxicity of investigated COs. This is a rule-based tool having the accuracy of predictions higher than 70% (Lagorce et al., 2017). FAF-Drugs4 tool allows filtering against Lipinski's rule (Lipinski et al., 2001), Egan's rule (Egan et al., 2000), and Veber's rule (Veber et al., 2002) for predicting

TABLE 1 | Chito-oligomers considered in this study, their computed molecular weights (MW), and known medical and side effects (NA means not available data).

DD	Acetylation pattern	MW (g/mol)	Medical effects	Side effects
0%	A	221.21	N-acetyl-D-glucosamine is used in treating osteoarthritis, cancer, and wounds (Jordan et al., 2003; Masuda et al., 2014). It proved to be useful for treating colds and pain (Konno, 2002) and is found in cosmetic products being able to reduce the facial hyperpigmentation (Bissett et al., 2007).	A study concerning oral administration of GlcNAc at doses of 500 and 1000 mg/day for 68 female revealed no side effects (Kubomura et al., 2017).
	2A	424.40	Di-N-acetyl chitobiose and tri-N-acetyl chitotriose did not show anti-oxidant activity *in vitro* (Chen et al., 2003) but proved to be useful for treating colds and pain (Konno, 2002).	NA
	3A	627.59		
	4A	870.79	Tetra-N acetyl-chitotetraose and penta N-acetyl chitopentaose have been used for treating colds and pain (Konno, 2002). Tetra-N acetyl-chitotetraose significantly improved both learning and of rats suffering of Alzheimer's disease (Jiang et al., 2019).	NA
	5A	1,033.98		
	6A	1,237.17	Hexa N -acetyl chitohexaose revealed a tumor grows inhibitory effect (Xiong et al., 2009) and had favorable influence in treating colds and pain (Konno, 2002). Chitohexaose blocks the induction of inflammatory mediators both *in vitro* and *in vivo* (Das et al., 2019) and significantly improved both learning and of rats suffering of Alzheimer's disease (Jiang et al., 2019).	NA
	8A	1,643.56	Octa N -acetyl chitooctose had favorable influence in treating colds and pain (Konno, 2002).	NA
33%	ADA	585.56	N,N′-diacetylchitotriose exhibited an anti-oxidant activity *in vitro* (Li et al., 2013).	NA
50%	DA	382.36	NA	NA
	DADA	746.71	NA	NA
	ADAD	746.71	NA	NA
	AADD	746.71	NA	NA
	DDAA	746.71	NA	NA
	DAAD	746.71	NA	NA
	ADDA	746.71	NA	NA
	DADADA	1,475.41	NA	NA
	ADADAD	1,475.41	NA	NA
	DADADADA	1,857.77	NA	NA
67%	DDA	543.52	N-acetylchitotriose revealed an anti-oxidant activity *in vitro* (Li et al., 2013).	NA
	ADDDAD	1,069.02	NA	NA
	DDDADA	1,069.02	NA	NA
100%	D	179.17	Glucosamine is a popular food supplement used for treating osteoarthritis, but clinical trials on humans did not reveal results supporting its efficacy for every human subject (Chan and Fat, 2011; Liu et al., 2018). Glucosamine administration is expected to promote wound healing by enhancing hyaluronic acid production (Esfahani et al., 2012). It has anti-inflammatory, anti-aging, anti-oxidant, anti-cancer, anti-fibrotic, anti-fungal, neuro-protective, cardio-protective, skin hydration, and wrinkle reduction properties (Masuda et al., 2014; Zahedipour et al., 2017; Fawzya et al., 2019). It induced weight loss and reduced triglyceride and cholesterol levels in serum (Huang et al., 2015).	Clinical trial data obtained for 3063 human subjects revealed non effects of the oral administration of glucosamine on glucose metabolism and on urine, blood, and fecal parameters (Anderson et al., 2005). It may induce mild gastrointestinal disorders (Dalirfardouei et al., 2016).
	2D	340.33	Chitobiose had a strong anti-oxidant activity *in* (Chen et al., 2003) and has been used for treating common colds and pain (Konno, 2002). Chitobiose revealed a significant inhibitory effect on hepatic lipid accumulation *in vitro* (Li et al., 2018; Zhao et al., 2019) and anti-bacterial effect on Gram-positive bacteria (Li et al., 2014).	NA
	3D	501.48	Chitotriose revealed potency to treat colds and pain (Konno, 2002), strong anti-oxidant activity *in vitro* (Chen et al., 2003), a low inhibitory effect on hepatic lipid accumulation *in vitro* (Li et al., 2018; Zhao et al., 2019) and an anti-bacterial effect on Gram-positive bacteria (Li et al., 2014). Chitotriose seems to have beneficial effects on the nervous system (Jiang et al., 2014).	NA

(Continued)

TABLE 1 | Continued

DD	Acetylation pattern	MW (g/mol)	Medical effects	Side effects
	4D	662.64	Chitotetraose revealed a low inhibitory effect on hepatic lipid accumulation *in vitro* (Li et al., 2018) and an anti-bacterial effect on Gram-positive bacteria (Li et al., 2014). It had favorable properties for treating pain and colds (Konno, 2002).	NA
	5D	823.79	Chitopentaose revealed a low inhibitory effect on hepatic lipid accumulation *in vitro* (Li et al., 2018), an enhanced anti-bacterial effect on Gram-positive bacteria (Li et al., 2014) and anti-inflammatory action *in vitro* (Li et al., 2012).	NA
	6D	984.95	Chitohexaose revealed a low inhibitory effect on hepatic lipid accumulation *in vitro* (Li et al., 2018), exhibited a high anti-tumor activity *in vitro* (Xiong et al., 2009; Li et al., 2016) and anti-fungal activity (Fawzya et al., 2019).	NA
	8D	1,307.26	Chitooctose had favorable influence in treating colds and pain (Konno, 2002).	NA

bioavailability and of Pfizer's and GSK rules for predicting the overall toxicity (Gleeson, 2008).

SwissADME is a web tool that allows the computation of the physicochemical parameters of a chemical compound, its pharmacokinetic profile, drug likeness and medicinal chemistry, starting from the SMILES formula, the accuracy of predictions being between 72 and 94% (Daina et al., 2017).

AdmetSAR2.0 (Cheng et al., 2012; Yang et al., 2019) tool has been used to predict pharmacokinetic profiles and organ (eye, heart, liver) and genomic toxicity of investigated COs. with a predictive accuracy of 72.3–76.7% (Yang et al., 2019). Furthermore, every prediction made by this tool is quantitatively described by a probability output.

PreADMET is also a web tool having four parts: (i) molecular descriptors calculation; (ii) drug likeness prediction considering well known rules; (iii) ADME prediction; and (iv) toxicity prediction [mutagenicity by Ames test and rodent carcinogenicity; (Lee et al., 2003, 2004)].

Because occupational exposure to chitin and chitosan may also occur through dermal contact and skin sensitization, it may have a significant impact on individual working capacity and quality of life, we have assessed the skin sensitizer potential of investigated COs using Pred-Skin computational tool (Braga et al., 2017; Alves et al., 2018b). This information is also important when we take into account the fact that chitosan is approved to be used in wound healing purposes. Pred-Skin is a web-based computational facility considering QSAR models of skin sensitization potential. It performs the following predictions: (i) binary predictions of human skin sensitization potential established taking into account human data (prediction accuracy being 73–76%); (ii) binary predictions of murine skin sensitization potential taking into account animal data (LLNA, prediction accuracy being 70–84%); (iii) binary predictions based on Direct Peptide Reactivity Assay (DPRA), KeratinoSens, and the human Cell Line Activation Test (h-CLAT) data (prediction accuracy being 80–86%); (iv) a consensus model that is generated by averaging the predictions of individual models (prediction accuracy being 70–84% (Braga et al., 2017; Alves et al., 2018b).

Predictions concerning carcinogenicity and mutagenicity are also obtained using Toxtree software, the accuracy of predictions being 70% (Patlewicz et al., 2008).

CarcinoPred-EL (Carcinogenicity Prediction using Ensemble Learning methods) utility has been used for accomplishing predictions concerning the carcinogenicity of investigated chemicals (Zhang et al., 2017). It is a free prediction online server that is based on twelve different molecular fingerprints and three ensemble machine learning models (Ensemble RF, Ensemble SVM, and Ensemble XGBoost) permitting the identification of the structural features related to carcinogenic effects of chemical compounds (Zhang et al., 2017).

Pred-hERG is another free accessible web tool that builds predictive models of the ability of a chemical compound to inhibit the human ether-à-go-go related gene (hERG) K^+ channels. This hERG K^+ channel blockage may result in cardiac side effects such as heart arrhythmia and even possibly death (Braga et al., 2015). Consequently, hERG K^+ channel blockage is one of the most important toxicological endpoints to be considered when assessing the safety of chemical compounds. There are two outcomes when using Pred-hERG tool: a binary prediction (hERG non-blocker or blocker) and a multiclass prediction (hERG non-blocker, weak/moderate blocker, strong blocker) along with the probability of the prediction for each class. The predictions have an accuracy of up to 89% (Braga et al., 2015).

Endocrine disruption potential is evaluated using ENDOCRINE DISRUPTOME computational tool (Kolšek et al., 2014). This tool uses the molecular docking approach for predicting interactions between the explored compound with 12 distinct human nuclear receptors, those binding sites are known: androgen receptor (AR), estrogen receptors α (ERα) and β (ERβ), glucocorticoid receptor (GR), liver X receptors α (LXRα) and β (LRXβ), peroxisome proliferator-activated receptors α (PPRAα), β/δ (PPRAβ), and γ (PPRAγ), retinoid X receptor α (RXRα) and thyroid receptors α (TRα), and β (TRβ). Both agonistic and antagonistic (an) effects are predicted for AR, ERα, ERβ, and GR. Predictions are based on computation of the sensitivity (SE) parameter and compounds are categorized in four classes: (i)

TABLE 2 | Short presentation of the computational tools that were used in the current study.

Tool	Inputs	Method	Output	References
FAF-Drugs4	Structural data files (2D SDF) of COs	expert-rules based	Oral bioavailability and safety profiles	Lagorce et al., 2017
SwissADME	SMILES formulas of COs	expert-rules based 2D QSAR	Druglikeness Pharmacokinetic profile	Daina et al., 2017
PreADMET	Structural data files (2D SDF) of COs	expert-rules based 2D-QSAR	Druglikeness Pharmacokinetic profile Toxicological endpoint	Lee et al., 2003, 2004
admetSAR2.0	SMILES formulas of COs	2D QSAR	Pharmacokinetic profiles, organ (eye, heart, liver) and genomic toxicity	Cheng et al., 2012; Yang et al., 2019
Pred-Skin	SMILES formulas of COs	2D-QSAR	Skin sensitization potential	Braga et al., 2017; Alves et al., 2018b
Toxtree	SMILES formulas of COs	Expert-rules based	Carcinogenic and mutagenic potential	Patlewicz et al., 2008
CarcinoPred-EL	SMILES formulas of COs	2D QSAR	Carcinogenic potential	Zhang et al., 2017
Pred-hERG	SMILES formulas of COs	2D QSAR	hERG K+ channel blockage potential	Braga et al., 2015
ENDOCRINE DISRUPTOME	SMILES formulas of COs	Molecular docking and calculation of a sensitivity parameter	Probability of binding to nuclear receptors	Kolšek et al., 2014

compounds with SE<0.25 expose a high probability of binding to nuclear receptors; (ii) compounds with 0.25<SE<0.50 reflect a medium probability of binding to the nuclear receptors; (iii) compounds having 0.50<SE<0.75 emphasize minor probability of binding and (iv) compounds with SE>0.75 reveal a low probability of binding to the nuclear receptors (Kolšek et al., 2014).

A summary of the computational tools that we have used in this study is presented in **Table 2**.

The computational tools that are used in this study have been elaborated for assessing the pharmacological profiles and toxicological endpoints of new drugs, but they were successfully applied for other classes of chemicals: cosmetic ingredients and pesticides (Alves et al., 2018c; Roman et al., 2018a; Gridan et al., 2019), synthetic steroids found on the market as food supplements or veterinary drugs (Roman et al., 2018b), water soluble derivatives of chitosan (Isvoran et al., 2017). It illustrates their applicability for predicting pharmacological properties and toxicological endpoints for many classes of compounds.

RESULTS

Estimation of the oral bioavailability and overall toxicity of investigated COs is obtained using FAF-Drugs4 tool and is based on filtering the physicochemical properties of investigated compounds in accordance with the rules mentioned above. FAF-Drugs4 tool also estimates if the investigated compounds are able to produce phospholipidosis (PI). The outcomes are presented in **Table 3**.

With the exceptions of the monomeric and some of the dimeric chito-oligomers, the outcomes of FAF-Drugs4 indicate the lack of oral bioavailability of the other investigated COs because of their molecular weight and extensive hydrogen bonding potential. Similar results concerning the lack of human oral bioavailability of investigated COs containing more than 2 monomeric units have been obtained using admetSAR2.0 (**Figure 1**), PreADMET and SwissADME tools (**Supplementary Table 1**).

As expected, the oral bioavailability decreases with increasing molecular weight and increases with the deacetylation degree. PreADMET predictions concerning the percent of the human intestinal absorption (HIA, **Supplementary Table 2**) reveal a mean absorbance (20%<HIA<70%) (Aswathy et al., 2018) for the monomeric units, the highest value (60.25%) being registered for the GlcN oligomer. Chito-oligomers containing two monomeric units reflect a poor absorption (HIA<20%) and the other COs do not reflect intestinal absorption (HIA=0). Predictions obtained using SwissADME tool reveal low gastrointestinal absorption (GI) for all investigated oligomers (**Supplementary Table 3**). All of these results suggest that smaller and deacetylated COs could be better absorbed at the gastrointestinal level and it facilitates their access to systemic circulation and distribution through the human body.

Predictions concerning the distribution (expressed as the probability of plasma protein binding—PPB, being P-glycoprotein substrate and/or inhibitor, being able to penetrate the blood-brain barrier– BBB) of the investigated COs have been obtained using admetSAR2.0 tool and the outcomes are illustrated in **Figure 2**. Negative values of the probabilities illustrate that the investigated activity is absent.

Data presented in **Figure 2** illustrate that investigated COs reveal a very low probability to bind to plasma proteins, they are not able to penetrate the blood brain barrier and to affect the central nervous system, oligomers with more than 3 monomeric units reflect a small probability to inhibit the P-glycoprotein and none of the investigated COs is considered as P-glycoprotein substrate. There are small differences in the values of predicted probabilities for a given activity between oligomers with the same DP and different DDA, reflecting the influence of the deacetylation degree on the activity of chito-oligomers. Almost similar predictions

TABLE 3 | Estimation of oral bioavailability and overall toxicity of chito-oligomers: green cells correspond to respected rules (0 violations), yellow cells correspond to partially respected rules (maximum 2 violations for Lipinski's rule and 1 violation for Veber's and Eagan's rules), light red cells correspond to broken rules.

Compound	Oral bioavailability			Overall toxicity		
	Lipinski's rule	Veber's rule	Eagan's rule	Pfizer's rule	GSK rule	PI
A						No
2A	2 violations HBA>10 HBD>5					No
3A, 4A, 5A, 6A, 8A	3 violations MW>500 HBA>10 HBD>5					No
ADA, DAD	3 violations MW>500 HBA>10 HBD>5					Yes
AD	2 violations HBA>10 HBD>5					Yes
ADAD, DADA, DAAD, DDAA, AADD ADDA ADADAD, DADADA DDDADA ADDDAD, DADADADA	3 violations MW>500 HBA>10 HBD>5					Yes
D	2 violations HBD>5, HBA>5					Yes
2D, 3D, 4D, 5D, 6D, 8D	3 violations MW>500 HBA>10 HBD>5					Yes

The number of violation for every considered rule is specified. Compounds expected to not induce phospholipidosis (PI) are marked by "No" in green cells and compounds expected to induce phospholipidosis are marked by "yes" in light red cells. (MW-molecular weight, HBA – hydrogen bond acceptors, HBD- hydrogen bonds donors).

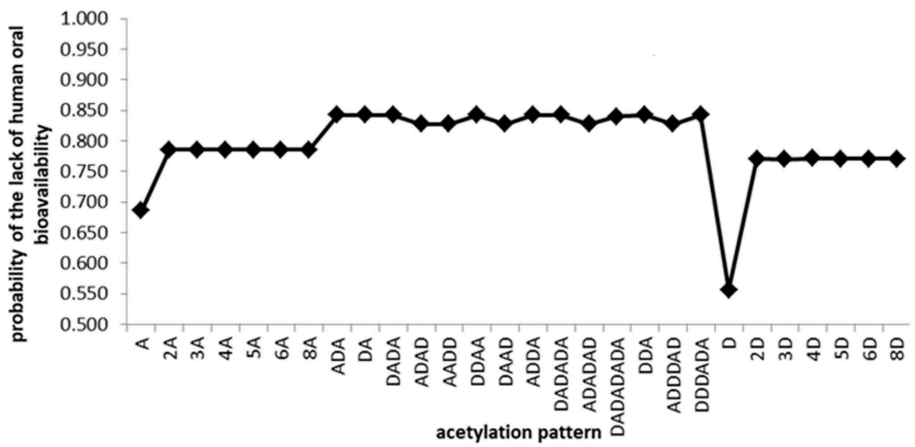

FIGURE 1 | Predictions obtained using admetSAR2.0 tool concerning the lack of the human oral bioavailability of investigated chito-oligomers. The predicted probabilities of the lack of oral bioavailability may take values between 0 and 1. As the value is closer to 1, the oral bioavailability is missing.

are obtained using PreADMET (**Supplementary Table 2**) and SwissADME (**Supplementary Table 3**) tools. PreADMET reveals that investigated COs are not inhibitors of the P-glycoprotein and outcomes values for the blood brain barrier penetration that are lower than 0.1 that correspond to a low absorbance to central nervous system (Aswathy et al., 2018). The PPB binding assessment (percentage of drug bound in plasma protein) reveals that investigated COs exhibit low binding energy with plasma proteins (PPB<90%) (Kandagalla et al., 2017) with the exception of the oligomer 6D that shows a high binding energy to plasma proteins (93.384%). SwissADME predicts that investigated compounds are not able to penetrate the blood brain barrier and are considered as substrates of P-glycoprotein.

SwissADME, PreADMET, and admetSAR2.0 tools have been also used to assess the metabolism of COs by predicting the probability for every compound to be a substrate or to inhibit the human cytochromes P450 (CYP) involved in the metabolism of xenobiotics. The outcomes of SwissADME and admetSAR2.0 tools indicate that COs considered in this study are not substrates and inhibitors of CYPs (**Supplementary Tables 3, 4**).

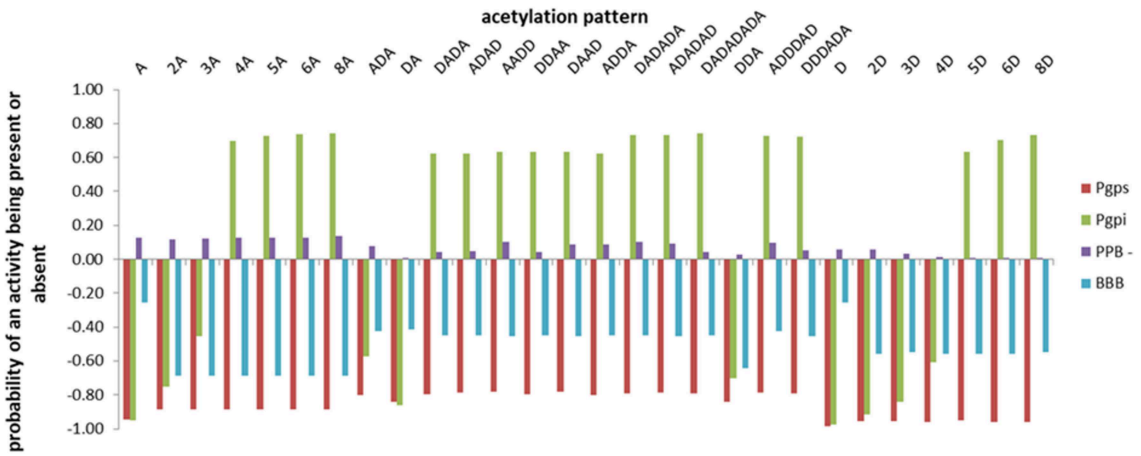

FIGURE 2 | The distribution profiles of the investigated chito-oligomers expressed as the probabilities of binding to plasma proteins (PPB), being substrate/inhibitor of the P-glycoprotein (P-gpS/P-gpI), being able to penetrate the blood-brain barrier (BBB). The predicted probabilities may take values between 0 and 1 when the investigated activity is present and between −1 and 0 when the activity is considered absent. Values closer to 1 correspond to effects that are highly probable and values closer to −1 correspond to highly improbable effects.

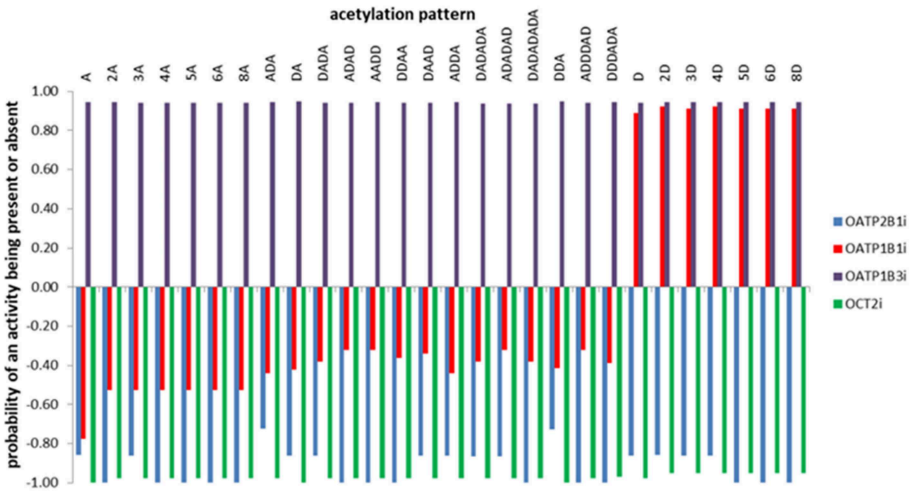

FIGURE 3 | Predictions concerning the probability of the inhibition of the organic anion and cation transporter peptides by the investigated COs. The predicted probabilities may take values between 0 and 1 when the investigated activity is present, and between −1 and 0 when the activity is considered absent. Values closer to 1 correspond to effects that are highly probable and values closer to −1 correspond to highly improbable effects.

The predictions obtained using PreADMET are not similar, they indicate that investigated COs are not considered as substrates and inhibitors of CYP2C9 and CYP2C19, but the oligomers containing deacetylated units are possible dual inhibitors and substrates of CYP2D6 and CYP3A4. It may be due to complex modulation of CYP enzymes and this aspect should be further analyzed.

Predictions concerning the probability of the inhibition of the organic anion and cation transporter peptides by the investigated COs are also obtained using admetSAR2.0 tool and are illustrated in **Figure 3**. This figure suggests the inhibitory potential of all investigated COs against organic anion polypeptide transporter OATP1B3. Deacetylated oligomers also illustrate the inhibitory potential against OATP1B1 and underline the influence of the DDA on the activity of investigated COs.

Predictions concerning the organ (eye, heart, liver) and genomic toxicity of investigated COs obtained using admetSAR2.0 and PreADMET tools are revealed in **Table 4**.

None of the investigated oligomers have carcinogenic potential, does not produce eye irritations and corrosion. Excepting the monomeric and dimeric units that are not predicted to block the hERG, the other oligomers reveal moderate potentials of hERG channel blocking. Totally acetylated oligomers and small oligomers containing deacetylated units are predicted by the PreADMET tool as displaying mutagenic potential. Besides admetSAR2.0 and PreADMET tools,

TABLE 4 | Predictions obtained using admetSAR and PreADMET tools concerning the probabilities of organ and genomic toxicity of investigated COs: hERG – potassium channel blocking potential (cardiotoxicity), EC-eye corrosion, EI – eye irritation, HEPT – hepatotoxicity.

Compound/ tool	admetSAR2.0	Pre-ADMET	admet SAR2.0	Pre-ADMET	admetSAR2.0	Pre-ADMET	admetSAR2.0		
	hERG		Ames mutagenesis		Mouse carcinogenicity	Mouse and rat carcinogenicity	EC	EI	HEPT
A	−0.62	low_risk	−0.54	Mutagen	−0.94	Negative	−0.99	−1.00	−0.65
2A	−0.44	Low_risk	−0.57	Mutagen	−0.96	negative	−0.99	−0.97	−0.58
3A	0.76	Ambiguous	−0.57	Mutagen	−0.96	Negative	−0.99	−0.92	0.63
4A	0.79	Ambiguous	−0.57	Mutagen	−0.96	Negative	−0.99	−0.90	0.78
5A	0.80	Ambiguous	−0.57	Mutagen	−0.96	Negative	−0.99	−0.90	0.78
6A	0.80	Ambiguous	−0.57	Mutagen	−0.96	Negative	−0.99	−0.90	−0.50
8A	0.80	Ambiguous	−0.57	Mutagen	−0.96	Negative	−0.99	−0.90	−0.60
ADA	0.73	Ambiguous	−0.51	Non-mutagen	−0.96	Negative	−0.99	−0.94	0.58
DA	−0.49	Low_risk	−0.57	Mutagen	−0.96	negative	−0.99	−0.99	−0.55
DADA	0.86	Ambiguous	−0.56	Non-mutagen	−0.96	Negative	−0.99	−0.92	0.65
ADAD	0.77	Ambiguous	−0.52	Non-mutagen	−0.96	Negative	−0.99	−0.92	0.68
AADD	0.79	ambiguous	−0.51	Non-mutagen	−0.95	Negative	−0.99	−0.92	0.68
DDAA	0.79	Ambiguous	−0.56	Non-mutagen	−0.96	Negative	−0.99	−0.91	0.70
DAAD	0.80	Ambiguous	−0.59	Non-mutagen	−0.96	Negative	−0.99	−0.91	0.72
ADDA	0.76	Ambiguous	−0.51	non-mutagen	−0.95	Negative	−0.99	−0.91	0.70
DADADA	0.82	Ambiguous	−0.56	Non-mutagen	−0.96	Negative	−0.99	−0.90	0.60
ADADAD	0.81	Ambiguous	−0.51	Non-mutagen	−0.96	Negative	−0.99	−0.90	0.55
DADADADA	0.77	Ambiguous	−0.61	Non-mutagen	−0.95	Negative	−0.99	−0.90	−0.56
DDA	0.68	Ambiguous	−0.57	Mutagen	−0.96	Negative	−0.99	−0.96	−0.50
ADDDAD	0.82	Ambiguous	−0.52	Non-mutagen	−0.95	Negative	−0.99	−0.90	0.58
DDDADA	0.81	Ambiguous	−0.56	Non-mutagen	−0.95	Negative	−0.99	−0.90	0.55
D	−0.67	Low_risk	−0.70	Mutagen	−0.97	Negative	−0.99	−0.99	−0.90
2D	−0.43	low_risk	−0.71	Mutagen	−0.97	Negative	−0.99	−0.98	−0.95
3D	0.72	Ambiguous	−0.71	Mutagen	−0.97	Negative	−0.99	−0.94	−0.85
4D	0.73	Ambiguous	−0.71	Non-mutagen	−0.99	Negative	−0.99	−0.92	−0.68
5D	0.73	Ambiguous	−0.71	Non-mutagen	−0.99	Negative	−0.99	−0.90	0.53
6D	0.82	Ambiguous	−0.71	Non-mutagen	−0.97	Negative	−0.99	−0.90	0.53
8D	0.83	Too big to be computed	−0.71	Too big to be computed	−0.97	Too big to be computed	−0.99	−0.90	−0.50

Negative values of the probabilities illustrate that the investigated activity is absent. These probabilities may take values between −1 and 0 when the predicted activity is absent and between 0 and 1.00 when the predicted activity is present.

TABLE 5 | Outcomes of the Pred-hERG computational tool concerning the blockage of the potassium channel by the investigated chito-oligomers: red cells illustrate predictions of hERG blocking potential and green cells illustrate hERG non-blocking potential.

Compound	Pred-hERG	
	Prediction by binary model	Prediction by multiclass model non-blocker
A	0.5	0.8
2A	0.6	0.7
3A	0.6	0.7
4A	0.6	0.7
5A	0.6	0.7
6A	0.6	0.7
8A	0.6	0.7
ADA	0.7	0.7
DA	0.6	0.7
ADAD	0.7	0.7
DADA	0.7	0.7
ADDA	0.7	0.7
AADD	0.7	0.7
DAAD	0.7	0.7
DDAA	0.7	0.7
ADADAD	0.7	0.7
DADADA	0.7	0.7
DADADADA	0.7	0.7
DDA	0.7	0.7
ADDDAD	0.7	0.7
DDDADA	0.7	0.7
D	0.5	0.8
2D	0.6	0.7
3D	0.6	0.7
4D	0.6	0.7
5D	0.6	0.7
6D	0.7	0.7
8D	0.6	0.7

Number in every cell represents the probability of the prediction for each class. The values vary between 0 and 1.

carcinogenicity and mutagenicity of investigated COs have also been assessed using CarcinoPred-EL and Toxtree and their outcomes displayed no carcinogenicity and no Ames toxicity for every considered oligomer (**Supplementary Table 5**). The consensus of the predictions made by the majority of these computational tools emphasizes that none of the investigated COs is expected to be carcinogen and mutagen. Data presented in **Table 4** reveal different values for the predicted probabilities for COs with distinct DDA and AP and it underlines the dependence of the biological activities of investigated COs on their properties, DDA, and AP.

For assessing cardiotoxicity of investigated COs we have also considered Pred-hERG prediction tool and the results are presented in **Table 5**.

Predictions made using the binary model illustrate that, except GlcN and GlcNAc monomers, that are considered as non-hERG K+ blockers, the other investigated COs are predicted as having hERG K+ blocking potential but the probabilities of these predictions are relatively small. Predictions based on the multiclass models reveal non-hERG blocking potential for all investigated COs, also with relatively small probabilities. Predictions reliability reported using Pred-hERG are ranging between 83 and 84% for the binary model and between 66 and 79% for the multiclass models (Braga et al., 2015). Consequently, we deliberate that, excepting the monomers, the other investigated COs reveal a weak hERG K+ blocking potential, this outcome being in very good correlation with predictions made by admetSAR2.0 and PreADMET tools (see **Table 4**).

The use of Pred-Skin computational tool reveals that investigated oligomers reflect no skin sensitizer potential (**Supplementary Table 6**). It is an important result as skin sensitization is known to be a common occupational health issue (Anderson and Meade, 2014). SwissADME and PreADMET tools also predicted very small values of the skin permeability parameters (**Supplementary Tables 2, 3**). The value of skin permeability parameter computed using SwissADME tool for diclofenac (an anti-inflammatory drug known to permeate the skin) is logKp = −4.96 cm/s (Daina et al., 2017). The use of PreADMET tool to compute the skin permeability coefficient for betulinic acid conducted to the value of logKp = −2.11 cm/h proving that betulinic acid is not permeable through the skin (Khan et al., 2018). The values of logKp computed for investigated COs by using SwissADME and PreADMET tools are much smaller that the two indicated values and it illustrates that these compounds are not permeable through skin.

Endocrine disruption potential is another toxicological endpoint that must be considered when using chemical compounds. Assessment of the endocrine disruption potential of investigated COs has been obtained using ENDOCRINE DISRUPTOME prediction tool and the results are presented in **Table 6**. Monomers and dimers of GlcNAc and GlcN, and chitobiose (DA) have the moderate ability (0.75>SE>0.50, yellow cells in **Table 6**) to bind to the androgen receptor and to produce antagonistic effects. The dimers AA and DA and the trimers ADA and DDD reflect a moderate potential to bind to the glucocorticoid receptor and to produce agonistic effects (0.75>SE>0.50, yellow cells in **Table 6**).

It means that smaller COs may inhibit the androgen and the glucocorticoid receptors and could be capable of deleterious effects on the male reproductive tract or to affect the immune response of the organism. COs containing more than 4 monomers are too big to accommodate in the binding site of the human nuclear receptors considered by the ENDOCRINE DISRUPTOME prediction tool and there are not outcomes, calculations being aborted. It seems that molecular weight is an important property for the COs that are able to interact with nuclear receptors. This outcome is in good agreement with literature data revealing that small organic non-steroidal molecules (MW between 430 and 600 Da) are capable to act as AR antagonists (Song et al., 2012; Tesei et al., 2013) and to interact with GR (Harcken et al., 2014; Sundahl et al., 2015).

TABLE 6 | Outcomes of the ENDOCRINE DISRUPTOME prediction tool concerning the potential binding of investigated COs to the human nuclear receptors: androgen receptor (AR), estrogen receptors α (ERα) and β (ERβ), glucocorticoid receptor (GR), liver X receptors α (LXRα), and β (LRXβ), peroxisome proliferator-activated receptors α (PPRAα), β/δ (PPRAβ), and γ (PPRAγ), retinoid X receptor α (RXRα) and thyroid receptors α (TRα) and β (TRβ), an - antagonistic effect.

Acetylation pattern	AR	AR an	ERα	ERα an	ERβ	ERβ an	GR	GR an	LXRα	LXRβ	PPARα	PPARβ	PPARγ	RXR α	TRα	TRβ
A																
AA																
AAA																
DA																
ADA																
DADA																
AADD																
DAAD																
DDAA																
ADDA																
DDA																
ADAD																
D																
DD																
DDD																
DDDD																

Results are color coded taking into account the values of the sensitivity parameter. Class "yellow" corresponds to 0.50<SE<0.75 and indicates compounds with moderate probability of binding, and class "green" corresponds to SE>0.75 and illustrates compounds with low probability of binding to the nuclear receptors.

DISCUSSION

The outcomes of the computational tools have been used to study the chito-oligomers pharmacological profiles and their toxicity. It has been shown that the results obtained with the different computational tools are usually in accordance with each other. The results obtained using FAF-Drugs4, admetSAR2.0, and PreADMET reveal that oligomers GlcNAc, GlcN, and GlcNAc-GlcN may have a higher oral bioavailability by comparison to the other COs, showing that oral bioavailability seems to be decreasing with increasing molecular weight. This outcome is in good correlation with published data considering that chitosan's systemic absorption and distribution is dependent on the molecular weight, oligomers could reveal some absorption whereas larger polymers are excreted (Kean and Thanou, 2010). Other studies revealed that the absorption of chito-oligomers was significantly influenced by the molecular weight, the absorption decreased with increasing molecular weight (Chae et al., 2005; Naveed et al., 2019). Moreover, low molecular weight COs produced by depolymerization are usually preferred for pharmaceutical applications (Quiñones et al., 2018) as they have been reported to show remarkable biological activities (Adhikari and Yadav, 2018).

The action of chemicals depends on their interactions with plasma proteins, with unbound molecules usually reflecting better interactions with their targets and influencing the efficacy of the molecules (Kandagalla et al., 2017). All computational facilities that we have used reveal that COs considered in this study exhibit low potential to bind to plasma proteins. Consequently, these compounds exist freely being available for transport across the cell membranes, for the interaction with specific/non-specific targets and for excretion.

Predictions concerning the potential of the investigated chito-oligomers of being substrates and/or inhibitors of the P-glycoprotein (an efflux membrane transporter that is responsible for limiting cellular uptake and the distribution of xenobiotics within the human body) are not consistent between the computational tools that were used in this study. SwissADME tool predicts that all investigated COs are substrates of P-gp, but admetSAR2.0 illustrate the contrary. PreADMET tool reveals that investigated COs are not inhibitors of P-glycoprotein, but admetSAR2.0 displays that oligomers containing at least 4 monomeric units are potential inhibitors of P-glycoprotein. It illustrates that the activity of P-glycoprotein may be affected by the presence of COs and absorption and retention of COs in the cells could be impaired. This aspect must be further considered in experimental studies. Investigated COs reveal no potential to penetrate the blood brain barrier and it underlines their minimal side effects against the central nervous system. An *in vitro* study emphasized that COs with MW < 2,000 Da reflected neuroprotective effects (Santos-Moriano et al., 2018).

Investigated COs reveal no toxicity, but partially and totally deacetylated chitin oligomers are predicted to produce phospholipidosis, a disorder characterized by the accumulation in excess of phospholipids in tissues. This prediction is not unexpected as chitosan is a cationic polymer and it is known that cationic amphiphilic drugs may produce phospholipidosis (Anderson and Borlaka, 2006; Muehlbacher et al., 2012).

Literature data reflect that some xenobiotics (including drugs) are able to inhibit organic anion polypeptide transporters

OATP1B1, OATP1B3, and OATP2B1. OATP1B1 and OATP1B3 are exclusively expressed in the liver, this organ being responsible for the hepatic uptake of some drugs, bile acids and some endogenous compounds. OATP2B1 is found in the liver and other tissues being associated with the oral absorption of chemicals. The inhibition of these transporters conducts to clinically relevant drug-drug interactions and to modified pharmacological effects and adverse reactions of drugs (Maeda, 2015; Alam et al., 2018). Another transporter that may be affected by the presence of xenobiotics is the organic cation transporter expressed in the kidney, OCT2. OCT2 transports compounds that are positively charged from the blood to the tubular epithelial cells, its inhibition also conducting to adverse effects (Motohashi and Inui, 2013). Consequently, predicting the inhibition of these transporters is important. Predictions obtained using admetSAR2.0 reflect that all investigated chito-oligomers are considered as possible inhibitors of the OATP1B3 and the deacetylated oligomers are also inhibitors of the OATP1B1. The inhibition of organic anion transporters OATP1B1 and OPTAP1B3 by the investigated oligomers is not an unexpected result because *in silico* models revealed the importance of lipophilicity, polarity and hydrogen bonding for OATP inhibition (Karlgren et al., 2012). Deacetylated oligomers reveal higher lipophilicity and hydrogen bonding potential that may conduct to their inhibitory effect against OATP1B1 too. Furthermore, the role of computational methods in predicting clinically relevant transporter interactions has been recognized (Türková and Zdrazil, 2019).

The outcomes of both admetSAR2.0 and Pred-hERG revealed that investigated COs, excepting the monomers, illustrate moderate potentials of hERG channel blocking. The hERG blockage potential of investigated COs increases with the molecular weight and it slightly depends on the acetylation degree and pattern. Literature data reveal the cavity of the hERG pore is large and is able to accommodate compounds with very high molecular weight (Linder et al., 2016) and that hERG inhibition positively correlates to the logP, molecular weight and rotatable bonds (Yu et al., 2016).

The hepatotoxicity of investigated COs also seems to depend on the molecular weight, the oligomers having the molecular weights between 500 and 1500 Da reflecting a weak potential of hepatotoxicity. This result is also in good correlation with published data revealing that lipophilicity and molecular weight are the most important physicochemical properties that influence the drug induced liver injury (Leeson, 2018). Furthermore, there is a slight dependence of hepatotoxicity of COs on the deacetylation degree and pattern. Literature data concerning the organ, tissue and cellular distribution COs suggest that: (i) they are usually distributed to kidney, hepatic, and splenic cells (the highest detected concentration was in hepatic cells) and lower concentrations were distributed to cardiac and lung tissues; (ii) MW and DDA influence the tissue and cellular distribution of COs and (iii) the biodegradation of COs is considered to occurring in the liver (Naveed et al., 2019).

There are some potential lacunas when predicting the pharmacokinetic profiles and toxicological endpoints of COs that might limit their effectiveness and probably affect the experimental validations. These lacunas are common to *in silico* predictions and in the case of the present study, they refer to: (i) the models used for predictions could not be adequate as the data regarding the biological activities of well-defined COs are limited and these data are not considered when building the models used for predictions; (ii) these predictions do not take into account the quantity of COs and the basic variables of experimental studies (temperature, humidity, pH, etc.); (iii) there are difficulties concerning the modeling of the toxicological endpoint because the lack of a complete understanding of its biology and of the complexity of processes involved. These lacunas may affect the experimental validations as data that were used for model building may originate from various experimental approaches that are different from those used for validation, as it is recognized that inconsistencies between predictions and experiments can often be attributed to the fact that they do not test the same assumptions (Gallion et al., 2017). In order to minimize the effects of the quality of the models built on data originated from various experimental approaches we have used well-established and recognized computational tools that are based on models obtained considering data for numerous chemical compounds and that have high predictive accuracies (higher than 70%). Furthermore, we have used both computational tools that are able to predict many pharmacological and toxicological properties, but also computational tools that are associated with a defined toxicological endpoint. The consensus of the predictions obtained using these tools increase the probability that the results are further validated in experimental tests. Due to these limitations of *in silico* predictions, the results have to be handled carefully and should not be used isolated to determine the potential hazard of COs. However, official agencies consider that the combination of computational modeling with *in vitro* testing is needed for a more efficient safety assessment of all types of chemicals.

Experimental validations of the biological effects of chemicals should be reliable, precise, and performed on a sufficiently large scale to be meaningful. These conditions may require repetitive measurement with a given assay or testing the same biological action with various assays. Consequently, in most practical cases, it is challenging to evaluate whether the available data are acceptably and complete, and to assess whether the experimental design affects the relationship with computational prediction (Gallion et al., 2017). An exhaustive experimental campaign can be time- and money-consuming also because of the intrinsic high number of variables related to the material. Focusing on chitosan, an appropriate experimental design should explore the influence of molecular weight, acetylation degree and acetylation pattern, to name a few aspects to be considered and that have been included in this study.

The potential merits of the computational predictions obtained within this study are that they highlighted some trends that relate material properties and possible side effects, which can be included in a suitable design of experiment algorithms in order to minimize the experimental efforts number and maximize the outcomes. Initially, in *vitro* basic tests through experiments that closely match the conditions used for predictions are

preferably used for validation such as to avoid the complexity of the physiological pathways and possible interactions between various chemical molecules in the animal organisms. This approach could provide several advantages. First, it would lead to a structured experimental campaign, whose results can complement the fragmentary insights available in scientific literature. Secondly, experiments can be employed to assess the reliability of model predictions and thus the suitability of the chosen approach for pure predictive simulations. Thirdly, getting experimental data for well-characterized COs may provide an insight to define the applications of COs and will also drive the development of more rigorous models that also will conduct to improved predictions.

CONCLUSIONS

The pharmacokinetic profiles of chito-oligosaccharides are rarely experimentally studied, but taking into account their promising applications, their efficacy, and safety assessment are points to be considered. Obtaining well-defined COs in terms of length, degree acetylation, and acetylation pattern are still not straightforward and computational approaches offer an advantage in such cases. Within this study, we have used various computational tools to assess the pharmacokinetic profiles and toxicological endpoints of investigated COs. Computational predictions revealed that investigated small chito-oligomers, regardless of molecular weight, acetylation degree and acetylation pattern, reflect favorable pharmacological profiles: they are not able to penetrate the blood-brain barrier, do not produce eye irritation and corrosion, reveal no mutagenicity, no carcinogenicity, and no skin sensitization potential.

As possible harmful effects we have noticed the followings: (i) all investigated COs revealed high potential of inhibition of the OATP1B3 and COs containing only deacetylated units also reflect inhibition potential of the OATP1B1; (ii) COs containing more than 2 units reflect a moderate potential of cardiotoxicity; (iii) some of considered COs reflect small probabilities to produce hepatotoxicity; (iv) smaller oligomers ($n = 1$–3) reflect a weak disruption potential against AR and GR; (v) totally deacetylated oligomers are considered to produce phospholipidosis.

Predictions concerning the interactions of investigated COs with P-glycoprotein and CYPs are unclear and they must be further considered in experimental studies.

We have also examined the influence of the molecular weight, deacetylation degree, and pattern on the pharmacological profiles and toxicological endpoints of investigated COs. The oral bioavailability of investigated COs decreases with increasing MW and deacetylation degree. Taking into account that bioavailability profile could be the main factor limiting the efficiency of a drug, this information is of interest. There is a slightly dependence of hepatotoxicity and cardiotoxicity on the molecular weight and on the deacetylation degree and pattern of COs. The cardiotoxicity of investigated COs increases poorly with the molecular weight, decreases slightly with the deacetylation degree and is not influenced by deacetylation pattern. Hepatotoxicity increases with the molecular weight, decrease with the deacetylation degree and depends on the deacetylation pattern.

DATA AVAILABILITY

All datasets generated for this study are included in the manuscript/**Supplementary Files**.

AUTHOR CONTRIBUTIONS

DR performed the computations using FAF-Drugs, admetSAR, PreADMET, Pred-Skin, and Endocrine Disruptome, to results analysis and contributed to manuscript editing. MR performed computations using, SwissADME, Pred-hERG, CarcinoPred-El, and Toxtree, to results analysis and contributed to manuscript editing. CS, MS, EH, PW, TC, and GP contributed to the analysis of results, conception, and design of the manuscript. VO furnished the SMILES and structural formulas of oligomers and contributed to the conception and design of the manuscript. AI conceived and planned the study and contributed to the conception and design of the manuscript. All authors contributed to revise the manuscript and approved the submitted version.

FUNDING

This study is part of the GoNanoBioMat project and has received funding from the Horizon 2020 framework program of the European Union, ProSafe Joint Transnational Call 2016; from the CTI (1.1.2018 Innosuisse), under grant agreement Number 19267.1 PFNM-NM; by the Rumanian funding agency Executive Unit for Financing Higher Education, Research, Development and Innovation (UEFISCDI) under the grant PN3-P3-285 for research work and under the grant PNIII 28 PFE BID for publication fee, and from FCT Foundation for Science and Technology under the project PROSAFE/0001/2016.

SUPPLEMENTARY MATERIAL

The Supplementary Material for this article can be found online at: https://www.frontiersin.org/articles/10.3389/fbioe.2019.00214/full#supplementary-material

REFERENCES

Adhikari, H. S., and Yadav, P. N. (2018). Anticancer activity of chitosan, chitosan derivatives, and their mechanism of action. *Int. J. Biomaterial.* 2018:2952085. doi: 10.1155/2018/2952085

Alam, K., Crowe, A., Wang, X., Zhang, P., Ding, K., Li, L., et al. (2018). Regulation of Organic Anion Transporting Polypeptides (OATP) 1B1- and OATP1B3-mediated transport: an updated review in the context of OATP-mediated drug-drug interactions. *Int. J. Mol. Sci.* 19:E855. doi: 10.3390/ijms19030855

Alves, V. M., Braga, R. C., Muratov, E., and Andrade, C. H. (2018a). Development of web and mobile applications for chemical toxicity prediction. *J. Braz. Chem. Soc.* 29, 982–988. doi: 10.21577/0103-5053.20180013

Alves, V. M., Capuzzi, S. J., Braga, R. C., Borba, J. V. B., Silva, A. C., Luechtefeld, T., et al. (2018b). A perspective and a new integrated computational strategy for skin sensitization assessment. *ACS Sustain. Chem. Eng.* 6, 2845–2859. doi: 10.1021/acssuschemeng.7b04220

Alves, V. M., Muratov, E. N., Zakharov, A., Muratov, N. N., Andrade, C. H., and Tropsha, A. (2018c). Chemical toxicity prediction for major classes of industrial chemicals: Is it possible to develop universal models covering cosmetics, drugs, and pesticides? *Food Chem. Toxicol.* 112, 526–534. doi: 10.1016/j.fct.2017.04.008

Anderson, J. W., Nicolosi, R. J., and Borzelleca, J. F. (2005). Glucosamine effects in humans: a review of effects on glucose metabolism, side effects, safety considerations and efficacy. *Food Chem. Toxicol.* 43, 187–201. doi: 10.1016/j.fct.2004.11.006

Anderson, N., and Borlaka, J. (2006). Drug-induced phospholipidosis. *FEBS Lett.* 580, 5533–5540. doi: 10.1016/j.febslet.2006.08.061

Anderson, S. E., and Meade, B. J. (2014). Potential health effects associated with dermal exposure to occupational chemicals. *Environ. Health Insights.* 8, 51–62. doi: 10.4137/EHI.S15258

Aswathy, L., Jisha, R. S., Masand, V. H., Gajbhiye, J. M., and Shibi, I. G. (2018). Design of novel amyloid β aggregation inhibitors using QSAR, pharmacophore modeling, molecular docking and ADME prediction. *In Silico Pharmacol* 6:12. doi: 10.1007/s40203-018-0049-1

Beddoes, C. M., Case, C. P., and Briscoe, W. H. (2015). Understanding nanoparticle cellular entry: a physicochemical perspective. *Adv. Colloid Interface Sci.* 218, 48–68. doi: 10.1016/j.cis.2015.01.007

Bissett, D. L., Robinson, L. R., Raleigh, P. S., Miyamoto, K., Hakozaki, T., Li, J., et al. (2007). Reduction in the appearance of facial hyperpigmentation by topical N-acetyl glucosamine. *J. Cosmet. Dermatol.* 6, 20–26. doi: 10.1111/j.1473-2165.2007.00295.x

Braga, R. C., Alves, V. M., Muratov, E. N., Strickland, J., Kleinstreuer, N., Trospsha, A., et al. (2017). Pred-Skin: a fast and reliable web application to assess skin sensitization effect of chemicals. *J. Chem. Inf. Model.* 57, 1013–1017. doi: 10.1021/acs.jcim.7b00194

Braga, R. C., Alves, V. M., Silva, M. F., Muratov, E., Fourches, D., Lião, L. M., et al. (2015). Pred-hERG: a novel web-accessible computational tool for predicting cardiac toxicity. *Mol. Inform.*. 34, 698–701. doi: 10.1002/minf.201500040

Chae, S. Y., Jang, M. K., and Nah, J. W. (2005). Influence of molecular weight on oral absorption of water soluble chitosans. *J. Control. Release.* 102, 383–394. doi: 10.1016/j.jconrel.2004.10.012

Chan, K., and Fat, G. Y. (2011). A review on the effects of glucosamine for knee osteoarthritis based on human and animal studies. *Hong Kong Physiother. J.* 29, 42–52. doi: 10.1016/j.hkpj.2011.06.004

Chen, A. S., Taguchi, T., Sakai, K., Kikuchi, K., Wang, M. W., and Miwa, I. (2003). Antioxidant activities of chitobiose and chitotriose. *Biol. Pharm. Bull.* 26, 1326–1330. doi: 10.1248/bpb.26.1326

Cheng, F., Li, W., Zhou, Y., Shen, J., Wu, Z., Liu, G., et al. (2012). admetSAR: a comprehensive source and free tool for evaluating chemical ADMET properties. *J. Chem. Inf. Model.* 52, 3099–3105. doi: 10.1021/ci300367a

Cheung, R. C., Ng, T. B., Wong, J. H., and Chan, W. Y. (2015). Chitosan: an update on potential biomedical and pharmaceutical applications. *Mar. Drugs* 13, 5156–5186. doi: 10.3390/md13085156

Choi, J. S., Ha, M. K., Trinh, T. X., Yoon, T. H., and Byun, H. G. (2018). Towards a generalized toxicity prediction model for oxide nanomaterials using integrated data from different sources. *Sci. Rep.* 8:6110. doi: 10.1038/s41598-018-24483-z

Daina, A., Michielin, O., and Zoete, V. (2017). SwissADME: a free web tool to evaluate pharmacokinetics, drug-likeness and medicinal chemistry friendliness of small molecules. *Sci. Rep.* 7:42717. doi: 10.1038/srep42717

Dalirfardouei, R., Karimi, G., and Jamialahmadi, K. (2016). Molecular mechanisms and biomedical applications of glucosamine as a potential multifunctional therapeutic agent. *Life Sci.* 159, 21–29. doi: 10.1016/j.lfs.2016.03.028

Das, P., Panda, S. K., Agarwal, B., Behera, S., Ali, S. M., Pulse, M. E., et al. (2019). Novel chitohexaose analog protects young and aged mice from CLP induced polymicrobial sepsis. *Sci. Rep.* 9:2904. doi: 10.1038/s41598-019-38731-3

Egan, W. J., Merz, K. M. Jr., and Baldwin, J. J. (2000). Prediction of drug absorption using multi variate statistics. *J. Med. Chem.* 43, 3867–3877. doi: 10.1021/jm000292e

El-Sayed, S. T., Omar, N. I., and El-Sayed, E.-S. M., Shousha, W. G. (2017). Evaluation Antioxidant and cytotoxic activities of novel chitooligosaccharides prepared from chitosan via enzymatic hydrolysis and ultrafiltration. *J. Appl. Pharmaceut. Sci.* 7, 50–55. doi: 10.7324/JAPS.2017.71107

Enescu, D., and Olteanu, C. E. (2008). Functionalized chitosan and its use in pharmaceutical, biomedical and biotechnological research. *Chem. Eng. Commun.* 195, 1269–1291. doi: 10.1080/00986440801958808

Esfahani, S., Emami, Y., Esmaeilzadeh, E., Bagheri, F., and Namazi, M. R. (2012). Glucosamine enhances tissue regeneration in the process of wound healing in rats as animal model. A stereological study. *J. Cytol Histol.* 3:150. doi: 10.4172/2157-7099.1000150

Fawzya, Y. N., Trisdayanti, W. S., and Noriko, N. (2019). "Antifungal activity of chitosan oligomer prepared using chitosanase of *Aeromonas media* KLU 11.16," in *IOP Conf. Series: Earth and Environmental Science 278:012026IOP* (Bristol). doi: 10.1088/1755-1315/278/1/012026

Fjodorova, N., Novich, M., Vracko M., and Benfenati, E. (2008). Regulatory assessment of chemicals within OECD member countries, EU and in Russia. *J. Environ. Sci. Health C* 26, 40–88. doi: 10.1080/10590500801907365

Gallion, J., Koire, A., Katsonis, P., Schoenegge, A.-M., Bouvier, M., and Lichtarge, O. (2017). Predicting phenotype from genotype: improving accuracy through more robust experimental and computational modeling. *Hum. Mutat.* 38, 569–580. doi: 10.1002/humu.23193

Giri, T. K., Thakur, A., Alexander, A., Ajazuddin, B. H., and Tripathi, D. K. (2012). Modified chitosan hydrogels as drug delivery and tissue engineering systems: present status and applications. *Acta Pharm. Sin. B.* 2, 439–449. doi: 10.1016/j.apsb.2012.07.004

Gleeson, M. P. (2008). Generation of a set of simple, interpretable ADMET rules of thumb. *J. Med. Chem.* 51, 817–834. doi: 10.1021/jm701122q

Gridan, I. M., Ciorsac, A. A., and Isvoran, A. (2019). Prediction of ADME-Tox properties and toxicological endpoints of triazole fungicides used for cereals protection. *ADMET&DMPK* 7, 161–173. doi: 10.5599/admet.668

Harcken, C., Riether, D., Kuzmich, D., Liu, P., Betageri, R., Ralph, M., et al. (2014). Identification of highly efficacious glucocorticoid receptor agonists with a potential for reduced clinical bone side effects. *J. Med. Chem.* 574, 1583–1598. doi: 10.1021/jm4019178

Huang, L., Chen, J., Cao, P., Pan, H., Ding, C., Xiao, T., et al. (2015). Anti-obese effect of glucosamine and chitosan oligosaccharide in high-fat diet-induced obese rats. *Mar. Drugs* 13, 2732–2756. doi: 10.3390/md13052732

Isvoran, A., Ciorsac, A., and Ostafe, V. (2017). ADME-Tox profiling of some low molecular weight water soluble chitosan derivatives. *ADMET & DMPK* 5, 192–200. doi: 10.5599/admet.5.3.423

Jerosch, J. (2011). Effects of glucosamine and chondroitin sulfate on cartilage metabolism in oa: outlook on other nutrient partners especially omega-3 fatty acids. *Int. J. Rheumatol.* 2011:969012. doi: 10.1155/2011/969012

Jiang, M., Guo, Z., Wang, C., Yang, Y., Liang, X., Ding, F., (2014). Neural activity analysis of pure chito-oligomer components separated from a mixture of chitooligosaccharides. *Neurosci. Lett.* 581, 32–36. doi: 10.1016/j.neulet.2014.08.014

Jiang, Z., Liu, G., Yang, Y., Shao, K., Wang, Y., Liu, W., et al. (2019). N-Acetyl chitooligosaccharides attenuate amyloid β-induced damage in animal and cell models of Alzheimer's disease. *Process Biochem.* 184, 161–171. doi: 10.1016/j.procbio.2019.06.014

Jordan, K. M., Arden, N. K., Doherty, M., Bannwarth, B., Bijlsma, J. W., Dieppe, P., et al. (2003). EULAR Recommendations 2003: an evidence based approach to the management of knee osteoarthritis: Report of a Task Force of the Standing Committee for International Clinical Studies Including Therapeutic Trials (ESCISIT). *Ann. Rheum. Dis.* 62, 1145–1155. doi: 10.1136/ard.2003.011742

Kandagalla, S., Sharath, B. S., Bharath, B. R., Hani, U., and Manjunatha, H. (2017). Molecular docking analysis of curcumin analogues against kinase domain of ALK5. *In Silico Pharmacol.* 5:15. doi: 10.1007/s40203-017-0034-0

Kar, S., and Leszczynski, J. (2019). Exploration of computational approaches to predict the toxicity of chemical mixtures. *Toxics* 7:15. doi: 10.3390/toxics7010015

Karlgren, M., Vildhede, A., Norinder, U., Wisniewski, J. R., Kimoto, E., Lai, Y., et al. (2012). Classification of inhibitors of hepatic organic anion transporting polypeptides (OATPs): influence of protein expression on drug-drug interactions. *J. Med. Chem.* 55, 4740–4763. doi: 10.1021/jm300212s

Kean, T., and Thanou, M. (2010). Biodegradation, biodistribution and toxicity of chitosan. *Adv. Drug Deliv. Rev.* 62, 3–11. doi: 10.1016/j.addr.2009.09.004

Khan, M. F., Nahar, N., Rashid, R. B., Chowdhury, A., and Rashid, M. A. (2018). Computational investigations of physicochemical, pharmacokinetic, toxicological properties and molecular docking of betulinic acid, a constituent of *Corypha taliera* (Roxb.) with Phospholipase A2 (PLA2). *BMC Complement. Alternat. Med.* 18:48. doi: 10.1186/s12906-018-2116-x

Kleandrova, V. V., and Speck-Planche, A. (2013). Regulatory issues in management of chemicals in OECD member countries. *Front. Biosci.* 1, 375–398.

Kolšek, K., Mavri, J., Sollner Dolenc, M., Gobec, S., and Turk, S. (2014). Endocrine disruptome - an open source prediction tool for assessing endocrine disruption potential through nuclear receptor binding. *J. Chem. Inf. Model.* 54, 1254–1267. doi: 10.1021/ci400649p

Konno, A. I. (2002). Administering a water soluble mixture of chitin and chitosans. *US Patent*. 6492350 (accessed July 17, 2018).

Kubomura, D., Ueno, T., Yamada, M., Tomonaga, A., and Nagaoka, I. (2017). Effect of N-acetyl glucosamine administration on cartilage metabolism and safety in healthy subjects without symptoms of arthritis: A case report. *Exp. Ther. Med.* 13, 1614–1621. doi: 10.3892/etm.2017.4140

Lagorce, D., Bouslama, L., Becot, J., Miteva, M. A., and Villoutreix, B. O. (2017). FAF-Drugs4: free ADME-tox filtering computations for chemical biology and early stages drug discovery. *Bioinformatics* 33, 3658–3660. doi: 10.1093/bioinformatics/btx491

Lee, S. K., Chang, G. S., Lee, I. H., Chung, J. E., Sung, K. Y., and No, K. T. (2004). "The PreADME: PC-based program for batch prediction of ADME properties", in *EuroQSAR 2004, Designing Drugs and Crop Protectants: Processes, Problems and Solutions*, ed M. G. Ford (Malden, MA: Blackwell Pub Istanbul), 9–10.

Lee, S. K., Lee, I. H., Kim, H. J., Chang, G. S., Chung, J. E., and No, K. T. (2003). "The PreADME Approach: Web-based program for rapid prediction of physico-chemical, drug absorption and drug-like properties," in *EuroQSAR 2002 Designing Drugs and Crop Protectants: Processes, Problems and Solutions* (Blackwell Publishing), 418–420.

Leeson, P. D. (2018). Impact of physicochemical properties on dose and hepatotoxicity of oral drugs. *Chem. Res. Toxicol.* 31, 494–505. doi: 10.1021/acs.chemrestox.8b00044

Li, K., Liu, S., Xing, R., Qin, Y., and Li, P. (2013). Preparation, characterization and antioxidant activity of two partially N-acetylated chitotrioses. *Carbohydr. Polym.* 92, 1730–1736. doi: 10.1016/j.carbpol.2012.11.028

Li, K., Xing, R., Liu, S., and Li, P. (2016). Advances in preparation, analysis and biological activities of single chitooligosaccharides. *Carbohydrate Polymers.* 139, 178–190. doi: 10.1016/j.carbpol.2015.12.016

Li, K., Xing, R., Liu, S., Qin, Y., Yu, H., and Li, P. (2014). Size and pH effects of chitooligomers on antibacterial activity against *Staphylococcus aureus*. *Int. J. BiolMacromol.* 64, 302–305. doi: 10.1016/j.ijbiomac.2013.11.037

Li, X., Zhao, M., Fan, L., Cao, X., Chen, L., Chen, J., et al. (2018). Chitobiose alleviates oleic acid-induced lipid accumulation by decreasing fatty acid uptake and triglyceride synthesis in HepG2 cells. *J. Funct. Foods.* 46, 202–211. doi: 10.1016/j.jff.2018.04.058

Li, X., Zhou, C., Chen, X., Wang, J., and Tian, J. (2012). Effects of five chitosan oligosaccharides on nuclear factor-kappa B signalling pathway. *J. Wuhan Univ. Technol. Mat. Sci. Edit.* 27, 276–279. doi: 10.1007/s11595-012-0452-0

Liaqat, F., and Eltem, R. (2018). Chitooligosaccharides and their biological activities: a comprehensive review. *Carbohydr. Polym.* 184, 243–259. doi: 10.1016/j.carbpol.2017.12.067

Linder, T., Bernsteiner, H., Saxena, P., Bauer, F., Erker, T., Timin, E., et al. (2016). Drug trapping in hERG K+ channels: (not) a matter of drug size? *Med. Chem. Comm.* 7, 512–518. doi: 10.1039/c5md00443h

Lipinski, C. A., Lombardo, F., Dominy, B. W., and Feeney, P. J. (2001). Experimental and computational approaches to estimate solubility and permeability in drug discovery and development settings. *Adv. Drug Deliv. Rev.* 46, 3–26. doi: 10.1016/S0169-409X(96)00423-1

Liu, X., Machado, G. C., Eyles, J. P., Ravi, V., and Hunter, D. J. (2018). Dietary supplements for treating osteoarthritis: a systematic review and meta-analysis. *Br. J. Sports Med.* 52, 167–175. doi: 10.1136/bjsports-2016-097333

Lo Piparo, E., and Worth, A. (2010). *Review of QSAR Models and Software Tools for Predicting Developmental and Reproductive Toxicity*. EU JRC, EUR 24522 EN – 2010.

Long, T., Yu, J., Wang, J., Liu, J., and He, B. S. (2018). Orally administered chitooligosaccharides modulate colon microbiota in normal and colitis mice. *Int. J. Pharmacol.* 14, 291–300. doi: 10.3923/ijp.2018.291.300

Lu, J., Chen, Q., Pan, B., Qin, Z., Fan, L., Xia, Q., et al. (2019). Efficient inhibition of Cronobacter biofilms by chitooligosaccharides of specific molecular weight. *World J. Microbiol. Biotechnol.* 35:87. doi: 10.1007/s11274-019-2662-5

Luechtefeld, T., and Hartung, T. (2017). Computational approach to chemical hazard assessment. *ALTEX* 34, 459–478. doi: 10.14573/altex.1710141

Maeda, K. (2015). Organic anion transporting polypeptide (OATP)1B1 and OATP1B3 as important regulators of the pharmacokinetics of substrate drugs. *Biol. Pharm. Bull.* 38, 155–168. doi: 10.1248/bpb.b14-00767

Masuda, S., Azuma, K., Kurozumi, S., Kiyose, M., Osaki, T., Tsuka, T., et al. (2014). Anti-tumor properties of orally administered glucosamine and N-acetyl-d-glucosamine oligomers in a mouse model. *Carbohydr. Polym.* 111, 783–787. doi: 10.1016/j.carbpol.2014.04.102

Mohammed, M. A., Syeda, J. T. M., Wasan, K. M., and Wasan, E. K. (2017). An overview of chitosan nanoparticles and its application in non-parenteral drug delivery. *Pharmaceutics* 9:E53. doi: 10.3390/pharmaceutics9040053

Motohashi, H., and Inui, K. (2013). Organic cation transporter OCTs (SLC22) and MATEs (SLC47) in the human kidney. *AAPS J.* 15, 581–588. doi: 10.1208/s12248-013-9465-7

Mourya, V. K., Inamdar, N. N., and Choudhari, Y. M. (2011). Chitooligosaccharides: synthesis, characterization and applications. *Polym. Sci. Ser. A.* 53, 583–612. doi: 10.1134/S0965545X11070066

Muanprasat, C., and Chatsudthipong, V. (2017). Chitosan oligosaccharide: biological activities and potential therapeutic applications. *Pharmacol. Ther.* 170, 80–97. doi: 10.1016/j.pharmthera.2016.10.013

Muehlbacher, M., Tripal, P., Roas, F., and Kornhuber, J. (2012). Identification of drugs inducing phospholipidosis by novel *in vitro* data. *ChemMedChem.* 7, 1925–1934. doi: 10.1002/cmdc.201200306

Myatt, G. J., Ahlberg, E., Akahori, Y., Allen, D., Amberg, A., Angere, L.T., et al. (2018). *In silico* toxicology protocols. *Regulat. Toxicol. Pharmacol.* 96, 1–17. doi: 10.1016/j.yrtph.2018.04.014

Naveed, M., Phil, L., Sohail, M., Hasnat, M., Baig, M. M. F. A, Ihsan, A. U., et al. (2019). Chitosan oligosaccharide (COS): an overview. *Int. J. Biol. Macromol.* 129, 827–843. doi: 10.1016/j.ijbiomac.2019.01.192

Nel, A. E., Mädler, L., Velegol, D., Xia, T., Hoek, E. M., Somasundaran, P., et al. (2009). Understanding biophysicochemical interactions at the nano-bio interface. *Nat. Mater.* 8, 543–557. doi: 10.1038/nmat2442

O'Boyle, N. M., Banck, M., James, C. A., Morley, C., Vandermeersch, T., and Hutchison, G. R. (2011). Open babel: an open chemical toolbox. *J. Cheminform.* 3:33. doi: 10.1186/1758-2946-3-33

Park, J. K., Chung, M. J., Choi, H. N., and Park, Y. I. (2011). Effects of the molecular weight and the degree of deacetylation of chitosan oligosaccharides on antitumor activity. *Int. J. Mol. Sci.* 12, 266–277. doi: 10.3390/ijms12010266

Patlewicz, G., Jeliazkova, N., Safford, R. J., Worth, A. P., and Aleksiev, B. (2008). An evaluation of the implementation of the Cramer classification scheme in the Toxtree software. *SAR QSAR Environ. Res.* 19, 495–524. doi: 10.1080/10629360802083871

Patrulea, V., Ostafe, V., Borchard, G., and Jordan, O. (2015). Peptide-decorated chitosan derivatives enhance fibroblast adhesion and proliferation in wound healing. *Eur. J. Pharm. Biopharm.* 97, 417–426. doi: 10.1016/j.carbpol.2016.01.045

Pettersen, E. F., Goddard, T. D., Huang, C. C., Couch, G. S., Greenblatt, D. M., Meng, E. C., et al. (2004). UCSF Chimera-a visualization system for exploratory research and analysis. *J. Comput. Chem.* 25, 1605–1612. doi: 10.1002/jcc.20084

Phil, L., Naveed, M., Mohammad, I. S., Bo, L., and Bin, D. (2018). Chitooligosaccharide: an evaluation of physicochemical and biological properties with the proposition for determination of thermal degradation products. *Biomed. Pharmacother.* 102, 438–451. doi: 10.1016/j.biopha.2018.03.108

Quiñones, J. P., Peniche, H., and Peniche, C. (2018). Chitosan based self-assembled nanoparticles in drug delivery. *Polymers* 10:235. doi: 10.3390/polym10030235

Raafat, D., and Sahl, H. G. (2009). Chitosan and its antimicrobial potential – a critical literature survey. *Microb. Biotechnol.* 2, 186–101. doi: 10.1111/j.1751-7915.2008.00080.x

Rinaudo, M. (2006). Chitin and chitosan: properties and applications. *Prog. Polym. Sci.* 31, 603–632. doi: 10.1016/j.progpolymsci.2006.06.001

Roman, M., Roman, D. L., Ostafe, V., Ciorsac, A., and Isvoran, A. (2018b). Computational assessment of pharmacokinetics and biological effects of some anabolic and androgenic steroids. *Pharm. Res.* 35:41. doi: 10.1007/s11095-018-2353-1

Roman, M., Roman, D. L., Ostafe, V., and Isvoran, A. (2018a). Computational assessment of biological effects of methyl-ethyl-, propyl- and butyl-parabens. *JSM Bioinform. Genom. Proteomics*. 3:1029.

Saikia, C., Gogoi, P., and Maji, T. K. (2015). Chitosan: a promising biopolymer in drug delivery applications. *J. Mol. Genet. Med. S*4:006. doi: 10.4172/1747-0862.S4-006

Sánchez, Á., Mengíbar, M., Rivera-Rodríguez, G., Moerchbacher, B., Acosta, N., and Heras, A. (2017). The effect of preparation processes on the physicochemical characteristics and antibacterial activity of chitooligosaccharides. *Carbohydr. Polym.* 157 (Suppl. C), 251–257. doi: 10.1016/j.carbpol.2016.09.055

Santos-Moriano, P., Fernandez-Arrojo, L., Mengibar, M., Belmonte-Reche, E., Peñalver, P., Acosta, F. N., et al. (2018). Enzymatic production of fully deacetylated chitooligosaccharides and their neuroprotective and anti-inflammatory properties. *Biocatal. Biotransform.* 36, 57–67. doi: 10.1080/10242422.2017.1295231

Song, C. H., Yang, S. H., Park, E., Cho, S. H., Gong, E. Y., Khadka, D. B., et al. (2012). Structure-based virtual screening and identification of a novel androgen receptor antagonist. *J. Biol. Chem.* 287, 30769–30780. doi: 10.1074/jbc.M112.379107

Sundahl, N., Bridelance, J., Libert, C., De Bosscher, K., and Beck, I. M. (2015). Selective glucocorticoid receptor modulation: new directions with non-steroidal scaffolds. *Pharmacol. Ther.* 152, 28–41. doi: 10.1016/j.pharmthera.2015.05.001

Tesei, A., Leonetti, C., Di Donato, M., Gabucci, E., Porru, M., Varchi, G., et al. (2013). Effect of small molecules modulating androgen receptor (sarms) in human prostate cancer models. *PLoS ONE* 8:e62657. doi: 10.1371/journal.pone.0062657

Türková, A., and Zdrazil, B. (2019). Current advances in studying clinically relevant transporters of the solute carrier (slc) family by connecting computational modeling and data science. *Comput. Struct. Biotechnol. J.* 17, 390–405. doi: 10.1016/j.csbj.2019.03.002

van de Poel, I., and Robaey, Z. (2017). Safe-by-design: from safety to responsibility. *Nanoethics* 11, 297–306. doi: 10.1007/s11569-017-0301-x

Veber, D. F., Johnson, S. R., Cheng, H. Y., Smith, B. R., Ward, K. W., and Kopple, K. D. (2002). Molecular properties that influence the oral bioavailability of drug candidates. *J. Med. Chem.* 45, 2615–2623. doi: 10.1021/jm020017n

Ways, T. M. M., Lau, W. M., and Khutoryanskiy, V. V. (2018). Chitosan and its derivatives for application in mucoadhesive drug delivery systems. *Polymers* 10:267. doi: 10.3390/polym10030267

Wedmore, I., McManus, J. G., Pusateri, A. E., and Holcomb, J. B. (2000). A special report on the chitosan-based hemostatic dressing: experience in current combat operations. *J. Trauma*. 66, 655–658. doi: 10.1097/01.ta.0000199392.91772.44

Xiong, C., Wu, H., Wei, P., Pan, M., Tuo, Y., and Kusakabe, I. (2009). Potent angiogenic inhibition effects of deacetylated chitohexaose separated from chitooligosaccharides and its mechanism of action *in vitro*. *Carbohydr. Res.* 344, 1975–1983. doi: 10.1016/j.carres.2009.06.036

Yang, H., Lou, C., Sun, L., Li, J., Cai, Y., Wang, Z., et al. (2019). admetSAR 2.0: web-service for prediction and optimization of chemical ADMET properties. *Bioinformatics* 35, 1067–1069. doi: 10.1093/bioinformatics/bty707

Yang, H., Sun, L., Li, W., Liu, G., and Tang, Y. (2018). *In silico* prediction of chemical toxicity for drug design using machine learning methods and structural alerts. *Front Chem*. 6:30. doi: 10.3389/fchem.2018.00129

Yu, H. B., Zou, B. Y., Wang, X. L., and Li, M. (2016). Investigation of miscellaneous hERG inhibition in large diverse compound collection using automated patch-clamp assay. *Acta Pharmacol. Sin.* 37, 111–123. doi: 10.1038/aps.2015.143

Zahedipour, F., Dalirfardouei, R., Karimi, G., and Jamialahmadi, K. (2017). Molecular mechanisms of anticancer effects of glucosamine. *Biomed. Pharmacother.* 95, 51–8. doi: 10.1016/j.biopha.2017.08.122

Zhang, L., Ai, H., Chen, W., Yin, Z., Hu, H., Zhu, J., et al. (2017). CarcinoPred-EL: novel models for predicting the carcinogenicity of chemicals using molecular fingerprints and ensemble learning methods. *Sci. Rep.* 7:2118. doi: 10.1038/s41598-017-02365-0

Zhao, M., Shen, X., Li, X., Chen, B., Fan, L., Xia, Q., et al. (2019). Chitooligosaccharide supplementation prevents the development of high fat diet-induced non-alcoholic fatty liver disease (NAFLD) in mice via the inhibition of cluster of differentiation 36 (CD36). *J. Funct. Foods* 57, 7–18. doi: 10.1016/j.jff.2019.03.048

Conflict of Interest Statement: The authors declare that the research was conducted in the absence of any commercial or financial relationships that could be construed as a potential conflict of interest.

frontiers in Bioengineering and Biotechnology

REVIEW
published: 11 October 2019
doi: 10.3389/fbioe.2019.00259

A Perspective on Polylactic Acid-Based Polymers Use for Nanoparticles Synthesis and Applications

Tommaso Casalini[1]*, *Filippo Rossi*[2], *Andrea Castrovinci*[1] and *Giuseppe Perale*[1,3]

[1] Polymer Engineering Laboratory, Department of Innovative Technologies, Institute for Mechanical Engineering and Materials Technology, University of Applied Sciences of Southern Switzerland, Manno, Switzerland, [2] Department of Chemistry, Materials and Chemical Engineering "Giulio Natta", Politecnico di Milano, Milan, Italy, [3] Ludwig Boltzmann Institute for Experimental and Clinical Traumatology, Vienna, Austria

Polylactic acid (PLA)—based polymers are ubiquitous in the biomedical field thanks to their combination of attractive peculiarities: biocompatibility (degradation products do not elicit critical responses and are easily metabolized by the body), hydrolytic degradation *in situ*, tailorable properties, and well-established processing technologies. This led to the development of several applications, such as bone fixation screws, bioresorbable suture threads, and stent coating, just to name a few. Nanomedicine could not be unconcerned by PLA-based materials as well, where their use for the synthesis of nanocarriers for the targeted delivery of hydrophobic drugs emerged as a new promising application. The purpose of the here presented review is two-fold: on one side, it aims at providing a broad overview of PLA-based materials and their properties, which allow them gaining a leading role in the biomedical field; on the other side, it offers a specific focus on their recent use in nanomedicine, highlighting opportunities and perspectives.

Keywords: polylactic acid, degradation, processing, nanomedicine, nanoparticles

OPEN ACCESS

Edited by:
Anderson Oliveira Lobo, Federal University of Piauí, Brazil

Reviewed by:
Jianxun Ding, Changchun Institute of Applied Chemistry (CAS), China
Edson Cavalcanti Silva-Filho, Federal University of Piauí, Brazil

***Correspondence:**
Tommaso Casalini
tommaso.casalini@supsi.ch

Specialty section:
This article was submitted to Biomaterials, a section of the journal Frontiers in Bioengineering and Biotechnology

Received: *05 July 2019*
Accepted: *26 September 2019*
Published: *11 October 2019*

Citation:
Casalini T, Rossi F, Castrovinci A and Perale G (2019) A Perspective on Polylactic Acid-Based Polymers Use for Nanoparticles Synthesis and Applications. Front. Bioeng. Biotechnol. 7:259. doi: 10.3389/fbioe.2019.00259

INTRODUCTION

Polylactic acid (PLA), classified as an aliphatic polyester because of the ester bonds that connect the monomer units, has gained a key role in the biomedical field for a wide range of applications: suture threads, bone fixation screws, devices for drug delivery, just to scratch the surface. PLA merges several interesting properties that make it an ideal candidate for biomedical applications.

PLA naturally degrades *in situ* through hydrolysis mechanism: water molecules break the ester bonds that constitute polymer backbone. This eliminates the necessity of additional surgeries in order to remove the device, improving patient recovery and optimizing health system costs.

The main phenomena involved in the degradation mechanisms and the most important factors that influence hydrolysis rate are currently well-established in scientific literature, thanks to a devoted research activity that reached the peak between the 1980s and the 1990s. Consequently, degradation kinetics and mechanical properties can be tailored by properly tuning few polymer properties (such as composition or molecular weight), thus leading to the development of biomedical devices optimized for each specific application. Degradation products (composed of lactic acid and its short oligomers) are recognized and metabolized by the body itself: this gives PLA an intrinsic biocompatibility that dampens the attainment of critical immune responses.

In addition, PLA can be processed with standard and established technologies, such as injection molding, extrusion, etc.

After this brief summary, whose main points will be discussed in the following sections, it should be no more surprising why PLA attracted a lot of attention and enthusiasm in the biomedical field. These features make PLA a suitable option also for the new paradigm recently introduced by nanomedicine, where nanomaterials (whose size is similar to molecules of biological interest, such as proteins or viruses) are distributed within the human body and can be internalized by cells.

Nanomedicine offers new unprecedented chances, thanks to the synthesis of nanoparticles, which can be employed for the targeted delivery of drugs, vaccines and genes. On the other hand, nanomaterials can also give rise to new side effects due to specific interactions with the biological components (proteins, carbohydrates, lipids) present in body fluids (blood, plasma, interstitial fluids).

The first part of this review guides the interested reader through the main peculiarities of PLA, underlining the reasons why it emerged as a material of choice in the biomedical field. The second part of the manuscript is focused on the use of PLA for the synthesis and application of nanoparticles, from the synthetic routes of nanovectors to perspectives and opportunities.

POLYLACTIC ACID-BASED MATERIALS: GENERAL DESCRIPTION AND SYNTHESIS ROUTES

Polylactic acid is a hydrophobic polymer that belongs to the class of biomaterials commonly referred as poly-α-hydroxy acids, poly-α-esters or aliphatic polyesters. It is synthesized starting from lactic acid (LA; 2-hydroxypropanoic acid), which a water-soluble monomer that exhibits two enantiomeric forms, namely L-(+)-LA and D-(-)-LA, as shown in **Figure 1**.

Although both enantiomers are employed in industrial practice, L-(+)-LA is the isomer of interest for biomedical applications since it is involved in the cellular metabolism of the human body and reduces the risk of adverse reactions. In *in vivo* environment L-(+)-LA can be either incorporated into the Krebs' cycle or converted into glycogen in the liver; eventually it is eliminated as water and carbon dioxide from the lungs (Sheikh et al., 2015). PLA can be produced starting from pure L-lactic and D-lactic isomers, which leads to poly-L-lactic (PLLA) acid and poly-D-lactic acid (PDLA) homopolymers, respectively; if a racemic mixture of L- and D-monomers is employed, poly-D,L-lactic acid (PDLLA) copolymer is obtained. The stereochemistry has a relevant impact on material properties: PLLA is a semi-crystalline polymer, while PDLLA is an amorphous polymer with no melting point. In addition, degradation rate of PLLA is significantly slower than PDLLA, because of the presence of crystalline regions. Main advantages and disadvantages of PLA use and production are summarized in **Table 1**.

Focusing on lactic acid itself, synthesis can be performed in different ways; the most popular route is the following one (Storti and Lattuada, 2017):

$$CH_3CHO + HCN \rightarrow CH_3CH\,(OH)\,CN \quad (1)$$

$$CH_3CH\,(OH)\,CN + 2H_2O + HCl \rightarrow CH_3CH\,(OH)\,COOH + NH_4Cl \quad (2)$$

$$CH_3CH\,(OH)\,COOH + CH_3OH \leftrightarrow CH_3CH\,(OH)\,COOCH_3 + H_2O \quad (3)$$

Lactonitrile, obtained from acetaldehyde and hydrogen cyanide (1), is hydrolysed at low pH in order to lactic acid (2); it is subsequently converted to methyl lactate (3) through esterification and eventually recovered and purified by distillation. Lactic acid and methanol are obtained through hydrolysis from lactate; methanol is recycled in step (3). Anyway, this kinetic pathway leads to a racemic mixture.

Bacterial fermentation of sugar solutions is currently the most employed process; this process leads to high yields and, depending on the chosen type of bacteria, it allows obtaining one given stereoisomer or the racemic mixture. It is estimated that about 90% of the total LA produced worldwide is currently obtained with this procedure.

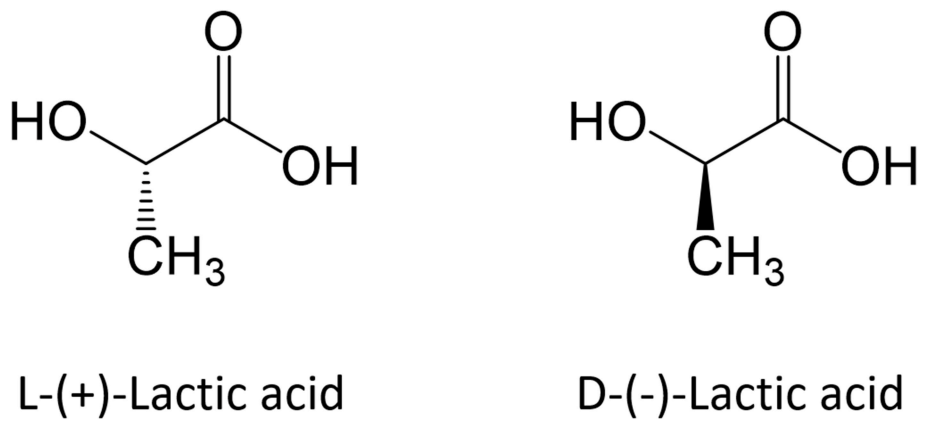

FIGURE 1 | Enantiomeric forms of lactic acid.

TABLE 1 | Main advantages and disadvantages of PLA.

Advantages	Disadvantages
Eco-friendliness: PLA is produced from renewable sources (corn, wheat, rice). In addition, it is biodegradable, recyclable and compostable. Its production consumes CO_2.	**Poor thoughness:** PLA is a very brittle material, whose elongation at break is <10%. This can represent a limit for those applications that need plastic deformation at high stress levels.
Biocompatibility: main PLA degradation product, lactic acid, is non-toxic and metabolized by the organism itself.	**Slow degradation rate:** PLA naturally degrades through hydrolysis, whose rate depends on may factors, such as crystallinity and molecular weight. Slow PLA degradation leads to high life time of devices *in vivo*, and can raise issues for the disposal of commodities.
Processability: PLA has a better thermal processability than other biopolymers. It can be processed through injection molding, film extrusion, blow molding, thermoforming, fiber spinning, and film forming.	**Hydrophobicity:** PLA is a relatively hydrophobic material (static water contact angle value is about 80°). This results in low cell affinity and can lead to inflammatory response upon direct contact to biological fluids.
Energy saving: PLA requires 25–55% less energy than petroleum-based polymers.	**Lack of reactive side chain groups:** PLA is chemically inert, which makes surface functionalization and bulk modification challenging tasks.

Adapted from Farah et al. (2016).

In this framework, the critical step is the subsequent LA purification, which is expensive and determines process profitability. Commonly used techniques are liquid extraction, membrane separation, ion exchange, electrodialysis, and reactive distillation.

Polymer synthesis can be carried out through step growth polymerization or ring opening polymerization. Step growth polymerization simply takes advantage of the reactivity of the two LA functional groups: indeed, the polycondensation of hydroxyl and carboxyl moieties leads to the formation of the ester bonds that constitute polymer backbone. This synthetic route has several drawbacks: long residence times are required for longer chains (leading to unwanted side reactions, like transesterification), challenging reaction conditions (temperatures up to 250°C and vacuum up to 100 mbar) and continuous water (side product of polycondensation) removal. Chain extenders (e.g., isocyanates or epoxides) can be in principle employed, although this approach has an inevitable impact on material purity and quality.

At industrial scale ROP is the most popular process because of its advantages: mild process conditions, short residence times, absence of side products and high molecular weights. The most widely used catalyst is 2-ethylhexanoic tin(II) salt (also referred as stannous octoate [$Sn(Oct)_2$]), approved by United Stated Food and Drug Administration (FDA) and usually employed along with an alcohol as cocatalyst. The real bottleneck of ROP is the availability of cyclic monomers as well as their optical and chemical purity, since impurities have detrimental effects on material properties due to the sensitivity of the reaction to residual non-cyclic monomers. The cyclic raw material for PLA is constituted by cyclic dimer lactide, which exhibits three stereoisomeric forms, as shown in **Figure 2**: LL-, DD-, and D,L- (also referred a meso-lactide).

Lactide is usually produced through backbiting kinetic mechanism is then (promoted with suitable process conditions) starting from low molecular weight prepolymer; cycles are eventually collected by distillation. Other synthesis routes are azeotropic dehydration and enzymatic polymerization. PLA-based polymers synthesis routes are summarized in **Figure 3**.

PLA is widely employed in the biomedical field because of its biocompatibility and its processability, since it can be processed with a wide range of techniques, such as extrusion, injection molding, injection stretch blow molding, film and sheet casting, extrusion blow film, thermoforming, foaming, fiber spinning, electro spinning, blending, compounding, and nanocompositing.

PHYSICAL AND CHEMICAL PROPERTIES

PLA can be seen as a "family" of polymers, which include homopolymers PLLA and PDLA (synthesized from mixtures of pure L- or D-lactic acid) and the copolymer PDLLA (obtained from the racemic mixture). This has a remarkable impact on material properties because of the involved stereochemistry: PLLA and PDLA are semicrystalline polymers, while PDLLA is usually amorphous. The final crystallinity depends also on the thermal and mechanical history, mainly due to fabrication processes. Mechanical properties are summarized in **Table 2**; values are expressed as ranges, since they strongly depend on the characteristic of the tested material (molecular weight, crystallinity, processing, etc.) as well as testing procedure (Van De Velde and Kiekens, 2002).

Polymer crystallinity influences mechanical and physical properties such as hardness, modulus, tensile strength, stiffness, and melting points. If the amount of PLLA is higher than 90% the polymer is semicrystalline, while lower amounts (and thus a lower optical purity) lad to an amorphous polymer. The density values lie in small range depending on the composition, as shown in **Table 2**.

PLA is soluble in dioxane, acetonitrile, chloroform, methylene chloride, 1,1,2-trichloroethane and dichloroacetic acid, while it is only partially soluble in ethyl benzene, toluene, acetone and tetrahydrofuran, only when heated to boiling temperature. PLA is not soluble in water, alcohols, and linear hydrocarbons. Crystalline PLLA cannot be dissolved in acetone, ethyl acetate, or tetrahydrofuran.

It is worth mentioning that polymer properties can change after processing, because of thermal and mechanical stresses. PLA undergoes thermal degradation above 200°C, although degradation rate and extent depend on variables like time, temperature, low molecular weight impurities, and catalyst amount (Carrasco et al., 2010).

The success of PLA passes also through its versatility, since material properties can be modified in several ways. They can

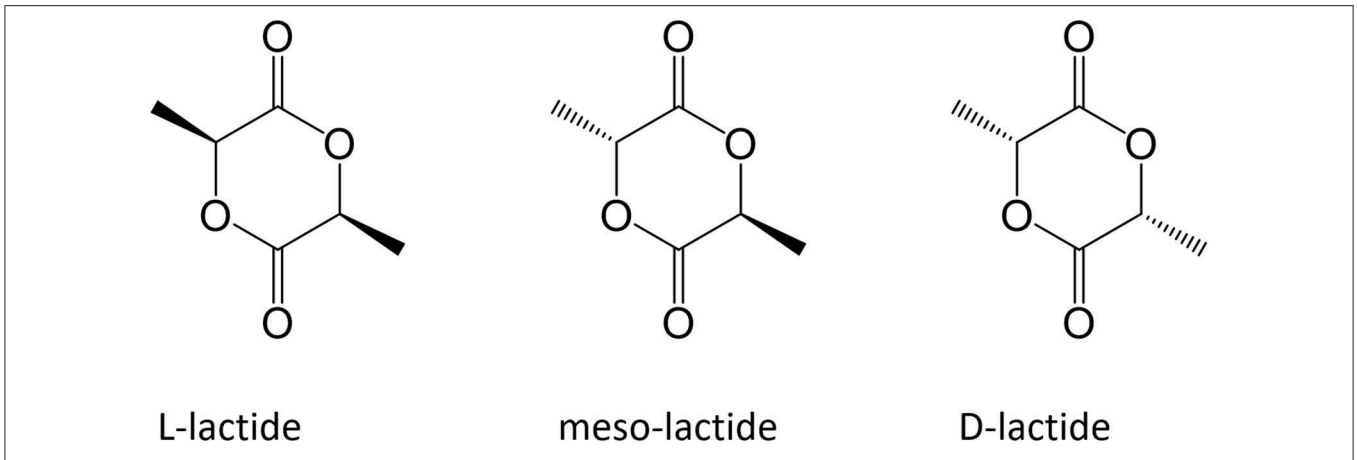

FIGURE 2 | Cyclic dimers for ROP process.

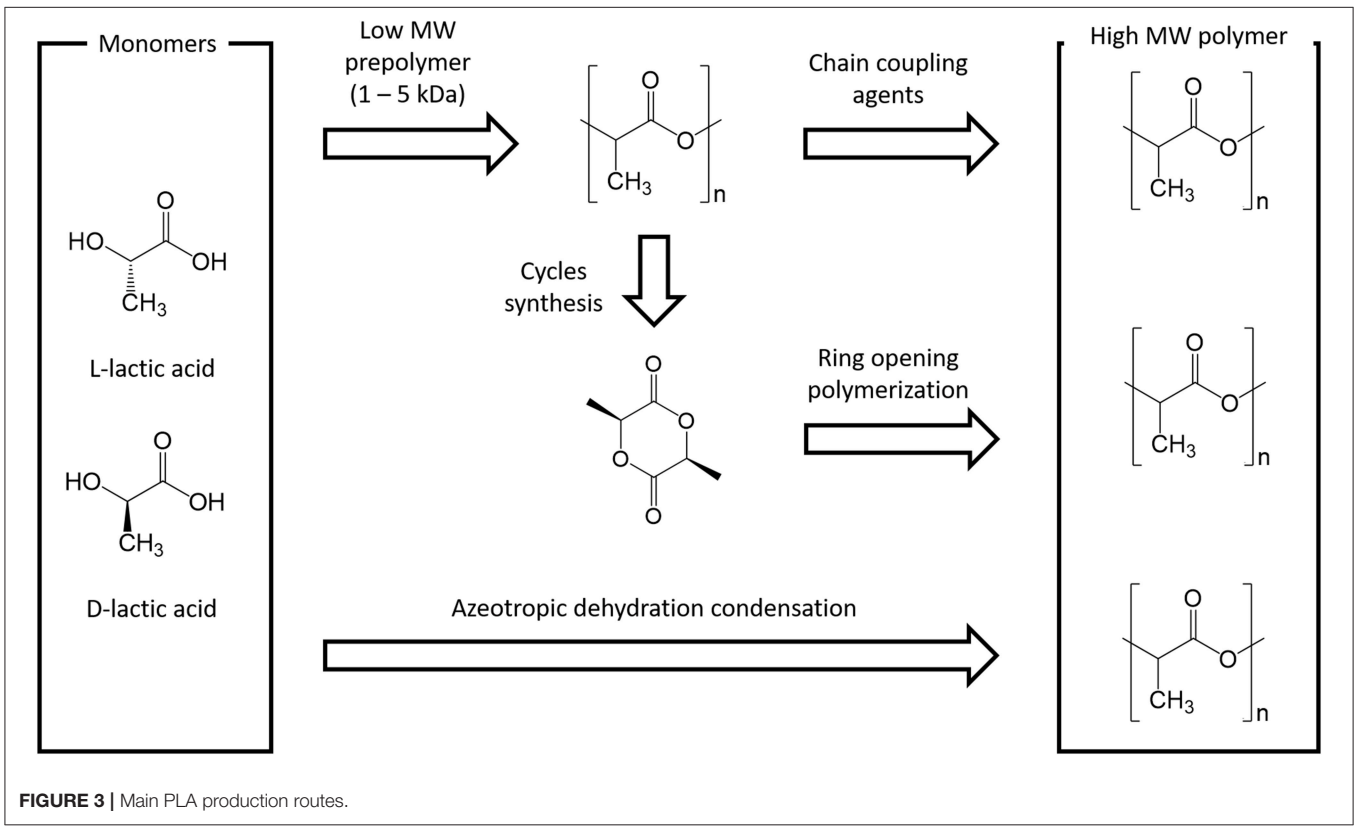

FIGURE 3 | Main PLA production routes.

be tuned, e.g., through the addition of suitable plasticizers, widely used in order to improve processability and flexibility of polymers. Focusing on semicrystalline PLA, plasticizer addition decreases T_g, as well as T_m and crystallinity.

PLA can be blended with biodegradable or non-biodegradable polymers (such as polyethylene, polypropylene, chitosan, polystyrene, polyethylene terephthalate, and polycarbonates) (Saini et al., 2016) or by making composite materials (Murariu and Dubois, 2016) through the addition of carbon nanotubes, ceramic nanoparticles, natural fibers, and cellulose (Hamad et al., 2018). A relevant example is constituted by PLA/hydroxyapatite (HA) composites for devices for bone healing, where HA micro or nanoparticles are dispersed into the polymer matrix (Rodenas-Rochina et al., 2015).

Another is the formation of stereocomplexes (Tsuji, 2016), which can be obtained by blending PLLA with PDLA (that is, the homopolymer composed by D-lactide units only) or adopting PLLA/PDLA block copolymers. The strong interactions between PDLA and PLLA blocks that derive from the formation of stereocomplex crystallization improves mechanical properties

TABLE 2 | Mechanical properties of PLA-based polymers.

Property	PLA	PLLA	PDLLA
ρ [g cm^{-3}]	1.21–1.25	1.24–1.30	1.25–1.27
σ [MPa]	21–60	15.5–150	27.6–50
E [GPa]	0.35–0.5	2.7–4.14	1–3.45
ε [%]	2.5–6	3.0–10.0	2.0–10.0
T_g [°C]	45–60	55–65	50–60
T_m [°C]	150–162	170–200	amorphous–no melt point

ρ, density; σ, tensile strength; E, elastic modulus; ε, ultimate strain; T_g, glass transition temperature; T_m, melting temperature. Taken from Farah et al. (2016).

and thermal stability, slows down degradation rate and increase PLA barrier properties, allowing a more prolonged drug release. PLA-based stereocomplexed materials, by virtue of their improved stability, attracted a lot of interest also for biomedical applications, such as fibers and nanoparticles for drug delivery applications (Jing et al., 2016).

PLA-based materials can be also assembled in complex molecular architectures (Corneillie and Smet, 2015), leading to branched polymer chains, star-shaped structures (Michalski et al., 2019), grafted chains (Nagahama et al., 2007), and cross-linked matrices (Tsuji, 2016). If synthesized with both PLLA and PDLA blocks, stereocomplexation can be achieved also with these complex structures (Nagahama et al., 2007; Fan et al., 2013; Sveinbjornsson et al., 2014), which found as well-potential applications in the biomedical field for the synthesis of hydrogels, nanoparticles and micelles for drug delivery purposes.

Another popular way to tune material properties is the copolymerization with glycolic acid, which leads to the well-known polylactic-co-glycolic random copolymer (PLGA). Copolymerization is also performed with caprolactone, which allows obtaining polylactic-co-caprolactone (PLCL). Another strategy to improve material hydrophilicity is the synthesis of PLA and polyethylene glycol (PEG) block copolymers.

PLA (as well as its copolymers) degrades because of hydrolysis mechanism: water breaks the ester bonds that constitute polymer backbone, according to the following mechanism:

$$P_{n+m} + H_2O + H^+ \leftrightarrow P_n + P_m + H^+ \quad (4)$$

where P_{n+m}, P_n, and P_m are polymer chains composed by $n+m$, n, and m monomer units, respectively, H_2O is a water molecule and H^+ indicates that hydrolysis is catalyzed in acidic environment. The most important phenomena that govern PLA degradation are currently rationalized and accepted in scientific literature (Casalini, 2017). Two degradation regime can be distinguished. If hydrolysis rate is higher than diffusion rate, surface, or heterogeneous degradation takes place; only polymer surface experiences degradation and erosion (i.e., mass loss), while the bulk remains intact. The shape of the device remains unchanged, but its volume decreases in time. On the other hand, if water penetration is much faster than water consumption, homogeneous, or bulk degradation occurs: degradation rate is essentially equal in every point of the matrix and the volume does not appreciably change in time. Mass loss is observed after a certain time interval, when chain scission has created oligomers that are mobile enough to diffuse through the matrix toward the environment. Another relevant aspect is autocatalysis: polymer degradation creates small fragment that lower pH-value by virtue of their dissociated carboxyl terminal group, thus enhancing hydrolysis rate. In other words, pH decreases as degradation continues and this results in an autocatalytic behavior. Notably, when mass transport resistances and/or mean diffusive paths are relevant, a transition from homogeneous to heterogeneous degradation may occur. In this case, oligomers accumulate in the core of the device, locally lowering the pH; consequently, degradation is faster in the bulk than close to the surface. In order to discriminate the degradation mechanism, Von Burkersroda et al. (2002) proposed a distinctive parameter called critical thickness L_{crit}; if the characteristic size of the device (e.g., the radius of a sphere) is larger than the critical thickness surface degradation occurs, otherwise bulk degradation govern matrix hydrolysis mechanism.

A scheme is provided in **Figure 4**.

The discussed mechanisms represent asymptotic cases and the observed experimental behavior is usually one of the many shades of gray in between.

L_{crit} depends on the interplay between degradation and diffusion kinetics, and at a first glance, it depends on the specific material. Von Burkersroda et al. (2002) computed the values of L_{crit} for some polymers of interest; the reference value for aliphatic polyesters is 7.4 cm. The main phenomena behind PLA degradation can be summarized as follows (Casalini, 2017):

- Water penetrates into the polymer matrix from the surrounding environment through diffusion. PLA is hydrophobic and polymer dissolution is absent; volumetric swelling is negligible;
- While water diffuses, it breaks the ester bonds and causes chain scission;
- The resulting small oligomers diffuse out of the matrix; if their concentration in the core is high because of mass transport resistances, degradation is locally faster due to autocatalysis;
- Diffusivities of each compound increase as molecular weight decreases, since chain scission creates new and wider diffusive paths;
- In *in vivo* environment, an additional contribution to degradation is given by enzymes, which contribute to the erosion of device surface (*vide infra*).

Degradation rate depends on several factors, such as (Alexis, 2005):

- *Polymer composition*: Generally speaking, degradation increases as material hydrophilicity increases. PLLA degradation is slower than PDLLA because of the presence of crystalline regions.
- *pH*: As mentioned, hydrolysis of ester bond is favored at low pH-values, although there are some experimental evidences that basic conditions can speed up chain scission.
- *Device geometry*: Device size can discriminate the attainment of bulk or surface degradation (*vide supra*).

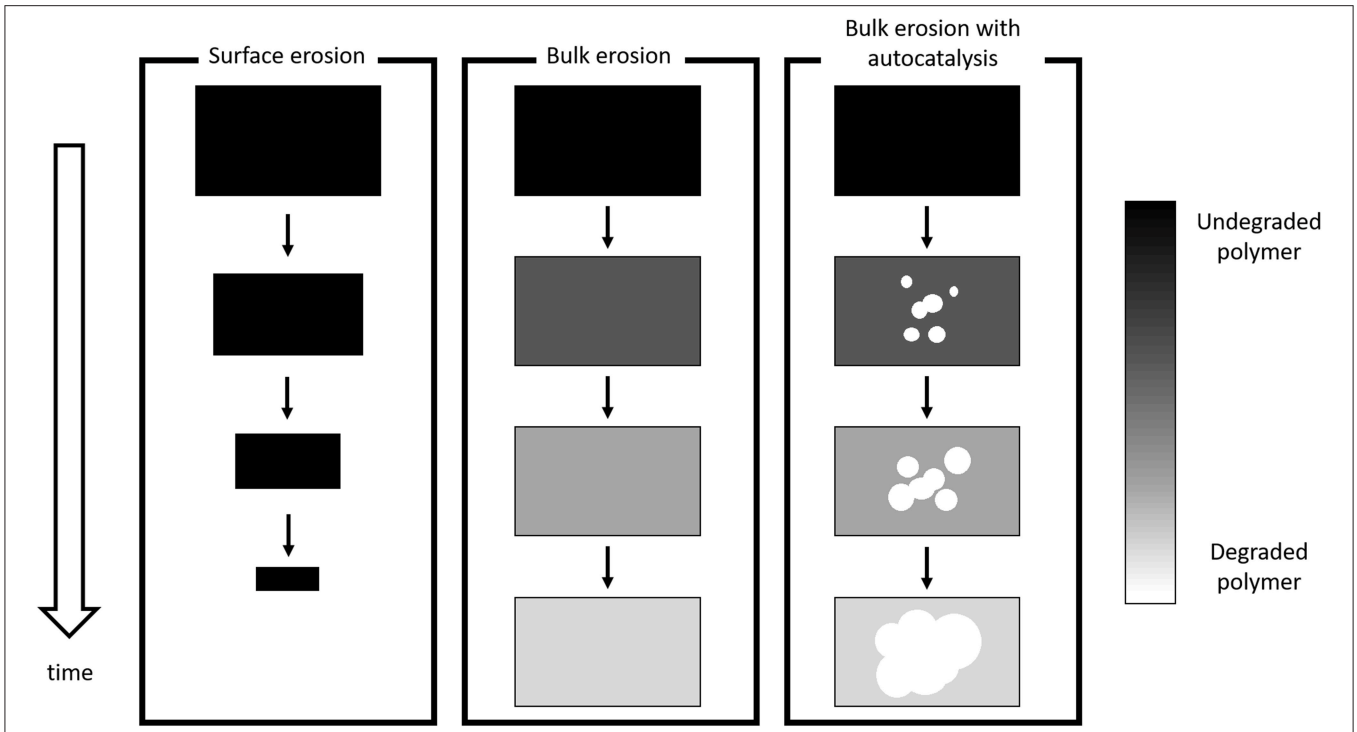

FIGURE 4 | Schematic of degradation mechanisms.

- *Molecular weight*: Degradation rate decreases as molecular weight increases, because of the lower water uptake. In addition, high molecular weight values imply a lower concentration of carboxyl end groups.
- *Crystallinity*: Broadly, semicrystalline polymers are characterized by a slower degradation rate than amorphous ones, since crystallites regions are less subjected to hydrolysis. However, there are still some inconsistent results, which may depend on the different process methodologies. It has also been observed that the short chains that derive from the degradation of amorphous regions gain enough mobility to organize themselves in crystalline regions.
- *Addition of drugs and/or additives*: The addition of acidic compounds can enhance hydrolysis rate, while basic compounds can neutralize carboxyl end groups and enhance degradation through base catalysis. The addition of plasticizers can promote water diffusion and water uptake, enhancing degradation rate.
- *Sterilization*: The use of beta or gamma irradiation or sterilization results in undesired reactions such as chain scissions and cyclization, that lower molecular weight and enhance degradation rate.
- *Mechanical stress*: Stress fields due to specific applications (e.g., fixation screw) enhance degradation rate.
- *Fabrication processing*: Thermal and mechanical stresses experienced by the polymer during commonly employed processing techniques (extrusion, injection molding, etc.) can lead to decrease in molecular weight and increase of degradation rate.

By virtue of a critical thickness equal to 7.4 cm, PLA-based devices usually experience homogeneous degradation, which can become heterogeneous when oligomer accumulation in the bulk occurs.

In *in vivo* environment, there is an additional contribution to degradation due to enzymes that cleave ester bonds, such as lipases, cutinases, serine proteases, PHB depolymerase, PCL depolymerase, elastase esterase, proteinase K, and trypsin. This enzymatic degradation is a heterogeneous process since involves only device surface: enzymes are not able to diffuse in the polymer matrix and contribute to surface erosion through ester bonds cleavage (Armentano et al., 2018).

PLA-based materials are also subjected to thermal degradation; while this is not relevant for biomedical applications themselves (at body temperature, thermal degradation is absent), this should be taken into account in the fabrication process. Indeed, for temperature values above 200°C (Garlotta, 2001), PLA experiences not only hydrolysis but also lactide reformation, oxidative chain scission, intra- or intermolecular transesterification reactions.

PROCESSES FOR NANOPARTICLES SYNTHESIS

PLA-based materials experienced a wide success in biomedical field for several reasons: biocompatibility, low toxicity, degradation through hydrolysis and tailored physical and chemical properties through the selection of molecular weight or

TABLE 3 | Overview of PLA biomedical applications.

Field	Application
Orthopedic	Peripheral nerve and spinal cord injury regeneration Bioadsorbable screws Meniscus repair Guided bone regeneration
Cardiac	Chest wall reconstruction Stent
Dentistry	Guided tissue regeneration Biocompatible space fillers
Plastic surgery	Suture Reconstructive surgery Dermal fillers Skin draft
General surgery	Hemia mesh
Gynecology	Stress incontinence mesh
Radiology	Theranostic imaging
Oncology	Nanoparticles for drug delivery

Adapted from Tyler et al. (2016).

through copolymerization, blending, or building more complex molecular architectures and processability. A proper tuning of polymer properties allows assuring the desired performances (in terms, e.g., of tensile strength or release rate) over a suitable time span, before an appreciable onset of degradation reactions. The natural degradation of PLA-based devices due to hydrolysis avoids the need of additional surgery for device removal, improving patient care.

All these advantages led to a wide range of applications, summarized in **Table 3** for the sake of completeness.

Nanomedicine is an emerging field, focused on the development and application of engineered nanomaterials, whose size (from 1 to 1,000 nm according to the FDA draft guideline form 2017) is comparable to many molecules of biological interest, such as proteins and viruses. Devices like polymer nanoparticles, by virtue of their small size, can be internalized by cells and this opens a wide range of new opportunities for the development, e.g., of new carriers for the targeted delivery of drugs and vaccines or image contrast agents for diagnostic purposes. Because of the interesting properties of PLA-based polymers, it is not surprising that they experienced and are still experiencing a great interest as starting materials for the synthesis of nanoparticles.

The most frequently used and promising methods to formulate nanosized particles can be divided in four categories according to the fundamental physical principles, as summarized by Lee et al. (2016). The main challenges are the control of particle size and an efficient drug encapsulation.

Emulsion-Based Methods

The single-emulsion/solvent-extraction method is the simplest approach for the synthesis of micro- and nanoparticles, including drug-loaded carriers. The polymer and, if needed, the hydrophobic drug are dissolved in a water-immiscible organic solvent and an emulsion in water phase is subsequently realized by adding a stabilizer and stirring. For the sake of completeness, oil in water (o/w) as well as oil in oil (o/o) and water in oil (w/o) emulsions can be suitable for this process.

The removal of the organic phase is carried out through evaporation at low pressure or vacuum or by solvent extraction; polymer particles are recovered by centrifugation or filtration and washed with water or buffer solutions in order to remove possible traces of solvent, stabilizer and free drug before lyophilization.

Single-emulsion approach leads to a poor encapsulation efficiency of hydrophilic drugs (such as peptides), which are mainly dispersed in the aqueous phase rather than the organic one. Double-emulsions methods aim at overcoming this issue. A water solution containing the hydrophilic active molecule is added to an organic solvent where the polymer is dissolved under stirring, in order to form a w/o (or an o/w) emulsion that is subsequently added to a second water phase containing a stabilizer. This leads to the formation of a w/o/w (or an o/w/o) emulsion. The organic solvent is removed by means of evaporation under low pressure or vacuum and the resulting particles are washed (to safely remove traces of solvent, stabilizer, and free drug) before lyophilization.

Emulsion-based methods, despite their simplicity, need the optimization of several process parameters, such as phase volumes (oil and water), polymer, drug and stabilizer concentration, type of solvents, and stirring rate.

Examples of particles produced with emulsion-based methods are provided in **Table 4**.

Precipitation-Based Methods

Nanoprecipitation, also referred as solvent displacement, is a one-step process suitable for producing nanoparticles loaded with hydrophobic drugs. The underlying physical principle is the interfacial deposition of a polymer, following the displacement of a water-compatible solvent from a lipophilic solution. Polymer and drug are dissolved in a semi-polar organic solvent (acetone, methanol, ethanol, acetonitrile); the resulting organic phase is mixed drop-wise in a water solution containing a stabilizer. This technique leads a narrow particle size distribution and allows avoiding the use of large amounts of toxic solvents as well as external energy sources. On the other hand, it is limited by drug solubility in the organic phase and it is thus not suitable for hydrophilic drugs; another drawback is the removal of the residual solvent.

Salting-out method is based on the addition of a polymer and drug solution in a water-compatible solvent (acetone, acetonitrile, tetrahydrofuran) to an aqueous solution that contains the salting-out agent (electrolytes like magnesium chloride and calcium chloride or non-electrolytes like sucrose) and a stabilizer, under stirring. This allows obtaining an o/w emulsion that is subsequently diluted with large volumes of water, promoting the formation of particles by virtue of the diffusion of the water-compatible solvent toward the aqueous phase. Particles are recovered and purified by means of centrifugation or filtration. In particular, salt residues must be removed before utilization.

Salting-out is the ideal process for encapsulating heat-sensitive molecules (such as proteins, DNA, RNA) because no heating

TABLE 4 | Examples of nanoparticles synthesis by means of emulsion-based methods.

Loaded drug	Preparation method	Particle size [nm]	References
Bovine Serum Albumin	Double emulsion	140–250	Gao et al., 2005
Nimesulide	Emulsion-solvent evaporation	160–2,150	Freitas and Marchetti, 2005
Tetanus toxoid	Double emulsion	353–1,153	Bilati et al., 2005
Lysozyme	Double emulsion	369–459	Bilati et al., 2005
Insulin	Double emulsion	1,000–1,400	Bilati et al., 2005
Betamethasone phosphate	O/w emulsion	90–250	Ishihara et al., 2005
Vanillin	O/w emulsion	240	Dalmolin et al., 2016
Hemoglobin	Double emulsion	122–185	Sheng et al., 2009
Neurotoxin-I	Double emulsion	65	Cheng et al., 2008
Triclosan	Double emulsion	207–286	Pinon-Segundo et al., 2005
Paclitaxel	Single emulsion	110	Feng et al., 2015

TABLE 5 | Examples of nanoparticles synthesis by means of precipitation-based methods.

Loaded drug	Preparation method	Particle size [nm]	References
Sodium cromoglycate	Nanoprecipitation	470–1,300	Peltonen et al., 2004
Lysozyme	Nanoprecipitation	137–351	Bilati et al., 2005
Tyrphostin	Nanoprecipitation	65–143	Chorny et al., 2002
Cloricromene	Nanoprecipitation	120–340	Leo et al., 2004
–	Nanoprecipitation	100–300	Legrand et al., 2007
–	Salting out	100–400	Zweers et al., 2003
–	Salting out	279	Nguyen et al., 2003
–	Salting out	248	Zweers et al., 2004
Savoxepine	Salting out	274–736	Leroux et al., 1996
–	Dialysis	40–250	Lo et al., 2005
Epirubicin	Dialysis	128–1,088	Liu et al., 2007
Paclitaxel	Dialysis	367–475	Zhang et al., 2008
HIV p24 protein	Dialysis	200	Aline et al., 2009

steps are required. Anyway, the process requires the optimization of parameters like salt type and concentration, type of polymer and solvent, and their relative amounts. The principal limitations are the intensive purification of the resulting nanoparticles as well as incompatibility issues concerning most of the employed salts with bioactive compounds.

Dialysis emerged as a simple process that allows obtaining small particles with a narrow size distribution. The polymer is dissolved in an organic solvent and placed in a dialysis tube of suitable pore size; dialysis is subsequently carried out in a solvent that is miscible with the organic phase but not compatible with the polymer. This leads to the formation of polymer particles due to the loss in solubility. Selected examples from literature of particles synthesized by means of precipitation based-methods are reported in **Table 5**.

Compositing Methods

In spray drying technique, polymer and drug are dissolved in an organic solvent and subsequently dispersed as ultra-fine droplets in a hot air flow. The solvent evaporates instantaneously and dried particles are collected under low pressure in dry air flow. Spray drying process is easy to perform and can be potentially employed at industrial scale. However, productivity can be hindered by the adhesion of the particles to the walls of the spray dryer and their agglomeration. Moreover, it is challenging to control drug distribution.

Melting technique allows avoiding the use of organic solvents but implies the dissolution of the drug in a polymer melt; therefore, it is not suitable for encapsulating active compound that are subjected to thermal degradation. Drug/polymer melt is subsequently solidified and cooled down with water or dry air. Particles are obtained through grounding or milling; in order to achieve small particles with narrower size distribution, the ground melt can be emulsified in a hot solution with a stabilizer. Despite the absence of organic solvents, this approach is limited by the thermal treatment of the drug/polymer system and the high number of steps needed to obtain smooth particles.

In situ-forming techniques aim at overcoming the most common drawbacks of the discussed processes, such as solvent removal, particles recovering, and resuspension. A drug/polymer solution (in a water-miscible solvent) is prepared and injected in the target site. When in contact with physiological fluids, polymer phase hardens and precipitates forming microparticles that entrap the active compound. The main drawback lies in a careful choice of the solvent, whose side-effects must be previously investigated.

Other Approaches

Supercritical fluids-based methods attracted a lot of interest because of their advantages, such as the use of environmentally friendly solvent and the possibility to obtain nanoparticles with (virtually) no traces of residual solvents. There are two main processes that involve supercritical fluids: rapid expansion of supercritical solution (RESS) and rapid expansion of a supercritical solution into a liquid solvent (RESOLV).

In RESS technique, the polymer is dissolved into the supercritical fluid; the solution is then subjected to a rapid expansion across a nozzle in ambient air. The sudden reduction in pressure leads to a substantial supersaturation, which, in

turn, promotes homogeneous nucleation and the formation of well-dispersed particles. RESOLV process is based on the same principle, but the expansion does not take place in air but in a liquid solvent. The liquid phase hinders particle growth, leading to the synthesis of nanoparticles. The most important limitation of RESS and RESOLV technique is the poor solubility of the polymer in the supercritical fluid. In addition, it is difficult to control particle size and morphology.

With microfluidic techniques it is possible to obtain uniform particles with a narrow particle size distribution, which, in turn, allows a finer control of the release rate. The starting point is usually the attainment of an o/w emulsion in the microfluidic device, where monodisperse droplets can be achieved, followed by droplet solidification by means of solvent evaporation, diffusion or extraction. Particle size can be controlled by tuning the properties of oil and water phases (density, interfacial tension, and viscosity) and flow rates. Because of the inherent micron length scale, the challenge lies in the synthesis of particles at nanoscale. The underlying principle of hydrogel template method is the possibility to control sol-gel transition of physical gel by changing the environmental conditions (e.g., temperature). A warm aqueous gelling solution is distributed on a hard master template and placed at low temperature, in order to obtain a hydrogel mold. Polymer and drug are dissolved in a suitable solvent and poured on the hydrogel mold; solvent is removed through evaporation and particles are recovered by centrifugation or filtration and washed after dissolving the mold in water. Polyvinyl alcohol water-soluble molds are also employed. Similarly to microfluidic techniques, the drawback lies in the particle size, which is still limited to the micron length scale. In principle, nanoparticles can be obtained by means of nanostructured mold templates. Notably, nanoparticles can be produced not only from preformed polymers but also starting from monomers, including the polymerization process in the nanoparticle production step. This can be achieved my means of emulsion polymerization (George et al., 2019).

Summary

For the sake of completeness, the main advantages and disadvantages of the most common employed methods are summarized in **Table 6**.

As mentioned in the previous sections, several parameters are involved in process optimization and strongly influence the final particle size distribution. The most important degrees of freedom, as well as their influence on the final outcome are summarized in **Table 7**.

TABLE 6 | Advantages and disadvantages of the most common nanoparticles production methods.

Process	Advantages	Disadvantages
Single/double emulsion	Particle size can be tuned acting on several variables (**Table 7**)	High shear rate High volumes of water to be removed
Nanoprecipitation	Nanoparticles have a well-defined size and a narrow size distribution Less toxic solvents No use of external energy sources	Extensive optimization of polymer/solvent/non solvent system Not suitable only for hydrophilic compounds
Salting out	No heating process required No hazardous/chlorinated solvents are employed	Extensive optimization of process conditions (type of salt and its concentration, type of polymer and solvent, and their ratio) Extensive purification to remove salting-out agent Possible incompatibility of salting out agents and drugs
Supercritical fluids-based technology	Environmentally friendly solvents Few traces of solvent in the final product	Limited by polymer solubility in the supercritical fluid Difficult to control particle size and morphology;
Spray drying	Residual organic phase is immediately evaporated Easy to set up	It is difficult to control drug distribution into the nanoparticles Adhesion of nanoparticles to the inner walls of spray dryer
Melting techniques	No solvents required	Not suitable for thermally-sensitive compounds (e.g., proteins) Many steps are required
In situ forming techniques	No need to recover particles	Solvent toxicity must be previously investigated.

TABLE 7 | Process variables and their effect on particle size.

Process variable	Effect on average particle size
Solvent	It depends on the specific solvent, i.e., its effect on emulsification.
Surfactant/stabilizer	It depends on the chemical nature of the stabilizer (ionic/non-ionic).
Shear rate	High shear rate decreases particle size.
PLA molecular weight	Size increases as molecular weight increases (the viscosity of dispersed phase increases).
PLA concentration	Size increases as polymer concentration increases (the viscosity of dispersed phase increases).
Stabilizer concentration	High stabilizer concentration (3% w/v or higher) decreases particle size.
Viscosity of the dispersed phase	Size increases as viscosity increases.

THE NEW PARADIGM INTRODUCED BY NANOPARTICLES

While devices at macroscale (suture treads, polymer-coated stents, bone fixation screws, etc.) remain at the implantation site, nanoparticles, because of their size, are able to spread all over the body and to penetrate into cells. This introduces a new paradigm in the engineering of polymeric nanocarriers, since they must be designed so that they remain in the systemic circulation long enough to accomplish their task and they are able to target the desired objective. Particle behavior, in terms of clearance, biodistribution (i.e., distribution in the organs), cellular uptake, and toxicity are mainly influenced by particle size, shape, morphology, surface chemistry, and charge (Blanco

TABLE 8 | Experimental techniques for nanoparticles characterization (Crucho and Barros, 2017).

Experimental technique	Nanoparticle property
Atomic Force Microscopy	• Size and size distribution • Shape • Structure • Aggregation • Surface properties
Differential scanning calorimetry	• Physicochemical state and possible interactions between drug and polymer
Dynamic light scattering	• Particle size distribution (hydrodynamic radius);
Fluorescence microscopy	• Critical association concentration • Drug content • *In vitro* drug release
High performance liquid chromatography	• Drug content • *In vitro* drug release
Infrared spectroscopy	• Structure and conformation of bioconjugates • Functional group analysis
Mass spectrometry	• Molecular weight • Composition • Structure • Surface properties
Near-field scanning optical microscopy	• Size • Shape
Nuclear magnetic resonance	• Structure • Composition • Purity • Conformational change
Scanning electron microscopy	• Size and particle size distribution • Shape • Aggregation
Transmission electron microscopy	• Size and particle size distribution • Shape heterogeneity • Aggregation
X-ray photoelectron spectroscopy	• Elemental and chemical composition a the surface
Zeta potential	• Stability referring to surface charge

et al., 2015). The techniques that can be used to characterize experimentally nanoparticles are summarized in **Table 8** (Crucho and Barros, 2017).

The acquired knowledge led to the development of proper design strategies, as shown below (*vide infra*). Nanoparticles synthesized from PLA-based materials are mainly employed as devices for drug delivery for cancer treatment and for imaging purposes (Kim et al., 2019). Nanoparticles are potentially able to penetrate selectively within the cancer, where they can release the loaded active compound at the desired rate, so that a therapeutic effective drug concentration is maintained for a given time period. This allows minimizing the amount of administered drug, since it mainly diffuses in the tumor following nanoparticles permeation through cancer cells, dampening potential side effects and optimizing costs for health systems.

There are various administration routes for nanoparticles, such as oral, parenteral (intravenous, subcutaneous, intradermal, and intramuscular), respiratory, and transdermal routes (Kaialy and Al Shafiee, 2016). In any case, nanoparticles must be able to cross certain barriers (which can vary according to the administration route) in order to be effective (Blanco et al., 2015). Depending on the administration route, the first barrier can be constituted by endothelial or epithelial cells.

Epithelium is essentially constituted by the skin and mucosal membranes, while endothelium separates the blood flow from the surrounding tissues. The endothelium that separates blood vessel and central nervous system is the well-known blood brain barrier (BBB), which is very challenging to cross.

Another barrier is constituted by the immune system; after injection, nanoparticles experience opsonization, which involves the adsorption of plasma proteins on the surface of the device that leads to the formation of the protein corona (*vide infra*). After the attainment of the layer of adsorbed proteins, nanoparticles bind to a macrophage receptor and are subsequently internalized and removed from circulation. This problem can be overcome through surface modification, hindering protein adsorption, and interactions with macrophages receptors. The most popular route is PEGylation, that is, the addition of PEG brushes on nanoparticle surface that constitute an obstacle for protein adsorption (Partikel et al., 2019). Other strategies involve surface functionalization with *ad hoc* peptides that delay phagocytic clearance (Rodriguez et al., 2013), or coating with cell membranes from red blood cells or leukocytes (Blanco et al., 2015). In general, the objective is to prolong the persistence in the blood circulation avoiding a rapid clearance by the immune system.

Focusing on PEGylation of PLA-based particles, three main approaches can be identified (Betancourt et al., 2009). In direct conjugation, PEG chains are covalently bound to the end groups of polymer chains already assembled in nanoparticles. This approach has the advantage that PEGylation is performed after the encapsulation of an active principle with standard techniques but it is not very efficient because of the limited exposure of the end groups on particle surface. When active conjugation in solution is chosen, preformed long polymer chains are activated and conjugated with PEG chains. Despite the moderate conjugation efficiency, the attainment of high yields is hindered by a difficult recover of the copolymer and the possible formation of PEG-PEG conjugates that can affect the purity of the product. The most used technique is ring opening polymerization, where preformed OH-PEG-COOH chains (that is, with a hydroxyl and a carboxyl end groups) are polymerized with lactide (and glycolide, if PLGA is needed) cyclic dimers. In these conditions, the hydroxyl end group of PEG acts as a protic agent initiating the reaction, while carboxyl end group remains intact. This leads to the synthesis of block PLA-PEG block copolymers.

Eventually, nanoparticles can experience cellular uptake mainly through endocytosis, which can be due to different pathways (Sahay et al., 2010; Kim et al., 2019). In receptor-mediated endocytosis, nanoparticles can be internalized by interacting with a specific receptor expressed on cellular membrane; a key role is played by clathrin and caveolin. Clathrin-mediated endocytosis is present in essentially all mammalian cells and is responsible for the uptake of essential nutrients; caveolae-mediated endocytosis exploits the presence of caveolin

proteins in the caveolae (lipid rafts along cellular membranes) and attracted some interest since this pathway allows bypassing lysosomes and thus avoiding lysosomal degradation. Carrier-mediated endocytosis exploits the presence of carrier proteins on cellular membrane; this pathway can be exploited to pass challenging barriers like the BBB. Since the cellular membrane, at physiological pH, has a slight negative charge, electrostatic interactions with positively charged carriers can promote particle internalization through an adsorption-mediated endocytosis. Pinocytosis implies the formation of membrane-based vesicles from the cell surface, which captures solute and fluid from the environment.

From an experimental point of view, it is possible to identify the specific endocytosis pathway by suppressing some mechanisms with suitable inhibitors and assessing the cellular uptake.

In this regard, it useful to introduce the concept of targeting. In order to maximize their effect, nanoparticles should be able to selectively penetrate within the tumor, minimizing their accumulation in healthy organs. There are two different targeting approaches: passive and active targeting.

Passive targeting exploits the so called enhanced permeation and retention (EPR) effect; according to EPR, cancer exhibits an enhanced permeation due to the hyperpermeable vasculature and an enhanced retention because of the ineffective lymphatic drainage. Although EPR concept seems to be quite well-assessed in literature, its effectiveness is still debated since it is well-documented for small animal models but human clinical data are less clear (Danhier, 2016).

Active targeting implies the functionalization of nanoparticle surface with suitable ligands (small molecules, proteins, carbohydrates, etc.), which can interact in a specific way with receptors that are overexpressed in diseased organs, tissues and cells (Bertrand et al., 2014). Since PLA has no reactive side groups, functionalization needs the synthesis of polymer chains with end groups that can be activated for further conjugation. In this regard, two strategies can be identified; pre-conjugation, where conjugated chains are obtained and subsequently assembled in nanoparticles with a suitable technique. This approach can be used for small ligands and peptides, while it is not suitable for proteins, since they can affect self-assembling process and conjugation needs organic solvents that can influence the secondary structure. Pre-conjugation allows introducing multiple ligands with one-step formulation procedure and a good control of particle properties. Post-conjugation involves the functionalization of preformed nanoparticles; this strategy is suitable for both small and big ligands (proteins, antibodies).

Notably, functionalization can be achieved also through the physical (that is, non-covalent) adsorption of targeting moieties on nanoparticle surface (Bertrand et al., 2014).

Summarizing, Dawidczyk et al. (2014) proposed general guidelines for the design of nanoparticles as carriers of active compounds, as shown in **Table 9**.

In the following paragraphs, some relevant examples from scientific literature are reported concerning PLA-based nanoparticles for drug delivery and imaging purposes. Given the extent of the topic, the following discussion does not claim to be exhaustive, but aims at presenting some opportunities in the field.

TABLE 9 | Design criteria for nanoparticles for drug delivery purposes (Dawidczyk et al., 2014).

Function	Design requirements	Possible strategies
Circulation	• Stable under flow at 37°C	• Avoid binding with components of blood • Neutral or slightly negative zeta potential
Distribution	• Minimize tissue (peripheral) volume • Minimize binding to endothelium • Minimize paracellular transport	
Elimination	• Minimize opsonization • Minimize recognition by phagocytic cells • Maximize circulation time • Minimize rapid clearance by the kidneys	• Stealth coating • diameter > 8 mm to avoid rapid clearance in kidneys
Tumor accumulation	• Maximize extravasation across tumor vasculature	• Diameter < 200 nm for transport across leaky vasculature through EPR • Maintain high plasma concentration • Enhance EPR effect
Tumor cell uptake	• Maximize binding/uptake by tumor cells • Trafficking to cellular compartment	• Active or passive drug release at tumor site • Maximize cell death/particle • Maximize dose/particle • Maximize endosomal escape for particles taken up by endocytosis

Nanoparticles for Drug Delivery

Shalgunov et al. (2017) systematically investigated the effect of PEG coverage, injected dose and release kinetics on the performance of PLA-PEG nanoparticles loaded with vincristine (an anticancer active compound), determining their impact on pharmacokinetics and biodistribution in *in vivo* animal model.

Pavot et al. (2013) synthesized PLA nanoparticles containing Nod1 and Nod2 receptors ligand; the aim is to induce a systemic immune response to improve the efficacy of vaccine delivery applications. Experimental outcomes showed promising results.

Zhou et al. (2018) developed nanoparticles based on hydroxyehyl starch-polylactide (HES-PLA) polymer, where they loaded two active compounds: doxorubicin and the TGF-β inhibitor LY2157299. This strategy involving combined delivery aims at suppressing both tumor growth and metastasis.

Medel et al. (2017) developed PLA-PEG nanoparticles loaded with anticancer drugs curcumin and bortezomib. These active compounds are highly hydrophobic and show synergistic effects; in addition, they can form a covalent complex stable at physiological pH but labile at midly acidic pH (such as cancer microenvironment). The use of nanoparticles improved the

cytotoxicity provided by curcumin-bortezomib if compared to free, not-encapsulated drugs.

Raudszus et al. (2018) synthesized PLA nanoparticles using a newly developed stabilizer, a vinyl sulphone-modified poly(vinyl alcohol) (VS-PVA) derivative. By virtue of its enhanced reactivity, VS-PVA derivative allowed an easy functionalization of particle surface with targeting moieties such as Ovalbumin, Apolipoprotein E (ApoE), and Penetratin. In particular, ApoE and Penetratin functionalized particles exhibited a higher cellular uptake, associated to a specific interactions with cellular receptors.

Zhu et al. (2016) developed nanoparticles made of D-α-tocopherol polyethylene glycol succinate-poly(lactide) (TPGS-PLA) loaded with docetaxel, an anticancer compound. Nanoparticles were coated with polydopamine and functionalized with glucosamine in order to enhance cellular uptake in the liver through ligand-mediated endocytosis.

Zhang et al. (2016) synthesized PLA-PEG nanoparticles loaded with paclitaxel and functionalized with EGFP-EGF1 covalently bound to PEG brushes. *In vivo* experiments showed that such particles are able to target multiple types of key cells in tumor tissues.

Turino et al. (2017) developed paclitaxed-loaded PLGA nanoparticles functionalized with ferritin. Functionalization was possible thanks to the use of PLGA-NHS polymer, where one end group is constituted by succinimidyl ester, which reacts with protein amine groups. Nanoparticles were also loaded with a guanidinium-based (Gd-DOTAMA) agent for magnetic resonance imaging (MRI). Experimental studies *in vitro* proved the targeting capability using breast cancer cell lines.

Gourdon et al. (2017) investigated PLA-PEG nanoparticles loaded with acyclovir (antiviral drug) and functionalized with single amino acids or short peptides in order to target PepT1 intestinal transporter. Functionalization was performed by covalently linking amino acids to PEG chains with an amine end group. Valine-functionalized nanoparticles showed the best outcomes in terms of targeting.

Cui and Zhu (2016) prepared doxorubicin-loaded PLA nanoparticles, covered with polyethylene imine (PEI) that was functionalized with Herceptin, a monoclonal antibody, which targets the human epidermal growth factor receptor 2 (HER2), overexpressed in breast cancer. Functionalization improved cellular uptake and nanoparticles proved to enhance the therapeutic effect of the drug reducing side effects.

Xiong et al. (2016) synthesized a block copolymer containing folic acid, pluronic (a polyethylene oxide-poly propylene oxide-polyethylene oxide block copolymer) and lactic acid. Resulting product was employed to produce paclitaxel-loaded nanoparticles. Experimental data proved that folate included in polymer chain could be used for active targeting with folate receptor expressed in ovarian cancer cells.

Coolen et al. (2019) synthesized PLA nanoparticles, which exhibit a negative charge on the surface due to lactic acid resulting from degradation. In order to non-covalently bind mRNA on the surface (they are both negatively charged), the authors firstly created a non-covalent complex between mRNA and cationic cell penetrating peptides (CPPs), which could be adsorbed on PLA surface.

Tang et al. (2018) obtained PLA-PEG micelles loaded with paclitaxel, an anticancer drug. They functionalized the surface with a CPP linked to PEG polymer with a pH-sensitive sequence composed of histidine and glutamic acid. At physiological pH, CPP, and the linker are strongly bound through electrostatic interactions between glutamic acid (in the linker) and arginine (in the CPP). The mildly acidic pH of the tumor microenvironment leads to the protonation of some histidine residues of the linker, which interfere with the linker/CPP electrostatic interactions. The immediate consequence is an increased exposure of the CPP in the cancer and thus a more effective targeting, which could be achieved with stimuli responsive device (pH, in this case).

Song et al. (2016) developed PLA-PEG nanoparticles loaded with AZD2811, a hydrophobic anticancer active compound. The authors extensively tested the hydrophobic ion pairing (HIP) approach in order to maximize drug loading and encapsulation efficiency. They evaluated different hydrophobic counterions (such as oleic acid, cholic acid, and so on) that increase AZD2811 hydrophobicity through the formation of ion pairs. Different counterions led to different release kinetics, which allowed obtaining a library of particle formulations.

Medina et al. (2019) synthesized PLA-PEG and PLGA nanoparticles, blended with low molecular weight PLA and PCL and lipid-conjugate PEG, respectively. They observed that this blending improved the encapsulation efficiency of adapalene (a topical retinoid). Blending had a moderate impact on release kinetics.

Discussed examples are summarized in **Table 10**.

Nanoparticles for Imaging

Banerjee et al. (2017) radiolabeled with ^{111}In-containing moieties and IRDye680RD PLA-PEG nanoparticles functionalized with prostate-specific membrane antigen (PSMA) moieties. *In vivo* and *ex vivo* imaging allowed determining the distribution of both PSMA-functionalized and not-functionalized particles in the tumor. Xiong et al. (2017) treated Fe_3O_4 iron oxide nanoparticles with PLA-PEG chains for MRI purposes. End groups of PLA-PEG chains where functionalized with D-glucosamine as targeting agent. *In vivo* MRI in tumor-bearing mice confirmed the ability of the nanoparticles to target the cancer and their potential as contrast agents.

Dos Santos et al. (2017) synthesized PLA nanoparticles loaded with betamethasone and dexamethasone (antiflammatory drugs) and labeled with technetium-99m. Experiments showed that betamethasone loaded particles were able to accumulate in the inflammation site in an *in vivo* model of *S. aureus* infection.

Kerr et al. (2017) synthesized dye-PLLA-conjugates using Difluoroboron β-Diketonates as dyes, which were subsequently employed to obtain nanoparticles (average diameter 55 nm) for imaging purposes. In order to improve stability, the authors added PDLA-PEG to promote stereocomplexation. *In vivo* experiments proved the ability of such particles to target tumors.

TABLE 10 | Summary of discussed examples of nanoparticles for drug delivery.

System	Preparation method	Average size [nm]	Loaded compounds	Main features	*In vivo*	References
PLA-PEG	Single emulsion	100	Vincristine	Systematic investigation of PEG coverage, release kinetics and injected dose	Yes	Shalgunov et al., 2017
PLA	Nanoprecipitation	200	Nod receptor ligands	Induced systemic immune response for vaccine delivery	Yes	Pavot et al., 2013
HES-PLA	Single emulsion	155	Doxorubicin and TGF-β inhibitor LY2157299	Co-delivery of two active compounds	Yes	Zhou et al., 2018
PLA-PEG	Nanoprecipitation	100–150	Curcumin, curcumin and bortezomib	Synergistic effects with co-delivery	No	Medel et al., 2017
PLA-VS-PVA	Double emulsion	220	Lumogen Red (dye)	New stabilizer for easier surface functionalization	No	Raudszus et al., 2018
TPGS-PLA	Single emulsion	200	Docetaxel	Nanoparticles coated with polydopamine and functionalized with galactosamine	Yes	Zhu et al., 2016
PLA-PEG	Single emulsion	100–120	Paclitaxel	Surface functionalization with EGFP-EGF1 protein to enhance active targeting	Yes	Zhang et al., 2016
PLGA-PEG	Single emulsion	150	Paclitaxel	Surface functionalization with ferritin for targeting, Gd-DOTAMA as imaging agent	No	Turino et al., 2017
PLA-PEG	Nanoprecipitation	30–50	Acyclovir	Surface functionalization with amino acids	Yes	Gourdon et al., 2017
PLA-PEI	Single emulsion	140–220	Doxorubicin hydrochloride	Surface functionalization with antibodies	Yes	Cui and Zhu, 2016
FA-Pluronic-PLA	Dialysis	190–260	Paclitaxel	Synthesis of block copolymer with folate groups that target folate receptors	Yes	Xiong et al., 2016
PLA	Nanoprecipitation	200–240	mRNA	mRNA adsorbed on surface through electrostatic interactions	No	Coolen et al., 2019
PLA-PEG micelles	Thin-film hydration	25	Paclitaxel	pH-responsive system	Yes	Tang et al., 2018
PLA-PEG	Single emulsion	90–130	AZD2811	Development of a formulation library with different release kinetics	Yes	Song et al., 2016
PLA-PEG PLGA	Single emulsion	115–130	Adapalene	Blending with short chains of aliphatic polyesters or lipid improves encapsulation	Yes	Medina et al., 2019

TOXICITY OF POLYLACTIC-BASED NANOPARTICLES

Nanoparticles behavior mainly depends on size, shape, morphology, and surface charge; this holds also for their unwanted side effects. Entering into cells, nanoparticles can provide cytotoxic effects, leading to the disruption of cell membranes or cytosolic components or to programmed cell death (apoptosis). Typical adverse effects are oxidative stress [an excess of reactive oxygen species (ROS) or reactive nitrogen species (RNS) usually neutralized by cells], apoptosis, cytokine activation (due to inflammatory response), loss of mitochondrial, and lysosomal stability. They can also be a source of genotoxic effects, damaging DNA (Ganguly et al., 2018).

In addition, nanoparticles may induce haemolysis (disruption of red blood cells) or blood coagulation (causing thrombosis) (Dobrovolskaia and McNeil, 2007). PLA-based nanoparticles may provide additional side effects through their degradation products.

Toxicity assessment *in vitro* in usually performed by exposing cells to given dose of the potential toxic agent and measuring, e.g., cell viability and proliferation, mitochondrial activity, ROS production, cytokine activation through suitable assays.

In vivo experiments aim at assessing the pharmacokinetics of nanoparticles, their distribution in the organ and their clearance.

While *in vitro* and *in vivo* testing are usually performed when a new formulation is discussed (*vide* supra) up to author's best knowledge, there are few systematic

studies concerning toxicity of PLA-based nanoparticles (Da Luz et al., 2017; Da Silva et al., 2019).

Singh and Ramarao (2013), e.g., observed that PLA nanoparticles *in vitro* did not provide detrimental effect concerning RNS, cytokine activation, mitochondrial or lysosomal integrity. At high concentration, they stimulated ROS production and inflammation; this was linked to the accumulation of polymer degradation products in the cell.

There is an additional intrinsic risk of toxic responses when nanoparticles are used and injected in the blood stream. Nanoparticles interact with the components present in the environment (proteins, carbohydrates, small molecules, etc.) through their surface. The driving force leading to the formation of this nano-bio interface are already known in scientific literature and are basically due to electrostatic and Van der Waals interactions as well as hydrophobic and depletion effects (Nel et al., 2009). One of the main outcomes from this network of interactions is the attainment of a layer of adsorbed proteins on nanoparticle surface, usually referred as protein corona (Cedervall et al., 2007). Because of the interactions with the surface, adsorbed proteins can be subjected to relevant structural changes, which can lead to aggregation and fibrillation, loss of enzymatic activity, or the exposure of new antigenic epitopes. Such side effects emerge from the specific protein-surface interactions: while, as mentioned, driving forces are known, they depend on many factors (materials, pH, ionic strength, etc.) and are challenging to be determined *a priori*.

In vitro experiments allow a rapid and cost-effective evaluation of toxicity if compared to *in vivo* experiments with animal models (and the related ethical concerns). However, the possible lack of correlation between *in vitro-in vivo* tests, the challenging extrapolation of animal data to human patients and the shortage of harmonized protocols are still obstacles for extensive clinical trials (Dobrovolskaia and McNeil, 2013).

CONCLUSIONS

PLA—based polymers have been extensively studied in literature and are currently an established reality in the biomedical field, thanks to their interesting properties. This led to a growing interest also in the nanomedicine field for the synthesis of nanoparticles for drug delivery and imaging purposes. Nanoparticles showed a great potential as nanocarriers to deliver poorly soluble drugs, proteins, and genes targeting the tumor and releasing the active compound at the desired rate, enhancing in the therapeutic effect.

The new perspective introduced by nanoparticles also brings new sources of toxicity connected with cytotoxicity and haemolysis; also protein corona can provide undesired side effects that are not easily predictable *a priori*.

Nowadays, an extensive clinical application of nanoparticles is still hindered by an exhaustive assessment of potential toxic effects, which does not allow nanoparticles unleashing their full potential.

AUTHOR CONTRIBUTIONS

TC performed literature research and wrote the first draft of the paper. All authors discussed and approved the contents of the manuscript and contributed to its final version by reading and editing.

FUNDING

This study is part of the GoNanoBioMat project and has received funding from the Horizon 2020 framework program of the European Union, ProSafe Joint Transnational Call 2016, from the CTI (1.1.2018 Innosuisse) under grant agreement number 19267.1 PFNM-NM and from FCT Foundation for Science and Technology under the project PROSAFE/0001/2016.

REFERENCES

Alexis, F. (2005). Factors affecting the degradation and drug-release mechanism of poly(lactic acid) and poly[(lactic acid)-co-(glycolic acid)]. *Polym. Int.* 54, 36–46. doi: 10.1002/pi.1697

Aline, F., Brand, D., Pierre, J., Roingeard, P., Severine, M., Verrier, B., et al. (2009). Dendritic cells loaded with HIV-1 p24 proteins adsorbed on surfactant-free anionic PLA nanoparticles induce enhanced cellular immune responses against HIV-1 after vaccination. *Vaccine* 27, 5284–5291. doi: 10.1016/j.vaccine.2009.05.028

Armentano, I., Gigli, M., Morena, F., Argentati, C., Torre, L., and Martino, S. (2018). Recent advances in nanocomposites based on aliphatic polyesters: design, synthesis, and applications in regenerative medicine. *Appl. Sci.* 8:1452. doi: 10.3390/app8091452

Banerjee, S. R., Foss, C. A., Horhota, A., Pullambhatla, M., McDonnell, K., Zale, S., et al. (2017). In-111- and IRDye800CW-labeled PLA-PEG nanoparticle for imaging prostate-specific membrane antigen-expressing tissues. *Biomacromolecules* 18, 201–209. doi: 10.1021/acs.biomac.6b01485

Bertrand, N., Wu, J., Xu, X. Y., Kamaly, N., and Farokhzad, O. C. (2014). Cancer nanotechnology: the impact of passive and active targeting in the era of modern cancer biology. *Adv. Drug Deliv. Rev.* 66, 2–25. doi: 10.1016/j.addr.2013.11.009

Betancourt, T., Byrne, J. D., Sunaryo, N., Crowder, S. W., Kadapakkam, M., Patel, S., et al. (2009). PEGylation strategies for active targeting of PLA/PLGA nanoparticles. *J. Biomed. Mater. Res. A* 91a, 263–276. doi: 10.1002/jbm.a.32247

Bilati, U., Allemann, E., and Doelker, E. (2005). Nanoprecipitation versus emulsion-based techniques for the encapsulation of proteins into biodegradable nanoparticles and process-related stability issues. *AAPS PharmSciTech.* 6, E594–E604. doi: 10.1208/pt060474

Blanco, E., Shen, H., and Ferrari, M. (2015). Principles of nanoparticle design for overcoming biological barriers to drug delivery. *Nat. Biotechnol.* 33, 941–951. doi: 10.1038/nbt.3330

Carrasco, F., Pages, P., Gamez-Perez, J., Santana, O. O., and Maspoch, M. L. (2010). Processing of poly(lactic acid): characterization of chemical structure, thermal stability and mechanical properties. *Polym. Degrad. Stab.* 95, 116–125. doi: 10.1016/j.polymdegradstab.2009.11.045

Casalini, T. (2017). Bioresorbability of polymers: chemistry, mechanisms, and modeling. *Bioresor. Polymers Biomed. Appl.* 120, 65–83. doi: 10.1016/B978-0-08-100262-9.00003-3

Cedervall, T., Lynch, I., Lindman, S., Berggard, T., Thulin, E., Nilsson, H., et al. (2007). Understanding the nanoparticle-protein corona using methods to quantify exchange rates and affinities of proteins for nanoparticles. *Proc. Natl. Acad. Sci. U.S.A.* 104, 2050–2055. doi: 10.1073/pnas.0608582104

Cheng, Q. Y., Feng, J., Chen, J. M., Zhu, X., and Li, F. Z. (2008). Brain transport of neurotoxin-I with PLA nanoparticles through intranasal

administration in rats: a microdialysis study. *Biopharm. Drug Dispos.* 29, 431–439. doi: 10.1002/bdd.621

Chorny, M., Fishbein, I., Danenberg, H. D., and Golomb, G. (2002). Lipophilic drug loaded nanospheres prepared by nanoprecipitation: effect of formulation variables on size, drug recovery and release kinetics. *J. Controlled Release* 83, 389–400. doi: 10.1016/S0168-3659(02)00211-0

Coolen, A. L., Lacroix, C., Mercier-Gouy, P., Delaune, E., Monge, C., Exposito, J. Y., et al. (2019). Poly(lactic acid) nanoparticles and cell-penetrating peptide potentiate mRNA-based vaccine expression in dendritic cells triggering their activation. *Biomaterials* 195, 23–37. doi: 10.1016/j.biomaterials.2018.12.019

Corneillie, S., and Smet, M. (2015). PLA architectures: the role of branching. *Polym. Chem.* 6, 850–867. doi: 10.1039/C4PY01572J

Crucho, C. I. C., and Barros, M. T. (2017). Polymeric nanoparticles: a study on the preparation variables and characterization methods. *Mater. Sci. Eng. C Mater. Biol. Appl.* 80, 771–784. doi: 10.1016/j.msec.2017.06.004

Cui, N., and Zhu, S. H. (2016). Monoclonal antibody-tagged polyethylenimine (PEI)/poly(lactide) (PLA) nanoparticles for the enhanced delivery of doxorubicin in HER-positive breast cancers. *RSC Adv.* 6, 79822–79829. doi: 10.1039/C6RA12616B

Da Luz, C. M., Boyles, M. S. P., Falagan-Lotsch, P., Pereira, M. R., Tutumi, H. R., Santos, E. D., et al. (2017). Poly-lactic acid nanoparticles (PLA-NP) promote physiological modifications in lung epithelial cells and are internalized by clathrin-coated pits and lipid rafts. *J. Nanobiotechnol.* 15:11. doi: 10.1186/s12951-016-0238-1

Da Silva, J., Jesus, S., Bernardi, N., Coleco, M., and Borges, O. (2019). Poly(D,L-Lactic Acid) nanoparticle size reduction increases its immunotoxicity. *Front. Bioeng. Biotechnol.* 7:137. doi: 10.3389/fbioe.2019.00137

Dalmolin, L. F., Khalil, N. M., and Mainardes, R. M. (2016). Delivery of vanillin by poly(lactic-acid) nanoparticles: development, characterization and *in vitro* evaluation of antioxidant activity. *Mater. Sci. Eng. C Mater. Biol. Appl.* 62, 1–8. doi: 10.1016/j.msec.2016.01.031

Danhier, F. (2016). To exploit the tumor microenvironment: since the EPR effect fails in the clinic, what is the future of nanomedicine? *J. Controlled Release* 244, 108–121. doi: 10.1016/j.jconrel.2016.11.015

Dawidczyk, C. M., Kim, C., Park, J. H., Russell, L. M., Lee, K. H., Pomper, M. G., et al. (2014). State-of-the-art in design rules for drug delivery platforms: lessons learned from FDA-approved nanomedicines. *J. Controlled Release* 187, 133–144. doi: 10.1016/j.jconrel.2014.05.036

Dobrovolskaia, M. A., and McNeil, S. E. (2007). Immunological properties of engineered nanomaterials. *Nat. Nanotechnol.* 2, 469–478. doi: 10.1038/nnano.2007.223

Dobrovolskaia, M. A., and McNeil, S. E. (2013). Understanding the correlation between *in vitro* and *in vivo* immunotoxicity tests for nanomedicines. *J. Controlled Release* 172, 456–466. doi: 10.1016/j.jconrel.2013.05.025

Dos Santos, S. N., Dos Reis, S. R. R., Pinto, S. R., Cerqueira-Coutinho, C., Nigro, F., Barja-Fidalgo, T. C., et al. and Santos-Oliveira, R. (2017). Anti-inflammatory/infection PLA nanoparticles labeled with technetium 99m for *in vivo* imaging. *J. Nanoparticle Res.* 19:345. doi: 10.1007/s11051-017-4037-x

Fan, X. S., Wang, M. A., Yuan, D., and He, C. B. (2013). Amphiphilic conetworks and gels physically cross-linked via stereocomplexation of polylactide. *Langmuir* 29, 14307–14313. doi: 10.1021/la403432y

Farah, S., Anderson, D. G., and Langer, R. (2016). Physical and mechanical properties of PLA, and their functions in widespread applications - A comprehensive review. *Adv. Drug Deliv. Rev.* 107, 367–392. doi: 10.1016/j.addr.2016.06.012

Feng, X. Y., Gao, X. L., Kang, T., Jiang, D., Yao, J. H., Jing, Y. X., et al. (2015). Mammary-derived growth inhibitor targeting peptide-modified PEG-PLA nanoparticles for enhanced targeted glioblastoma therapy. *Bioconjug. Chem.* 26, 1850–1861. doi: 10.1021/acs.bioconjchem.5b00379

Freitas, M. N., and Marchetti, J. M. (2005). Nimesulide PLA microspheres as a potential sustained release system for the treatment of inflammatory diseases. *Int. J. Pharm.* 295, 201–211. doi: 10.1016/j.ijpharm.2005.03.003

Ganguly, P., Breen, A., and Pillai, S. C. (2018). Toxicity of nanomaterials: exposure, pathways, assessment, and recent advances. *ACS Biomater. Sci. Eng.* 4, 2237–2275. doi: 10.1021/acsbiomaterials.8b00068

Gao, H., Wang, Y. N., Fan, Y. G., and Ma, J. B. (2005). Synthesis of a biodegradable tadpole-shaped polymer via the coupling reaction of polylactide onto mono(6-(2-aminoethyl)amino-6-deoxy)-beta-cyclodextrin and its properties as the new carrier of protein delivery system. *J. Controlled Release* 107, 158–173. doi: 10.1016/j.jconrel.2005.06.010

Garlotta, D. (2001). A literature review of poly(lactic acid). *J. Polym. Environ.* 9, 63–84. doi: 10.1023/A:1020200822435

George, A., Shah, P. A., and Shrivastav, P. S. (2019). Natural biodegradable polymers based nano-formulations for drug delivery: a review. *Int. J. Pharm.* 561, 244–264. doi: 10.1016/j.ijpharm.2019.03.011

Gourdon, B., Chemin, C., Moreau, A., Arnauld, T., Baumy, P., Cisternino, S., et al. (2017). Functionalized PLA-PEG nanoparticles targeting intestinal transporter PepT1 for oral delivery of acyclovir. *Int. J. Pharm.* 529, 357–370. doi: 10.1016/j.ijpharm.2017.07.024

Hamad, K., Kaseem, M., Ayyoob, M., Joo, J., and Deri, F. (2018). Polylactic acid blends: the future of green, light and tough. *Prog. Polym. Sci.* 85, 83–127. doi: 10.1016/j.progpolymsci.2018.07.001

Ishihara, T., Izumo, N., Higaki, M., Shimada, E., Hagi, T., Mine, L., et al. (2005). Role of zinc in formulation of PLGA/PLA nanoparticles encapsulating betamethasone phosphate and its release profile. *J. Controlled Release* 105, 68–76. doi: 10.1016/j.jconrel.2005.02.026

Jing, Y. H., Quan, C. Y., Liu, B., Jiang, Q., and Zhang, C. (2016). A mini review on the functional biomaterials based on poly (lactic acid) stereocomplex. *Polymer Rev.* 56, 262–286. doi: 10.1080/15583724.2015.1111380

Kaialy, W., and Al Shafiee, M. (2016). Recent advances in the engineering of nanosized active pharmaceutical ingredients: promises and challenges. *Adv. Colloid Interface Sci.* 228, 71–91. doi: 10.1016/j.cis.2015.11.010

Kerr, C., Derosa, C. A., Daly, M. L., Zhang, H. T., Palmer, G. M., and Fraser, C. L. (2017). Luminescent difluoroboron beta-diketonate PLA-PEG nanoparticle. *Biomacromolecules* 18, 551–561. doi: 10.1021/acs.biomac.6b01708

Kim, K. T., Lee, J. Y., Kim, D. D., Yoon, I. S., and Cho, H. J. (2019). Recent progress in the development of poly(lactic-co-glycolic acid)-based nanostructures for cancer imaging and therapy. *Pharmaceutics* 11:E280. doi: 10.3390/pharmaceutics11060280

Lee, B. K., Yun, Y., and Park, K. (2016). PLA micro- and nano-particles. *Adv. Drug Deliv. Rev.* 107, 176–191. doi: 10.1016/j.addr.2016.05.020

Legrand, P., Lesieur, S., Bochot, A., Gref, R., Raatjes, W., Barratt, G., et al. (2007). Influence of polymer behaviour in organic solution on the production of polylactide nanoparticles by nanoprecipitation. *Int. J. Pharm.* 344, 33–43. doi: 10.1016/j.ijpharm.2007.05.054

Leo, E., Brina, B., Forni, F., and Vandelli, M. A. (2004). *In vitro* evaluation of PLA nanoparticles containing a lipophilic rug in water-soluble or insoluble form. *Int. J. Pharm.* 278, 133–141. doi: 10.1016/j.ijpharm.2004.03.002

Leroux, J. C., Allemann, E., Dejaeghere, F., Doelker, E., and Gurny, R. (1996). Biodegradable nanoparticles - from sustained release formulations to improved site specific drug delivery. *J. Controlled Release* 39, 339–350. doi: 10.1016/0168-3659(95)00164-6

Liu, M., Zhou, Z. M., Wang, X. F., Xu, J., Yang, K., Cui, Q., et al. (2007). Formation of poly(L,D-lactide) spheres with controlled size by direct dialysis. *Polymer* 48, 5767–5779. doi: 10.1016/j.polymer.2007.07.053

Lo, C. L., Lin, K. M., and Hsiue, G. H. (2005). Preparation and characterization of intelligent core-shell nanoparticles based on poly(D,L-lactide)-g-poly(N-isopropyl-acrylamide-co-methacrylic acid). *J. Controlled Release* 104, 477–488. doi: 10.1016/j.jconrel.2005.03.004

Medel, S., Syrova, Z., Kovacik, L., Hrdy, J., Hornacek, M., Jager, E., et al. (2017). Curcumin-bortezomib loaded polymeric nanoparticles for synergistic cancer therapy. *Eur. Polym. J.* 93, 116–131. doi: 10.1016/j.eurpolymj.2017.05.036

Medina, D. X., Chung, E. P., Bowser, R., and Sirianni, R. W. (2019). Lipid and polymer blended polyester nanoparticles loaded with adapalene for activation of retinoid signaling in the CNS following intravenous administration. *J. Drug Deliv. Sci. Technol.* 52, 927–933. doi: 10.1016/j.jddst.2019.04.013

Michalski, A., Brzezinski, M., Lapienis, G., and Biela, T. (2019). Star-shaped and branched polylactides: synthesis, characterization, and properties. *Prog. Polym. Sci.* 89, 159–212. doi: 10.1016/j.progpolymsci.2018.10.004

Murariu, M., and Dubois, P. (2016). PLA composites: from production to properties. *Adv. Drug Deliv. Rev.* 107, 17–46. doi: 10.1016/j.addr.2016.04.003

Nagahama, K., Mori, Y., Ohya, Y., and Ouchi, T. (2007). Biodegradable nanogel formation of polylactide-grafted dextran copolymer in dilute aqueous solution and enhancement of its stability by stereocomplexation. *Biomacromolecules* 8, 2135–2141. doi: 10.1021/bm070206t

Nel, A. E., Madler, L., Velegol, D., Xia, T., Hoek, E. M. V., Somasundaran, P., et al. (2009). Understanding biophysicochemical interactions at the nano-bio interface. *Nat. Mater.* 8, 543–557. doi: 10.1038/nmat2442

Nguyen, C. A., Allemann, E., Schwach, G., Doelker, E., and Gurny, R. (2003). Synthesis of a novel fluorescent poly(D,L-lactide) end-capped with 1-pyrenebutanol used for the preparation of nanoparticles. *Eur. J. Pharm. Sci.* 20, 217–222. doi: 10.1016/S0928-0987(03)00196-9

Partikel, K., Korte, R., Stein, N. C., Mulac, D., Herrmann, F. C., Humpf, H. U., et al. (2019). Effect of nanoparticle size and PEGylation on the protein corona of PLGA nanoparticles. *Eur. J. Pharm. Biopharm.* 141, 70–80. doi: 10.1016/j.ejpb.2019.05.006

Pavot, V., Rochereau, N., Primard, C., Genin, C., Perouzel, E., Lioux, T., et al. (2013). Encapsulation of Nod1 and Nod2 receptor ligands into poly(lactic acid) nanoparticles potentiates their immune properties. *J. Controlled Release* 167, 60–67. doi: 10.1016/j.jconrel.2013.01.015

Peltonen, L., Aitta, J., Hyvonen, S., Karjalainen, M., and Hirvonen, J. (2004). Improved entrapment efficiency of hydrophilic drug substance during nanoprecipitation of poly(l)lactide nanoparticles. *AAPS Pharmscitech.* 5:E16. doi: 10.1007/BF02830584

Pinon-Segundo, E., Ganem-Quintanar, A., Alonso-Perez, V., and Quintanar-Guerrero, D. (2005). Preparation and characterization of triclosan nanoparticles for periodontal treatment. *Int. J. Pharm.* 294, 217–232. doi: 10.1016/j.ijpharm.2004.11.010

Raudszus, B., Mulac, D., and Langer, K. (2018). A new preparation strategy for surface modified PLA nanoparticles to enhance uptake by endothelial cells. *Int. J. Pharm.* 536, 211–221. doi: 10.1016/j.ijpharm.2017.11.047

Rodenas-Rochina, J., Vidaurre, A., Cortazar, I. C., and Lebourg, M. (2015). Effects of hydroxyapatite filler on long-term hydrolytic degradation of PLLA/PCL porous scaffolds. *Polym. Degrad. Stab.* 119, 121–131. doi: 10.1016/j.polymdegradstab.2015.04.015

Rodriguez, P. L., Harada, T., Christian, D. A., Pantano, D. A., Tsai, R. K., and Discher, D. E. (2013). Minimal "Self" peptides that inhibit phagocytic clearance and enhance delivery of nanoparticles. *Science* 339, 971–975. doi: 10.1126/science.1229568

Sahay, G., Alakhova, D. Y., and Kabanov, A. V. (2010). Endocytosis of nanomedicines. *J. Controlled Release* 145, 182–195. doi: 10.1016/j.jconrel.2010.01.036

Saini, P., Arora, M., and Kumar, M. N. V. R. (2016). Poly(lactic acid) blends in biomedical applications. *Adv. Drug Deliv. Rev.* 107, 47–59. doi: 10.1016/j.addr.2016.06.014

Shalgunov, V., Zaytseva-Zotova, D., Zintchenko, A., Levada, T., Shilov, Y., Andreyev, D., et al. (2017). Comprehensive study of the drug delivery properties of poly(L-lactide)-poly (ethylene glycol) nanoparticles in rats and tumor-bearing mice. *J. Controlled Release* 261, 31–42. doi: 10.1016/j.jconrel.2017.06.006

Sheikh, Z., Najeeb, S., Khurshid, Z., Verma, V., Rashid, H., and Glogauer, M. (2015). Biodegradable materials for bone repair and tissue engineering applications. *Materials* 8, 5744–5794. doi: 10.3390/ma8095273

Sheng, Y., Yuan, Y., Liu, C. S., Tao, X. Y., Shan, X. Q., and Xu, F. (2009). *In vitro* macrophage uptake and *in vivo* biodistribution of PLA-PEG nanoparticles loaded with hemoglobin as blood substitutes: effect of PEG content. *J. Mater. Sci. Mater. Med.* 20, 1881–1891. doi: 10.1007/s10856-009-3746-9

Singh, R. P., and Ramarao, P. (2013). Accumulated polymer degradation products as effector molecules in cytotoxicity of polymeric nanoparticles. *Toxicol. Sci.* 136, 131–143. doi: 10.1093/toxsci/kft179

Song, Y. H., Shin, E., Wang, H., Nolan, J., Low, S., Parsons, D., et al. (2016). A novel *in situ* hydrophobic ion paring (HIP) formulation strategy for clinical product selection of a nanoparticle drug delivery system. *J. Controlled Release* 229, 106–119. doi: 10.1016/j.jconrel.2016.03.026

Storti, G., and Lattuada, M. (2017). Synthesis of bioresorbable polymers for medical applications. *Bioresor. Polymers Biomed. Appl.* 120, 153–179. doi: 10.1016/B978-0-08-100262-9.00008-2

Sveinbjornsson, B. R., Miyake, G. M., El-Batta, A., and Grubbs, R. H. (2014). Stereocomplex formation of densely grafted brush polymers. *ACS Macro Lett.* 3, 26–29. doi: 10.1021/mz400568j

Tang, B. Q., Zaro, J. L., Shen, Y., Chen, Q., Yu, Y. L., Sun, P. P., et al. (2018). Acid-sensitive hybrid polymeric micelles containing a reversibly activatable cell-penetrating peptide for tumor-specific cytoplasm targeting. *J. Controlled Release* 279, 147–156. doi: 10.1016/j.jconrel.2018.04.016

Tsuji, H. (2016). Poly(lactic acid) stereocomplexes: a decade of progress. *Adv. Drug Deliv. Rev.* 107, 97–135. doi: 10.1016/j.addr.2016.04.017

Turino, L. N., Ruggiero, M. R., Stefania, R., Cutrin, J. C., Aime, S., and Crich, S. G. (2017). Ferritin decorated PLGA/paclitaxel loaded nanoparticles endowed with an enhanced toxicity toward MCF-7 breast tumor cells. *Bioconjug. Chem.* 28, 1283–1290. doi: 10.1021/acs.bioconjchem.7b00096

Tyler, B., Gullotti, D., Mangraviti, A., Utsuki, T., and Brem, H. (2016). Polylactic acid (PLA) controlled delivery carriers for biomedical applications. *Adv. Drug Deliv. Rev.* 107, 163–175. doi: 10.1016/j.addr.2016.06.018

Van De Velde, K., and Kiekens, P. (2002). Biopolymers: overview of several properties and consequences on their applications. *Polym. Test.* 21, 433–442. doi: 10.1016/S0142-9418(01)00107-6

Von Burkersroda, F., Schedl, L., and Gopferich, A. (2002). Why degradable polymers undergo surface erosion or bulk erosion. *Biomaterials* 23, 4221–4231. doi: 10.1016/S0142-9612(02)00170-9

Xiong, F., Hu, K., Yu, H. L., Zhou, L. J., Song, L. N., Zhang, Y., et al. (2017). A functional iron oxide nanoparticles modified with PLA-PEG-DG as tumor-targeted MRI contrast agent. *Pharm. Res.* 34, 1683–1692. doi: 10.1007/s11095-017-2165-8

Xiong, X. Y., Tao, L., Qin, X., Li, Z. L., Gong, Y. C., Li, Y. P., et al. (2016). Novel folated Pluronic/poly(lactic acid) nanoparticles for targeted delivery of paclitaxel. *RSC Adv.* 6, 52729–52738. doi: 10.1039/C6RA09271C

Zhang, B., Jiang, T., Ling, L., Cao, Z. L., Zhao, J. J., Tuo, Y. Y., et al. (2016). Enhanced antitumor activity of EGFP-EGF1-conjugated nanoparticles by a multitargeting strategy. *ACS Appl. Mater. Interfaces* 8, 8918–8927. doi: 10.1021/acsami.6b00036

Zhang, Z. P., Lee, S. H., Gan, C. W., and Feng, S. S. (2008). *In vitro* and *in vivo* investigation on PLA-TPGS nanoparticles for controlled and sustained small molecule chemotherapy. *Pharm. Res.* 25, 1925–1935. doi: 10.1007/s11095-008-9611-6

Zhou, Q., Li, Y. H., Zhu, Y. H., Yu, C., Jia, H. B., Bao, B. H., et al. (2018). Co-delivery nanoparticle to overcome metastasis promoted by insufficient chemotherapy. *J. Controlled Release* 275, 67–77. doi: 10.1016/j.jconrel.2018.02.026

Zhu, D. W., Tao, W., Zhang, H. L., Liu, G., Wang, T., Zhang, L. H., et al. (2016). Docetaxel (DTX)-loaded polydopamine-modified TPGS-PLA nanoparticles as a targeted drug delivery system for the treatment of liver cancer. *Acta Biomater.* 30, 144–154. doi: 10.1016/j.actbio.2015.11.031

Zweers, M. L. T., Engbers, G. H. M., Grijpma, D. W., and Feijen, J. (2004). *In vitro* degradation of nanoparticles prepared from polymers based on DL-lactide, glycolide and poly(ethylene oxide). *J. Controlled Release* 100, 347–356. doi: 10.1016/j.jconrel.2004.09.008

Zweers, M. L. T., Grijpma, D. W., Engbers, G. H. M., and Feijen, J. (2003). The preparation of monodisperse biodegradable polyester nanoparticles with a controlled size. *J. Biomed. Mater. Res. B Appl. Biomater.* 66b, 559–566. doi: 10.1002/jbm.b.10046

Conflict of Interest: The authors declare that the research was conducted in the absence of any commercial or financial relationships that could be construed as a potential conflict of interest.

frontiers in Bioengineering and Biotechnology

REVIEW
published: 17 October 2019
doi: 10.3389/fbioe.2019.00268

Molecular Modeling for Nanomaterial–Biology Interactions: Opportunities, Challenges, and Perspectives

Tommaso Casalini[1]*, *Vittorio Limongelli*[2,3], *Mélanie Schmutz*[4], *Claudia Som*[4], *Olivier Jordan*[5], *Peter Wick*[6], *Gerrit Borchard*[5] and *Giuseppe Perale*[1,7]

[1] Polymer Engineering Laboratory, Department of Innovative Technologies, Institute for Mechanical Engineering and Materials Technology, University of Applied Sciences and Arts of Southern Switzerland (SUPSI), Manno, Switzerland, [2] Faculty of Biomedical Sciences, Center for Computational Medicine in Cardiology, Institute of Computational Science, Università della Svizzera italiana (USI), Lugano, Switzerland, [3] Department of Pharmacy, University of Naples "Federico II", Naples, Italy, [4] Technology and Society Laboratory, Swiss Federal Laboratories for Materials Science and Technology (Empa), St. Gallen, Switzerland, [5] School of Pharmaceutical Sciences, University of Geneva, Genève, Switzerland, [6] Laboratory for Particles – Biology Interactions, Swiss Federal Laboratories for Materials Science and Technology (Empa), St. Gallen, Switzerland, [7] Ludwig Boltzmann Institute for Experimental and Clinical Traumatology, Wien, Austria

OPEN ACCESS

Edited by:
Roberto Molinaro, University of Urbino Carlo Bo, Italy

Reviewed by:
Giosuè Costa, University of Catanzaro, Italy
Isabella Romeo, University of Calabria, Italy

***Correspondence:**
Tommaso Casalini
tommaso.casalini@supsi.ch

Specialty section:
This article was submitted to Nanobiotechnology, a section of the journal Frontiers in Bioengineering and Biotechnology

Received: *09 July 2019*
Accepted: *27 September 2019*
Published: *17 October 2019*

Citation:
Casalini T, Limongelli V, Schmutz M, Som C, Jordan O, Wick P, Borchard G and Perale G (2019) Molecular Modeling for Nanomaterial–Biology Interactions: Opportunities, Challenges, and Perspectives. Front. Bioeng. Biotechnol. 7:268. doi: 10.3389/fbioe.2019.00268

Injection of nanoparticles (NP) into the bloodstream leads to the formation of a so-called "nano–bio" interface where dynamic interactions between nanoparticle surfaces and blood components take place. A common consequence is the formation of the protein corona, that is, a network of adsorbed proteins that can strongly alter the surface properties of the nanoparticle. The protein corona and the resulting structural changes experienced by adsorbed proteins can lead to substantial deviations from the expected cellular uptake as well as biological responses such as NP aggregation and NP-induced protein fibrillation, NP interference with enzymatic activity, or the exposure of new antigenic epitopes. Achieving a detailed understanding of the nano–bio interface is still challenging due to the synergistic effects of several influencing factors like pH, ionic strength, and hydrophobic effects, to name just a few. Because of the multiscale complexity of the system, modeling approaches at a molecular level represent the ideal choice for a detailed understanding of the driving forces and, in particular, the early events at the nano–bio interface. This review aims at exploring and discussing the opportunities and perspectives offered by molecular modeling in this field through selected examples from literature.

Keywords: molecular dynamics, metadynamics, molecular modeling, protein corona, coarse grain, lipid bilayer, cellular membrane

INTRODUCTION

Nanomedicine is an emerging discipline that is providing novel impulses to the biomedical field thanks to the use of nanotechnologies and the continuous development of engineered nanomaterials such as polymer-, metal- or metal oxide-based nanoparticles. Nanomaterials, by virtue of their small size (1–1000 nm, comparable to many biological molecules like proteins and viruses) open up a wide range of new opportunities and applications, for example as devices for targeted drug delivery and diagnostic purposes and as image contrast agents. However, as with every

novel technology, the potential negative side effects have to be assessed early in the development process to avoid adverse social and economic effects.

Indeed, the injection of nanomaterials into an organism leads to complex interactions between the surface of the device and the components of the medium, such as proteins, carbohydrates, fatty acids, *et cetera*. These interactions play a key role in determining not only the fate of the nanomaterial (in terms of clearance and *in vivo* biodistribution) but also the attainment of undesired side effects. The fundamental driving forces governing the formation of this nano-bio interface have already been identified and discussed (Nel et al., 2009) and include van der Waals and electrostatic interactions and hydrophobic and depletion effects. The challenge lies in the rationalization of the synergistic effects of intrinsic nanomaterial properties (chemical composition, size, surface functionalization, *et cetera*), the characteristics of the surrounding medium (pH, ionic strength, *et cetera*), and the phenomena occurring at the interface and their impact on nanomaterial behavior.

One of the most relevant consequences is the formation of the protein corona, i.e., a layer of adsorbed proteins on the NP surface (Cedervall et al., 2007a,b; Lundqvist et al., 2008; Dell'orco et al., 2010). The attainment of such a network alters the surface properties of the nanomaterial, which may cause substantial deviations from the expected behavior concerning colloidal stability, cellular uptake, clearance, distribution within the organs, and immune response.

On top of that, the formation of the protein corona can lead to changes in the protein structure and thus to undesired consequences (not easily predictable *a priori*), such as (Nel et al., 2009):

- Enhanced or hampered cellular uptake with specific kinds of cells due to the interactions of adsorbed proteins with particular receptors;
- Protein aggregation and fibrillation at the nanocarrier surface;
- Interference with enzymatic activity;
- Exposure of new antigenic epitopes.

Experimental protocols for the investigation of the protein corona are currently well-established (Walkey and Chan, 2012; Wei et al., 2014; Pederzoli et al., 2017), although they have some intrinsic limitations concerning spatial and temporal resolution; indeed, they do not allow the characterization of the early events leading to protein corona formation and do not provide a clear overview of specific nanomaterial/protein interactions or changes in protein structure.

Computational approaches at the molecular scale, such as molecular dynamics (MD) simulations, constitute the natural complement to experimental techniques. This is due to several factors, such as the accessible time and length scales (microsecond and nanometer, respectively), the full atomistic description of the system (which allows the specific protein/nanomaterial interactions to be identified) and its dynamic behavior (thus identifying conformational changes after binding), and the inclusion of environmental effects.

This review aims at exploring and discussing the opportunities and limitations of nano-bio as well as giving some perspectives on the use of molecular modeling techniques for characterizing these interactions. After giving a brief theoretical background, relevant applications of simulations at the molecular scale are discussed through selected examples from the scientific literature.

MOLECULAR MODELING—A BRIEF OVERVIEW

Molecular modeling can be seen as the sum of two components: a molecular model and a computational technique to properly characterize the behavior of the molecules.

Building a suitable molecular model, that is, how the system under investigation is rationalized and represented in the framework of a meaningful simulation, is the first fundamental step. In this framework, molecular models can be essentially divided into two categories; on the one side, full atomistic models provide the highest level of detail since all atoms (considered as the smallest constitutive units of the model) are explicitly accounted for. On the other side, coarse-grained models summarize the atomic detail by enclosing groups of atoms into beads that lump the main peculiarities (in terms of charge, polarity, *et cetera*) of the atoms that they embed. This simplification is unavoidable for complex systems whose atomistic representation would be prohibitive from a computational point of view, in terms of the system size and/or time and length scales needed to investigate the phenomena of interest. Despite the loss of detail, a coarse-grained model that retains the main features of the system is able to provide meaningful insights at a reasonable computational cost (*vide infra*). For the sake of completeness, there exist more detailed representations where electrons are the smallest constitutive units and are explicitly included. Such models are treated with quantum chemistry methods, which are not considered or discussed here since their application in the field of nanomedicine is hindered by their computational inefficiency.

In a broader sense, a molecular model also includes unavoidable simplifications that allow for the simulation of complex systems, either at a full atomistic or coarse-grained level of detail, which could not be treated otherwise. The simulation of protein adsorption on a microparticle surface, for example, is unfeasible because of the system size. Such a system is usually simplified by adopting a molecular model that involves the adsorption of a protein on a flat surface with a suitable thickness. This approach is reasonable since the phenomena of interest are restricted to the solvent/particle interface; in addition, since protein size is much smaller than microparticle radius, curvature effects can be reasonably neglected.

The second component of molecular modeling is constituted by suitable computational methods that allow the characterization of the dynamics, energetics, and conformational sampling of the system of interest. Full atomistic models are usually treated with molecular dynamics, while other

techniques such as coarse-grained molecular dynamics and dissipative particle dynamics are employed along with coarse-grained models.

Each method has its own strengths and limitations, as well as characteristic accessible time and length scales, as discussed in the following paragraphs.

Full Atomistic Models—Molecular Dynamics

In molecular dynamics simulations, atoms are represented as spheres that interact with each other by virtue of a potential energy function, usually called the force field (FF). Molecular coordinates and velocities as a function of simulation time can be evaluated by solving Newton's equation of motion with a suitable numerical integration scheme, as shown in Equation (1) (Frenkel and Smit, 2002):

$$m_i \frac{d^2 r_i}{dt^2} = F_i = -\nabla U(r) \quad (1)$$

where m_i is the mass of the i-th atom, r_i are the spatial coordinates of the i-th atom, t is time, F_i is the force acting on the i-th atom, and $U(r)$ is the potential energy (that is, the force field), which is a function of the coordinates of all atoms present in system r. Such an approach essentially implies a couple of assumptions, as follows. First, the motion of electrons can be reasonably described by the dynamics of the corresponding nuclei (Born–Oppenheimer approximation). Second, the motion of the atomic nuclei (which are heavier than electrons) can be described as point particles that follow classical mechanics; this is an acceptable approximation when quantum effects are not important (Frenkel and Smit, 2002). Generally speaking, a force field takes into account both intramolecular and intermolecular interactions, in terms of bonds, angles, dihedrals, and long-range interactions, namely van der Waals and electrostatic.

FFs contain several parameters that are computed in order to reproduce the conformational energies and minimum energy structures obtained from high-level quantum mechanics calculations and/or experimental data, such as hydration enthalpies or structural parameters from NMR experiments (Riniker, 2018). There are "general purpose" force fields, usually employed to describe small ligands, as well as FFs specifically tailored for given categories of molecules, like proteins, nucleic acids, carbohydrates, and lipids (Riniker, 2018). The choice and the quality of the force field cannot be underestimated, since they strongly affect the reliability of the simulation outcome.

MD simulations do not explicitly consider electrons, so chemical reactions and excited states cannot be investigated; however, they constitute the ideal tool for those systems that are mainly governed by non-covalent interactions, like electrostatic and Van der Waals forces. MD also allows environmental conditions to be included through the addition of explicit solvent molecules, ions, and other solute molecules into the system. The main outputs from an MD simulation are molecular trajectories, the post-processing of which can provide structural information (binding poses, protein conformation) as well as energetic information such as interaction energies.

Enhanced Sampling Methods

The characteristic time and length scales of MD simulations are in the tens to hundreds of nanoseconds (up to 1000 ns) and tens of nanometers (up to 20 nm), respectively. However, many phenomena of interest (e.g., molecular binding, protein unfolding) need large time scales to occur (up to minutes), and their investigation through MD would be in principle unfeasible; this is due to the presence of metastable states separated by high free energy barriers. A way to overcome this issue is to use enhanced sampling methods, which allow enhancement of the transitions between different metastable states separated by energy barriers higher than the thermal energy k_BT, which would not be crossed in a standard simulation at temperature T (where k_B is the Boltzmann constant and T is absolute temperature). As recently reviewed (Camilloni and Pietrucci, 2018), there are three different suitable approaches: i) increasing the temperature T; ii) changing the potential $U(r)$, and iii) adding an external bias potential $V(r)$. Each approach has its own methods, the discussion of which (along with their theoretical basis) is well beyond the purpose of this review; the interested reader is referred to *ad hoc* reviews (Miao and Mccammon, 2016; Camilloni and Pietrucci, 2018). Some of the popular enhanced sampling techniques are Replica Exchange (RE, first approach) (Miao and Mccammon, 2016) and Well-Tempered Metadynamics (WTM) (Valsson et al., 2016), which belongs to the third group. In particular, WTM and its variant forms allow the free energy of the system under investigation to be recovered by adding an external bias on a selected number of degrees of freedom, commonly referred to as collective variables (CVs). CVs are generally functions of atomic coordinates and can range from simple quantities, such as distances and dihedral angles, to more complicated variables, like the number of hydrogen bonds/hydrophobic contacts, alpha helix-content in a protein, or Debye–Hückel interaction energy. Collective variables must be chosen so that they can discriminate between metastable states and can be representative of the transition mechanism. Typical applications of WTM and WTM-based methods are the study of protein conformations (also in the presence of denaturants) (Owczarz et al., 2015), the binding poses of small ligands to target proteins (Tiwary et al., 2015), and the conformation and self-assembly of polymeric and supramolecular systems (Bochicchio and Pavan, 2018). Some phenomena, such as protein folding, require a relevant number of collective variables to perform meaningful simulations. Although conceptually feasible, running a WTM simulation with many CVs introduces some issues such as a drop in computational efficiency and a non–trivial analysis of the results obtained. In order to overcome this issue, some WTM variants have been proposed, discussed, and validated in literature (mainly for protein folding), namely Parallel Tempering Metadynamics (PTMD) (Bussi et al., 2006), Parallel Tempering Metadynamics in the Well-Tempered Ensemble (PTMD-WTE) (Deighan et al., 2012), and Bias Exchange Metadynamics (BEMD) (Piana and Laio, 2007). The discussion of the theoretical basis of these methods is beyond the purpose of this review; the interested reader is referred to the corresponding papers.

Coarse-Grained Models—Molecular Dynamics, Dissipative Particle Dynamics

The aim of coarse-grained (CG) models is to perform meaningful simulations of systems whose analysis would be challenging or unfeasible with full atomistic MD methods by building simplified representations that allow the main physical/chemical features (like the interplay between hydrophobic and hydrophilic effects) to be retained.

In the coarse-graining procedure, groups of atoms are enclosed into "beads" or "interaction sites" that are representative of the embedded atoms in terms of charge, size, hydrophobicity/hydrophilicity, *et cetera*. Beads interact with each other by virtue of a potential energy function, which takes into account both bonded interactions (that is, bond, angles, and dihedrals) and non-bonded interactions and which is parameterized in order to optimally reproduce some experimental properties (like water/octanol partition) or the behavior of more detailed full atomistic simulations.

Trajectories can be computed by integrating Newton's equation of motion and also adding other components to the force such as friction due to the solvent (if implicit solvent methods are used) (*vide infra*).

It is worth mentioning that the coarse-graining procedure can be performed to different extents, since a bead can enclose a group of atoms (3–4 heavy atoms), a group of monomers (or amino acids), an entire protein or an entire microparticle, according to the aim of the simulation. In this review, the term "coarse-grained models" is employed for all those approaches where there is a loss of degrees of freedom with respect to a full atomistic description.

A common drawback of CG models is that parameterization is strictly tailored for the system under investigation and in principle should be repeated for every new system; in other words, parameters are not transferable. In this regard, the MARTINI force field (Marrink et al., 2007) attracted a lot of interest due to its reliability and straightforward coarse-graining procedure. Beads (which include groups of 3–4 heavy atoms) still interact with each other through a simple potential energy function, as described for MD (*vide supra*). MARTINI offers a library of parameterized beads, mainly divided into four categories: polar, non-polar, apolar, and charged; in addition, each group includes subgroups representative of polarity and hydrogen bond capability. Parameters for bonded interactions (bonds, angle, dihedrals) must be determined from detailed MD simulations, while non-bonded interactions are tuned in order to reproduce thermodynamic properties like free energy of hydration, free energy of vaporization, and partitioning between water and different solvents. Explicit water and ions can also be added (a MARTINI water bead is representative of four water molecules). An example of MARTINI mapping from a full atomistic to a coarse-grained system is shown in **Figure 1**.

Bead parameterization can be further refined by the user in order to improve agreement with full atomistic simulations. Even with simulations based on the MARTINI force field, some phenomena of interest can be still characterized at a time scale that is not accessible. In this framework, enhanced sampling methods like Metadynamics can be employed to alleviate this issue, as already shown in the literature (Lelimousin et al., 2016).

Another widely employed method with CG models is Dissipative Particle Dynamics (DPD). Bead trajectories are still obtained by means of Newton's equation of motion, assuming that each i-th particle is subjected to three pair-additive forces that arise from the interactions with the other j-th particles: a conservative force, a dissipative force, and a random force (Liu et al., 2015):

$$m_i \frac{d^2 r_i}{dt^2} = f_i = \sum\nolimits_{j \neq i} F_{ij}^c + F_{ij}^d + F_{ij}^r \quad (2)$$

The conservative force F^c is due to the interaction potential of particles and accounts for both bonded and long-range interactions through an elastic force and a soft repulsion force, respectively. F^d is a dissipative force that damps the relative motion between particles, and F^r is a random force directed along the line that connects beads centers. Dissipative and random forces are momentum-conserving and represent the minimal model that takes into account viscous forces and thermal noise between particles.

Full Atomistic vs. Coarse-Grained Models: Strengths and Weaknesses for Nanomaterial–Biology Interactions

In this framework, full atomistic models provide the highest level of detail, since all atoms are explicitly included. On the one side, they account for all those fundamental interactions that are essential for a suitable description of the nano–bio interface, such as van der Waals, electrostatic, hydrogen bonding, π-π stacking, and π – cation interactions (provided the intrinsic limits and the accuracy of the FF). On the other side, the inclusion of explicit solvent molecules, ions, and other solute molecules allows environmental effects to be taken into account; the impact of pH is accounted for by appropriately changing protonation states. Focusing on proteins, by means of molecular dynamics simulations and their resolution at atomic scale it is possible to highlight the most relevant amino acids that drive the interactions at the nano–bio interface and protein structural changes at the single amino acid level, achieving a level of detail that is usually out of reach from an experimental point of view. On top of this, the reliability of the simulation results can be assessed by comparing theoretical quantities such as circular dichroism spectra with the corresponding experimental outcomes. The importance of this aspect cannot be underestimated since it strengthens the connection between experiments and simulations. Molecular dynamics simulations are still limited by the characteristic time and length scales accessible by the method: microseconds and nanometers, respectively. The direct use of enhanced sampling methods is still prohibitive for complex and/or large systems. In this regard, switching to coarse-grained models is a forced but attractive choice due to the longer accessible time and length scales (tens of microseconds and tens of nanometers, respectively). The drawback is the loss of the atomic detail, which implies that some

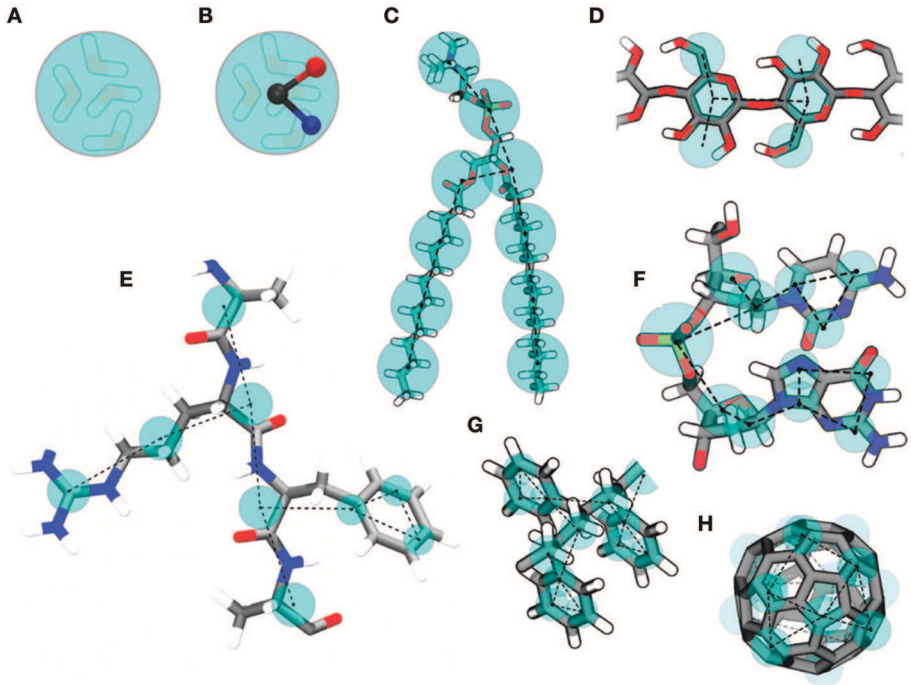

FIGURE 1 | Examples of MARTINI mapping. Standard water bead embedding four water molecules **(A)**. Polarizable water bead with embedded charges **(B)**. DMPC lipid **(C)**. Polysaccharide fragment **(D)**. Peptide **(E)**. DNA fragment **(F)**. Polystyrene fragment **(G)**. Fullerene **(H)**. Reproduced from Marrink and Tieleman (2013) under a CC-BY 3.0 license. Published by the Royal Society of Chemistry.

interactions (strong electrostatic interactions, hydrogen bonds, solvation effects) are accounted for only in a roughly qualitative way. Anyway, if the fundamental physical/chemical peculiarities of the system (such as the balance between hydrophobic and hydrophilic groups) are well reproduced in the CG model and if the interaction potentials (that govern the interactions between beads) are accurately parameterized against experimental data or validated simulations at atomic scale, simulations at CG scale are a powerful tool to complement the insights obtained with MD simulations. CG simulations can also provide some input guess structures for, e.g., protein–protein interactions (that would be challenging to obtain with MD simulations), which can be further employed for a more accurate analysis at atomic scale. On top of that, enhanced sampling methods (in particular, Well-Tempered Metadynamics) have proved to be useful for simulations at CG scale when the time scale is still not accessible.

All these aspects are discussed in detail, along with selected examples, in the following paragraphs.

APPLICATIONS FOR NANOMATERIAL–BIOLOGY INTERACTIONS

Molecular modeling is essentially employed for two purposes in the framework of nanomaterial–biology interactions. On the one side, it can shed light on the early events leading to the protein corona, highlighting the main mechanisms behind protein adsorption on the nanomaterial surface (hydrophobic effects, hydrogen bonds, electrostatic interactions, *et cetera*), the most important amino acids involved in the binding and the attainment of conformational changes. On the other side, simulations at the molecular scale allow the evaluation (in a trend-wise manner) of the impact of environmental effects, nanoparticle material, and surface functionalization on cellular uptake; some preliminary theoretical insights can also be obtained concerning the effect of protein corona formation.

Protein Corona

Molecular modeling, thanks to its resolution at the atomic scale, represents the natural choice for the study of early events that lead to protein corona formation. Knowledge of the structural changes experienced by the protein after adsorption is essential for understanding system behavior, as discussed in the introduction (*vide supra*). Molecular modeling can offer an exhaustive overview of the structural transitions thanks to the resolution at a molecular level, highlighting the portion of proteins subjected to structural changes (along with the most important amino acids that cause this) and the main driving forces (electrostatic interactions, hydrophobic effects, *et cetera*). This allows information to be obtained that is challenging or impossible to achieve experimentally, and this is why molecular modeling has emerged as the natural and ideal complement to experiments. A typical application is constituted by detailed MD simulations of the interactions between a protein and a particle and the resulting changes in protein structure. The particle is

usually modeled as a flat surface. On the one hand, there is no need to account for the entire sphere, since the interactions occur only at the interface. On the other hand, if the size of the protein is much smaller than the particle size, surface curvature effects can be safely neglected; this approximation is not valid for nanoparticles, whose size is comparable to those of proteins, and particle curvature must be accounted for by building the molecular model of the NP surface properly.

In this framework, full atomistic simulations can provide a detailed picture of the structural changes experienced by the protein after adsorption at the surface in terms of modifications of its secondary and tertiary structure (increase/decrease of alpha-helix and beta-sheet motifs and their arrangement). The specific structural changes of the protein can be directly correlated with experimental data, circular dichroism results, or NMR spectra. In addition, since protein adsorption modifies the properties of the particle surface (in terms of charge, hydrophobicity, *et cetera*), the insights obtained can be correlated, e.g., to differences in the colloidal stability of the particle suspension or other phenomena related to the protein corona such as protein aggregation and fibrillation.

Environmental effects can be taken into account thanks to the addition of explicit solvent molecules and ions, so that given salt concentrations (i.e., ionic strength) can be included in the simulation. The effect of pH can be included by changing the protonation state of the protein and the NP surface accordingly; anyway, protonation states in MD simulations are fixed and not dynamic since proton exchanges are not simulated. In other words, a positively charged amino acid remains protonated during the entire simulation, although the proton may be exchanged with surrounding water molecules according to the environmental pH. On top of that, the acid dissociation constant can be heavily influenced by local environmental effects such as the neighboring units and exposure to the solvent. This issue can be overcome by means of constant pH methods, which are currently available and validated only for proteins (Swails et al., 2014).

Simulations can also account for surface functionalization and its impact on the interactions with the protein. Through trajectory post-processing, it is possible to identify the main driving forces behind adsorption (hydrophobic effects, hydrogen bonds, *et cetera*) and to compute interaction energies in order to obtain a quantitative estimation of the strength of the binding.

Although the results of such simulations can surely contribute to increasing understanding and rationalizing experimental data, this approach also has some limitations and drawbacks.

The accuracy and reliability of the simulated protein structural changes are strongly related to the robustness of the force field; if FF parameterization leads to, e.g., an overestimation of alpha-helix content, this will unavoidably affect the simulation results. Several articles where force field performances are systematically analyzed, as well as reference FF papers, address such limitations in detail, which are therefore known *a priori*. It is also worth mentioning that force field improvements are continuously carried out, and updated FF versions are periodically released. In principle, changes in protein secondary and tertiary structure can occur on time scales beyond those accessible to standard MD simulations (ns–μs), so the use of enhanced sampling methods often becomes an inescapable necessity to achieve meaningful results. Standard MD simulations provide an ensemble of conformations according to the given conditions (temperature, solvent, ionic strength, *et cetera*), but if two metastable states are separated by an energy barrier much higher than the thermal energy, k_BT, some relevant protein conformations are not accounted for because this barrier would not be crossed and simulation outcomes can provide only a partial description of the event under investigation. The use of enhanced sampling methods alleviates this issue.

Simulations are usually focused on the adsorption of a single protein on a surface, which is essentially representative of particles in a very dilute protein solution; in other words, the overall protein–protein interactions are neglected since they can occur on long time scales and their description is usually challenging, even with enhanced sampling methods. Although simulations provide interesting insights, systematic and rational validation of the molecular models is still lacking. This currently hinders the extensive use of molecular simulations for practical applications, such as the engineering of nanoparticles in order to promote or discourage the adsorption of given proteins.

In this regard, the use of coarse-grained models, along with suitable techniques to study system dynamics, represents an inescapable choice, although the atomic detail is lost. CG models allow longer time and length scales to be explored than do full atomistic models coupled with MD simulations and can thus be used to investigate the impact of protein–protein interactions, overcoming the infinite dilution condition. Small nanoparticles can be explicitly included, and the surface curvature effect can be taken into account. However, the coarse-graining procedure is not painless due to its intrinsic limits: strong electrostatic interactions, solvation effects, and anisotropic interactions like hydrogen bonding are poorly described. Focusing on proteins, it is still challenging to account for changes in secondary structures. Therefore, an accurate parameterization of interaction potentials is an essential step in obtaining reliable results. Simulations at CG scale, despite the mentioned drawbacks, can still provide useful insights and can also be employed to obtain input guess structures for protein–protein interactions that can subsequently be investigated at an atomic level. The interaction potentials are usually parameterized against more accurate simulations with full atomistic models, whose validity, in turn, must be evaluated through comparison with experimental data. This further reinforces the need for systematic experimental validation.

The advantages and disadvantages (related to both MD and CG approaches) are summarized in **Table 1**.

As mentioned above, molecular models still need to be validated against comparison with experimental data. Indeed, for every property of interest, it is possible to highlight reference experimental techniques as well as computational techniques, as summarized in **Table 2**.

The literature offers several examples of MD simulations of protein adsorption on different materials, such as graphene sheets (Chong et al., 2015), carbon nanotubes (Ge et al., 2011; Gu et al., 2015), gold nanoparticles/surfaces (Wang et al., 2013; Brancolini et al., 2014; Tavanti et al., 2015; Bellucci et al., 2016; Yang et al.,

TABLE 1 | Advantages and disadvantages in protein–surface simulation.

Advantages	Disadvantages
Detailed overview of protein structural changes after adsorption at single amino acid level	Intrinsic limits due to the accuracy of the employed force field
Explicit solvent molecules and ions allow environmental effects to be accounted for	Standard simulation may not be sufficient to account for protein structural changes due to time scale limitations; results from enhanced sampling methods still heavily depend on FF accuracy, which must be assessed with experiments
pH effects through protonation state of protein and surface	Protein–protein interactions are usually neglected; they can be accounted for with CG models, but systematic model validation is still lacking
Impact of particle material and surface functionalization on protein structure and adsorption	Lack of systematic validation through comparison with experimental data

TABLE 2 | Reference experimental and computational techniques for properties of interest of the protein corona.

Property of interest	Experimental technique	Computational technique
Particle stability	Dynamic light scattering, zeta potential	Assessment of surface hydrophilicity/hydrophobicity changes upon protein adsorption
Protein conformational changes	Circular dichroism, nuclear magnetic resonance	Standard molecular dynamics simulations and enhanced sampling methods provide insights into conformational changes at single amino acid level Theoretical circular dichroism spectra can be obtained from simulations
Adsorption thermodynamics	Isothermal titration calorimetry	Protein–surface interaction energy or binding free energy from post-processing of molecular trajectory; binding free energy from enhanced sampling methods

2017; Ma et al., 2018), hydroxyapatite surfaces (Dong et al., 2007, 2011), fullerenes (Leonis et al., 2015), titanium oxide surfaces (Utesch et al., 2011; Mudunkotuwa and Grassian, 2014), and molybdenum disulfide (Gu et al., 2018), highlighting the specific interactions behind the binding and the attainment of structural changes. Interestingly, there are no relevant computational studies of protein adsorption on polymer surfaces. To our best knowledge, this may be due to the limited availability of validated FF parameters for polymers and to intrinsic issues with the design of molecular models. Whereas inorganic nanoparticles are characterized by an ordered atomic arrangement, a model of a disordered polymer random coil can be more challenging to build.

Among many theoretical works, only a few papers combine experimental and computational components in order to achieve an all-round understanding of the mechanisms that lead to hard corona formation. Chong et al. (2015) adopted MD simulations to study the affinity of four abundant plasma proteins (bovine fibrinogen, immunoglobulin, transferrin, and bovine serum albumin) on graphene oxide and reduced graphene oxide surfaces. The affinity trend predicted by MD is in agreement with the experimental trend for all investigated proteins. Simulations also allowed determination of the most relevant residues for the binding. Gu et al. (2018) studied the interactions of MoS_2 nanoflakes with potassium channels proteins highlighting potential toxic effects of the binding, which can alter the biological function. The results were further corroborated by experimental data.

As mentioned, enhanced sampling methods are currently also applied for the study of protein–surface interactions with both MD simulations (where the system is described at full atomistic level) and CG simulations (where the atomic detail is lost for the sake of computational efficiency). Indeed, the accessible time scale may not be adequate for the phenomena under investigation, and the use of enhanced sampling methods is a good solution for both MD and CG simulations.

Even if standard simulations are sufficient for small peptides, the application of enhanced sampling methods improves the efficiency of the sampling and provides additional information about the system thanks to the possibility of reconstructing the free energy as a function of the degrees of freedom of interest. In this regard, Metadynamics-based methods have proved to be a promising choice. Prakash et al. (2018) systematically analyzed the use of Metadynamics-based methods for the adsorption of GGKGG peptide on a silica surface, explicitly including the influence of ionic strength and ion charge; the authors discussed the performances of each method and suggested the best collective variables to account for, thus providing useful guidelines for meaningful simulations. Deighan and Pfaendtner (2013) employed Metadynamics to study the influence of surface functionalization on the adsorption of Lkα14 and Lkβ15 peptides on self-assembled monolayers; the model outcomes were in good agreement with experimental findings. Bellucci et al. (2016) investigated the adsorption of $A\beta_{16-22}$ peptide on a gold surface in order to investigate the impact of the binding on fibrillation. Their simulations revealed that binding poses are mainly influenced by the affinity between gold and phenylalanine, as shown in **Figure 2A**. The model was also validated through a comparison between experimental and calculated spectra obtained through sum generation frequency (SFG) spectroscopy (**Figure 2B**).

Hildebrand et al. (2018) employed Metadynamics-based methods to examine the conformational changes of Chymotrypsin after adsorption on silica. Simulations highlighted that the enzyme loses part of its helical content with minor perturbation of the tertiary structure; the model results were used to compute a theoretical circular dichroism spectrum that was in good agreement with the experimental spectrum.

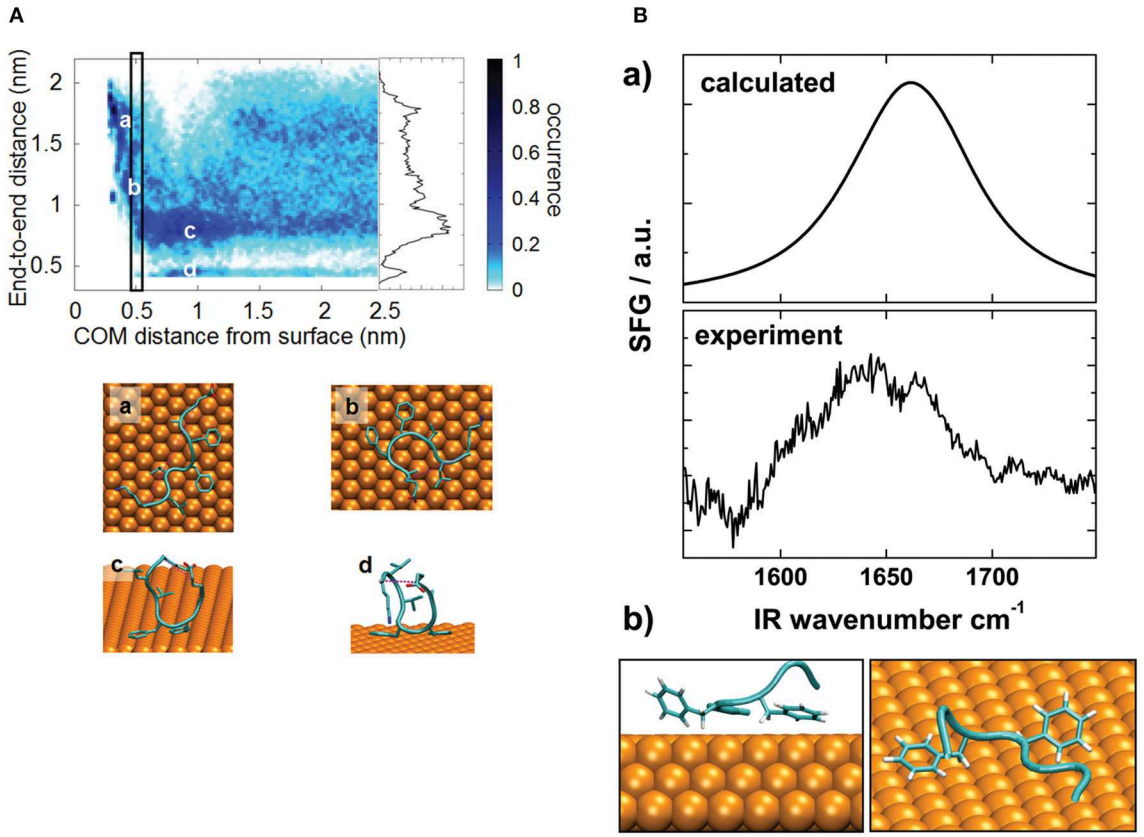

FIGURE 2 | (A) Distribution fraction of peptide end-to-end distance (computed considering terminal C_α atoms) as a function of peptide–surface distance. The rectangle identifies the free energy minimum as a function of the peptide–surface distance. The inset represents the distribution of the end-to-end distance in the bulk region (COM distance from the surface larger than 1.25 nm). (a–d) show representative conformations. **(B)** Comparison between calculated and experimental SFG spectra (a) and simulated structure used for spectral calculation (b). Reproduced from Bellucci et al. (2016) under a CC-BY 3.0 license. Published by the Royal Society of Chemistry.

CG models are also extensively used (Bellion et al., 2008; Vilaseca et al., 2013; Ding and Ma, 2014; Lopez and Lobaskin, 2015; Tavanti et al., 2015; Yu and Zhou, 2016; Hu et al., 2017; Wei et al., 2017), since they allow the characteristic accessible time and length scales of full atomistic simulations to be extended and the computational cost to be reduced. It thus becomes possible to simulate entire nanoparticles whose size is equal to or less than about 20 nm (at least when MARTINI is employed), fully covered by one or more kinds of proteins. The investigation of larger particles is still also challenging for CG methods because of the required computational effort.

Adopting CG models implies the loss of the atomic detail at the single amino acid level and a less accurate description of the system. While hydrophobic effects are reasonably accounted for, it is challenging to take into account properly, e.g., water structuring, cation–π interactions, strong electrostatic interactions, and hydrogen bonds, which lose their directionality because of the coarse-graining procedure (Marrink and Tieleman, 2013). Focusing on proteins, changes in tertiary structure can be reasonably described, while it is still non-trivial to account for changes in secondary structure due to the intrinsic limitations of the method (Marrink and Tieleman, 2013).

Despite such limitations, CG models can be employed for qualitative insights or to obtain guess structures for subsequent more detailed full atomistic simulations, as is commonly done, e.g., for the non-covalent protein–protein interaction and oligomerization of membrane proteins (Lelimousin et al., 2016). Anyway, a systematic use for more quantitative results must first be corroborated through comparison with more accurate and, above all, validated atomistic MD simulations.

Yu and Zhou (2016) used CG simulations with the MARTINI force field to understand the influence of nanoparticle curvature on lysozyme adsorption on silica at different values of ionic strength. They found that while salt concentration had a modest effect, surface curvature greatly influenced structural changes.

Ding and Ma (2014) used dissipative particle dynamics to characterize the adsorption of human serum albumin (HSA) on generic hydrophobic, hydrophilic, and charged nanoparticles for different size and pH values. By computing binding free energy as a function of the distance between the protein and particle centers of mass (COM), they showed that HSA could be bound only to hydrophobic and positively charged nanoparticles. They further studied the attainment of the protein corona by computing the

number of adsorbed proteins as a function of particle size at neutral pH for hydrophobic and positively charged particles.

The reported studies are summarized in **Table 3**.

Although the reported examples of simulations at the CG scale provide interesting findings, they are not coupled with validation against experimental data; therefore, the results should be taken as qualitative theoretical considerations. Notably, the literature offers many examples concerning inorganic nanoparticles (gold, silica) or carbon-based materials (graphene, carbon nanotubes). To our best knowledge, polymeric systems are not widely investigated. This is due to a lack of validated parameters as well as intrinsic issues related to system modeling since, by virtue of their ordered atomic arrangement, inorganic surfaces can be more easily described than a polymer surface composed of a disordered random coil.

To summarize, at this stage, molecular modeling of the protein corona cannot replace experimental activity, and its use as a purely predictive tool is currently premature. This is due, on the one side, to the intrinsic complexity of the system under investigation and, on the other side, to the lack of systematic validation against experimental data. Many examples discussed in the literature are purely theoretical, and only a few recent studies have critically validated simulation outcomes with experiments. In addition, comparison with experimental data is only performed *in vitro*; the complexity of the *in vivo* environment still constitutes an arduous challenge because of

TABLE 3 | Detailed summary of computational protein corona studies.

Device material	Protein	Method	Experimental data	Outcomes	References
Graphene	Bovine fibrinogen Immunoglobulin Transferrin Bovine serum albumin	MD	Protein adsorption (fluorescence spectroscopy) Atomic Force Microscopy Circular dichroism	Protein affinity with the surface Structural changes	Chong et al., 2015; Gu et al., 2015
Carbon nanotubes	Bovine fibrinogen Immunoglobulin Transferrin Bovine serum albumin	MD	Atomic Force Microscopy Circular dichroism	Protein affinity with the surface Structural changes	Ge et al., 2011; Gu et al., 2015
Gold particles/rods/slabs	β_2-microglobulin Bovine serum albumin Bovine beta-lactoglobulin Glutathione S-transferase	MD	Circular dichroism X-ray spectroscopy UV spectroscopy Surface plasmon resonance	Structural changes	Wang et al., 2013; Brancolini et al., 2014; Yang et al., 2017; Ma et al., 2018
Gold slab	$A\beta_{16-22}$ peptide	MD + Metadynamics	Sum generation frequency spectroscopy	Structural changes Affinity with the surface	Bellucci et al., 2016
Hydroxyapatite	Bone morphogenetic protein 2	MD	No	Affinity with the surface Structural changes	Dong et al., 2007, 2011
Fullerene	Human serum albumin	MD	Comparison with data from the literature	Binding energies Structural changes	Leonis et al., 2015
Titanium oxide	L–histidine Bone morphogenetic protein 2	MD	Attenuated total reflectance fourier transform infrared spectroscopy	Binding energies Structural changes	Utesch et al., 2011; Mudunkotuwa and Grassian, 2014
Graphite	Bone morphogenetic protein 2	MD	No	Binding energies Structural changes	Utesch et al., 2011
Molybdenum disulfide nanoflakes	K+ channels	MD	Electrophysiology	Binding affinity Consequences on protein functionality as K+ channel	Gu et al., 2018
Functionalized self-assembled monolayers	LKα14 LKβ15	MD + Metadynamics	Comparison with literature	Binding free energies Structural changes	Deighan and Pfaendtner, 2013
Silica surface	GGKGG peptide Chymotrypsin	MD + Metadynamics	Circular dichroism spectra	Binding free energies at different environmental conditions Structural changes	Hildebrand et al., 2018; Prakash et al., 2018
Generic hydrophobic nanoparticle	α_1-antitrypsin human serum albumin transferrin immunoglobulin G Fibrinogen α_2-macroglobulin	CG	No	Binding energies Structural changes	Lopez and Lobaskin, 2015
Gold nanoparticles	Insulin Fibrinogen	CG	No	Competitive binding Structural changes	Tavanti et al., 2015; Quan et al., 2017
Silica nanoparticles	Lysozyme	CG (MARTINI)	No	Curvature effects on lysozyme adsorption	Yu and Zhou, 2016
Generic hydrophobic/hydrophilic nanoparticle	Bovine serum albumin	CG (DPD)	No	Binding energy as a function of size and surface characteristics	Ding and Ma, 2014

the wide range of proteins present in the blood flow and their mutual interactions.

It is important to take into account another limitation of the method: usually, the investigation is focused only on the proteins directly adsorbed on the nanoparticle, usually modeled as a flat surface if the particle size is much larger than that of the protein. Small nanoparticles can be entirely included in the simulations, while in intermediate cases the molecular model of the surface must account for curvature effects.

Molecular simulations must be intended as the ideal complement to experimental activity *in vitro*. As shown in **Table 2**, simulation outcomes can be compared with the corresponding experimental information, providing a deeper understanding thanks to the detail provided at the molecular level.

The road toward purely predictive simulations is still long and arduous, but the main points to be addressed are clear. On the one side is the development of more reliable force fields that can accurately capture the structural transitions of proteins (in terms of both secondary and tertiary structure) after adsorption. On the other side is a systematic validation of simulations with experimental data, which can clearly highlight the strong and weak points of the molecular model and the computational technique and thus where and how to improve them. The link between experiments and simulations is becoming stronger and tighter, since it is possible to compute theoretical quantities (such as circular dichroism spectra) that can be directly compared with the corresponding experimental outcomes. The validation of full atomistic models is an unavoidable condition for exploiting the main advantages of coarse-grained models, which must be properly parameterized against more accurate simulations at the molecular level in order to obtain robust and reliable results.

Nanoparticle–Cellular Membrane Interactions

Molecular modeling can also be employed to investigate the interactions of drug molecules and nanocarriers with lipid bilayers that act as a simplified description of the complex and heterogeneous cellular membrane. Full atomistic MD simulations are the method of choice when small drug molecules are involved, while CG models are the only opportunity if the interest lies in bigger entities like polymer nanoparticles. A detailed molecular model of a cellular membrane, which includes several kinds of lipid molecules as well as transmembrane proteins, is still out of reach, although progress has recently been made in this direction (Ingolfsson et al., 2014), as recently reviewed (Ingolfsson et al., 2016; Marrink et al., 2019). This is due not only to the long time scales needed for achieving converged results but also to the lack of the experimental data for complex membranes (that is, composed of different lipid molecules) needed to parameterize and validate molecular models. For this reason, the cellular membrane is usually represented as a homogeneous bilayer (i.e., which contains only one kind of lipid molecule such as dipalmitoylphosphatidylcholine) or a simple heterogeneous membrane (with two different lipid molecules and sometimes cholesterol). In this framework, molecular modeling can be used to qualitatively understand the impact of nanocarrier formulation and the presence of adsorbed proteins on non-specific cellular uptake (that is, not mediated by a receptor).

A typical application of MD simulations is the study of the permeation of drug molecules through lipid bilayers, which mimic cellular membranes. Because of the energy barrier related to membrane crossing, the application of enhanced sampling methods becomes unavoidable. Further post-processing by means of an inhomogeneous solubility–diffusion model allows the evaluation of a position-dependent diffusion coefficient through the lipid bilayer as well as the overall permeation coefficient (Dickson et al., 2017). In another study, Bruno et al. (2015) elucidated the binding mechanism of the multiple sclerosis biomarker CSF-114 peptide to membrane using an unbiased atomistic MD approach inspired by the binding free-energy method, funnel metadynamics (Limongelli et al., 2013).

This approach provides very useful insights, since it allows the relation of the observed permeation of different drug molecules to the specific interactions at the atomic level, such as hydrogen bonds. On the other hand, the use of full atomistic simulations limits the applicability of this analysis to small drug/peptide molecules (up to a few hundreds of Da). The study of nanoparticle permeation with atomic detail would lead to unfeasible or extremely challenging simulations due to the size of the system and the long time scales needed to reach converged results. Because of this, coarse-grained simulations are the method of choice for the study of nanoparticle–cell membrane interactions, as widely discussed in the literature (Rossi and Monticelli, 2014, 2016; Ding and Ma, 2015; Ge and Wang, 2016). For the same reasons, there has been an increase of interest in the use of CG simulations for the study of transmembrane proteins (Lelimousin et al., 2016). In a recent study (Molinaro et al., 2018), a MARTINI model was employed to study the introduction of a membrane protein in biomimetic vesicles (leukosomes) obtained through a microfluidic-based setup. CG simulations allowed the impact of glycosylation, steric hindrance of the protein extracellular domain versus the intracellular domain, and relative to vesicle curvature on protein orientation to be highlighted.

Another limitation is shared by both full atomistic and coarse-grained methods: as has been mentioned, cellular membranes are very heterogeneous environments because of the wide range of lipids involved and the presence of several transmembrane proteins and receptors, and simplified models are needed for affordable simulations. Lipid bilayers made of dioleoylphosphatidylcholine (DOPC) and dipalmitoylphosphatidylcholine (DPPC) are commonly used as cell membrane models thanks to the availability of validated parameters for the force fields. Simulations of bilayers with heterogeneous compositions (that is, composed by many different lipid molecules), which would constitute a more realistic cellular membrane model, are hindered by the lack of experimental data for force field validation (Poger et al., 2016). Transmembrane proteins are not included unless the investigation is focused on the interactions with a specific receptor or on the behavior of such proteins.

In summary, simulations at the molecular level of nanoparticle–cellular membrane interactions are usually performed by means of CG methods and are focused on simplified systems made up of a mimicking lipid bilayer and a

small nanoparticle (up to 10–20 nm). The investigation of larger particles, although of potential interest, is still limited by the computational effort required and the difficulty of achieving converged results.

The advantages and disadvantages, for both MD and CG, are summarized in **Table 4**.

In general, the comparison with experimental data is more challenging. Simulation of naked and decorated particles (i.e., with surface functionalization and/or a hard protein corona) can highlight the different interactions with the cellular membrane and can be compared with the expected and the experimental cellular uptake. In this framework, simulations are expected to give those insights at molecular resolution, which cannot be obtained experimentally; this reinforces the need to have previously validated models of protein–particle interactions and model lipid bilayers. Computational efforts are currently focused on parametric simulations, where the influence of particle hydrophilicity/hydrophobicity (including charge), coating (e.g., PEGylation), shape, and size on membrane permeation and induced stresses are qualitatively evaluated.

The examples offered by the literature involve generic nanoparticles with different shapes or functionalization (Yang and Ma, 2010; Ding and Ma, 2012, 2014; Li and Hu, 2014; Li et al., 2014), gold nanoparticles (Lin et al., 2010; Rossi and Monticelli, 2016; Salassi et al., 2017; Lunnoo et al., 2019), and polymer systems (Schulz et al., 2012) such as dendrimers (Rossi and Monticelli, 2014, 2016), polystyrene (Rossi and Monticelli, 2016), and polyelectrolytes (Rossi and Monticelli, 2016).

Ding and Ma (2014) employed dissipative particle dynamics to study the influence of human serum albumin corona (*vide supra*) around hydrophobic or positively charged nanoparticles on membrane permeation. They found that at physiological pH, the HSA corona promotes particle adhesion on a DPPC lipid bilayer model of a cell membrane thanks to the specific interactions with the protein coating of a 3-nm hydrophobic particle. They also investigated the impact of pH and membrane charge.

Li et al. (2014) studied through a coarse-grained model and dissipative particle dynamics the effect of PEG grafting density (0.2–1.6 chains nm^{-2}) and molecular weight (550–5000 Da) on the internalization of an 8-nm particle, proposing a optimal choice of parameters for maximizing cellular uptake. They also characterized the uptake process in detail, identifying three stages: membrane bending ($0 < t < 122$ ns), membrane monolayer protruding ($122 < t < 750$ ns), and equilibrium ($t > 750$ ns).

Recently, Lunnoo et al. (2019) employed the MARTINI CG model to simulate the cellular uptake of gold nanoparticles. Notably, they employed a more complex mammalian cell model previously proposed by Ingolfsson et al. (2014), which includes 63 different lipid species asymmetrically distributed in the bilayer. This allowed the limitations of simple models to be overcome and the complexity of a more realistic cellular membrane to be accounted for; indeed, they found that neutral 10-nm nanoparticles experienced an endocytic pathway with a DSPC/DSPG model membrane, while they exhibited direct translocation across the more complex model of a mammalian membrane. They also characterized the energy barrier related to membrane crossing by changing the shape and charge density, also taking particle aggregation into account.

Similarly to protein corona simulations, in this framework, molecular modeling must still be considered as a complementary tool to experimental activity and not as an alternative. Although it provides interesting insights, the lack of systematic experimental validation hinders the application of molecular simulations as a predictive tool. It is also necessary to take into account the inherent approximations of coarse-grained models, where some kinds of interactions are poorly accounted for. In addition, there are still some limitations concerning the size of the device; according to examples in the literature, the maximum investigated nanoparticle size is about 20 nm. Simulations of larger devices not only increase the number of beads but also require very long calculations to achieve converged results: the required computational effort is not always feasible. This issue could in principle be overcome by employing, e.g., implicit solvent methods, which further improve computational efficiency by representing the solvent as a continuum (and thus reducing the number of explicit beads in the system) at the price of an additional approximation. The implicit solvent parameterization of the MARTINI force field, called Dry MARTINI, is currently validated only for lipid bilayers, although it has been shown that it can also be used for polymeric systems after a proper re-parameterization (Bochicchio and Pavan, 2017). In general, the use of implicit solvent methods requires an accurate parameterization and validation with experimental data or more detailed simulations at an atomic scale. Currently, only qualitative insights concerning more realistic systems (in terms of particle size) can be obtained through the simulation of smaller devices.

TABLE 4 | Advantages and disadvantages for nanoparticle–cellular membrane interactions.

Advantages	Disadvantages
Availability of validated parameters for the simulation of lipid bilayers	Only homogeneous bilayers can be reliably simulated
Particle–membrane interactions at molecular level	Only CG models can be fruitfully used, because of the size of the system, which is still limited to 10–20 nm nanoparticles
Simulation of membrane-crossing by the naked or functionalized particle	Simulation of the non-specific permeation across a simplified model system The influence of receptors is not taken into account
Protein corona and/or nanoparticle surface modification can be accounted for	Hard corona description is very qualitative and must be validated in a previous step

CONCLUSIONS AND PERSPECTIVES

Simulations at the molecular level, despite the discussed limitations and drawbacks, constitute a powerful tool for improving understanding of the governing phenomena at the nano–bio interface. The intrinsic peculiarities of molecular modeling, which account for the synergistic effects of several

factors (particle material, protein adsorption, environmental effects, interactions with cellular membranes, *et cetera*), can provide some insights that are challenging or impossible obtain experimentally, thanks to the molecular resolution. The increasing availability of computational resources, the development of improved force fields (that are more accurate), algorithm optimization, and theoretical advancements are constantly pushing molecular simulations beyond their limits, slowly overcoming the current issues.

Focusing on the protein corona, the *conditio sine qua non* for a meaningful simulation is a validated force field, which allows a reasonable description of secondary and tertiary structures to be obtained and a robust sampling of the most relevant conformation. Indeed, discrepancies in the description of protein structural transitions inevitably affect result reliability and the subsequent steps (e.g., the study of the interaction of a protein-decorated particle with a cellular membrane). Descriptive capabilities are known *a priori*, since they are addressed in detail in several papers and FF reference papers. The development and the improvement of force fields (not only for proteins) are always ongoing, and updates are periodically released and discussed in the scientific literature. This refinement process is currently taking advantage of new state-of-the-art techniques such as machine learning (Debiec et al., 2016).

Molecular dynamics simulations provide detail at an atomic level, but they are limited by the time scale of many phenomena of interest (such as protein folding/unfolding, slow binding/unbinding kinetics), which is beyond that accessible through standard simulations. The development of enhanced sampling methods allows this issue to be alleviated and allows a more comprehensive ensemble of conformations to be obtained. Currently, the extensive application of such methods is still hindered by the size of the molecules under investigation, which cannot exceed, in the case of proteins, a few tens of amino acids in order to obtain reliable and converged results. Further improvements of the method itself and optimization of computational protocols and algorithms could allow the investigation to be focused on larger and more complex proteins.

Coarse-grained models, along with suitable methods to study system dynamics, have emerged as an attractive choice when molecular dynamics simulations are unfeasible because of the time and length scales involved. Indeed, despite the loss of atomic detail, CG models have proved that the fundamental physical/chemical peculiarities lie at the molecular model. However, in order to obtain reliable results, careful parameterization and validation against experimental data still represent essential steps that are not always addressed.

Simulations are mainly focused on inorganic particles (gold, silica) or carbon-based devices (graphene, carbon nanotubes), while there are no relevant examples concerning polymer nanoparticles. This can be attributed to the fact that molecular models of inorganic particles are easier to build given the availability of reliable force field parameters together with their known and well-parametrized structural properties.

Many efforts are also being devoted to the development of more realistic models of cellular membranes, as recently reviewed (Ingolfsson et al., 2016; Marrink et al., 2019). This aspect cannot be underestimated, because the reliability of the results concerning drug or nanocarrier–cell membrane interactions of course requires a robust description of a cell membrane with a suitable level of approximation.

The available force fields provide validated parameters for small sets of lipid molecules (although the number of available compounds increases in every FF update), and it is difficult to validate simulations of heterogeneous membranes (that is, made up of several kinds of different lipid molecules) because of the lack of suitable experimental data. In this regard, a first attempt has been performed by Ingolfsson et al. (2014), who employed a CG MARTINI model to simulate an idealized mammalian plasma membrane, including more than 63 lipid species asymmetrically distributed in the bilayer. Marrink et al. (2019) recently published a comprehensive review that summarizes all the advancements in the field and clearly describes the ultimate goal for comprehensive modeling: the simulation of a membrane with hundreds of different lipids, with a large variety of transmembrane as well as peripherally bound proteins and realistic gradients of metabolites, ions, and pH. Although this "definitive" simulation is still far off, there are in the literature some interesting attempts to model complex systems, such as viral envelopes and mesoscale simulations remodeling eukaryotic cell membranes (Marrink et al., 2019).

In conclusion, simulations at the molecular scale have emerged as a fruitful tool to complement the insights provided by experimental activity and obtain a deeper understanding of the main phenomena behind the observed behavior. Despite their use becoming more and more widespread, there are still some points that need to be addressed in the near future to overcome the current limitations:

- Extensive application of plain and enhanced sampling simulative methods to study the conformational changes of the most abundant plasma proteins;
- Availability of force fields of increased accuracy;
- Extension of the study of protein–particle interactions to polymeric systems prone to bind to the NP surface;
- Systematic and rational validation of molecular models with *ad hoc* experimental data;
- Extensive validation of CG models for nanoparticle–cellular membrane interactions;
- More realistic models of cellular membranes.

AUTHOR CONTRIBUTIONS

TC performed the literature research and wrote the first draft of the paper. All authors discussed and approved the contents of the manuscript and contributed to the final version by reading and editing.

FUNDING

This study is part of the GoNanoBioMat project and has received funding from the Horizon 2020 framework program of the European Union, ProSafe Joint Transnational Call 2016, from the CTI (1.1.2018 Innosuisse) under grant agreement

Number 19267.1 PFNM-NM and from the FCT Foundation for Science and Technology under the project PROSAFE/0001/2016. VL thanks the Swiss National Science Foundation (Project N. 200021_163281) and the COST action CA15135 (Multi-target paradigm for innovative ligand identification in the drug discovery process MuTaLig) for the support.

REFERENCES

Bellion, M., Santen, L., Mantz, H., Hahl, H., Quinn, A., Nagel, A., et al. (2008). Protein adsorption on tailored substrates: long-range forces and conformational changes. *J. Phys. Condens. Matter* 20:404226. doi: 10.1088/0953-8984/20/40/404226

Bellucci, L., Ardevol, A., Parrinello, M., Lutz, H., Lu, H., Weidner, T., et al. (2016). The interaction with gold suppresses fiber-like conformations of the amyloid beta (16-22) peptide. *Nanoscale* 8, 8737–8748. doi: 10.1039/C6NR01539E

Bochicchio, D., and Pavan, G. M. (2017). Effect of concentration on the supramolecular polymerization mechanism via implicit-solvent coarse-grained simulations of water-soluble 1,3,5-benzenetricarboxamide. *J. Phys. Chem. Lett.* 8, 3813–3819. doi: 10.1021/acs.jpclett.7b01649

Bochicchio, D., and Pavan, G. M. (2018). Molecular modelling of supramolecular polymers. *Adv. Phys. X* 3, 315–337. doi: 10.1080/23746149.2018.1436408

Brancolini, G., Toroz, D., and Corni, S. (2014). Can small hydrophobic gold nanoparticles inhibit beta(2)-microglobulin fibrillation? *Nanoscale* 6, 7903–7911. doi: 10.1039/C4NR01514B

Bruno, A., Scrima, M., Novellino, E., D'errico, G., D'ursi, A. M., and Limongelli, V. (2015). The glycan role in the glycopeptide immunogenicity revealed by atomistic simulations and spectroscopic experiments on the multiple sclerosis biomarker CSF114(Glc). *Sci. Rep.* 5:9200. doi: 10.1038/srep09200

Bussi, G., Gervasio, F. L., Laio, A., and Parrinello, M. (2006). Free-energy landscape for beta hairpin folding from combined parallel tempering and metadynamics. *J. Am. Chem. Soc.* 128, 13435–13441. doi: 10.1021/ja062463w

Camilloni, C., and Pietrucci, F. (2018). Advanced simulation techniques for the thermodynamic and kinetic characterization of biological systems. *Adv. Phys. X* 3:1477531. doi: 10.1080/23746149.2018.1477531

Cedervall, T., Lynch, I., Foy, M., Berggad, T., Donnelly, S. C., Cagney, G., et al. (2007a). Detailed identification of plasma proteins adsorbed on copolymer nanoparticles. *Angew. Chem. Int. Ed.* 46, 5754–5756. doi: 10.1002/anie.200700465

Cedervall, T., Lynch, I., Lindman, S., Berggard, T., Thulin, E., Nilsson, H., et al. (2007b). Understanding the nanoparticle-protein corona using methods to quantify exchange rates and affinities of proteins for nanoparticles. *Proc. Natl. Acad. Sci. U.S.A.* 104, 2050–2055. doi: 10.1073/pnas.0608582104

Chong, Y., Ge, C. C., Yang, Z. X., Garate, J. A., Gu, Z. L., Weber, J. K., et al. (2015). Reduced cytotoxicity of graphene nanosheets mediated by blood-protein coating. *ACS Nano* 9, 5713–5724. doi: 10.1021/nn5066606

Debiec, K. T., Cerutti, D. S., Baker, L. R., Gronenborn, A. M., Case, D. A., and Chong, L. T. (2016). Further along the road less traveled: AMBER ff15ipq, an original protein force field built on a self-consistent physical model. *J. Chem. Theory Comput.* 12, 3926–3947. doi: 10.1021/acs.jctc.6b00567

Deighan, M., Bonomi, M., and Pfaendtner, J. (2012). Efficient simulation of explicitly solvated proteins in the well-tempered ensemble. *J. Chem. Theory Comput.* 8, 2189–2192. doi: 10.1021/ct300297t

Deighan, M., and Pfaendtner, J. (2013). Exhaustively sampling peptide adsorption with metadynamics. *Langmuir* 29, 7999–8009. doi: 10.1021/la4010664

Dell'orco, D., Lundqvist, M., Oslakovic, C., Cedervall, T., and Linse, S. (2010). Modeling the time evolution of the nanoparticle-protein corona in a body fluid. *PLoS ONE* 5:e10949. doi: 10.1371/journal.pone.0010949

Dickson, C. J., Hornak, V., Pearlstein, R. A., and Duca, J. S. (2017). Structure-kinetic relationships of passive membrane permeation from multiscale modeling. *J. Am. Chem. Soc.* 139, 442–452. doi: 10.1021/jacs.6b11215

Ding, H. M., and Ma, Y. Q. (2012). Role of physicochemical properties of coating ligands in receptor-mediated endocytosis of nanoparticles. *Biomaterials* 33, 5798–5802. doi: 10.1016/j.biomaterials.2012.04.055

Ding, H. M., and Ma, Y. Q. (2014). Computer simulation of the role of protein corona in cellular delivery of nanoparticles. *Biomaterials* 35, 8703–8710. doi: 10.1016/j.biomaterials.2014.06.033

Ding, H. M., and Ma, Y. Q. (2015). Theoretical and computational investigations of nanoparticle-biomembrane interactions in cellular delivery. *Small* 11, 1055–1071. doi: 10.1002/smll.201401943

Dong, X. L., Qi, W., Tao, W., Ma, L. Y., and Fu, C. X. (2011). The dynamic behaviours of protein BMP-2 on hydroxyapatite nanoparticles. *Mol. Simul.* 37, 1097–1104. doi: 10.1080/08927022.2011.582108

Dong, X. L., Wang, Q., Wu, T., and Pan, H. H. (2007). Understanding adsorption-desorption dynamics of BMP-2 on hydroxyapatite (001) surface. *Biophys. J.* 93, 750–759. doi: 10.1529/biophysj.106.103168

Frenkel, D., and Smit, B. (2002). *Understanding Molecular Simulation: From Algorithms to Applications*. San Diego: Academic Press.

Ge, C. C., Du, J. F., Zhao, L. N., Wang, L. M., Liu, Y., Li, D. H., et al. (2011). Binding of blood proteins to carbon nanotubes reduces cytotoxicity. *Proc. Natl. Acad. Sci. U.S.A.* 108, 16968–16973. doi: 10.1073/pnas.1105270108

Ge, Z., and Wang, Y. (2016). Computer simulation and modeling techniques in the study of nanoparticle-membrane interactions. *Annu. Rep. Comput. Chem.* 12, 159–200. doi: 10.1016/bs.arcc.2016.05.001

Gu, Z. L., Plant, L. D., Meng, X. Y., Perez-Aguilar, J. M., Wang, Z. G., Dong, M. D., et al. (2018). Exploring the nanotoxicology of MoS2: a study on the interaction of MoS2 nanoflakes and K+ channels. *ACS Nano* 12, 705–717. doi: 10.1021/acsnano.7b07871

Gu, Z. L., Yang, Z. X., Chong, Y., Ge, C. C., Weber, J. K., Bell, D. R., et al. (2015). Surface curvature relation to protein adsorption for carbon-based nanomaterials. *Sci. Rep.* 5:10886. doi: 10.1038/srep10886

Hildebrand, N., Michaelis, M., Wurzler, N., Li, Z., Hirst, J. D., Micsonai, A., et al. (2018). Atomistic details of chymotrypsin conformational changes upon adsorption on silica. *ACS Biomater. Sci. Eng.* 4, 4036–4050. doi: 10.1021/acsbiomaterials.8b00819

Hu, Q. L., Bai, X., Hu, G. Q., and Zuo, Y. Y. (2017). Unveiling the molecular structure of pulmonary surfactant corona on nanoparticles. *ACS Nano* 11, 6832–6842. doi: 10.1021/acsnano.7b01873

Ingolfsson, H. I., Arnarez, C., Periole, X., and Marrink, S. J. (2016). Computational 'microscopy' of cellular membranes. *J. Cell Sci.* 129, 257–268. doi: 10.1242/jcs.176040

Ingolfsson, H. I., Melo, M. N., Van Eerden, F. J., Arnarez, C., Lopez, C. A., Wassenaar, T. A., et al. (2014). Lipid organization of the plasma membrane. *J. Am. Chem. Soc.* 136, 14554–14559. doi: 10.1021/ja507832e

Lelimousin, M., Limongelli, V., and Sansom, M. S. P. (2016). Conformational changes in the epidermal growth factor receptor: role of the transmembrane domain investigated by coarse-grained metadynamics free energy. *J. Am. Chem. Soc.* 138, 10611–10622. doi: 10.1021/jacs.6b05602

Leonis, G., Avramopoulos, A., Papavasileiou, K. D., Reis, H., Steinbrecher, T., and Papadopoulos, M. G. (2015). A comprehensive computational study of the interaction between human serum albumin and fullerenes. *Journal of Physical Chemistry B* 119, 14971–14985. doi: 10.1021/acs.jpcb.5b05998

Li, Y., and Hu, Y. (2014). Computational investigation of the influence of chain length on the shielding effect of PEGylated nanoparticles. *RSC Adv.* 4, 51022–51031. doi: 10.1039/C4RA11142G

Li, Y., Kroger, M., and Liu, W. K. (2014). Endocytosis of PEGylated nanoparticles accompanied by structural and free energy changes of the grafted polyethylene glycol. *Biomaterials* 35, 8467–8478. doi: 10.1016/j.biomaterials.2014.06.032

Limongelli, V., Bonomi, M., and Parrinello, M. (2013). Funnel metadynamics as accurate binding free-energy method. *Proc. Natl. Acad. Sci. U.S.A.* 110, 6358–6363. doi: 10.1073/pnas.1303186110

Lin, J. Q., Zhang, H. W., Chen, Z., and Zheng, Y. G. (2010). Penetration of lipid membranes by gold nanoparticles: insights into cellular uptake, cytotoxicity, and their relationship. *ACS Nano* 4, 5421–5429. doi: 10.1021/nn1010792

Liu, M. B., Liu, G. R., Zhou, L. W., and Chang, J. Z. (2015). Dissipative particle dynamics (DPD): an overview and recent developments. *Arc. Comput. Methods Eng.* 22, 529–556. doi: 10.1007/s11831-014-9124-x

Lopez, H., and Lobaskin, V. (2015). Coarse-grained model of adsorption of blood plasma proteins onto nanoparticles. *J. Chem. Phys.* 143:243138. doi: 10.1063/1.4936908

Lundqvist, M., Stigler, J., Elia, G., Lynch, I., Cedervall, T., and Dawson, K. A. (2008). Nanoparticle size and surface properties determine the protein corona with possible implications for biological impacts. *Proc. Natl. Acad. Sci. U.S.A.* 105, 14265–14270. doi: 10.1073/pnas.0805135105

Lunnoo, T., Assaeakhajornsak, J., and Puangmali, T. (2019). In silico study of gold nanoparticle uptake into a mammalian cell: interplay of size, shape, surface charge and aggregation. *J. Phys. Chem. C.* 123, 3801–3810. doi: 10.1021/acs.jpcc.8b07616

Ma, W. W., Saccardo, A., Roccatano, D., Aboagye-Mensah, D., Alkaseem, M., Jewkes, M., et al. (2018). Modular assembly of proteins on nanoparticles. *Nat. Commun.* 9:1489. doi: 10.1038/s41467-018-03931-4

Marrink, S. J., Corradi, V., Souza, P. C. T., Ingolfsson, H. I., Tieleman, D. P., and Sansom, M. S. P. (2019). Computational modeling of realistic cell membranes. *Chem. Rev.* 119, 6184–6226. doi: 10.1021/acs.chemrev.8b00460

Marrink, S. J., Risselada, H. J., Yefimov, S., Tieleman, D. P., and De Vries, A. H. (2007). The MARTINI force field: coarse grained model for biomolecular simulations. *J. Phys. Chem. B* 111, 7812–7824. doi: 10.1021/jp071097f

Marrink, S. J., and Tieleman, D. P. (2013). Perspective on the Martini model. *Chem. Soc. Rev.* 42, 6801–6822. doi: 10.1039/c3cs60093a

Miao, Y. L., and Mccammon, J. A. (2016). Unconstrained enhanced sampling for free energy calculations of biomolecules: a review. *Mol. Simul.* 42, 1046–1055. doi: 10.1080/08927022.2015.1121541

Molinaro, R., Evangelopoulos, M., Hoffman, J. R., Corbo, C., Taraballi, F., Martinez, J. O., et al. (2018). Design and development of biomimetic nanovesicles using a microfluidic approach. *Adv. Mater.* 30:e1702749. doi: 10.1002/adma.201702749

Mudunkotuwa, I. A., and Grassian, V. H. (2014). Histidine adsorption on TiO2 nanoparticles: an integrated spectroscopic, thermodynamic, and molecular-based approach toward understanding nano-bio interactions. *Langmuir* 30, 8751–8760. doi: 10.1021/la500722n

Nel, A. E., Madler, L., Velegol, D., Xia, T., Hoek, E. M. V., Somasundaran, P., et al. (2009). Understanding biophysicochemical interactions at the nano-bio interface. *Nat. Mater.* 8, 543–557. doi: 10.1038/nmat2442

Owczarz, M., Casalini, T., Motta, A. C., Morbidelli, M., and Arosio, P. (2015). Contribution of electrostatics in the fibril stability of a model ionic-complementary peptide. *Biomacromolecules* 16, 3792–3801. doi: 10.1021/acs.biomac.5b01092

Pederzoli, F., Tosi, G., Vandelli, M. A., Belletti, D., Forni, F., and Ruozi, B. (2017). Protein corona and nanoparticles: how can we investigate on? *Wiley Interdiscip. Rev. Nanomed. Nanobiotechnol.* 9:e1467. doi: 10.1002/wnan.1467

Piana, S., and Laio, A. (2007). A bias-exchange approach to protein folding. *J. Phys. Chem. B* 111, 4553–4559. doi: 10.1021/jp067873l

Poger, D., Caron, B., and Mark, A. E. (2016). Validating lipid force fields against experimental data: progress, challenges and perspectives. *Biochim. Biophys. Acta Biomembr.* 1858, 1556–1565. doi: 10.1016/j.bbamem.2016.01.029

Prakash, A., Sprenger, K. G., and Pfaendtner, J. (2018). Essential slow degrees of freedom in protein-surface simulations: a metadynamics investigation. *Biochem. Biophys. Res. Commun.* 498, 274–281. doi: 10.1016/j.bbrc.2017.07.066

Quan, X. B., Peng, C. W., Zhao, D. H., Li, L. B., Fan, J., and Zhou, J. (2017). Molecular understanding of the penetration of functionalized gold nanoparticles into asymmetric membranes. *Langmuir* 33, 361–371. doi: 10.1021/acs.langmuir.6b02937

Riniker, S. (2018). Fixed-charge atomistic force fields for molecular dynamics simulations in the condensed phase: an overview. *J. Chem. Inf. Model.* 58, 565–578. doi: 10.1021/acs.jcim.8b00042

Rossi, G., and Monticelli, L. (2014). Modeling the effect of nano-sized polymer particles on the properties of lipid membranes. *J. Phys. Condens. Matter* 26:503101. doi: 10.1088/0953-8984/26/50/503101

Rossi, G., and Monticelli, L. (2016). Simulating the interaction of lipid membranes with polymer and ligand-coated nanoparticles. *Adv. Phys. X* 1, 276–296. doi: 10.1080/23746149.2016.1177468

Salassi, S., Simonelli, F., Bochicchio, D., Ferrando, R., and Rossi, G. (2017). Au nanoparticles in lipid bilayers: a comparison between atomistic and coarse-grained models. *J. Phys. Chem. C* 121, 10927–10935. doi: 10.1021/acs.jpcc.6b12148

Schulz, M., Olubummo, A., and Binder, W. H. (2012). Beyond the lipid-bilayer: interaction of polymers and nanoparticles with membranes. *Soft Matter* 8, 4849–4864. doi: 10.1039/c2sm06999g

Swails, J. M., York, D. M., and Roitberg, A. E. (2014). Constant pH replica exchange molecular dynamics in explicit solvent using discrete protonation states: implementation, testing, and validation. *J. Chem. Theory Comput.* 10, 1341–1352. doi: 10.1021/ct401042b

Tavanti, F., Pedone, A., and Menziani, M. C. (2015). Competitive binding of proteins to gold nanoparticles disclosed by molecular dynamics simulations. *J. Phys. Chem. C* 119, 22172–22180. doi: 10.1021/acs.jpcc.5b05796

Tiwary, P., Limongelli, V., Salvalaglio, M., and Parrinello, M. (2015). Kinetics of protein-ligand unbinding: predicting pathways, rates, and rate-limiting steps. *Proc. Natl. Acad. Sci. U.S.A.* 112, E386–E391. doi: 10.1073/pnas.1424461112

Utesch, T., Daminelli, G., and Mroginski, M. A. (2011). Molecular dynamics simulations of the adsorption of bone morphogenetic protein-2 on surfaces with medical relevance. *Langmuir* 27, 13144–13153. doi: 10.1021/la202489w

Valsson, O., Tiwary, P., and Parrinello, M. (2016). Enhancing important fluctuations: rare events and metadynamics from a conceptual viewpoint. *Annu. Rev. Phys. Chem.* 67, 159–184. doi: 10.1146/annurev-physchem-040215-112229

Vilaseca, P., Dawson, K. A., and Franzese, G. (2013). Understanding and modulating the competitive surface-adsorption of proteins through coarse-grained molecular dynamics simulations. *Soft Matter* 9, 6978–6985. doi: 10.1039/c3sm50220a

Walkey, C. D., and Chan, W. C. W. (2012). Understanding and controlling the interaction of nanomaterials with proteins in a physiological environment. *Chem. Soc. Rev.* 41, 2780–2799. doi: 10.1039/C1CS15233E

Wang, L. M., Li, J. Y., Pan, J., Jiang, X. M., Ji, Y. L., Li, Y. F., et al. (2013). Revealing the binding structure of the protein corona on gold nanorods using synchrotron radiation-based techniques: understanding the reduced damage in cell membranes. *J. Am. Chem. Soc.* 135, 17359–17368. doi: 10.1021/ja406924v

Wei, Q., Becherer, T., Angioletti-Uberti, S., Dzubiella, J., Wischke, C., Neffe, A. T., et al. (2014). Protein interactions with polymer coatings and biomaterials. *Angew. Chem. Int. Ed.* 53, 8004–8031. doi: 10.1002/anie.201400546

Wei, S., Ahlstrom, L. S., and Brooks, C. L. (2017). Exploring protein-nanoparticle interactions with coarse-grained protein folding models. *Small* 13:1603748. doi: 10.1002/smll.201603748

Yang, J., Wang, B., You, Y. S., Chang, W. J., Tang, K., Wang, Y. C., et al. (2017). Probing the modulated formation of gold nanoparticles-beta-lactoglobulin corona complexes and their applications. *Nanoscale* 9, 17758–17769. doi: 10.1039/C7NR02999C

Yang, K., and Ma, Y. Q. (2010). Computer simulation of the translocation of nanoparticles with different shapes across a lipid bilayer. *Nat. Nanotechnol.* 5, 579–583. doi: 10.1038/nnano.2010.141

Yu, G. B., and Zhou, J. (2016). Understanding the curvature effect of silica nanoparticles on lysozyme adsorption orientation and conformation: a mesoscopic coarse-grained simulation study. *Phys. Chem. Chem. Phys.* 18, 23500–23507. doi: 10.1039/C6CP01478J

Conflict of Interest: The authors declare that the research was conducted in the absence of any commercial or financial relationships that could be construed as a potential conflict of interest.

frontiers in Bioengineering and Biotechnology

REVIEW
published: 23 October 2019
doi: 10.3389/fbioe.2019.00261

Hazard Assessment of Polymeric Nanobiomaterials for Drug Delivery: What Can We Learn From Literature So Far

Sandra Jesus[1], *Mélanie Schmutz*[2], *Claudia Som*[2], *Gerrit Borchard*[3], *Peter Wick*[4] *and Olga Borges*[1,5]*

[1] Center for Neuroscience and Cell Biology, University of Coimbra, Coimbra, Portugal, [2] Laboratory for Technology and Society, Empa Swiss Laboratories for Materials Science and Technology, St. Gallen, Switzerland, [3] School of Pharmaceutical Sciences, University of Geneva, Geneva, Switzerland, [4] Laboratory for Particles-Biology Interactions, Empa Swiss Laboratories for Materials Science and Technology, St. Gallen, Switzerland, [5] Faculty of Pharmacy, University of Coimbra, Coimbra, Portugal

OPEN ACCESS

Edited by:
Michele Iafisco,
Italian National Research Council (CNR), Italy

Reviewed by:
Smilja Markovic,
Institute of Technical Sciences (SASA), Serbia
Ching-Yun Chen,
National Health Research Institutes, Taiwan

***Correspondence:**
Olga Borges
olga@ci.uc.pt

Specialty section:
This article was submitted to Nanobiotechnology, a section of the journal Frontiers in Bioengineering and Biotechnology

Received: 02 August 2019
Accepted: 26 September 2019
Published: 23 October 2019

Citation:
Jesus S, Schmutz M, Som C, Borchard G, Wick P and Borges O (2019) Hazard Assessment of Polymeric Nanobiomaterials for Drug Delivery: What Can We Learn From Literature So Far. Front. Bioeng. Biotechnol. 7:261. doi: 10.3389/fbioe.2019.00261

The physicochemical properties of nanobiomaterials, such as their small size and high surface area ratio, make them attractive, novel drug-carriers, with increased cellular interaction and increased permeation through several biological barriers. However, these same properties hinder any extrapolation of knowledge from the toxicity of their raw material. Though, as suggested by the Safe-by-Design (SbD) concept, the hazard assessment should be the starting point for the formulation development. This may enable us to select the most promising candidates of polymeric nanobiomaterials for safe drug-delivery in an early phase of innovation. Nowadays the majority of reports on polymeric nanomaterials are focused in optimizing the nanocarrier features, such as size, physical stability and drug loading efficacy, and in performing preliminary cytocompatibility testing and proving effectiveness of the drug loaded formulation, using the most diverse cell lines. Toxicological studies exploring the biological effects of the polymeric nanomaterials, particularly regarding immune system interaction are often disregarded. The objective of this review is to illustrate what is known about the biological effects of polymeric nanomaterials and to see if trends in toxicity and general links between physicochemical properties of nanobiomaterials and their effects may be derived. For that, data on chitosan, polylactic acid (PLA), polyhydroxyalkanoate (PHA), poly(lactic-co-glycolic acid) (PLGA) and policaprolactone (PCL) nanomaterials will be evaluated regarding acute and repeated dose toxicity, inflammation, oxidative stress, genotoxicity, toxicity on reproduction and hemocompatibility. We further intend to identify the analytical and biological tests described in the literature used to assess polymeric nanomaterials toxicity, to evaluate and interpret the available results and to expose the obstacles and challenges related to the nanomaterial testing. At the present time, considering all the information collected, the hazard assessment and thus also the SbD of polymeric nanomaterials is still dependent on a case-by-case evaluation. The identified obstacles prevent the identification of toxicity trends and the generation of an

assertive toxicity database. In the future, *in vitro* and *in vivo* harmonized toxicity studies using unloaded polymeric nanomaterials, extensively characterized regarding their intrinsic and extrinsic properties should allow to generate such database. Such a database would enable us to apply the SbD approach more efficiently.

Keywords: hazard assessment, exposure assessment, *in vivo* toxicity, oxidative stress, genotoxicity, toxicity on reproduction, hemocompatibility, polymeric nanobiomaterials

INTRODUCTION

Over the last decades, several nanomaterials (NMs) have been developed and studied as promisor drug delivery vehicles and medical devices, including magnetic, metallic, ceramic and polymeric nanomaterials. At present, there is fragile consensus regarding the "nano" definition among different regulatory organizations. In detail, considering medical regulatory authorities, such as the European Medicines Agency (EMA) or the United States Food and Drug Administration (FDA) some considerations can be made. In a reflection paper about nanotechnology-based medicinal products for human use published in 2006, EMA defined nanotechnology as "the production and application of structures, devices and systems by controlling the shape and size of materials at nanometer scale," considering that "the nanometer scale ranges from the atomic level at around 0.2 nm (2 Å) up to around 100 nm" (European Medicines Agency, 2006). On its turn, FDA guidance for considering whether an FDA-regulated product involves the application of nanotechnology (Food Drug Aministration, 2014) refers that it should be considered "the evaluation of materials or end products engineered to exhibit properties or phenomena attributable to dimensions up to 1,000 nm, as a means to screen materials for further examination and to determine whether these materials exhibit properties or phenomena attributable to their dimension(s) and associated with the application of nanotechnology." Therefore, for the context of academic research and to the context of this review the following definition of nanomaterial applies: materials in the size range of 1 nm to 1,000 nm and a function or mode of action based on its nanotechnological properties. In addition, by "nanobiomaterial" we considered NMs intended to interact with biological systems. The application of nanobiomaterials in the medicine field present several advantages as they can (Moritz and Geszke-Moritz, 2015; Banik et al., 2016):

- Transport higher drug payloads
- Enable targeted drug delivery
- Increase the bioavailability of poorly water-soluble drugs
- Promote controlled drug delivery
- Increase the stability of drugs in biological fluids
- Increase drug circulation time in the body
- Confer drugs protection from biological fluids
- Permeate through various biological barriers
- Enable surface modifications to increase interaction with biological targets.

Considering polymeric NMs in particular, they can be assembled in different pharmaceutical nanosystems, such as nanoparticles (NPs), dendrimers, polymeric micelles and drug conjugates (Bhatia, 2016). On its turn, polymeric NPs comprise both vesicular systems (nanocapsules) and matrix systems (nanospheres) (Bhatia, 2016). The polymeric nature of these NMs provides additional advantages that are worth exploring, such as enhanced biocompatibility, biodegradability and low immunogenicity (Egusquiaguirre et al., 2016; Rana and Sharma, 2019).

All considered, most of these advantages are frequently attributed to their distinctive size which contributes to their high surface area to mass ratio, and is also responsible for the different toxicokinetic fate of the NMs (Landsiedel et al., 2012; Boyes et al., 2017). Indeed, small sizes facilitate cell uptake, penetration through endothelial and epithelial cells, interaction with tissues and accumulation in the liver, kidney and spleen (Khan and Shanker, 2015). The increased cellular interaction can have a modulatory effect on the immune system, triggering inflammation, increased susceptibility to infectious diseases, or even to autoimmune diseases or cancer (Kononenko et al., 2015).

The unique physicochemical properties of the NMs restricts the extrapolation of toxicological data from raw materials, and makes it necessary to have specific toxicological studies adequate to the nanoscale (Ge et al., 2011). Moreover, there is a need for specific and optimized methods for NMs toxicity evaluation, since interactions between NMs and current toxicity testing protocols can lead to false positive or false negative results (Khan and Shanker, 2015; Kononenko et al., 2015).

Understanding the toxicokinetics of NMs and their modulation of the immunological system is necessary to implement their Safe-by-Design based on the literature. This is an up-to-date subject, currently widely discussed among the scientific community, but most commonly for metallic NM (Gatto and Bardi, 2018; Kanwal et al., 2019).

Therefore, the objective of this review is to summarize what is known about the toxic effects of polymeric NMs, with special focus on polymeric NPs that could be correlated to human health risks. We intend to identify the analytical and biological tests described in the literature used to assess NMs toxicity and to evaluate and interpret the available results. Furthermore, we intend to understand the obstacles and challenges related to the nanomaterial testing that are still preventing a harmonized regulation on polymeric NMs for drug delivery and biomedical applications.

We started this review by discussing the pillars of human health risk assessment: exposure assessment and hazard assessment. Next, in order to analyze the state of the art about the toxic effects of polymeric NMs, peer reviewed original research articles from the last 10 years were analyzed and discussed,

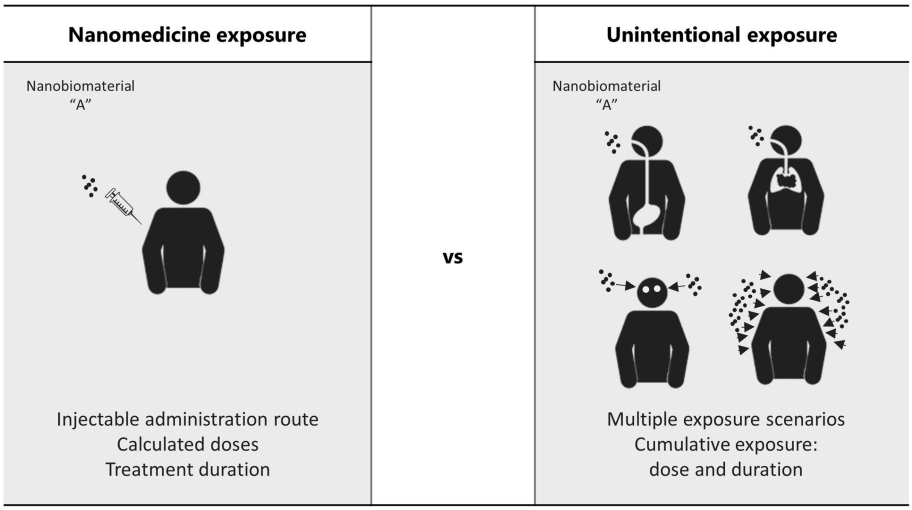

FIGURE 1 | Hypothetical scenarios of exposure: comparison between the administration route and doses foreseen in medical applications and the exposure routes and cumulative doses difficult to predict in unintentional exposures, such as occupational scenarios.

addressing the following endpoints: (1) *in vivo* toxicity (acute and repeated-dose), (2) oxidative stress, (3) inflammation, (4) genotoxicity, (5) toxicity on reproduction and (6) hemolysis. Importantly, articles were carefully examined regarding minimal characterization parameters, such as chemical composition, particle size, surface charge and endotoxin contamination (when relevant).

PILLARS FOR HUMAN HEALTH RISK ASSESSMENT

To perform human health risk assessment of any material is necessary to integrate the exposure assessment with hazard assessment. The first intends to determine routes of exposure and estimate exposure dosages (dose, duration and frequency) while the second intends to characterize the possible hazards (toxic effects) of polymeric NMs when in contact with the human body.

Exposure Assessment

Human exposure to polymeric NMs should be considered in the context of intentional nanomedicine applications, and in the context of occupational exposures of workers during the manufacturing processes, testing methods, distribution and handling/administration of polymeric NMs. Moreover, it cannot be disregarded situations where misuse and overuse are easily attained (Sayes et al., 2016). While in nanomedicine exposure scenarios, the administration route, the dose and duration of the exposure are well-defined, occupational exposure can happen through multiple and non-expected routes (**Figure 1**) and result in potentially cumulative levels of exposure and organ accumulation, whose impact in human health might be very different from the one predicted (Sayes et al., 2016). In fact, working with NMs involves challenges different from when working with bulk size materials, since they have increased ability to enter the human body, particularly through the respiratory airways, and to be translocated to the bloodstream and different organs (Yah et al., 2012). The lack of testing methods to detect and quantify the unintentional absorbed cumulative doses of these materials in the organism is currently, one of the main difficulties for designing predictive toxicological assays for occupational exposures. Therefore, exposure modeling arises as one alternative to allow occupational risk assessment. In the context of the FP7 NanoReg project a number of risk assessment tools for manufactured NMs, such as the CB NanoTool, the Nanosafer, and the Stoffenmanager-Nano have been examined and a new two-box nano specific exposure model (I-Nano) has been implemented (Jiménez et al., 2016). However, the need to rely on detailed input data (rate of particulate release from the source as well as the particle size distribution) which is not always available and its only application to inhalable exposures are some of the limitations present (Jiménez et al., 2016).

In the main, the NM routes of administration and exposure include respiratory, oral, ocular, dermal, and parenteral (injectable and implantable), each route presenting its own biodistribution pattern, resulting in different effects on human health. Indeed, the same composition, size and surface charge of the polymeric NM, might produce a different effect only by changing the exposure route (Sharma et al., 2016; Boyes et al., 2017). Importantly, it cannot be disregarded that the characteristics of the individual exposed, such as its age and health status, might also influence the NMs effect (Boyes et al., 2017). **Table 1** below summarizes the most common administration/exposure routes and the most important characteristics of NMs related to each one.

Hazard Assessment

The NMs toxic effects might occur in the administration site or they can result from the nano-sized materials ability to cross biological barriers (mucosal barriers, air-blood

TABLE 1 | Common routes of administration/exposure: important considerations relating nanomaterials characteristics and the various routes of exposure (Agrawal et al., 2014; Blanco et al., 2015; Date et al., 2016; Palmer and DeLouise, 2016; Boyes et al., 2017).

Route of exposure	Considerations on the exposure route	Nanomaterials characteristics and its relation with the exposure route	
Respiratory	- The most common route of exposure in the workplace - Nanomaterials inhaled for drug delivery must overcome bronchial mucociliary clearance - Inhaled nanomaterials may translocate to various regions of the brain, without crossing the blood–brain barrier - Inhaled nanomaterials can cross the alveoli–blood barrier, reaching the systemic-circulation portion of the cardiovascular system, without gastric passage or a first-pass metabolism	Size	Particles of about 20 nm have the highest proportional deposition rate in the alveolar region Particles smaller than 55 nm will penetrate the alveoli more efficiently than particles of 200 nm or greater
		Charge	Positively charged nanomaterials will exhibit greater interaction with the mucus' negative charge, thus avoiding fast mucociliary clearance
		Others	Inhalation flow-rate influences which region of the respiratory tract nanomaterials will reach The mucoadhesive properties of nanomaterials may increase their residence time in nasal mucosa, increasing drug absorption
Oral	- The first choice, non-invasive route - Inhaled nanomaterials cleared by the mucociliary system may be ingested - Ingested nanomaterials can reach and interact with different organs of the GI tract, such as the esophagus, stomach, small and large intestine and colon - Ingested nanoparticles can translocate into the systemic-circulation portion of the cardiovascular system, but to do so they must resist a wide range of pH environments and enzymatic degradation until they reach the small intestine - The absorption of ingested nanomaterials can be hindered by the poor permeability of the intestinal epithelium - Before reaching systemic circulation, ingested nanomaterials and cargo drugs will undergo a first-pass metabolism in the liver	Size	Particles with a diameter of <50 nm are known to cross epithelial barriers via paracellular passage, whereas larger particles are endocytosed by intestinal enterocytes (<500 nm) or taken up by M cells in Peyer's patches (<5 mm)
		Charge	Positively charged nanomaterials may exhibit greater interaction with intestinal mucus, therefore improving nanoparticle retention, but also decreasing nanoparticle absorption Neutrally charged nanomaterials diffuse more efficiently through the mucus layers
		Others	Surface coating nanomaterials with enteric polymers improves their resistance in the gastrointestinal (GI) tract Hydrophilicity and poor chemical or enzymatic stability in the GI tract diminish intestinal absorption
Injectable	- Most commonly used routes for injectables include intravenous, intramuscular, subcutaneous and intradermal administration - Injectables are the first choice for active pharmaceutical ingredients with narrow therapeutic indices, poor bioavailability or administration to unconscious patients - Intravenously injected nanoparticles are distributed throughout the circulatory system, reaching different organs - Intradermal injection leads to uptake by the lymphatic system - Intramuscularly injected particles are taken up via the neuronal and lymphatic systems - Intravenously injected nanoparticles are rapidly cleared by the kidneys and liver, or via the reticuloendothelial system (res)	Size	Smaller nanomaterials are mostly absorbed into capillaries, whereas larger nanomaterials are drained by the lymphatic system
		Charge	Nanomaterials with positively charged surfaces exhibit greater interactions with blood components and are therefore more rapidly cleared by the mononuclear phagocyte system Nanomaterials with neutral and negatively charged surfaces have longer circulation half-lives
		Others	Nanomaterial surface hydrophobicity increases interaction with blood components and therefore increases nanomaterial clearance via the mononuclear phagocyte system Nanomaterial surfaces coated with hydrophilic polymers or surfactants exhibit decreased clearance by opsonisation
Dermal	- Mostly used for the topical delivery of molecules intended to act locally (sunscreens, antifungals, anti-inflammatory or keratolytic agents, etc.) - Accumulation in hair follicles can increase the penetration of nanomaterials and cargo drugs - Damaged skin is more permeable to larger nanomaterials - Small, lipophilic molecules can penetrate easily into the skin and eventually reach the bloodstream or the lymphatic system	Size	Nanomaterials <20 nm may penetrate or permeate intact skin Nanomaterials <45 nm may penetrate damaged skin Nanomaterials >45 nm may translocate or be stored in skin appendages (i.e., air follicles)
		Charge	Cationic nanoparticles have an affinity for the negatively charged skin pores (which can limit their subsequent diffusion)
		Others	Physicochemical methods, such as the application of low-frequency ultrasound or surfactants (i.e., sodium lauryl sulfate), are used to disturb the skin barrier and promote nanomaterial absorption

barrier, blood-brain barrier, placenta barrier) reaching cells and tissues that are generally protected from bulk size materials (Buzea et al., 2007; Ai et al., 2011). This improved penetration of nanoparticles may increase the toxicity, but at the same time be advantageous in order to improve current therapies.

The uncertainties about using NMs for drug delivery and other biomedical applications result mainly from particle size reduction which is linked to increased reactivity and augmented toxicity (Ai et al., 2011). Nonetheless, several other properties can contribute to the effects of these nano-sized delivery systems, such as chemical composition, hydrophobicity/hydrophilicity, surface charge or shape. In the literature, there is a significant amount of data relating physicochemical features of NMs with cellular interaction, biodistribution, cytotoxicity and immune system activation, as reviewed elsewhere (Fröhlich, 2012; Ma et al., 2013; Salatin et al., 2015; Hoshyar et al., 2016; Jindal, 2017; Zhang et al., 2017). Nevertheless, general conclusions indicating toxicity trends for a specific nanoparticle physicochemical property, are limited to cautious hypotheses, only verified in particular scenarios (i.e., depending on the administration route, dose metrics, etc.). A review published in 2014 by Gatoo et al. (2014) discusses the correlation between the physicochemical properties of NMs and its toxicity. Briefly, smaller particles are often correlated with a higher toxicity, due to their increasing ability to cross biological barriers and reach different organs without being recognized by the reticuloendothelial system (RES) (Gatoo et al., 2014). Other characteristics, such as the non-spherical shape or the positive surface charge are also believed to contribute to an increased toxicity of NMs (Gatoo et al., 2014). Importantly, most of these conclusions are based on studies using inorganic NMs. Since chemical composition is one of the variables affecting the NMs toxicity, different behaviors can derive from the polymer composition and therefore, extensive extrapolations among all classes of NMs should be avoided. Moreover, most toxicity trends consider one characteristic at a time, but it is important to consider a holistic approach of the NM: all physicochemical characteristics are interconnected and together will influence its toxicological profile.

The key aspect to test polymeric NM for human toxic effects is the simulation of realistic human exposures. Those scenarios are difficult to simulate mainly due to: (1) the difficulty on transposing accurately human effective doses to *in vitro* settings; and (2) the difficulty to have complex *in vitro* systems, based on human cells or primary cell lines, that mimic the physiological complexity of the human body and its interaction with the materials (Sharma et al., 2016). Actually, most of the results of the application of *in vitro* studies to polymeric NMs might not reflect the realistic exposures, since the tests are performed at much higher concentrations than those that can be achieved in *in vivo* experiments (Landsiedel et al., 2017). Moreover, *in vitro* testing commonly use mass-based exposure metrics, which is believed to be a limiting factor, as particle number, surface areas and the formed agglomerates in suspension greatly influence the effective concentration delivered to cells (Hinderliter et al., 2010; DeLoid et al., 2014).

The intrinsic and distinctive characteristics inherent to the nanoscale dimension, might interfere with reagents and detection methods of *in vitro* assays recommended for bulk materials (Dobrovolskaia et al., 2009). For instance, NMs may bind to the marker enzyme lactate dehydrogenase (LDH) or they may interact with dyes and dye products, such as neutral red and the tetrazolium salt (MTT) (Landsiedel et al., 2017). On the other hand, polymeric NMs also go through modifications when in contact with biological matrices, such as: bio-corona formation, aggregation/agglomeration, dissolution, generation of new nano-sized particles (as a result of ionic salvation or degradation of surface coatings) (Sharma et al., 2016). These transformations of the NM can interfere with its toxicological effect, and most of the times are not considered during *in vitro* testing. Lastly, the selection of relevant positive and negative nano-sized controls is most of the times ignored, mainly because there is no clear knowledge-base on the toxicity (and especially immunotoxicity) of the different NMs (Dobrovolskaia and McNeil, 2013).

It is widely accepted that *in vitro* assays based on cell lines are an inexpensive and direct method to evaluate nanoparticle related toxicity in target tissues. However, results significantly depend on the chosen cell line (commonly immortalized cancer cells), incubation time, cell culture media or cell culture supplementation (Lorscheidt and Lamprecht, 2016). For instance, cell culture media supplementation with serum is highly likely to induce a protein corona in the surface of positively charged nanoparticles, changing its size and zeta potential, and therefore modifying the nanoparticle-cell interaction and uptake, and ultimately its biological effect (Khang et al., 2014; Lorscheidt and Lamprecht, 2016).

Overall, despite the great effort in developing high-throughput *in vitro* assays, there is still much variables to accurately mimic real exposure scenarios, and the results are often in disagreement with those of animal studies (DeLoid et al., 2014). Even so, nanotechnology laboratories are still searching for the best *in vitro* assays to replace *in vivo* testing and predict real exposure scenarios. This issue has been extensively discussed by Dobrovolskaia and McNeil (2013).

The urge to replace *in vivo* testing of toxicity, is motivated by the high costs and relatively low throughput of the assays, the inter-species variability particularly on the structure and function of the immune system, the low sensitivity of standard *in vivo* toxicity tests toward mild immunomodulation reactions, and most importantly, the ethical concerns about animal use (Dobrovolskaia and McNeil, 2013).

Altogether, it is widely accepted that efficient and cost-effective toxicological testing is required (DeLoid et al., 2014). For that reason, international organizations including OECD and ISO have developed official papers with considering the NMs properties and their influence on testing methods (Sharma et al., 2016; Dusinska et al., 2017).

In 2006, the OECD started a nanosafety programme overseen a Working Party on Manufactured Nanomaterials (WPMN), which aims to promote international cooperation on the human health and environmental safety of manufactured NMs, and involves the safety testing and risk assessment of manufactured NMs. Over the years they have published numerous reports and some test guidelines which are published in the OECD Series on the Safety of Manufactured Nanomaterials to provide up-to-date information on the OECD activities in this area (OECD[1]).

[1]OECD. Available online at: http://www.oecd.org/science/nanosafety/publications-series-safety-manufactured-nanomaterials.htm (accessed June 15, 2018).

In 2005, the Technical Committee ISO/TC 229 was created. It aims at the standardization in the field of nanotechnologies. The specific tasks of this committee include developing standards for terminology and nomenclature, metrology and instrumentation, test methodologies, modeling and simulations, and science-based health, safety, and environmental practices (Behzadi et al., 2014). Over the years, the committee has published several standards, from which we can highlight the recent ISO/TS 19006:2016 [Nanotechnologies-5-(and 6)-Chloromethyl-2′,7′-Dichloro-dihydrofluorescein diacetate (CM-H2DCF-DA) assay for evaluating nanoparticle-induced intracellular reactive oxygen species (ROS) production in RAW 264.7 macrophage cell line] and the ISO 19007:2018 (Nanotechnologies–*in vitro* MTS assay for measuring the cytotoxic effect of nanoparticles), discussed below (Bazile et al., 1995; Behzadi et al., 2017). In addition to the specific standards generated by this committee, in 2017, the part 22—Guidance on nanomaterials, was implemented in ISO 10993 (Biological evaluation of medical devices) (Barratt, 2000). Although this technical report represents the current technical knowledge related to NMs for medical devices it does not contain detailed testing protocols.

An important contribution to this field is being given by the US National Cancer Institute Nanotechnology Characterization Laboratory, whose main objective is to facilitate the development and translation of nanoscale particles and devices for clinical applications. In fact, they have described several protocols for *in vitro* characterization as well as for *in vivo*, and for the physicochemical characterization of NMs (Assay Cascade Protocols—https://ncl.cancer.gov/resources/assay-cascade-protocols). In parallel, the European Nanomedicine Characterization Laboratory (EUNCL) is also developing standard operating procedures (SOPs) to allow the physical, chemical, *in vitro* and *in vivo* testing of nanobiomaterials (http://www.euncl.eu/).

HAZARD CHARACTERIZATION OF POLYMERIC NANOMATERIALS—LITERATURE REVIEW

NMs toxicity should be evaluated by *in vivo* and *in vitro* assays considering its effect in the host physiological and immunological integrity (Yildirimer et al., 2011). Most of *in vitro* assays available for testing a NM toxicological effects are focused on the molecular mechanisms underlying toxicity (i.e., oxidative stress generation and inflammation), while *in vivo* assays, particularly acute and repeated dose toxicity assays assess the effects on vital organ functions [i.e., biomarkers of liver function, such as aspartate aminotransferase (AST) and alanine aminotransferase (ALT)].

Table 2 summarizes the studies collected from the literature of the last 10 years, assessing the toxicity of polymeric NMs for the endpoints studied. The polymers considered for analysis were chitosan, polylactic acid (PLA), polyhydroxyalkanoate (PHA), poly(lactic-co-glycolic acid) (PLGA) and policaprolactone (PCL). From the table systematization we can highlight three main issues: (1) chitosan based NPs are the most studied polymeric

TABLE 2 | Systematization of the toxicity results described in the literature for chitosan, PLA, PHA, PLGA, and PCL nanomaterials.

		Acute toxicity					Repeated-dose toxicity			Inflammation	Oxidative stress	Genotoxicity*	Toxicity on Reproduction	Haemolysis
		Via inhalation	Via ingestion	Via ocular contact	Via injection (i.v.)	Via injection (others)	Via ingestion	Via injection (i.v.)	Via injection (others)					
Chitosan	Bare[a]			1						1 1	3 1		2 2	2 1
	Blend[b]	1	2		1		6	1		2	1	1	1	1
PLA	Bare[a]				1					1	2			1
	Blend[b]				1			1		1	1			2 1
PHA	Bare[a]													
	Blend[b]													
PLGA	Bare[a]				1					3	1			
	Blend[b]	1			3 1	1	2	2	1	1 2	4	2 1	2	3 2 1
PCL	Bare[a]				1					1	1			
	Blend[b]				2									

The number in each cell represents the number of studies supporting each conclusion according to the following color scheme: red indicates studies where all the concentrations tested induced an effect; orange indicates studies where at least one concentration tested induced an effect; green indicates studies that revealed no toxicity for any of the concentrations tested; (blank) no data available. Further details on each study are described in ***Tables 3–8****.*

[a]*"Bare" polymer nanomaterials produced using crosslinkers or surfactants only, and which were not loaded with drugs, genes or proteins.*

[b]*"Blend" polymeric nanomaterials, functionalized/chemically modified polymers or particles loaded with drugs, genes, or proteins).*

**Genotoxicity includes Mutagenicity and Carcinogenicity.*

NMs followed by PLGA based NPs; (2) the different colors illustrating the generation or absence of effect for each endpoint according to the different studies, reflects the inconsistency in the results found for the same type of NM; (3) No data on PHA based NMs is available regarding those endpoints. The inconsistent results must be carefully analyzed because in fact they may be complementary results, as the NM characteristics, their concentrations, the cellular and animal models used and even the experimental methodology are significantly different among authors. Therefore, in the next sub-chapters each endpoint and respective studies will be discussed in detail in an attempt to scrutiny possible toxicity trends for polymeric NMs. To note, over the following discussion, the effect of some other polymers, such as alginate, polyethylene glycol (PEG), pluronic and polyvinyl alcohol (PVA) are addressed as they are often used as surface coatings and blends in chitosan, PLGA, PLA and PCL based nanomaterials.

In vivo Toxicity Studies

To study the toxicity of the NMs and to identify possible risks to the human health, researchers perform *in vivo* tests in animals (most time non-primates) to evaluate acute and repeated-dose (subacute, sub-chronic or chronic) toxicity. These studies, although highly valuable to understand the adsorption, distribution, metabolism and excretion (ADME) of the NMs as well as the immune system interactions, should be limited to a minimum according to the 3Rs strategy (replacement, reduction and refinement) (Oostingh et al., 2011; Dusinska et al., 2017). To note, in 2018, OECD guidelines for the testing of chemicals were adapted to accommodate the testing of NMs (OECD, 2018b,c).

As illustrated in **Table 3**, the available research articles testing *in vivo* the toxicity of NMs are characterized by a great variability between the rodent's species (or other animals, such as carps) used in the assays, the number of days (for the repeated-dose toxicity studies) and even for the endpoints that are analyzed. Some of the most reported endpoints are the clinical appearance of the animal, clinical signs of infection, hematological parameters, serum hemoglobin levels and albumin/globulin ratio, organ weights, and enhanced histopathology evaluation different organs (Dusinska et al., 2017).

As already stated, chitosan NMs are the most studied polymeric NMs regarding toxicity. Several studies were found in the literature evaluating the toxicity of blend chitosan NPs upon repeated oral administrations. Despite the great heterogeneity among the used NPs (chitosan/alginate NPs, chitosan/glutamic acid NPs, oleoyl-carboxy methyl chitosan NPs, chitosan coated PLGA NPs and α-tocopherol succinate-g-carboxymethyl chitosan NPs), the animal models (Wistar and Sprague Dawley rats, ICR mice and Carps) and the dosing schedules (7–19 days), all revealed no *in vivo* toxicity (Sonaje et al., 2009; Liu et al., 2013; Jena and Sangamwar, 2016; Aluani et al., 2017; Maity et al., 2017; Radwan et al., 2017b; Sharma et al., 2017). Moreover, the conclusion of no toxicity was based on different evaluated parameters for each study, except for the histopathological analysis, which was performed in all studies (generally liver and intestine histopathology with no signs of tissue damage). Among these studies, only Sonaje et al. (2009), Maity et al. (2017), and Radwan et al. (2017b) have evaluated biochemical parameters in blood, and in common have tested serum alanine transaminase (ALT), alkaline phosphatase (ALP) and aspartate transaminase (AST) activities, and their results were in agreement (no changes in comparison to the control group). Moreover, chitosan based NPs lack of oral toxicity was also reported for single dose administrations (Mukhopadhyay et al., 2015; Leng et al., 2018). Therefore, considering these reports, we may hypothesize that chitosan NPs (as well as bulk chitosan Chang et al., 2014) do not present oral toxicity. On the other hand, although only 2 reports were found testing chitosan NPs toxicity through the injectable route (Yuan et al., 2015; Shan et al., 2017), a dose dependent toxicity was found, even though chitosan and chitosan NPs appear to be hemocompatible in some hemolysis assays (Fernandes et al., 2010; Lü et al., 2011; Wang et al., 2014; Kumar et al., 2017; Leng et al., 2018).

On its turn, PLGA NPs also exhibited no toxicity on repeated oral administration studies (Moraes Moreira Carraro et al., 2017; Sharma et al., 2017), as well as on the majority of intravenous (i.v.) administration studies (VasanthaKumar et al., 2014; Fasehee et al., 2016; Radwan et al., 2017a). Only one article described some toxicity when using danorubicin loaded PEG-PLL-PLGA NPs (Guo et al., 2015). Unfortunately, the formulations in those reports were loaded with the active drug and no information was given on blank NPs. Therefore, not only the effects might be associated with the drugs (rather than the NPs polymers or characteristics), but also no comparison on the dose of the NPs administered can be made between articles, as they only refer to the equivalent amount of drug administered. Similarly (Li et al., 2014), tested two mPEG-PLA NPs (with different copolymerization degrees) loaded with paclitaxel in beagle dogs by i.v. administration in the foreleg. Despite the results had revealed differences between the NPs, being the ones with the 50/50 ratio mPEG:PLA more toxic than the ones with the 40/60, no experiments were made with unloaded NPs, restricting the extrapolation of data.

Oxidative Stress

Reactive oxygen species (ROS) are produced during cellular metabolism in the forms of hydrogen peroxide (H_2O_2), superoxide anion ($O2^{-\bullet}$) and hydroxyl ($^{\bullet}OH$) radicals (Ngo and Kim, 2014; Lorscheidt and Lamprecht, 2016). Besides its role in cell signaling and regulation, excessive oxidative stress can induce oxidative damage to cells through lipid peroxidation, DNA disruption, interference with signaling functions, gene transcription modulation and inadvertent enzyme activation, causing several health disorders, such as hypertensive, cardiovascular, inflammatory, aging, diabetes mellitus, and neurodegenerative and cancer diseases (Sharifi et al., 2012; Ngo and Kim, 2014; Lorscheidt and Lamprecht, 2016).

The most used probe to access ROS is the H_2O_2 specific 2′,7′-dichlorodihydrofluorescein diacetate (H_2DCFDA or DCFH-DA), which diffuses freely through the cell membrane and is hydrolyzed inside the cells into H_2DCF carboxylate anion form, which is in its turn non-permeable (Kalyanaraman et al., 2012; Oparka et al., 2016). Then, H_2DCF is oxidized and results in the formation of the fluorescent product (DCF), which is excited at 495 nm and emits at 520 nm (Kalyanaraman et al.,

TABLE 3 | Review of original articles assessing *in vivo* the toxicity of polymeric nanoparticles.

Nanomaterial	Polymer characterization	Nanomaterial characterization	Testing method	Model	Administration route	Dose/ concentration range	Results	References
Chitosan NPs	Chitosan hydrochloride salt (Protasan CL 110)	289 nm + 36 Mv (phosphate buffer)	*In vivo* exposure (acute toxicity)	New Zealand rabbits	Ocular	30 μL of the 0.5 mg/mL CSNP formulation in the right eye every 30 min for 6 h	No signs of discomfort in rabbits eyes 24 h after the administration No histopathological changes in the eye compared to control	de Salamanca A et al., 2006
Insulin (ins) loaded alginate/chitosan (Alg/chi) NPs	Depolymerized chitosan (65 and 25 kDa, and 86% DD[a]) Alginate (M/G[b] content 64.5/35.5%)	3:1:1[c] 104 nm, + 4 mV 3:2:1[c] 157 nm, + 10 mV 3:3:1[c] 216 nm, + 16 mV	*In vivo* exposure (acute toxicity)	Swiss albino mice	Oral	150 mg/kg b.w. (ratio alg:chi:ins 3:1:1)	No mortality No change in biochemical or histopathological parameters No liver or renal toxicity	Mukhopadhyay et al., 2015
Eudragit® S100/alginate-enclosed chitosan-calcium phosphate-loaded lactoferrin nanocapsules	na	240 nm −2.6 mV	*In vivo* exposure (acute toxicity: 24 h)	*Artemia salina* (brine shrimp)	Oral (diluted in the water)	20–5,000 μg/mL	No lethality	Leng et al., 2018
Pluronic coated PLGA NPs	75:25 Resomer® RG756 and Pluronic F68	240 nm −35 mV	*In vivo* exposure (acute toxicity)	Balb/cJ mice	Intratracheal (nebulization)	250 μg/50 μL in 5% glucose	Coated PLGA NPs did not induce an inflammatory response in mice, with no alterations of cellular population, protein quantity or expression of cytokines in BAL	Aragao-Santiago et al., 2015
PVA coared PLGA NPs	75:25 Resomer® RG756 and PVA (87–89% hydrolyzed, 30–70 kDa)	220 nm −4 mV	*In vivo* exposure (acute toxicity)	Balb/cJ mice	Intratracheal (nebulization)	250 μg/50 μL in 5% glucose	Coated PLGA NPs did not induce an inflammatory response in mice, with no alterations of cellular population, protein quantity or expression of cytokines in BAL	Aragao-Santiago et al., 2015
Chitosan coated PLGA NPs	75:25 Resomer® RG756 and Protasan® UP CL113,75–90% deacetylation, 50–150 kDa	200 nm + 18 mV	*In vivo* exposure (acute toxicity)	Balb/cJ mice	Intratracheal (nebulization)	250 μg/50 μL in 5% glucose	Coated PLGA NPs did not induce an inflammatory response in mice, with no alterations of cellular population, protein quantity or expression of cytokines in BAL	Aragao-Santiago et al., 2015

(Continued)

TABLE 3 | Continued

Nanomaterial	Polymer characterization	Nanomaterial characterization	Testing method	Model	Administration route	Dose/ concentration range	Results	References
Dissulfiram loaded PLGA nanoparticles, coated with PEG and functionalized with folate	PLGA (RG 504 H, acid terminated, lactide:glycolide 50:50, Mw: 38,000) and PEG-bis-amine (Mn: 10,000)	204 nm −5.24 mV	*In vivo* exposure (acute toxicity)	BALB/C mice	Intravenous	Equivalent to 120 and 60 mg/kg b.w. of dissulfiram	No lethality, no hematological parameters changes *(2,000 mg/kg of loaded NPs ∼100 mg/kg equivalent of disulfiram)*	Fasehee et al., 2016
Dissulfiram loaded PLGA nanoparticles, coated with PEG and functionalized with folate	PLGA (RG 504 H, acid terminated, lactide:glycolide 50:50, Mw: 38,000) and PEG-bis-amine (Mn: 10,000)	204 nm −5.24 mV	*In vivo* exposure (acute toxicity)	BALB/C mice	Intraperitoneal	Equivalent to 2,000 and 225 mg/kg b.w. of dissulfiram	No lethality, hematological parameters altered *(2,000 mg/kg of loaded NPs ∼100 mg/kg equivalent of disulfiram)*	Fasehee et al., 2016
Poly(ε-caprolactone)-poly(ethylene glycol)-poly(ε-caprolactone) (PCEC) nanoparticles	PCEC copolymer with a molecular weight of 17,500 (1H NMR spectrum)	40 nm	*In vivo* exposure (acute toxicity)	Sprague-Dawley rats	Intravenous	2.4 g/kg (divided in 2 administration within 12 h)	No clinical symptoms 14-days post-injection No histopathological findings after animal's sacrifice	Huang et al., 2010
Paclitaxel loaded PLA NPs	Inherent viscosity 0.55–0.75 dL/g and average molecular weight 75,000–1,20,000	150–175 nm, and zeta potentials lower than −15 mV	*In vivo* exposure (acute toxicity)	Wistar rats	Intravenous	10 mg/kg b.w.of paclitaxel	No induction of histopathological alterations (number, arrangement and architecture of cells) of the heart, lungs, liver, spleen, kidney, and brain Blank nanoparticles (unspecified dose) did not cause any toxicity as well	VasanthaKumar et al., 2014
Paclitaxel loaded PLGA NPs	Lactide:glycolide 50/50 and average molecular weight 5000–1,5000	150–175 nm <-15 mV	*In vivo* exposure (acute toxicity)	Wistar rats	Intravenous	10 mg/kg b.w.of paclitaxel	No induction of histopathological alterations (number, arrangement and architecture of cells) of the heart, lungs, liver, spleen, kidney, and brain Blank nanoparticles (unspecified dose) did not cause any toxicity as well	VasanthaKumar et al., 2014

(Continued)

TABLE 3 | Continued

Nanomaterial	Polymer characterization	Nanomaterial characterization	Testing method	Model	Administration route	Dose/ concentration range	Results	References
Paclitaxel loaded PCL NPs	Average molecular weight 14,000 and average molecular number 10,000	150–175 nm, and zeta potentials lower than −15 mV	*In vivo* exposure (acute toxicity)	Wistar rats	Intravenous	10 mg/kg b.w.of paclitaxel	No induction of histopathological alterations (number, arrangement and architecture of cells) of the heart, lungs, liver, spleen, kidney, and brain Blank nanoparticles (unspecified dose) did not cause any toxicity as well	VasanthaKumar et al., 2014
Danorubicin loaded polyethylene glycol-poly L-lysine-poly lactic-co-glycolic acid (PEG-PLL-PLGA) NPs	na	229 nm −20 mV	*In vivo* exposure (Acute toxicity)	Kunming mice	Intravenous	40, 30, 22, 17, and 13 mg/kg b.w.of Danunorubicin (DNR) loaded in the particles	LD_{50}: 464.4 mg/kg b.w.(23.22 mg/kg b.w.of DNR) 95% confidence interval: 399–542 mg/kg b.w.(20–27 mg/kg b.w.OF DNR) No significant pathological changes of organizational structure and cell morphology	Guo et al., 2015
Danorubicin loaded polyethylene glycol-poly L-lysine-poly lactic-co-glycolic acid (PEG-PLL-PLGA) NPs	na	229 nm −20 mV	*In vivo* exposure (Acute toxicity)	Kunming mice	Intravenous	200 mg/kg b.w.of DNR loaded in the particles	No lethality No physical signs of toxicity No changes in hepatic or renal markers	Guo et al., 2015
Amphotericin loaded PEG-PLGA nanoparticles	Copolymer produced with 6,000 Da PLGA (lactic to glycolic acid molar ratio of 1:1) and 15% PEG	25 nm	*In vivo* exposure (acute toxicity)	Albino Sprague-Dawley rats	Intravenous	Equivalent to 1 mg/kg of amphotericin and blank NPs	No nephrotoxicity (evaluated by renal injury biomarkers BUN and PCr) Although described no results presented for blank nanoparticles group	Radwan et al., 2017a
Angiopoietin-2 (Ang2) small interfering (si)RNA plasmid chitosan magnetic nanoparticles (CMNPs)	Chitosan polysaccharides (Mw[d] 1,38,0000, 90% DD)	na[e]	*In vivo* exposure (acute toxicity)	Kunming mice	Intravenous	92, 153, 255, 424, and 707 mg/kg b.w.	All doses: no mortality, no changes in b.w. Higher doses: short-term staggering, reduced activities and accelerated breathing, as well as transient reduction of eating, lung uneven dark red coloring and particles aggregated inside the lungs *Based on the conversion method of equivalent dose co efficient, the non-toxic dose in humans should be < 222 mg/kg per day for 14 day, overall a total of 3117 mg/kg, which is significantly higher compared with the quantity required clinically*	Shan et al., 2017

(Continued)

TABLE 3 | Continued

Nanomaterial	Polymer characterization	Nanomaterial characterization	Testing method	Model	Administration route	Dose/ concentration range	Results	References
Tween 80 modified chitosan nanoparticles (TmCS-NPs)	Chitosan (100 kDa, 85% DD)	251 nm +26.5 mV	*In vivo* exposure (7 days)	Sprague-Dawley rats	Intravenous	3, 10, and 30 mg/kg b.w.	Body weight of rats remarkably decreased dose-dependently Dose-dependent neuron apoptosis and slight inflammatory response in the frontal cortex, and downregulation of GFAP expression in the cerebellum Study aim: neurotoxicity	Yuan et al., 2015
Chitosan/alginate (Chi/alg) NPs	Chitosan (Mv^f of 1,10,000–1,50,000) Sodium alginate (very low viscosity)	1:10[g] 300 nm, −30 mV (water) 900 nm, −25 mV (cell culture medium) 10:1[g] 500 nm, + 30 mV (water) 1,100 nm, + 10 mV (cell culture medium)	*In vivo* exposure (14 days)	Wistar albino rats	Oral	9 mg/kg b.w. (in 0.5 ml/100 g b.w.)	No mortality No behavioral changes No changes in body weight or relative liver weight No changes in MDA levels GSH levels decreased for the 10:1 (chit:alg) ratio No hematological parameters altered	Aluani et al., 2017
Chitosan/alginate (Chi/alg) NPs	Chitosan (low molecular weight; 200 cp viscosity) Sodium Alginate (low viscosity −0.02 Pa.s)	1:9[g] 254 nm, −35 mV	*In vivo* exposure (14 days)	Wistar albino rats	Oral	24.5 mg (in 2 mL)	No mortality No adverse reaction in the condition of the eye, nose and motor activity No histopathological alteration in animal's organs Normal feed intake and weight gain	Radwan et al., 2017b
pH sensitive chitosan/poly-γ-glutamic acid (Chi/PGA) NPs	Chitosan (80 kDa, 85% DD) γ -PGA (60 kDa)	218 nm +25.3 mV	*In vivo* exposure (14 days)	ICR mice	Oral	100 mg/kg b.w.	No clinical signs or weight loss No change in hematological or biochemical parameters No pathological changes in liver, kidney and intestinal segments *The dose (100 mg/kg) was 18 times higher than the dose they used in the pharmacokinetic study of insulin-loaded nanoparticles (5.5 mg/kg)*	Sonaje et al., 2009
α-tocopherol succinate-grafted carboxymethyl chitosan polymeric micelles	low molecular weight chitosan: 22 kDa	114–187 nm −20 to −22 mV	*In vivo* exposure (14 days)	Sprague Dawley rats	Oral	500 mg/kg b.w.	No mortality Normal weight gain Normal red blood cells morphology No pathological changes in the liver, kidney, and intestine	Jena and Sangamwar, 2016

(Continued)

TABLE 3 | Continued

Nanomaterial	Polymer characterization	Nanomaterial characterization	Testing method	Model	Administration route	Dose/ concentration range	Results	References
Alginate coated CS core-shell NPs	Sodium alginate (ALG) of low viscosity, ∼50 kDa Low molecular weight CS (25 kDa, DDA 82%)	216 nm −36 mV (with naringenin encapsulated)	*In vivo* exposure (19 days)	Wistar rats	Oral	50 mg/kg b.w. (blank NPs)	No significant differences in hair texture or color, water and food intake No hepatic toxicity No abnormalities found in the hepatic or intestinal tissues No hematological parameters change (glucose and lipids)	Maity et al., 2017
Oleoyl-carboxymethyl-chitosan (OCMCS) nanoparticles	170 kDa chitosan, 92.56% DD modified with chloroactic acid and oleoyl chloride	171 nm + 19 mV	*In vivo* exposure (7 days)	Carp	Oral (catheter)	2 mg/mL (500 μL)	No lethality or histopathological signs of inflammation (liver, spleen, kidneys)	Liu et al., 2013
Amphotericin loaded PEG-PLGA NPs	PLGA lactic to glycolic acid 50:50 with 40–75 KDa and PEG with 10 KDa	170 nm	*In vivo* exposure (7 days)	Wistar rats	Intraperitoneal and oral	Equivalent to 10 mg/kg b.w.of amphotericin	No lethality, no body weight loss, no hematological parameters alterations, no histopathological changes in liver, and kidneys	Moraes Moreira Carraro et al., 2017
Amphotericin loaded PLGA NPs	PLGA lactic to glycolic acid 50:50 with 40–75 KDa	190 nm						
Chitosan/alginate (Chi/alg) NPs	Chitosan (Mv^h of 1,10,000–1,50,000) Sodium alginate (very low viscosity)	1:10[i] 300 nm, −30 mV (water) 900 nm, −25 mV (cell culture medium) 10:1[i] 500 nm, + 30 mV (water) 1,100 nm, + 10 mV (cell culture medium)	*In vivo* exposure (14 days)	Wistar albino rats	Oral	9 mg/kg b.w. (in 0.5 ml/100 g b.w.)	No mortality No behavioral changes No changes in body weight or relative liver weight No changes in MDA levels GSH levels decreased for the 10:1 (chit:alg) ratio No hematological parameters altered	Aluani et al., 2017
Chitosan/alginate (Chi/alg) NPs	Chitosan (low molecular weight; 200 cp viscosity) Sodium Alginate (low viscosity −0.02 Pa.s)	1:9[i] 254 nm, −35 mV	*In vivo* exposure (14 days)	Wistar albino rats	Oral	24.5 mg (in 2 mL)	No mortality No adverse reaction in the condition of the eye, nose, and motor activity No histopathological alteration in animal's organs Normal feed intake and weight gain	Radwan et al., 2017b

(Continued)

TABLE 3 | Continued

Nanomaterial	Polymer characterization	Nanomaterial characterization	Testing method	Model	Administration route	Dose/ concentration range	Results	References
pH sensitive chitosan/poly-γ-glutamic acid (Chi/PGA) NPs	Chitosan (80 kDa, 85% DD) γ -PGA (60 kDa)	218 nm +25.3 mV	*In vivo* exposure (14 days)	ICR mice	Oral	100 mg/kg b.w.	No clinical signs or weight loss No change in hematological or biochemical parameters No pathological changes in liver, kidney, and intestinal segments *The dose (100 mg/kg) was 18 times higher than the dose they used in the pharmacokinetic study of insulin-loaded nanoparticles (5.5 mg/kg)*	Sonaje et al., 2009
Dissulfiram loaded PLGA nanoparticles, coated with PEG and functionalized with folate	PLGA (RG 504 H, acid terminated, lactide:glycolide 50:50, Mw: 38,000) and PEG-bis-amine (Mn: 10,000)	204 nm −5.24 mV	*In vivo* exposure (7 days)	BALB/C mice	Intravenous	Equivalent to 120, 60, 30, and 15 mg/kg of dissulfiram 120 mg/kg b.w. blank nanoparticles	No lethality, no hematological parameters changes *(2,000 mg/kg of loaded NPs ∼100 mg/kg equivalent of disulfiram)*	Fasehee et al., 2016
Polyphenolic bio-enhancers with oleanolic acid in chitosan coated PLGA NPs (CH-OA-B-PLGA NPs)	chitosan (molecular weight 150 kDa, deacetylation degree 85%), Poly (lactide-coglycolide) (PLGA) 50:50, mw 40–75 kDa	342 nm + 34 mV	*In vivo* exposure (15 days)	Sprague Dawley rats	Oral	100 mg/kg b.w. of OA	No mortality No histopathological changes No abnormal behavior *(100 mg/kg is the double of the OA effective dose)*	Sharma et al., 2017
Polyphenolic bio-enhancers with oleanolic acid in PLGA NPs (OA-B-PLGA NPs)	chitosan (molecular weight 150 kDa, deacetylation degree 85%), Poly (lactide-coglycolide) (PLGA) 50:50, mw 40–75 kDa	221 nm −19 mV	*In vivo* exposure (15 days)	Sprague Dawley rats	Oral	100 mg/kg b.w. of OA	No mortality No histopathological changes No abnormal behavior *(100 mg/kg is the double of the OA effective dose)*	Sharma et al., 2017
Amphotericin loaded PEG-PLGA nanoparticles	Copolymer produced with 6,000 Da PLGA (lactic to glycolic acid molar ratio of 1:1) and 15% PEG	25 nm	*In vivo* exposure (7 days)	Albino Sprague-Dawley rats	Intravenous	Equivalent to 1 mg/kg of amphotericin and blank NPs	No nephrotoxicity (evaluated by renal injury biomarkers BUN and PCr) No histopathological damage of the kidney Although described no results presented for blank nanoparticles group	Radwan et al., 2017a

(Continued)

TABLE 3 | Continued

Nanomaterial	Polymer characterization	Nanomaterial characterization	Testing method	Model	Administration route	Dose/ concentration range	Results	References
Paclitaxel loaded monomethoxypoly (ethylene glycol)-b-poly(lactic acid) (mPEG-PLA) polymeric micelles	mPEG-PLA copolymer (40/60) with a number average molecular weight of 4488.4	(40/60): 37 nm After incubation with BSA: 40 nm (50/50): 44 nm After ncubation with BSA: 71 nm	*In vivo* exposure (4 weeks, 1 injection per week)	Beagle dogs	Injection in the foreleg (intravenous)	Equivalent to 0.5 mg/mL of paclitaxel	mPEG-PLA (40/60): no sign of pathological changes except the lung congestion. mPEG-PLA (50/50): liver index was higher and the thymus index was lower;pylorus and small intestine congestion were also observed The toxicity of paclitaxel loaded mPEG-PLA (40/60) polymeric micelles was significantly lower than those of mPEG-PLA (50/50)	Li et al., 2014
Angiopoietin-2 (Ang2) small interfering (si)RNA plasmid chitosan magnetic nanoparticles (CMNPs)	Chitosan polysaccharides (Mw[j] 13,80,000, 90% DD)	na[e]	*In vivo* exposure (14 days)	Sprague-Dawley rats	Intravenous	35, 70, and 353 mg/kg b.w.	Higher doses: chronic pulmonary congestion in Sprague-Dawley rats, as well as simultaneous pulmonary inflammation and partial fibrosis All doses: total number of white blood was significantly higher *Based on the conversion method of equivalent dose co-efficient, the non-toxic dose in humans should be <222 mg/kg per day for 14 day, overall a total of 3,117 mg/kg, which is significantly higher compared with the quantity required clinically*	Shan et al., 2017

[a] *DD, deacetylation degree.*
[b] *M/G, β-D-mannuronic acid/α-L-guluronic acid.*
[c] *Ratio alg:chi:ins.*
[d] *Mw, molecular weight number.*
[e] *na, not available.*
[f] *Mv, viscosity molecular weight.*
[g] *Ratio chi:alg.*

2012; Oparka et al., 2016). Using this probe, the intracellular signal can be monitored by several techniques, such as confocal microscopy and flow cytometry (Kalyanaraman et al., 2012). During the H_2DCF oxidation, there is a formation of a superoxide radical that can stimulate the auto-amplification of the DCF signal (Oparka et al., 2016). On the other hand, DCF is cell permeable, which means it leaks out of cells over time and can induce measurement errors depending on the analysis time (Lorscheidt and Lamprecht, 2016). A variant of the DCFH-DA probe is the 5-(and 6)-chloromethyl-derivative, that leads to the formation of fluorescent CM-DCF, which displays a lower passive leakage from the cell (Oparka et al., 2016). Alternatively, the fluorescence read-out can also be performed using a fluorescence microplate reader and in this situations errors can result from nanoparticle quenching effect over the DCF fluorescence (Aranda et al., 2013).

Free radical production is the highest in macrophages (Singh and Ramarao, 2013) which is in line with the protocol suggested in ISO/TS 19006:2016-Nanotechnologies-5-(and 6)-Chloromethyl-2′,7′-Dichloro-dihydrofluorescein diacetate (CM-H_2DCF-DA) assay for evaluating nanoparticle-induced intracellular reactive oxygen species (ROS) production in RAW 264.7 macrophage cell line. Nonetheless, according to this ISO, other cell lines similar to RAW 264.7 (BEAS-2B, RLE-6TN, HEPA-1, HMEC and A10) can be used with due validations. In this technical specification, the protocol was validated for conducting the assay in 24 well-plates, for 6 and 24 h incubation with the NPs and controls, and 30 min incubation with the probe before flow cytometry analysis. To note, the recommendation is the use of Sin-1 as positive control (maximum ROS production due to cell death) and polystyrene NPs as negative control.

As it is possible to observe from **Table 4**, most studies reported in the literature do not use RAW 264.7 cells, neither do they employ 6 and 24 h incubation.

In detail, Grabowski et al. found a transient production of ROS with chitosan stabilized PLGA NPs in THP-1 cells (Grabowski et al., 2015), Sharma et al. verified an increased oxidative effect of oleanolic acid when delivered by chitosan coated PLGA NPs in MDAMB-231 cells (Sharma et al., 2017), Sarangapani et al. found an increase in ROS production in BCL2(AAA) Jurkat cells with chitosan NPs (Sarangapani et al., 2018) and Gao et al. found an increase in ROS production in zebrafish embryos incubated with chitosan NPs (Hu et al., 2011). In contrast, Bor et al. found a reduction in ROS production with plasmid loaded chitosan NPs and chitosan NPs in Hela, THP-1 and MDAMB-231 cells (Bor et al., 2016). These inconsistent results, obtained with different chitosan based nanomaterials, different cellular models and concentrations do not allow for a straightforward interpretation of the oxidative effect of nanoscale chitosan. Among these articles, only Sarangapani et al. compared the activity of chitosan NPs with bulk chitosan (at the same concentrations) and verified a similar but lower concentration dependent effect for the polymer (Sarangapani et al., 2018). Also, it is important to note, that the tested concentrations (10–50 μg/mL), caused increasing cell death as verified by the MTT assay, and therefore, the oxidative stress was the mechanism identified as responsible for cellular toxicity. In contrast, Bor et al. verified that chitosan NPs reduced ROS production in several cell lines (also tumor derived cells), but they used a concentration that did not cause cell death (Bor et al., 2016). Therefore, although at first sight the results are conflicting, they cannot be directly compared, but we can hypothesize that chitosan NPs might influence ROS production in a concentration dependent manner. One of the widely reported characteristics of bulk chitosan is its anti-oxidant activity, attributed to its scavenging activity against several radicals, such as hydroxyl ($^{\bullet}$OH), superoxide anion ($O_2^{\bullet -}$), 1,1-diphenyl-2-picryl-hydrazy (DPPH) and alkyl (Ngo and Kim, 2014). This scavenging activity, has been widely demonstrated by cell-free *in vitro* assays (Je et al., 2004; Yen et al., 2008; Ngo and Kim, 2014). In fact, in the article discussed before (Sarangapani et al., 2018), although reporting that chitosan and chitosan NPs increased ROS production in BCL2(AAA) Jurkat cells, they also verified that the same concentrations increased free radical scavenging activity using chemical assays. Therefore, some compounds may demonstrate chemically some antioxidant activity, which is not verified at cellular and physiological level (Lü et al., 2010).

Regarding bare PLGA NPs its effect on ROS production was documented by 3 authors Platel, Singh, and Granbowski (Singh and Ramarao, 2013; Grabowski et al., 2015; Platel et al., 2016) all using different cellular models. Nevertheless, Platel tested only one low concentration of PLGA NPs (40 μg/mL) and found no effect on ROS production (Platel et al., 2016), while the other 2 authors found an increase in ROS production that was dose dependent (Singh and Ramarao, 2013; Grabowski et al., 2015). Curiously, both tested 1 mg/mL, but Singh et al. reported that this concentration quenched the fluorescence of the probe, therefore interfering with the results (Singh and Ramarao, 2013). On its turn, Grabowski et al. found that at the concentration of 1 mg/mL only a transient production of ROS was verified at 5 min after the incubation with PLGA NPs, and at longer incubation times, no significant ROS increase was verified (Grabowski et al., 2015). Although the authors do not explore this achievement, we could hypothesize that a similar interference as reported by Singh and Ramarao might be occurring.

Overall, not only PLGA NPs, but in general the polyester NPs appear to induce ROS production in a concentration dependent manner. Other studies confirm this effect for concentrations above 300 μg/mL (Singh and Ramarao, 2013; Legaz et al., 2016; Da Silva et al., 2019). Nevertheless, this conclusion has reservations since for instance, Da Silva et al. tested two different PLA NPs, and only one of these induced ROS production.

Inflammation

Presently, inflammation is acknowledged as a mechanism of immune defense and repair, in addition to its widely accepted role in passive cell injury and cell death (Wallach et al., 2013; Khanna et al., 2015). Interestingly, several molecules are associated with inflammation and cell death. For instance TNF-α, IL-1β, IL-6, IFN-γ, IL-17, IL-8, IL-2, GM-CSF, TGF-β, and IL-12 are examples of pro-inflammatory mediators frequently evaluated in the context of cellular toxicity induced by nanomaterials (Khanna et al., 2015; Lorscheidt and Lamprecht, 2016).

TABLE 4 | Review of original articles assessing oxidative stress induction by polymeric nanoparticles.

Nanomaterial	Polymer characterization	Nanomaterial characterization	Testing method	Cellular model	Dose/ concentration range	Results	Observations	References
Chitosan NPs	Low molecular weight chitosan (50–190 kDa, 75–85% DD[a])	92 nm +32 mV	2′,7′-dichlorodihydro-fluorescein diacetate (H_2DCF-DA) probe (72 h incubation)	HeLa, MDA-MB-231 and THP-1 cells	1%	Significant reduction in the generation of reactive oxygen species when compared to control	Similar results for plasmid loaded chitosan NPs	Bor et al., 2016
Chitosan NPs	80% DD 400 kDa	100 nm + 19 mV	Dichlorofluorescin diacetate (DCFH-DA) probe (6/12/24 h incubation)	Hela and SMMC-7721 cells	10; 100 μg/mL	Chitosan NPs increase ROS production in a concentration-dependent manner	–	Wang et al., 2018
Chitosan NPs	Low molecular weight chitosan (85% DD)	≤100 nm + 40 mV	Dichlorofluorescin diacetate (DCFH-DA) probe (unknown h incubation)	BCL2(AAA) Jurkat cells	10–50 μg/mL	All concentrations induced ROS production (concentration dependent manner)	Bulk chitosan was tested at the same concentrations. ROS production was concentration dependent but lower than with chitosan NPs	Sarangapani et al., 2018
Chitosan NPs	na	164 nm; + 63 mV 385 nm; + 62 mV 459 nm; +72 mV 475 nm; +71 mV 685 nm; +74 mV	Dihydroethidium (DHE) probe (72 h incubation)	Mouse bone marrow-derived hematopoietic stem cells	250–1,000 μg/mL	ROS production was not significantly altered following exposure to chitosan NPs	–	Omar Zaki et al., 2015
Chitosan NPs	75–85% 50–190 kDa	173 nm + 23 mV	Dichlorofluorescin diacetate (DCFH-DA) probe (24 h incubation)	HEK-293 cells	100 μg/mL	Chitosan NPs had no effect on ROS production	Bulk chitosan was also tested and had no effect in ROS production	Arora et al., 2016
PLA NPs	Poly(D,L-lactide) (PDLLA) 1,01,782 g/mol and 0.68 dL/g	188 nm −24 mV (water) 78 nm −0.4 mV (DMEM [b])	2′,7′-Dichlorofluorescin diacetate (DCFH-DA) probe (24 h incubation)	RAW 264.7 cells	4.3, 17, 34, 340 μg/mL	PLA NPs with 78 nm in DMEM caused a significant increase in ROS production for the highest concentration tested (340 μg/mL)	The increase in ROS production was related to cytotoxicity. The sample and concentration that induced ROS production decreased cell viability to values close to 70%. All the other concentrations were close to 100%	Da Silva et al., 2019
PLA NPs	Poly(D,L-lactide) (PDLLA) 1,01,782 g/mol and 0.68 dL/g	109 nm −7 mV (water) 154 nm −0.7 mV (DMEM)	2′,7′-Dichlorofluorescin diacetate (DCFH-DA) probe (24 h incubation)	RAW 264.7 cells	8.6, 34, 69, 690 μg/mL	No ROS production observed	–	Da Silva et al., 2019

(Continued)

TABLE 4 | Continued

Nanomaterial	Polymer characterization	Nanomaterial characterization	Testing method	Cellular model	Dose/ concentration range	Results	Observations	References
PLA NPs	na	176 nm −58 mV In cell culture: 212 nm −24 mV	2′,7′-Dichlorofluorescin diacetate (DCFH-DA) probe (72 h incubation)	Schneider's *Drosophila melanogaster* line 2 (S2) cells	0.5–500 μg/mL	ROS production was only observed at the highest tested concentration (500 μg/mL) indicating a concentration dependent effect	–	Legaz et al., 2016
PLGA NPs	Resomer® RG503H, acid terminated, 50:50, Mw 24,000–38,000	80 nm −25 mV	2′,7′-Dichlorofluorescin diacetate (DCFH-DA) probe (3 h incubation)	16HBE14o-, L5178Y, and TK6 cells	40 μg/mL	No increase in ROS production in 16HBE14o-, L5178Y, and TK6 cells, in comparison to the control	The L5178Y mouse lymphoma and TK6 human B-lymphoblastoid cells, are routinely used in *in vitro* regulatory genotoxic assays. The human bronchial epithelial cells 16HBE14o-, a cell line is suitable for toxicity studies of inhaled NPs as it is highly similar to the primary bronchial epithelium	Platel et al., 2016
hexadecyltrimethylammonium bromide (CTAB) stabilized PLGA NPs	Resomer® RG503H, acid terminated, 50:50, Mw 24,000–38,000 and PEG 2,000	82 nm +15 mV	2′,7′-Dichlorofluorescin diacetate (DCFH-DA) probe (3 h incubation)	16HBE14o-, L5178Y, and TK6 cells	40 μg/mL	Significant increase in ROS production in 16HBE14o-, L5178Y, and TK6 cells, in comparison to the control	The L5178Y mouse lymphoma and TK6 human B-lymphoblastoid cells, are routinely used in *in vitro* regulatory genotoxic assays. The human bronchial epithelial cells 16HBE14o-, a cell line is suitable for toxicity studies of inhaled NPs as it is highly similar to the primary bronchial epithelium	Platel et al., 2016
Polyphenolic bio-enhancers with oleanolic acid in chitosan coated PLGA NPs (CH-OA-B-PLGA NPs)	Chitosan (molecular weight 150 kDa, deacetylation degree 85%), Poly (lactide-coglycolide) (PLGA) 50:50, mw 40–75 kDa	342 nm + 34 mV	2′,7′-Dichlorofluorescin diacetate (DCFH-DA) probe (24 h incubation)	MDAMB-231 cells	na	Increased proxidant effect of CH-OA-B-PLGA was two times higher than plain OA	100 mg/kg is the double of the OA effective dose	Sharma et al., 2017
Poly-lactic-co-glycolic acid–polyethylene oxide (PLGA–PEO) NPs	(Purchased from Advancell)	140 nm −43 mV (in cell culture medium)	Hydroethidine probe (24–48 h incubation)	16HBE14o- and A549 cells	37.5 and 75 $\mu g/cm^2$	Weak production of intracellular ROS at the highest concentrations used, only in the A549 cell line	–	Guadagnini et al., 2013b

(Continued)

TABLE 4 | Continued

Nanomaterial	Polymer characterization	Nanomaterial characterization	Testing method	Cellular model	Dose/ concentration range	Results	Observations	References
PLGA NPs	75:25 Resomer® RG756	170 nm −45 mV (200 nm in cell culture medium)	2′,7′- Dichlorofluorescin diacetate (DCFH-DA) probe (5 min−48 h incubation)	THP-1 cell culture	0.1 or 1 mg/mL	No Induction of ROS production at 0.1 mg/mL At 1 mg/mL, a transient increase in ROS production was verified at 5 min	THP-1 monocytes differentiation into macrophages was performed using 12-o-tetradecanoylphorbol-13-acetate (PMA)	Grabowski et al., 2015
PVA stabilized PLGA NPs	75:25 Resomer® RG756 and PVA (87–89% hydrolyzed, 30–70 kDa)	Ratio PVA:PLGA 11.5:100 230 nm −1 mV (210 nm in cell culture medium)	2′,7′- Dichlorofluorescin diacetate (DCFH-DA) probe (5 min−48 h incubation)	THP-1 cell culture	0.1 or 1 mg/mL	No Induction of ROS production at 0.1 mg/mL At 1 mg/mL, a transient increase in ROS production was verified at 5 min	THP-1 monocytes differentiation into macrophages was performed using 12-o-tetradecanoylphorbol-13-acetate (PMA)	Grabowski et al., 2015
Chitosan stabilized PLGA NPs	75:25 Resomer® RG756 and Protasan® UP CL113, 75–90% deacetylation, 50–150 kDa	Ratio chi:PVA:PLGA 15.3:30.4:100 230 nm + 40 mV (270 nm in cell culture medium)	2′,7′- Dichlorofluorescin diacetate (DCFH-DA) probe (5 min−48 h incubation)	THP-1 cell culture	0.1 or 1 mg/mL	No Induction of ROS production at 0.1 mg/mL At 1 mg/mL, a transient increase in ROS production was verified at 5 min	THP-1 monocytes differentiation into macrophages was performed using 12-o-tetradecanoylphorbol-13-acetate (PMA)	Grabowski et al., 2015
Pluronic stabilized PLGA NPs	75:25 Resomer® RG756 and Pluronic F68	Ratio F68:PLGA 15.5:100 230 nm −30 mV (315 nm in cell culture medium)	2′,7′- Dichlorofluorescin diacetate (DCFH-DA) probe (5 min−48 h incubation)	THP-1 cell culture	0.1 or 1 mg/mL	No Induction of ROS production at 0.1 and 1 mg/mL	THP-1 monocytes differentiation into macrophages was performed using 12-o-tetradecanoylphorbol-13-acetate (PMA)	Grabowski et al., 2015
PLGA NPs	50:50[c] (intrinsic viscosity 0.60 g/dl) 65:35[c] (intrinsic viscosity 0.64 g/dl) 75:25[c] (intrinsic viscosity 0.72 g/dl) 85:15[c] (intrinsic viscosity 0.62 g/dl)	210 nm −14 mV 211 nm −8.70 mV 218 nm −12.7 mV 243 nm −12.7 mV	2′,7′- Dichlorofluorescin diacetate (DCFH-DA) probe (24 h incubation)	RAW 264.7 cells	10, 30, 100, and 300 μg/mL	No effect on ROS production up to 100 μg/ml concentration; 300 μg/ml showed 1.5- to 2-fold stimulation of ROS production A further increase in NPs concentration to 1,000 μg/ ml interfered with ROS assay due to fluorescence quenching	No significant differences were found in these assays between these NPs	Singh and Ramarao, 2013

(Continued)

TABLE 4 | Continued

Nanomaterial	Polymer characterization	Nanomaterial characterization	Testing method	Cellular model	Dose/ concentration range	Results	Observations	References
PLA NPs	DL-PLA (MW 10,000)	256 nm −17.1 mV	2′,7′-Dichlorofluorescin diacetate (DCFH-DA) probe (24 h incubation)	RAW 264.7 cells	10, 30, 100, and 300 μg/mL	No effect on ROS production up to 100 μg/ml concentration; 300 μg/ml showed 1.5- to 2-fold stimulation of ROS production A further increase in NPs concentration to 1,000 μg/ ml interfered with ROS assay due to fluorescence quenching	–	Singh and Ramarao, 2013
PCL NPs	PCL (intrinsic viscosity 1.07 g/dl)	268 nm −9.10 mV	2′,7′-Dichlorofluorescin diacetate (DCFH-DA) probe (24 h incubation)	RAW 264.7 cells	10, 30, 100, and 300 μg/mL	No effect on ROS production up to 100 μg/ml concentration; 300 μg/ml showed 1.5- to 2-fold stimulation of ROS production A further increase in NPs concentration to 1,000 μg/ ml interfered with ROS assay due to fluorescence quenching	–	Singh and Ramarao, 2013
Poly(lactide-co-caprolactone) (PLCL) NPs	PLCL 25:75 (intrinsic viscosity 0.71 g/dl) PLCL 80:20 (intrinsic viscosity 0.77 g/dl	261 nm −15.3 mV 261 nm −15.4 mV	2′,7′-Dichlorofluorescin diacetate (DCFH-DA) probe (24 h incubation)	RAW 264.7 cells	10, 30, 100, and 300 μg/mL	No effect on ROS production up to 100 μg/ml concentration; 300 μg/ml showed 1.5- to 2-fold stimulation of ROS production A further increase in NPs concentration to 1,000 μg/ ml interfered with ROS assay due to fluorescence quenching	–	Singh and Ramarao, 2013

[a] *DD, deacetylation degree.*
[b] *DMEM, Dulbecco's Modified Eagle Medium.*
[c] *PLGA lactic to glycolic acid.*

Regarding the methodologies, the enzyme-linked immunosorbent assay (ELISA) is widely applied as a simple mean to perform a qualitative and quantitative analysis of cytokines, chemokines, growth factors and immunoglobulins, with a spectrophotometric readout (Lorscheidt and Lamprecht, 2016). In this assay, the pro- and anti-inflammatory mediators are released into cell supernatant, which is collected and then analyzed. Therefore, the release of cytokines or other molecules by cells during the incubation with nanoparticles can be underestimated due to the nanoparticles ability to adsorb biomolecules at its surface (Lorscheidt and Lamprecht, 2016). Kroll et al. (2012) tested the potential interference of 4 types of engineered nanoparticles on IL-8 secretion, and verified that a specific pre-dispersion of TiO_2 nanoparticles was able to reduce the measurable levels of the cytokine, under the assay conditions. Similarly, Guadagnini et al. (2013a), tested 4 types of nanoparticles in acellular conditions and verified that TiO_2, SiO_2, and Fe_3O_4 NPs decreased the cytokines levels due to surface adsorption. In the same experiment, PLGA-PEO NPs induced an apparent increase in GM-CSF levels, which the authors believe may be due to the stabilization of the peptides, their protection from proteolysis or by avoiding the interaction of this cytokine with the plastic of the culture plates (Guadagnini et al., 2013a). Although most of the reported interferences are for inorganic nanoparticles, these are good examples that can be overlooked when performing ELISA in cell supernatants previously incubated with polymeric nanoparticles. When studying pro- and anti-inflammatory molecules release due to NPs stimulation, it can be useful to previously study the adsorption or interaction of the NPs with the molecules (i.e., cytokine standards) in acellular conditions.

Alternatively, instead of measuring cell secreted pro- and anti-inflammatory molecules by ELISA, the mRNA levels inside the cell can be measured with RT-qPCR (Real-Time quantitative Polymerase Chain Reaction) or the intracellular levels of the cytokines can be measured by flow cytometry analysis using specific antibodies fluorescently labeled (Lorscheidt and Lamprecht, 2016). In the first alternative, however, an increase of mRNA expression does not necessarily lead to an increase of protein secretion (Guadagnini et al., 2013a).

Lastly, besides the masking/enhancing effect of NPs, the presence of contaminants, such as endotoxins can induce itself increased levels of pro-inflammatory molecules in cells (Oostingh et al., 2011). Endotoxins, commonly referred to as lipopolysaccharide (LPS), are present in the outer cell membrane of Gram negative bacteria and are released during multiple processes, such as cell death, growth and division (Magalhaes et al., 2007; Lieder et al., 2013). Therefore, due to the bacteria ability to growth and adapt in several environments, LPS is easily found in numerous media, including poor nutrient media (water, saline and buffers) and its removal is a struggle since it is highly resistant to extreme temperatures pHs (Magalhaes et al., 2007). LPS is comprised by a O-antigen region, a hydrophilic core oligosaccharide and a hydrophobic Lipid A (LipA) (Davydova et al., 2000; Magalhaes et al., 2007; Steimle et al., 2016). The lipid A structure, highly conserved, differs among bacterial species, and determines the molecule immunogenicity (Steimle et al., 2016). On the whole, LPS is a pathogen associated molecular pattern (PAMP), which is recognized and activates the mammalian innate immune system, leading for instance to cellular release of pro-inflammatory cytokines and free radicals, particularly by monocytes and macrophages (Yermak et al., 2006; Lieder et al., 2013; Steimle et al., 2016). Consequently, *in vitro* testing of LPS contaminated polymeric NMs might generate misleading results and false assumptions of bioactivity or toxicity, ultimately affecting the evaluation of possible human health effects (Lieder et al., 2013).

Table 5 summarizes the results found in the literature for polymeric NPs stimulation of cytokines.

For chitosan NPs, it is interesting to notice that one author referred chitosan NPs induced several cytokines in BMDCs (Koppolu and Zaharoff, 2013), while other did not (Han et al., 2016). Nevertheless, in both papers, no endotoxin contamination was assessed, no concentrations of NPs were given and the chitosan polymers and NPs characteristics were not the same. Furthermore, it must be considered that cytokine secretion highly depends on the cellular model under study. Indeed, Koppolu and Zaharoff, upon stimulation with chitosan NPs, reported the production of IL-1β in BMDCs and the absence of the same cytokine in RAW 264.7 (Koppolu and Zaharoff, 2013).

The fact that no endotoxin control was made in both papers can rise several questions, mainly in the results that suggest a positive stimulation of chitosan NPs. Chitosan has a cationic charge, resultant from the N-acetyl group removal during chitin deacetylation. This positive charge, mediates for instance the electrostatic interactions with cargo molecules, allowing high loading efficacies, but it also enables chitosan interactions with the negatively charged phosphate, pyrophosphate, and carboxylic groups of LPS (Davydova et al., 2000). Actually, chitosan has been used as a selective filtration membrane for endotoxin removal due to these extensive interactions (Machado et al., 2006; Lieder et al., 2013).

But not only chitosan should be evaluated regarding endotoxin contamination. For instance, Grabowski et al. have published two reports, comparing the inflammatory ability of different PLGA NPs based on the *in vitro* assessment of cytokines, such as IL-6, TNF-α, IL-8 and MCP-1 (Grabowski et al., 2015, 2016). The differences among PLGA NPs resulted from the inclusion of chitosan, PVA and P68 in order to obtain, positive, neutral and negatively charged particles. In one of the reports the authors do not evaluate or discuss the presence of endotoxin contamination in the formulations (Grabowski et al., 2015). Nonetheless, in the other report, using the same methods and polymers, the authors mentioned that all formulations presented 0.1 to 0.3 EU/mL of LPS depending on the concentration used (Grabowski et al., 2016). In both reports, this information was imperative, since the authors tested IL-8, IL-6 and TNF-α, cytokines whose production is induced by LPS (Agarwal et al., 1995; Grabowski et al., 2016). Therefore, despite their conclusions, as illustrated in **Table 5** (Grabowski et al., 2015, 2016), and despite the authors attribute the observed effects to the nanoparticulate form of the formulations, the effect of LPS contamination might be interfering with the results. A simple control that could be adopted in this situation, was

TABLE 5 | Review of original articles assessing inflammatory cytokines induced by polymeric nanoparticles in different cells.

Nanomaterial	Polymer characterization	Nanomaterial characterization	Testing method	Cellular model	Dose/ concentration range	Results	Endotoxin contamination	References
Chitosan NPs	95 ± 20 kDa	290 nm +37 ± 1.4	*In vitro* cytokine production (24 h incubation) (IL-1β, IL-6, TNF-α, MCP-1α, and MIP-1)	RAW 264.7 and BMDCs	–	RAW 264.7: production of MIP1 and TNF-α, IL6, and MCP1 but not of IL-1β BMDCs: production of MIP1, TNF-α, IL-1β, IL6, and MCP1 [a]	–	Koppolu and Zaharoff, 2013
Chitosan NPs	50–190 KDa	70 nm + 15 mV	*In vitro* cytokine production (30 min incubation + 24 h) (IL-1β, IL-6, IL-12p70, and TNF-α)	BMDCs	–	No cytokine production	–	Han et al., 2016
Poly-lactic-co-glycolic acid–polyethylene oxide (PLGA–PEO) NPs	(Purchased from advancell)	140 nm −43 mV (in cell culture medium)	*In vitro* cytokine production (24–48 h incubation) (GM-CSF, IL-6, IL-8, IL-1β)	16HBE14o- and A549 cells	75 $\mu g/cm^2$	No significant increase of any cytokine mRNA after 24 or 48 h Interestingly, there was a decreased level of all cytokine mRNA in A549 cells after PLGA-PEO NP exposure	mRNA cytokine analysis was performed through RT-qPCR	Guadagnini et al., 2013b
PLGA NPs	75:25 Resomer® RG756	170 nm −45 mV (200 nm in cell culture medium)	*In vitro* cytokine production (24 h incubation) (IL-8, IL-6, TNF-α, and MCP-1)	A549 and THP-1-D cell co-culture	0.1 or 1 mg/mL	0.1 mg/mL did not induce cytokine secretion 1 mg/mL induced IL-6, TNF-α and MCP-1[16]	Endotoxin (LPS) determination was performed in the supernatant (12,000 g, 30′) of all formulations diluted in cell culture medium for the used *in vitro* concentrations with LAL chromogenic endotoxin quantitation kit. Results showed endotoxin values between 0.1 and 0.3 EU/mL.	Grabowski et al., 2016
PVA stabilized PLGA NPs	75:25 Resomer® RG756 and PVA (87–89% hydrolyzed, 30–70 kDa)	230 nm −1 mV (210 nm in cell culture medium)	*In vitro* cytokine production (24 h incubation) (IL-8, IL-6, TNF-α, and MCP-1)	A549 and THP-1-D cell co-culture	0.1 or 1 mg/mL	0.1 mg/mL induced IL-8 and MCP-1 1 mg/mL induced IL-6 [b]	Endotoxin (LPS) determination was performed in the supernatant (12,000 g, 30′) of all formulations diluted in cell culture medium for the used *in vitro* concentrations with LAL chromogenic endotoxin quantitation kit. Results showed endotoxin values between 0.1 and 0.3 EU/mL.	Grabowski et al., 2016

(Continued)

TABLE 5 | Continued

Nanomaterial	Polymer characterization	Nanomaterial characterization	Testing method	Cellular model	Dose/ concentration range	Results	Endotoxin contamination	References
Chitosan stabilized PLGA NPs	75:25 Resomer® RG756 and Protasan® UP CL113, 75–90% deacetylation, 50–150 kDa	230 nm +40 mV (270 nm in cell culture medium)	*In vitro* cytokine production (24 h incubation) (IL-8, IL-6, TNF-α and MCP-1)	A549 and THP-1-D cell co-culture	0.1 or 1 mg/mL	0.1 mg/mL induced IL-8 and MCP-1 1 mg/mL induced IL-6 and MCP-1[16]	Endotoxin (LPS) determination was performed in the supernatant (12,000 g, 30′) of all formulations diluted in cell culture medium for the used *in vitro* concentrations with LAL chromogenic endotoxin quantitation kit. Results showed endotoxin values between 0.1 and 0.3 EU/mL.	Grabowski et al., 2016
Pluronic F68 stabilized PLGA NPs	75:25 Resomer® RG756 and Pluronic PF68 (BASF)	230 nm −30 mV (315 nm in cell culture medium)	*In vitro* cytokine production (24 h incubation) (IL-8, IL-6, TNF-α, and MCP-1)	A549 and THP-1-D cell co-culture	0.1 or 1 mg/mL	0.1 mg/mL induced MCP-1 1 mg/mL induced il-8. Il-6 and MCP-1[16]	Endotoxin (LPS) determination was performed in the supernatant (12,000 g, 30′) of all formulations diluted in cell culture medium for the used *in vitro* concentrations with LAL chromogenic endotoxin quantitation kit. Results showed endotoxin values between 0.1 and 0.3 EU/mL.	Grabowski et al., 2016
PLGA NPs	75:25 Resomer® RG756	170 nm −45 mV (200 nm in cell culture medium)	*In vitro* cytokine production (24 h incubation) (IL-8, IL-6, TNF-α, and MCP-1)	THP-1 cell culture (differentiated into macrophages)	0.1 or 1 mg/mL	0.1 mg/mL did not induce cytokine secretion 1 mg/mL induced IL-8 and TNF-α	–	Grabowski et al., 2015
PVA stabilized PLGA NPs	75:25 Resomer® RG756 and PVA (87–89% hydrolyzed, 30–70 kDa)	230 nm −1 mV (210 nm in cell culture medium)	*In vitro* cytokine production (24 h incubation) (IL-8, IL-6, TNF-α, and MCP-1)	THP-1 cell culture (differentiated into macrophages)	0.1 or 1 mg/mL	0.1 mg/mL did not induce cytokine secretion 1 mg/mL induced IL-8	–	Grabowski et al., 2015
Chitosan stabilized PLGA NPs	75:25 Resomer® RG756 and Protasan® UP CL113,75–90% deacetylation, 50–150 kDa	230 nm + 40 mV (270 nm in cell culture medium)	*In vitro* cytokine production (24 h incubation) (IL-8, IL-6, TNF-α, and MCP-1)	THP-1 cell culture (differentiated into macrophages)	0.1 or 1 mg/mL	0.1 mg/mL and 1 mg/mL did not induce cytokine secretion[c]	–	Grabowski et al., 2015

(Continued)

TABLE 5 | Continued

Nanomaterial	Polymer characterization	Nanomaterial characterization	Testing method	Cellular model	Dose/ concentration range	Results	Endotoxin contamination	References
Pluronic stabilized PLGA NPs	75:25 Resomer® RG756 and Pluronic F68	230 nm −30 mV (315 nm in cell culture medium)	*In vitro* cytokine production (24 h incubation) (IL-8, IL-6, TNF-α and MCP-1)	THP-1 cell culture (differentiated into macrophages)	0.1 or 1 mg/mL	0.1 mg/mL did not induce cytokine secretion 1 mg/mL induced IL-6	–	Grabowski et al., 2015
PLGA NPs	PLGA lactic to glycolic acid 50:50 (intrinsic viscosity 0.60 g/dl) PLGA lactic to glycolic acid 65:35 (intrinsic viscosity 0.64 g/dl) PLGA lactic to glycolic acid 75:25 (intrinsic viscosity 0.72 g/dl) PLGA lactic to glycolic acid 85:15 (intrinsic viscosity 0.62 g/dl)	210 nm −14 mV 211 nm −8.70 mV 218 nm −12.7 mV 243 nm −12.7 mV	*In vitro* cytokine production (24 h incubation) (IL-6 and TNF-α)	RAW 264.7 cells	300 μg/mL	No induction of the IL-6 release 1.5- to 2-fold increase in TNF-α release	–	Singh and Ramarao, 2013
PLA NPs	DL-PLA (MW 10,000)	256 nm −17.1 mV	*In vitro* cytokine production (24 h incubation) (IL-6 and TNF-α)	RAW 264.7 cells	300 μg/mL	No induction of the IL-6 release 1.5- to 2-fold increase in TNF-α release	–	Singh and Ramarao, 2013
PCL NPs	PCL (intrinsic viscosity 1.07 g/dl)	268 nm −9.10 mV	*In vitro* cytokine production (24 h incubation) (IL-6 and TNF-α)	RAW 264.7 cells	300 μg/mL	No induction of the IL-6 release 1.5- to 2-fold increase in TNF-α release	–	Singh and Ramarao, 2013
poly(lactide-co-caprolactone) (PLCL) NPs	PLCL 25:75 (intrinsic viscosity 0.71 g/dl) PLCL 80:20 (intrinsic viscosity 0.77 g/dl)	261 nm −15.3 mV 261 nm −15.4 mV	*In vitro* cytokine production (24 h incubation) (IL-6 and TNF-α)	RAW 264.7 cells	300 μg/mL	No induction of the IL-6 release 1.5- to 2-fold increase in TNF-α release	–	Singh and Ramarao, 2013

[a] *Inferred results from the graphs. The authors do not show or discuss the comparison with non-treated cells.*

[b] *Only statistically significant increases were considered in the results.*

[c] *According to the authors, IL-6 levels were not statically different from the control but neither were LPS levels. Considering this, chitosan stabilized PLGA NPs induced IL-6 levels similar to LPS.*

to use the LPS concentration the authors quantified in the formulations, incubate with the cell and assess the cytokine secretion. In these articles, the relationship between the 0.1–0.3 EU/ml of contamination and the 0.1–10 μg/mL of LPS as control was not given, and therefore, no further conclusions could be drawn regarding the effect of the LPS contamination in the formulations. Another relevant aspect to highlight, is the fact that nanoparticles, particularly polymeric nanoparticles interfere with most endotoxin quantification assays. This fact was denoted by the authors of these reports, who overcame the interference, by centrifuging the formulations and measuring the contamination in the supernatant (Grabowski et al., 2016). Unfortunately, due to what was discussed previously, the polymers, and particularly the positively charged, might adsorb the LPS through electrostatic interactions, which means the quantification on the supernatant can be underestimated. Overall, in this example, the conclusions about the mild inflammatory ability of PLGA and PLGA stabilized NPs should be extrapolated with caution, since the use of endotoxin free materials, or the presence of endotoxin inhibitor (i.e., polymycin B) might generate different results.

Genotoxicity

Genotoxicity describes the capacity of the compounds to affect the DNA structure or the cellular apparatus and topoisomerases, modifying the genome fidelity (Słoczynska et al., 2014). Genotoxic effects are not always related with mutations but they can have serious implications for risks of cancer or chronic/heritable diseases (Słoczynska et al., 2014; Lorscheidt and Lamprecht, 2016; Dusinska et al., 2017).

NMs can cause damage to cell's DNA through direct and indirect interactions (Magdolenova et al., 2013; Lorscheidt and Lamprecht, 2016; Dusinska et al., 2017). In fact, upon cellular uptake, NMs might reach the nucleus and contact with cell genetic material, leading to physical or chemical alterations (Magdolenova et al., 2013; Lorscheidt and Lamprecht, 2016; Dusinska et al., 2017). Importantly, this direct interaction is limited by the particle size. Particles ranging between 8 and 10 nm of diameter may reach the nuclear compartment through nuclear pores, whether 15–60 nm particles will only access the nucleus during cellular division when the nuclear wall is disrupted (Barillet et al., 2010). However, indirect interactions have a greater significance for genotoxicity, since several biomolecules involved in normal gene function (i.e., DNA repair) and cell division (i.e., DNA transcription and replication) can interact with even larger NMs, altering its function and consequently leading to DNA injury or chromosome malformation (Lorscheidt and Lamprecht, 2016; Dusinska et al., 2017). For instance, oxidative stress is a key mechanism by which NMs can cause DNA injury (Dusinska et al., 2017). Therefore, data showing non-cytotoxic increase of ROS should imply genotoxicity studies to assess the degree of damage caused by the oxidative stress (Lorscheidt and Lamprecht, 2016).

Several assays are described in the literature for genotoxicity assessment and include *in vitro* and *in vivo* approaches. *In vitro* assays are commonly performed in cell lines, such as the mouse lymphoma L5178Y $TK^{+/-}$ 3.7.2C cells, the TK6 human lymphoblastoid cells and rodent fibroblastic cell lines (CHL-IU, CHO and V79 cells) (Lorge et al., 2016). Regarding *in vivo* studies, the bacterial reverse mutation test (AMES test) is the most commonly used initial screening performed. Also, the *Allium cepa* model, allows for a simple and cost-effective assay where DNA damage is assessed after the roots of the plant grow in direct contact with the substance of interest (Bosio and Laughinghouse IV, 2012). Alternatively, other *in vivo* studies comprise the use of Zebrafish (*Danio rerio*) due to their molecular and physiological similarities with humans, therefore giving a high-throughput for genotoxicity (Chakravarthy et al., 2014). Rodents and other mammals are also widely used for genotoxicity assessment. In all these models, the comet assay, the micronucleus assay and the chromosome aberrations test are the most common used tests to evaluate nanoparticles toxicity (Magdolenova et al., 2013).

Importantly, some considerations have been published by OECD regarding the protocols to assess genotoxicity of NMs, namely the "2018 Report No. 85—Evaluation of *in vitro* methods for human hazard assessment applied in the OECD Testing Programme for the Safety of Manufactured Nanomaterials" and "2014 Report No. 43—Genotoxicity of Manufactured Nanomaterials: Report of the OECD expert meeting" (OECD, 2014, 2018a).

Data collected from the literature assessing genotoxicity of polymeric NMs is summarized in **Table 6**. Again, most of the data collected refers to chitosan and PLGA based NPs and should be carefully analyzed. First, we must recognize we are comparing NPs comprising a particular polymer (chitosan or PLGA) but whose chemical specifications can differ and whose composition and characteristics are very diverse. Also, comparisons should ideally be performed only when the same test is applied. In detail, chitosan/poly(methacrylic acid) NPs induced a concentration dependent genotoxic effect according to the cytogenetic test using human lymphocyte culture (De Lima et al., 2010). However, the same report reported no evidence for DNA alterations using the *Allium Cepa* assay (De Lima et al., 2010). In another study, Eudragit® S100/alginate enclosed chitosan calcium phosphate-loaded lactoferrin nanocapsules, was considered non-genotoxic based on the *Allium Cepa* and the comet assay in Vero cells (Leng et al., 2018). Overall, these two studies comprising nanoparticles with chitosan in their composition, presented a different conclusion for the NM genotoxicity, but if we compare only the same assay (*Allium Cepa* assay), the results were similar. Another interesting fact, is the heterogeneity of results that may be achieved with different cell lines. For instance, Platel et al. used three different cell lines, and three different PLGA NPs and evaluated genotoxicity using the comet assay and the micronucleus test (Platel et al., 2016). For bare PLGA NPs, no genotoxicity effects were verified in none of the 3 cell lines with both tests (Platel et al., 2016). On the other hand, CTAB stabilized PLGA NPs induced an increase in the number of micronuclei only in one of the cell lines (micronucleous test in HBE14o- cells) (Platel et al.,

2016). These examples illustrate how an extrapolation based on one single genotoxicity assay (or cellular/animal model) can be misleading.

Toxicity on Reproduction

The extrapolation to human health of toxic effects on reproduction using *in vitro* and animal models presents several specific limitations, such as the differences in reproductive structures and endocrine functions or the duration of gestation or spermatogenesis period (Das et al., 2016). Also, alike other studies, the tested concentrations and doses are much higher than the clinically relevant doses in humans (Das et al., 2016). Nevertheless, the toxicity on reproduction is a valuable endpoint since it allows the prediction of health effects not only of individuals but also of the next generation (Dusinska et al., 2017).

As mentioned before, toxicity on reproduction might be evaluated using *in vitro* and *in vivo* studies. For instance, *in vitro* assays test the toxicity of nanoparticles in cells from reproductive organs (such as blastocysts and granulosa cells) or use *ex vivo* placentae or sperm from healthy donors (Ema et al., 2010; Sun et al., 2013; Brohi et al., 2017). In these examples, the authors expect to see direct toxicity of the NPs in reproductive system cells, or to evaluate the ability of the NPs to cross for instance the placental barrier (Ema et al., 2010; Brohi et al., 2017).

Regarding *in vivo* testing, the use of mice as a mammalian model provides analogous experimental conditions to humans. However, the investigation of early embryonic developmental effects occurring *in utero* are not easily detectable (Sun et al., 2013). Interestingly, the zebrafish model has been widely applied as a rapid and cost-effective whole animal model to assess reproductive toxicity (Hu et al., 2011). Characteristics like the small size, rapidity to reach sexual maturity, great number of eggs (200–300) and the possibility to examine every stage of embryonic development through its transparency, make zebrafish one of the most used animal models (Wang et al., 2016).

Results from toxicity on reproduction assays with polymeric NMs are summarized in **Table 7**. The results for chitosan NPs (blend and bare) are consistent between reports. In fact, it appears that chitosan based NPs induce embryonic malformations when directly in contact with embryos, or intravenously administered to animal models (Hu et al., 2011; Park et al., 2013; Choi et al., 2016; Wang et al., 2016; Yostawonkul et al., 2017). However, this effect is not verified in when PLGA NPs coated with chitosan are administered through the oral route in Sprague Dawley rats (Sharma et al., 2017). Though, this conclusion is only speculative. In order to have a proven conclusion, the oral route should be tested for toxicity on reproduction using the same NPs as were used for the intravenous administration and embryonic incubation experiments. Otherwise, we cannot be sure if the result is due to the administration route, or the NPs composition and characteristics. Nevertheless, other study using PLGA based NPs also tested toxicity on reproduction through the *in vitro* zebrafish embryonic model, and found no toxicity for those nanoparticles (Chen et al., 2017).

Hemocompatibility

Hemocompatibility is frequently assessed as an endpoint of biocompatibility for chemicals and particularly NMs. In fact, blood is the first target when considering intravenous injections of NMs, but it is also a surrogate target model for other routes of exposure, since its high complexity allows for an approximation the overall body response (Tulinska et al., 2015).

In particular, hemolysis which is associated to red blood cells damage is believed to have a good correlation with toxicity, since the *in vitro* hemolytic assays show results that greatly relate with *in vivo* toxicity studies (Dobrovolskaia and McNeil, 2013).

In 2008, Dobrovolskaia et al. published a report describing the validation of an *in vitro* assay for the analysis of nanoparticle hemolytic properties and main interferences (Dobrovolskaia et al., 2008). In 2013, ASTM International standards organization published the Standard Test Method for Analysis of Hemolytic Properties of Nanoparticles and defined a material as hemolytic if the hemolysis values are above 5% and as moderately hemolytic if they are between 2 and 5% (ASTM International, 2013; Dobrovolskaia and McNeil, 2013). Therefore, the existence of this protocol contributes to the use of standardized procedures among research groups, allowing comparisons and extrapolations of results.

From **Table 8** we can acknowledge several authors reporting the hemolytic activity of diverse polymeric NMs. An important remark is the fact that a number of papers describe the hemolytic activity of drug loaded formulations and compare it to the free drug, but not with the unloaded nanocarrier (Essa et al., 2012; Gupta et al., 2012; Altmeyer et al., 2016; Radwan et al., 2017a). These results generally demonstrate a lower hemolysis rate of the drug loaded polymeric NM in comparison to the free drug, but still a significant hemolysis (>5%) (Essa et al., 2012; Gupta et al., 2012; Radwan et al., 2017a). In these situations, no conclusion regarding the hemolytic activity of the polymeric NM itself can be drawn. On the other hand, some other authors, test the unloaded nanoparticles but make no disclosure of their concentration (Altmeyer et al., 2016; Moraes Moreira Carraro et al., 2017).

Nevertheless, polymeric NMs appear to present good hemocompability profile, as in most tested cases, hemolysis is a concentration dependent phenomenon, reaching significant values only for high NM concentrations. Also, the encapsulation of hemolytic drugs in polymeric NMs decreases their hemolytic activity.

DISCUSSION

Most information available on nanotoxicity is related to inorganic NMs, such as zinc oxide NPs, nanoscale silver clusters, and titanium dioxide NPs or carbon nanotubes (Yuan et al., 2015). Information related to polymeric NMs toxicity that could be correlated with their effects on human health is still scarce and poorly harmonized.

The majority of reports on polymeric NMs are focused in optimizing the nanocarrier features, such as size, physical stability and drug loading efficacy, and in performing preliminary cytocompatibility testing (mainly through MTT and LDH assays)

TABLE 6 | Review of original articles assessing the genotoxicity of polymeric nanoparticles according to different testing methodologies.

Nanomaterial	Polymer Characterization	Nanomaterial Characterization	Testing method	Model	Administration route (if applicable)	Dose/ concentration range	Results	Observations	References
Chitosan/poly(methacrylic acid) (CS/PMAA) NPs	Chitosan with 71.3 kDa and 94 % DD	60 nm 82 nm 111 nm	*Allium cepa* assay (24 h)	*Allium cepa* bulbs	–	1.8, 18, and 180 mg/L	No significant numerical or structural changes in DNA	Smaller particles were not toxic at higher concentrations, by opposition to larger size nanoparticles	De Lima et al., 2010
Chitosan/poly(methacrylic acid) (CS/PMAA) NPs	Chitosan with 71.3 kDa and 94 % DD	60 nm 82 nm 111 nm	Cytogenetic test	Human blood (lymphocyte culture)	–	1.8, 18, and 180 mg/L	The 82 and 111 nm NPs reduced mitotic index values at the highest concentration tested (180 mg/L)	Smaller particles were not toxic at higher concentrations, by opposition to larger size nanoparticles	De Lima et al., 2010
Eudragit® S100/alginate-enclosed chitosan-calcium phosphate-loaded lactoferrin nanocapsules	na	240 nm −2.6 mV	*Allium cepa* assay (24 h)	*Allium cepa* bulbs	Roots immersed in formulations	125, 250, 500, and 1000 μg/mL	No genotoxicity	–	Leng et al., 2018
Eudragit® S100/alginate-enclosed chitosan-calcium phosphate-loaded lactoferrin nanocapsules	na	240 nm −2.6 mV	Comet assay (24 h)	Vero cells	–	100 μg/mL	No genotoxicity	–	Leng et al., 2018
Poly-lactic-co-glycolic acid–polyethylene oxide (PLGA–PEO) NPs	na	143–180 nm −43 mV	Comet assay (24 h)	Human peripheral blood	–	3, 15, or 75 $\mu g/cm^2$	No induction of SBs or oxidized DNA bases	–	Tulinska et al., 2015
Poly-lactic-co-glycolic acid–polyethylene oxide (PLGA–PEO) NPs	na	143–180 nm −43 mV	Micronucleous test (24 h)	Human peripheral blood	–	3, 15, or 75 $\mu g/cm^2$	No increase in the number of micronucleated binucleated cells	–	Tulinska et al., 2015
PLGA NPs	Resomer® RG503H, acid terminated, 50:50, Mw 24,000–38,000	80 nm −25 mV	Comet assay (3 h) and micronucleus test (3 + 40 h recovery time)	16HBE14o-, L5178Y and TK6 cells	–	50–500 μg/mL (16HBE14o-, L5178Y, and TK6 cells)	No primary DNA, no chromosomal damage and no increase in the number of micronulei on L5178Y and TK6 and 16HBE14o- cells	The L5178Y mouse lymphoma and TK6 human B-lymphoblastoid cells, are routinely used in *in vitro* regulatory genotoxic assays. The human bronchial epithelial cells 16HBE14o-, a cell line is suitable for toxicity studies of inhaled NPs as it is highly similar to the primary bronchial epithelium	Platel et al., 2016

(Continued)

TABLE 6 | Continued

Nanomaterial	Polymer Characterization	Nanomaterial Characterization	Testing method	Model	Administration route (if applicable)	Dose/ concentration range	Results	Observations	References
PEG stabilized PLGA NPs	Resomer® RG503H, acid terminated, 50:50, Mw 24,000–38,000	78 nm −1 mV	Comet assay (3 h) and Micronucleus test (3 + 40 h recovery time)	L5178Y and TK6 cells	–	50–500 μg/mL (L5178Y and TK6 cells)	No primary DNA, no chromosomal damage and no increase in the number of micronulei on L5178Y and TK6 cells	The L5178Y mouse lymphoma and TK6 human B-lymphoblastoid cells, are routinely used in *in vitro* regulatory genotoxic assays	Platel et al., 2016
hexadecyltrimethylammonium bromide (CTAB) stabilized PLGA NPs	Resomer® RG503H, acid terminated, 50:50, Mw 24,000–38,000 and PEG 2000	82 nm +15 mV	Comet assay (3 h) and micronucleus test (3 + 40 h recovery time)	16HBE14o-, L5178Y and TK6 cells	–	25–100 μg/mL (L5178Y and TK6 cells) 25–100 μg/mL (16HBE14o- cells)	No primary DNA or chromosomal damage on L5178Y and TK6 cells; concentration-related increase in the number of micronuclei in 16HBE14o- cells	The L5178Y mouse lymphoma and TK6 human B-lymphoblastoid cells, are routinely used in *in vitro* regulatory genotoxic assays. The human bronchial epithelial cells 16HBE14o-, a cell line is suitable for toxicity studies of inhaled NPs as it is highly similar to the primary bronchial epithelium	Platel et al., 2016
Danorubicin loaded polyethylene glycol-poly L-lysine-poly lactic-co-glycolic acid (PEG-PLL-PLGA) NPs	na	229 nm −20 mV	*In vivo* exposure /bone marrow micronucleus assay	Kunming mice	Intravenous	1/2 LD_{50}, 1/4 LD_{50}, 1/8 LD_{50} per kg	No teratogenic or mutagenic effects		Guo et al., 2015
Poly(ε-caprolactone)-poly(ethylene glycol)-poly(ε-caprolactone) (PCEC) nanoparticles	PCEC copolymer with a molecular weight of 17,500 (1H NMR spectrum)	40 nm	Ames test (48 h)	*Salmonella typhimurium*	–	150–5,000 μg/mL	No mutagenicity to the *Salmonella typhimurium* strains TA97, TA98, TA100, TA102, and TA1535	–	Huang et al., 2010
Poly(ε-caprolactone)-poly(ethylene glycol)-poly(ε-caprolactone) (PCEC) nanoparticles	PCEC copolymer with a molecular weight of 17,500 (1H NMR spectrum)	40 nm	Chromosomal aberration test (6, 24, 48 h)	Chinese hamster lung (CHL) cells	–	150–5,000 μg/mL	No significant increases in the incidence of chromosomal aberrations	–	Huang et al., 2010
Poly(ε-caprolactone)-poly(ethylene glycol)-poly(ε-caprolactone) (PCEC) nanoparticles	PCEC copolymer with a molecular weight of 17,500 (1H NMR spectrum)	40 nm	Mouse micronucleus test (*in vivo* exposure, 1 or 2 administrations, 24 or 48 h)	ICR mice	Intraperitoneal	0, 0.4, 0.8, and 1.6 g/kg	No increase in micronuclei	–	Huang et al., 2010

TABLE 7 | Review of original articles assessing toxicity on reproduction induced by polymeric nanoparticles.

Nanomaterial	Polymer characterization	Nanomaterial characterization	Testing method	Model	Administration route (if applicable)	Dose/ concentration range	Results	Observations	References
Chitosan NPs	na	100 nm	*In vivo* reproduction model/*in vitro* culture of embryos	ICR mice: Mouse pre-implantation embryos	–	10–200 μg/mL	Impaired blastocyst expansion and hatching Higher rates of resorption after embryo transfer Decreased implantation and increased embryonic death *in vivo*	Authors refer the use of different molecular-weight chitosan, derived from crab shell, without further distinctions	Park et al., 2013
Chitosan NPs	100 kDa and 85 % DD	200 nm	*In vitro* embryo model (72 h)	Zebrafish	–	5, 10, 20, and 40 μg/mL	Decrease in hatching rate (30 and 40 μg/mL) All embryos dies with 40 μg/mL Malformation with (5 μg/mL) Enhanced expression of ROS (5 μg/mL) Overexpression of HSP70 (5 μg/mL)	Dose dependent effect 200 nm nanoparticles showed higher toxicity than the 300 nm nanoparticles Results for ROS production were only presented for 5 μg/mL	Hu et al., 2011
Chitosan NPs	100 kDa and 95 % DD	85 nm	*In vitro* embryo model (5 days)	Zebrafish	–	100, 150, 200, 250, 300, 350, and 400 μg/mL	Dose-dependent effect in terms of malformation, mortality and hatching rates	The comparison between the toxicity of chitosan nanoparticles and chitosan powder suggested the nano assembly of chitosan was relatively more secure than normal chitosan particles	Wang et al., 2016
Chitosan NPs	na	100 nm	*In vitro* culture of embryos (24 h)	Mouse morula-stage embryos	–	100 μg/mL	Induce endoplasmic reticulum (ER) stress and double- and multi-membraned autophagic vesicles, that lead to cell death of blastocoels	–	Choi et al., 2016
Chitosan NPs	na	100 nm	*In vivo* reproduction model	ICR mice	Intravenous	500 μg/kg or 1,000 μg/kg b.w.[a]	Significant reduction in the number of developing follicles	–	Choi et al., 2016
Nanostructured lipid carrier (NLC)-oleoyl-quaternized-chitosan (CS)-coated	Chitosan (CS) (molecular weight 600 kDa)	147 nm + 44.9 mV	*In vitro* embryo model (incubation for 72 h)	Zebrafish	–	2.5, 5, 10, 20, and 40 μM	Embryonic survival was dose dependent exposure to 40 μM−100% embryo mortality Survivor embryos of the 5, 10, and 20 μM exposure presented some malformations (e.g., eye/head abnormalities, pericardial edema, and yolk sac edema)	Chitosan coating increased the toxicity of the NLC	Yostawonkul et al., 2017

(Continued)

TABLE 7 | Continued

Nanomaterial	Polymer characterization	Nanomaterial characterization	Testing method	Model	Administration route (if applicable)	Dose/ concentration range	Results	Observations	References
Poly(lactic-*co*-glycolic acid) (PLGA)–polyethylene glycol (PEG)–folic acid (FA) NPs	PEG – MW 2kDa PLGA – MW 90 kDa (lactic to glycolic acid 50:50), carboxyl-terminated	131 nm −25 mV	*In vitro* embryo model (12 and 36 h) Zebrafish	Zebrafish	–	–	No serious malformation or death was observed at the embryo-development stage or for hatched zebrafish larva	–	Chen et al., 2017
Poly(lactic-*co*-glycolic acid) (PLGA) NPs	PEG – MW 2kDa PLGA – MW 90 kDa (lactic to glycolic acid 50:50), carboxyl-terminated	83 nm −27 mV	*In vitro* embryo model (12 and 36 h)	Zebrafish	–	–	No serious malformation or death was observed at the embryo-development stage or for hatched zebrafish larva	–	Chen et al., 2017
Polyphenolic bio-enhancers with oleanolic acid in chitosan coated PLGA NPs (CH-OA-B-PLGA NPs)	Chitosan (molecular weight 150 kDa, deacetylation degree 85%), Poly (lactide-coglycolide) (PLGA) 50:50, mw 40–75 kDa	342 nm + 34 mV	*In vivo* exposure (21 days)	Sprague Dawley rats	Oral	100 mg/kg b.w. of OA	Normal mating Major increase in the weight Higher number of pups at parturition No sign of abnormality or deformation on pups	100 mg/kg is the double of the OA effective dose	Sharma et al., 2017
Polyphenolic bio-enhancers with oleanolic acid in PLGA NPs (OA-B-PLGA NPs)	Poly (lactide-coglycolide) (PLGA) 50:50, mw 40–75 kDa	221 nm −19 mV	*In vivo* exposure (21 days)	Sprague Dawley rats	Oral	100 mg/kg b.w. of OA	Authors do not present or discuss the result	100 mg/kg is the double of the OA effective dose	Sharma et al., 2017

[a] *b.w., body weight.*

TABLE 8 | Review of original articles assessing hemolysis induced by polymeric nanoparticles.

Nanomaterial	Polymer characterization	Nanomaterial characterization	Testing method	Model	Dose/concentration range	Results	Observations	References
Chitosan NPs	270 kDa	367 nm +5 mV	Erythrocyte incubation (2 h)	Human blood	2000 μg/mL	Chitosan NPs were slightly hemolytic (~7%)	–	Shelma and Sharma, 2011
Chitosan NPs	Low molecular weight chitosan ≥75% DD	180 nm + 48 mV (acetic acid) 150 nm +39 mV (lactic acid) 140–160 nm +(20–25) mV (saline)	Whole blood incubation (3 h)	Human blood	50 μg/mL	NPs prepared in acetic acid medium showed high % hemolysis compared to those prepared in lactic acid medium, whereas the saline-dispersed NPs were found to be hemocompatible	The authors also tested the molecular chitosan and was hemocompatible	Nadesh et al., 2013
Chitosan NPs	Low molecular weight chitosan (85% DD)	≤100 nm +40 mV	Erythrocyte incubation (2 h)	Human blood	50–300 μg/mL	No significant hemolysis	Bulk chitosan was tested at the same concentrations.	Sarangapani et al., 2018
Chitosan NPs	50 kDa and 85% DD	~300 nm +35 mV	Erythrocyte incubation (2, 4 h)	Wistar rat	2.5 and 3.75 mg/mL	Low hemolysis rates		Kumar et al., 2017
Oleoyl-carboxymethyl-chitosan (OCMCS) nanoparticles	170 kDa chitosan, 92.56% DD modified with chloroactic acid and oleoyl chloride	171 nm +19 mV	Erythrocyte incubation (30, 60 min)	Carp blood	1 and 2 mg/mL	No hemolysis		Liu et al., 2013
PLA NPs	Poly(D,L-lactide) (PDLLA) 101782 g/mol and 0.68 dL/g	188 nm −24 mV (water) 109 nm −7 mV (water)	Whole blood incubation (3 h)	Human blood	38, 50, 200, 250 μg/mL	No hemolysis		Da Silva et al., 2019
PLA NPs	Poly(D,L-lactide) (PDLLA) 101782 g/mol and 0.68 dL/g	188 nm −24 mV (water) 109 nm −7 mV (water)	Whole blood incubation (3 h)	Human blood	75, 100, 300, 400 μg/mL	No hemolysis		Da Silva et al., 2019
Amphotericin loaded PEG-PLGA NPs	Copolymer produced with 6000 Da PLGA (lactic to glycolic acid molar ratio of 1:1) and 15% PEG	25 nm	Erythrocyte incubation (8 and 24 h)	Sprague Dawley Rat blood	Equivalent to 20, 50, and 100 μg/mL of amphotericin	Low hemolysis rate (<15%) Concentration dependent	Reduced hemolysis when compared to amphotericin commercial formulation (same dose)	Radwan et al., 2017a
Amphotericin loaded PEG-PLGA NPs	PLGA lactic to glycolic acid 50:50 with 40–75 KDa and PEG with 10 KDa	170 nm	Erythrocyte incubation (1 h)	Human blood	Equivalent to 25 μg/mL of amphotericin	Nanoparticles reduced the hemolytic activity of amphotericin in more than 95% Blank nanoparticles induced negligible hemolysis (unknown concentration)		Moraes Moreira Carraro et al., 2017

(Continued)

TABLE 8 | Continued

Nanomaterial	Polymer characterization	Nanomaterial characterization	Testing method	Model	Dose/concentration range	Results	Observations	References
Amphotericin loaded PLGA NPs	PLGA lactic to glycolic acid 50:50 with 40–75 KDa	190 nm	Erythrocyte incubation (1 h)	Human blood	Equivalent to 25 μg/mL of amphotericin	Nanoparticles reduced the hemolytic activity of amphotericin in more than 95% Blank nanoparticles induced negligible hemolysis (unknown concentration)		Moraes Moreira Carraro et al., 2017
Casein stabilized PLGA NPs	PLGA lactic to glycolic acid 75:25, 5,000 kDa PEI: 25 kDa	165 nm −21 mV	Diluted whole blood incubation (3 h)	Human blood	0.01–10 mg/mL	No hemolysis		Pillai et al., 2015
PVA stabilized PLGA NPs	PLGA lactic to glycolic acid 75:25, 5,000 kDa PEI: 25 kDa	159 nm −0.14 mV	Diluted whole blood incubation (3 h)	Human blood	0.01–10 mg/mL	No hemolysis		Pillai et al., 2015
PEI stabilized PLGA NPs	PLGA lactic to glycolic acid 75:25, 5,000 kDa PEI: 25 kDa	158 nm +30 mV	Diluted whole blood incubation (3 h)	Human blood	0.01–10 mg/mL	7% hemolysis at the highest concentration tested (10 mg/ml)		Pillai et al., 2015
Acyclovir loaded Galactosylated (Gal)-PLGA NPs	na	173 nm −20 mV	Erythrocyte incubation (3 h)	na	0.1 mM of acyclovir	3.3% hemolysis	Free acyclovir in the same concentration induced 16.7% hemolysis	Gupta et al., 2012
Acyclovir loaded PLGA NPs	na	198 nm −8.5 mV	Erythrocyte incubation (3 h)	na	0.1 mM of acyclovir	9.8% hemolysis	Free acyclovir in the same concentration induced 16.7% hemolysis	Gupta et al., 2012
Poly(lactic-*co*-glycolic acid) (PLGA)–polyethylene glycol (PEG)–folic acid (FA) NPs	PEG – MW 2kDa PLGA – MW 90 kDa (lactic to glycolic acid 50:50), carboxyl-terminated	131 nm −25 mV	Diluted whole blood incubation (1 h)	New Zeeland Rabbit blood	0.033, 0.05, and 0.1 mg/mL	No significant hemolysis (<4%)		Chen et al., 2017
Poly(lactic-*co*-glycolic acid) (PLGA) NPs	PEG – MW 2 kDa PLGA – MW 90 kDa (lactic to glycolic acid 50:50), carboxyl-terminated	83 nm −27 mV	Diluted whole blood incubation (1 h)	New Zeeland Rabbit blood	0.033, 0.05, and 0.1 mg/mL	No significant hemolysis (<4%)		Chen et al., 2017

(Continued)

TABLE 8 | Continued

Nanomaterial	Polymer characterization	Nanomaterial characterization	Testing method	Model	Dose/concentration range	Results	Observations	References
Danorubicin loaded polyethylene glycol-poly L-lysine-poly lactic-co-glycolic acid (PEG-PLL-PLGA) NPs	na	229 nm −20 mV	Erythrocyte incubation (15 min−3 h)	New Zeeland Rabibit blood	50 mg/mL (unloaded)	No hemolysis		Guo et al., 2015
Tamoxifen loaded PLA NPs	85–160 kDa PLA	155 nm −21.7 mV	Erythrocyte incubation (4, 12, 24,48, 72, 96 h)	Human blood	4.4 or 1.1 μM of tamoxifen	Negligible hemolysis at both concentrations and all incubations times	No results presented for blank NPs but is stated they cause no cellular damage to erythrocytes	Altmeyer et al., 2016
Itraconazole loaded PLA NPs	PLA (molecular weight: 56,000	284 nm ∼0 mV	Erythrocyte incubation (3 h)	Wistar rat blood	5–20 μg/mL of ITZ i.e., 53–212 μg/mL of NPs	Significant hemolysis (>5%), concentration dependent	Reduced hemolysis when compared to free itraconazol (same dose). Hemolysis is suggested to be caused by the drug release during incubation	Essa et al., 2012
Itraconazole loaded PEG-PLA NPs	PEG7%-g-PLA, molecular weight: 8,300	197 nm ∼0 mV	Erythrocyte incubation (3 h)	Wistar rat blood	5–20 μg/mL of ITZ i.e., 35–142 μg/mL of NPs	Significant hemolysis (>5%), concentration dependent	Reduced hemolysis when compared to free itraconazol (same dose). Hemolysis is suggested to be caused by the drug release during incubation	Essa et al., 2012
Itraconazole loaded PEG-PLA NPs	[PLA–PEG–PLA]n, molecular weight: 3,900	185 nm ∼0 mV	Erythrocyte incubation (3 h)	Wistar rat blood	5–20 μg/mL of ITZ i.e., 40–159 μg/mL of NPs	Significant hemolysis (>5%), concentration dependent	Reduced hemolysis when compared to free itraconazol (same dose). Hemolysis is suggested to be caused by the drug release during incubation	Essa et al., 2012
Paclitaxel loaded monomethoxypoly (ethylene glycol)-b-poly(lactic acid) (mPEG-PLA) polymeric micelles	mPEG-PLA copolymer (40/60) with a number average molecular weight of 4488.4 and mPEG-PLA copolymer (50/50)	(40/60): 37 nm After incubation with BSA: 40 nm (50/50): 44 nm After ncubation with BSA: 71 nm	Erythrocyte incubation (1 h)	New Zeeland rabbit blood	2–10%	Minimal hemolysis (<6%)	The toxicity of paclitaxel loaded mPEG-PLA (40/60) polymeric micelles was significantly lower than those of mPEG-PLA (50/50)	Li et al., 2014

and proving effectiveness of the drug loaded formulation, using the most diverse cell lines (Lorscheidt and Lamprecht, 2016). Toxicological studies exploring the biological effects of the polymeric NMs, particularly regarding immune system interaction are often disregarded. Though, as suggested by the safe-by-design concept, the toxicity study of NMs should be the starting point for the formulation development.

After our research on original peer reviewed articles, we selected the following endpoints to analyze that are crucial to understand the toxicity of nanobiomaterials for drug delivery: acute toxicity, repeated-dose toxicity, inflammation, oxidative stress, genotoxicity (including carcinogenicity and mutagenicity) toxicity on reproduction, and hemolysis. Importantly, one of the first conclusions to retain is that among different research groups, the methodologies, the animal or cellular model, the dose or concentration, the assay duration and notably, the polymeric NM properties, are not the same, making it difficult to compare and establish trends. This issue derives in part from the absence of regulatory binding and standardized methodologies and guidelines which hardens the comparison of safety/toxicity assessments in different reports (Dhawan and Sharma, 2010), and ultimately, makes it difficult to extrapolate safety profiles for human health. A similar conclusion was achieved by Park and coworkers, who discussed the status of *in vitro* toxicity studies for wide-ranging NMs, particularly cytotoxicity, oxidative stress, inflammation and genotoxicity and established that important limitations were preventing their use for human health risk assessment (Park et al., 2009).

Among the different polymeric NMs available, the most studied and reported are chitosan and PLGA nanoparticles. "Chitosan nanoparticles" and "PLGA nanoparticles" are general terms used for an endless number of different nanoparticles comprising multiple polymeric combinations, cross-links and surfactants, and therefore, displaying diverse physical and chemical properties as illustrated by the first 3 columns of **Tables 3**–**8**. As expected, these variables, together with the great diversity of protocols employed by different authors for the same assays, generates ambiguous results that prevent the establishment of trends between the nanocarriers characteristics and the expected toxicological endpoints.

An adequate characterization of the polymeric NMs is crucial for a comprehensive interpretation of the results but also to allow a comparison between different NMs. In 2018, in the context of EU FP-7 GUIDEnano project, it was published the development of a systematic method to assess similarity between NMs that would allow the extrapolation of results for human hazard evaluation purpose (Park et al., 2018). In that methodology they defined the following parameters for assessing similarities between NMs: chemical composition, crystalline form, impurities, primary size distribution, aggregate/agglomerate size distribution, density, and shape. Importantly, those parameters should be tested and compared in relevant media accordingly to the exposure route or toxicity test. However, in the process of developing such methodology, the authors identified several challenges that prevented the establishment of thresholds for establishing similarity. They suggest that the awareness of researchers for the relevance of characterizing NMs when performing hazard assessments is increasing which can lead to the establishment of the thresholds in the future, facilitating the extrapolation of hazard endpoints between similar NMs. Indeed, among the different research articles analyzed, the lack of broad characterization is frequent, sometimes even ignoring important parameters, such as the polymer molecular weight or the nanoparticle size.

Another aspect that should be taken into consideration when characterizing the polymeric NMs to study their biological effects is the endotoxin contamination. In fact, when discussing for instance cytokine stimulation or oxidative stress, endotoxin contamination should not be neglected. Nevertheless, endotoxin quantification (or its acknowledgment) on chitosan and other polymeric NMs is still scarce, which compromises some of the results found in the literature regarding their bioactivity and toxicity. In addition, despite testing the presence of endotoxins is a common procedure in laboratory and several commercial tests are available, they need to be validated for use with NMs, since most are based on optical assays and may be affected by the optical density of NPs (Dobrovolskaia et al., 2010).

Not only endotoxin detection assays are susceptible of interference from NMs and consequently misinterpretation of the results. Therefore, one way of trying to overcome this problem is to use different assays to evaluate the same endpoint. Additionally, experiment controls, such as the incubation of probes (without biological matrixes) and positive controls with NMs, can reveal whether these NMs might be generating false positive or negative results.

The obstacles identified in this review prevent the identification of toxicity trends and the generation of a useful database where we can rely for the Safe-by-Design. Only by performing *in vitro* and *in vivo* harmonized toxicity studies using unloaded polymeric NMs, extensively characterized regarding their intrinsic and extrinsic properties and by performing all necessary controls it is possible to generate such database. At the present time, taking everything into account, the human health risk assessment of polymeric NMs is still dependent on a case-by-case evaluation, and it should comprise the evaluation of parameters, such as the route of administration and dose, among others, to define the required tests for the hazard assessment (i.e., type of *in vitro* and *in vivo* studies).

AUTHOR CONTRIBUTIONS

SJ gathered the information, analyzed, and wrote the first draft of the manuscript. SJ, MS, CS, GB, PW, and OB defined the subjects for discussion. All authors contributed to manuscript revision, read, and approved the submitted version.

FUNDING

This work was financed by the European Regional Development Fund (ERDF), through the Centro 2020 Regional Operational Programme under project CENTRO-01-0145-FEDER-00008:BrainHealth 2020, and through the COMPETE 2020—Operational Programme for Competitiveness and

Internationalization and Portuguese national funds via FCT—Fundação para a Ciência e a Tecnologia, I.P., under project PROSAFE/0001/2016, and the strategic projects POCI-01-0145-FEDER-030331 and POCI-01-0145-FEDER-007440 (UID/NEU/04539/2019). This work is part of the GoNanoBioMat project and has received funding from the Horizon 2020 framework program of the European Union, ProSafe Joint Transnational Call 2016 and from the CTI (1.1.2018 Innosuisse), under grant agreement Number 19267.1 PFNM-NM.

REFERENCES

Agarwal, S., Piesco, N. P., Johns, L. P., and Riccelli, A. E. (1995). Differential expression of IL-1 beta, TNF-alpha, IL-6, and IL-8 in human monocytes in response to lipopolysaccharides from different microbes. *J. Dent. Res.* 74, 1057–1065. doi: 10.1177/00220345950740040501

Agrawal, U., Sharma, R., Gupta, M., and Vyas, S. P. (2014). Is nanotechnology a boon for oral drug delivery? *Drug Discov. Today* 19, 1530–1546. doi: 10.1016/j.drudis.2014.04.011

Ai, J., Biazar, E., Jafarpour, M., Montazeri, M., Majdi, A., Aminifard, S., et al. (2011). Nanotoxicology and nanoparticle safety in biomedical designs. *Int. J. Nanomedicine* 1117–1127. doi: 10.2147/IJN.S16603

Altmeyer, C., Karam, T. K., Khalil, N. M., and Mainardes, R. M. (2016). Tamoxifen-loaded poly(L-lactide) nanoparticles: development, characterization and *in vitro* evaluation of cytotoxicity. *Mater. Sci. Eng. C* 60, 135–142. doi: 10.1016/j.msec.2015.11.019

Aluani, D., Tzankova, V., Kondeva-Burdina, M., Yordanov, Y., Nikolova, E., Odzhakov, F., et al. (2017). Evaluation of biocompatibility and antioxidant efficiency of chitosan-alginate nanoparticles loaded with quercetin. *Int. J. Biol. Macromol.* 103, 771–782. doi: 10.1016/j.ijbiomac.2017.05.062

Aragao-Santiago, L., Hillaireau, H., Grabowski, N., Mura, S., Nascimento, T. L., Dufort, S., et al. (2015). Compared *in vivo* toxicity in mice of lung delivered biodegradable and non-biodegradable nanoparticles. *Nanotoxicology* 10, 292–302. doi: 10.3109/17435390.2015.1054908

Aranda, A., Sequedo, L., Tolosa, L., Quintas, G., Burello, E., Castell, J. V., et al. (2013). Dichloro-dihydro-fluorescein diacetate (DCFH-DA) assay: a quantitative method for oxidative stress assessment of nanoparticle-treated cells. *Toxicol. in vitro* 27, 954–963. doi: 10.1016/j.tiv.2013.01.016

Arora, D., Dhanwal, V., Nayak, D., Saneja, A., Amin, H., ur Rasool, R., et al. (2016). Preparation, characterization and toxicological investigation of copper loaded chitosan nanoparticles in human embryonic kidney HEK-293 cells. *Mater. Sci. Eng. C* 61, 227–234. doi: 10.1016/j.msec.2015.12.035

ASTM International (2013). *ASTM E2524-08(2013)–Standard Test Method for Analysis of Hemolytic Properties of Nanoparticles.*

Banik, B. L., Fattahi, P., and Brown, J. L. (2016). Polymeric nanoparticles: the future of nanomedicine. *Wiley Interdiscip. Rev. Nanomed. Nanobiotechnol.* 8, 271–299. doi: 10.1002/wnan.1364

Barillet, S., Jugan, M. L., Laye, M., Leconte, Y., Herlin-Boime, N., Reynaud, C., et al. (2010). *In vitro* evaluation of SiC nanoparticles impact on A549 pulmonary cells: Cyto-, genotoxicity and oxidative stress. *Toxicol. Lett.* 198, 324–330. doi: 10.1016/j.toxlet.2010.07.009

Barratt, G. M. (2000). Therapeutic applications of colloidal drug carriers. *Pharm. Sci. Technol. Today* 3, 163–171. doi: 10.1016/S1461-5347(00)00255-8

Bazile, D., Prud'homme, C., Bassoullet, M. T., Marlard, M., Spenlehauer, G., and Veillard, M. (1995). Stealth Me.PEG-PLA nanoparticles avoid uptake by the mononuclear phagocytes system. *J. Pharm. Sci.* 84, 493–498. doi: 10.1002/jps.2600840420

Behzadi, S., Serpooshan, V., Sakhtianchi, R., Muller, B., Landfester, K., Crespy, D., et al. (2014). Protein corona change the drug release profile of nanocarriers: the "overlooked" factor at the nanobio interface. *Colloids Surf. B Biointerfaces* 123, 143–149. doi: 10.1016/j.colsurfb.2014.09.009

Behzadi, S., Serpooshan, V., Tao, W., Hamaly, M. A., Alkawareek, M. Y., Dreaden, E. C., et al. (2017). Cellular uptake of nanoparticles: journey inside the cell. *Chem. Soc. Rev.* 46, 4218–4244. doi: 10.1039/C6CS00636A

Bhatia, S. (2016). "Nanoparticles types, classification, characterization, fabrication methods and drug delivery applications," in *Natural Polymer Drug Delivery Systems* (Cham: Springer), 33–93.

Blanco, E., Shen, H., and Ferrari, M. (2015). Principles of nanoparticle design for overcoming biological barriers to drug delivery. *Nat. Biotechnol.* 33, 941–951. doi: 10.1038/nbt.3330

Bor, G., Mytych, J., Zebrowski, J., Wnuk, M., and Sanli-Mohamed, G. (2016). Cytotoxic and cytostatic side effects of chitosan nanoparticles as a non-viral gene carrier. *Int. J. Pharm.* 513, 431–437. doi: 10.1016/j.ijpharm.2016.09.058

Bosio, S., and Laughinghouse IV, H. D. (2012). "Bioindicator of genotoxicity: the Allium cepa test," in *Environmental Contamination*, ed J. Srivastava (IntechOpen).

Boyes, W. K., Thornton, B. L. M., Al-Abed, S. R., Andersen, C. P., Bouchard, D. C., Burgess, R. M., et al. (2017). A comprehensive framework for evaluating the environmental health and safety implications of engineered nanomaterials. *Crit. Rev. Toxicol.* 47, 767–810. doi: 10.1080/10408444.2017.1328400

Brohi, R. D., Wang, L., Talpur, H. S., Wu, D., Khan, F. A., Bhattarai, D., et al. (2017). Toxicity of nanoparticles on the reproductive system in animal models: a review. *Front. Pharmacol.* 8:606. doi: 10.3389/fphar.2017.00606

Buzea, C., Pacheco, I. I., and Robbie, K. (2007). Nanomaterials and nanoparticles: sources and toxicity. *Biointerphases* 2, MR17–MR71. doi: 10.1116/1.2815690

Chakravarthy, S., Sadagopan, S., Nair, A., and Sukumaran, S. K. (2014). Zebrafish as an *in vivo* high-throughput model for genotoxicity. *Zebrafish* 11, 154–166. doi: 10.1089/zeb.2013.0924

Chang, Y.-M., Lee, Y.-J., Liao, J.-W., Jhan, J.-K., Chang, C.-T., and Chung, Y.-C. (2014). *In vitro* and *in vivo* safety evaluation of low molecular weight chitosans prepared by hydrolyzing crab shell chitosans with bamboo shoots chitosanase. *Food Chem. Toxicol.* 71, 10–16. doi: 10.1016/j.fct.2014.05.016

Chen, J., Wu, Q., Luo, L., Wang, Y., Zhong, Y., Dai, H., et al. (2017). Dual tumor-targeted poly(lactic-co-glycolic acid)–polyethylene glycol–folic acid nanoparticles: a novel biodegradable nanocarrier for secure and efficient antitumor drug delivery. *Int. J. Nanomed.* 12, 5745–5760. doi: 10.2147/IJN.S136488

Choi, Y.-J., Gurunathan, S., Kim, D., Jang, H. S., Park, W.-J., Cho, S.-G., et al. (2016). Rapamycin ameliorates chitosan nanoparticle-induced developmental defects of preimplantation embryos in mice. *Oncotarget* 7, 74658–74677. doi: 10.18632/oncotarget.10813

Da Silva, J., Jesus, S., Bernardi, N., Colaço, M., and Borges, O. (2019). Poly(D,L-lactic acid) nanoparticle size reduction increases its immunotoxicity. *Front. Bioeng. Biotechnol.* 7:137. doi: 10.3389/fbioe.2019.00137

Das, J., Choi, Y.-J., Song, H., and Kim, J.-H. (2016). Potential toxicity of engineered nanoparticles in mammalian germ cells and developing embryos: treatment strategies and anticipated applications of nanoparticles in gene delivery. *Hum. Reprod. Update* 22, 588–619. doi: 10.1093/humupd/dmw020

Date, A. A., Hanes, J., and Ensign, L. M. (2016). Nanoparticles for oral delivery: Design, evaluation and state-of-the-art. *J. Control. Release* 240, 504–526. doi: 10.1016/j.jconrel.2016.06.016

Davydova, V. N., Yermak, I. M., Gorbach, V. I., Krasikova, I. N., and Solov'eva, T. F. (2000). Interaction of bacterial endotoxins with chitosan. Effect of endotoxin structure, chitosan molecular mass, and ionic strength of the solution on the formation of the complex. *Biochemistry 65*, 1082–1090.

De Lima, R., Feitosa, L., Pereira A, D. E. S., De Moura, M. R., Aouada, F. A., Mattoso L. H. C., et al. (2010). Evaluation of the genotoxicity of chitosan nanoparticles for use in food packaging films. *J. Food Sci.* 75, N89–N96. doi: 10.1111/j.1750-3841.2010.01682.x

de Salamanca A. E. D., Diebold, Y., Calonge, M., Garci'a-Vazquez, C., Callejo, S., Vila, A., et al. (2006). Chitosan nanoparticles as a potential drug delivery system for the ocular surface: toxicity, uptake mechanism and *in vivo* tolerance. *Investig. Opthalmol. Vis. Sci.* 47, 1416–1425. doi: 10.1167/iovs.05-0495

DeLoid, G., Cohen, J. M., Darrah, T., Derk, R., Rojanasakul, L., Pyrgiotakis, G., et al. (2014). Estimating the effective density of engineered nanomaterials for *in vitro* dosimetry. *Nat. Commun.* 5:3514. doi: 10.1038/ncomms4514

Dhawan, A., and Sharma, V. (2010). Toxicity assessment of nanomaterials: methods and challenges. *Anal. Bioanal. Chem.* 398, 589–605. doi: 10.1007/s00216-010-3996-x

Dobrovolskaia, M. A., Clogston, J. D., Neun, B. W., Hall, J. B., Patri, A. K., and McNeil, S. E. (2008). Method for analysis of nanoparticle hemolytic properties *in vitro*. *Nano Lett.* 8, 2180–2187. doi: 10.1021/nl0805615

Dobrovolskaia, M. A., Germolec, D. R., and Weaver, J. L. (2009). Evaluation of nanoparticle immunotoxicity. *Nat. Nanotechnol.* 4, 411–414. doi: 10.1038/nnano.2009.175

Dobrovolskaia, M. A., and McNeil, S. E. (2013). Understanding the correlation between *in vitro* and *in vivo* immunotoxicity tests for nanomedicines. *J. Control. Release* 172, 456–466. doi: 10.1016/j.jconrel.2013.05.025

Dobrovolskaia, M. A., Neun, B. W., Clogston, J. D., Ding, H., Ljubimova, J., and McNeil, S. E. (2010). Ambiguities in applying traditional Limulus amebocyte lysate tests to quantify endotoxin in nanoparticle formulations. *Nanomedicine* 5, 555–562. doi: 10.2217/nnm.10.29

Dusinska, M., Tulinska, J., El Yamani, N., Kuricova, M., Liskova, A., Rollerova, E., et al. (2017). Immunotoxicity, genotoxicity and epigenetic toxicity of nanomaterials: new strategies for toxicity testing? *Food Chem. Toxicol.* 109(Pt 1), 797–811. doi: 10.1016/j.fct.2017.08.030

Egusquiaguirre, S. P., Pedraz, J. L., Hernández, R. M., and Igartua, M. (2016). "Nanotherapeutic platforms for cancer treatment: from preclinical development to clinical application," in *Nanoarchitectonics for Smart Delivery and Drug Targeting,* eds A.-M. Holban, A. Mihai (Oxford: William Andrew) 813–869. doi: 10.1016/B978-0-323-47347-7.00029-X

Ema, M., Kobayashi, N., Naya, M., Hanai, S., and Nakanishi, J. (2010). Reproductive and developmental toxicity studies of manufactured nanomaterials. *Reproduct. Toxicol.* 30, 343–352. doi: 10.1016/j.reprotox.2010.06.002

Essa, S., Louhichi, F., Raymond, M., and Hildgen, P. (2012). Improved antifungal activity of itraconazole-loaded PEG/PLA nanoparticles. *J. Microencapsul.* 30, 205–217. doi: 10.3109/02652048.2012.714410

European Medicines Agency (2006). *EMEA/CHMP/79769/2006–Reflection Paper on Nanotechnology-Based Medicinal Products for Human Use*.

Fasehee, H., Dinarvand, R., Ghavamzadeh, A., Esfandyari-Manesh, M., Moradian, H., Faghihi, S., et al. (2016). Delivery of disulfiram into breast cancer cells using folate-receptor-targeted PLGA-PEG nanoparticles: *in vitro* and *in vivo* investigations. *J. Nanobiotechnol.* 14:32. doi: 10.1186/s12951-016-0183-z

Fernandes, J. C., Eaton, P., Nascimento, H., Gião, M. S., Ramos, Ó. S., Belo, L., et al. (2010). Antioxidant activity of chitooligosaccharides upon two biological systems: Erythrocytes and bacteriophages. *Carbohydr. Polym.* 79, 1101–1106. doi: 10.1016/j.carbpol.2009.10.050

Food and Drug Aministration (2014). *Considering Whether an FDA-Regulated Product Involves the Application of Nanotechnology: Guidance for Industry*. Food and Drug Aministration (FDA).

Fröhlich, E. (2012). The role of surface charge in cellular uptake and cytotoxicity of medical nanoparticles. *Int. J. Nanomedicine* 7, 5577–5591. doi: 10.2147/IJN.S36111

Gatoo, M. A., Naseem, S., Arfat, M. Y., Mahmood Dar, A., Qasim, K., and Zubair, S. (2014). Physicochemical properties of nanomaterials: implication in associated toxic manifestations. *Biomed Res. Int.* 2014:498420. doi: 10.1155/2014/498420

Gatto, F., and Bardi, G. (2018). Metallic nanoparticles: general research approaches to immunological characterization. *Nanomaterials* 8:E753. doi: 10.3390/nano8100753

Ge, C. C., Du, J. F., Zhao, L. N., Wang, L. M., Liu, Y., Li, D. H., et al. (2011). Binding of blood proteins to carbon nanotubes reduces cytotoxicity. *Proc. Natl. Acad. Sci. U.S.A.* 108, 16968–16973. doi: 10.1073/pnas.1105270108

Grabowski, N., Hillaireau, H., Vergnaud, J., Tsapis, N., Pallardy, M., Kerdine-Romer, S., et al. (2015). Surface coating mediates the toxicity of polymeric nanoparticles towards human-like macrophages. *Int. J. Pharm.* 482, 75–83. doi: 10.1016/j.ijpharm.2014.11.042

Grabowski, N., Hillaireau, H., Vergnaud-Gauduchon, J., Nicolas, V., Tsapis, N., Kerdine-Römer, S., et al. (2016). Surface-modified biodegradable nanoparticles' impact on cytotoxicity and inflammation response on a co-culture of lung epithelial cells and human-like macrophages. *J. Biomed. Nanotechnol.* 12, 135–146. doi: 10.1166/jbn.2016.2126

Guadagnini, R., Halamoda Kenzaoui, B., Walker, L., Pojana, G., Magdolenova, Z., Bilanicova, D., et al. (2013a). Toxicity screenings of nanomaterials: challenges due to interference with assay processes and components of classic *in vitro* tests. *Nanotoxicology* 9, 13–24. doi: 10.3109/17435390.2013.829590

Guadagnini, R., Moreau, K., Hussain, S., Marano, F., and Boland, S. (2013b). Toxicity evaluation of engineered nanoparticles for medical applications using pulmonary epithelial cells. *Nanotoxicology* 9, 25–32. doi: 10.3109/17435390.2013.855830

Guo, L., Chen, B., Liu, R., Liu, P., Xia, G., Wang, Y., et al. (2015). Biocompatibility assessment of polyethylene glycol-poly L-lysine-poly lactic-co-glycolic acid nanoparticles *in vitro* and *in vivo*. *J. Nanosci. Nanotechnol.* 15, 3710–3719. doi: 10.1166/jnn.2015.9509

Gupta, S., Agarwal, A., Gupta, N. K., Saraogi, G., Agrawal, H., and Agrawal, G. P. (2012). Galactose decorated PLGA nanoparticles for hepatic delivery of acyclovir. *Drug Develop. Industr. Pharm.* 39, 1866–1873. doi: 10.3109/03639045.2012.662510

Han, H. D., Byeon, Y., Jang, J.-H., Jeon, H. N., Kim, G. H., Kim, M. G., et al. (2016). *In vivo* stepwise immunomodulation using chitosan nanoparticles as a platform nanotechnology for cancer immunotherapy. *Sci. Rep.* 6:38348. doi: 10.1038/srep38348

Hinderliter, P. M., Minard, K. R., Orr, G., Chrisler, W. B., Thrall, B. D., Pounds, J. G., et al. (2010). ISDD: a computational model of particle sedimentation, diffusion and target cell dosimetry for *in vitro* toxicity studies. *Part. Fibre Toxicol.* 7:36. doi: 10.1186/1743-8977-7-36

Hoshyar, N., Gray, S., Han, H., and Bao, G. (2016). The effect of nanoparticle size on *in vivo* pharmacokinetics and cellular interaction. *Nanomedicine* 11, 673–692. doi: 10.2217/nnm.16.5

Hu, Y., Wang, H., and Gao, J. (2011). Toxicity evaluation of biodegradable chitosan nanoparticles using a zebrafish embryo model. *Int. J. Nanomedicine* 6, 3351–339. doi: 10.2147/IJN.S25853

Huang, Y., Gao, H., Gou, M., Ye, H., Liu, Y., Gao, Y., et al. (2010). Acute toxicity and genotoxicity studies on poly(ε-caprolactone)-poly(ethylene glycol)-poly(ε-caprolactone) nanomaterials. *Mutat. Res. Genet. Toxicol. Environ. Mutage.* 696, 101–106. doi: 10.1016/j.mrgentox.2009.12.016

Je, J.-Y., Park, P.-J., and Kim, S.-K. (2004). Free radical scavenging properties of hetero-chitooligosaccharides using an ESR spectroscopy. *Food Chem. Toxicol.* 42, 381–387. doi: 10.1016/j.fct.2003.10.001

Jena, S. K., and Sangamwar, A. T. (2016). Polymeric micelles of amphiphilic graft copolymer of α -tocopherol succinate- g -carboxymethyl chitosan for tamoxifen delivery: synthesis, characterization and *in vivo* pharmacokinetic study. *Carbohydr. Polym.* 151, 1162–1174. doi: 10.1016/j.carbpol.2016.06.078

Jiménez, A. S., MacCalman, L., Belut, E., Goekce, S., Sirokova, L., Cowie, H., et al. (2016). *NANoREG Deliverable 3.08–Improved and Validated Occupational Exposure Models of Release, Exposure, Dispersion and Transfer*. National Institute for Public Health and the Environment Ministry of Health, Welfare and Sport

Jindal, A. B. (2017). The effect of particle shape on cellular interaction and drug delivery applications of micro- and nanoparticles. *Int. J. Pharm.* 532, 450–465. doi: 10.1016/j.ijpharm.2017.09.028

Kalyanaraman, B., Darley-Usmar, V., Davies, K. J. A., Dennery, P. A., Forman, H. J., Grisham, M. B., et al. (2012). Measuring reactive oxygen and nitrogen species with fluorescent probes: challenges and limitations. *Free Radical Biol. Med.* 52, 1–6. doi: 10.1016/j.freeradbiomed.2011.09.030

Kanwal, Z., Raza, M., Manzoor, F., Riaz, S., Jabeen, G., Fatima, S., et al. (2019). A comparative assessment of nanotoxicity induced by metal (silver, nickel) and metal oxide (cobalt, chromium) nanoparticles in *Labeo rohita*. *Nanomaterials* 9:309. doi: 10.3390/nano9020309

Khan, H. A., and Shanker, R. (2015). Toxicity of nanomaterials. *Biomed Res. Int.* 2015:521014. doi: 10.1155/2015/521014

Khang, D., Lee, Y. K., Choi, E.-J., Webster, T. J., and Kim, S.-H. (2014). Effect of the protein corona on nanoparticles for modulating cytotoxicity and immunotoxicity. *Int. J. Nanomedicine* 10, 97–113. doi: 10.2147/IJN.S72998

Khanna, P., Ong, C., Bay, B., and Baeg, G. (2015). Nanotoxicity: an interplay of oxidative stress, inflammation and cell death. *Nanomaterials* 5, 1163–1180. doi: 10.3390/nano5031163

Kononenko, V., Narat, M., and Drobne, D. (2015). Nanoparticle interaction with the immune system/Interakcije nanodelcev z imunskim sistemom. *Arch. Industr. Hyg. Toxicol.* 66, 97–108. doi: 10.1515/aiht-2015-66-2582

Koppolu, B., and Zaharoff, D. A. (2013). The effect of antigen encapsulation in chitosan particles on uptake, activation and presentation by antigen presenting cells. *Biomaterials* 34, 2359–2369. doi: 10.1016/j.biomaterials.2012.11.066

Kroll, A., Pillukat, M. H., Hahn, D., and Schnekenburger, J. (2012). Interference of engineered nanoparticles with *in vitro* toxicity assays. *Arch. Toxicol.* 86, 1123–1136. doi: 10.1007/s00204-012-0837-z

Kumar, V., Leekha, A., Tyagi, A., Kaul, A., Mishra, A. K., and Verma, A. K. (2017). Preparation and evaluation of biopolymeric nanoparticles as drug delivery system in effective treatment of rheumatoid arthritis. *Pharm. Res.* 34, 654–667. doi: 10.1007/s11095-016-2094-y

Landsiedel, R., Fabian, E., Ma-Hock, L., Wohlleben, W., Wiench, K., Oesch, F., et al. (2012). Toxico-/biokinetics of nanomaterials. *Arch. Toxicol.* 86, 1021–1060. doi: 10.1007/s00204-012-0858-7

Landsiedel, R., Ma-Hock, L., Wiench, K., Wohlleben, W., and Sauer, U. G. (2017). Safety assessment of nanomaterials using an advanced decision-making framework, the DF4nanoGrouping. *J. Nanopart. Res.* 19:171. doi: 10.1007/s11051-017-3850-6

Legaz, S., Exposito, J.-Y., Lethias, C., Viginier, B., Terzian, C., and Verrier, B. (2016). Evaluation of polylactic acid nanoparticles safety using Drosophila model. *Nanotoxicology* 10, 1136–1143. doi: 10.1080/17435390.2016.1181806

Leng, K. M., Vijayarathna, S., Jothy, S. L., Sasidharan, S., and Kanwar, J. R. (2018). *In vitro* and *in vivo* toxicity assessment of alginate/eudragit S 100-enclosed chitosan–calcium phosphate-loaded iron saturated bovine lactoferrin nanocapsules (Fe-bLf NCs). *Biomed. Pharmacother.* 97, 26–37. doi: 10.1016/j.biopha.2017.10.121

Li, C., Shen, Y., Sun, C., Nihad, C., and Tu, J. (2014). Immunosafety and chronic toxicity evaluation of monomethoxypoly(ethylene glycol)-b-poly(lactic acid) polymer micelles for paclitaxel delivery. *Drug Deliv.* 23, 888–895. doi: 10.3109/10717544.2014.971196

Lieder, R., Gaware, V. S., Thormodsson, F., Einarsson, J. M., Ng, C.-H., Gislason, J., et al. (2013). Endotoxins affect bioactivity of chitosan derivatives in cultures of bone marrow-derived human mesenchymal stem cells. *Acta Biomater.* 9, 4771–4778. doi: 10.1016/j.actbio.2012.08.043

Liu, Y., Kong, M., Feng, C., Yang, K. K., Li, Y., Su, J., et al. (2013). Biocompatibility, cellular uptake and biodistribution of the polymeric amphiphilic nanoparticles as oral drug carriers. *Colloids Surfaces B* 103, 345–353. doi: 10.1016/j.colsurfb.2012.11.012

Lorge, E., Moore, M. M., Clements, J., O'Donovan, M., Fellows, M. D., Honma, M., et al. (2016). Standardized cell sources and recommendations for good cell culture practices in genotoxicity testing. *Mutat. Res. Genet. Toxicol. Environ. Mutage.* 809, 1–15. doi: 10.1016/j.mrgentox.2016.08.001

Lorscheidt, S., and Lamprecht, A. (2016). Safety assessment of nanoparticles for drug delivery by means of classic *in vitro* assays and beyond. *Expert Opin. Drug Deliv.* 13, 1545–1558. doi: 10.1080/17425247.2016.1198773

Lü, J.-M., Lin, P. H., Yao, Q., and Chen, C. (2010). Chemical and molecular mechanisms of antioxidants: experimental approaches and model systems. *J. Cell. Mol. Med.* 14, 840–860. doi: 10.1111/j.1582-4934.2009.00897.x,

Lü, X., Zheng, B., Tang, X., Zhao, L., Lu, J., Zhang, Z., et al. (2011). *In vitro* biomechanical and biocompatible evaluation of natural hydroxyapatite/chitosan composite for bone repair. *J. Appl. Biomater. Biomech.* 9, 11–18. doi: 10.5301/JABB.2011.6474

Ma, N., Ma, C., Li, C., Wang, T., Tang, Y., Wang, H., et al. (2013). Influence of nanoparticle shape, size, and surface functionalization on cellular uptake. *J. Nanosci. Nanotechnol.* 13, 6485–6498. doi: 10.1166/jnn.2013.7525

Machado, R. L., de Arruda, E. J., Santana, C. C., and Bueno, S. M. A. (2006). Evaluation of a chitosan membrane for removal of endotoxin from human IgG solutions. Process Biochem. 41, 2252–2257. doi: 10.1016/j.procbio.2006.05.015

Magalhaes, P. O., Lopes, A. M., Mazzola, P. G., Rangel-Yagui, C., Penna, T. C., and Pessoa, A., et al. (2007). Methods of endotoxin removal from biological preparations: a review. *J. Pharm. Pharm. Sci.* 10, 388–404.

Magdolenova, Z., Collins, A., Kumar, A., Dhawan, A., Stone, V., and Dusinska, M. (2013). Mechanisms of genotoxicity. *A review of in vitro and in vivo studies with engineered nanoparticles. Nanotoxicology* 8, 233–278. doi: 10.3109/17435390.2013.773464

Maity, S., Mukhopadhyay, P., Kundu, P. P., and Chakraborti, A. S. (2017). Alginate coated chitosan core-shell nanoparticles for efficient oral delivery of naringenin in diabetic animals—an *in vitro* and *in vivo* approach. *Carbohydr. Polym.* 170, 124–132. doi: 10.1016/j.carbpol.2017.04.066

Moraes Moreira Carraro, T. C., Altmeyer, C., Maissar Khalil, N., and Mara Mainardes, R. (2017). Assessment of *in vitro* antifungal efficacy and *in vivo* toxicity of Amphotericin B-loaded PLGA and PLGA-PEG blend nanoparticles. *J. Mycol. Méd.* 27, 519–529. doi: 10.1016/j.mycmed.2017.07.004

Moritz, M., and Geszke-Moritz, M. (2015). Recent developments in application of polymeric nanoparticles as drug carriers. *Adv. Clin. Exper. Med.* 24, 749–758. doi: 10.17219/acem/31802

Mukhopadhyay, P., Chakraborty, S., Bhattacharya, S., Mishra, R., and Kundu, P. P. (2015). pH-sensitive chitosan/alginate core-shell nanoparticles for efficient and safe oral insulin delivery. *Int. J. Biol. Macromol.* 72, 640–648. doi: 10.1016/j.ijbiomac.2014.08.040

Nadesh, R., Narayanan, D., PR, S., Vadakumpully, S., Mony, U., Koyakkutty, M., et al. (2013). Hematotoxicological analysis of surface-modified and -unmodified chitosan nanoparticles. *J. Biomed. Mater. Res. Part A* 101, 2957–2966. doi: 10.1002/jbm.a.34591

Ngo, D.-H., and Kim, S.-K. (2014). Antioxidant effects of chitin, chitosan, and their derivatives. *Adv. Food Nutr. Res.* 73, 15–31. doi: 10.1016/B978-0-12-800268-1.00002-0

OECD (2014). "Genotoxicity of manufactured nanomaterials: report of the OECD expert meeting," in *Series on the Safety of Manufactured Nanomaterials No. 43* (Paris: OECD Environment, Health and Safety Publications).

OECD (2018a). "Evaluation of *in vitro* methods for human hazard assessment applied in the OECD Testing Programme for the Safety of Manufactured Nanomaterials," in *Series on the Safety of Manufactured Nanomaterials No. 85* (Paris: OECD Environment, Health and Safety Publications).

OECD (2018b). "Test No. 412: subacute inhalation toxicity: 28-day study," in *OECD Guidelines for the Testing of Chemicals, Section 4: Health Effects* (Paris: OECD Publishing).

OECD (2018c). "Test No. 413: subchronic inhalation toxicity: 90-day study," in *OECD Guidelines for the Testing of Chemicals, Section 4: Health Effects* (Paris: OECD Publishing).

Omar Zaki, S. S., Katas, H., and Hamid, Z. A. (2015). Lineage-related and particle size-dependent cytotoxicity of chitosan nanoparticles on mouse bone marrow-derived hematopoietic stem and progenitor cells. *Food Chem. Toxicol.* 85, 31–44. doi: 10.1016/j.fct.2015.05.017

Oostingh, G. J., Casals, E., Italiani, P., Colognato, R., Stritzinger, R., Ponti, J., et al. (2011). Problems and challenges in the development and validation of human cell-based assays to determine nanoparticle-induced immunomodulatory effects. *Part. Fibre Toxicol.* 8:8. doi: 10.1186/1743-8977-8-8

Oparka, M., Walczak, J., Malinska, D., van Oppen, L. M. P. E., Szczepanowska, J., Koopman, W. J. H., et al. (2016). Quantifying ROS levels using CM-H 2 DCFDA and HyPer. *Methods* 109, 3–11. doi: 10.1016/j.ymeth.2016.06.008

Palmer, B., and DeLouise, L. (2016). Nanoparticle-enabled transdermal drug delivery systems for enhanced dose control and tissue targeting. *Molecules* 21:E1719. doi: 10.3390/molecules21121719

Park, M.-R., Gurunathan, S., Choi, Y.-J., Kwon, D.-N., Han, J.-W., Cho, S.-G., et al. (2013). Chitosan nanoparticles cause pre- and post-implantation embryo complications in mice. *Biol. Reprod.* 88:88. doi: 10.1095/biolreprod.112.107532

Park, M. V. D. Z., Catalán, J., Ferraz, N., Cabellos, J., Vanhauten, R., Vázquez-Campos, S., et al. (2018). Development of a systematic method to assess similarity between nanomaterials for human hazard evaluation purposes–lessons learnt. *Nanotoxicology* 12, 652–676. doi: 10.1080/17435390.2018.1465142

Park, M. V. D. Z., Lankveld, D. P. K., van Loveren, H., and de Jong, W. H. (2009). The status of *in vitro* toxicity studies in the risk assessment of nanomaterials. *Nanomedicine* 4, 669–685. doi: 10.2217/nnm.09.40

Pillai, G. J., Greeshma, M. M., and Menon, D. (2015). Impact of poly(lactic-co-glycolic acid) nanoparticle surface charge on protein, cellular and haematological interactions. *Colloids Surf. B Biointerfaces* 136, 1058–1066. doi: 10.1016/j.colsurfb.2015.10.047

Platel, A., Carpentier, R., Becart, E., Mordacq, G., Betbeder, D., and Nesslany, F. (2016). Influence of the surface charge of PLGA nanoparticles on their *in vitro* genotoxicity, cytotoxicity, ROS production and endocytosis. *J. Appl. Toxicol.* 36, 434–444. doi: 10.1002/jat.3247

Radwan, M. A., AlQuadeib, B. T., Šiller, L., Wright, M. C., and Horrocks, B. (2017a). Oral administration of amphotericin B nanoparticles: antifungal activity, bioavailability and toxicity in rats. *Drug Deliv.* 24, 40–50. doi: 10.1080/10717544.2016.1228715

Radwan, S. E.-S., Sokar, M. S., Abdelmonsif, D. A., and El-Kamel, A. H. (2017b). Mucopenetrating nanoparticles for enhancement of oral bioavailability of furosemide: *in vitro* and *in vivo* evaluation/sub-acute toxicity study. *Int. J. Pharm.* 526, 366–379. doi: 10.1016/j.ijpharm.2017.04.072

Rana, V., and Sharma, R. (2019). "Recent advances in development of nano drug delivery," in *Applications of Targeted Nano Drugs and Delivery Systems*, eds S.S. Mohapatra, S. Ranjan, N. Dasgupta, R.K. Mishra, and S. Thomas (Oxford: Elsevier), 93–131. doi: 10.1016/B978-0-12-814029-1.00005-3

Salatin, S., Maleki Dizaj, S., and Yari Khosroushahi, A. (2015). Effect of the surface modification, size, and shape on cellular uptake of nanoparticles. *Cell Biol. Int.* 39, 881–890. doi: 10.1002/cbin.10459

Sarangapani, S., Patil, A., Ngeow, Y. K., Elsa Mohan, R., Asundi, A., and Lang, M. J. (2018). Chitosan nanoparticles' functionality as redox active drugs through cytotoxicity, radical scavenging and cellular behaviour. *Integr. Biol.* 10, 313–324. doi: 10.1039/C8IB00038G

Sayes, C. M., Aquino, G. V., and Hickey, A. J. (2016). Nanomaterial drug products: manufacturing and analytical perspectives. *AAPS J.* 19, 18–25. doi: 10.1208/s12248-016-0008-x

Shan, X., Xu, T., Liu, Z., Hu, X., Zhang, Y.-D., and Wang, B. (2017). Safety and toxicology of the intravenous administration of Ang2-siRNA plasmid chitosan magnetic nanoparticles. *Mol. Med. Rep.* 15, 736–742. doi: 10.3892/mmr.2016.6090

Sharifi, S., Behzadi, S., Laurent, S., Laird Forrest, M., Stroeve, P., and Mahmoudi, M. (2012). Toxicity of nanomaterials. *Chem. Soc. Rev.*. 41, 2323–2343. doi: 10.1039/C1CS15188F

Sharma, M., Sharma, S., Sharma, V., Sharma, K., Yadav, S. K., Dwivedi, P., et al. (2017). Oleanolic–bioenhancer coloaded chitosan modified nanocarriers attenuate breast cancer cells by multimode mechanism and preserve female fertility. *Int. J. Biol. Macromol.* 104, 1345–1358. doi: 10.1016/j.ijbiomac.2017.06.005

Sharma, M., Shatkin, J. A., Cairns, C., Canady, R., and Clippinger, A. J. (2016). Framework to evaluate exposure relevance and data needs for risk assessment of nanomaterials using *in vitro* testing strategies. *Risk Analysis* 36, 1551–1563. doi: 10.1111/risa.12581

Shelma, R., and Sharma, C. P. (2011). Development of lauroyl sulfated chitosan for enhancing hemocompatibility of chitosan. *Colloids and Surfaces B: Biointerfaces* 84, 561–570. doi: 10.1016/j.colsurfb.2011.02.018

Singh, R. P., and Ramarao, P. (2013). Accumulated polymer degradation products as effector molecules in cytotoxicity of polymeric nanoparticles. *Toxicol. Sci.* 136, 131–143. doi: 10.1093/toxsci/kft179

Słoczynska, K., Powroznik, B., Pekala, E., and Waszkielewicz, A. M. (2014). Antimutagenic compounds and their possible mechanisms of action. *J. Appl. Genet.* 55, 273–285. doi: 10.1007/s13353-014-0198-9

Sonaje, K., Lin, Y.-H., Juang, J.-H., Wey, S.-P., Chen, C.-T., and Sung, H.-W. (2009). *In vivo* evaluation of safety and efficacy of self-assembled nanoparticles for oral insulin delivery. *Biomaterials* 30, 2329–2339. doi: 10.1016/j.biomaterials.2008.12.066

Steimle, A., Autenrieth, I. B., and Frick, J.-S. (2016). Structure and function: lipid A modifications in commensals and pathogens. *Int. J. Med. Microbiol.* 306, 290–301. doi: 10.1016/j.ijmm.2016.03.001

Sun, J., Zhang, Q., Wang, Z., and Yan, B. (2013). Effects of nanotoxicity on female reproductivity and fetal development in animal models. *Int. J. Mol. Sci.* 14, 9319–9337. doi: 10.3390/ijms14059319

Tulinska, J., Kazimirova, A., Kuricova, M., Barancokova, M., Liskova, A., Neubauerova, E., et al. (2015). Immunotoxicity and genotoxicity testing of PLGA-PEO nanoparticles in human blood cell model. *Nanotoxicology* 9(Suppl. 1), 33–43. doi: 10.3109/17435390.2013.816798

VasanthaKumar, S., Ahamed, H. N., and Saha, R. N. (2014). Nanomedicine I: *in vitro* and *in vivo* evaluation of paclitaxel loaded poly-(ε-caprolactone), poly (dl-lactide-co-glycolide) and poly (dl-lactic acid) matrix nanoparticles in wistar rats. *Eur. J. Drug Metab. Pharmacokinet.* 40, 137–161. doi: 10.1007/s13318-014-0189-6

Wallach, D., Kang, T.-B., and Kovalenko, A. (2013). Concepts of tissue injury and cell death in inflammation: a historical perspective. *Nat. Rev. Immunol.* 14, 51–59. doi: 10.1038/nri3561

Wang, H., Yu, X., Su, C., Shi, Y., and Zhao, L. (2018). Chitosan nanoparticles triggered the induction of ROS-mediated cytoprotective autophagy in cancer cells. *Artif. Cells Nanomed. Biotechnol.* 46(Suppl. 1.):293–301. doi: 10.1080/21691401.2017.1423494

Wang, Q., Liu, P., Liu, P., Gong, T., Li, S., Duan, Y., et al. (2014). Preparation, blood coagulation and cell compatibility evaluation of chitosan-graft-polylactide copolymers. *Biomed. Mater.* 9:015007. doi: 10.1088/1748-6041/9/1/015007

Wang, Y., Zhou, J., Liu, L., Huang, C., Zhou, D., and Fu, L. (2016). Characterization and toxicology evaluation of chitosan nanoparticles on the embryonic development of zebrafish, *Danio rerio*. *Carbohydr. Polym.* 141, 204–210. doi: 10.1016/j.carbpol.2016.01.012

Yah, C. S., Simate, G. S., and Iyuke, S. E. (2012). Nanoparticles toxicity and their routes of exposures. *Pak. J. Pharm. Sci.* 25, 477–491.

Yen, M.-T., Yang, J.-H., and Mau, J.-L. (2008). Antioxidant properties of chitosan from crab shells. *Carbohydr. Polym.* 74, 840–844. doi: 10.1016/j.carbpol.2008.05.003

Yermak, I. M., Davidova, V. N., Gorbach, V. I., Luk'yanov, P. A., Solov'eva, T. F., Ulmer, A. J., et al. (2006). Forming and immunological properties of some lipopolysaccharide–chitosan complexes. *Biochimie* 88, 23–30. doi: 10.1016/j.biochi.2005.07.004

Yildirimer, L., Thanh, N. T. K., Loizidou, M., and Seifalian, A. M. (2011). Toxicology and clinical potential of nanoparticles. *Nano Today* 6, 585–607. doi: 10.1016/j.nantod.2011.10.001

Yostawonkul, J., Surassmo, S., Iempridee, T., Pimtong, W., Suktham, K., Sajomsang, W., et al. (2017). Surface modification of nanostructure lipid carrier (NLC) by oleoyl-quaternized-chitosan as a mucoadhesive nanocarrier. *Colloids Surfaces B* 149, 301–311. doi: 10.1016/j.colsurfb.2016.09.049

Yuan, Z.-Y., Hu, Y.-L., and Gao, J.-Q. (2015). Brain Localization and neurotoxicity evaluation of polysorbate 80-modified chitosan nanoparticles in rats. *PLoS ONE* 10:e0134722. doi: 10.1371/journal.pone.0134722

Zhang, J., Tang, H., Liu, Z., and Chen, B. (2017). Effects of major parameters of nanoparticles on their physical and chemical properties and recent application of nanodrug delivery system in targeted chemotherapy. *Int. J. Nanomedicine* 12, 8483–8493. doi: 10.2147/IJN.S148359

Conflict of Interest: The authors declare that the research was conducted in the absence of any commercial or financial relationships that could be construed as a potential conflict of interest.

frontiers in Bioengineering and Biotechnology

SYSTEMATIC REVIEW
published: 17 December 2019
doi: 10.3389/fbioe.2019.00405

Meta-Analysis of Pharmacokinetic Studies of Nanobiomaterials for the Prediction of Excretion Depending on Particle Characteristics

*Marina Hauser and Bernd Nowack**

Empa, Swiss Federal Laboratories for Materials Science and Technology, St. Gallen, Switzerland

The growth in development and use of nanobiomaterials (NBMs) has raised questions regarding their possible distribution in the environment. Because most NBMs are not yet available on the market and exposure monitoring is thus not possible, prospective exposure modeling is the method of choice to get information on their future environmental exposure. An important input for such models is the fraction of the NBM excreted after their application to humans. The aim of this study was to analyze the current literature on excretion of NBMs using a meta-analysis. Published pharmacokinetic data from *in vivo* animal experiments was collected and compiled in a database, including information on the material characteristics. An evaluation of the data showed that there is no correlation between the excretion (in % of injected dose, ID) and the material type, the dose, the zeta potential or the size of the particles. However, the excretion is dependent on the type of administration with orally administered NBMs being excreted to a larger extent than intravenously administered ones. A statistically significant difference was found for IV vs. oral and oral vs. inhalation. The database provided by this work can be used for future studies to parameterize the transfer of NBMs from humans to wastewater. Generic probability distributions of excretion for oral and IV-administration are provided to enable excretion modeling of NBMs without data for a specific NBM.

Keywords: nanobiomaterials, pharmacokinetic, meta-analysis, excretion, prediction

OPEN ACCESS

Edited by:
Olga Borges,
University of Coimbra, Portugal

Reviewed by:
Domenico Cassano,
Joint Research Centre (Italy), Italy
Po-Chang Chiang,
Genentech, Inc., United States

****Correspondence:***
Bernd Nowack
nowack@empa.ch

Specialty section:
This article was submitted to Nanobiotechnology, a section of the journal Frontiers in Bioengineering and Biotechnology

Received: *08 October 2019*
Accepted: *27 November 2019*
Published: *17 December 2019*

Citation:
Hauser M and Nowack B (2019) Meta-Analysis of Pharmacokinetic Studies of Nanobiomaterials for the Prediction of Excretion Depending on Particle Characteristics. Front. Bioeng. Biotechnol. 7:405. doi: 10.3389/fbioe.2019.00405

INTRODUCTION

In the past decade, nanobiomaterials (NBMs) have been increasingly investigated for the use in pharmaceutics and biomedical engineering (Küster and Adler, 2014). A wide range of different nanomaterials are being suggested for these purposes. For example, metals or metal oxides are very common in nanomedicine. Their relatively simple generation and surface modification as well as biocompatibility make gold (Au) nanoparticles attractive for the utilization in medical imaging or cancer detection and treatment (Hirn et al., 2011; Bonakdar and Mashinchian, 2015; Rambanapasi et al., 2015). Silver (Ag) nanoparticles are applied as coatings for indwelling catheters, antibacterial agents, wound dressing, orthopedic implants, and tissue-engineered scaffolds (Lin et al., 2015). Silica nanoparticles (SiO_2) are easy to synthesize, exhibit low toxicity and have an ease for surface modification. These properties make silica applicable as biomarkers, biosensors, DNA or drug delivery, and cancer therapy (Lee et al., 2014). Also organic nanomaterials are often used in medical applications, especially due to their high biological safety, good biodegradability,

low environmental toxicity (Hauser et al., 2019), and easy production and modification (Han et al., 2018). Commonly used organic NBMs are chitosan, polylactic acid (PLA), or poly(lactic-glycolic acid) (PLGA). They may be preferred to other types of nanoparticles due to their flexibility, biodegradability, and relatively low levels of toxicity (Navarro et al., 2017). Chitosan is a polysaccharide which is found in the exoskeleton of crustaceans and is applied in fast wound healing or as a blood clotting agent (Singh et al., 2017). PLA is used in cartilage regeneration, bone tissue engineering, and cartilage repair due to its good elastic modulus, thermal formability, and mechanical strength. PLGA is widely used in nanoparticles, microspheres, pellets, sutures, implantable scaffolds, and microcapsules (Navarro et al., 2017; Han et al., 2018). Additionally, also carbon-based nanomaterials are used in nanomedicine. Fullerenes and carbon nanotubes (CNTs) are highly promising for medical applications as carriers in drug delivery (Yamashita et al., 2012).

NBMs can be administered to the patient's body in different ways. The most commonly used routes of administration in humans are oral, intravenous and inhalation. From these, the oral route is the most convenient one as it is non-invasive and therefore widely accepted by most patients (Schleh et al., 2012). Besides, it also has the potential to be taken at home and not necessarily in a hospital or clinic setting (Navarro et al., 2017). However, the absorption into the bloodstream after oral absorption is generally very low (Park et al., 2011; Lin et al., 2015). The lungs are considered the most important entry of nanoparticles into the human body for example via occupational inhalation of airborne particles during manufacturing (Li X. et al., 2012; Laux et al., 2017). The advantage of intravenous injection is the direct access of the NBM to the blood circulation and thereby a quick distribution throughout the entire body (Hirn et al., 2011). In animal studies also intratracheal (introduction of the material directly into the trachea) or intraperitoneal (into the body cavity) administration is common.

Increasing applications and usage of NBMs leads to an increase in the potential for environmental exposure (Laux et al., 2017; Kabir et al., 2018). Depending on the material, a NBM can biodegrade, accumulate in tissues and organs or get excreted via urine or feces. From urine and feces, they enter the sewage system and are eventually discharged into surface water from where they are distributed throughout the whole biosphere. We expect NBMs to behave similarly to pharmaceuticals as they have the same mode of application and are also excreted in urine and feces from where they reach the sewage system. The German Federal Environment Agency reported the detection of 156 pharmaceuticals in environmental media such as surface water, groundwater and drinking water (Umwelt Bundesamt, 2018). Pharmaceuticals were detected in surface water at a concentration of 0.1–10.0 μg/l (Bergmann et al., 2011).

In order to be able to assess the environmental exposure, one needs knowledge of the presence of nanomaterials in different products but also about their release throughout the life cycle (Som et al., 2010; Keller et al., 2013). The release of nanomaterials into the environment has previously been modeled for a range of engineered nanomaterials (Mueller and Nowack, 2008; Gottschalk et al., 2009, 2010; Sun et al., 2014, 2016, 2017; Wang et al., 2016). However, only one modeling study has been published for NBMs, covering the environmental exposure of gold-nanoparticles from medical applications in the United States and the United Kingdom (Mahapatra et al., 2015).

In exposure modeling the whole life cycle of the material needs to be taken into consideration. For NBMs, the excretion of the NBM from the body is the starting point from where they flow to the sewage system, the waste water treatment plant and finally can be distributed throughout the biosphere to reach different environmental compartments such as soil, ground water, oceans, as well as the atmosphere. In recent years, the number of published physiologically based pharmacokinetic models (PBPK) of NBMs has increased significantly (Grass and Sinko, 2002; Li et al., 2010; Li M. et al., 2012; Li M. et al., 2016; Moss and Siccardi, 2014; Carlander et al., 2016; Li D. et al., 2016). These studies are mostly interested in the distribution of the NBMs in the body to different organs and tissues but the excretion of the material in feces or urine is in many cases also considered.

The aim of our study was to collect data from published pharmacokinetic studies of NBMs and make predictions based on this data set about the excretion of the NBM from the body. As different studies used different materials, coatings, administrations, doses, animals, and evaluation time spans, we aimed to incorporate the different materials and particle properties or study designs into the evaluation and to make general predictions about the excretion of NBMs.

METHODS

The literature was searched for pharmacokinetic studies of NBM or nanoparticles in general that specifically quantified excretion of the nanoparticles. The time frame of the search includes all studies until the end of April 2019. Google Scholar was used with search terms such as "pharmacokinetics nanoparticles excretion," or "pharmacokinetics nanomaterials excretion," "pharmacokinetics metallic/polymeric/organic/etc. nanoparticles/nanomaterials excretion" in all variations, or just "nanoparticles excretion." For each search term, the first ten pages each containing 10 articles were looked at. Besides, the cited articles of these studies were also evaluated.

Only studies with a time frame of a least 1 day were considered. As we were only interested in the total excretion of the nanoparticles, studies with a time frame of <1 day were deemed too short to fully excrete the nanoparticles. Additionally, only studies where the excretion in feces and/or urine is mentioned in %ID (percent of injected dose) or total excretion with the amount administered mentioned in the article (so the %ID could be calculated) were considered. Within one study, only the data point at the longest time was collected per material as it was assumed that this shows the total excretion. Only one data point was collected per material per study to avoid overrepresentation of studies with many measurements. However, several data points were collected from one study if materials with different size, zeta potential, surface coating, dose, etc. were used.

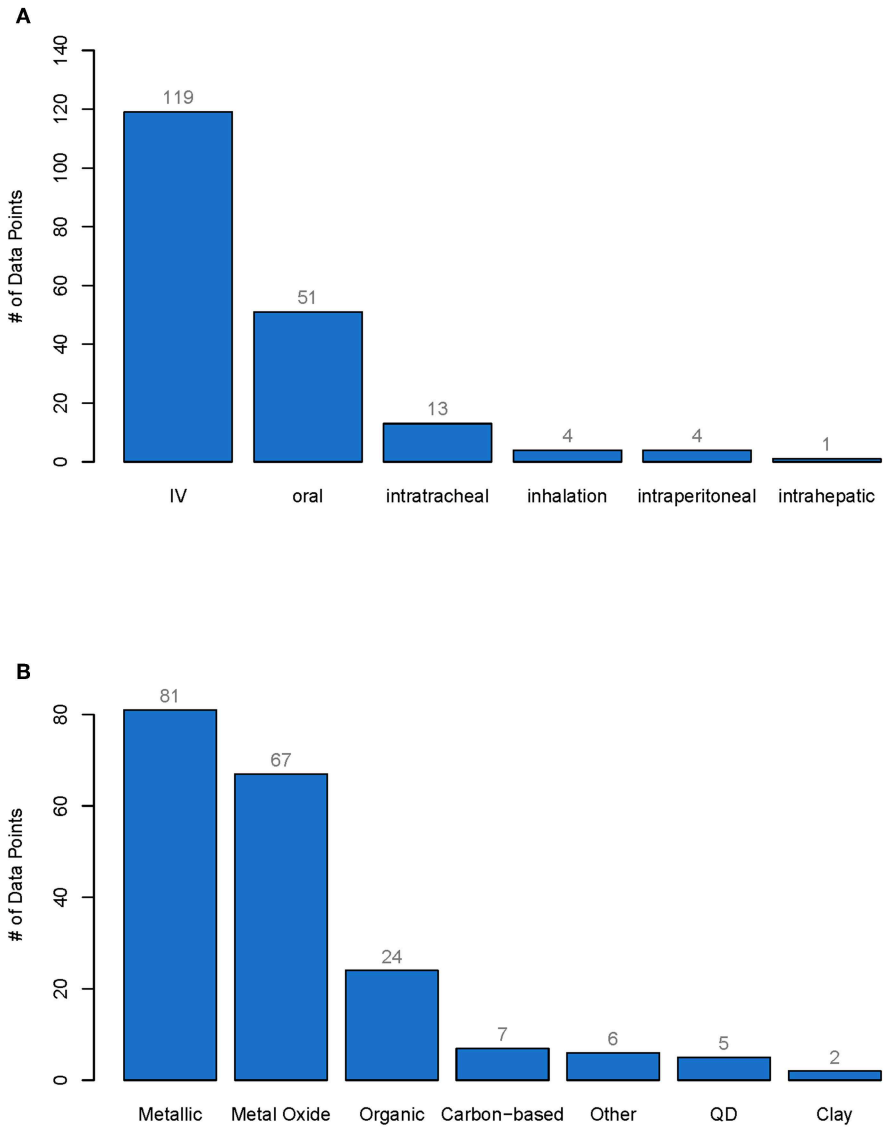

FIGURE 1 | Number of data points for each type of administration **(A)** and for each type of material class **(B)**. From each pharmacokinetic study of nanobiomaterials only one data point was extracted per specific material and the cumulative excretion as well as the material properties were reported. The whole database with all data points can be found in the Supporting Information. IV, Intravenously administered, QD, Quantum dots.

For each material, the material class, the particle size (TEM measurements), the test animal, the route of administration, the zeta potential of the material, the administered dose, and the cumulative excretion (in %ID) were noted. We have taken these material characteristics as they were mentioned in other articles to be of significance for the excretion of the material (Soo Choi et al., 2007; Semmler-Behnke et al., 2008; Alric et al., 2013; Xu et al., 2018). TEM measurements of the primary particle size were preferred over hydrodynamic size as TEM measurements were more widely available and as the nanoparticles get rapidly modified by protein adsorption after administration in the body (Kreyling et al., 2014).

RESULTS AND DISCUSSION

Presentation of the Database

In total, 192 data points were collected from 66 studies. The whole database can be found in the **Table S1**. More than 60% of the nanomaterials were administered intravenously (IV), 30% orally, 7% intratracheally, and <3% by inhalation or intraperitoneal or intrahepatic injection (see **Figure 1A**). Of all the materials investigated, 40% were metallic, 35% metal oxides, 12% organic and <4% carbon-based, Quantum Dots (QD), clays or other (see **Figure 1B**).

Not all studies reported all relevant material or study characteristics. For almost 45% of the data points, the full data set

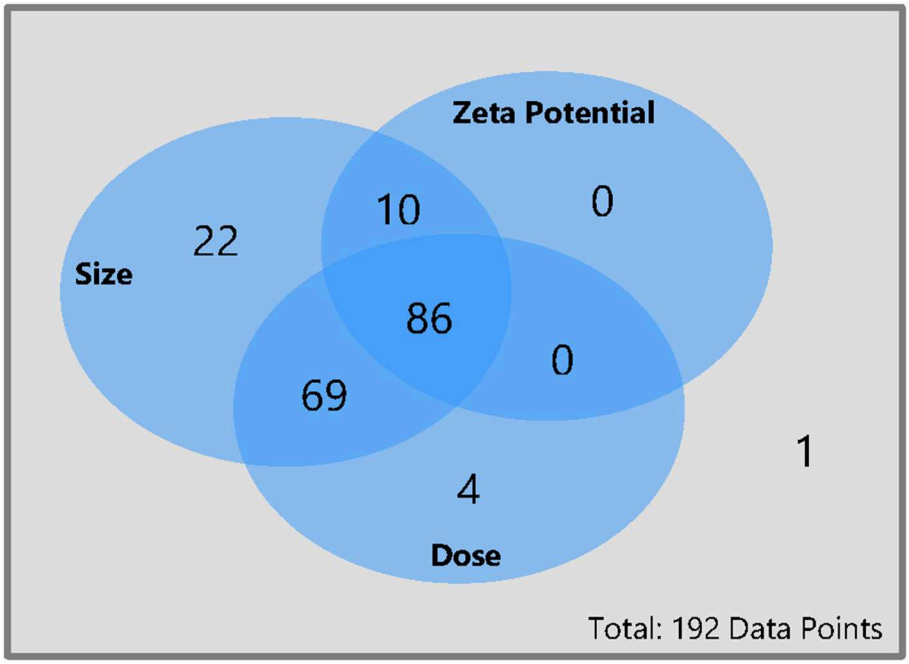

FIGURE 2 | Availability of size, dose, and zeta potential for all data points collected for this meta-analysis. From each pharmacokinetic study of nanobiomaterials only one data point was extracted per specific material and the cumulative excretion as well as the material properties were reported. The whole database with all data points can be found in the Supporting Information.

with zeta potential, size, and administered dose was available (86 data points), see **Figure 2**. For six data points the zeta potential was only listed as positive or negative. These data points were counted as only size and dose available. For 36% of the data points only the size and the dose were mentioned but not the zeta potential, whereas for 5% of the data points only the size and the zeta potential was available but not the dose. For more than 10% of the data points only the size and for 2% of the data points only the dose could be found. For one data point, neither the size nor the dose or the zeta potential was mentioned in the article (see **Figure 2**). The particles ranged in size from 1.1 to 360 nm, the zeta potential ranged from −76 to 106.2 mV, and the administered dose ranged from 0.0032 to 2,000 mg/kg body weight.

The amounts excreted through urine and feces were added together to get the total excretion of the nanomaterial. In order to evaluate if there is a relationship between the size of the material, the zeta potential, or the administered dose, each of these properties were plotted against the cumulative excretion. The dots were color-coded either for the type of administration (**Figures 3B,D**) or the material class (**Figures 3A,C**) to see if there was any relationship. Only material classes or administration types with at least three data points were used. Categories with <3 data points are shown together as "All other" just for illustrative purposes. Not all graphs have the same amount of points as for some data points the specific information was missing. For example, only 96 of the 192 data points have a zeta potential mentioned in the original study, therefore there are only 96 points in the graph for zeta potential and not 192. Plotting all data points together (**Figure 3A**), it can be seen that most (94%) of the materials are below 200 nm in size, the majority (79%) even below 100 nm, which would be the currently accepted threshold for the nanoparticle definition (European Commission, 2011). Regarding the zeta potential (**Figure 3C**), the majority (67%) of the data points have a negative zeta potential, only a few (33%) have a positive zeta potential. The doses used in most studies are below 100 mg/kg or even less, only a very small amount of studies used higher doses (**Figure 3D**). The plots for cumulative excretion versus zeta potential of the nanomaterial color-coded by type of administration and cumulative excretion versus dose of the nanomaterial color-coded by material class can be found in the Supporting Information in **Figures S1**, **S2**, respectively.

Data Evaluation

Several studies report size and surface charge of nanoparticles to be of major influence for their biodistribution and excretion. Small particles (Soo Choi et al., 2007; Semmler-Behnke et al., 2008; Li D. et al., 2016; Jasinski et al., 2018) and positively-charged particles (Alric et al., 2013) are reported to be excreted faster than larger or negatively and neutrally-charged particles. However, looking at the graphs above, there seems to be no correlation between size or zeta potential and excretion neither for different types of administration nor for different material classes. Therefore, a multilinear regression was calculated for the 86 data points for which the size, dose, and zeta potential was available to check if there was any relationship. Size, dose and zeta potential were used as input values and the cumulative excretion of feces and urine in percent as the output. The calculations show

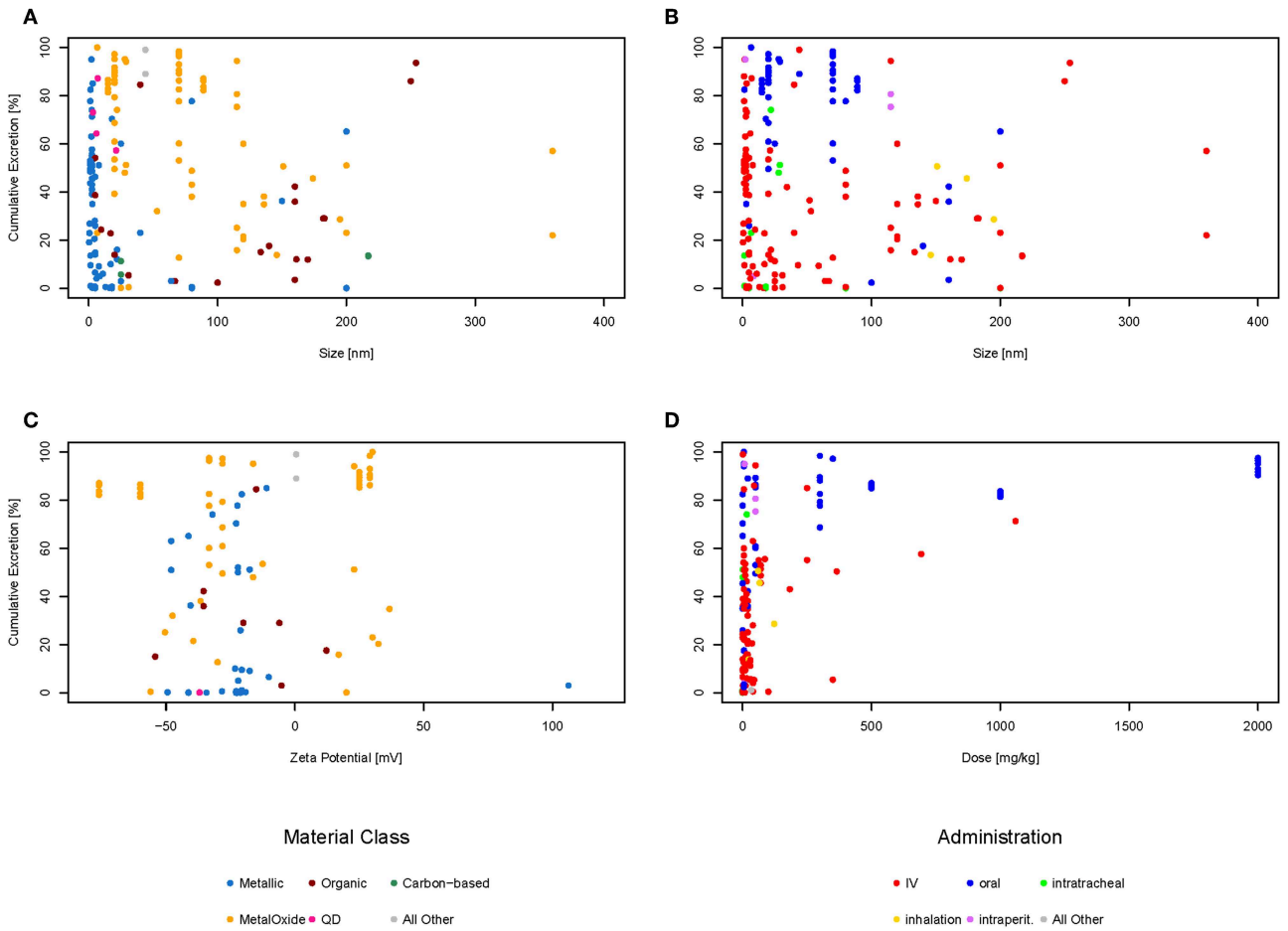

FIGURE 3 | Cumulative excretion vs. size of nanoparticle color-coded by material class **(A)**, cumulative excretion vs. size of nanoparticle color-coded by type of administration **(B)**, cumulative excretion vs. zeta potential of nanoparticle color-coded by material class **(C)**, and cumulative excretion vs. dose of nanoparticle color-coded by type of administration **(D)**.

that using zeta potential, size, and dose of nanomaterials, the accuracy of predicting the cumulative excretion is low with R^2 being only 0.29. The plot of observed vs. predicted values shown in the **Figure S3** reveals that the multilinear regression does not result in an acceptable fit. Taking all data together, it is therefore not possible to predict the amount excreted based on size, zeta potential and amount administered.

Regarding dose dependencies, Xu et al. (2018) have found strong dose-dependent renal clearance of glutathione-coated gold nanoparticles. At higher doses, the same can be seen in the graphs considering all types of nanoparticles. This might be explained by the fact that these doses are so high that the tissues are saturated with the material and the body cannot take up more of the nanomaterial and it is therefore excreted.

Looking at **Figure 3B** showing the size against excretion color-coded by type of administration, there seems to be a general trend of orally administered particles (blue dots) being excreted more than intravenously administered particles (red dots). Therefore, we have plotted the cumulative excretion vs. the administration for all administration types with three or more data points. **Figure 4** shows a boxplot of the cumulative excretion distribution for the five types of administration. The data points are plotted in red circles for each type of administration and the number of data points available for each type of administration is written in brackets next to the administration type.

To test whether the cumulative excretion of the different types of administration is statistically different, we applied a one-way analysis of variance (ANOVA) followed by a *post-hoc* Turkey test on the data set (**Table 1**). The criterion for statistical significance was $p < 0.05$. We found that only IV-oral, oral-intratracheal, oral-inhalation, and intratracheal-intraperitoneal were significantly different.

Prediction of Excretion for Environmental Risk Assessment

In environmental risk assessments, the potential hazard of a material is compared to the extent the material will come in contact with an organism (ECHA, 2016). Several environmental hazard assessments have been performed on various nanomaterials: Coll et al. (2016) for nano-Ag, CNT,

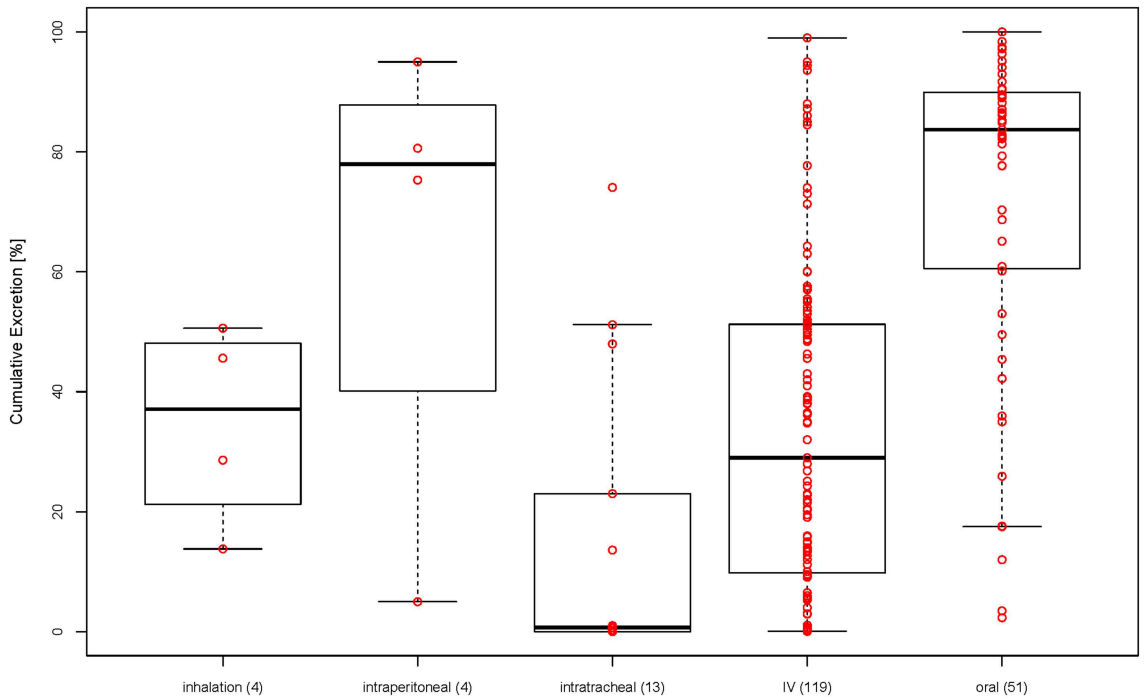

FIGURE 4 | Cumulative excretion for different types of administration (in brackets: number of data points for each type of administration).

TABLE 1 | *p*-values from ANOVA for testing statistical difference between different types of administration ($p < 0.05$ in green, $p > 0.05$ in red).

	Oral	Intratracheal	Inhalation	Intraperitoneal
IV	<0.001	0.202	0.999	0.154
Oral		<0.001	0.045	0.964
Intratracheal			0.748	0.017
Inhalation				0.524

nano-TiO_2, and nano-ZnO in freshwater; Hauser et al. (2019) for chitosan, nano-chitosan and HAP in freshwater, and chitosan in soil; Mahapatra et al. (2018) for nano-Au in freshwater; Wang and Nowack (2018) for nano-Al_2O_3, nano-SiO_2, nano iron oxides, nano-CeO_2, and QDs in freshwater. On the other hand, only one study has been performed so far on environmental exposure to NBMs (Mahapatra et al., 2015 for nano-Au). Therefore, more research is needed on the exposure side before environmental risk assessments of NBMs can be performed. As often the NBMs in question are only in the development stage and not yet on the market, the only way to estimate the prospective environmental concentration is through mathematical models (Gottschalk et al., 2009). The amount of a nanomaterial released into a technical or environmental compartment is a central point in any release model (Gottschalk and Nowack, 2011). For NBMs the main relevant release process is the excretion from the human body. If most of the NBM is excreted, it will end up in the wastewater, if it stays in the body or is metabolized, there is no immediate release into water.

The excretion data collected in the database (**Table S1**) can be used to predict excretion for a specific NBM or be used to obtain a generic excretion rate for NBM with a specific administration. So if a specific material has its own data, then the real excretion for this material can be used in the model. If however for the material in question, no own data is available, then data from the database can be used in the form of probability distributions. Therefore, for each type of administration, a histogram was prepared to show the distribution of the data points. For IV and oral administration, there are enough data points to see the distribution (see **Figures 5A,B** below). For inhalation only four data points were available. The histogram for inhalation can be found in the **Figure S4**. As intratracheal and intraperitoneal administration are not used on humans, their data are not shown here and will not be further evaluated. The distributions shown in **Figure 5** represent the probability that a NBM is excreted to a certain extent and can be used as input value to parameterize excretion in probabilistic exposure models such as DPMFA (dynamic probabilistic material flow analysis) (Bornhöft et al., 2016).

Recently published studies have focused on evaluating small difference in particles characteristics and their influence on the biodistribution and excretion. It is generally believed that particles below 5.5 nm in size get rapidly cleared from the body through urinary excretion (Soo Choi et al., 2007). Du et al. (2017) evaluated urinary excretion of sub-nm gold particles with the same surface ligands but different sizes after IV injection. They found that a size reduction of just a few atoms resulted in a decrease in urinary clearance. As in our database, no other

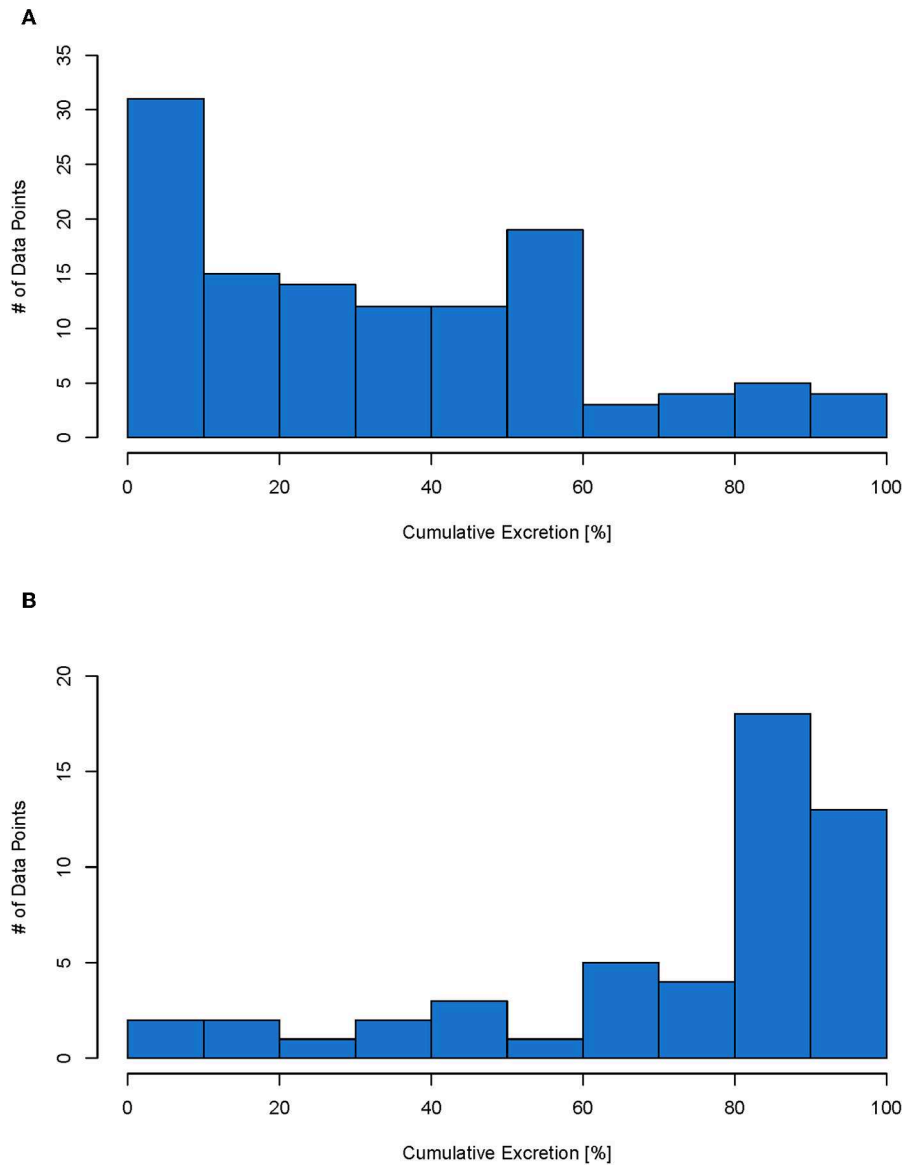

FIGURE 5 | Histogram for IV (total of 114 data points) **(A)** and oral (total of 51 data points) **(B)** administration. Each data point represents the cumulative excretion of a material with specific material properties from one study.

materials were in the sub-nm size-range, we could not confirm this on a general basis with other materials. As mentioned before, we have not found a size dependent relationship. Cassano et al. (2019) compared the excretion of silver, gold and platinum nanoparticles and found that while gold nanoparticles are predominantly excreted in urine, silver nanoparticles were almost completely found in feces. We have only analyzed the total excretion, however, it would be interesting to evaluate the route of excretion for the different NBMs. Jasinski et al. (2018) evaluated the effect of shape of RNA nanoparticles on their biodistribution. They compared squared, triangular and pentagon-shaped RNA nanoparticles of 10 nm size. Fluorescent images showed a high fluorescence in kidneys after 12 h for nanosquared, but none for the triangle and very little for the pentagon-shaped nanoparticles. Most studies used round nanoparticles, so to study the general effect of shape, more studies using differently shaped nanoparticles would be needed in the future.

The data collected in the database are all from animal studies. No study is available in which pharmacokinetic profiles for NBMs are compared between animals and humans to get an indication on the extrapolation of animal data to humans with regard to excretion. Data on excretion for other pharmaceuticals are available for different animals and humans. Mamidi et al. (2014) performed an excretion study of orally administered canagliflozin (used for the treatment of type 2 diabetes) in mice, rats, dogs, and humans. They have found a total excretion of canagliflozin and its metabolites of 97.8 and 98.3% for male and female

mice, respectively, 96.9 and 98.4% for male and female rats, 99.1% for male dogs, and 92.9% for male humans. Maurer et al. (1983) administered bromocriptine (used for the treatment of Parkinson's disease) orally to mice, rats, monkeys, and humans. They have found a total excretion 94.2% and 101.6% for mice with a dose of 3 and 50 mg/kg, respectively, 83.4% for rats, 101.7% for monkeys, and 88.0% for humans. Comparing these studies, the total excretion from humans is in a similar range as the excretion from the animals included in our database. Therefore, we can assume that the excretion of NBMs in humans would also be in a similar range to animals and thus we can use the calculated excretion profiles for further modeling of NBMs administered to humans.

DATA AVAILABILITY STATEMENT

The raw data supporting the conclusions of this manuscript will be made available by the authors, without undue reservation, to any qualified researcher.

AUTHOR CONTRIBUTIONS

MH collected, prepared, evaluated the input data, created the figures and tables for the manuscript, and wrote the manuscript. BN supervised the study, gave inputs on the data, and contributed to the writing of the manuscript. All authors read and approved the final manuscript.

FUNDING

This work was supported by the BIORIMA project which received funding from the European Union Horizon 2020 framework under grant agreement #760928.

SUPPLEMENTARY MATERIAL

The Supplementary Material for this article can be found online at: https://www.frontiersin.org/articles/10.3389/fbioe.2019.00405/full#supplementary-material

REFERENCES

Alric, C., Miladi, I., Kryza, D., Taleb, J., Lux, F., Bazzi, R., et al. (2013). The biodistribution of gold nanoparticles designed for renal clearance. *Nanoscale* 5, 5930–5939. doi: 10.1039/c3nr00012e

Bergmann, A., Fohrmann, F., and Weber, F.-A. (2011). *Zusammenstellung von Monitoringdaten Zu Umweltkonzentrationen von Arzneimitteln*. Umwelt Bundesamt, 1–99. Available online at: https://www.umweltbundesamt.de/sites/default/files/medien/461/publikationen/4188.pdf (accessed December 9, 2019).

Bonakdar, S., and Mashinchian, O. (2015). "Toxicology of nanobiomaterials," in *Stem Cell Nanoengineering*, eds H. Baharvand and N. Aghdami (Hoboken, NJ: John Wiley & Sons, Inc.), 171–84. doi: 10.1002/9781118540640.ch10

Bornhöft, N. A., Sun, T. Y., Hilty, L. M., and Nowack, B. (2016). A dynamic probabilistic material flow modeling method. *Environ. Model. Softw.* 76, 69–80. doi: 10.1016/j.envsoft.2015.11.012

Carlander, U., Li, D., Jolliet, O., Emond, C., and Johanson, G. (2016). Toward a general physiologically-based pharmacokinetic model for intravenously injected nanoparticles. *Int. J. Nanomed.* 11, 625–640. doi: 10.2147/IJN.S94370

Cassano, D., Mapanao, A. K., Summa, M., Vlamidis, Y., Giannone, G., Santi, M., et al. (2019). Biosafety and biokinetics of noble metals: the impact of their chemical nature. *ACS Appl. Bio Mater.* 2, 4464–4470. doi: 10.1021/acsabm.9b00630

Coll, C., Notter, D., Gottschalk, F., Sun, T., Som, C., and Nowack, B. (2016). Probabilistic environmental risk assessment of five nanomaterials (Nano-TiO_2, Nano-Ag, Nano-ZnO, CNT, and Fullerenes). *Nanotoxicology* 10, 436–444. doi: 10.3109/17435390.2015.1073812

Du, B., Jiang, X., Das, A., Zhou, Q., Yu, M., Jin, R., et al. (2017). Glomerular barrier behaves as an atomically precise bandpass filter in a sub-nanometre regime. *Nature Nanotech.* 12, 1096–1102. doi: 10.1038/nnano.2017.170

ECHA (2016). *Guidance on Information Requirements and Chemical Safety Assessment - Part E: Risk Characterisation*. Helsinki: European Chemicals Agency.

European Commission (2011). Commission recommendation of 18 October 2011 on the definition of nanomaterial (2011/696/EU). *Off. J. Eur. Union* 38–40.

Gottschalk, F., and Nowack, B. (2011). The release of engineered nanomaterials to the environment. *J. Environ. Monitor.* 13, 1145–1155. doi: 10.1039/c0em00547a

Gottschalk, F., Scholz, R. W., and Nowack, B. (2010). Probabilistic material flow modeling for assessing the environmental exposure to compounds: methodology and an application to engineered nano-TiO_2 particles. *Environ. Model. Softw.* 25, 320–332. doi: 10.1016/j.envsoft.2009.08.011

Gottschalk, F., Sondere, T., Schols, R., and Nowack, B. (2009). Modeled environmental concentrations of engineered nanomaterials for different regions. *Environ. Sci. Technol.* 43, 9216–9222. doi: 10.1021/es9015553

Grass, G. M., and Sinko, P. J. (2002). Physiologically-based pharmacokinetic simulation modelling. *Adv. Drug Deliv. Rev.* 54, 433–451. doi: 10.1016/S0169-409X(02)00013-3

Han, J., Zhao, D., Li, D., Wang, X., Jin, Z., and Zhao, K. (2018). Polymer-based nanomaterials and applications for vaccines and drugs. *Polymers* 10, 1–14. doi: 10.3390/polym10010031

Hauser, M., Li, G., and Nowack, B. (2019). Environmental hazard assessment for polymeric and inorganic nanobiomaterials used in drug delivery. *J. Nanobiotech.* 17, 1–10. doi: 10.1186/s12951-019-0489-8

Hirn, S., Semmler-Behnke, M., Schleh, C., Wenk, A., Lipka, J., Schäffler, M., et al. (2011). Particle size-dependent and surface charge-dependent biodistribution of gold nanoparticles after intravenous administration. *Eur. J. Pharm. Biopharm.* 77, 407–416. doi: 10.1016/j.ejpb.2010.12.029

Jasinski, D. L., Li, H., and Guo, P. (2018). The effect of size and shape of RNA nanoparticles on biodistribution. *Mol. Ther.* 26, 784–792. doi: 10.1016/j.ymthe.2017.12.018

Kabir, E., Kumar, V., Kim, K. H., Yip, A. C. K., and Sohn, J. R. (2018). Environmental impacts of nanomaterials. *J. Environ. Manag.* 225, 261–271. doi: 10.1016/j.jenvman.2018.07.087

Keller, A. A., McFerran, S., Lazareva, A., and Suh, S. (2013). Global life cycle releases of engineered nanomaterials. *J. Nanop. Res.* 15:1692. doi: 10.1007/s11051-013-1692-4

Kreyling, W. G., Hirn, S., Möller, W., Schleh, C., Wenk, A., Celik, G., et al. (2014). Air-blood barrier translocation of tracheally instilled gold nanoparticles inversely depends on particle size. *ACS Nano* 8, 222–233. doi: 10.1021/nn403256v

Küster, A., and Adler, N. (2014). Pharmaceuticals in the environment: scientific evidence of risks and its regulation. *Philos. Trans. R Soc. B* 369:20130587. doi: 10.1098/rstb.2013.0587

Laux, P., Riebeling, C., Booth, A. M., Brain, J. D., Brunner, J., Cerrillo, C., et al. (2017). Biokinetics of nanomaterials: the role of biopersistence. *NanoImpact* 6, 69–80. doi: 10.1016/j.impact.2017.03.003

Lee, J. A., Kim, M. K., Paek, H. J., Kim, Y. R., Kim, M. K., Lee, J. K., et al. (2014). Tissue distribution and excretion kinetics of orally administered silica nanoparticles in rats. *Int. J. Nanomed.* 2, 251–260. doi: 10.2147/IJN.S57939

Li, D., Morishita, M., Wagner, J. G., Fatouraie, M., Wooldridge, M., Eagle, W. E., et al. (2016). *In vivo* biodistribution and physiologically based pharmacokinetic modeling of inhaled fresh and aged cerium oxide nanoparticles in rats. *Particle Fibre Toxicol.* 13:45. doi: 10.1186/s12989-016-0156-2

Li, M., Al-Jamal, K. T., Kostarelos, K., and Reineke, J. (2010). Physiologically based pharmacokinetic modeling of nanoparticles. *ACS Nano* 4, 6303–6317. doi: 10.1021/nn1018818

Li, M., Panagi, Z., Avgoustakis, K., and Reineke, J. (2012). Physiologically based pharmacokinetic modeling of PLGA nanoparticles with varied MPEG content. *Int. J. Nanomed.* 7, 1345–1356. doi: 10.2147/IJN.S23758

Li, M., Zou, P., Tyner, K., and Lee, S. (2016). Physiologically based pharmacokinetic (PBPK) modeling of pharmaceutical nanoparticles. *AAPS J.* 19, 26–42. doi: 10.1208/s12248-016-0010-3

Li, X., Wang, L., Fan, Y., Feng, Q., and Cui, F. Z. (2012). Biocompatibility and toxicity of nanoparticles and nanotubes. *J. Nanomater.* 2012:548389. doi: 10.1155/2012/548389

Lin, Z., Monteiro-Riviere, N. A., and Riviere, J. E. (2015). Pharmacokinetics of metallic nanoparticles. *Wiley Interdisc. Rev.* 7, 189–217. doi: 10.1002/wnan.1304

Mahapatra, I., Clark, J. R. A., Dobson, P. J., Owen, R., Lynch, I., and Lead, J. R. (2018). Expert perspectives on potential environmental risks from nanomedicines and adequacy of the current guideline on environmental risk assessment. *Environ. Sci. Nano* 5, 1873–1889. doi: 10.1039/C8EN00053K

Mahapatra, I., Sun, T. Y., Clark, J. R. A., Dobson, P. J., Hungerbuehler, K., Owen, R., et al. (2015). Probabilistic modelling of prospective environmental concentrations of gold nanoparticles from medical applications as a basis for risk assessment. *J. Nanobiotechnol.* 13, 1–14. doi: 10.1186/s12951-015-0150-0

Mamidi, R. N. V. S., Cuyckens, F., Chen, J., Scheers, E., Kalamaridis, D., Lin, R., et al. (2014). Metabolism and excretion of canagliflozin in mice, rats, dogs, and humans. *Drug Metab. Dispos.* 42, 903–916. doi: 10.1124/dmd.113.056440

Maurer, G., Schreier, E., Delaborde, S., Nufer, R., and Shukla, A. P. (1983). Fate and disposition of bromocriptine in animals and man. II: absorption, elimination and metabolism. *Eur. J. Drug Metab. Pharmacokinetics* 8, 51–62. doi: 10.1007/BF03189581

Moss, D. M., and Siccardi, M. (2014). Optimizing nanomedicine pharmacokinetics using physiologically based pharmacokinetics modelling. *Br. J. Pharmacol.* 171, 3963–3979. doi: 10.1111/bph.12604

Mueller, N. C., and Nowack, B. (2008). Exposure modelling of engineered nanoparticles in the environment. *Environ. Sci. Technol.* 42, 44447–44453. doi: 10.1021/es7029637

Navarro, S. M., Swetledge, S., Morgan, T., Astete, C. E., Stout, R., Coulon, D., et al. (2017). Biodistribution of orally administered poly(lactic-co-glycolic) acid nanoparticles for 7 days followed by 21 day recovery in F344 rats. *NanoImpact* 5, 1–5. doi: 10.1016/j.impact.2016.12.002

Park, K., Park, E. J., Chun, I. K., Choi, K., Lee, S. H., Yoon, J., et al. (2011). Bioavailability and toxicokinetics of citrate-coated silver nanoparticles in rats. *Arch. Pharmacal. Res.* 34, 153–158. doi: 10.1007/s12272-011-0118-z

Rambanapasi, C., Barnard, N., Grobler, A., Buntting, H., Sonopo, M., Jansen, D., et al. (2015). Dual radiolabeling as a technique to track nanocarriers: the case of gold nanoparticles. *Molecules* 20, 12863–12879. doi: 10.3390/molecules200712863

Schleh, C., Semmler-Behnke, M., Lipka, J., Wenk, A., Hirn, S., Schäffler, M., et al. (2012). Size and surface charge of gold nanoparticles determine absorption across intestinal barriers and accumulation in secondary target organs after oral administration. *Nanotoxicology* 6, 36–46. doi: 10.3109/17435390.2011.552811

Semmler-Behnke, M., Kreyling, W. G., Lipka, J., Fertsch, S., Wenk, A., Takenaka, S., et al. (2008). Biodistribution of 1.4- and 18-Nm gold particles in rats. *Small* 4, 2108–2111. doi: 10.1002/smll.200800922

Singh, P., Mall, B. B., Singh, R. R., Chandra, R., and Saxena, A. (2017). Nanobiomaterial in dental medicine : a review. *IOSR J. Dental Med. Sci.* 16, 68–71. doi: 10.9790/0853-1602018490

Som, C., Berges, M., Chaudhry, Q., Dusinska, M., Fernandes, T. F., Olsen, S. I., et al. (2010). The importance of life cycle concepts for the development of safe nanoproducts. *Toxicology* 269, 160–169. doi: 10.1016/j.tox.2009.12.012

Soo Choi, H., Liu, W., Misra, P., Tanaka, E., Zimmer, J. P., Itty Ipe, B., et al. (2007). Renal clearance of quantum dots. *Nat. Biotechnol.* 25, 1165–1170. doi: 10.1038/nbt1340

Sun, T. Y., Bornhöft, N. A., Hungerbühler, K., and Nowack, B. (2016). Dynamic probabilistic modeling of environmental emissions of engineered nanomaterials. *Environ. Sci. Tech.* 50, 4701–4711. doi: 10.1021/acs.est.5b05828

Sun, T. Y., Gottschalk, F., Hungerbühler, K., and Nowack, B. (2014). Comprehensive probabilistic modelling of environmental emissions of engineered nanomaterials. *Environ. Pollut.* 185, 69–76. doi: 10.1016/j.envpol.2013.10.004

Sun, T. Y., Mitrano, D. M., Bornhöft, N. A., Scheringer, M., Hungerbühler, K., and Nowack, B. (2017). Envisioning nano release dynamics in a changing world: using dynamic probabilistic modeling to assess future environmental emissions of engineered nanomaterials. *Environ. Sci. Technol.* 51, 2854–2863. doi: 10.1021/acs.est.6b05702

Umwelt Bundesamt (2018). "Database - pharmaceuticals in the environment," in *Pharmaceuticals*. Available online at: https://www.umweltbundesamt.de/en/database-pharmaceuticals-in-the-environment-0 (accessed December 9, 2019).

Wang, Y., Kalinina, A., Sun, T., and Nowack, B. (2016). Probabilistic modeling of the flows and environmental risks of nano-silica. *Sci. Total Environ.* 545–546, 67–76. doi: 10.1016/j.scitotenv.2015.12.100

Wang, Y., and Nowack, B. (2018). Environmental risk assessment of engineered nano-SiO_2, nano iron oxides, nano-CeO_2, Nano-Al_2O_3, and quantum dots. *Environ. Toxicol. Chem.* 37, 1387–1395. doi: 10.1002/etc.4080

Xu, J., Yu, M., Peng, C., Carter, P., Tian, J., Ning, X., et al. (2018). Dose dependencies and biocompatibility of renal clearable gold nanoparticles: from mice to non-human primates. *Angew. Chem. Int. Edn.* 57, 266–271. doi: 10.1002/anie.201710584

Yamashita, T., Yamashita, K., Nabeshi, H., Yoshikawa, T., Yoshioka, Y., Tsunoda, S., et al. (2012). Carbon nanomaterials: efficacy and safety for nanomedicine. *Materials* 5, 350–363. doi: 10.3390/ma5020350

Conflict of Interest: The authors declare that the research was conducted in the absence of any commercial or financial relationships that could be construed as a potential conflict of interest.

frontiers in Bioengineering and Biotechnology

REVIEW
published: 31 January 2020
doi: 10.3389/fbioe.2020.00032

A Review of Nanotechnology for Targeted Anti-schistosomal Therapy

*Tayo Alex Adekiya, Pierre P. D. Kondiah, Yahya E. Choonara, Pradeep Kumar and Viness Pillay**

Wits Advanced Drug Delivery Platform Research Unit, Department of Pharmacy and Pharmacology, School of Therapeutic Science, Faculty of Health Sciences, University of the Witwatersrand, Johannesburg, South Africa

Schistosomiasis is one of the major parasitic diseases and second most prevalent among the group of neglected diseases. The prevalence of schistosomiasis may be due to environmental and socio-economic factors, as well as the unavailability of vaccines for schistosomiasis. To date, current treatment; mainly the drug praziquantel (PZQ), has not been effective in treating the early forms of schistosome species. The development of drug resistance has been documented in several regions globally, due to the overuse of PZQ, rate of parasitic mutation, poor treatment compliance, co-infection with different strains of schistosomes and the overall parasite load. Hence, exploring the schistosome tegument may be a potential focus for the design and development of targeted anti-schistosomal therapy, with higher bioavailability as molecular targets using nanotechnology. This review aims to provide a concise incursion on the use of various advance approaches to achieve targeted anti-schistosomal therapy, mainly through the use of nano-enabled drug delivery systems. It also assimilates the molecular structure and function of the schistosome tegument and highlights the potential molecular targets found on the tegument, for effective specific interaction with receptors for more efficacious anti-schistosomal therapy.

Keywords: schistosomiasis, nanoparticles, drug delivery, targeted agents, molecular receptors, antibody, aptamers

OPEN ACCESS

Edited by:
Olga Borges,
University of Coimbra, Portugal

Reviewed by:
Pradipta Ranjan Rauta,
University of Texas MD Anderson Cancer Center, United States
Stefano Leporatti,
Institute of Nanotechnology (NANOTEC), Italy

***Correspondence:**
Viness Pillay
viness.pillay@wits.ac.za

Specialty section:
This article was submitted to Nanobiotechnology, a section of the journal Frontiers in Bioengineering and Biotechnology

Received: *03 November 2019*
Accepted: *14 January 2020*
Published: *31 January 2020*

Citation:
Adekiya TA, Kondiah PPD, Choonara YE, Kumar P and Pillay V (2020) A Review of Nanotechnology for Targeted Anti-schistosomal Therapy. Front. Bioeng. Biotechnol. 8:32. doi: 10.3389/fbioe.2020.00032

INTRODUCTION

Schistosomiasis is recognized as the second most prevalent among the group of NTDs in sub-Saharan Africa, following hookworm infection (Adekiya et al., 2017). Schistosomiasis is an infectious disease caused by parasitic worms that belong to the group of trematode and genus of *Schistosoma*, that results in chronic and acute disease (Adekiya et al., 2017). It poses a significant challenge on agricultural productivity and the life, growth and development of pregnant women and school children in afflicted areas. The disease-causing species of *Schistosoma* are *Schistosoma mansoni*, *Schistosoma haematobium*,

Abbreviations: Ach, acetylcholine; AChE, acetylcholinesterase; ACS, american cancer society; AD, alzheimer's disease; AFM, atomic force microscopy; AuNP, gold nanoparticle; BBB, blood-brain barrier; CNS, central nervous system; IgGs, immunoglobulins; IVM, ivermectin; LBNPs, lipid-based nanoparticles; LGIC, ligand-gated ion channel; LNCs, lipid nanocapsules; MB, methylene blue; nAChR, nicotinic acetylcholine receptor; NK, natural killer; NLCs, nano-lipid carriers; NTDs, neglected tropical diseases; pRBCs, *plasmodium*-infected red blood cells; PZQ, praziquantel; RBCs, red blood cells; SEM, scanning electron microscopy; SGTP1, schistosome glucose transporter 1; SGTP4, schistosome glucose transporter 4; SLN, solid lipid nanoparticle; TEM, transmission electron microscopy; TSPs, tetraspanins; Th1, T-helper 1 cells; Th2, T-helper 2 cells; WHO, world health organisation.

Schistosoma japonicum, *Schistosoma intercalatum,* and *Schistosoma mekongi* (Adekiya et al., 2017; da Paixão Siqueira et al., 2017). For these worms to cause disease, the intermediate hosts (freshwater snails) need to be infected with the miracidia in freshwater where it develops into cercaria. Following human-water exposure, the cercaria penetrates the intact skin of humans.

Schistosomiasis affects the world's poorest countries where there is no safe water, basic sanitation and hygiene education (da Paixão Siqueira et al., 2017). Currently, over 200 million people have been affected by schistosomiasis, including 40 million women of reproductive age and approximately 600–779 million individuals are at risk of becoming infected. The mortality rate has been estimated at 280,000 deaths annually in Sub-Saharan countries (Cioli et al., 2014).

The parasitizing of this infectious disease results in fever, malaise, abdominal pain, and skin rashes in an acute state, while intestinal, liver, urinary tract and lung diseases are the result of chronic infection. Acute and chronic disease is solely reliant on the type of species that infects an individual. Reappearance of schistosomiasis over latent periods can result in blockage of the urinary tract and pulmonary hypertension that can lead to fatal complications. In addition, schistosome infection promotes the severity of infection with additional pathogens such as; *Plasmodium falciparum, Toxoplasma gondii, Leishmania* spp., *Mycobacteria, Staphylococcus aureus, Salmonella,* and *Entamoeba histolytica* (Abruzzi and Fried, 2011).

The incidence of schistosomiasis is predominant in Sub-Saharan Africa, and with the increasing rate of infection, due to climate change and other socio-economic factors. To date, PZQ remains the only drug for the treatment of this debilitating disease. PZQ has the following benefits: (1) its effective against all forms of Schistosomes, (2) it is inexpensive and readily available and (3) it has a low side-effect profile, well tolerated in patients of all ages. Unfortunately, the use of PZQ is limited by the following: (1) drug resistance, (2) poor patient compliance to treatment in certain populations, (3) its ineffective against immature forms of the *Schistosoma* species and (4) it cannot prevent re-infection of Schistosomiasis. Furthermore, there is an increase in parasite alteration and modification, the global parasite load and co-infection with several strains of *Schistosoma* parasites (Caffrey, 2007; Doenhoff et al., 2008; Fenwick et al., 2009). Coupled with cases of cerebral schistosomiasis in some regions globally, there is an urgent need for an alternative anti-schistosomal drug molecule or to improve the delivery efficacy of PZQ using approaches such as nanotechnology to achieve targeted anti-schistosomal therapy, for example in the CNS.

There has not been a considerable impetus placed on developing novel and new drug treatments for schistosomiasis. However, based on the debilitating impact of the disease, researchers need to be alerted on exploring several essential target proteins found in the *Schistosoma species* and could play a significant role in ensuring the possibility of designing new drug molecules for schistosomiasis (Garcia-Salcedo et al., 2016). In the absence of any meaningful drug discovery programs for identifying new drug targets and molecules for schistosomiasis, pharmaceutical researchers have turned to providing more efficacious delivery systems for the gold-standard drug PZQ. Hence, nanotechnology and the use of nano-enable drug delivery systems (**Figure 1**), has been a major focus to potentially provide better treatment outcomes for schistosomiasis using PZQ (Veerasamy et al., 2011). Nano-enabled drug delivery systems can enhance the bioavailability and therapeutic efficacy of PZQ (or other drugs) and reduce the side effect profile by having more targeted drug delivery. Nanoparticulate systems currently researched involve, but are not limited to, lipid-based nanoparticles (liposomes, micelles, solid lipid nanoparticles, nanostructured lipid carriers and nanodiscs). Others include polymeric-based nanoparticles (nanospheres, nanocapsules, nanofibers/nanotubes, nanodiscs and micelles), metallic/inorganic-based nanoparticles (nanospheres, nanocapsules, nanodiscs and nanowires/nanotubes) and metal nanoparticles; fabricated by green chemistry (gold, silver, copper, platinum, palldium and zinc nanoparticles).

The emergence of smart LBNPs (**Figure 2**) has offers secure platforms for the use of nano-biomaterials in medical applications such as encapsulation of therapeutic drugs for the targeted delivery of drugs for the treatment of diseases in biomedicine. Recently, the use of LBNPs has gained much interest, particularly in treating schistosomiasis, due to a better absorbed tegument of the schistosomes, which has an affinity for the phospholipid bilayer. LBNPs amphipathic nature allows them to play a pivotal role in the solubility modification and rate at which drugs such as PZQ can be targeted, for enhancing drug absorption across biological barriers (Cheng et al., 2017). Furthermore, targeted LBNPs can improve the efficacy and specificity of drugs to cells or tissues by upregulating surface molecular receptors such as antigens, unregulated selectin and serpin enzyme complex-receptor (Cheng et al., 2017). The *Schistosoma* parasite consists of different molecules that are found on the surface of the parasite tegument, which are needed for the parasite survival. This is a largely unexplored approach for targeted drug delivery in anti-schistosomal therapy. To this end, nanotechnology has played a central role in the design of systems intended to target the parasite tegument. Hence, this review aims to provide a concise incursion into the molecular structure and function of the schistosome tegument and assimilate the potential targeting proteins/molecules on the tegument to identify new targets and targeting molecules in anti-schistosomiasis therapy.

OVERVIEW OF THE PAST AND PRESENT ANTI-SCHISTOSOMIASIS THERAPIES

In 1984, the WHO Expert Committee proposed chemotherapy as the best treatment approach to eliminate schistosomiasis (Conlon, 2005). Ever since, chemotherapy continues to be the only measure for the control of schistosomiasis and depends only on a single dose treatment with PZQ. Among other anti-schistosomal drugs that have been explored, PZQ is the most widely used. PZQ is active against all forms of *Schistosoma* species that cause schistosomiasis. It reduces the parasitic load and is able to reduce the severity of symptoms. It is also the most preferred drug because of its simple administration,

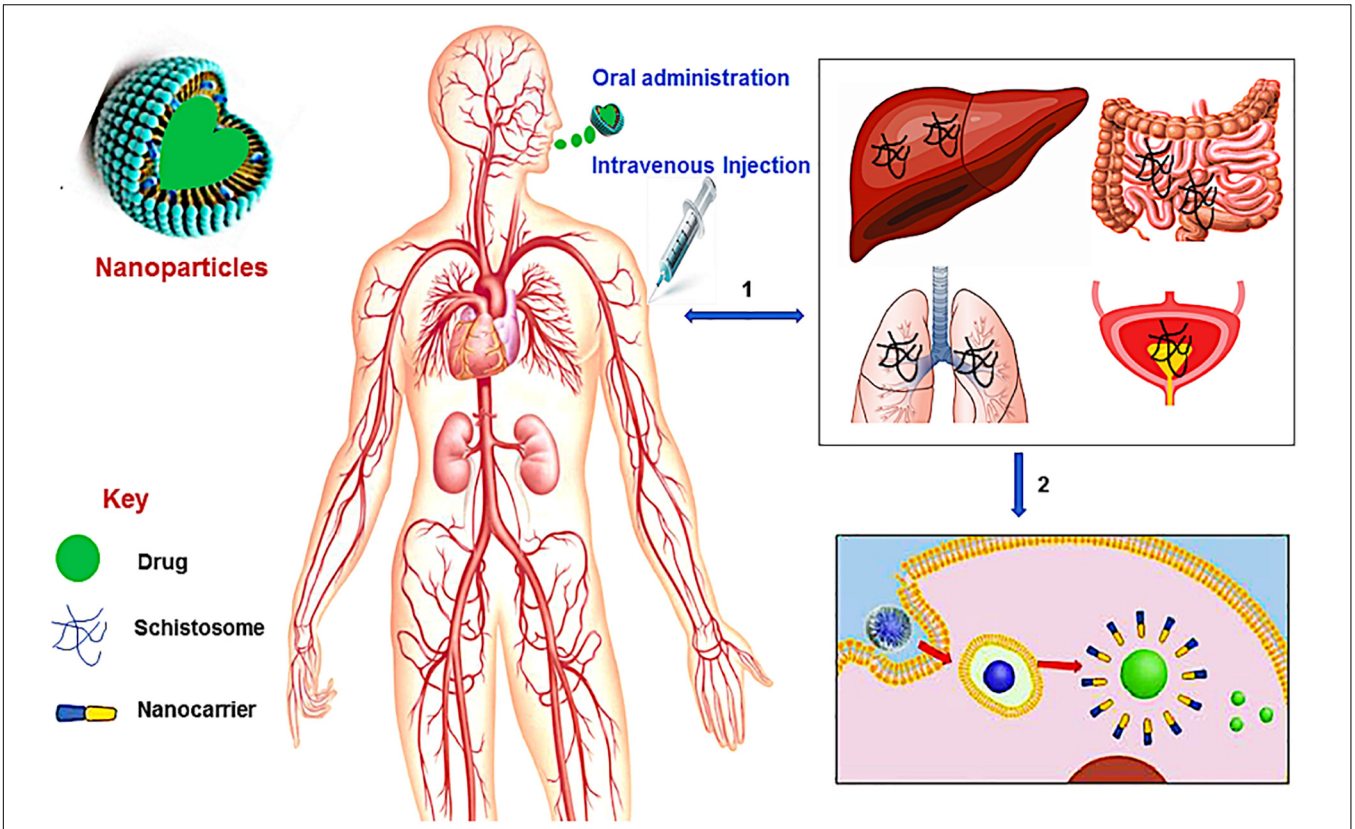

FIGURE 1 | A schematic overview of nanotechnology in schistosomiasis treatment. **(1)** The Schistosoma parasites penetrates the human skin and enter the bloodstream where they travel via the blood vessels of the liver and lungs, and then to the vein around the intestines and bladder, **(2)** the administration (oral or intravenous injection) of nanotechnological-based drug leads to the disruption of the membrane (tegument) of the worms thereby releasing the drug to kill the worms.

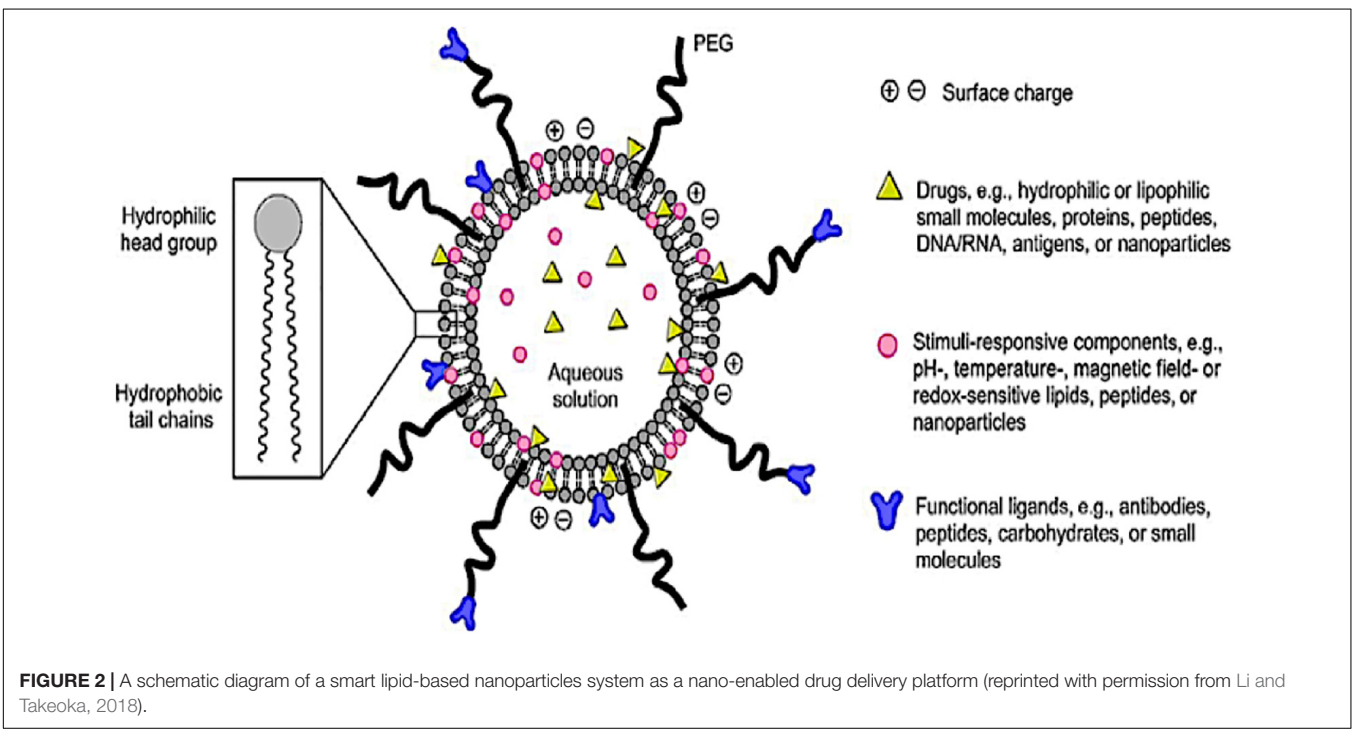

FIGURE 2 | A schematic diagram of a smart lipid-based nanoparticles system as a nano-enabled drug delivery platform (reprinted with permission from Li and Takeoka, 2018).

efficacy and affordability. Although, the mechanism of action in treating schistosomiasis is not well understood, a widely proposed mechanism is the immediate alteration in the worm musculature. This was reported by Pax et al. (1978) when they noticed that the alteration in the worm musculature causes contraction probably due to rapid influx of Ca^{2+} into the schistosome. This assertion was corroborated by interesting work undertaken by Kohn et al. (2001) that drew attention to the voltage-gated calcium channels of schistosomes as the potential target for PZQ. In their study, the mechanism of action for PZQ was suggested to be consistent with the observed effects of PZQ on Ca^{2+} homeostasis in schistosomes. It was noted that β-subunits of schistosome channels had a unique form of β-subunit structure that was different from other common β-subunits which inhibit flow of current through the α_1 subunit of schistosome with which they are associated. The study further hypothesized that PZQ facilitated the opening of more channels for current to flow leading to the disruption of α1/β interaction in these channels resulting in disruption of Ca^{2+} homeostasis (Kohn et al., 2001). It has also been reported that PZQ causes morphological transitions in the schistosomes tegument. This was initially indicated by the formation of vacuoles within the tegument and blebbing at the surface (Becker et al., 1980; Mehlhorn et al., 1981; Cioli and Pica-Mattoccia, 2003). These morphological transitions cause increased exposure of antigens on the surface of the parasite (Harnett and Kusel, 1986). Harnett and Kusel suggested that the action of PZQ on the exposed antigens may be due to its lipophilicity that makes it easier to interact with hydrophobic cores of the tegument.

Due to the shortcomings of the drugs listed in **Table 1**, researchers have resorted to the use of drug delivery technologies such as nanotechnology to provide more targeted therapies to all stages of the Schistosoma parasite such that drugs can be more effective in treating the immature forms of the parasite. These novel approaches can also reduce drug resistance and avert re-infection by clearing the schistosomes in the human host.

TABLE 1 | Drugs that have been used to treat schistosomiasis to date, with their shortcomings evaluated.

Anti-schistosomal drugs	Shortcomings	Reference
Metrifonate	Metrifonate is selective to only *S. haematobium* and due to medical standards and economic operations, the drug has been withdrawn from the market.	Eissa et al., 2011; de Moraes, 2012; Aruleba et al., 2018
Oltripaz	Oltripaz is another anti-schistosomal drug which has been used in the past, but not in the market again and discontinued in treating schistosomes infection due to its photosensitivity induction and longer time in curing the infections; approximately 2 months.	Nare et al., 1992
Niridazole	Niridazole was jettisoned due to its unpleasant adverse effects which include non-specificity destruction to the T waves electrocardiogram (ECG), toxicity to the renal and central nervous system, it has also been revealed to be a carcinogenic material.	Urman et al., 1975; Katz, 1977; Nare et al., 1992; Thetiot-Laurent et al., 2013
Oxamniquine	Oxamniquine has also been used in the past, but it is ineffective against all schistosomes type, only effective to *S. mansoni,* and due to cost effectiveness, drug resistance and some side effects, the drug has been replaced by praziquantel in treating schistosomiasis.	Saconato and Atallah, 2000; Morgan et al., 2001; Richter, 2003; El Ridi and Tallima, 2013; Aruleba et al., 2018

THE SCHISTOSOME TEGUMENT: REVISIT OF THE MOLECULAR STRUCTURE AND FUNCTION FOR TARGETED DRUG DELIVERY

The outer-surface of the schistosome is enclosed with an uncommon structure known as the tegument where some probable receptors for targeted nano-delivery system are found. It is a rare double layered membrane structure that plays a pivotal role in protecting the worm from harsh conditions in the host system. There are several organelles present in the tegument (**Figure 3**). The heptalaminate tegumental surface is enclosed by a typical plasma membrane structure that is superimposed by a secreted membranocalyx (generated by the multi-laminate vesicles found in the tegument cytoplasm) and fuses with lateral channels protruding out into the base of the surface from the cytoplasm which also host some potential proteins for nano-delivery systems. The membranocalyx can be active by interacting with proteins and glycans via the extracellular loops of the tetraspanins protein, this depicts tetraspanins as a probable target for nano-delivery systems.

The initiation of heptalaminate membrane surface alongside dyneins protein starts from the outer membrane of the cercarial trilaminate 30 min after invasion of cercarial into the host skin, and within 3 h, the change in cercarial membrane from the trilaminate to the heptalaminate mature membrane structure is accomplished in an immature schistosome (schistosomulum) (Mansour and Mansour, 2002), with the help of several molecules which are potential target for nano-delivery systems. The surface spines of schistosomes are made-up of paracrystalline arrangements of filamentous actin, which are found outside the tegument and basal membranes with protruding tip which is above the general level of the tegument. The dorsal surface spines protrude into the endothelial cells surface of the human host blood vessels with the help of different molecular proteins such as; dyneins, SGTP4 and tetraspanins (some of the potential targets for nano-enabled drug delivery systems), where it helps the schistosomes to hold fast against the blood flow when the

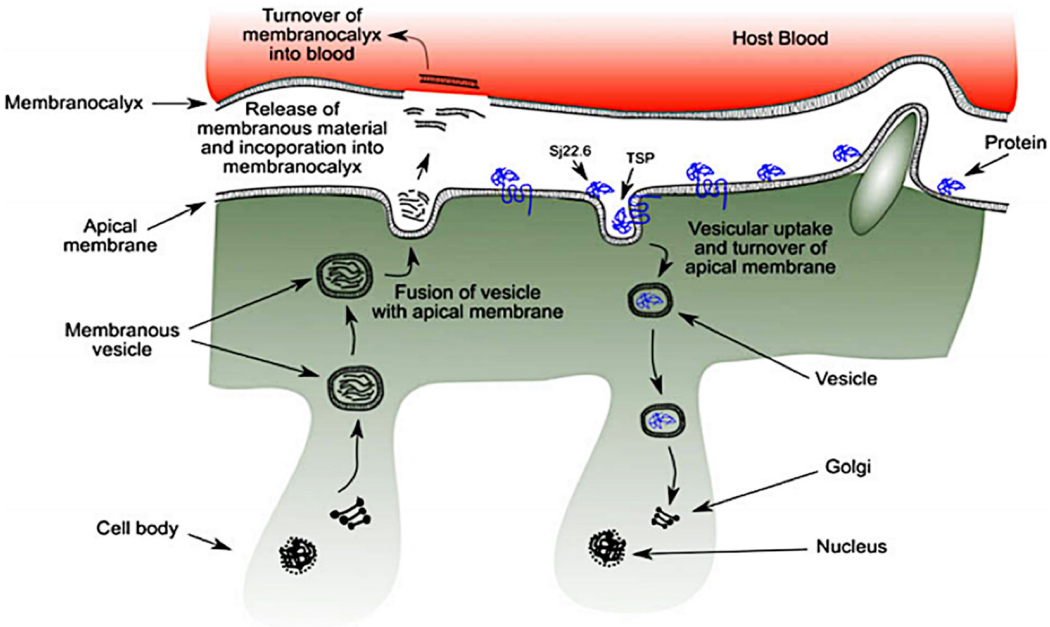

FIGURE 3 | Schematic diagram of schistosome tegument structure with several organelles and the position of targeted proteins (as seen in blue) (reprinted with permission from Mulvenna et al., 2010).

schistosomes are living in the host mesenteric blood vessels (Kašný et al., 2017).

The syncytium of the tegument consists of trilaminate vesicles that comprise membranous material, and they are either elongated or spherical in shape and are known as membranous bodies and elongate bodies. The syncytium is linked to nucleated cell bodies (cytons) by cytoplasmic tubes that are coated with microtubules. Although, cytons are not considered to be part of the tegument, they are found under the circular and longitudinal muscle fibers of the tegument where some potential targeted proteins and molecules are secreted. They consist of mitochondria, nuclei, Golgi complexes, ribosomes and glycogen particles (Mansour and Mansour, 2002). The biogenesis of new membrane material including tegumental proteins, and the maintenance of the schistosomes tegument are equipped inside the cytons, under the muscular layer and syncytium vesicles (El Ridi et al., 2017). Though, the process has not been well studied, both the elongated bodies and membranous bodies transport membranous material which are found to be scattered in the cytons in conjunction with Golgi complexes where they are possibly generated. These vesicles carry membranous material and some targeted proteins produced within the cytons and move them via the tubules of the cytoplasm to the syncytium, and thereafter, migrate to the outside of the surface tegument of the membrane (El Ridi et al., 2017; Gobert et al., 2017; Kašný et al., 2017). More so, the incorporation of membrane vesicles content with other tegumental proteins (potential targeted molecules for nano-delivery systems) take place in the cytons where a fresh heptalaminate membrane is produced. This activity is not only restricted to schistosomula developments, also to adult schistosomes after the shedding or the rupture of the exterior schistosomes surface. Surface pits is another organelle found on the surface of the schistosomes tegument. The pits have an ability to increase the surface area of the worm not less than tenfold where it provides an avenue for the worm to absorb nutrients such as glucose and other molecules from the exterior milieu using its tegumental proteins and receptors.

Wendt et al. (2018) developed a new fluorescent schistosome tegument label technique. This proved that the schistosome parasite usually repairs and replaces the tegument continuously with a half-life of 5 days in order to survive harsh conditions in the host system (Wendt et al., 2018). This corroborated with the work of Wilson and Barnes (1977), where they showed that there is a possibility for the membranocalyx of the schistosome tegument to replace itself at a variable rate and was dependent on the external environmental conditions in which the worm was found. This view was supported by Perez and Terry (1973) where they observed that the surface of the schistosome was turning over more rapidly when schistosomes cultured in monkey anti-mouse serum were selected from the schistosome mice model.

This unique membrane structure allows the schistosome tegument to play a significant role in protecting the schistosome to survive in the host, some of which include; host response modulation that causes host immune response evasion (Elzoheiry et al., 2018). This immune evasion occurs by rendering the infected host's antibody responses ineffective, hence fails to clear the established parasites (Han et al., 2009). In addition, the tegument of the schistosomes has some other functions such as absorption of nutrients.

Trematodes have an incomplete digestive tract, and the *Schistosoma species* can survive under prolonged *in vitro* incubation in the absence of nutrient absorption within the

intestine (Isseroff and Read, 1974; Popiel and Basch, 1984). Glucose absorption in trematodes is noticed during immature stages of the trematode's life cycle, which lacks a developed intestine (Uglem and Lee, 1985). Both, immature and mature schistosomes rely mainly on plasma glucose from the host for energy. Physiological investigations demonstrated that the influx of glucose within the tegument occurred by a carrier-mediated process (Rogers and Bueding, 1975; Uglem and Read, 1975). Several enzymes function for the absorption of amino acids on the tegument (Skelly et al., 2014), and other enzymes, for instance, leucine aminopeptidase is absent in the gut. Cholesterol is also acquired by schistosomes from the host via the tegument where it is redistributed throughout the schistosomes body (Haseeb et al., 1985; Popiel and Basch, 1986).

In terms of parasite motility control, the mature *Schistosoma* species move based on several degrees of flow and confinement. Zhang et al. (2019) observed that movement mechanics of schistosomes may be an important factor for the specific morphological qualities of an adult male worm, some of which include tegument topography and the strength as well as the nature of its suckers. In addition, the regulation of osmotic and electrochemical gradients of the worms is also control by the tegument. Faghiri and Skelly (2009) revealed that the schistosomes tegument controlled the movement of drug molecules and water into the parasites. This highlighted the role of the tegument in the uptake of drugs and in the osmoregulatory control of the parasite. The tegument also controls the excretion of certain metabolic products like amino acids, lactate, NH_4^+ and H^+ (Faghiri et al., 2010; Skelly et al., 2014).

POTENTIAL MOLECULAR TARGETS IN THE SCHISTOSOME TEGUMENT

There are several targets which have been identified on the surface of the tegument (**Table 2**). These are essential for engineered drug-loaded nanoparticles to target SGTP1 and SGTP4 as well as AChE and a nicotinic type of acetylcholine receptor (nAChR) that are predominantly found on the surface of the male schistosomes tegument. Other major surface proteins found on the tegument that can be targeted include dynein, aquaporins and tetraspanins among others. These molecules located on the surface of the tegument can serve as major molecular targets for the design and development of novel drug molecules and vaccines against the Schistosoma parasite.

Glucose Transporters as a Potential Molecular Target for Nano-Delivery Systems

Several studies (Skelly et al., 1994, 1998, 2014; Skelly and Shoemaker, 2000; Krautz-Peterson et al., 2010) have shown that *Schistosoma* parasites rely on energy (glucose) to survive. Energy (glucose) is consumed by the tegument first and not by the intestinal cecum. Uptake within the tegument is facilitated by the glucose transporters found on the tegument (Skelly et al., 1994, 1998). Skelly et al. (1994) isolated and characterized three different cDNAs with predicted protein sequences that indicate a high degree of structural and sequence similarity to that of facilitated diffusion transporters in animals, bacteria and plants. It was discovered that two cDNAs encoded for two different glucose transporters in the tegument namely SGTP1 and SGTP4. In addition, the study described that the SGTP 1 and 4 genes are expressed in adult and larval female and male schistosomes to facilitate the uptake of glucose from the host. In another related study by Cabezas-Cruz et al. (2015) four glucose transporters were encoded in the *Schistosoma mansoni* genome and only two out of the four facilitated glucose diffusion. Their results further proposed that *Schistosoma mansoni* class 1 glucose transporters failed to carry glucose and that this function developed independently in the schistosomes-specific glucose transporter.

There is a dynamic difference from the glucose transport of the platyhelminthes-specific transporters of the schistosomes when compared with humans (Cabezas-Cruz et al., 2015). It has been shown that the sequence of SGTP1 and 4 are 60% similar. Zhong et al. (1995) used electron microscopy to map the various locations of the transporters on the tegument. They observed that localization of SGTP1 was at the basal lamina and to a lesser extent under the muscle cells. This may help in transporting free glucose inside the tegument into the interstitial fluids that paddle the interior organs of the parasite. It was also demonstrated that SGTP4 was evenly distributed on the dorsal and ventral surfaces of female and male teguments with an extraordinary structure of a double lipid bilayer (Zhong et al., 1995). The distinct location of SGTP4 on the outer tegumental membrane reveals that SGTP4 facilitated glucose transport into the parasite tegument from the host bloodstream (Skelly et al., 1998; Skelly and Shoemaker, 2001). In addition, SGTP4 is involved in the development of the free-living cercariae into schistosomula. Through maturation they satisfy the needs of the parasite for high glucose uptake as soon as they enter the host (schistosomula stage) and throughout adulthood (Skelly and Shoemaker, 1996; Skelly et al., 1998).

Thus, proposing SGTP proteins as a potential target for nano-delivery systems, this postulation was supported by Krautz-Peterson et al. (2010) where RNAi was used to knock down the upregulation of SGTP4 and SGTP1 genes in schistosomula and in the life stages of adult worms. This study was undertaken to investigate the significance of these proteins to the parasite. Downregulation of either SGTP4 or SGTP1 displayed impairment in the ability of the protein to transport glucose when compared with the control. The study further showed that the simultaneous downregulation of both SGTP1 and SGTP4 reduced the ability of the parasite to transport glucose when compared with a single downregulated SGTP gene. It was also demonstrated that none of the parasites exhibited phenotypic distinction after prolonged incubation of all the suppressed parasites in enriched medium when compared to the control. Finally, it was suggested that SGTP1 and SGTP4 were important for transporting exogenous glucose from the mammalian host for normal parasite development. This was based on the observation that parasites with suppressed SGTPs showed decrease viability *in vivo* after infection of experimental animals (Krautz-Peterson et al., 2010). This notion was supported by a study performed by

TABLE 2 | Different potential targets found on the schistosomes tegument for conjugated nanoparticles and their functions.

Potential targets	Functions	References
Schistosome Glucose Transporters	Facilitate the uptake of glucose required for energy production in schistosomes directly from the host bloodstream.	Skelly et al., 1994, 1998, 2014; Skelly and Shoemaker, 2000; Krautz-Peterson et al., 2010
Acetylcholinesterase (AChE) and a nicotinic type of acetylcholine receptor (nAChR)	They maintain the schistosomes ion channels and nervous system, and they have glucose scavenging modulatory activity from the mammalian host blood.	Camacho and Agnew, 1995; MacDonald et al., 2014
Microtubule liked-proteins (dyneins, actin, tubulin and paramyosin)	Microtube liked-proteins can play a role in schistosomes mobility. Dyneins helps in the attachment and detachment of the adjacent membranous organelles along microtubules. Also, they are implicated in the assembling of spindle which are used for chromosome movement in mitosis.	Braschi et al., 2006a,b; Githui et al., 2009; Simanon et al., 2019
Aquaporins	They control the flow of water molecules in and out of the schistosomes. Some associates of aquaporins family also helps in metabolites (e.g., lactate) diffusion in and out of the cell. In other words, aquaporins control the osmotic regulation of the schistosomes.	Tsukaguchi et al., 1998, 1999; Braschi et al., 2006a,b; Gonen and Walz, 2006; Faghiri and Skelly, 2009; Faghiri et al., 2010
Tetraspanins	They play an essential role in maintaining the plasma membrane structure of the schistosomes where they interact with one another. Also, interacts with many others, particularly associate proteins such as, integrins, MHC and co-stimulatory molecules to generate a huge signal transduction complexes known as tetraspanin-enriched microdomains (TEMs).	Braschi et al., 2006a; Tran et al., 2010; Sotillo et al., 2015
Molecular chaperone (heat shock proteins 70, 16, and 60)	They help the schistosomes to withstand stress by inducing heat shock responses. They may likely also be responsible for the dramatic changes in niche environments of the earlier stages of intra-mammalian schistosomula development.	Braschi et al., 2006a,b; Van Hellemond et al., 2006; Sotillo et al., 2015, 2016, 2019
Enzymes (Esterases, carbonic anhydrase, Phosphodrolases, Thoredoxin peroxidase, Glyceraldehyde-3-phosphate dehydrogenase, protein disulfide isomerase, Glutathione S-transferase etc.)	Carbonic anhydrase is responsible for the hydration of CO_2 released by schistosomes during respiration. Phosphodrolases facilitate the removal of phosphate groups from organic molecules so that both could enter into the schistosomes via the plasma membrane. All other enzymes found on schistosomes tegument contribute toward the survival of the schistosomes.	Braschi et al., 2006a; Van Hellemond et al., 2006; Mulvenna et al., 2010; Sotillo et al., 2015, 2016, 2019

McKenzie et al. (2017), where the uptake of glucose was regulated in *Schistosoma mansoni* by Akt/Protein kinase B signaling. It was observed that Akt can be triggered by the host L-arginine, more so, insulin was shown to be effective in the layer of adult and schistosomula teguments. The inhibition of Akt decreased the upregulation and development of SGTP4 at the exterior of the host-invading larval stage of the parasite. The suppression of the SGTP4 upregulation at the tegument in adult worms was associated with a decrease in glucose uptake.

Hence, the functionalization of nanoparticles with targeted agents (antibodies, aptamers, antibody-like ligands, peptides and small molecules) with high specificity to SGTP proteins may be a superior alternative to anti-schistosomal treatment to nano-enabled the delivery of anti-schistosomal drugs. In achieving the desired selectivity of drug delivery, nanotechnology has allowed researchers to design nanoparticulate systems and incorporate therapeutic drugs to acts as nanocarriers. This is due to the overexpression of receptor molecules (SGTP proteins) which can serve as docking/interacting sites for targeting potential therapeutic drugs. Theoretically, the therapeutic drugs can be concentrated in a specific site in organ and tissues by functionalizing drug-containing nano-delivery systems with ligands against the receptors. Thus, nano-delivery systems with ligands specific to SGTPs as a receptor can be a potential target for designing, developing and delivering of anti-schistosomal drug.

Acetylcholine (nAChRs), AChE and Nicotinic Receptors; Possible Targets for Nano-Delivery Systems

Acetylcholine (ACh) is an essential neurotransmitter, both in invertebrates and vertebrates. The neuromuscular consequences of ACh are normally mediated by postsynaptic nAChRs due to their high-affinity for nicotine. Based on the structure of nAChRs, they belong to the Cys-loop LGIC superfamily (Albuquerque et al., 2009; MacDonald et al., 2014). nAChRs generate hetero and homo-pentameric structures that are arranged in a barrel shape around a central ion-selective hole. nAChRs in invertebrates are anion and cation-selective (Cl_2) ACh-gated channels while in vertebrates nAChRs are cation-selective (Ca^{2+}, Na^{+}, K^{+}) and facilitate excitatory responses.

Both the nicotinic type of the acetylcholine receptor (nAChR) and AChE are potential target for nano-enabled drug delivery system, because they are both found on the exterior surface of the

tegument where they play an essential role in the schistosomes ion channels and nervous system (Mansour and Mansour, 2002; MacDonald et al., 2014). AChE and nAChR are predominantly found on the surface of adult male schistosomes. The adult female schistosomes usually lodges in the gynaecophoral canal of the male containing a lower number of these proteins. AChE has been shown to have glucose scavenging modulatory activity from the human host bloodstream. The uptake of glucose is controlled by the interaction of ACh with the nAChR and AChE on the surface of the tegument (Camacho and Agnew, 1995). It has also been discovered that the exposure of low concentrations of ACh to *S. haematobium* or *S. bovis* and not *S. mansoni* improved the uptake of the glucose by the parasites in the host blood. At higher concentrations of ACh, the uptake of glucose in the host by parasites was inhibited. This specificity between the nicotinic receptor and ACh was supported by showing the effect of α-bungarotoxin and D-tubocurarine as antagonists to ACh. Therefore, it is significant when instituting a nanotechnology approach to deliver antagonistic drug molecules to the binding sites of nAChR and AChE in order to inhibit their glucose scavenging activities from the host bloodstream.

Dyneins as a Possible Molecular Targets for Nano-Delivery Systems

Dyneins is a protein that produces force and movement on microtubules for biological processes such as ciliary beating, intracellular transportation and cell division, it performs these functions through the help of ATP hydrolysis (Roberts et al., 2013). Dyneins could serve as a possible target for nano-delivery system in the treatment of schistosomiasis owing to its biological function in the survival of the parasite. Several studies have employed immunostaining to identify various microtubule related proteins inside the schistosomes tegument such as actin, tubulin, paramyosin, and dyneins. Studies have suggested that cytoplasmic dyneins may have a role to play in transporting of vesicles to the surface bilayers and tegument cytoplasm from the sub-tegumental cells. Dynein chains are part of a huge enzyme complex comprising heavy, intermediate and light chains. Dyneins are implicated in the assembly of spindles that are used for chromosome movement in mitosis. The upregulation of dyneins are involved in the developmental of *S. mansoni.* In addition, they are found in the schistosomula stage that occurs after the penetration of the intact skin of the host by the parasite and at the lung stage in adult worms. At this stage, early upregulation of the heptalaminate exterior membranes are exhibited. Meanwhile, dynein light chains are not found in the cercariae or ciliated miracidia (Hoffmann and Strand, 1996).

The dynein light chain protein discovered recently was shown to have high affinity to other proteins tegument with which they form highly complex associations. Another dynein light chain protein has been considered as a tegument antigen with the molecular weight of 20.8 kDa. Githui et al. (2009) investigated the normal motor constituents of vesicular transport present in the schistosomes tegument. The NCBI database blast search analysis recognized clones that are myosin and dynein light chains genes. After subjecting the genes of schistosome dynein to further analysis in the databases, they detected three dynein light chains families. They also observed that the Tctex family sequences of the dynein light chains are different significantly when compare to the mammalian homologs, Hence, could serve as probable drug/vaccine target against schistosomes infection. The three dynein light chains, *S. japonicum* dynein light chain-1, *S. mansoni* dynein light chain and SM10 studied via the immunolocalization of microtubule-related motor protein components show a specific and strong immunolocalization in the distal cytoplasm of the tegument (Kohlstädt et al., 1997; Yang et al., 1999). The tegument-associated protein of the *S. japonicum* which has 22.6 kDa displays similar localization arrangements (Li et al., 2000). In view of these aforementioned roles of dyneins in schistosomes survival, the delivery of targeted drug to localize and bind to dynein using nanotechnology approach will be a potential technique in eradicating schistosomiasis. Nanotechnology-based targeted delivery system functionalized with specific targeted molecules (antibodies, peptides, antibody-like molecule and aptamer) can recognize and selectively bind onto the dynein protein (receptors) on its active region thereby conferring targeted delivery.

Aquaporins as a Potential Molecular Targets for Nano-Delivery Systems

Aquaporins is another promising target for the delivery of surface-engineered drug-loaded nanoparticles. They are small integral membrane proteins that are mostly upregulated in animal and plant kingdoms. Aquaporins consist of two short and six transmembrane helical segments that enclose cytoplasmic and extracellular vestibules linked by a narrow aqueous pore. They consist of several conserved motifs, and aquaporin monomers are assembled as tetramers in membranes, with every monomer working independently (Verkman, 2013). Aquaporins act as channels to selectively control the influx and efflux of water molecules within cells. Certain aquaporins allow the diffusion of metabolites in and out of the cell (Tsukaguchi et al., 1998, 1999; Gonen and Walz, 2006).

The nano-enabling drug delivery activity of aquaporins was corroborated by Braschi et al. (2006a) where a proteomic study of the schistosome tegument was described. The presence of aquaporins was revealed on the surface of the tegument which indicated that aquaporins assisted with the influx of water and solutes within the plasma membrane of the schistosomes. The tegument (*S. mansoni*) as an excretory organ was investigated by Faghiri et al. (2010), where they observed that aquaporins on the surface of the tegument acted as a lactate transporter. In addition, it was also shown that the aquaporin found on the tegument was competent in transporting mannitol, water, alanine and fructose, but not glucose. Their further analysis of the tegument using immunofluorescent and immune-EM suggested that the function of the tegument was far above the known ability as an organ of nutrient uptake, but rather, it also helped in excretion of waste metabolites (Faghiri et al., 2010). The study supported the notion that the tegument controlled the osmoregulation and drug uptake in parasites (Faghiri and Skelly, 2009). It was also shown that the existence of aquaporins on the tegument controlled the

movement of water following the suppression of *S. mansoni* aquaporins with iRNAs (Faghiri and Skelly, 2009).

It has also been shown that aquaporin-4 (a homolog of aquaporins) enhanced the granulomatous response with an increase in the accumulation of macrophages and eosinophils around the *S. japonicum* eggs in the liver of the mice model. Similarly, the study showed that aquaporin-4 mice enhanced Th2, but decreased Th1 and Treg cell formation in *S. japonicum*., This accounts for the improvements of the liver granuloma formation (Zhang et al., 2015). These findings collectively indicate that aquaporins may be a desirable target for anti-schistosomal therapy using high precision delivery of drug-loaded nanostructures.

Tetraspanins as a Potential Molecular Target for Nano-Delivery Systems

Tetraspanins (TSPs) is a family of integral membrane proteins expressed by schistosomes, found in the exterior surface of the membrane of the schistosomes tegument. Braschi et al. (2006a) identified five tetraspanins in the schistosomes membrane surface, and the abundant components of these proteins are found in the tegument periphery. They speculated that the schistosome tetraspanins play an important role in the structure of the schistosomes plasma membrane, based on their analogy with other organisms (Braschi et al., 2006a). They also showed that, some tetraspanins are recognized more readily than others, and the concentrations and locations of only three biotinylated are suggested to vary within the surface of schistosomes tegument. The capacity of tetraspanins homologous interaction to generate a tetraspanin web may help scaffold organization in the lipid bilayer upon which there are assemblage of other proteins within the tegument. More so, the extracellular loops of the tetraspanins may provide platforms for gylcans and proteins which interact with the membranocalyx (Braschi et al., 2006a).

The functions of tetraspanins in the tegument of *S. mansoni* was investigated with the inhibition of the upregulation of Sm-tsp-1 and Sm-tsp-2 mRNAs using RNA. The ultrastructural morphology of mature schistosomes treated with Sm-tsp-2 dsRNA, show a thinner tegument and there is a visible formation of vacuoles on the schistosomes tegument. More so, schistosomula exposed to Sm-tsp-2 dsRNA showed a drastic thinner and extensive vacuolated tegument, and this morphological observation depends on failure of tegumentary invaginations (Tran et al., 2010). In another related study by Sotillo et al. (2015), it was reported that tetraspanins were found in biotinylated and unbound tegument tissues. It was also reported that tetraspanin-2 found in *S. mansoni* is essential for the formation of the schistosomes tegument and is a target of protective immunity in naturally resistant human and vaccinated mice. On the other hand, *S. mansoni* tetraspanin-1 are detected on the apical membrane of schistosomula. Tetraspanin-2 was found only in the unbound sample, which corroborates with other findings, which shows that the localization of tetraspanin-2 within the inner compartments of the schistosomes; relates with the exterior invaginations and vesicles in the tegument (Sotillo et al., 2015). Targeted nanocarriers has three main components that is; as a targeting moiety-penetration enhancer, an apoptosis-inducing agent and also, as a carrier. Therefore, the inhibition of tetraspanin by the means of nanotechnology-based approach will stop the interaction of glycans and proteins to the schistosomes membranocalyx, because, nanomaterials can preferentially accumulate in the parasite via tetraspanin in an active targeting mechanism thereby, release the encapsulated drugs in a regulated manner. This will provide the benefits of increasing the anti-schistosomal drug concentration and its therapeutic efficacy.

Other Potential Molecular Targets for Nano-Delivery Systems

Several studies have used proteomic in identifying constituents found within the tegument of schistosomes which potential targets for nano-delivery systems are. Braschi et al. (2006a) used proteomics to detect molecules found within the *S. mansoni* tegument. In their study, they identified transporters for sugars, inorganic ions, amino acids and water, which indicated that the tegument plasma membrane was crucial for schistosomes to acquire nutrients from the host and help maintain solute levels. They also identified enzymes such as esterases, phosphohydrolases and carbonic anhydrase with their catalytic domains found in the outer core of the plasma membrane, more so, annexin, five tetraspanins and dysferlin were shown to play a pivotal role in the architecture of the membrane. The study was corroborated by another proteomic analysis of *S. mansoni* proteins that was performed in the same year by Braschi et al. (2006b) not less than fifty-one (51) proteins were identified based on homology with known proteins in other organisms. Some of the identified proteins were enolase which involves energy metabolism; several cytoskeletal and molecular motor proteins such as severin, actin and dynein light chains. Others include molecular chaperone heat shock proteins 17, 19, and 20, calmodulin; vesicle proteins, and plasma membrane transporters; mitochondrial proteins for example ATP synthase; structural molecules and enzymes such as glucose transporter protein, calcium ATPase, annexin, alkaline phosphatase and tetraspanins A, B, and C (Braschi et al., 2006b).

As shown in **Figure 4** Sotillo et al. (2015) used the same approach to detect novel therapeutic targets for nanocarriers in *S. mansoni* schistosomula. Over 450 proteins were detected on the apical membrane of *S. mansoni* schistosomula, in which the expression of 200 have significant controlled profiles at diverse stages of schistosomula development *in vitro* which are potential targets for nano-delivery systems, such as glucose transporters, heat shock proteins, sterols, antioxidant enzymes and peptidases. In addition, current vaccine antigens were also detected on the apical membrane such as calpain, Sm-TSP-1 or Sm-TSP-2, Sm29 found on sub-tegumental fractions of the schistosomula showing localization patterns that differ in some instances from those found on the adult stage of the worm. Another study used S. mansoni genome project, concurrently with proteomic and lipidomic approaches, which allowed the study to characterize the lipids and proteins within the tegument plasma membrane in details. This study detected

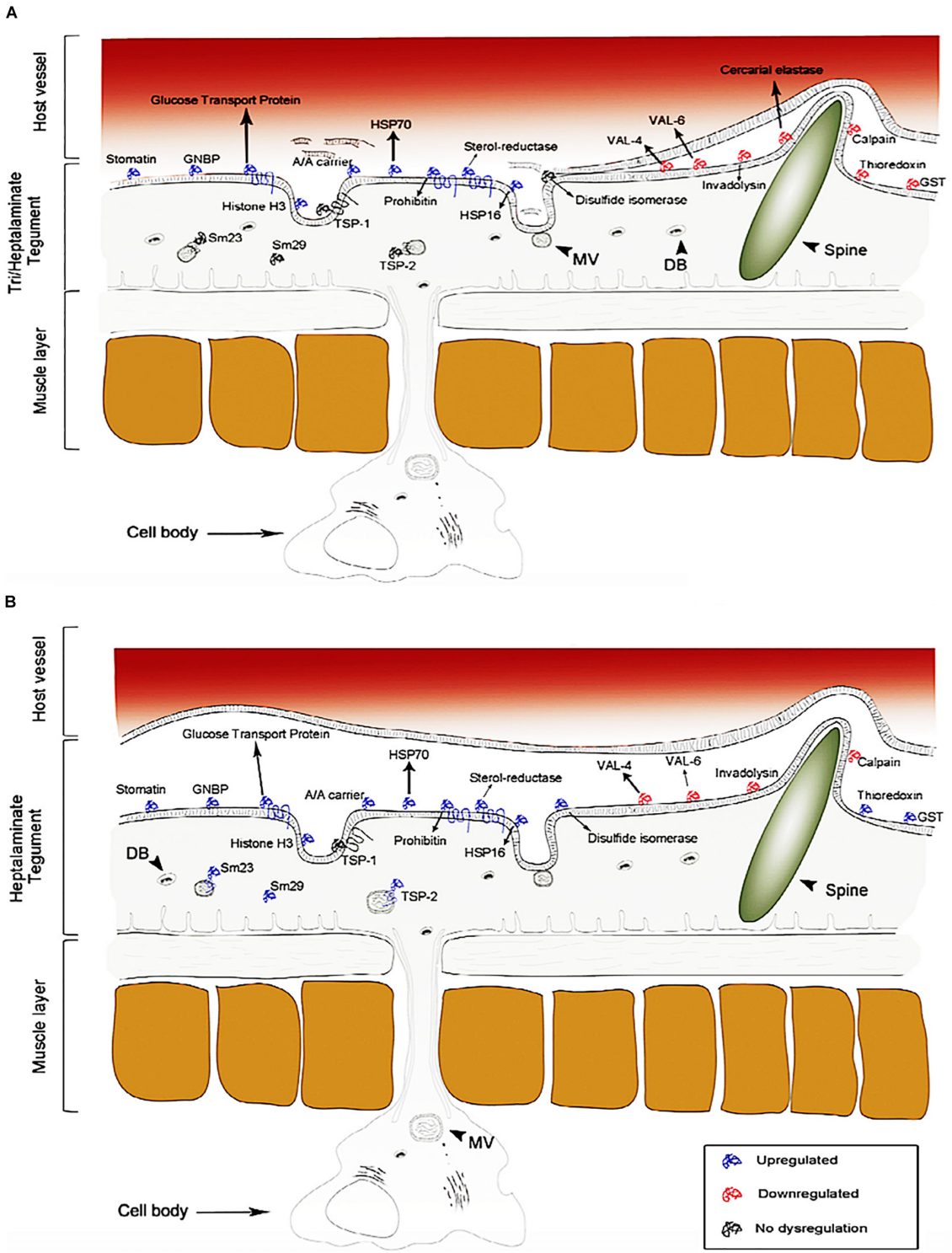

FIGURE 4 | Proteome identification of upregulated, downregulated and no dysregulation proteins found on the tegument of *S. mansoni* (schistosomula). The dysregulation of these proteins changes over time. **(A)** 3 h of infection and **(B)** 5 days of infection (reprinted with permission from Sotillo et al., 2015).

some tegumental targeted proteins and lipids, which depicts the role of the tegument in the uptake of nutrients from the host, and in the evasion of immune response. Furthermore, the study demonstrated that the tegument of the worm is enriched in lipids which are not found in the host. Similarly, the schistosome tegument possess proteins which have no sequence similarity

with any other sequence found in databases of species excepts in schistosomes (Van Hellemond et al., 2006). Several other studies (Liu et al., 2006; Pérez-Sánchez et al., 2006; Mulvenna et al., 2010; Castro-Borges et al., 2011; Sotillo et al., 2016, 2019) have employed proteomics technique in identification of several molecular receptors which are druggable and vaccine candidates for schistosomiasis treatment.

To date, there is no effective vaccine for schistosomiasis. Although, several potential promising vaccine candidates for *S. mansoni* and, to a lesser extent, *S. haematobium* have been discovered and published in literature. There is one vaccine, namely, BILHVAX, or the 28-kDa GST from *S. haematobium*, which has entered clinical trials (Capron et al., 2005). Unfortunately, published data is not available on the clinical efficacy of this vaccine, but nonetheless, it is of concern that other vaccines have not progressed to this stage. More so, there are several nanotechnology approaches in developing vaccines for schistosomiasis published in literature, but have not entered clinical trials. Some include oral vaccination with chitosan nanoparticles loaded with plasmid DNA encoding a Rho1-CTPase protein of *S. mansoni* (Oliveira et al., 2012). Another approach includes a novel nanoparticle formulation of the Sj26GST DNA vaccine; although there was no significant reduction in worm burden, a highly significant decline in tissue egg burden and the fecundity of female adult worms was reported (Mbanefo et al., 2015).

AN OVERVIEW OF NANO-DELIVERY SYSTEMS

Nanomedicine is the application of nanotechnology for treatment, prevention, monitoring, and control of biological diseases. In applying nanomedicine in the treatment of diseases, the precise targets (cells and/or receptors) specific to the clinical disease is identified and the suitable nanoparticles for the delivery system to minimize the side effects and improve the efficacy of the original drug is selected. One of these precise targets are macrophages, endothelial cells, proteins, dendritic cells as well as tumor cells. Some typical examples of nano-delivery systems (**Figure 5**) used over the years in the treatment of diseases includes; liposomes, micelles, dendrimer, polymeric nanoparticles, polymeric micelles, metallic nanoparticles, nanotubes and nanocrystals.

Morphological characteristics such as rigidity, size and aspect ratio play a vital role in, and affect the impact and fate of nanocarrier properties *in vivo* (Wang et al., 2018). The properties of nano-delivery systems are critically dependent on the morphological characteristics of the particle, and it is of importance to deliver drug into a specific site during the treatment of disease, such as the delivery of an anti-tumor drug into the site of a solid tumor (Wang et al., 2018). The characterization of the nanoparticles morphology and dimensions can be determine using SEM, TEM, and AFM. Although, the most appropriate technique depends on the sample type and the desired information to be measured and in some cases, researchers usually adopt techniques which are available and well-known to them in a characteristic dimension of the nanoparticles. A typical example of TEM, SEM and AFM of nanoparticle are shown in **Figure 6**.

Several studies have explored the use of nano-delivery system in improving the therapeutic efficacy of different drug molecules in the treatment of diseases. Mehrizi et al. (2018) carried out the synthesis of a novel nanosized chitosan-betulinic acid delivery system, against resistant Leishmania, with the first clinical observation of this parasite in the kidney. It was discovered that chitosan nanoparticles synthesized using phase separation; and drug loading by phase separation, improved the therapeutic dose of betulinic acid to 20 mg/kg. More so, the successful improvement in the

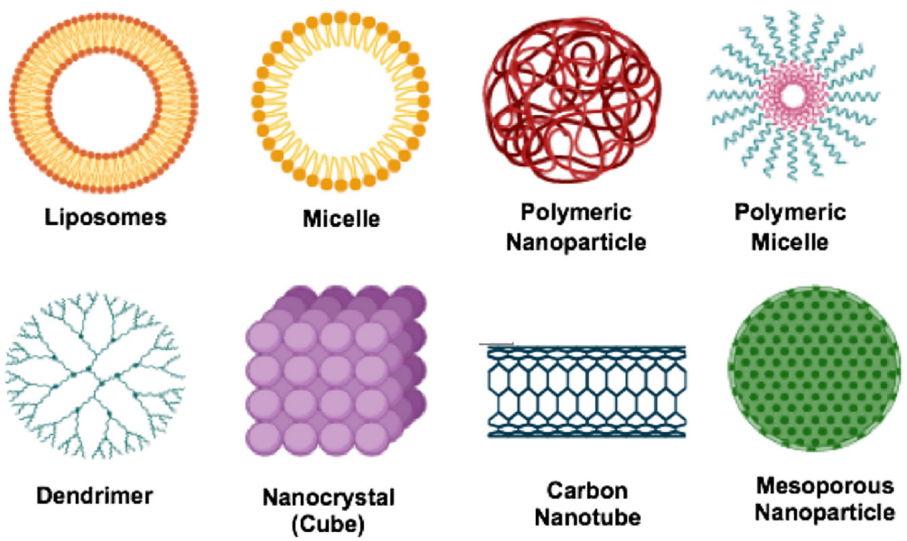

FIGURE 5 | Types of nanocarriers for drug delivery.

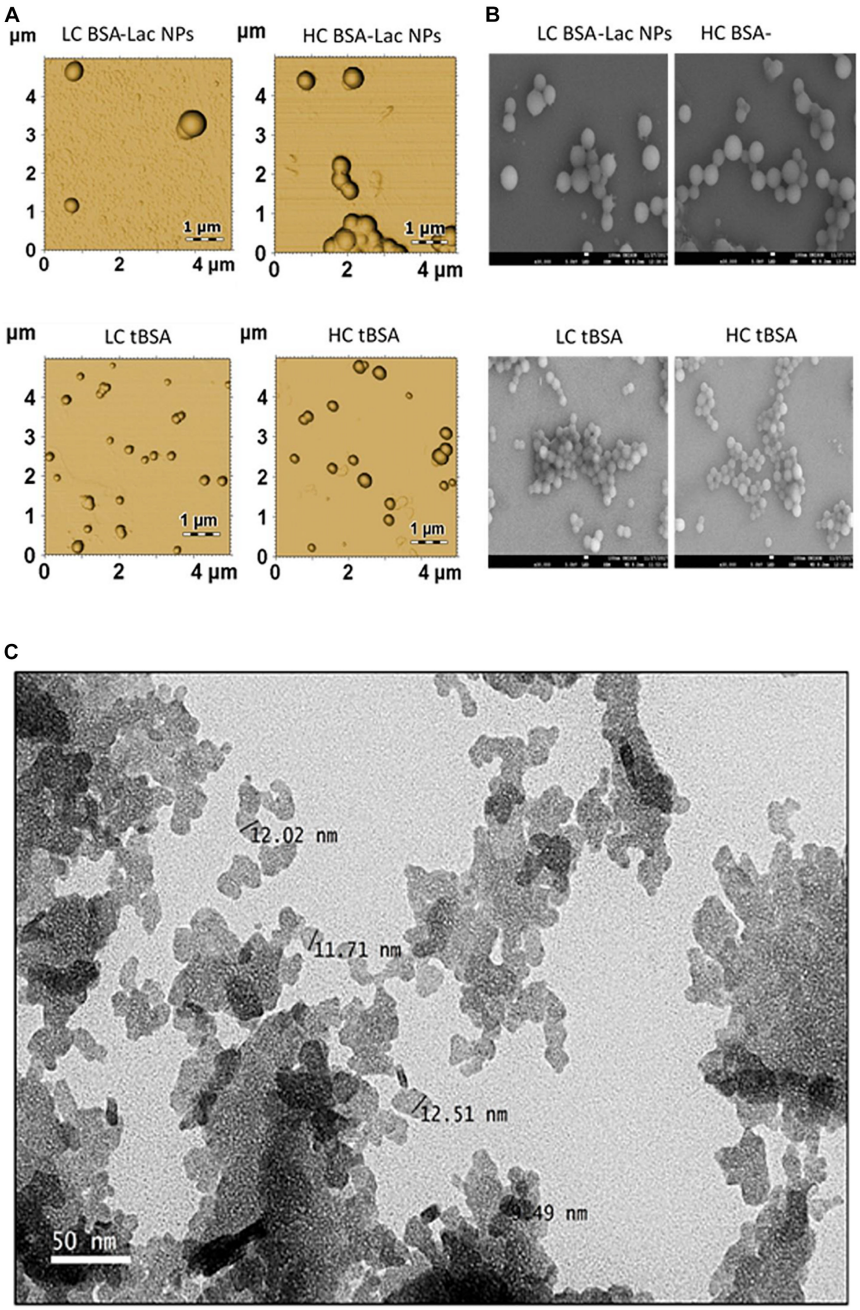

FIGURE 6 | Morphology of HC and LC BSA-Lac and tBSA NPs **(A)** atomic force microscopy (AFM) and **(B)** Scanning electron microscopy (SEM). **(C)** Transmission electron microscopy (TEM) image of Citral-loaded self nano-emulsifying drug delivery system (CIT-SNEDDS). Adapted from Izham et al. (2019) and Teran-Saavedra et al. (2019).

use of the nanosystem loaded betulinic acid in the treatment of leishmania, displayed both in *in vitro* and *in vivo* efficacy (Mehrizi et al., 2018).

The effectiveness of IVM was investigated using nanostructured lipid carriers in the treatment of hydatidosis, with some limitations and resistance associated with the drug overcome by the carriers in *in vitro* experimentation. It was observed that NLCs-loaded IVM induced higher mRNA caspase-3 expression which suggested a more potent apoptotic effect on the parasite (Ahmadpour et al., 2019). In another related study, nucleoside-lipid-based nanocarriers was used to encapsulate MB; a positively charged tricyclic phenothiazine molecule used in malaria treatment. This approach showed that the nanoparticles partially protected MB from oxido-reduction reactions, thereby preventing early degradation during storage, and the carrier also prolonged the pharmacokinetics in plasma.

It was concluded that this approach was an interesting technique in improving MB stability and the delivery in malaria treatment (Kowouvi et al., 2019).

Hence, the utilization of lipid nanoparticle-based drugs in the treatment of schistosomiasis will be beneficial in terms of cost, since solid lipid nanoparticles are easy to scale-up and involves lower cost production, relative non-toxic nature, biodegradable composition and stability against aggregation. More so, lipid-based formulations have the ability to enhance the bioavailability of drugs through solubility modification and the rate at which drugs can be released for the improvement and enhancement of drug absorption across biological barriers (Cheng et al., 2017), reducing side-effects associated with these drugs. This type of approach will be beneficial and effective in treating all forms of schistosomes (both mature and immature), by functionalizing the nanoparticles with targeted molecules which has ability to recognize and bind to molecular receptors present in all forms of schistosomes. Thus, preventing reinfection by specifically targeting overexpressed schistosomes antigens present in the human host, it has been reported that nanoparticles have the ability to induce heightened T cell immunity, which can prevent disease reactivation and reinfection (Tousif et al., 2017). The list of various nano-delivery systems used in improving the therapeutic efficacy of PZQ in the treatment of *Schistosomal* infections are reported in **Table 3**.

TARGETED NANO-ENABLED DRUG DELIVERY

Targeted nano-enabled therapies are able to recognize or detect molecules that are highly expressed on the surface of specific cells. This approach has gained popularity in treating various cancers due to the overexpression of specific receptors on the membrane surface of cancer cells. In the field of cancer, targeted nanotherapies inhibit particular cell surface proteins or genes which are responsible for cancer growth and metastasis. It has been hypothesized that targeted nanotherapies may be desirable over other forms of treatment (Joo et al., 2013; Camidge, 2014). According to a 2018 review published by the ACS, targeted nanotherapies have been approved for various anti-cancer therapies. Thus, employing a nanotherapeutic approach to target overexpressed proteins or genes on the surface of the schistosome tegument will assist in overcoming PZQ resistant, reduce the burden of immature schistosomes (schistosomula), and finally, put an end to the morbidity and mortality of schistosomiasis (**Figure 7**). More so, this approach and can be employed in the treatment of various parasitic infections. Although there are no reports of targeted nano-enabled drug delivery against Schistosoma species to date; there are few reports of this type of approach on other similar parasites such as; the preparation of the primaquine-containing liposomes functionalized with covalently bound heparin for the targeted delivery of antimalarial drugs to pRBCs.

Heparin covalently linked with targeted nano-enabled drug delivery to pRBCs was carried out to reduce anticoagulation risks. The study showed that heparin-based targeting can be designed to have a greater half-life, further relying on antibodies with exposed antigens, whose expression is constantly modified by successive generations of the parasite (Marques et al., 2017). Further to this, targeted nano-enabled drug delivery of a 19-amino peptide from the circumsporozoite protein of *Plasmodium berghei* which contained a conserved region, as a consensus heparin sulfate proteoglycan-binding sequence attached to the distal end of a lipid-polyethylene glycol bioconjugated, was prepared by the incorporation into phosphatidylcholine liposomes, reflecting favorable *in vitro* results (Longmuir et al., 2006).

Jain et al. (2014) developed a chitosan-assisted immunotherapy for the intervention of experimental leishmaniasis via amphotericin B -SLPs to activate the macrophages in order to impart a specific immune response by improving the production of TNF-α and IL-12 (Jain et al., 2014). This study also reflected a positive hypothesis for targeted nano-drug delivery for site specific targeting.

Antibody-Functionalized Drug Delivery Systems for Targeted Therapy in Schistosomes Infection

Antibodies are mostly IgGs or their fragments and have ability to recognize and interact virtually with any molecular target with high affinity and high specificity. Antibodies have gained special interest in targeted therapies due to their nanosized. They are biological materials which are part of the specific immune system, and they are toxin or pathogens neutralizers in nature. They help in recruitments of immune elements such as; improving phagocytosis, complement, cytotoxicity antibody dependent by NK cells. They can also help in carrying several elements such as; toxins, nanoparticles, drugs and fluorochroms to where they can be used in therapy to destroy a specific target, and for several other diagnostic procedures (Arruebo et al., 2009). Antibody-functionalized nanoparticulate systems are more site-specific, causing higher accumulation on the target region and subsequently, reduces dosage requirements.

The bioconjugation of antibodies with nanoparticles to generate a unique product which is composed of both the properties of the antibodies and nanoparticles can take place by adsorption process that is, at the isoelectrical point of the antibody through electrostatic interaction (Arruebo et al., 2009; Greene et al., 2018). More so, the conjugation can take place by direct covalent bonding between the surface of the antibody and the nanoparticles (that is, coupling of the antibodies to nanoparticles by free carboxyl or amine functionalities on aspartic/glutamic acid or lysine residues or by thio-maleimide reaction) (Arruebo et al., 2009). Another means by which the bioconjugation of the antibodies to the nanoparticles can be achieved is through the use of adapter molecules that is, bio-recognitions like streptavidin and biotin, which usually involves the formation of the complex. Greene et al. (2018), developed a novel approach for the site-specific conjugation of nanoparticulate systems which promotes the uniform and outward projection of paratopes for utmost target interaction. They demonstrated a successful re-bridging of the inter-chain

TABLE 3 | List of some nano-delivery systems which have been used in improving the therapeutic efficacy of PZQ in treating *schistosoma* infection.

S/N	Test nanoparticles	Test *schistosoma* species	Efficacy	References
1	PZQ-Liposomes	*S. mansoni*	Lip.PZQ causes a great significant reduction in the number of worm count, eggs/gram liver tissue and intestine. The nanosystem also reduced the number and diameter of hepatic granuloma in the histopathological studies.	Labib El Gendy et al., 2019
2	SLN-PZQ	*S. mansoni*	SLN-PZQ enhanced the bioavailability and antischistosomal efficacy against *S. mansoni* and reduced both the hepatic and intestinal tissue egg loads. In addition, the SLN-PZQ approximately cause complete disappearance on immature deposited eggs.	Radwan et al., 2019
3	Lipid nanocapsules (LNCs)-PZQ	*S. mansoni*	Oral LNCs-PZQ enhanced the efficacy of PZQ by targeting the distal postabsorption sites	Amara et al., 2018
4	Gold nanoparticles	*S. mansoni*	Gold NP showed to regulate gene expression impaired by *S. mansoni* infection	Dkhil et al., 2016
5	PZQ-Liposomes combined with hyperbaric oxygen therapy (HBO)	*S. mansoni*	100 mg/kg concentration of lip.PZQ + HBO was more effective (48.0% reduction of worms, 83.3% reduction of eggs/gram of feces) and 100% of the mice had altered of oograms; indicating interruption of oviposition. Additionally, HBO was able to stimulate the immune system, hence, HBO can work as an adjuvant in the treatment of the infection.	Frezza et al., 2015
6	PZQ-Liposomes	*S. mansoni*	There is improvement in the efficacy of the treatment with lip.PZQ, especially when administered 45 days following infection. More so, lip.PZQ is better absorbed by the tegument of *S. mansoni*, which has an affinity for phospholipids	Frezza et al., 2013
7	PZQ-Liposomes	*S. mansoni*	PZQ-liposomes caused a decrease in amounts of eggs and parasites. Liposomes improve the antischistosomal activity of praziquantel.	Mourão et al., 2005

disulfide linkage with a heterobifunctional linker and successive coupling to nanoparticles bearing complementary azide moieties in TRAZ F(ab) model. In a study by Mohammad et al., the administration of the antimalarial drug (chloroquine) loaded liposomes, targeted to infected RBCs with a tagged antibody against infected erythrocytes surface antigens on the chloroquine liposomes against drug-resistant *Plasmodium berghei*, presented a cure rate of 75–90% on days 4–6 post infection in mice (Mohammad et al., 1995).

Secret et al. (2013) described the preparation of antibody-functionalized biodegradable porous silicon nanoparticles loaded with the hydrophobic anticancer drug camptothecin. Using a novel semicarbazide based bioconjugation technique in chemistry, the specific orientation of the immobilized antibody on the nanoparticles was achieved. Three antibodies mAb528 a monoclonal antibody to EGFR; MLR2 a monoclonal antibody to p75NTR and Rituximab a monoclonal antibody to CD20 were used to target glioblastoma, neuroblastoma and B lymphoma cells, respectively in an *in vitro* study. The successful targeting was demonstrated by means of immunocytochemistry and flow cytometry both with cell lines and primary cells. The incubation of the antibody-functionalized nanoparticles with the cell lines for cell viability, showed selective killing of cells expressing the receptor, which correspond to the antibody coupled on the porous silicon nanoparticles. Also, the incorporation of camptothecin an anticancer drug into a nanoparticle functionalized with the antibodies showed to be very effective and efficient in targeting and killing cancer cells (Secret et al., 2013). In another recent study by Li et al. (2019), they developed an antibody-functionalized gold nanoparticle (cetuximab-AuNP) to selectively target cancer cells and probe for their potential radiosensitizing impacts under proton irradiation. It was discovered that cetuximab-AuNP interacts and bound specifically and accumulate in EGRF-overexpressing A431 cells when compared with EGFR-negative MDA-MB-453 cells. It was further shown that, cetuximab-AuNP improved the influence of proton irradiation in A431 cells but not in MDA-MB453 cells (Li et al., 2019). There are several other studies (Day et al., 2010; Dai et al., 2015; Korkmaz et al., 2016) which have employed antibody-functionalized nanoparticles to selectively target some specific receptors on the cancer cells either for treatments or imaging (diagnostics).

Aptamer-Functionalized Drug Delivery System for Targeted Therapy in Schistosomes Infection

Aptamers are short single-stranded oligonucleotide (RNA or DNA ligands) or peptides that bind to their target molecules; either small chemicals, large molecular cell-surface or transmembrane proteins with high specificity, affinity and versatility. They have been developed for over two decades against several targets and for different applications. Aptamers have emerged as promising molecules to target specific cancer antigens in therapy and clinical diagnosis (Cerchia and De Franciscis, 2010; Catuogno et al., 2016). Nucleic acid aptamers have gained attention as an attractive molecular vehicle because of their ability to bind to specific ligands with high affinity,

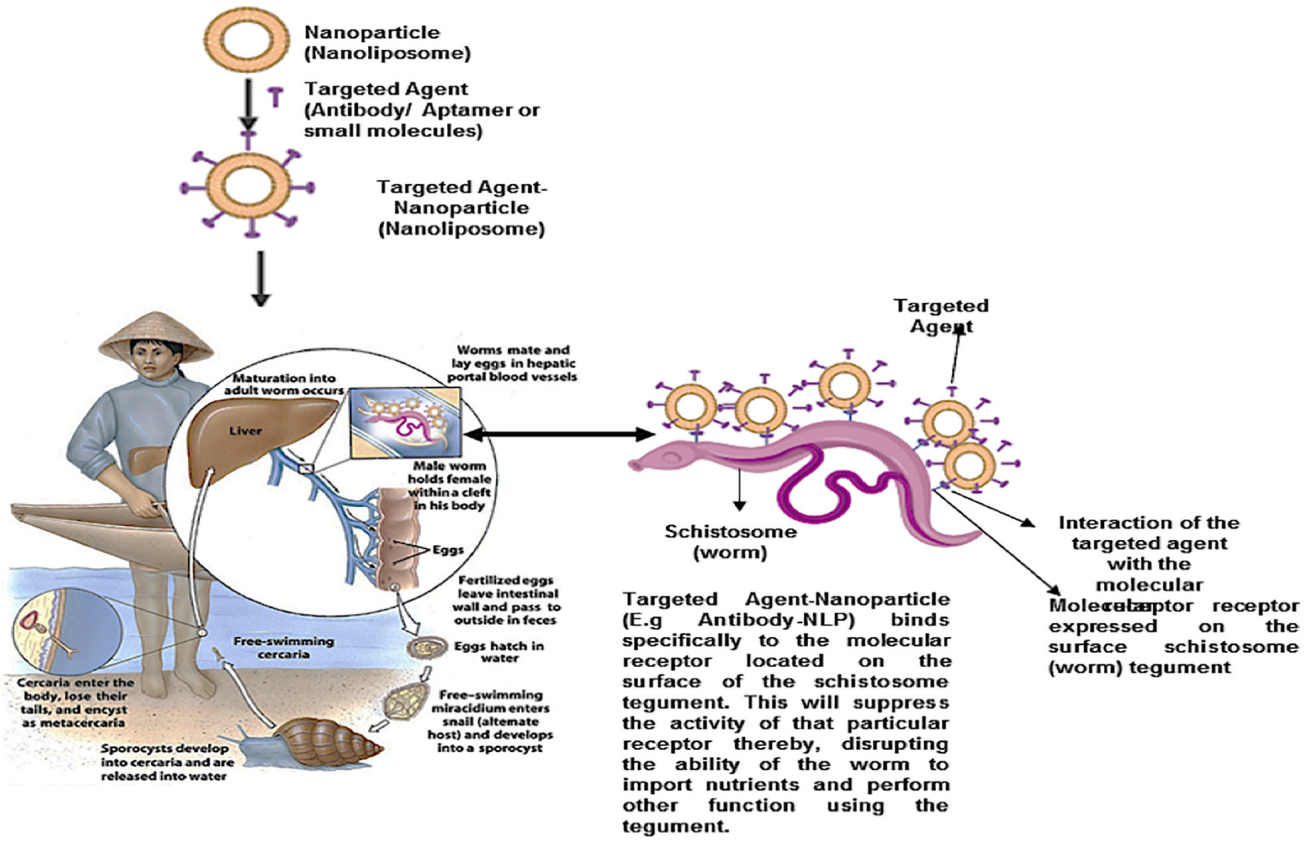

FIGURE 7 | Proposed schematic for nanoparticle (nanoliposome) surface engineered (functionalized) with targeted agents (Antibodies, aptamers, antibody-like ligands or small molecules). This targeted nanoparticle localized/detected as molecular receptors, located within the exterior of the schistosome tegument, and specifically binds to it. Thus, suppressing the activity of the receptor, as well as disrupt the ability of the worm to import nutrients from the host, and perform other activities.

they have high ability to penetrate cells, tissues and organs, and they also possess high chemical flexibility (Catuogno et al., 2016). Whereas, peptide aptamers, otherwise known as affimers are small stable proteins that are selected to interact and attach with high binding affinity to specific sites (surface) on their target molecules. They contain short amino acid of about 5–20 residues long sequences which are normally embedded as a loop inside a stable protein scaffold (Reverdatto et al., 2015). Aptamer based sensing platforms for the recognition of peptides, small molecules, proteins and cells have gained a huge interest due to their high sensitivity and selectivity. In general, aptamers are molecules that can generate unique 3-dimentional structure and has the ability to bind almost any molecular targets with higher binding affinity in the nanomolar level compared to monoclonal or polyclonal antibody.

Due to aptamers properties such as; high affinity, chemical stability, small size, ease of synthesis, low-immunogenicity and controllable chemical modification, owing to these multiple attributes, aptamer conjugated nanoparticles are well qualified nanosystems for the development of biomedical devices for imaging, analytical, drug delivery and some other medical applications. The bioconjugation of the aptamers onto the nanoparticulate systems can be attained via non-covalent (affinities interaction e.g., streptavidin-biotin or metal ion co-ordination) and covalent (1-ethyl-3-carbodiimide or succinimdyl ester-amine chemistry and *N*-hydroxysuccinimide activation chemistry which cross link the carboxylic acid group on the surface of the nanoparticles and the amino group of the ligands) interactions. The covalent interaction strategies can also be achieved by maleimide-thiol chemistry that is, the cross linking of the thiol group on the targeting moiety and the maleimide functional group on the surface of the nanoparticulate systems.

Yu et al. (2011) developed a novel aptamer bioconjugated nanoparticles in order to enhance the delivery of paclitaxel anticancer drug to MUC1-positive cancer cells. The aptamer was engineered into the surface of the nanoparticles via a DNA spacer. The flow cytometry analysis shown the higher uptake of the nanoparticulate systems conjugated with MUC1 specific aptamer into the target cells via the overexpression of MUC1. The results further showed that, paclitaxel loaded aptamer functionalized nanoparticles improved the *in vitro* drug delivery and cytotoxicity to MUC1 cancerous cells when compared to non-targeted nanoparticulate systems which lack the MUC1

aptamer. In Yang et al. (2013) developed a DNA aptamer envelope protein for the inhibition of hepatitis C virus. In their study, it was shown that selected aptamers for E1E2 particularly recognized the recombinant E1E2 protein and E1E2 protein from hepatitis C virus-infected cells. The aptamers exert antiviral properties via the inhibition of the virus binding to the host cell (Yang et al., 2013). Several other studies (Mathieu et al., 2016; Corda et al., 2018; Dou et al., 2018; Tan et al., 2019) have employed aptamer-conjugate as a targeted delivery system for therapeutics and diagnostics.

Other Functionalized Drug Delivery Systems for Targeted Therapy in Schistosomes Infection

Other small molecules or peptides that are highly specific for certain molecular receptors with high affinity, can also be screened or developed in order to localize and bind with the molecular receptors found on the tegument of the schistosomes. Lei et al. (2019) designed a novel alendronate-modified nanoparticle loaded with paclitaxel and coated with polydopamine for osteosarcoma-targeted therapy. In this study, it was reported that the polymerization of dopamine in a versatile modification method was not limited by the absence of functional groups on the surfaces of the compound and do not affect the chemical properties. The successful bioconjugation of the polydopamine with nanoparticles with a surface modifier which consist of a precise affinity for osteosarcoma cells was attained. They posit further that, the targeting nano-delivery systems exhibited a higher *in vitro* cytotoxicity on K7M2 of osteosarcoma cells when compared with the native nanosystems. Furthermore, the *in vivo* study showed that the targeting nano-delivery systems could accumulate within the tumor to a greater extent with remarkable decrease in the adverse effects of paclitaxel when compared with non-targeted nanosystems (Lei et al., 2019).

Säälik et al. (2019) investigated the effect of a novel penetrating peptide-guided nanoparticles that targets cell surface LinTT1, p32 for glioblastoma targeting. In this study, the coupling of LinTT1 to albumin-paclitaxel nano-delivery systems was achieved by sulfosuccinimidyl 4-(*N*-maleimidomethyl) cyclohexane-1-carboxylate as a linker. They demonstrated that the novel p32 targeting peptide, LinTT1 promotes the targeted accumulation of nanoparticles to tumors across a panel of high-grade glioma mouse model effectively. They further showed that the treatment of mice with LinTT1-guided nanoparticles extend the survival rate of mice with the tumor; due to the ability of LinTT1-nanopaticles to recognize the upregulation of p32 on glioblastoma (Säälik et al., 2019).

Ahlschwede et al. (2019) employed targeted nano-delivery approach in treating cerebral amyloid angiopathy and detecting cerebrovascular amyloid observed in AD. A targeted nano-delivery system was developed by a cationic blood brain barrier penetrating peptide using a covalent bioconjugation technique. The results from the targeted nanosystem depicted a higher significant brain uptake due to the high binding affinity of the peptide (K16ApoE)-nano-delivery system to amyloid plaques. In another study carried out by Colombo et al. (2019) where the targeted biodegradable nano-delivery system for CD34 + endothelial precursors in the treatment of rheumatoid arthritis was achieved. The bioconjugation of the targeting molecule was activated by *N*-hydroxysuccinimide in order to exploit its primary amino groups. The results in this study showed that, the targeted nano-delivery system possess a greater advantage in delivery the drug to inflamed synovia via the synovium-homing peptide as a targeting molecular receptor.

Silva et al. (2015) carried out mannose-functionalized polymeric nanoparticles to target the mannose receptors on antigen-presenting cells and therapeutic anti-tumor immune responses in a melanoma model. It was discovered that mannose-functionalized nanoparticles potentiated the Th1 immune activity, and the nanoparticulated vaccines reduced the rate of murine B16F10 melanoma tumors growth in prophylactic and therapeutic settings (Silva et al., 2015). Also, Mufamadi et al. (2013) carried out a ligand-functionalized nanoliposomes for targeted delivery of galantamine in AD. It was shown that ligand-functionalized nanoliposomes enhanced the uptake of galantamine into PC12 neuronal cells through the receptor of Serpin Enzyme Complex (Mufamadi et al., 2013). Ruff et al. (2017) investigated the effect of gold nanoparticles surface engineered with amyloidogenic β-amyloid specific peptides in a BBB in an *in vitro* model. This study was carried out in order to increase the BBB permeability, as well as the nanoparticle concentration in the brain by the peptides. It was discovered that, the multivalent peptides bind selectively to Aβ-amyloid fibrils, thereby posing a strongly effect on the integrity of BBB, thus, actively cause the transport of the gold nanoparticle conjugates via the BBB.

CONCLUSION

Incidences of schistosomiasis continue to increase globally across sub-Saharan Africa and other tropical regions. However, the development of resistance against the only drug PZQ necessitates the design of more effective drug molecules to tackle the continual increase in Schistosomiasis cases. In this review, the molecular structure and function of the schistosomal tegument was described and several molecular targets have been identified to potentially target the schistosomes tegument as a site for enhanced PZQ delivery in anti-schistosomal therapy. In addition, potential agents that could target the molecular receptors identified have been highlighted. In general, surface functionalization of nanoparticles with antibodies, aptamers, antibody-like ligands, peptides and small molecules to specifically target and bind to the schistosomes tegument receptor genes and proteins presents a viable option for researchers to explore. This approach will suppress the activity of receptor genes/proteins, thereby impairing the ability of schistosomes to import nutrients from the host as well as disrupt the ability of the parasite to maintain solute balancing and evasion of the host immune response. Hence, exploration of the schistosomes tegument may be a possible and

potential focus for designing and developing anti-schistosomal drug which can target receptors and proteins present on the worm tegument.

AUTHOR CONTRIBUTIONS

All authors contributed to the manuscript completion and approved the final submission. TA, PK, YC, PK, and VP contributed to this study from framework design and manuscript content to manuscript optimization.

FUNDING

This work was supported by the National Research Foundation (NRF) of South Africa (Grant name: SARChI).

REFERENCES

Abruzzi, A., and Fried, B. (2011). Coinfection of Schistosoma (Trematoda) with bacteria, protozoa and helminths. *Adv. Parasitol.* 77, 1–85. doi: 10.1016/B978-0-12-391429-3.00005-8

Adekiya, T. A., Kappo, A. P., and Okosun, K. O. (2017). Temperature and rainfall impact on schistosomiasis. *Glob. J. Pure Appl. Math.* 13, 8453–8469.

Ahlschwede, K. M., Curran, G. L., Rosenberg, J. T., Grant, S. C., Sarkar, G., Jenkins, R. B., et al. (2019). Cationic carrier peptide enhances cerebrovascular targeting of nanoparticles in Alzheimer's disease brain. *Nanomed. Nanotechnol. Biol. Med.* 16, 258–266. doi: 10.1016/j.nano.2018.09.010

Ahmadpour, E., Godrati-Azar, Z., Spotin, A., Norouzi, R., Hamishehkar, H., Nami, S., et al. (2019). Nanostructured lipid carriers of ivermectin as a novel drug delivery system in hydatidosis. *Parasit. Vectors* 12, 1–9. doi: 10.1186/s13071-019-3719-x

Albuquerque, E. X., Pereira, E. F., Alkondon, M., and Rogers, S. W. (2009). Mammalian nicotinic acetylcholine receptors: from structure to function. *Physiol. Rev.* 89, 73–120. doi: 10.1152/physrev.00015.2008

Amara, R. O., Ramadan, A. A., El-Moslemany, R. M., Eissa, M. M., El-Azzouni, M. Z., El-Khordagui, L. K., et al. (2018). Praziquantel–lipid nanocapsules: an oral nanotherapeutic with potential *Schistosoma mansoni* tegumental targeting. *Int. J. Nanomed.* 13, 4493–4505. doi: 10.2147/IJN.S167285

Arruebo, M., Valladares, M., and González-Fernández, Á (2009). Antibody-conjugated nanoparticles for biomedical applications. *J. Nanomater.* 2009, 37. doi: 10.1155/2009/439389

Aruleba, R. T., Adekiya, T. A., Oyinloye, B. E., Masamba, P., Mbatha, L. S., Pretorius, A., et al. (2018). PZQ therapy: how close are we in the development of effective alternative anti-schistosomal drugs? *Infect. Disord. Drug Targets* 19, 337–349. doi: 10.2174/1871526519666181231153139

Becker, B., Mehlhorn, H., Andrews, P., Thomas, H., and Eckert, J. (1980). Light and electron microscopic studies on the effect of praziquantel on *Schistosoma mansoni*, *Dicrocoelium dendriticum*, and *Fasciola hepatica* (Trematoda) in vitro. *Zeitschrift für Parasitenkunde* 63, 113–128. doi: 10.1007/bf00927527

Braschi, S., Borges, W. C., and Wilson, R. A. (2006a). Proteomic analysis of the shistosome tegument and its surface membranes. *Mem. Inst. Oswaldo Cruz.* 101, 205–212. doi: 10.1590/s0074-02762006000900032

Braschi, S., Curwen, R. S., Ashton, P. D., Verjovski-Almeida, S., and Wilson, A. (2006b). The tegument surface membranes of the human blood parasite *Schistosoma mansoni*: a proteomic analysis after differential extraction. *Proteomics* 6, 1471–1482. doi: 10.1002/pmic.200500368

Cabezas-Cruz, A., Valdés, J. J., Lancelot, J., and Pierce, R. J. (2015). Fast evolutionary rates associated with functional loss in class I glucose transporters of *Schistosoma mansoni*. *BMC Genomics* 16:980. doi: 10.1186/s12864-015-2144-2146

Caffrey, C. R. (2007). Chemotherapy of schistosomiasis: present and future. *Curr. Opin. Chem. Biol.* 11, 433–439. doi: 10.1016/j.cbpa.2007.05.031

Camacho, M., and Agnew, A. (1995). Schistosoma: rate of glucose import is altered by acetylcholine interaction with tegumental acetylcholine receptors and acetylcholinesterase. *Exp. Parasitol.* 81, 584–591. doi: 10.1006/expr.1995.1152

Camidge, D. R. (2014). Targeted therapy vs chemotherapy: which has had more impact on survival in lung cancer? Does targeted therapy make patients live longer? Hard to prove, but impossible to ignore. *Clin. Adv. Hematol. Oncol.* 12, 763–766.

Capron, A., Riveau, G., Capron, M., and Trottein, F. (2005). Schistosomes: the road from host-parasite interactions to vaccines in clinical trials. *Trends Parasitol.* 21, 143–149. doi: 10.1016/j.pt.2005.01.003

Castro-Borges, W., Dowle, A., Curwen, R. S., Thomas-Oates, J., and Wilson, R. A. (2011). Enzymatic shaving of the tegument surface of live schistosomes for proteomic analysis: a rational approach to select vaccine candidates. *PLoS Neg. Trop. Dis.* 5:e993. doi: 10.1371/journal.pntd.0000993

Catuogno, S., Esposito, C., and de Franciscis, V. (2016). Aptamer-mediated targeted delivery of therapeutics: an update. *Pharmaceuticals* 9:69. doi: 10.3390/ph9040069

Cerchia, L., and De Franciscis, V. (2010). Targeting cancer cells with nucleic acid aptamers. *Trends Biotechnol.* 28, 517–525. doi: 10.1016/j.tibtech.2010.07.005

Cheng, W., Li, X., Zhang, C., Chen, W., Yuan, H., and Xu, S. (2017). Preparation and in vivo-in vitro evaluation of polydatin-phospholipid complex with improved dissolution and bioavailability. *Int. J. Drug Dev. Res.* 9, 39–43.

Cioli, D., and Pica-Mattoccia, L. (2003). Praziquantel. *Parasitol. Res.* 90, S3–S9. doi: 10.1007/s00436-002-0751-z

Cioli, D., Pica-Mattoccia, L., Basso, A., and Guidi, A. (2014). Schistosomiasis control: praziquantel forever? *Mol. Biochem. Parasitol.* 195, 23–29. doi: 10.1016/j.molbiopara.2014.06.002

Colombo, F., Durigutto, P., De Maso, L., Biffi, S., Belmonte, B., Tripodo, C., et al. (2019). Targeting CD34+ cells of the inflamed synovial endothelium by guided nanoparticles for the treatment of rheumatoid arthritis. *J. Autoimmun.* 03:102288. doi: 10.1016/j.jaut.2019.05.016

Conlon, C. P. (2005). Schistosomiasis. *Medicine* 33, 64–67.

Corda, E., Du, X., Shim, S. Y., Klein, A. N., Siltberg-Liberles, J., and Gilch, S. (2018). Interaction of peptide aptamers with prion protein central domain promotes α-cleavage of PrP C*. *Mol. Neurobiol.* 55, 7758–7774. doi: 10.1007/s12035-018-0944-9

da Paixão Siqueira, L., Fontes, D. A. F., Aguilera, C. S. B., Timóteo, T. R. R., Ângelos, M. A., Silva, L. C. P. B. B., et al. (2017). Schistosomiasis: drugs used and treatment strategies. *Acta Trop.* 176, 179–187. doi: 10.1016/j.actatropica.2017.08.002

Dai, Q., Yan, Y., Ang, C. S., Kempe, K., Kamphuis, M. M., Dodds, S. J., et al. (2015). Monoclonal antibody-functionalized multilayered particles: targeting cancer cells in the presence of protein coronas. *ACS Nano* 9, 2876–2885. doi: 10.1021/nn506929e

Day, E. S., Bickford, L. R., Slater, J. H., Riggall, N. S., Drezek, R. A., and West, J. L. (2010). Antibody-conjugated gold-gold sulfide nanoparticles as multifunctional agents for imaging and therapy of breast cancer. *Int. J. Nanomed.* 5:445. doi: 10.2147/ijn.s10881

de Moraes, J. (2012). "Antischistosomal natural compounds: present challenges for new drug screens," in *Current Topics in Tropical Medicine*, ed. A. J. Rodriguez-Morales, (London: IntechOpen).

Dkhil, M. A., Khalil, M. F., Bauomy, A. A., Diab, M. S., and Al-Qura, S. (2016). Efficacy of gold nanoparticles against nephrotoxicity induced by Schistosoma mansoni Infection in mice. *Biomed. Environ. Sci.* 29, 773–781. doi: 10.3967/bes2016.104

Doenhoff, M. J., Cioli, D., and Utzinger, J. (2008). Praziquantel: mechanisms of action, resistance and new derivatives for schistosomiasis. *Curr. Opin. Infect. Dis.* 21, 659–667. doi: 10.1097/QCO.0b013e328318978f

Dou, X. Q., Wang, H., Zhang, J., Wang, F., Xu, G. L., Xu, C. C., et al. (2018). Aptamer–drug conjugate: targeted delivery of doxorubicin in a her3 aptamer-functionalized liposomal delivery system reduces cardiotoxicity. *Int. J. Nanomed.* 13:763. doi: 10.2147/IJN.S149887

Eissa, M. M., El Bardicy, S., and Tadros, M. (2011). Bioactivity of miltefosine against aquatic stages of Schistosoma mansoni, Schistosoma haematobium and their snail hosts, supported by scanning electron microscopy. *Parasit. Vectors* 4:73. doi: 10.1186/1756-3305-4-73

El Ridi, R., Tallima, H., and Migliardo, F. (2017). Biochemical and biophysical methodologies open the road for effective schistosomiasis therapy and vaccination. *Biochim. Biophys. Acta* 1861, 3613–3620. doi: 10.1016/j.bbagen.2016.03.036

El Ridi, R. A. F., and Tallima, H. A. M. (2013). Novel therapeutic and prevention approaches for schistosomiasis: review. *J. Adv. Res.* 4, 467–478. doi: 10.1016/j.jare.2012.05.002

Elzoheiry, M., Da'dara, A. A., Bhardwaj, R., Wang, Q., Azab, M. S., El-Kholy, E. S. I., et al. (2018). Intravascular *Schistosoma mansoni* cleave the host immune and hemostatic signaling molecule sphingosine-1-phosphate via tegumental alkaline phosphatase. *Front. Immunol.* 9:1746. doi: 10.3389/fimmu.2018.01746

Faghiri, Z., Camargo, S. M., Huggel, K., Forster, I. C., Ndegwa, D., Verrey, F., et al. (2010). The tegument of the human parasitic worm *Schistosoma mansoni* as an excretory organ: the surface aquaporin SmAQP is a lactate transporter. *PLoS One* 5:e10451. doi: 10.1371/journal.pone.0010451

Faghiri, Z., and Skelly, P. J. (2009). The role of tegumental aquaporin from the human parasitic worm, *Schistosoma mansoni*, in osmoregulation and drug uptake. *FASEB J.* 23, 2780–2789. doi: 10.1096/fj.09-130757

Fenwick, A., Webster, J. P., Bosque-Oliva, E., Blair, L., Fleming, F. M., Zhang, Y., et al. (2009). The Schistosomiasis Control Initiative (SCI): rationale, development and implementation from 2002–2008. *Parasitology* 136, 1719–1730. doi: 10.1017/S0031182009990400

Frezza, T. F., de Souza, A. L. R., César, C. R. P., Claudineide, N. F. O., and Gremião, M. P. D. (2015). Effectiveness of hyperbaric oxygen for experimental treatment of schistosomiasis mansoni using praziquantel-free and encapsulated into liposomes: assay in adult worms and oviposition. *Acta Trop.* 150, 182–189. doi: 10.1016/j.actatropica.2015.07.022

Frezza, T. F., Gremião, M. P. D., Zanotti-Magalhães, E. M., Magalhães, L. A., and de Souza, A. L. R. (2013). Liposomal-praziquantel: efficacy against Schistosoma mansoni in a preclinical assay. *Acta Trop.* 128, 70–75. doi: 10.1016/j.actatropica.2013.06.011

Garcia-Salcedo, J. A., Unciti-Broceta, J. D., Valverde-Pozo, J., and Soriano, M. (2016). New approaches to overcome transport related drug resistance in trypanosomatid parasites. *Front. Pharmacol.* 7:351. doi: 10.3389/fphar.2016.00351

Githui, E. K., Damian, R. T., Aman, R. A., Ali, M. A., and Kamau, J. M. (2009). *Schistosoma* spp.: isolation of microtubule associated proteins in the tegument and the definition of dynein light chains components. *Exp. Parasitol.* 121, 96–104. doi: 10.1016/j.exppara.2008.10.007

Gobert, G. N., Schulte, L., and KJones, M. (2017). "Tegument and external features of Schistosoma (with particular reference to ultrastructure)," in *Schistosoma*, ed. B. Jamieson, (Boca Raton, FL: CRC press), 213–238. doi: 10.1201/9781315368900-11

Gonen, T., and Walz, T. (2006). The structure of aquaporins. *Q. Rev. Biophy.* 39, 361–396. doi: 10.1017/S0033583506004458

Greene, M. K., Richards, D. A., Nogueira, J. C., Campbell, K., Smyth, P., Fernández, M., et al. (2018). Forming next-generation antibody–nanoparticle conjugates through the oriented installation of non-engineered antibody fragments. *Chem. Sci.* 9, 79–87. doi: 10.1039/c7sc02747h

Han, Z. G., Brindley, P. J., Wang, S. Y., and Chen, Z. (2009). Schistosoma genomics: new perspectives on schistosome biology and host-parasite interaction. *Ann. Rev. Genomics Hum. Genet.* 10, 211–240. doi: 10.1146/annurev-genom-082908-150036

Harnett, W., and Kusel, J. R. (1986). Increased exposure of parasite antigens at the surface of adult male *Schistosoma mansoni* exposed to praziquantel in vitro. *Parasitology* 93, 401–405. doi: 10.1017/S0031182000051568

Haseeb, M. A., Eveland, L. K., and Fried, B. (1985). The uptake, localization and transfer of [4-14C] cholesterol in Schistosoma mansoni males and females maintained in vitro. *Comp. Biochem. Physiol. A Comp. Physiol.* 82, 421–423. doi: 10.1016/0300-9629(85)90877-1

Hoffmann, K. F., and Strand, M. (1996). Molecular identification of a *Schistosoma mansoni* tegumental protein with similarity to cytoplasmic dynein light chains. *J. Biol. Chem.* 271, 26117–26123. doi: 10.1074/jbc.271.42.26117

Isseroff, H., and Read, C. P. (1974). Studies on membrane transport—VIII. Absorption of monosaccharides by *Fasciola hepatica*. *Comp. Biochem. Physiol. Part A* 47, 141–152. doi: 10.1016/0300-9629(74)90060-7

Izham, M., Nadiah, M., Hussin, Y., Aziz, M. N. M., Yeap, S. K., Rahman, H. S., et al. (2019). Preparation and characterization of self nano-emulsifying drug delivery system loaded with citraland its antiproliferative effect on colorectal cells in vitro. *Nanomaterials* 9:1028. doi: 10.3390/nano9071028

Jain, V., Gupta, A., Pawar, V. K., Asthana, S., Jaiswal, A. K., Dube, A., et al. (2014). Chitosan-assisted immunotherapy for intervention of experimental leishmaniasis via amphotericin B-loaded solid lipid nanoparticles. *Appl. Biochem. Biotechnol.* 174, 1309–1330. doi: 10.1007/s12010-014-1084-y

Joo, W. D., Visintin, I., and Mor, G. (2013). Targeted cancer therapy–are the days of systemic chemotherapy numbered? *Maturitas* 76, 308–314. doi: 10.1016/j.maturitas.2013.09.008

Kašný, M., Haas, W., Jamieson, B. G., and Horák, P. (2017). "Cercaria of Schistosoma," in *Schistosoma*, Vol. 149, ed. B. Jamieson, (Boca Raton, FL: CRC Press),

Katz, M. (1977). Antihelmintics. *Drugs* 13, 124–136.

Kohlstädt, S., Couissinier-Paris, P., Bourgois, A., Bouchon, B., Piper, K., Kolbe, H., et al. (1997). Characterization of a schistosome T cell-stimulating antigen (Sm10) associated with protective immunity in humans. *Mol. Biochem. Parasitol.* 84, 155–165. doi: 10.1016/S0166-6851(96)02787-9

Kohn, A. B., Anderson, P. A., Roberts-Misterly, J. M., and Greenberg, R. M. (2001). Schistosome calcium channel β subunits unusual modulatory effects and potential role in the action of the antischistosomal drug praziquantel. *J. Biol. Chem.* 276, 36873–36876. doi: 10.1074/jbc.C100273200

Korkmaz, E., Friedrich, E. E., Ramadan, M. H., Erdos, G., Mathers, A. R., Ozdoganlar, O. B., et al. (2016). Tip-loaded dissolvable microneedle arrays effectively deliver polymer-conjugated antibody inhibitors of tumor-necrosis-factor-alpha into human skin. *J. Pharm. Sci.* 105, 3453–3457. doi: 10.1016/j.xphs.2016.07.008

Kowouvi, K., Alies, B., Gendrot, M., Gaubert, A., Vacher, G., Gaudin, K., et al. (2019). Nucleoside-lipid-based nanocarriers for methylene blue delivery: potential application as anti-malarial drug. *RSC Adv.* 9, 18844–18852. doi: 10.1039/c9ra02576f

Krautz-Peterson, G., Simoes, M., Faghiri, Z., Ndegwa, D., Oliveira, G., Shoemaker, C. B., et al. (2010). Suppressing glucose transporter gene expression in schistosomes impairs parasite feeding and decreases survival in the mammalian host. *PLoS Pathog.* 6:e1000932. doi: 10.1371/journal.ppat.1000932

Labib El Gendy, A. E. M., Mohammed, F. A., Abdel-Rahman, S. A., Shalaby, T. I. A., Fathy, G. M., Mohammad, S. M., et al. (2019). Effect of nanoparticles on the therapeutic efficacy of praziquantel against *Schistosoma mansoni* infection in murine models. *J. Parasit. Dis.* 43, 416–425. doi: 10.1007/s12639-019-01106-6

Lei, Z., Mengying, Z., Dongdong, B., Xiaoyu, Q., Yifei, G., Xiangtao, W., et al. (2019). Alendronate-modified polydopamine-coated paclitaxel nanoparticles for osteosarcoma-targeted therapy. *J. Drug Deliv. Sci. Technol.* 53, 101133. doi: 10.1016/j.jddst.2019.101133

Li, S., Bouchy, S., Penninckx, S., Marega, R., Fichera, O., Gallez, B., et al. (2019). Antibody-functionalized gold nanoparticles as tumor-targeting radiosensitizers for proton therapy. *Nanomedicine* 14, 317–333. doi: 10.2217/nnm-2018-0161

Li, T., and Takeoka, S. (2018). "Smart Liposomes for Drug Delivery," in *Smart Nanoparticles for Biomedicine*, Edn 1st Edn, ed. G. Ciofani, (Amsterdam: Elsevier), 31–47. doi: 10.1016/B978-0-12-814156-4.00003-3

Li, Y., Auliff, A., Jones, M. K., Yi, X., and McManus, D. P. (2000). Immunogenicity and immunolocalization of the 22.6 kDa antigen of *Schistosoma japonicum*. *Parasit. Immunol.* 22, 415–424. doi: 10.1046/j.1365-3024.2000.00319.x

Liu, F., Lu, J., Hu, W., Wang, S. Y., Cui, S. J., Chi, M., et al. (2006). New perspectives on host-parasite interplay by comparative transcriptomic and proteomic analyses of *Schistosoma japonicum*. *PLoS Pathog.* 2:e29. doi: 10.1371/journal.ppat.0020029

Longmuir, K. J., Robertson, R. T., Haynes, S. M., Baratta, J. L., and Waring, A. J. (2006). Effective targeting of liposomes to liver and hepatocytes in vivo by incorporation of a *Plasmodium amino* acid sequence. *Pharm. Res.* 23, 759–769. doi: 10.1007/s11095-006-9609-x

MacDonald, K., Buxton, S., Kimber, M. J., Day, T. A., Robertson, A. P., and Ribeiro, P. (2014). Functional characterization of a novel family of acetylcholine-gated chloride channels in *Schistosoma mansoni*. *PLoS Pathog.* 10:e1004181. doi: 10.1371/journal.ppat.1004181

Mansour, T., and Mansour, J. (2002). "Targets in the Tegument of Flatworms," in *Chemotherapeutic Targets in Parasites: Contemporary Strategies*, ed. J. M. Mansour, (Cambridge: Cambridge University Press), 189–214. doi: 10.1017/cbo9780511546440.009

Marques, J., Valle-Delgado, J. J., Urbán, P., Baró, E., Prohens, R., Mayor, A., et al. (2017). Adaptation of targeted nanocarriers to changing requirements in antimalarial drug delivery. *Nanomed. Nanotechnol. Biol. Med.* 13, 515–525. doi: 10.1016/j.nano.2016.09.010

Mathieu, S., Cisse, C., Vitale, S., Ahmadova, A., Degardin, M., Perard, J., et al. (2016). From peptide aptamers to inhibitors of FUR, bacterial transcriptional regulator of iron homeostasis and virulence. *ACS Chem. Bol.* 11, 2519–2528. doi: 10.1021/acschembio.6b00360

Mbanefo, E. C., Takashi, K., Yukinobu, K., Tomoaki, K., Rieko, F., Mahamoud, S. C., et al. (2015). Immunogenicity and anti-fecundity effect of nanoparticle coated glutathione S-transferase (SjGST) DNA vaccine against murine *Schistosoma japonicum* infection. *Parasitol. Int.* 64, 24–31. doi: 10.1016/j.parint.2015.01.005

McKenzie, M., Kirk, R. S., and Walker, A. J. (2017). Glucose Uptake in the Human Pathogen *Schistosoma mansoni* is regulated through Akt/protein kinase B signaling. *J. Inf. Dis.* 218, 152–164. doi: 10.1093/infdis/jix654

Mehlhorn, H., Becker, B., Andrews, P., Thomas, H., and Frenkel, J. K. (1981). In vivo and in vitro experiments on the effects of praziquantel on *Schistosoma mansoni*. A light and electron microscopic study. *Arzneimittel-Forschung* 31, 544–554.

Mehrizi, T. Z., Ardestani, M. S., Hoseini, M. H. M., Khamesipour, A., Mosaffa, N., and Ramezani, A. (2018). Novel Nanosized Chitosan-Betulinic Acid Against Resistant Leishmania Major and First Clinical Observation of such parasite in Kidney. *Sci. Rep.* 8:11759. doi: 10.1038/s41598-018-30103-7

Mohammad, O., Varshney, G. C., Subhash Chandra, A. C., and Gupta, C. M. (1995). Chloroquine encapsulated in malaria-infected erythrocyte-specific antibody-bearing liposomes effectively controls chloroquine-resistant *Plasmodium berghei* infections in mice. *Antimicrob. Agents Chemother.* 39, 180–184. doi: 10.1128/aac.39.1.180

Morgan, J. A., de Jong, R. J., Snyder, S. D., Mkoji, G. M., and Loker, E. S. (2001). *Schistosoma mansoni* and *Biomphalaria*: past history and future trends. *Parasitology* 123, S211–S228. doi: 10.1017/s0031182001007703

Mourão, S. C., Costa, P. I., Salgado, H. R., and Gremião, M. P. D. (2005). Improvement of antischistosomal activity of praziquantel by incorporation into phosphatidylcholine-containing liposomes. *Int. J. Pharm.* 295, 157–162. doi: 10.1016/j.ijpharm.2005.02.009

Mufamadi, M. S., Choonara, Y. E., Kumar, P., Modi, G., Naidoo, D., Vuuren, S., et al. (2013). Ligand-functionalized nanoliposomes for targeted delivery of galantamine. *Int. J. Pharm.* 448, 267–281. doi: 10.1016/j.ijpharm.2013.03.037

Mulvenna, J., Moertel, L., Jones, M. K., Nawaratna, S., Lovas, E. M., Gobert, G. N., et al. (2010). Exposed proteins of the *Schistosoma japonicum* tegument. *Intl. J. Parasitol.* 40, 543–554. doi: 10.1016/j.ijpara.2009.10.002

Nare, B., Smith, J. M., and Prichard, R. K. (1992). Mechanisms of inactivation of and mammalian glutathione -transferase activity by the anti- schistosomal drug oltipraz. *Biochem. Pharm.* 43, 1345–1351. doi: 10.1016/0006-2952(92)90512-h

Oliveira, C. R., Rezende, C. M., Silva, M. R., Borges, O. M., Pêgo, A. P., and Goes, A. M. (2012). Oral vaccination based on DNA-chitosan nanoparticles against *Schistosoma mansoni* infection. *Sci. World J.* 2012:938457. doi: 10.1100/2012/938457

Pax, R., Bennett, J. L., and Fetterer, R. (1978). A benzodiazepine derivative and praziquantel: effects on musculature of *Schistosoma mansoni* and *Schistosoma japonicum*. *Naunyn-Schmiedebergs Arch. Pharmacol.* 304, 309–315. doi: 10.1007/bf00507974

Perez, H., and Terry, R. J. (1973). The killing of adult *Schistosoma mansoni* in vitro in the presence of antisera to host antigenic determinants and peritoneal cells. *Int. J. Parasitol.* 3, 499–503. doi: 10.1016/0020-7519(73)90046-5

Pérez-Sánchez, R., Ramajo-Hernández, A., Ramajo-Martín, V., and Oleaga, A. (2006). Proteomic analysis of the tegument and excretory-secretory products of adult *Schistosoma bovis* worms. *Proteomics* 6, S226–S236. doi: 10.1002/pmic.200500420

Popiel, I., and Basch, P. F. (1984). Reproductive development of female *Schistosoma mansoni* (Digenea: Schistosomatidae) following bisexual pairing of worms and worm segments. *J. Exp. Zool.* 232, 141–150. doi: 10.1002/jez.1402320117

Popiel, I., and Basch, P. F. (1986). *Schistosoma mansoni*: cholesterol uptake by paired and unpaired worms. *Exp. Parasitol.* 61, 343–347. doi: 10.1016/0014-4894(86)90189-x

Radwan, A., El-Lakkany, N. M., William, S., El-Feky, G. S., and Al-Shorbagy, M. Y. (2019). A novel praziquantel solid lipid nanoparticle formulation shows enhanced bioavailability and antischistosomal efficacy against murine *S. mansoni* infection. *Parasit. Vectors* 12:304. doi: 10.1186/s13071-019-3563-z

Reverdatto, S., Burz, D. S., and Shekhtman, A. (2015). Peptide aptamers: development and applications. *Curr. Topics Med. Chem.* 15:1082. doi: 10.2174/1568026615666150413153143

Richter, J. (2003). The impact of chemotherapy on morbidity due to schistosomiasis. *Acta Trop.* 86, 161–183. doi: 10.1016/s0001-706x(03)00032-9

Roberts, A. J., Kon, T., Knight, P. J., Sutoh, K., and Burgess, S. A. (2013). Functions and mechanics of dynein motor proteins. *Nat. Rev. Mol. Cell Biol.* 14:713. doi: 10.1038/nrm3667

Rogers, S. H., and Bueding, E. (1975). Anatomical localization of glucose uptake by Schistosoma mansoni adults. *Int. J. Parasitol.* 5, 369–371. doi: 10.1016/0020-7519(75)90086-7

Ruff, J., Hüwel, S., Kogan, M. J., Simon, U., and Galla, H. J. (2017). The effects of gold nanoparticles functionalized with ß-amyloid specific peptides on an in vitro model of blood–brain barrier. *Nanomedicine: Nanotechnol. Biol. Med.* 13, 1645–1652. doi: 10.1016/j.nano.2017.02.013

Säälik, P., Lingasamy, P., Toome, K., Mastandrea, I., Rousso-Noori, L., Tobi, A., et al. (2019). Peptide-guided nanoparticles for glioblastoma targeting. *J. Control Release.* 308, 109–118. doi: 10.1016/j.jconrel.2019.06.018

Saconato, H., and Atallah, A. (2000). Interventions for treating *Schistosomiasi mansoni*. *Cochrane Data Syst. Rev.* 1999:CD000528. doi: 10.1002/14651858.CD000528

Secret, E., Smith, K., Dubljevic, V., Moore, E., Macardle, P., Delalat, B., et al. (2013). Antibody-functionalized porous silicon nanoparticles for vectorization of hydrophobic drugs. *Adv. Healthc. Mater.* 2, 718–727. doi: 10.1002/adhm.201200335

Silva, J. M., Eva, Z., Gaëlle, V., Vanessa, G. O., Ana, S., Mafalda, V., et al. (2015). In vivo delivery of peptides and Toll-like receptor ligands by mannose-functionalized polymeric nanoparticles induces prophylactic and therapeutic anti-tumor immune responses in a melanoma model. *J. Contr. Release* 198, 91–103. doi: 10.1016/j.jconrel.2014.11.033

Simanon, N., Adisakwattana, P., Thiangtrongjit, T., Limpanont, Y., Chusongsang, P., Chusongsang, Y., et al. (2019). Phosphoproteomics analysis of male and female Schistosoma mekongi adult worms. *Sci. Rep.* 9:10012. doi: 10.1038/s41598-019-46456-6

Skelly, P. J., Da'dara, A. A., Li, X. H., Castro-Borges, W., and Wilson, R. A. (2014). Schistosome feeding and regurgitation. *PLoS Pathog.* 10:e1004246. doi: 10.1371/journal.ppat.1004246

Skelly, P. J., Kim, J. W., Cunningham, J., and Shoemaker, C. B. (1994). Cloning, characterization, and functional expression of cDNAs encoding glucose transporter proteins from the human parasite *Schistosoma mansoni*. *J. Biol. Chem.* 269, 4247–4253.

Skelly, P. J., and Shoemaker, C. B. (1996). Rapid appearance and asymmetric distribution of glucose transporter SGTP4 at the apical surface of intramammalian-stage *Schistosoma mansoni*. *Pro. Nat. Aca. Sci. U.S.A.* 93, 3642–3646. doi: 10.1073/pnas.93.8.3642

Skelly, P. J., and Shoemaker, C. B. (2000). Induction cues for tegument formation during the transformation of *Schistosoma mansoni* cercariae. *Int. J. Parasitol.* 30, 625–631. doi: 10.1016/s0020-7519(00)00031-x

Skelly, P. J., and Shoemaker, C. B. (2001). The *Schistosoma mansoni* host-interactive tegument forms from vesicle eruptions of a cyton network. *Parasitology* 122, 67–73. doi: 10.1017/s0031182000007071

Skelly, P. J., Tielens, A. G. M., and Shoemaker, C. B. (1998). Glucose transport and metabolism in mammalian-stage schistosomes. *Parasitol. Today* 14, 402–406. doi: 10.1016/s0169-4758(98)01319-2

Sotillo, J., Pearson, M., Becker, L., Mulvenna, J., and Loukas, A. (2015). A quantitative proteomic analysis of the tegumental proteins from *Schistosoma mansoni* schistosomula reveals novel potential therapeutic targets. *Int. J. Parasitol.* 45, 505–516. doi: 10.1016/j.ijpara.2015.03.004

Sotillo, J., Pearson, M., Potriquet, J., Becker, L., Pickering, D., Mulvenna, J., et al. (2016). Extracellular vesicles secreted by *Schistosoma mansoni* contain protein vaccine candidates. *Int. J. Parasitol.* 46, 1–5. doi: 10.1016/j.ijpara.2015.09.002

Sotillo, J., Pearson, M. S., Becker, L., Mekonnen, G., Amoah, A. S., van Dam, G., et al. (2019). In-depth proteomic characterization of *Schistosoma haematobium*:

towards the development of new tools for elimination. *PLoS Neg. Trop. Dis.* 13:e0007362. doi: 10.1371/journal.pntd.0007362

Tan, K. X., Danquah, M. K., Pan, S., and Yon, L. S. (2019). Binding characterization of aptamer-drug layered microformulations and in vitro release assessment. *J. Pharm. Sci.* 108, 2934–2941. doi: 10.1016/j.xphs.2019.03.037

Teran-Saavedra, N. G., Sarabia-Sainz, J. A. I., Silva-Campa, E., Burgara-Estrella, A. J., Guzmán-Partida, A. M., Ramos-Clamont Montfort, G., et al. (2019). Lactosylated albumin nanoparticles: potential drug nanovehicles with selective targeting toward an in vitro model of hepatocellular carcinoma. *Molecules* 24:1382. doi: 10.3390/molecules24071382

Thetiot-Laurent, S. A. L., Boissier, J., Robert, A., and Meunier, B. (2013). Schistosomiasis chemotherapy. *Angewandte Chemie* 52, 7936–7956. doi: 10.1002/anie.201208390

Tousif, S., Singh, D. K., Mukherjee, S., Ahmad, S., Arya, R., Nanda, R., et al. (2017). nanoparticle-formulated curcumin prevents Posttherapeutic Disease reactivation and reinfection with *Mycobacterium tuberculosis* following isoniazid therapy. *Front. Immunol.* 8:739. doi: 10.3389/fimmu.2017.00739

Tran, M. H., Freitas, T. C., Cooper, L., Gaze, S., Gatton, M. L., Jones, M. K., et al. (2010). Suppression of mRNAs encoding tegument tetraspanins from *Schistosoma mansoni* results in impaired tegument turnover. *PLoS Pathog.* 6:e1000840. doi: 10.1371/journal.ppat.1000840

Tsukaguchi, H., Shayakul, C., Berger, U. V., Mackenzie, B., Devidas, S., Guggino, W. B., et al. (1998). Molecular characterization of a broad selectivity neutral solute channel. *J. Biol. Chem.* 273, 24737–24743. doi: 10.1074/jbc.273.38.24737

Tsukaguchi, H., Weremowicz, S., Morton, C. C., and Hediger, M. A. (1999). Functional and molecular characterization of the human neutral solute channel aquaporin-9. *Am. J. Physiol. Renal. Physiol.* 277, F685–F696. doi: 10.1152/ajprenal.1999.277.5.F685

Uglem, G. L., and Lee, K. J. (1985). Proterometra macrostoma (Trematoda: Azygiidae): functional morphology of the tegument of the redia. *Int. J. Parasitol.* 15, 61–64. doi: 10.1016/0020-7519(85)90102-X

Uglem, G. L., and Read, C. P. (1975). Sugar transport and metabolism in *Schistosoma mansoni*. *J. Parasitol.* 61, 390–397.

Urman, H. K., Bniay, O., Clayson, B. D., and Shubik, P. (1975). Carcinogenic effects of niridazole. *Cancer Lett.* 1, 69–74. doi: 10.1016/s0304-3835(75)95362-8

Van Hellemond, J. J., Retra, K., Brouwers, J. F., van Balkom, B. W., Yazdanbakhsh, M., Shoemaker, C. B., et al. (2006). Functions of the tegument of schistosomes: clues from the proteome and lipidome. *Int. J. Parasitol.* 36, 691–699. doi: 10.1016/j.ijpara.2006.01.007

Veerasamy, R., Xin, T. Z., Gunasagaran, S., Xiang, T. F. W., Yang, E. F. C., Jeyakumar, N., et al. (2011). Biosynthesis of silver nanoparticles using mangosteen leaf extract and evaluation of their antimicrobial activities. *J. Saudi Chem. Soc.* 15, 113–120. doi: 10.1016/j.jscs.2010.06.004

Verkman, A. S. (2013). Aquaporins. *Curr. Biol.* 23, R52–R55. doi: 10.1016/j.cub.2012.11.025

Wang, Z., Wu, Z., Liu, J., and Zhang, W. (2018). Particle morphology: an important factor affecting drug delivery by nanocarriers into solid tumors. *Expert Opin. Drug Deliv.* 15, 379–395. doi: 10.1080/17425247.2018.1420051

Wendt, G. R., Collins, J. N., Pei, J., Pearson, M. S., Bennett, H. M., Loukas, A., et al. (2018). Flatworm-specific transcriptional regulators promote the specification of tegumental progenitors in *Schistosoma mansoni*. *eLife* 7:e33221. doi: 10.7554/eLife.33221

Wilson, R. A., and Barnes, P. E. (1977). The formation and turnover of the membranocalyx on the tegument of *Schistosoma mansoni*. *Parasitology* 74, 61–71. doi: 10.1017/s0031182000047533

Yang, D., Meng, X., Yu, Q., Xu, L., Long, Y., Liu, B., et al. (2013). Inhibition of hepatitis C virus infection by DNA aptamer against envelope protein. *Antimicro. Agents Chemother.* 57, 4937–4944. doi: 10.1128/AAC.00897-13

Yang, W., Jones, M. K., Fan, J., Hughes-Stamm, S. R., and McManus, D. P. (1999). Characterisation of a family of *Schistosoma japonicum* proteins related to dynein light chains. *Biochim. Biophys. Acta* 1432, 13–26. doi: 10.1016/s0167-4838(99)00089-8

Yu, C., Hu, Y., Duan, J., Yuan, W., Wang, C., Xu, H., et al. (2011). Novel aptamer-nanoparticle bioconjugates enhances delivery of anticancer drug to MUC1-positive cancer cells in vitro. *PLoS One* 6:e24077. doi: 10.1371/journal.pone.0024077

Zhang, S., Skinner, D., Joshi, P., Criado-Hidalgo, E., Yeh, Y. T., Lasheras, J. C., et al. (2019). Quantifying the mechanics of locomotion of the schistosome pathogen with respect to changes in its physical environment. *J. R. Soc. Interf.* 16, 2018–2675. doi: 10.1098/rsif.2018.0675

Zhang, W., Zhu, J., Song, X., Xu, Z., Xue, X., Chen, X., et al. (2015). An association of Aquaporin-4 with the immunoregulation of liver pathology in mice infected with *Schistosoma japonicum*. *Parasit. Vectors* 8:37. doi: 10.1186/s13071-015-0650-7

Zhong, C., Skelly, P. J., Leaffer, D., Cohn, R. G., Caulfield, J. P., and Shoemaker, C. B. (1995). Immunolocalization of a *Schistosoma mansoni* facilitated diffusion glucose transporter to the basal, but not the apical, membranes of the surface syncytium. *Parasitology* 110(Pt 4), 383–394. doi: 10.1017/s0031182000064726

Conflict of Interest: The authors declare that the research was conducted in the absence of any commercial or financial relationships that could be construed as a potential conflict of interest.

frontiers in Bioengineering and Biotechnology

REVIEW
published: 11 February 2020
doi: 10.3389/fbioe.2020.00048

The Design of Poly(lactide-co-glycolide) Nanocarriers for Medical Applications

*Divesha Essa, Pierre P. D. Kondiah, Yahya E. Choonara and Viness Pillay**

Wits Advanced Drug Delivery Platform, Department of Pharmacy and Pharmacology, School of Therapeutic Sciences, Faculty of Health Sciences, University of the Witwatersrand, Johannesburg, South Africa

Polymeric biomaterials have found widespread applications in nanomedicine, and poly(lactide-co-glycolide), (PLGA) in particular has been successfully implemented in numerous drug delivery formulations due to its synthetic malleability and biocompatibility. However, the need for preconception in these formulations is increasing, and this can be achieved by selection and elimination of design variables in order for these systems to be tailored for their specific applications. The starting materials and preparation methods have been shown to influence various parameters of PLGA-based nanocarriers and their implementation in drug delivery systems, while the implementation of computational simulations as a component of formulation studies can provide valuable information on their characteristics. This review provides a critical summary of the synthesis and applications of PLGA-based systems in bio-medicine and outlines experimental and computational design considerations of these systems.

Keywords: poly(lactide-co-glycolide), drug delivery, biodegradable polymer, nanoparticle preparation, nanomedicine, computational simulation

OPEN ACCESS

Edited by:
Gianni Ciofani,
Italian Institute of Technology (IIT), Italy

Reviewed by:
Daniele Di Mascolo,
Italian Institute of Technology (IIT), Italy
Jyothi U. Menon,
The University of Rhode Island, United States

***Correspondence:**
Viness Pillay
viness.pillay@wits.ac.za

Specialty section:
This article was submitted to Nanobiotechnology, a section of the journal Frontiers in Bioengineering and Biotechnology

Received: *08 October 2019*
Accepted: *22 January 2020*
Published: *11 February 2020*

Citation:
Essa D, Kondiah PPD, Choonara YE and Pillay V (2020) The Design of Poly(lactide-co-glycolide) Nanocarriers for Medical Applications. Front. Bioeng. Biotechnol. 8:48. doi: 10.3389/fbioe.2020.00048

INTRODUCTION

The design of novel delivery systems using nanomaterials has experienced substantial growth since the application of nanotechnology to biomedical applications established the field of nanomedicine. As a result of the ongoing discovery of numerous new pharmaceutically active compounds which have shown excellent efficacy but inadequate clinical translation, there is a growing need to fill the gap between the formulations available and their successful inclusion into active treatment. This has urged scientists to investigate alternate forms of delivery to the biological target in order to overcome the hurdles associated with conventional drug delivery, such as poor drug entrapment, inadequate bioavailability and pharmacokinetics, as well as systemic toxicity and side effects. These novel delivery systems all strive for the "magic bullet" effect (Bosch and Rosich, 2008) which is a vehicle that can form favorable interactions with a lipophilic or hydrophilic drug to facilitate high drug loading (Aravind et al., 2013; Bauer et al., 2016), can shield the drug from physiological conditions, deliver it to the biological target with minimal loss, and then can release it at the site in a sustained manner and at therapeutic concentrations (Al-Jamal et al., 2016; Almoustafa et al., 2017). Moreover, the carrier is ideally biodegradable, biocompatible and non-immunogenic, with low systemic toxicity (Alshamsan, 2014; Ananta et al., 2016). Nanomaterials are a befitting source to meet these requirements because they can be tailored to a vast range of sizes and shapes and can suit various delivery mechanisms, while the interactions between the carrier and the physiological medium can be controlled by adapting the surface properties

of the carrier (Kakkar et al., 2017). This has given rise to the widespread implementation of nanomaterials as pharmaceutical carriers for medical diagnostics and therapeutics (theranostics) (Berthet et al., 2017; Singh et al., 2019). Nanostructures can be fabricated from organic, inorganic, metallic or non-metallic sources. Examples include carbon nanotubes (Singh et al., 2013), dendrimers, liposomes, micelles, and solid lipid nanoparticles (Mishra et al., 2014; Lombardo et al., 2019).

Polymeric nanoparticles are commonly implemented as components of drug delivery systems and the use of synthetic polymers in particular can enable the design of carriers in a well-controlled and reproducible manner in order to suit the desired application (Lai et al., 2014). Polymer-based nanoparticles act as drug delivery vehicles by encapsulating the active agent inside its polymeric matrix, by conjugating to the agent or by adsorbing it onto the surface of the polymer (Mahapatro and Singh, 2011; Ansary et al., 2014). Polymers can be constructed to be linear, branched or globular and their size and their properties can be modulated by the choice of synthetic process (Panyam and Labhasetwar, 2012; Chen et al., 2013). Biodegradable polymers are suitable as nanocarriers as they often self-assemble and are easily sourced. Natural biodegradable polymers are chitosan (Ali and Ahmed, 2018), alginate (Jana et al., 2016) and inorganic ceramic hydroxyapatite composites (Turon et al., 2017). Synthetic polymers such as poly lactide-co-glycolide (PLGA) are an attractive alternative as they can be precisely engineered from monomers to suit the target and physiological environment they are intended for Middleton and Tipton (2000).

Poly lactide-co-glycolide has become ubiquitous in the biomedical field for many reasons. Firstly, it is a synthetic, biodegradable polymer that is easily broken down *in vivo* by hydrolysis into lactic acid and glycolic acid. These monomers are biocompatible and are physiologically metabolized by the tricarboxylic acid cycle for final excretion in the lungs (Semete et al., 2010; Sequeira et al., 2018), as shown by **Figure 1** (Sun et al., 2017). Hence, PLGA as a nanocarrier is considered to produce minimal systemic toxicity when used for biomedical applications (Kumari et al., 2010) and has been used in various formulations including membranes, sponges and gels (Sun et al., 2017).

The appeal of PLGA also lies in the fact that its properties can be manipulated and adapted to modify the encapsulation profile and drug release kinetics of the nanostructure to suit the desired application (Mittal et al., 2007). PLGA is overall a hydrophobic polymer and is therefore detected by the RES and if unmodified, is bound by phagocytes for elimination by the liver or spleen and eliminated before delivering its payload to the target site (Danhier et al., 2012). To circumvent this, surface modification of PLGA is necessary. One such modification is the coating of hydrophilic poly ethylene glycol (PEG) groups on the surface of PLGA to shield the hydrophobic end groups from the reticulo endothelial system (RES), resulting in an amphiphilic di-block co-polymer (Salmaso and Caliceti, 2013). Other polymers used as surface modifiers include chitosan (Lu et al., 2019), polaxamer and poloxamines (Redhead et al., 2001) which work by altering the electrostatic and hydrophobic surface properties of the PLGA block co-polymer. To increase the therapeutic efficacy, the surface of the PLGA nanocarrier can be decorated with targeting ligands such as small molecules, antibodies, and aptamers. These molecules selectively bind to receptors on the target cell and guide the vehicle to the site of action (Jahan et al., 2017). Targeting moieties such as aptamers, have been shown to increase retention time at the site of action (Dinarvand et al., 2011).

The use of PLGA in biomedicine dates back to the 1970s when it was used as a component of biodegradable sutures and implants. With the advent of nanomedicine, it has found application as nanocarrier in various areas of medical research, including chemotherapeutics, immunology, and biomechanics (Swider et al., 2018). Numerous studies have also reported successful applications in antibiotics, antiseptics, imaging, wound healing, and as nano scaffolds (Sharma et al., 2016). The suitability and adaptability of PLGA as a nanocarrier is illustrated by **Figure 2** (Mir et al., 2017).

Optimizing the synthetic procedure by changing the parameters can affect other properties of nanocarriers and therefore a great deal of forethought should go into the design of the system for the particular application (Rezvantalab et al., 2018). During synthesis, parameters such as particle size, surface behavior, degree of crystallinity, degradation rate, and molecular weight can be modified to adapt the nanocarrier for desired dosage and site specific action (Mittal et al., 2007). Bio-nano interactions are important considerations in design as they determine the suitability of the nanostructure for the intended application as well as the undesired toxicity that may result from the engineering process. Previous research has indicated accumulation of PLGA in the liver when used as nanocarriers and therefore there could be toxicity challenges caused by dose dumping (Makadia and Siegel, 2011). While there are numerous reviews on PLGA based nanodelivery systems in general, this work considers the literature from a design perspective. Schrur's nano-toxicology editorial states "few studies offer consistent results that are of value, and it is difficult to compare studies because they are often carried out using poorly characterized nanomaterials and arbitrary experimental conditions" (Schrurs and Lison, 2012). With these considerations in mind, *in silico* design, which is an expanding field in drug delivery, could be used to model numerous parameters, including polymer degradation, drug loading and toxicity and hereby provide insight into the structure-behavior relationships of PLGA-based nanocarriers (Ramezanpour et al., 2016). The aim of this review is to collate research on PLGA based delivery vehicles that have been studied for common medical applications, to compare the choices of starting materials and synthetic methods on the properties and functions of the final polymer-drug systems, and to explore how computational investigations can assist in the design of these systems.

PLGA AS A NANOCARRIER

Properties

Poly lactide-co-glycolide is synthesized from its constituent monomers (Sun et al., 2017) and can be obtained commercially in varying ratios of these monomers

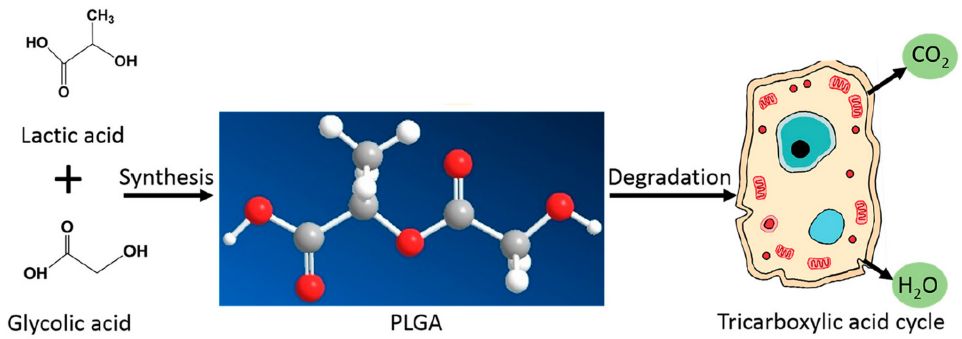

FIGURE 1 | The synthesis and physiological breakdown of PLGA, adapted from Sun et al. (2017).

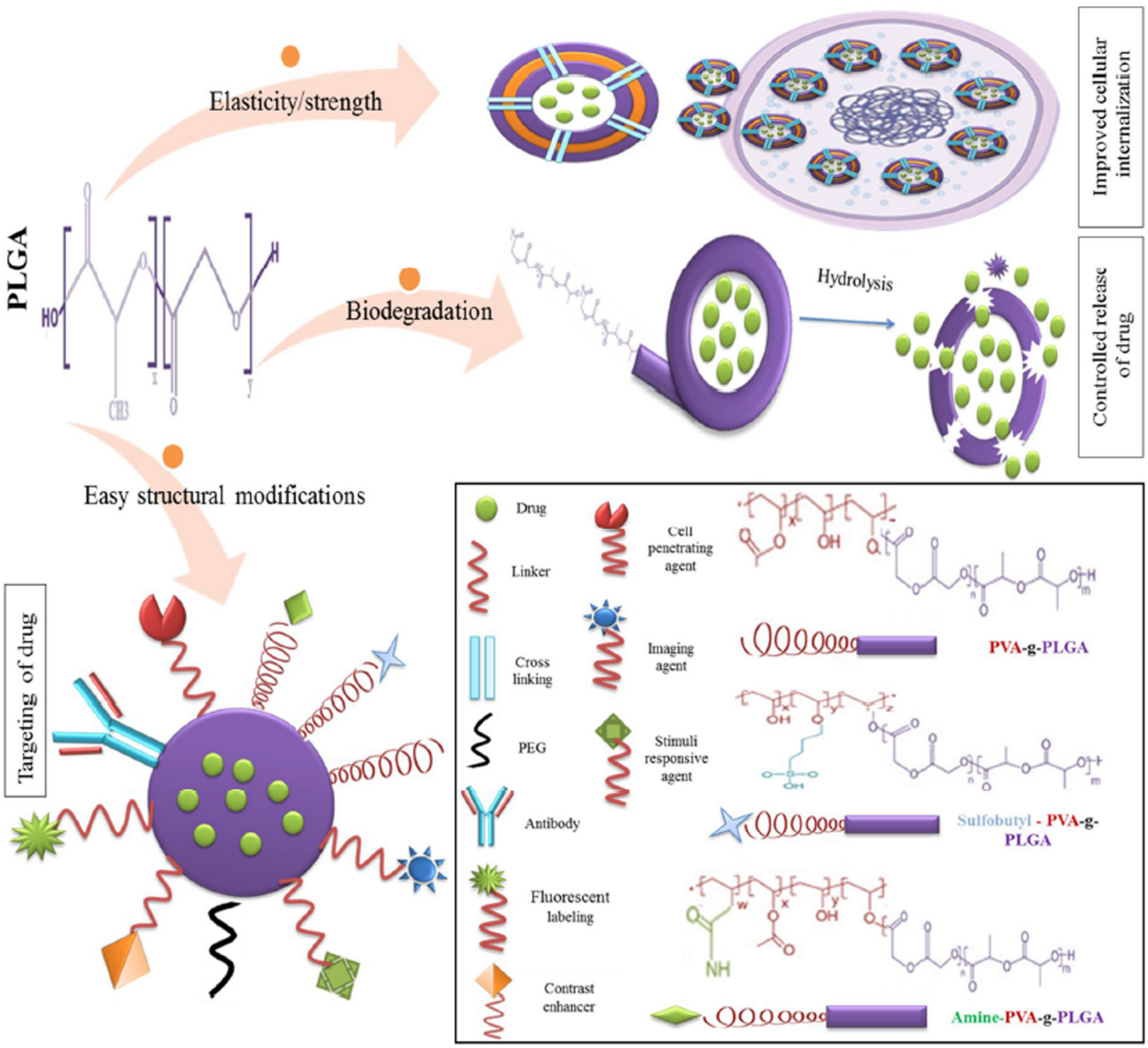

FIGURE 2 | Favorable characteristics of PLGA as a nano delivery system, reproduced from Mir et al. (2017).

(Sadat Tabatabaei Mirakabad et al., 2014). Each constituent has its own physical characteristics that it brings to the co-polymer. PLGA retains properties of both copolymers and can be customized using these properties, which are stiff, hydrophobic and slowly degrading lactic acid vs. malleable, less hydrophobic and faster degrading glycolic acid (Engineer et al., 2011). For example, poly-DL -lactic acid has a methyl group, as shown in **Figure 1**, and is therefore more hydrophobic than poly glycolic acid. Hence, adjusting the concentration of poly-lactic acid in PLGA varies the solubility of the final polymer (Makadia and Siegel, 2011). A study investigating the rate of hydrolysis of PLGA demonstrated that increasing glycolic acid to lactic acid ratio increases the hydrophilicity of the PLGA co-polymer and hence leads to faster degradation (Keles et al., 2015), while a separate study quantified the degradation constant to be 1.3 times higher for glycolic units than for lactic units in the PLGA co-polymers investigated (Vey et al., 2011). It has been shown that PLGA co polymer ratios can be varied to adapt the degradation rate from months to years (Sun et al., 2017). In general, the higher the glycolic acid content of the PLGA polymer, the more amorphous it is and the faster it degrades due to it being more hydrophilic. An exception is PLGA 50:50 lactic: glycolic units, which has exhibited the fastest degradation rate (Lü et al., 2009). It has been shown that increasing the glycolic acid ratio increases the wettability of PLGA for thin film applications (Ayyoob and Kim, 2018) and that increasing the lactic acid content has application in designing PLGA carriers for sustained release (Li, 1999). PLGA co-polymers with lactic acid content less than 70% have been characterized as amorphous and suitable for drug delivery applications (Habraken et al., 2006). As expected, the higher the molecular weight of PLGA, the more structural integrity it exhibits and the longer it has shown to degrade *in vivo* (Anderson and Shive, 2012). The PLGA co-polymer can be end-capped with different functional groups which have shown to affect the degradation kinetics of the delivery system. For example ester end-capped polymers exhibit a slower degradation rate than acid end-capped polymers and are therefore suitable for slower release applications (Gentile et al., 2014). Apart from degradation rate, it is also possible to control solubility and glass transition temperature of the PLGA system by varying the molecular weight, lactic/glycolic ratios, and end-cap functional groups of the starting material (Gentile et al., 2014).

Poly lactide-co-glycolide is also soluble in a variety of organic solvents including acetone, dichloromethane, chloroform, ethyl acetate, and THF (Sharma et al., 2016) and therefore is relatively simple to work with as carriers for both hydrophobic and hydrophilic drugs (Zhang et al., 2014).

Surface Functionalization

Shielding

In order to avoid elimination by the RES, a stealth coating around the hydrophobic PLGA nanoparticle surface has been achieved by incorporation of co-polymers with desired properties. The most frequently used co-polymer is polyethylene glycol (PEG) as it is biocompatible and easily grafted or adsorbed onto the surface of PLGA. The hydrophilic PEG shields the PLGA carrier from being taken up by opsonins (Vllasaliu et al., 2014) and it has been shown that the PEG shield dramatically increases the blood circulation half-life of the nanocarrier (Owens and Peppas, 2006). Some studies have shown that the nanoparticle *in vivo* residence time is dependent on the surface density of the PEG chains (Bertrand et al., 2017). PEGylation has also been associated with enhanced drug loading and tunable carrier degradation (Khalil et al., 2013). Chitosan, a natural polymer that is formed by partial deacetylation of chitin, is also commonly grafted onto the surface of PLGA based systems to increase biocompatibility. It is biodegradable and has mucoadhesive properties as it carries a positive charge and can efficiently bind to negatively charged cell membranes (Bruinsmann et al., 2019). Hence, a coating of chitosan on the PLGA nanostructure shields it from opsonins and promotes stronger cellular interaction and retention (Lima et al., 2018). Collagen is a highly hydrophilic protein that also increases cellular interaction and when blended with PLGA, can form a delivery system with superior hybrid properties such as increased biological compatibility and mechanical strength (Sadeghi-Avalshahr et al., 2017). Heparin, a biocompatible material that can be obtained both naturally and synthetically, has been used to impart specific binding properties to delivery systems when combined with polymers (Rodriguez-Torres et al., 2018). It is a sulfated glycosaminoglycan with high binding affinity for various growth factors and has been used in sustained delivery applications by immobilization on the surface of PLGA delivery systems (Chung et al., 2006).

Surfactants

One of the strategies employed in the nanofabrication process to increase colloidal stability is the use of surfactants. These are agents which usually have amphiphilic properties and reduce the interfacial tension between the hydrophobic and hydrophilic components, hence increasing miscibility and dispersion (Heinz et al., 2017) and preventing particle aggregation (Shkodra-Pula et al., 2019). A commonly used agent is polyvinyl alcohol (PVA), which is a hydrophilic polymeric surfactant that has been shown to decrease the size and increase the uniformity of PLGA nanocarriers, but is also associated with hypertension and central nervous system depression in animal studies (Menon et al., 2012). The use of Polysorbate 80, 60, and 20 has also shown increased residence time and enhanced permeation of the blood brain barrier (Sharma et al., 2016). However, it has shown in some cases to cause anaphylactoid reactions (Coors et al., 2005) and long-term infertility (Gajdova et al., 1993). Polaxamer is a thermo-reversible, non-toxic coating that has been used when encapsulating hydrophobic drugs and has been shown to preferentially target cancer cells. However, it has shown rapid erosion times and it is associated with hyperlipidemia and hypercholesterolemia (Miller and Drabik, 1984). Poloxamine is an amphiphilic block co-polymer and therefore has been used to stabilize hydrophobic drugs while increasing circulatory residence time (Alvarez-Lorenzo et al., 2010). Vitamin E TGPS is a water-soluble form of vitamin E and is used as a solubilizing and emulsifying agent in nano drug delivery. It is commonly used to enhance drug loading (Zhang and Feng, 2006) and nanoparticle degradation rates (Jalali et al., 2011).

Active Targeting

In active targeting, the surface of the nanoparticle is further decorated with ligands that specifically bind to receptors on the cells of interest and enables the carrier to enter the cell by receptor mediated endocytosis (Muhamad et al., 2018). These targeted delivery systems are designed to localize drug release at the disease site (Danhier et al., 2010). There are various different kinds of targeting ligands such as small molecules, peptides, antibodies, aptamers and polysaccharides, as shown in **Figure 3** (Yoo et al., 2019). These ligands can be either conjugated or adsorbed onto the surface of the nanocarrier after formation or can be linked to one of the components of the carrier before nanoparticle formation (Yoo et al., 2019). It has been shown that increasing the conjugation density of targeting ligands has an effect on the targeting ability of the nanocarrier.

Monoclonal antibodies have had a long history as targeting ligands (Friedman et al., 2013) since they have complementarity determining regions that enable them to bind to receptors on cell surfaces with high specificity and affinity (Carter et al., 2016). However, since they are large molecules, their conjugation density capacity on the nanocarrier is substantially decreased (Yoo et al., 2019) compared to other ligands, and furthermore, they raise immunogenicity concerns (Karra and Benita, 2012). Compared to antibodies, peptides have the advantage of smaller size and non-immunogenicity but they still are able to retain target specificity (Zhao et al., 2007). Aptamers are short strands of nucleic acids that can be synthetically designed to bind specific biological targets. They are non-immunogenic and non-toxic but their synthesis can be costly (Friedman et al., 2013). Despite their advantages for *in vivo* targeting, both peptides and aptamers are prone to enzymatic degradation (Yoo et al., 2019). Polysaccharides are advantageous because they are biocompatible and can be used as structural components of the nanocarrier (Choi et al., 2011) as well as to target carbohydrate binding receptors on cell surfaces. However, some polysaccharides could have solubility challenges and modification of the carbohydrate structure could result in unintended toxicity (Peng et al., 2018). Small molecules form a class of targeting ligands that comprise of synthetic compounds that are designed to target certain domains on cell surface receptors. They are usually chosen because of ease and control of synthesis but they often do not bind with high specificity and some target receptors can be expressed in healthy cells (Yoo et al., 2019), resulting in unintentional cell binding. Even though active targeting strategies provide an attractive avenue for site specific drug delivery, there are many challenges in this area, such as receptor accessibility and off-target binding. Particularly during different stages of tumor development, certain receptors can be up or down regulated, which provides an additional challenge for the use of targeting ligands in chemotherapeutic drug delivery (Vhora et al., 2014).

Toxicity

Despite biocompatibility and biodegradability of PLGA as a polymer, its toxicological profile in nanoformulations deserves to be investigated because of altered physicochemical properties, such as higher surface area to mass ratios. Furthermore, reports have suggested that particles of any material may acquire unique toxicological properties in the nanoscale

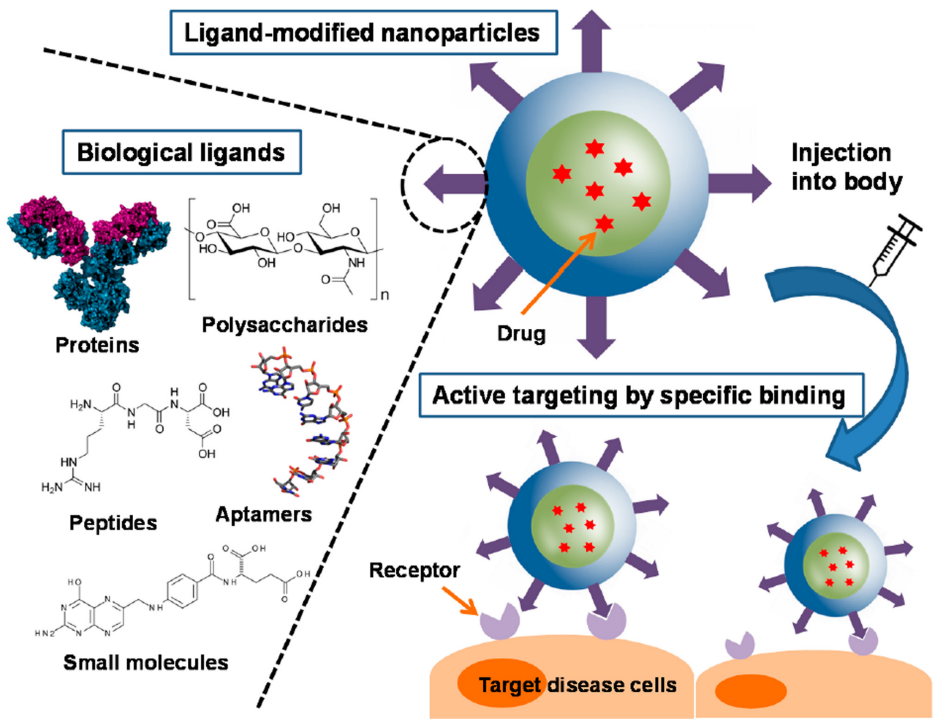

FIGURE 3 | Surface functionalized PLGA nanoparticles for active targeting and cellular binding reproduced from Yoo et al. (2019).

(Makadia and Siegel, 2011). Different effects such as acute toxicity, repeated dose toxicity, inflammation, oxidative stress, genotoxicity, and reproductive system toxicity of PLGA nanocarriers have been examined in order to obtain information on the possible risks of these materials in pharmaceutical preparations. A study of danorubicin loaded PEG-PLL-PLGA nanoparticles has described some toxicity in Kunming mice (Guo et al., 2015) but since no results were reported for blank nanoparticles, it is unclear whether the toxicity was due to the drug or nanocarrier (Jesus et al., 2019). Regarding oxidative stress, studies have reported an overall increase in the production of reactive oxidative species corresponding to increasing concentrations of the PLGA nanoformulations tested (Singh and Ramarao, 2013; Grabowski et al., 2015) and another study demonstrated mild inflammatory properties of different PLGA formulations (Grabowski et al., 2016). Several studies have confirmed no genotoxicity (Tulinska et al., 2015; Platel et al., 2016), no toxicity on reproduction (Chen et al., 2017; Sharma et al., 2017) and no hemolysis (Chen et al., 2017). A study comparing the toxicity of PLGA nanoparticles to silica-, iron-, and zinc-based nanoparticles showed that the PLGA system had no appreciable adverse *in vitro* or *in vivo* toxicological outcomes, and did not produce the toxicity commonly associated with the inorganic nanomaterials (Semete et al., 2010).

SYNTHETIC METHODS OF PLGA NANOCARRIERS

Poly lactide-co-glycolide nanocarriers may be fabricated by different methods and the choice of method has shown to affect properties such as particle size, colloidal stability, drug loading/encapsulation efficiency, and release behavior of the final product (Swider et al., 2018). Depending on the process of preparation, the structural organization may also be different. The drug is either encapsulated inside the carrier or adsorbed on the surface (Danhier et al., 2012). There are several methods that can be employed for the preparation of PLGA nanocarriers, and the following provides a brief overview on both the well-established and relatively recently developed techniques. The traditional methods based on emulsions are illustrated by **Figure 4** (Ding and Zhu, 2018).

Single and Double Emulsion

The emulsion methods have been the most frequently used methods of synthesis and they are suitable for a wide range of drugs with varying solubilities (Wang et al., 2016). The single emulsion (oil in water or O/W) method is suitable for hydrophobic drugs. PLGA and the drug is dissolved in a small volume of suitable volatile organic solvent and added dropwise to the aqueous phase containing a stabilizer, usually PVA. The mixture is sometimes sonicated and then stirred, often under sheer stress for a fixed amount of time to allow the organic solvent to evaporate. The double emulsion method is used when the active agent to be entrapped is hydrophilic, such as proteins and peptides. The active is dissolved in an aqueous phase and then added to PLGA which is dissolved in the organic phase, and this

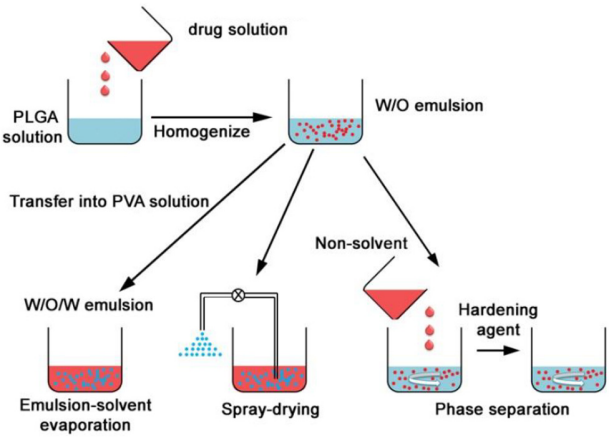

FIGURE 4 | Formation of PLGA nanoparticles by double (W/O/W) emulsion, spray drying and phase separation (coacervation) methods, adapted from Ding and Zhu (2018).

forms a primary water in oil (W/O) emulsion. This is then added to another aqueous phase containing a stabilizer and allowed to mix under stress, allowing the organic solvent to evaporate. The nanoparticles are therefore formed by a water in oil in water (W/O/W) emulsion (Makadia and Siegel, 2011). The product is isolated by centrifugation or ultrafiltration and washed to remove unreacted products. Thereafter it is freeze dried and can be stable for several months to years. Recently, a single emulsion method was used to successfully entrap proteins for vaccine application (Ospina-Villa et al., 2019) and a PLGA-PEG nanocarrier was formulated using the double emulsion method for intraperitoneal insulin delivery (Haggag et al., 2018). The emulsion methods can be adjusted by changing the drug to PLGA ratio, the organic solvent, the stabilizer concentration in the aqueous phase and the stirring speed and can hereby be adapted to control the size range of the nanocarriers to some extent. However, there are often batch to batch variation with these methods and the carriers prepared by this method for protein-based drugs have limited stability due to degradation of proteins at the aqueous interface and the sheer stress of homogenization leading to unfolding of the protein sheets (Ding and Zhu, 2018).

Spray Drying

This method involves the preparation of water in oil or solid in oil emulsions, which are sprayed in a thin stream of heated air. The type of drug (hydrophilic or hydrophobic) would determine the solvent used in the emulsion (Makadia and Siegel, 2011). Recently, spray drying was used in the preparation of a PLGA nanoformulation for sustained treatment of tuberculosis (TB) (Kalombo et al., 2019) and in the fabrication of a carrier for antibiotic coating of dental implants (Baghdan et al., 2019). This method is highly advantageous because it is suitable for hydrophobic and hydrophilic drugs and can be used for sensitive compounds since the conditions are mild. It is also a rapid method (Nie et al., 2008) which can be suitable for industrial scale-up due to the minimal processing parameters

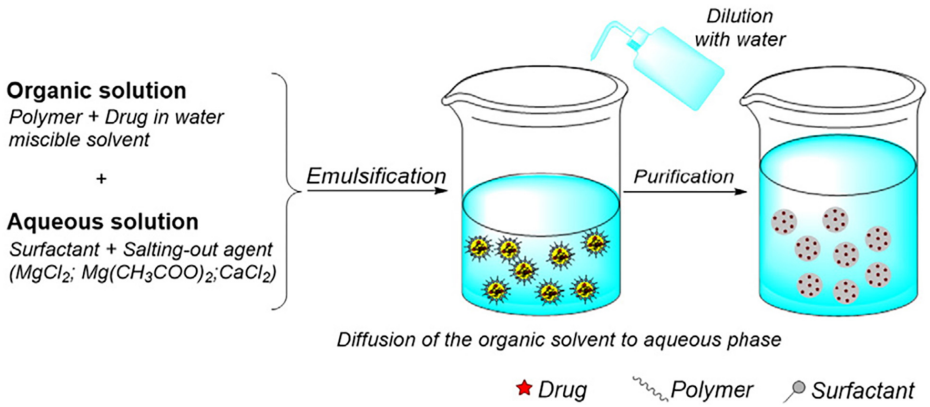

FIGURE 5 | Illustration of the salting out method of preparation, reproduced from Crucho and Barros (2017).

involved (Ding and Zhu, 2018). The main drawback of this technique is the wastage caused by inaccessible product that adheres to the inside of the nanosprayer (Wang et al., 2016). Parameters such as orientation of jets, temperature, and solvent choice can all affect the properties of the final nanoparticles (Berkland et al., 2004).

Coacervation

With coacervation or phase separation, the polymer and drug are prepared as O/W for hydrophobic drugs and W/O/W for hydrophilic drugs, and then a non-solvent, e.g., silicon oil is added dropwise under stirring (Verma et al., 2018). This reduces the solubility of PLGA in the organic solvent and results in the formation of a polymer-rich phase in which PLGA surrounds the drug molecules to form microdroplets (coacervates). These are rapidly quenched in a non-soluble medium to form the solid product (Wang et al., 2016). Parameters such as starting polymer, solvent choice, stirring rate and temperature can be varied to control the properties of the particles. Coacervation usually forms micrometer sized particles (Sharma et al., 2016) but has been used in protein nanoparticle preparation (Verma et al., 2018).

Salting Out

In the salting out method, drug and PLGA are dissolved in a miscible organic solvent and added to the aqueous phase containing stabilizer and a salt under sheer mechanical force. The salt usually used is magnesium chloride hexahydrate or magnesium acetate tetrahydrate (Wang et al., 2016) and is used at a ratio of 1:3 PLGA:salt (Eley et al., 2004). Upon addition of water, the organic solvent diffuses into the aqueous phase, causing the formation of PLGA-drug nanoparticles, illustrated by **Figure 5** (Crucho and Barros, 2017). This method is not suitable for lipophilic drugs and can be time intensive since isolation of the product involves several washing steps to remove reagents. However, it would suit drugs which are very temperature sensitive since heat is not required (Nagavarma et al., 2012). This method is robust and is suitable for nanoparticles with high polymer concentrations since the size of the particle is not generally affected by the amount of polymer (Swider et al., 2018).

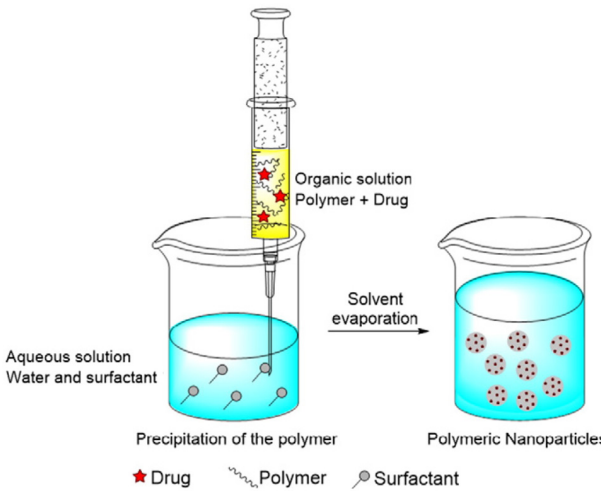

FIGURE 6 | The nanoprecipitation method, adapted from Crucho and Barros (2017).

Nanoprecipitation

In this method, PLGA and the drug is dissolved in a polar, water miscible solvent and added dropwise to the aqueous phase, which may contain a surfactant. The product is formed by rapid diffusion of the water miscible solvent into the aqueous phase, resulting in precipitation of the PLGA-drug nanoparticles, as shown in **Figure 6** (Crucho and Barros, 2017). The properties of the nanocarrier are controlled by PLGA content and molecular weight, PLGA to drug ratio and choice of solvent (Wang et al., 2016). Recently, an optimized nanoprecipitation method was developed for the preparation of PLGA encapsulated alendronate sodium, a drug for osteoporosis (Oz et al., 2019) and a modified procedure was reported for a PLGA hybrid nanocarrier for simvastatin (Zhang et al., 2018). Nanoprecipitation can be used to prepare particles in the 100 nm size range and is advantageous because of the absence of shear stress (Fessi et al., 1989). However, the unmodified nanoprecipitation method does not

usually work well for hydrophilic drugs as they do not form favorable interactions with PLGA in a water miscible solvent (Govender et al., 1999).

Supercritical Fluid Technology

Supercritical fluid technology, illustrated by **Figure 7** (Jog and Burgess, 2017), can provide an environmentally friendly method of generating nanoparticles since it reduces, and in some cases, eliminates the use of organic solvents (Koushik and Kompella, 2004). In this method, the polymer and drug are dissolved in a supercritical fluid which is then rapidly expanded and depressurized. The resultant mixture is then passed through a fine nozzle or capillary, resulting in supersaturation and formation of nanoparticles, which are collected separately (Mishima, 2008). This is an attractive method as it is highly tunable but the kind of nanoparticle products are restricted since not all starting materials are compatible with the supercritical fluid (Soh and Lee, 2019).

Microfluidics

The area of microfluidics deals with channels of the micrometer size range that are used to control and manipulate the movement of volumes of fluid from the nanolitre size range and below. When working at the nanoscale, the conditions of flow can be precisely controlled and constant laminar flow is maintained, which is impossible when conducting reactions at the macroscale level (Chiesa et al., 2018). Therefore this technique has lent itself to the synthesis of nanoparticles by the formation of emulsions using droplet microfluidics. In this method, the polymer and drug are combined and the emulsion is formed in the microfluidic mixer, which can have different channel architechtures (Collins et al., 2015). The most commonly used geometries for droplet based PLGA nanoparticle formation are the t-junction, flow focusing, and continuous flow microchannels, as shown in **Figure 8I** (Shembekar et al., 2016). In the t-junction geometry, channels are perpendicular to each other. The dispersed phase (aqueous) flows through one channel while the continuous phase (oil) flows through the other and droplets are formed at the junction. In the flow focusing system, the aqueous phase flows through a square capillary where shear force is provided on either side of it by the flow of the oil phase. The emulsion then flows through a narrow capillary and droplets are formed in a collection chamber. With continuous flow geometry channels, the aqueous phase flows through a capillary that resides in another capillary through which the oil flows in the same direction. Droplets begin to form once the two phases mix (Shembekar et al., 2016). SEM images of particles formed by this method are shown in **Figures 8II-D,E** (Xu et al., 2009).

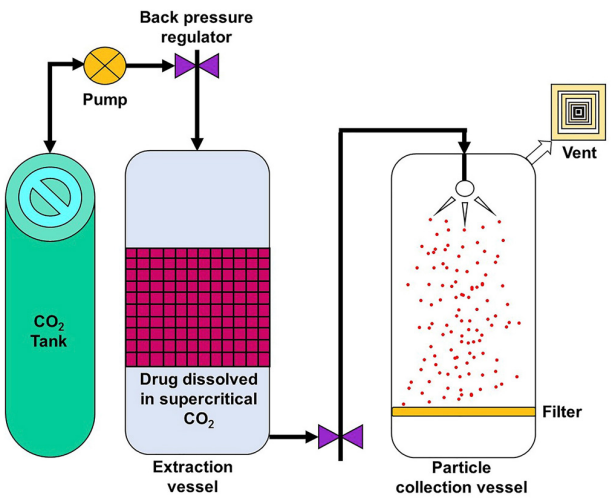

FIGURE 7 | Simple setup of a supercritical fluid technology method, reproduced from Jog and Burgess (2017).

These microchannels are used for O/W emulsions, but can be adapted for double (W/O/W) emulsions by using a combination of channels. Recently, a microfluidics method was developed for the encapsulation of cell penetrating peptides (Streck et al., 2019) and targeted delivery of taxanes (Martins and Sarmento, 2020). There are numerous advantages of microfluidics for nanoparticle synthesis. With this technique, the chemical composition of the final product can be preselected according to the desired application. The synthetic parameters can be controlled to the extent that there is a much larger particle size homogeneity compared to bulk methods, and there are also smaller volumes of solvent needed. However, the scale of nanoparticle production is limited and the microchannels are also susceptible to blockage and contamination. The time and temperature of mixing, flow rate, choice of solvents and payload type determine the properties of the final nanoparticles (Kim K.T. et al., 2019).

Membrane Extrusion Emulsification

With this technique, single or double emulsions of PLGA and drug are either initially prepared or formed when extruded through a membrane of predetermined pore size. There are two ways to do this – direct and pre-mix membrane extrusion (ME), as illustrated by **Figure 9A** (Guo et al., 2018), and a characteristic emulsion is shown in **Figure 9B**. In direct ME, the membrane emulsifies the dispersed phase into nanosized droplets, while in premix ME, the emulsion is formed via a conventional method and thereafter extruded through the membrane, which downsizes the coarse emulsion into uniform nanosized droplets. This method can be used for hydrophobic or hydrophilic drugs and is advantageous because the size of product can be controlled by varying the nanoporous membrane pore size to create particles of required dimensions, resulting in a large size homogeneity. Premix ME in particular has been shown to have a higher uniformity in dispersity of final nanoparticles as shown by **Figure 9C**, compared to direct ME. In general, it is a mild procedure with low energy requirements and can be easily scaled up. However, it is not suitable for emulsions with high viscosity (Guo et al., 2018).

Nanoimprint Lithography and the PRINT Technique

Nanoimprint lithography is used to form nanoparticles from a nanostructure template that is placed over a layer of precursor

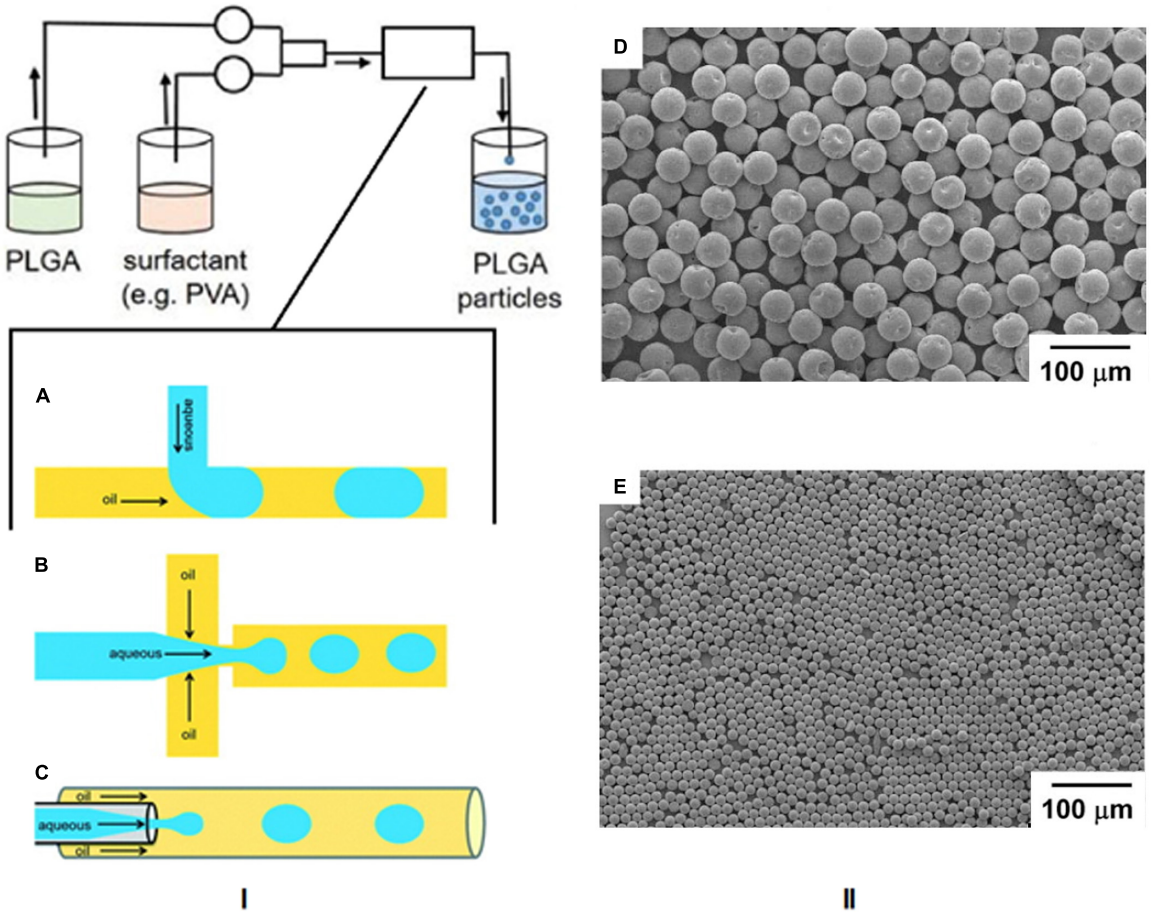

FIGURE 8 | (I) Schematic of the microfluidics method and the three most common microchannel geometries. **(A)** T junction, **(B)** flow focusing, **(C)** continuous flow. Reproduced from Shembekar et al. (2016)-published by the Royal Society of Chemistry. **(II-D,E)** SEM images of PLGA particles formed by this technique, adapted from Xu et al. (2009).

material which is heated to above the glass transition temperature of the polymer. Thereby, the malleable precursor material is molded into the desired size and shape, which is retained upon cooling. The template is then removed, leaving the product on the substrate base. Su et al. (2015) have successfully used this method for the nanofabrication of submicron PLGA grooves for the control of the length and direction of retraction fibers during cell division. The major drawback of this method is the residual interconnecting layer on the substrate base that prevents the formation of isolated nanostructures (Fu et al., 2018). The PRINT (particle replication in non-wetting template) technique involves the preparation of the PLGA-drug solution matrix and casting it on a delivering sheet. Thereafter a mold with nanosized cavities is placed over the delivering tray and it is passed through a nip and separated so that the polymeric material fills the mold cavities. The particles are then solidified and placed on a high energy adhesive layer and passed through the nip without separation. After the mold is removed, the nanoparticles are collected by washing with a solvent that dissolves the adhesive (Perry et al., 2011). The method is automated with a high degree of control over the individual parameters, and can be used for a wide variety of cargos including hydrophobic and hydrophilic drugs, vaccines, and proteins. However, it is a multistep process that can be labor intensive (Swider et al., 2018). The desired particle size, surface properties and composition can be preset and controlled in the initial step. The PRINT process is illustrated in **Figure 10** (Perry et al., 2011), while **Figure 11** shows SEM micrographs of the different shapes of PLGA nanoparticles that have been prepared by this method. Enlow and colleagues have reported the PRINT process whereby PLGA micro- and nanoparticles were prepared, with cylindrical, spherical, ridged, and fenestrated morphologies. These particles demonstrated > 40% drug loading and > 90% encapsulation efficiencies of docetaxel (Enlow et al., 2011).

MEDICAL APPLICATIONS

Cancer Research

Actively Targeted Chemotherapeutics

In the United States of America alone, 1,762,450 new cancer diagnoses and 606,880 cancer related deaths are expected to occur in 2019 Siegel et al. (2019). Despite the ubiquity of this

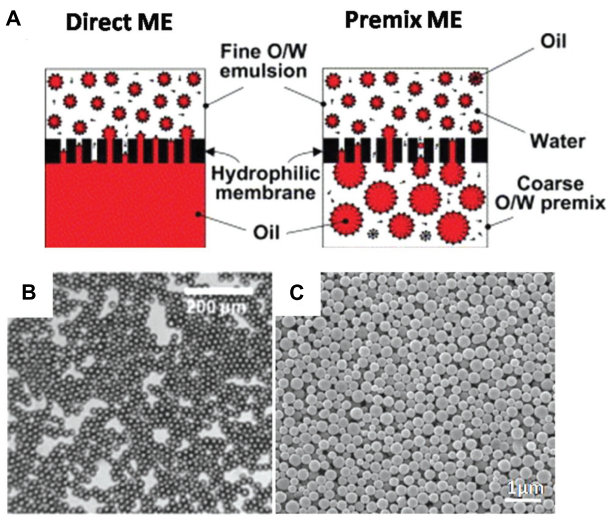

FIGURE 9 | (A) Direct- and premix- two common processes using membrane extrusion (ME). **(B)** SEM image of an emulsion formed by this method **(C)** SEM images of nanoparticles formed by premix ME, reproduced from Guo et al. (2018).

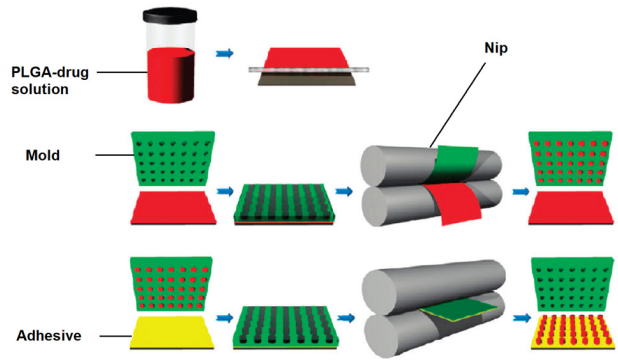

FIGURE 10 | Schematic showing PRINT procedure, reprinted with permission from Perry et al. (2011). Copyright (2019). American Chemical Society.

disease, treatment options are challenging due to the complex pathology of the different cancers. Current chemotherapy often leaves debilitating and life altering side effects since most drugs on the market that target the rapidly dividing cancer cells also inadvertently damage cells that are vital for normal life processes (Rizvi and Saleh, 2018). Actively targeting PLGA nanoparticles are able to circumvent this; Moku et al. (2019) have shown increased drug loading and efficacy against lung cancer by using transactivator of transcription (TAT) peptide ligands to target mesenchymal stem cells while Ganipineni et al. (2019) found that magnetically targeted paclitaxel- and SPIO-loaded PLGA-based nanoparticles effected increased cellular uptake in glioblastoma cells compared to the non-targeted carriers. Another type of nanoparticle targeting is the use of 'smart' carriers that are engineered to respond to a stimulus (Kapoor et al., 2015). Recently, a pH dependent aptamer functionalized PLGA nanocarrier system was reported to increase anti-cancer activity of doxorubicin to human lung cancer cells, with reduced toxicity to healthy cells (Saravanakumar et al., 2019) and a superparamagnetic iron oxide encapsulated nanocarrier

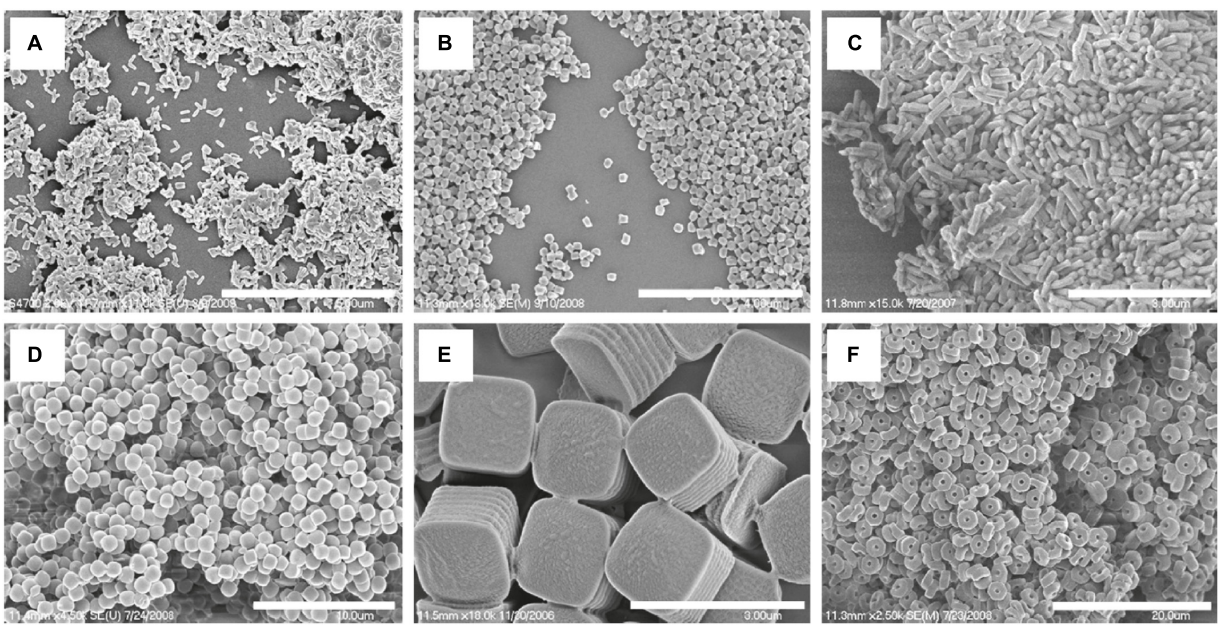

FIGURE 11 | SEM Images of PLGA PRINT particles. **(A–C)** Cylinders of different dimensions. **(D)** Spheres; **(E)** ridged cubes; (**F**, bottom right) particles with center fenestrations, reprinted with permission from Enlow et al. (2011). Copyright (2019) American Chemical Society.

for docetaxel demonstrated favorable pharmacokinetics and a greater degree of uptake in breast cancer cells (Panda et al., 2019).

Immunotherapy

Since Allison and Honjo were awarded the 2018 Nobel prize in Physiology and Medicine "for their discovery of cancer therapy by inhibition of negative immune regulation" (Guo, 2018), the area of nanomedical research into cancer immunotherapy has received substantial attention. This approach involves the use of pharmaceutical agents to activate a patient's immune system to fight cancers as opposed to traditional chemotherapy which involves directly drugging the cancer cells (Khalil et al., 2016). Chen et al. (2016) have described PLGA nanocarriers equipped with an immunostimulant and photothermal agent, and this formulation showed increased activation of the immune system of BALB mice compared to the free agent. More recently a sustained controlled release PLGA nanosystem was developed to activate the anti-tumor immune response in mice bearing melanoma and colon cancer (Yin, 2019) and a PLGA system containing an immune adjuvant together with an enzyme that increased the efficacy of radiation therapy demonstrated the feasibility of combination immunotherapy and targeted radiotherapy in BALB mice (Chen et al., 2019).

Imaging and Diagnostics

Poly lactide-co-glycolide has applications for tumor diagnostics as it is able to deliver imaging agents to cancer cells with specificity and controlled biodistribution. Advances in nanotheranostics, which is the incorporation of imaging and therapeutic agents in one nanocarrier, have shown promise for real time imaging throughout a patient's treatment course (Chapman et al., 2013). A novel theranostic PLGA nanocarrier with a near infrared imaging agent, further decorated with gold nanoparticles has been synthesized and shown to have increased activity and photodynamic properties in tumor grafted BALB mice (Xi et al., 2018) and a targeted PLGA-based nanobubble was designed with an ultrasound contrast agent, and demonstrated specificity and imaging capabilities to breast cancer in BALB mice (Du et al., 2018). More recently an image guided photothermal PLGA nanocarrier for doxorubicin showed promise for real time photoacoustic imaging in tumor bearing nude mice (Shen et al., 2019) and a near infra-red dye loaded PEGylated PLGA nanocarrier was also able to provide information on the circulation and distribution of the nanoparticles in nude mice (Kumar et al., 2019).

HIV Treatment

The delivery of anti-retro viral drugs faces many of the general limitations of conventional drug delivery and therefore biomaterials with low toxicity such as PLGA based nanocarriers are being implemented in formulations to treat HIV. Mannosylated PLGA nanoparticle carriers have shown promise for targeted delivery of anti-retro viral drugs to the brain (Patel et al., 2018) and the use of microfluidics technology enabled the novel synthesis of efiravine loaded PLGA nanoparticles (Martins et al., 2019). A recent study reported a PLGA based nanocarrier for the combination of the anti-retro virals griffithsin and dapirivine which showed a long acting treatment profile (Yang et al., 2019) and a separate proof of concept study showed promise for a long acting bictegravir encapsulated PLGA nanocarrier (Mandal et al., 2019).

Inflammatory Disorders

Many current treatments have proven to be inadequate at treating or alleviating symptoms of inflammation. The specific delivery of anti-inflammatory agents to the target site could potentially increase their therapeutic concentration in the inflamed tissue with reduced side effects (Gendelman et al., 2015), and the use of PLGA is particularly suitable to this application because of its favorable biodegradability and non-immunogenicity (Lamprecht et al., 2001). Davoudi et al. (2018) described a carrier within a carrier system using intestinal organoids to transport 5-ASA encapsulated PLGA nanoparticle to treat inflammatory bowel disease, and Perreira's research involved the development of a metformin loaded nanoformulation that showed efficacy against periodontal inflammation in diabetic rats (Pereira et al., 2018). Gholizadeh et al. (2018) have formulated a dactolisib-PLGA nanoparticle that showed activity against inflamed endothelial cells and more recently, Yang (2019) group reported the synthesis of a crocetin-loaded nanoparticles that reduced the level of pro-inflammatory cytokines in renal tissue and therefore shows potential for the treatment of diabetes induced nephropathy.

Other Applications

Poly lactide-co-glycolide has been adapted to treat conditions in many fields of biomedicine, as shown by **Figure 12** (Mir et al., 2017). A hyaluronic acid functionalized PLGA based nanocarrier for methatrexate has been developed for targeted treatment of rheumatoid arthritis (Trujillo-Nolasco et al., 2019), a PLGA nanoparticle with protease inhibitor has shown to overcome gastro-intestinal limitations of oral insulin delivery in rats (Faheem et al., 2019), a PLGA-chitosan based nanocarrier has been synthesized and shown to be selective for human antigen presenting cells (Durán et al., 2019), a potential DNA vaccine delivery system has been designed using a PLGA based nanocarrier (Besumbes et al., 2019), and a Vitamin D encapsulated PLGA based delivery system has recently shown activity against various markers for Alzheimer's disease in mice (Jeon et al., 2019). Gonzalez-Pizarro et al. (2018) have prepared an optimized fluoromethalone-PLGA nanoparticle that demonstrated increased efficacy in treating ocular inflammation compared to the commercial formula. The use of some of the available methods in PLGA nanocarrier synthesis and their applications are summarized in **Table 1**.

Inclusion of PLGA Formulations in the Clinic

The biocompatibility, biodegradability and versatility of PLGA has made it suitable for a wide range of clinical applications. PLGA was commercialized in the 1970s as a suture material under the trade name Vicryl® (Kamaly et al., 2016). Other sutures include Dolphin Sutures®, and Polysorb® which are both currently approved. PLGA-containing chemotherapeutic

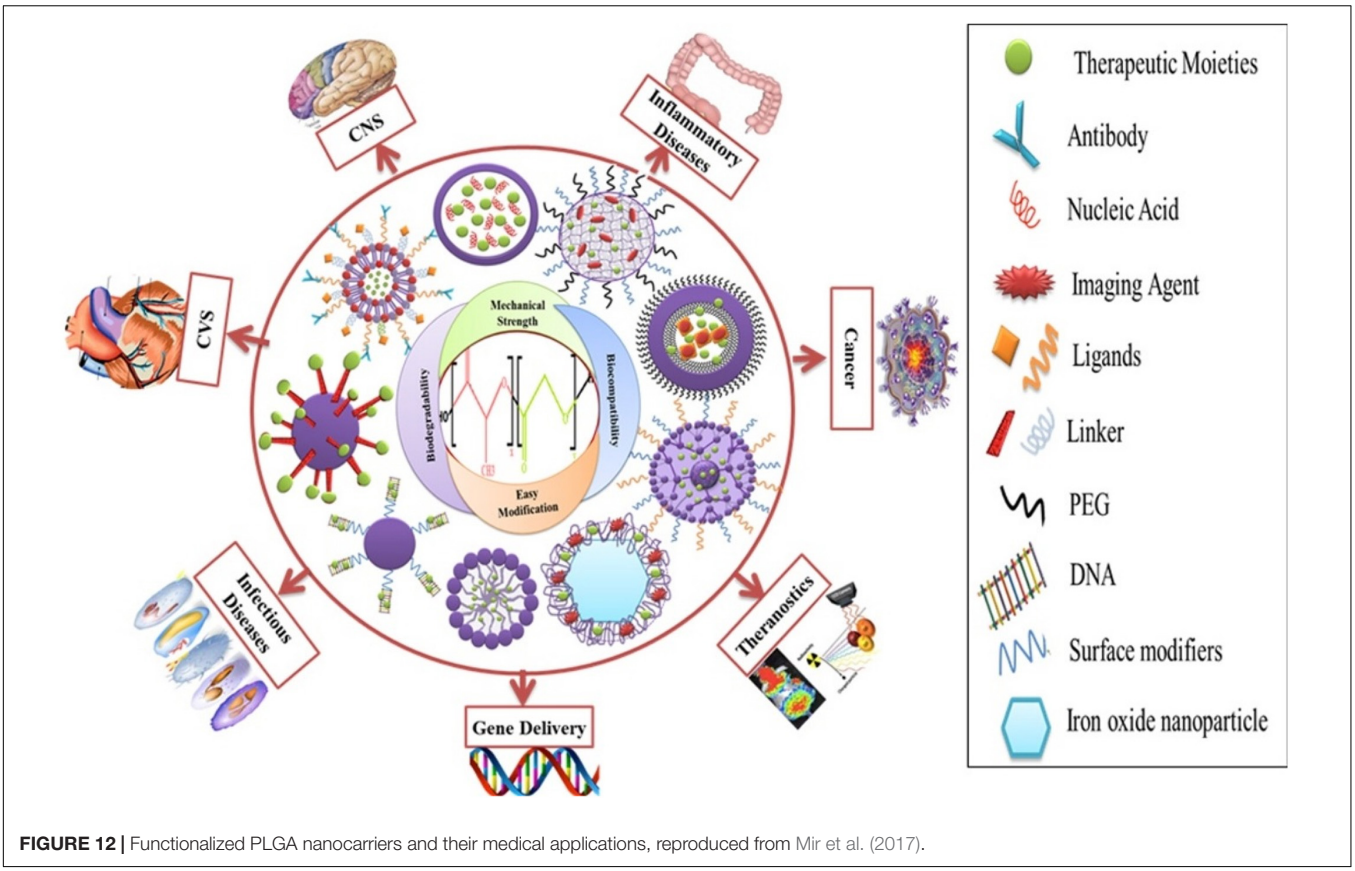

FIGURE 12 | Functionalized PLGA nanocarriers and their medical applications, reproduced from Mir et al. (2017).

formulations approved for clinical use include Lupron Depot®, for sustained release of leuprolide, which has application in the management of prostate cancer (Swider et al., 2018), Trelstar®, a triptorelin-containing suspension for the treatment of prostate cancer and Zoladex, a goserelin-containing implant used in the treatment of breast and prostate cancer and endometriosis. Formulations approved for other applications include Risperdal® Consta®(risperidone), Vivitrol®(naltrexone) and Arestin®(minocycline) for the treatment of schizophrenia, opioid dependence and periodontal disease respectively (Jain et al., 2016). A promising direction for clinical development is the engineering of PLGA based systems with imaging agents to monitor disease progress and/or relapse patterns using magnetic resonance imaging (MRI). Studies have shown these structures to be non-invasive and cost effective, with excellent safety profiles (Strohbehn et al., 2015). Furthermore, there are a number of PLGA based systems have been used in clinical trials that are ongoing or have been recently concluded (U.S. National Library of Medicine, 2019).

COMPUTATIONAL MODELING

Despite the numerous formulations and methods available for PLGA synthesis, there is a large discrepancy between *in vitro*, *in vivo* and clinical results. One of the reasons for this could be the fact that it is difficult to obtain mechanistic insight into nano-formulation behavior in the various systems by evaluation of results based solely on experimental methods (Huynh et al., 2012). Because of the ubiquity of PLGA across so many biomedical fields of research, there is an abundance of data at our fingertips for computational modeling (*in silico*). There are various levels of detail that can be used in computational simulations. The approach used most widely for nanoparticle drug delivery systems is molecular dynamics (MDs). This technique uses the motion of the molecules in the system to predict its behavior. The parameters it uses are the bonds, bond angles and dihedrals, and here the atoms are treated as point charges. If the degree of detail of atomistic interaction is not required, a coarse grained (CG) model can be used. Here, atoms are grouped into molecular fragments and their behavior in the system is modeled (Frenkel and Smit, 2001). Density functional theory is a model based on electronic density around atoms in the system and measures these interactions within the system of interest (Geerlings et al., 2003). Computational simulations at these levels can give insight into polymer interactions, drug-carrier miscibility, drug loading, drug release, and complex stability (Ramezanpour et al., 2016). Mathematical modeling such as finite element analysis and computational flow dynamics are particular useful when studying polymeric nanoparticle formation (Lince et al., 2011), diffusion and degradation (Kojic et al., 2017). Hence, coupled with experimental methods, they can be powerful tools in the rational design of PLGA nanocarriers for biomedical applications. A study of PLGA

TABLE 1 | Properties of some prepared PLGA nanocarriers, their methods of formation and biological targets.

Type of nanocarrier	Route of administration	LA:GA in PLGA	Mw of PLGA	Synthetic Method	Particle size range	Medical application	References
PLGA nanoparticle embedded in a microsphere	Inhalation	50:50	38.5 K	Single emulsion	~200 nm	Lung cancer treatment	Guo et al., 2014
PLGA-HDL hybrid nanoparticle	Injectable	50:50	30–60 K	Microfluidics	~100 nm	Cardiovascular disease treatment	Sanchez-Gaytan et al., 2015
Dye loaded PLGA nanoparticles	Intravenous	50:50	13.5 K	Spray drying	~500 nm	Photoacoustic imaging	Kohl et al., 2011
Paclitaxel loaded PLGA nanoparticle	Injectable	75:25	694 K	Membrane extrusion	~300 nm	Malignant melanoma treatment	Liang et al., 2013
Insulin loaded plga nanoparticle	Oral	50:50	10 K	Nano precipitation	~100 nm	Diabetes treatment	Chopra et al., 2017
Nimodipine loaded PLGA nanoparticle	Intravenous	85:15	–	Modified nano precipitation	~200 nm	Sustained release for cerebral vasospasm treatment	Mehta et al., 2007
Alendronate loaded PLGA nanoparticle	Intravenous	50:50	40–75 K	Double emulsion	~300 nm	Restenosis inhibition	Cohen-Sela et al., 2009
Docetaxel loaded PLGA nanoparticles	Injectable	50:50	33 K	PRINT	~300 nm	Cancer treatment	Enlow et al., 2011

binding to curcumin was conducted using MDs with the GROningen MAchine for Chemical Simulations (GROMACS) program, compared to laboratory findings and collated with the experimental results of 10 other PLGA-drug formulations. This study also predicted that PLGA could entrap curcumin with a higher encapsulation efficiency than tripalmitin, a lipid-based carrier, and this prediction was confirmed experimentally (Metwally and Hathout, 2015). A study on the drug release of the anti-cancer drug oxaliplatin in a PLGA matrix was conducted using the Large-scale Atomic/Molecular Massively Parallel Simulator (LAMMPS) program (Lange et al., 2016). A detailed insight into PLGA "patchy particles," which are particles made up of PLGA and lipid-polymer groups, was obtained from computational fluid dynamics, MDs and coarse grain simulations (Salvador-Morales et al., 2016). A study involving the simulation of PLGA-PEG co-polymer with the hydrophobic drug itraconazole, as shown in **Figure 13**, provided information about the drug loading limitations of this system (Wilkosz et al., 2018). A MDs simulation of the peptide Melittin showed that it constituted a more stable formulation with PLGA than PLA (Asadzadeh and Moosavi, 2019). The level of these studies as well as the information they provide is summarized in **Table 2**.

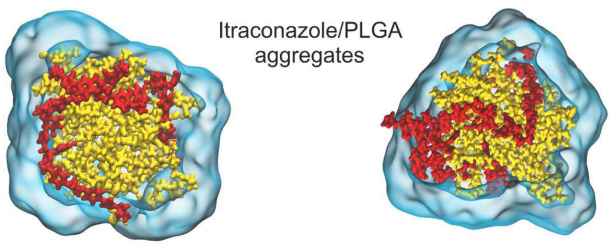

FIGURE 13 | Molecular dynamics (MDs) simulation showing (**A**, left) 12% w/w and (**B**, right) 24% itraconazole loading in a PLGA nanoparticle, adapted with permission from Wilkosz et al. (2018). Copyright (2019) American Chemical Society.

Another area of expansion of computational modeling on PLGA nanosystems is be the study of the transport of these nanocarriers in the circulatory system. One of the limitations of the clinical translation of nanosystems in general is the poor correlation between *in vitro* and *in vivo* results. The use of mathematical and computational methods to model the interactions between the drug, carrier, biological transport system and tumor vasculature can be used to gain insight into these complexities (Curtis et al., 2015). Finite element analysis can be employed to model the dynamics of a nanoparticles within a channel, hence simulating transport in a blood vessel while continuum models can also be used to simulate nanoparticles in a vascular network generated by physical input parameters (Liu et al., 2012).

While computational simulations can provide valuable information on the molecular interactions in various PLGA nanocarrier systems, they can be limited by computational cost and time intensive calculations (Ramezanpour et al., 2016). It has

TABLE 2 | Molecular simulations of PLGA and their significance to nanocarrier drug delivery properties.

Simulation type	Cargo	Property modeled	Experimental validation	Information obtained	References
Density functional theory	Doxorubicin, daunorubicin	Physicochemical properties, binding energy	Qualitative	Carrier-drug affinity, surface modification effects	Rahimi et al., 2012
Molecular dynamics	Curcumin, prednisolone, resveratrol	Binding energy	>85%	Carrier–drug affinity	Metwally and Hathout, 2015
Molecular dynamics	Oxaliplatin	Density Glass transition temperature	>96% >95%	Polymer degradation, drug release	Lange et al., 2016
Molecular dynamics, computational fluid dynamics, coarse grain	None	Shear stress, lipid-PLGA interaction energy	Qualitative	Loading capacity, release kinetics	Salvador-Morales et al., 2016
Finite element analysis	Rhodamine B	Diffusion, drug release	Qualitative	Polymer degradation, drug release	Milosevic et al., 2018
Molecular dynamics	Itraconazole	Binding energy	Qualitiative	Drug loading ability of carrier	Wilkosz et al., 2018
Molecular dynamcs	Melittin	Binding energy, radial distribution function	None	Protein-peptide interactions, encapsulation affinity	Asadzadeh and Moosavi, 2019

been proposed that a minimum reporting standard be instituted where researchers are required to present their results with enough information to make it useful for *in silico* modeling and future work (Faria et al., 2018).

Computational modeling could be immensely useful once it reaches a level where it can be used to select or eliminate certain experimental variables before laboratory research is conducted. Currently, even though simulation time scales are appropriate for the modeling of several nano-systems, the detailed investigation of the formation of nanoparticles by new methods, for example microfluidics, is beyond the abilities of current computational technology. The majority of studies conducted thus far involve the modeling of individual systems; however, more data is needed so that we can move away from specific systems to create profiles to generalize these delivery systems for rational design (Ramezanpour et al., 2016).

Optimizing nanoformulations especially with PLGA polymers which have numerous possible combinations of lactic acid to glycolic acid ratio, molecular weight, endcaps and surface functionalization, could be very time consuming, expensive and in some cases not experimentally feasible. Since computational simulations give a molecular insight to macroscopic properties (Huynh et al., 2012), it could provide a platform to model these initial parameters in order to narrow down the possibilities in a specific study.

DESIGN CONSIDERATIONS

Several studies have demonstrated the increase in particle size and decrease in drug release rate with increase in molecular weight and lactide:glycolide ratios (Song et al., 2008; Dinarvand et al., 2011). Recently, Lu et al. (2019) designed a 75:25 lactide:glycolide PLGA nanocarrier for the sustained release of paclitaxel. Surface functionalization is a component that needs to factor in when designing nanocarriers. Gu et al. (2008) conducted a study that optimized the *in vitro* release rate of docetaxel in PLGA, and additionally found that they could reduce the size of the nanoparticles from ∼291 to ∼160 nm by shortening the length of the PEG chains that were used for surface functionalization, while Bertrand et al. (2017) found that up to a point, increasing the density of PEG surface functionalization increased the blood circulation time of their nanoformulations. Gu's group also investigated an optimum targeting ligand density in order to provide maximum targeting ability without inhibiting the shielding effect of the PEG corona (Gu et al., 2008), while Lu's group found that increasing the density of the chitosan coating in their formulation increased the particle size from ∼133 to ∼173 nm (Lu et al., 2019).

Since the choice of fabrication methods and processes can determine the physicochemical characteristics of the resulting system, it is important to select an approach that is associated with the desired nanoparticle properties for the system of interest. For example Kim S.R. et al. (2019) reported that even though the preparation of their entacavir-loaded system by spray drying produced larger particle size diameters compared to emulsion techniques, the spray dried system showed a much more favorable drug loading and release profiles and hence was the better performing delivery system. Krishnamoorthy described a multi-criteria decision making approach to the synthesis of polymeric

nanoparticles which concluded that nanoprecipitation would be the best suited preparation method for a campthothecin-loaded system (Krishnamoorthy and Mahalingam, 2015), and an adapted approach could be implemented in the selection of synthetic methods for specific PLGA-based systems.

DISADVANTAGES OF PLGA AS A NANOCARRIER

Even though the versatility of PLGA makes it an attractive option as a nanocarrier, it does present several challenges in nanomedicine. PLGA co-polymers are usually readily commercially available, but to obtain it in a high purity, and the specificity required for different molecular weights, lactic/glycolic acid ratios and end capped options can make it very costly (Danhier et al., 2012). Many formulations show poor drug loading and therefore would require large doses in order to achieve therapeutic concentrations of cargo at the target site. Furthermore, these systems often exhibit burst release kinetics, which would result in off target *in vivo* delivery. The degradation rate of PLGA is often unpredictable and the acidic degradation products have shown to affect the activity of the encapsulated drug (Sharma et al., 2016), and despite its biodegradability, reports have shown that the use of PLGA in medical devices may produce localized reaction at the site of delivery (Makadia and Siegel, 2011). Even though targeted PLGA based carriers theoretically have more efficient site specific delivery properties, the targeting moieties in these nanosystems can induce additional immunogenocity (Danhier et al., 2010). There are various *in vivo* physiological barriers and up- and down-regulation of cell surface receptors and other targets can also decrease the efficacy of the targeting agents in these systems. The adaptability of PLGA as a polymer for its specific application has resulted in it being used in many delivery systems and therefore it is difficult to make comprehensive predictions at this stage about its general behavior and toxicity (Sharma et al., 2016).

CONCLUSION AND FUTURE WORK

Even though PLGA is a polymer with many desirable features, there are various areas in which research can be conducted to improve the viability of PLGA based nanocarriers for clinical translation. Since PLGA has been developed in drug delivery systems for such a wide berth of applications, it should be precisely designed in terms of cargo suitability, particle size, drug entrapment and degradation kinetics, for its specific target. This would determine the choice of starting materials and in some cases, the method of preparation and would therefore remove some of the uncertainty present in several trial-and-error attempts in previous drug delivery systems. The innovative fabrication techniques mentioned above could also be attempted to increase control over homogeneity of the products. The use of *in silico* modeling for PLGA nanoparticles as an element of experimental design and could have tremendous implications for the future of nanoparticle design.

AUTHOR CONTRIBUTIONS

DE, PK, YC, and VP from designing the framework and main content of the manuscript, revisions to optimize the manuscript, approved the final submission, and the manuscript was accomplished with contributions.

FUNDING

This work was supported by a National Research Foundation (NRF) SARChI grant.

REFERENCES

Ali, A., and Ahmed, S. (2018). A review on chitosan and its nanocomposites in drug delivery. *Int. J. Biol. Macromol.* 109, 273–286. doi: 10.1016/j.ijbiomac.2017.12.078

Al-Jamal, K. T., Bai, J., Wang, J. T.-W., Protti, A., Southern, P., Bogart, L., et al. (2016). Magnetic drug targeting: preclinical in vivo studies, mathematical modeling, and extrapolation to humans. *Nano Lett.* 16, 5652–5660. doi: 10.1021/acs.nanolett.6b02261

Almoustafa, H. A., Alshawsh, M. A., and Chik, Z. (2017). Technical aspects of preparing PEG-PLGA nanoparticles as carrier for chemotherapeutic agents by nanoprecipitation method. *Int. J. Pharm.* 533, 275–284. doi: 10.1016/j.ijpharm.2017.09.054

Alshamsan, A. (2014). Nanoprecipitation is more efficient than emulsion solvent evaporation method to encapsulate cucurbitacin I in PLGA nanoparticles. *Saudi Pharm. J.* 22, 219–222. doi: 10.1016/j.jsps.2013.12.002

Alvarez-Lorenzo, C., Rey-Rico, A., Sosnik, A., Taboada, P., and Concheiro, A. (2010). Poloxamine-based nanomaterials for drug delivery. *Front. Biosci.* 2, 424–440. doi: 10.2741/e102

Ananta, J. S., Paulmurugan, R., and Massoud, T. (2016). Temozolomide-loaded PLGA nanoparticles to treat glioblastoma cells: a biophysical and cell culture evaluation. *Neurol. Res.* 38, 51–59. doi: 10.1080/01616412.2015.1133025

Anderson, J. M., and Shive, M. S. (2012). Biodegradation and biocompatibility of PLA and PLGA microspheres. *Adv. Drug Deliv. Rev.* 64, 72–82. doi: 10.1016/j.addr.2012.09.004

Ansary, R. H., Awang, M. B., and Rahman, M. M. (2014). Biodegradable poly (D, L-lactic-co-glycolic acid)-based micro/nanoparticles for sustained release of protein drugs-A review. *Trop. J. Pharm. Res.* 13, 1179–1190.

Aravind, A., Nair, R., Raveendran, S., Veeranarayanan, S., Nagaoka, Y., Fukuda, T., et al. (2013). Aptamer conjugated paclitaxel and magnetic fluid loaded fluorescently tagged PLGA nanoparticles for targeted cancer therapy. *J. Magn. Magn. Mater.* 344, 116–123. doi: 10.1016/j.jmmm.2013.05.036

Asadzadeh, H., and Moosavi, A. (2019). Investigation of the interactions between Melittin and the PLGA and PLA polymers: molecular dynamic simulation and binding free energy calculation. *Mater. Res. Exp.* 6:055318. doi: 10.1088/2053-1591/ab06d3

Ayyoob, M., and Kim, Y. (2018). Effect of chemical composition variant and oxygen plasma treatments on the wettability of PLGA thin films, synthesized by direct copolycondensation. *Polymers* 10:E1132. doi: 10.3390/polym10101132

Baghdan, E., Raschpichler, M., Lutfi, W., Pinnapireddy, S. R., Pourasghar, M., Schäfer, J., et al. (2019). Nano spray dried antibacterial coatings for dental implants. *Eur. J. Pharm. Biopharm.* 139, 59–67. doi: 10.1016/j.ejpb.2019.03.003

Bauer, L. M., Situ, S. F., Griswold, M. A., and Samia, A. C. S. (2016). High-performance iron oxide nanoparticles for magnetic particle imaging–guided hyperthermia (hMPI). *Nanoscale* 8, 12162–12169. doi: 10.1039/c6nr01877g

Berkland, C., Pack, D. W., and Kim, K. K. (2004). Controlling surface nanostructure using flow-limited field-injection electrostatic spraying (FFESS) of poly(D,L-lactide-co-glycolide). *Biomaterials* 25, 5649–5658. doi: 10.1016/j.biomaterials.2004.01.018

Berthet, M., Gauthier, Y., Lacroix, C., Verrier, B., and Monge, C. (2017). Nanoparticle-based dressing: the future of wound treatment? *Trends Biotechnol.* 35, 770–784. doi: 10.1016/j.tibtech.2017.05.005

Bertrand, N., Grenier, P., Mahmoudi, M., Lima, E. M., Appel, E. A., Dormont, F., et al. (2017). Mechanistic understanding of in vivo protein corona formation on polymeric nanoparticles and impact on pharmacokinetics. *Nat. Commun.* 8:777. doi: 10.1038/s41467-017-00600-w

Besumbes, E. S., Fornaguera, C., Monge, M., García-Celma, M. J., Carrión, J., Solans, C., et al. (2019). PLGA cationic nanoparticles, obtained from nanoemulsion templating, as potential DNA vaccines. *Eur. Polym. J.* 120:109229. doi: 10.1016/j.eurpolymj.2019.109229

Bosch, F., and Rosich, L. J. P. (2008). The contributions of Paul Ehrlich to pharmacology: a tribute on the occasion of the centenary of his Nobel Prize. *Pharmacology* 82, 171–179. doi: 10.1159/000149583

Bruinsmann, F. A., Pigana, S., Aguirre, T., Dadalt Souto, G., Garrastazu Pereira, G., Bianchera, A., et al. (2019). Chitosan-coated nanoparticles: effect of chitosan molecular weight on nasal transmucosal delivery. *Pharmaceutics* 11:86. doi: 10.3390/pharmaceutics11020086

Carter, T., Mulholland, P., and Chester, K. (2016). Antibody-targeted nanoparticles for cancer treatment. *Immunotherapy* 8, 941–958. doi: 10.2217/imt.16.11

Chapman, S., Dobrovolskaia, M., Farahani, K., Goodwin, A., Joshi, A., Lee, H., et al. (2013). Nanoparticles for cancer imaging: the good, the bad, and the promise. *Nano Today* 8, 454–460. doi: 10.1016/j.nantod.2013.06.001

Chen, J., Wu, Q., Luo, L., Wang, Y., Zhong, Y., Dai, H. B., et al. (2017). Dual tumor-targeted poly(lactic-co-glycolic acid)-polyethylene glycol-folic acid nanoparticles: a novel biodegradable nanocarrier for secure and efficient antitumor drug delivery. *Int. J. Nanomedicine* 12, 5745–5760. doi: 10.2147/ijn.S136488

Chen, Q., Chen, J., Yang, Z., Xu, J., Xu, L., Liang, C., et al. (2019). Nanoparticle-enhanced radiotherapy to trigger robust cancer immunotherapy. *Adv. Mater.* 31:1802228. doi: 10.1002/adma.201802228

Chen, Q., Xu, L., Liang, C., Wang, C., Peng, R., and Liu, Z. (2016). Photothermal therapy with immune-adjuvant nanoparticles together with checkpoint blockade for effective cancer immunotherapy. *Nat. Commun.* 7:13193. doi: 10.1038/ncomms13193

Chen, Y., Yang, Z., Liu, C., Wang, C., Zhao, S., Yang, J., et al. (2013). Synthesis, characterization, and evaluation of paclitaxel loaded in six-arm star-shaped poly (lactic-co-glycolic acid). *Int. J. Nanomedicine* 8, 4315–4326. doi: 10.2147/IJN.S51629

Chiesa, E., Dorati, R., Pisani, S., Conti, B., Bergamini, G., Modena, T., et al. (2018). The microfluidic technique and the manufacturing of polysaccharide nanoparticles. *Pharmaceutics* 10:267. doi: 10.3390/pharmaceutics10040267

Choi, K. Y., Yoon, H. Y., Kim, J. H., Bae, S. M., Park, R. W., Kang, Y. M., et al. (2011). Smart nanocarrier based on PEGylated hyaluronic acid for cancer therapy. *ACS Nano* 5, 8591–8599. doi: 10.1021/nn202070n

Chopra, S., Bertrand, N., Lim, J. M., Wang, A., Farokhzad, O. C., and Karnik, R. (2017). Design of insulin-loaded nanoparticles enabled by multistep control of nanoprecipitation and zinc chelation. *ACS Appl. Mater. Interfaces* 9, 11440–11450. doi: 10.1021/acsami.6b16854

Chung, H. J., Kim, H. K., Yoon, J. J., and Park, T. G. (2006). Heparin immobilized porous PLGA microspheres for angiogenic growth factor delivery. *Pharm. Res.* 23, 1835–1841. doi: 10.1007/s11095-006-9039-9

Cohen-Sela, E., Chorny, M., Koroukhov, N., Danenberg, H. D., and Golomb, G. (2009). A new double emulsion solvent diffusion technique for encapsulating hydrophilic molecules in PLGA nanoparticles. *J. Control. Release* 133, 90–95. doi: 10.1016/j.jconrel.2008.09.073

Collins, D. J., Neild, A., deMello, A., Liu, A.-Q., and Ai, Y. (2015). The poisson distribution and beyond: methods for microfluidic droplet production and single cell encapsulation. *Lab Chip* 15, 3439–3459. doi: 10.1039/C5LC00614G

Coors, E. A., Seybold, H., Merk, H. F., and Mahler, V. (2005). Polysorbate 80 in medical products and nonimmunologic anaphylactoid reactions. *Ann. Allergy Asthma Immunol.* 95, 593–599. doi: 10.1016/s1081-1206(10)61024-1

Crucho, C. I. C., and Barros, M. T. (2017). Polymeric nanoparticles: a study on the preparation variables and characterization methods. *Mater. Sci. Eng. C Mater. Biol. Appl.* 80, 771–784. doi: 10.1016/j.msec.2017.06.004

Curtis, L. T., Wu, M., Lowengrub, J., Decuzzi, P., and Frieboes, H. B. (2015). Computational modeling of tumor response to drug release from vasculature-bound nanoparticles. *PLoS One* 10:e0144888. doi: 10.1371/journal.pone.0144888

Danhier, F., Ansorena, E., Silva, J. M., Coco, R., Le Breton, A., and Préat, V. (2012). PLGA-based nanoparticles: an overview of biomedical applications. *J. Control. Release* 161, 505–522. doi: 10.1016/j.jconrel.2012.01.043

Danhier, F., Feron, O., and Préat, V. (2010). To exploit the tumor microenvironment: passive and active tumor targeting of nanocarriers for anti-cancer drug delivery. *J. Control. Release* 148, 135–146. doi: 10.1016/j.jconrel.2010.08.027

Davoudi, Z., Peroutka-Bigus, N., Bellaire, B., Wannemuehler, M., Barrett, T. A., Narasimhan, B., et al. (2018). Intestinal organoids containing poly(lactic-co-glycolic acid) nanoparticles for the treatment of inflammatory bowel diseases. *J. Biomed. Mater. Res. Part A* 106, 876–886. doi: 10.1002/jbm.a.36305

Dinarvand, R., Sepehri, N., Manoochehri, S., Rouhani, H., and Atyabi, F. (2011). Polylactide-co-glycolide nanoparticles for controlled delivery of anticancer agents. *Int. J. Nanomedicine* 6, 877–895. doi: 10.2147/IJN.S18905

Ding, D., and Zhu, Q. (2018). Recent advances of PLGA micro/nanoparticles for the delivery of biomacromolecular therapeutics. *Mater. Sci. Eng. C Mater. Biol. Appl.* 92, 1041–1060. doi: 10.1016/j.msec.2017.12.036

Du, J., Li, X.-Y., Hu, H., Xu, L., Yang, S.-P., and Li, F.-H. (2018). Preparation and imaging investigation of dual-targeted C 3 F 8-filled PLGA nanobubbles as a novel ultrasound contrast agent for breast cancer. *Sci. Rep.* 8:3887.

Durán, V., Yasar, H., Becker, J., Thiyagarajan, D., Loretz, B., Kalinke, U., et al. (2019). Preferential uptake of chitosan-coated PLGA nanoparticles by primary human antigen presenting cells. *Nanomedicine* 21:102073. doi: 10.1016/j.nano.2019.102073

Eley, J. G., Pujari, V. D., and McLane, J. (2004). Poly (lactide-co-glycolide) nanoparticles containing coumarin-6 for suppository delivery: in vitro release profile and in vivo tissue distribution. *Drug Deliv.* 11, 255–261. doi: 10.1080/10717540490467384

Engineer, C., Parikh, J., Raval, A., and Organs, A. (2011). Review on hydrolytic degradation behavior of biodegradable polymers from controlled drug delivery system. *Trends Biomater. Artif. Organs* 25, 79–85. doi: 10.1002/wnan.10

Enlow, E. M., Luft, J. C., Napier, M. E., and DeSimone, J. M. (2011). Potent engineered PLGA nanoparticles by virtue of exceptionally high chemotherapeutic loadings. *Nano Lett.* 11, 808–813. doi: 10.1021/nl104117p

Faheem, A. M., Abdeåkader, D., Osman, M. A., McCarron, P. A., and El-Gizawy, S. A. (2019). Oral insulin delivery in diabetic rats by PLGA nanoparticles combined with a protease inhibitor (N-ethylmaleimide). *Br. J. Pharm.* 4, S2–3.

Faria, M., Björnmalm, M., Thurecht, K. J., Kent, S. J., Parton, R. G., Kavallaris, M., et al. (2018). Minimum information reporting in bio–nano experimental literature. *Nat. Nanotechnol.* 13, 777–785. doi: 10.1038/s41565-018-0246-4

Fessi, H., Puisieux, F., Devissaguet, J. P., Ammoury, N., and Benita, S. (1989). Nanocapsule formation by interfacial polymer deposition following solvent displacement. *Int. J. Pharm.* 55, R1–R4. doi: 10.1016/0378-5173(89)90281-0

Frenkel, D., and Smit, B. (2001). *Understanding Molecular Simulation: From Algorithms to Applications*, Vol. 1. San Diego, CA: Elsevier, 363.

Friedman, A. D., Claypool, S. E., and Liu, R. (2013). The smart targeting of nanoparticles. *Curr. Pharm. Des.* 19, 6315–6329. doi: 10.2174/13816128113199990375

Fu, X., Cai, J., Zhang, X., Li, W.-D., Ge, H., and Hu, Y. (2018). Top-down fabrication of shape-controlled, monodisperse nanoparticles for biomedical applications. *Adv. Drug Deliv. Rev.* 132, 169–187. doi: 10.1016/j.addr.2018.07.006

Gajdova, M., Jakubovsky, J., and Valky, J. (1993). Delayed effects of neonatal exposure to tween 80 on female reproductive organs in rats. *Food Chem. Toxicol.* 31, 183–190. doi: 10.1016/0278-6915(93)90092-d

Ganipineni, L. P., Ucakar, B., Joudiou, N., Riva, R., Jérôme, C., Gallez, B., et al. (2019). Paclitaxel-loaded multifunctional nanoparticles for the targeted treatment of glioblastoma. *J. Drug Target.* 27, 614–623. doi: 10.1080/1061186X.2019.1567738

Geerlings, P., De Proft, F., and Langenaeker, W. (2003). Conceptual density functional theory. *Chem. Rev.* 103, 1793–1873. doi: 10.1021/cr990029p

Gendelman, H. E., Anantharam, V., Bronich, T., Ghaisas, S., Jin, H., Kanthasamy, A. G., et al. (2015). Nanoneuromedicines for degenerative, inflammatory, and infectious nervous system diseases. *Nanomedicine* 11, 751–767. doi: 10.1016/j.nano.2014.12.014

Gentile, P., Chiono, V., Carmagnola, I., and Hatton, P. (2014). An overview of poly (lactic-co-glycolic) acid (PLGA)-based biomaterials for bone tissue engineering. *Int. J. Mol. Sci.* 15, 3640–3659. doi: 10.3390/ijms15033640

Gholizadeh, S., Kamps, J. A. A. M., Hennink, W. E., and Kok, R. J. (2018). PLGA-PEG nanoparticles for targeted delivery of the mTOR/PI3kinase inhibitor dactolisib to inflamed endothelium. *Int. J. Pharm.* 548, 747–758. doi: 10.1016/j.ijpharm.2017.10.032

Gonzalez-Pizarro, R., Silva-Abreu, M., Calpena, A. C., Egea, M. A., Espina, M., and Garcia, M. L. (2018). Development of fluorometholone-loaded PLGA nanoparticles for treatment of inflammatory disorders of anterior and posterior segments of the eye. *Int. J. Pharm.* 547, 338–346. doi: 10.1016/j.ijpharm.2018.05.050

Govender, T., Stolnik, S., Garnett, M. C., Illum, L., and Davis, S. S. (1999). PLGA nanoparticles prepared by nanoprecipitation: drug loading and release studies of a water soluble drug. *J. Control. Release* 57, 171–185. doi: 10.1016/s0168-3659(98)00116-3

Grabowski, N., Hillaireau, H., Vergnaud, J., Tsapis, N., Pallardy, M., Kerdine-Romer, S., et al. (2015). Surface coating mediates the toxicity of polymeric nanoparticles towards human-like macrophages. *Int. J. Pharm.* 482, 75–83. doi: 10.1016/j.ijpharm.2014.11.042

Grabowski, N., Hillaireau, H., Vergnaud-Gauduchon, J., Nicolas, V., Tsapis, N., Kerdine-Romer, S., et al. (2016). Surface-modified biodegradable nanoparticles' impact on cytotoxicity and inflammation response on a co-culture of lung epithelial cells and human-like macrophages. *J. Biomed. Nanotechnol.* 12, 135–146. doi: 10.1166/jbn.2016.2126

Gu, F., Zhang, L., Teply, B. A., Mann, N., Wang, A., Radovic-Moreno, A. F., et al. (2008). Precise engineering of targeted nanoparticles by using self-assembled biointegrated block copolymers. *Proc. Natl. Acad. Sci. U.S.A.* 105, 2586–2591. doi: 10.1073/pnas.0711714105

Guo, L., Chen, B., Liu, R., Xia, G., Wang, Y., Li, X., et al. (2015). Biocompatibility assessment of polyethylene glycol-poly L-lysine-poly lactic-co-glycolic acid nanoparticles in vitro and in vivo. *J. Nanosci. Nanotechnol.* 15, 3710–3719. doi: 10.1166/jnn.2015.9509

Guo, P., Huang, J., Zhao, Y., Martin, C. R., Zare, R. N., and Moses, M. A. (2018). Nanomaterial preparation by extrusion through nanoporous membranes. *Small* 14:e1703493. doi: 10.1002/smll.201703493

Guo, X., Zhang, X., Ye, L., Zhang, Y., Ding, R., Hao, Y., et al. (2014). Inhalable microspheres embedding chitosan-coated PLGA nanoparticles for 2-methoxyestradiol. *J. Drug Target.* 22, 421–427. doi: 10.3109/1061186x.2013.878944

Guo, Z. S. (2018). The 2018 Nobel Prize in medicine goes to cancer immunotherapy (editorial for BMC cancer). *BMC Cancer* 18:1086. doi: 10.1186/s12885-018-5020-3

Habraken, W. J., Wolke, J. G., Mikos, A. G., and Jansen, J. A. (2006). Injectable PLGA microsphere/calcium phosphate cements: physical properties and degradation characteristics. *J. Biomater. Sci. Polym. Ed.* 17, 1057–1074. doi: 10.1163/156856206778366004

Haggag, Y. A., Faheem, A. M., Tambuwala, M. M., Osman, M. A., El-Gizawy, S. A., O'Hagan, B., et al. (2018). Effect of poly(ethylene glycol) content and formulation parameters on particulate properties and intraperitoneal delivery of insulin from PLGA nanoparticles prepared using the double-emulsion evaporation procedure. *Pharm. Dev. Technol.* 23, 370–381. doi: 10.1080/10837450.2017.1295066

Heinz, H., Pramanik, C., Heinz, O., Ding, Y., Mishra, R. K., Marchon, D., et al. (2017). Nanoparticle decoration with surfactants: molecular interactions, assembly, and applications. *Surf. Sci. Rep.* 72, 1–58. doi: 10.1016/j.surfrep.2017.02.001

Huynh, L., Neale, C., Pomès, R., and Allen, C. (2012). Computational approaches to the rational design of nanoemulsions, polymeric micelles, and dendrimers for drug delivery. *Nanomedicine* 8, 20–36. doi: 10.1016/j.nano.2011.05.006

Jahan, S. T., Sadat, S. M. A., Walliser, M., and Haddadi, A. (2017). Targeted therapeutic nanoparticles: an immense promise to fight against cancer. *J. Drug Deliv.* 2017:9090325. doi: 10.1155/2017/9090325

Jain, A., Kunduru, K. R., Basu, A., Mizrahi, B., Domb, A. J., and Khan, W. (2016). Injectable formulations of poly(lactic acid) and its copolymers in clinical use. *Adv. Drug Deliv. Rev.* 107, 213–227. doi: 10.1016/j.addr.2016.07.002

Jalali, N., Moztarzadeh, F., Mozafari, M., Asgari, S., Motevalian, M., Alhosseini, S. N. J. C., et al. (2011). Surface modification of poly (lactide-co-glycolide) nanoparticles by d-α-tocopheryl polyethylene glycol 1000 succinate as potential carrier for the delivery of drugs to the brain. *Colloids Surf. A Physicochem. Eng. Asp.* 392, 335–342. doi: 10.1016/j.colsurfa.2011.10.012

Jana, S., Kumar Sen, K., and Gandhi, A. (2016). Alginate based nanocarriers for drug delivery applications. *Curr. Pharm. Des.* 22, 3399–3410. doi: 10.2174/1381612822666160510125718

Jeon, S. G., Cha, M.-Y., Kim, J.-I., Hwang, T. W., Kim, K. A., Kim, T. H., et al. (2019). Vitamin D-binding protein-loaded PLGA nanoparticles suppress Alzheimer's disease-related pathology in 5XFAD mice. *Nanomedicine* 17, 297–307. doi: 10.1016/j.nano.2019.02.004

Jesus, S., Schmutz, M., Som, C., Borchard, G., Wick, P., and Borges, O. (2019). Hazard assessment of polymeric nanobiomaterials for drug delivery: what can we learn from literature so far. *Front. Bioeng. Biotechnol.* 7:261. doi: 10.3389/fbioe.2019.00261

Jog, R., and Burgess, D. J. (2017). Pharmaceutical amorphous nanoparticles. *J. Pharm. Sci.* 106, 39–65. doi: 10.1016/j.xphs.2016.09.014

Kakkar, A., Traverso, G., Farokhzad, O. C., Weissleder, R., and Langer, R. (2017). Evolution of macromolecular complexity in drug delivery systems. *Nat. Rev. Chem.* 1:0063. doi: 10.1038/s41570-017-0063

Kalombo, L., Lemmer, Y., Semete-Makokotlela, B., Ramalapa, B., Nkuna, P., Booysen, L. L., et al. (2019). Spray-dried, nanoencapsulated, multi-drug anti-tuberculosis therapy aimed at once weekly administration for the duration of treatment. *Nanomaterials* 9:1167. doi: 10.3390/nano9081167

Kamaly, N., Yameen, B., Wu, J., and Farokhzad, O. C. (2016). Degradable controlled-release polymers and polymeric nanoparticles: mechanisms of controlling drug release. *Chem. Rev.* 116, 2602–2663. doi: 10.1021/acs.chemrev.5b00346

Kapoor, D. N., Bhatia, A., Kaur, R., Sharma, R., Kaur, G., and Dhawan, S. (2015). PLGA: a unique polymer for drug delivery. *Ther. Deliv.* 6, 41–58. doi: 10.4155/tde.14.91

Karra, N., and Benita, S. (2012). The ligand nanoparticle conjugation approach for targeted cancer therapy. *Curr. Drug Metab.* 13, 22–41. doi: 10.2174/138920012798356899

Keles, H., Naylor, A., Clegg, F., and Sammon, C. (2015). Investigation of factors influencing the hydrolytic degradation of single PLGA microparticles. *Polym. Degrad. Stab.* 119, 228–241. doi: 10.1016/j.polymdegradstab.2015.04.025

Khalil, D. N., Smith, E. L., Brentjens, R. J., and Wolchok, J. D. (2016). The future of cancer treatment: immunomodulation, CARs and combination immunotherapy. *Nat. Rev. Clin. Oncol.* 13, 273–290. doi: 10.1038/nrclinonc.2016.25

Khalil, N. M., do Nascimento, T. C., Casa, D. M., Dalmolin, L. F., de Mattos, A. C., Hoss, I., et al. (2013). Pharmacokinetics of curcumin-loaded PLGA and PLGA-PEG blend nanoparticles after oral administration in rats. *Colloids Surf. B Biointerfaces* 101, 353–360. doi: 10.1016/j.colsurfb.2012.06.024

Kim, K. T., Lee, J. Y., Kim, D. D., Yoon, I. S., and Cho, H. J. (2019). Recent progress in the development of poly(lactic-co-glycolic acid)-based nanostructures for cancer imaging and therapy. *Pharmaceutics* 11:E280. doi: 10.3390/pharmaceutics11060280

Kim, S. R., Ho, M. J., Choi, Y. W., and Kang, M. J. (2019). Improved drug loading and sustained release of entecavir-loaded PLGA microsphere prepared by spray drying technique. *Bull. Korean Chem. Soc.* 40, 306–312. doi: 10.1002/bkcs.11682

Kohl, Y., Kaiser, C., Bost, W., Stracke, F., Fournelle, M., Wischke, C., et al. (2011). Preparation and biological evaluation of multifunctional PLGA-nanoparticles designed for photoacoustic imaging. *Nanomedicine* 7, 228–237. doi: 10.1016/j.nano.2010.07.006

Kojic, M., Milosevic, M., Simic, V., Stojanovic, D., and Uskokovic, P. (2017). A radial 1D finite element for drug release from drug loaded nanofibers. *J. Serbian Soc. Comput. Mech.* 11, 82–93. doi: 10.24874/jsscm.2017.11.01.08

Koushik, K., and Kompella, U. B. (2004). Preparation of large porous deslorelin-PLGA microparticles with reduced residual solvent and cellular uptake using a supercritical carbon dioxide process. *Pharm. Res.* 21, 524–535. doi: 10.1023/B:PHAM.0000019308.25479.a4

Krishnamoorthy, K., and Mahalingam, M. (2015). Selection of a suitable method for the preparation of polymeric nanoparticles: multi-criteria decision making approach. *Adv. Pharm. Bull.* 5, 57–67. doi: 10.5681/apb.2015.008

Kumar, P., Van Treuren, T., Ranjan, A. P., Chaudhary, P., and Vishwanatha, J. K. J. N. (2019). In vivo imaging and biodistribution of near infrared dye loaded brain-metastatic-breast-cancer-cell-membrane coated polymeric nanoparticles. *Nanotechnology* 30:265101. doi: 10.1088/1361-6528/ab0f46

Kumari, A., Yadav, S. K., and Yadav, S. C. (2010). Biodegradable polymeric nanoparticles based drug delivery systems. *Colloids Surf. B Biointerfaces* 75, 1–18. doi: 10.1016/j.colsurfb.2009.09.001

Lai, P., Daear, W., Löbenberg, R., and Prenner, E. J. (2014). Overview of the preparation of organic polymeric nanoparticles for drug delivery based on gelatine, chitosan, poly (d, l-lactide-co-glycolic acid) and polyalkylcyanoacrylate. *Colloids Surf. B Biointerfaces* 118, 154–163. doi: 10.1016/j.colsurfb.2014.03.017

Lamprecht, A., Ubrich, N., Yamamoto, H., Schafer, U., Takeuchi, H., Maincent, P., et al. (2001). Biodegradable nanoparticles for targeted drug delivery in treatment of inflammatory bowel disease. *J. Pharmacol. Exp. Ther.* 299, 775–781.

Lange, J., de Souza, F. G., Nele, M., Tavares, F. W., Segtovich, I. S. V., and da Silva, G. C. Q. (2016). Molecular dynamic simulation of oxaliplatin diffusion in poly (lactic acid-co-glycolic acid). part a: parameterization and validation of the force-field CVFF. *Macromol. Theory Simul.* 25, 45–62. doi: 10.1002/mats.201500049

Li, S. (1999). Hydrolytic degradation characteristics of aliphatic polyesters derived from lactic and glycolic acids. *J. Biomed. Mater. Res.* 48, 342–353. doi: 10.1002/(sici)1097-4636(1999)48:3<342::aid-jbm20>3.0.co;2-7

Liang, R., Wang, J., Wu, X., Dong, L., Deng, R., Wang, K., et al. (2013). Multifunctional biodegradable polymer nanoparticles with uniform sizes: generation and in vitro anti-melanoma activity. *Nanotechnology* 24:455302. doi: 10.1088/0957-4484/24/45/455302

Lima, I. A. D., Khalil, N. M., Tominaga, T. T., Lechanteur, A., Sarmento, B., and Mainardes, R. M. (2018). Mucoadhesive chitosan-coated PLGA nanoparticles for oral delivery of ferulic acid. *Artif. Cells Nanomed. Biotechnol.* 46(Suppl. 2), 993–1002. doi: 10.1080/21691401.2018.1477788

Lince, F., Marchisio, D. L., and Barresi, A. A. (2011). A comparative study for nanoparticle production with passive mixers via solvent-displacement: use of CFD models for optimization and design. *Chem. Eng. Process.* 50, 356–368. doi: 10.1016/j.cep.2011.02.015

Liu, Y., Shah, S., and Tan, J. (2012). Computational modeling of nanoparticle targeted drug delivery. *Rev. Nanosci. Nanotechnol.* 1, 66–83. doi: 10.1166/rnn.2012.1014

Lombardo, D., Kiselev, M. A., and Caccamo, M. T. (2019). Smart nanoparticles for drug delivery application: development of versatile nanocarrier platforms in biotechnology and nanomedicine. *J. Nanomater.* 2019:3702518.

Lu, B., Lv, X., and Le, Y. (2019). Chitosan-modified PLGA nanoparticles for control-released drug delivery. *Polymers* 11:304. doi: 10.3390/polym11020304

Lü, J.-M., Wang, X., Marin-Muller, C., Wang, H., Lin, P. H., Yao, Q., et al. (2009). Current advances in research and clinical applications of PLGA-based nanotechnology. *Expert Rev. Mol. Diagn.* 9, 325–341. doi: 10.1586/erm.09.15

Mahapatro, A., and Singh, D. K. (2011). Biodegradable nanoparticles are excellent vehicle for site directed in-vivo delivery of drugs and vaccines. *J. Nanobiotechnol.* 9:55. doi: 10.1186/1477-3155-9-55

Makadia, H. K., and Siegel, S. (2011). Poly lactic-co-glycolic acid (PLGA) as biodegradable controlled drug delivery carrier. *Polymers* 3, 1377–1397. doi: 10.3390/polym3031377

Mandal, S., Prathipati, P. K., Belshan, M., and Destache, C. (2019). A potential long-acting bictegravir loaded nano-drug delivery system for HIV-1 infection: a proof-of-concept study. *Antiviral Res.* 167, 83–88. doi: 10.1016/j.antiviral.2019.04.007

Martins, C., Araújo, F., Gomes, M. J., Fernandes, C., Nunes, R., Li, W., et al. (2019). Using microfluidic platforms to develop CNS-targeted polymeric nanoparticles for HIV therapy. *Eur. J. Pharm. Biopharm.* 138, 111–124. doi: 10.1016/j.ejpb.2018.01.014

Martins, C., and Sarmento, B. (2020). Microfluidic manufacturing of multitargeted PLGA/PEG nanoparticles for delivery of taxane chemotherapeutics. *Methods Mol. Biol.* 2059, 213–224. doi: 10.1007/978-1-4939-9798-5_11

Mehta, A. K., Yadav, K. S., and Sawant, K. K. (2007). Nimodipine loaded PLGA nanoparticles: formulation optimization using factorial design, characterization and in vitro evaluation. *Curr. Drug Deliv.* 4, 185–193. doi: 10.2174/156720107781023929

Menon, J. U., Kona, S., Wadajkar, A. S., Desai, F., Vadla, A., and Nguyen, K. T. (2012). Effects of surfactants on the properties of PLGA nanoparticles. *J. Biomed. Mater. Rese. Part A* 100, 1998–2005. doi: 10.1002/jbm.a.34040

Metwally, A. A., and Hathout, R. M. (2015). Computer-assisted drug formulation design: novel approach in drug delivery. *Mol. Pharm.* 12, 2800–2810. doi: 10.1021/mp500740d

Middleton, J. C., and Tipton, A. (2000). Synthetic biodegradable polymers as orthopedic devices. *Biomaterials* 21, 2335–2346. doi: 10.1016/s0142-9612(00)00101-0

Miller, S. C., and Drabik, B. R. (1984). Rheological properties of poloxamer vehicles. *Int. J. Pharm.* 18, 269–276. doi: 10.1016/0378-5173(84)90142-x

Milosevic, M., Stojanovic, D., Simic, V., Milicevic, B., Radisavljevic, A., Uskokovic, P., et al. (2018). A computational model for drug release from PLGA implant. *Materials* 11:E2416. doi: 10.3390/ma11122416

Mir, M., Ahmed, N., and Ur Rehman, A. (2017). Recent applications of PLGA based nanostructures in drug delivery. *Colloids Surf. B Biointerfaces* 159, 217–231. doi: 10.1016/j.colsurfb.2017.07.038

Mishima, K. (2008). Biodegradable particle formation for drug and gene delivery using supercritical fluid and dense gas. *Adv. Drug Deliv. Rev.* 60, 411–432. doi: 10.1016/j.addr.2007.02.003

Mishra, A., Singh, S. K., Dash, D., Aswal, V. K., Maiti, B., Misra, M., et al. (2014). Self-assembled aliphatic chain extended polyurethane nanobiohybrids: emerging hemocompatible biomaterials for sustained drug delivery. *Acta Biomater.* 10, 2133–2146. doi: 10.1016/j.actbio.2013.12.035

Mittal, G., Sahana, D. K., Bhardwaj, V., and Ravi Kumar, M. N. (2007). Estradiol loaded PLGA nanoparticles for oral administration: effect of polymer molecular weight and copolymer composition on release behavior in vitro and in vivo. *J. Control. Release* 119, 77–85. doi: 10.1016/j.jconrel.2007.01.016

Moku, G., Layek, B., Trautman, L., Putnam, S., Panyam, J., and Prabha, S. J. C. (2019). Improving payload capacity and anti-tumor efficacy of mesenchymal stem cells using TAT peptide functionalized polymeric nanoparticles. *Cancers* 11:E491. doi: 10.3390/cancers11040491

Muhamad, N., Plengsuriyakarn, T., and Na-Bangchang, K. (2018). Application of active targeting nanoparticle delivery system for chemotherapeutic drugs and traditional/herbal medicines in cancer therapy: a systematic review. *Int. J. Nanomedicine* 13, 3921–3935. doi: 10.2147/ijn.S165210

Nagavarma, B., Yadav, H. K., Ayaz, A., Vasudha, L., and Shivakumar, H. J. A. (2012). Different techniques for preparation of polymeric nanoparticles-a review. *Asian J. Pharm. Clin. Res.* 5, 16–23.

Nie, H., Lee, L. Y., Tong, H., and Wang, C.-H. (2008). PLGA/chitosan composites from a combination of spray drying and supercritical fluid foaming techniques: new carriers for DNA delivery. *J. Control. Release* 129, 207–214. doi: 10.1016/j.jconrel.2008.04.018

Ospina-Villa, J. D., Gómez-Hoyos, C., Zuluaga-Gallego, R., and Triana-Chávez, O. (2019). Encapsulation of proteins from *Leishmania panamensis* into PLGA particles by a single emulsion-solvent evaporation method. *J. Microbiol. Methods* 162, 1–7. doi: 10.1016/j.mimet.2019.05.004

Owens, D. E. III, and Peppas, N. A. (2006). Opsonization, biodistribution, and pharmacokinetics of polymeric nanoparticles. *Int. J. Pharm.* 307, 93–102. doi: 10.1016/j.ijpharm.2005.10.010

Oz, U. C., Küçüktürkmen, B., Devrim, B., Saka, O. M., and Bozkir, A. (2019). Development and optimization of alendronate sodium loaded PLGA nanoparticles by central composite design. *Macromol. Res.* 27, 857–866. doi: 10.1007/s13233-019-7119-z

Panda, J., Satapathy, B. S., Majumder, S., Sarkar, R., Mukherjee, B., Tudu, B., et al. (2019). Engineered polymeric iron oxide nanoparticles as potential drug carrier for targeted delivery of docetaxel to breast cancer cells. *J. Magn. Magn. Mater.* 485, 165–173. doi: 10.1016/j.jmmm.2019.04.058

Panyam, J., and Labhasetwar, V. (2012). Biodegradable nanoparticles for drug and gene delivery to cells and tissue. *Adv. Drug Deliv. Rev.* 64, 61–71. doi: 10.1016/j.addr.2012.09.023

Patel, B. K., Parikh, R. H., and Patel, N. (2018). Targeted delivery of mannosylated-PLGA nanoparticles of antiretroviral drug to brain. *Int. J. Nanomedicine* 13, 97–100. doi: 10.2147/IJN.S124692

Peng, P., Yang, K., Tong, G., and Ma, L. (2018). Polysaccharide nanoparticles for targeted cancer therapies. *Curr. Drug Metab.* 19, 781–792. doi: 10.2174/1389200219666180511153403

Pereira, A. D. S. B. F., Brito, G. A. D. C., Lima, M. L. D. S., Silva Júnior, A. A. D., Silva, E. D. S., de Rezende, A. A., et al. (2018). Metformin hydrochloride-loaded PLGA nanoparticle in periodontal disease experimental model using diabetic rats. *Int. J. Mol. Sci.* 19:3488. doi: 10.3390/ijms19113488

Perry, J. L., Herlihy, K. P., Napier, M. E., and Desimone, J. M. (2011). PRINT: a novel platform toward shape and size specific nanoparticle theranostics. *ACC Chem. Res.* 44, 990–998. doi: 10.1021/ar2000315

Platel, A., Carpentier, R., Becart, E., Mordacq, G., Betbeder, D., and Nesslany, F. (2016). Influence of the surface charge of PLGA nanoparticles on their in vitro genotoxicity, cytotoxicity, ROS production and endocytosis. *J. Appl. Toxicol.* 36, 434–444. doi: 10.1002/jat.3247

Rahimi, F., Bahlake, A., Chamani, Z., and Bagheri, S. (2012). Theoretical study on the conjugation of PLGA and PLGA-PEG carriers to doxorubicin and daunorubicin. *Indian J. Exp. Biol.* 2, 2055–2060.

Ramezanpour, M., Leung, S., Delgado-Magnero, K., Bashe, B., Thewalt, J., and Tieleman, D. (2016). Computational and experimental approaches for investigating nanoparticle-based drug delivery systems. *Biochim. Biophys. Acta* 1858(7 Pt B), 1688–1709. doi: 10.1016/j.bbamem.2016.02.028

Redhead, H. M., Davis, S. S., and Illum, L. (2001). Drug delivery in poly(lactide-co-glycolide) nanoparticles surface modified with poloxamer 407 and poloxamine 908: in vitro characterisation and in vivo evaluation. *J. Control. Release* 70, 353–363. doi: 10.1016/s0168-3659(00)00367-9

Rezvantalab, S., Drude, N. I., Moraveji, M. K., Güvener, N., Koons, E. K., Shi, Y., et al. (2018). PLGA-based nanoparticles in cancer treatment. *Front. Pharmacol.* 9:1260. doi: 10.3389/fphar.2018.01260

Rizvi, S. A. A., and Saleh, A. M. (2018). Applications of nanoparticle systems in drug delivery technology. *Saudi Pharm. J.* 26, 64–70. doi: 10.1016/j.jsps.2017.10.012

Rodriguez-Torres, M. D. P., Acosta-Torres, L. S., and Diaz-Torres, L. A. (2018). Heparin-based nanoparticles: an overview of their applications. *J. Nanomater.* 2018:9780489. doi: 10.1155/2018/9780489

Sadat Tabatabaei Mirakabad, F., Nejati-Koshki, K., Akbarzadeh, A., Yamchi, M. R., Milani, M., Zarghami, N., et al. (2014). PLGA-based nanoparticles as cancer drug delivery systems. *Asian Pac. J. Cancer Prev.* 15, 517–535. doi: 10.7314/apjcp.2014.15.2.517

Sadeghi-Avalshahr, A., Nokhasteh, S., Molavi, A. M., Khorsand-Ghayeni, M., and Mahdavi-Shahri, M. (2017). Synthesis and characterization of collagen/PLGA biodegradable skin scaffold fibers. *Regen. Biomater.* 4, 309–314. doi: 10.1093/rb/rbx026

Salmaso, S., and Caliceti, P. (2013). Stealth properties to improve therapeutic efficacy of drug nanocarriers. *Nanotechnol. Cancer* 2013:374252.

Salvador-Morales, C., Brahmbhatt, B., Márquez-Miranda, V., Araya-Duran, I., Canan, J., Gonzalez-Nilo, F., et al. (2016). Mechanistic studies on the self-assembly of PLGA patchy particles and their potential applications in biomedical imaging. *Langmuir* 32, 7929–7942. doi: 10.1021/acs.langmuir.6b02177

Sanchez-Gaytan, B. L., Fay, F., Lobatto, M. E., Tang, J., Ouimet, M., Kim, Y., et al. (2015). HDL-mimetic PLGA nanoparticle to target atherosclerosis plaque macrophages. *Bioconjug. Chem.* 26, 443–451. doi: 10.1021/bc500517k

Saravanakumar, K., Hu, X., Shanmugam, S., Chelliah, R., Sekar, P., Oh, D.-H., et al. (2019). Enhanced cancer therapy with pH-dependent and aptamer functionalized doxorubicin loaded polymeric (poly D, L-lactic-co-glycolic acid) nanoparticles. *Arch. Biochem. Biophys.* 671, 143–151. doi: 10.1016/j.abb.2019.07.004

Schrurs, F., and Lison, D. (2012). Join the dialogue. *Nat. Nanotechnol.* 7, 545–545. doi: 10.1038/nnano.2012.150

Semete, B., Booysen, L., Lemmer, Y., Kalombo, L., Katata, L., Verschoor, J., et al. (2010). In vivo evaluation of the biodistribution and safety of PLGA nanoparticles as drug delivery systems. *Nanomedicine* 6, 662–671. doi: 10.1016/j.nano.2010.02.002

Sequeira, J. A. D., Santos, A. C., Serra, J., Veiga, F., and Ribeiro, A. J. (2018). "Chapter 10 - Poly(lactic-co-glycolic acid) (PLGA) matrix implants," in *Nanostructures for the Engineering of Cells, Tissues and Organs*, ed. A. M. Grumezescu, (Norwich, NY: William Andrew Publishing), 375–402. doi: 10.1016/b978-0-12-813665-2.00010-7

Sharma, M., Sharma, S., Sharma, V., Sharma, K., Yadav, S. K., Dwivedi, P., et al. (2017). Oleanolic-bioenhancer coloaded chitosan modified nanocarriers attenuate breast cancer cells by multimode mechanism and preserve female fertility. *Int. J. Biol. Macromol.* 104(Pt A), 1345–1358. doi: 10.1016/j.ijbiomac.2017.06.005

Sharma, S., Parmar, A., Kori, S., and Sandhir, R. (2016). PLGA-based nanoparticles: a new paradigm in biomedical applications. *TrAC Trends Anal. Chem.* 80, 30–40. doi: 10.1016/j.trac.2015.06.014

Shembekar, N., Chaipan, C., Utharala, R., and Merten, C. A. (2016). Droplet-based microfluidics in drug discovery, transcriptomics and high-throughput molecular genetics. *Lab Chip* 16, 1314–1331. doi: 10.1039/c6lc00249h

Shen, X., Li, T., Chen, Z., Xie, X., Zhang, H., Feng, Y., et al. (2019). NIR-light-triggered anticancer strategy for dual-modality imaging-guided combination therapy via a bioinspired hybrid PLGA nanoplatform. *Mol. Pharm.* 16, 1367–1384. doi: 10.1021/acs.molpharmaceut.8b01321

Shkodra-Pula, B., Grune, C., Traeger, A., Vollrath, A., Schubert, S., Fischer, D., et al. (2019). Effect of surfactant on the size and stability of PLGA nanoparticles encapsulating a protein kinase C inhibitor. *Int. J. Pharm.* 566, 756–764. doi: 10.1016/j.ijpharm.2019.05.072

Siegel, R. L., Miller, K. D., and Jemal, A. (2019). Cancer statistics, 2019. *CA Cancer J. Clin.* 69, 7–34. doi: 10.3322/caac.21551

Singh, A. P., Biswas, A., Shukla, A., and Maiti, P. (2019). Targeted therapy in chronic diseases using nanomaterial-based drug delivery vehicles. *Signal Transduct. Target. Ther.* 4:33. doi: 10.1038/s41392-019-0068-3

Singh, N. K., Singh, S. K., Dash, D., Gonugunta, P., Misra, M., and Maiti, P. (2013). CNT induced β-phase in polylactide: unique crystallization, biodegradation, and biocompatibility. *J. Phys. Chem. C* 117, 10163–10174. doi: 10.1021/jp4009042

Singh, R. P., and Ramarao, P. (2013). Accumulated polymer degradation products as effector molecules in cytotoxicity of polymeric nanoparticles. *Toxicol. Sci.* 136, 131–143. doi: 10.1093/toxsci/kft179

Soh, S. H., and Lee, L. Y. (2019). Microencapsulation and nanoencapsulation using supercritical fluid (SCF) techniques. *Pharmaceutics* 11:21. doi: 10.3390/pharmaceutics11010021

Song, X., Zhao, Y., Wu, W., Bi, Y., Cai, Z., Chen, Q., et al. (2008). PLGA nanoparticles simultaneously loaded with vincristine sulfate and verapamil hydrochloride: systematic study of particle size and drug entrapment efficiency. *Int. J. Pharm.* 350, 320–329. doi: 10.1016/j.ijpharm.2007.08.034

Streck, S., Clulow, A. J., Nielsen, H. M., Rades, T., Boyd, B. J., McDowell, A., et al. (2019). The distribution of cell-penetrating peptides on polymeric nanoparticles prepared using microfluidics and elucidated with small angle X-ray scattering. *J. Colloid Interface Sci.* 555, 438–448. doi: 10.1016/j.jcis.2019.08.007

Strohbehn, G., Coman, D., Han, L., Ragheb, R. R. T., Fahmy, T. M., Huttner, A. J., et al. (2015). Imaging the delivery of brain-penetrating PLGA nanoparticles in the brain using magnetic resonance. *J. Neurooncol.* 121, 441–449. doi: 10.1007/s11060-014-1658-0

Su, Y. H., Chiang, P. C., Cheng, L. J., Lee, C. H., Swami, N. S., and Chou, C. F. (2015). High aspect ratio nanoimprinted grooves of poly(lactic-co-glycolic acid) control the length and direction of retraction fibers during fibroblast cell division. *Biointerphases* 10:041008. doi: 10.1116/1.4936589

Sun, X., Xu, C., Wu, G., Ye, Q., and Wang, C. J. P. (2017). Poly (lactic-co-glycolic acid): applications and future prospects for periodontal tissue regeneration. *Polymers* 9:E189. doi: 10.3390/polym9060189

Swider, E., Koshkina, O., Tel, J., Cruz, L. J., de Vries, I. J. M., and Srinivas, M. (2018). Customizing poly(lactic-co-glycolic acid) particles for biomedical applications. *Acta Biomater.* 73, 38–51. doi: 10.1016/j.actbio.2018.04.006

Trujillo-Nolasco, R. M., Morales-Avila, E., Ocampo-García, B. E., Ferro-Flores, G., Gibbens-Bandala, B. V., Escudero-Castellanos, A., et al. (2019). Preparation and in vitro evaluation of radiolabeled HA-PLGA nanoparticles as novel MTX delivery system for local treatment of rheumatoid arthritis. *Mater. Sci. Eng. C Mater. Biol. Appl.* 103:109766. doi: 10.1016/j.msec.2019.109766

Tulinska, J., Kazimirova, A., Kuricova, M., Barancokova, M., Liskova, A., Neubauerova, E., et al. (2015). Immunotoxicity and genotoxicity testing of PLGA-PEO nanoparticles in human blood cell model. *Nanotoxicology* 9(Suppl. 1), 33–43. doi: 10.3109/17435390.2013.816798

Turon, P., del Valle, L., Alemán, C., and Puiggalí, J. (2017). Biodegradable and biocompatible systems based on hydroxyapatite nanoparticles. *Appl. Sci.* 7:60. doi: 10.3390/app7010060

U.S. National Library of Medicine (2019). Available at: https://clinicaltrials.gov/ct2/results?cond=&term=plga&cntry=&state=&city=&dist= (accessed December 10, 2019). doi: 10.1007/s13233-019-7119-z

Verma, D., Gulati, N., Kaul, S., Mukherjee, S., and Nagaich, U. (2018). Protein based nanostructures for drug delivery. *J. Pharm.* 2018:9285854. doi: 10.1155/2018/9285854

Vey, E., Rodger, C., Booth, J., Claybourn, M., Miller, A. F., and Saiani, A. (2011). Degradation kinetics of poly (lactic-co-glycolic) acid block copolymer cast films in phosphate buffer solution as revealed by infrared and Raman spectroscopies. *Polym. Degrad. Stab.* 96, 1882–1889. doi: 10.1016/j.polymdegradstab.2011.07.011

Vhora, I., Patil, S., Bhatt, P., Gandhi, R., Baradia, D., and Misra, A. (2014). Receptor-targeted drug delivery: current perspective and challenges. *Ther. Deliv.* 5, 1007–1024. doi: 10.4155/tde.14.63

Vllasaliu, D., Fowler, R., and Stolnik, S. (2014). PEGylated nanomedicines: recent progress and remaining concerns. *Expert Opin. Drug Deliv.* 11, 139–154. doi: 10.1517/17425247.2014.866651

Wang, Y., Li, P., Truong-Dinh Tran, T., Zhang, J., and Kong, L. (2016). Manufacturing techniques and surface engineering of polymer based nanoparticles for targeted drug delivery to cancer. *Nanomaterials* 6:E26. doi: 10.3390/nano6020026

Wilkosz, N., Łazarski, G., Kovacik, L., Gargas, P., Nowakowska, M., Jamroìz, D., et al. (2018). Molecular insight into drug-loading capacity of PEG–PLGA nanoparticles for itraconazole. *J. Phys. Chem. B* 122, 7080–7090. doi: 10.1021/acs.jpcb.8b03742

Xi, J., Wang, W., Da, L., Zhang, J., Fan, L., Gao, L., et al. (2018). Au-PLGA hybrid nanoparticles with catalase-mimicking and near-infrared photothermal activities for photoacoustic imaging-guided cancer therapy. *ACS Biomater. Sci. Eng.* 4, 1083–1091. doi: 10.1021/acsbiomaterials.7b00901

Xu, Q., Hashimoto, M., Dang, T. T., Hoare, T., Kohane, D. S., Whitesides, G. M., et al. (2009). Preparation of monodisperse biodegradable polymer microparticles using a microfluidic flow-focusing device for controlled drug delivery. *Small* 5, 1575–1581. doi: 10.1002/smll.200801855

Yang, H., Li, J., Patel, S. K., Palmer, K. E., Devlin, B., and Rohan, L. C. (2019). Design of poly (lactic-co-glycolic acid)(PLGA) nanoparticles for vaginal co-delivery of griffithsin and dapivirine and their synergistic effect for HIV prophylaxis. *Pharmaceutics* 11:E184.

Yang, X. (2019). Design and optimization of crocetin loaded PLGA nanoparticles against diabetic nephropathy via suppression of inflammatory biomarkers: a formulation approach to preclinical study. *Drug Deliv.* 26, 849–859. doi: 10.1080/10717544.2019.1642417

Yin, Q. (2019). *Abstract B142: Activation of Endogenous Anergic Self-Specific CD8+ T-Cells by Polymeric Nanoparticles for Enhanced Cancer Immunotherapy*. Philadelphia, PA: AACR.

Yoo, J., Park, C., Yi, G., Lee, D., and Koo, H. (2019). Active targeting strategies using biological ligands for nanoparticle drug delivery systems. *Cancers* 11:E640. doi: 10.3390/cancers11050640

Zhang, K., Tang, X., Zhang, J., Lu, W., Lin, X., Zhang, Y., et al. (2014). PEG–PLGA copolymers: their structure and structure-influenced drug delivery applications. *J. Control. Release* 183, 77–86. doi: 10.1016/j.jconrel.2014.03.026

Zhang, M., He, J., Zhang, W., and Liu, J. (2018). Fabrication of TPGS-stabilized liposome-PLGA hybrid nanoparticle via a new modified nanoprecipitation approach: *in vitro* and *in vivo* evaluation. *Pharm. Res.* 35:199. doi: 10.1007/s11095-018-2485-3

Zhang, Z., and Feng, S.-S. (2006). The drug encapsulation efficiency, in vitro drug release, cellular uptake and cytotoxicity of paclitaxel-loaded poly(lactide)–tocopheryl polyethylene glycol succinate nanoparticles. *Biomaterials* 27, 4025–4033. doi: 10.1016/j.biomaterials.2006.03.006

Zhao, P., Grabinski, T., Gao, C., Skinner, R. S., Giambernardi, T., Su, Y., et al. (2007). Identification of a met-binding peptide from a phage display library. *Clin. Cancer Res.* 13, 6049–6055. doi: 10.1158/1078-0432.CCR-07-0035

Conflict of Interest: The authors declare that the research was conducted in the absence of any commercial or financial relationships that could be construed as a potential conflict of interest.

frontiers in Bioengineering and Biotechnology

ORIGINAL RESEARCH
published: 21 February 2020
doi: 10.3389/fbioe.2020.00100

Chitosan Nanoparticles: Shedding Light on Immunotoxicity and Hemocompatibility

Sandra Jesus[1†], *Ana Patrícia Marques*[1†], *Alana Duarte*[1,2†], *Edna Soares*[1,2], *João Panão Costa*[1,2], *Mariana Colaço*[1,2], *Mélanie Schmutz*[3], *Claudia Som*[3], *Gerrit Borchard*[4], *Peter Wick*[5] *and Olga Borges*[1,2*]

[1] *Center for Neuroscience and Cell Biology, University of Coimbra, Coimbra, Portugal,* [2] *Faculty of Pharmacy, University of Coimbra, Coimbra, Portugal,* [3] *Laboratory for Technology and Society, Empa Swiss Laboratories for Materials Science and Technology, St. Gallen, Switzerland,* [4] *Institute of Pharmaceutical Sciences of Western Switzerland, University of Geneva, Geneva, Switzerland,* [5] *Laboratory for Particles-Biology Interactions, Empa Swiss Laboratories for Materials Science and Technology, St. Gallen, Switzerland*

OPEN ACCESS

Edited by:
Mustafa Culha,
Yeditepe University, Turkey

Reviewed by:
Subhra Mandal,
Creighton University, United States
Nanasaheb D. Thorat,
University of Limerick, Ireland

***Correspondence:**
Olga Borges
olga@ci.uc.pt

[†] *These authors have contributed equally to this work*

Specialty section:
This article was submitted to Nanobiotechnology, a section of the journal Frontiers in Bioengineering and Biotechnology

Received: *31 October 2019*
Accepted: *03 February 2020*
Published: *21 February 2020*

Citation:
Jesus S, Marques AP, Duarte A, Soares E, Costa JP, Colaço M, Schmutz M, Som C, Borchard G, Wick P and Borges O (2020) Chitosan Nanoparticles: Shedding Light on Immunotoxicity and Hemocompatibility. Front. Bioeng. Biotechnol. 8:100. doi: 10.3389/fbioe.2020.00100

Nanoparticles (NPs) assumed an important role in the area of drug delivery. Despite the number of studies including NPs are growing over the last years, their side effects on the immune system are often ignored or omitted. One of the most studied polymers in the nano based drug delivery system field is chitosan (Chit). In the scientific literature, although the physicochemical properties [molecular weight (MW) or deacetylation degree (DDA)] of the chitosan, endotoxin contamination and appropriate testing controls are rarely reported, they can strongly influence immunotoxicity results. The present work aimed to study the immunotoxicity of NPs produced with different DDA and MW Chit polymers and to benchmark it against the polymer itself. Chit NPs were prepared based on the ionic gelation of Chit with sodium tripolyphosphate (TPP). This method allowed the production of two different NPs: Chit 80% NPs (80% DDA) and Chit 93% NPs (93% DDA). In general, we found greater reduction in cell viability induced by Chit NPs than the respective Chit polymers when tested *in vitro* using human peripheral blood monocytes (PBMCs) or RAW 264.7 cell line. In addition, Chit 80% NPs were more cytotoxic for PBMCs, increased reactive oxygen species (ROS) production (above 156 μg/mL) in the RAW 264.7 cell line and interfered with the intrinsic pathway of coagulation (at 1 mg/mL) when compared to Chit 93% NPs. On the other hand, only Chit 93% NPs induced platelet aggregation (at 2 mg/mL). Although Chit NPs and Chit polymers did not stimulate the nitric oxide (NO) production in RAW 264.7 cells, they induced a decrease in lipopolysaccharide (LPS)-induced NO production at all tested concentrations. None of Chit NPs and polymers caused hemolysis, nor induced PBMCs to secrete TNF-α and IL-6 cytokines. From the obtained results we concluded that the DDA of the Chit polymer and the size of Chit NPs influence the *in vitro* immunotoxicity results. As the NPs are more cytotoxic than the corresponding polymers, one should be careful in the extrapolation of trends from the polymer to the NPs, and in the comparisons among delivery systems prepared with different DDA chitosans.

Keywords: chitosan nanoparticle, immunotoxicity, hemocompatibility, deacetylation degree, endotoxin-free, inflammation, reactive oxygen species, PBMCs

INTRODUCTION

Studies have shown that nanoparticles (NPs) can interact with different components of the immune system, resulting in immunosuppression and in immunostimulation (Dobrovolskaia and McNeil, 2007). Although these interactions can be purposeful and desirable in increasing the efficacy of vaccines, cancer immunotherapy or immunotherapies for autoimmune diseases, they can also be unexpected and undesirable, causing hypersensitivity reactions, anaphylaxis, coagulopathies and body defense decrease (Dobrovolskaia and McNeil, 2007).

Chitosan (Chit) is the common name given to a family of natural polysaccharide polymers obtained from the deacetylation of chitin. Chit is a cationic polymer, considered non-toxic, biodegradable and biocompatible and is therefore extensively investigated in nanobiomedical research (Ali and Ahmed, 2018). Chit has been granted FDA Generally Recognized As Safe (GRAS) designation (GRN n° 73, 170, 397 and 443) and is widely used in dietary supplements (U.S. FDA, 2019a) as well as in medical devices, such as wound dressings and gels (U.S. FDA, 2019b). Chit is known for its mucoadhesive properties and its ability to stimulate cells of the immune system, which supports the value of investigating Chit NPs as vaccine adjuvants (Dedloff et al., 2019). For this purpose, it has long been used by the group with various antigens, such as the hepatitis B surface antigen (HBsAg) (Borges et al., 2008; Lebre et al., 2016; Jesus et al., 2017, 2018; Soares et al., 2018a,b; Bento et al., 2019), the protective antigen (PA) from anthrax (Bento et al., 2015) or antigens from *Schistosoma mansoni* (Oliveira et al., 2012). Nevertheless, in the literature, Chit NPs have also been tested as drug delivery systems, without considering its immunomodulatory activity. An example of this situation is the numerous studies with the encapsulation of insulin into chitosan particles (Al Rubeaan et al., 2016). Furthermore, although there are several studies evaluating Chit NP toxicity *in vitro*, most of them do not assess the dysregulation of the immune system function (immunotoxicity). From the ones that do, the results are frequently contradictory. These contradictions and ambiguity may be due to differences in the used Chit polymers or *in vitro* methodology, namely the cellular model, NP concentration and incubation period. Moreover, it has been observed that most of the studies do not properly characterize, or at least do not report, both the polymer and the derived NPs, nor use or report adequate controls to screen NP interferences or monitor the presence of endotoxin contamination (Jesus et al., 2019). Notably, in the context of Safe-by-Design (SbD) of new polymeric NPs for drug delivery, it is necessary to rely on assertive results of immunotoxicity and hemocompatibility, obtained with properly characterized polymeric NPs.

The aim of this study is to explore the influence of the DDA of Chit polymer on immunotoxicity and hemocompatibility of Chit NPs. Therefore, murine RAW 264.7 cells, Peripheral Blood Mononuclear Cells (PBMCs) and whole blood were used as representative *in vitro* models for the immune system.

Nitric oxide (NO), reactive oxygen species (ROS) and cytokine production, cell viability, hemolysis, coagulation times and platelet aggregation were studied using appropriate controls under endotoxin-free conditions, and following protocols and recommendations, with slight changes, described by the European Nanomedicine Characterization Laboratory (EU-NCL) (EU-NCL, 2019).

MATERIALS AND METHODS

Chitosan Polymers

Two different low molecular weight (LMW) Chitosans (ChitoClear™) were kindly donated by Primex BioChemicals AS (Avaldsnes, Norway). According to the supplier's specifications, one Chit had a lower deacetylation degree (DDA) and a viscosity of 13 cP (1% solutions in 1% acetic acid), while the other had higher DDA and a viscosity of 71 cP. Their exact DDA was found to be 80 and 93%, respectively, using the methodology described below.

The polymers were purified using a routine technique used in our laboratory and previously described by us (Lebre et al., 2019). Briefly, 1 g of Chit was suspended in 10 mL NaOH (1 M) solution. This suspension was heated between 40 and 50°C under continuous magnetic stirring for 3 h. After this time, the suspension was allowed to reach room temperature and was filtered using a Buchner funnel. Insoluble Chit on the filter was washed with water and then recovered to be further dissolved in 200 mL of 1% acetic acid solution and stirred for 1 h at room temperature. The Chit solution was then filtered through a 0.45 μm filter and 1 M NaOH solution was used to adjust the pH of the filtrate to pH 8.0 to precipitate Chit. The precipitate was then washed with water through three consecutives 30 min centrifugations at 4500 × g. The precipitate was recovered and freeze dried. To note that deionized water was used to obtain the purified polymer for the first experiments, optimization of the NP production method and physicochemical characterization, while LPS-free water was used to obtain LPS-free chitosan for cell *in vitro* studies. The purified polymers were used in all the methods described below.

Chit deacetylation degree and mean molecular weight were obtained by nuclear magnetic resonance (^{1}H-NMR) and by size exclusion chromatography (SEC), respectively.

Deacetylation degree was determined as previously described (Lavertu et al., 2003). The DDA was calculated using the peaks of proton at the position 1 of deacetylated (H1D) and acetylated (H1A) monomer:

$$\text{DDA (\%)} = \left(\frac{\text{H1D}}{\text{H1D} + \text{H1A}}\right) \times 100 \quad (1)$$

where H1D is shifted at 5.21 ppm and H1A at 4.92 ppm.

For Chit molecular weight (MW) analysis, two types of Chit polymers (before and after purification) were dissolved in 0.1 M acetic buffer (pH 4.0) containing 0.3 M NaCl to obtain 1 mg/mL solutions. Then they were filtered through 0.22 μm filters and collected in the chromatographic sample vials. For each analysis, 100 μL were injected at a flow rate of 1 mL/min at room temperature. Each sample was measured in triplicate. The interpretation of the obtained results was done using Mnova software.

Chit polymer particle size (micrometer range) was also characterized in acetate buffer and cell culture media using Beckman Coulter LS 13 320 Laser Diffraction Particle Size Analyzer (Beckman Coulter Inc., Brea, CA, USA).

Preparation and Characterization of Chitosan Nanoparticles

To prepare both Chit NPs, each of the polymers (Chit 80% DDA and Chit 93% DDA) were dissolved at 0.1% (w/v) concentration in 1% (v/v) of acetic acid, and the pH was further adjusted to 4.6–4.8 using 10 N NaOH. Chit NPs spontaneously formed upon dropwise addition of 1.750 mL of sodium tripolyphosphate (TPP, 0.16% w/v) to 10 mL of Chit solution under high-speed homogenization. The final suspension remained in maturation during 30 min under magnetic stirring.

Chit NPs produced with Chit with 80% DDA were concentrated, washed with LPS-free water and concentrated again by centrifugation using Vivaspin 20 centrifugal concentrator (MWCO 300 kDa, 3,000 g). Chit NPs produced with Chit with 93% DDA were concentrated by centrifugation at 10,000 g (15 min) and centrifuged again at 7,000 g (15 min) with LPS-free water.

To evaluate if all the Chit polymer used for the NP production was effectively cross-linked with TPP, Cibacron Brilliant Red 3B-A dye assay (Muzzarelli, 1998) was used to quantify the free Chit that remained in solution after NPs preparation. The quantification was performed in 3 mL of the supernatants obtained by the previously described centrifugations, which were added to 100 μL of glycin/HCl buffer, 1 mL of the dye solution (0.015% dye in water, w/v) and 900 μL of ultra-pure water. The samples were left for 20 min in agitation and then the absorbance was read at 575 nm. The quantification was performed by interpolating the values with the values from a calibration curve ranging from 0.0004 to 0.0020% of Chit. The concentration of the Chit NPs was calculated subtracting to the initial mass of the chit used to prepare the NPs, the mas of free chitosan.

Delsa™ Nano C particle analyzer (Beckman Coulter, CA, USA) was used to measure NP size by dynamic light scattering (DLS) and the zeta potential through electrophoretic light scattering (ELS). Samples comprised the aqueous concentrated dispersions obtained after centrifugation, which were diluted with water before the measurements.

Concentrated samples of Chit NPs were tested for physicochemical stability when dispersed in cell culture media at 37°C for a maximum of 24 h. The resulting particle size and zeta potential were evaluated in Delsa™ Nano C particle analyzer (Beckman Coulter, CA, USA).

Images of Chit NPs, were acquired by two microscopy techniques. Transmission Electron Microscopy (TEM) using a FEI-Tecnai G2 Spirit Biotwin, (20–120) kV microscope (FEI company, Hillsboro, OR, USA) with NPs dispersed in water and subsequently dried out in the grid and observed with no contrast. For the second microscopy technique, a High resolution Scanning Electron CryoMicroscope (CryoSEM) (JEOL JSM 6301F/ Oxford INCA Energy 350/ Gatan Alto 2500) was used. The NP suspension was rapidly cooled in slush nitrogen, fractured and sublimated for 120 s at −90°C, before coating with Au/Pd. The sample was studied at −150°C.

For *in vitro* immunotoxicity studies, Chit purification and Chit NP production were conducted under endotoxin-free conditions following a methodology already published by our group (Lebre et al., 2019). All the reagents involved in NP production were tested with an endotoxin detection kit (Pyrochrome® Endpoint Chromogenic Endotoxin Testing, maximum sensitivity of 0.001 EU/mL, Associates of Cape Cod, Inc., East Falmouth, MA, USA) according to manufacturer's instructions.

In vitro Studies With RAW 264.7 Cell Line

RAW 264.7 cell line (ATCC® TIB-71™) was acquired from ATCC (Manassas, VA, USA), cultured in Dulbecco's modified eagle's medium (DMEM, supplemented with 10% heat inactivated fetal bovine serum (FBS), 1% Penicillin/Streptomycin, 10 mM HEPES and 3.7 g/L sodium bicarbonate) and used until passage 18.

Cell Viability

The Cell viability of Chit NP and polymers was evaluated in RAW 264.7 cells using the 3-(4,5-dimethylthiazol-2-yl)-2,5-diphenyltetrazolium bromide (MTT) assay, performed in 96-well plates and cells plated at a density of 2×10^4 cells per well. Serial dilutions of Chit NPs and Chit polymers ranged from 312 to 5,000 μg/mL final concentration in the well were incubated with the cells for 24 h, at 37°C and 5% CO_2. Simultaneously, the NPs solvent (supernatant from the last washing centrifugation) and the polymer solvent (acetate buffer) were also tested in a dilution equivalent to the most concentrated samples. Then, 20 μL of MTT solution (5 mg/mL, in PBS) were added to each well and incubated for additional 1 h 30 min. To ensure the dissolution of the formazan crystals, cell culture medium was replaced by 200 μL of dimethyl sulfoxide (DMSO).

The resultant colored solution OD was measured at 540 nm and 630 nm. Cell viability (%) was calculated by the following equation:

$$\text{Cell viability (\%)} = \frac{(\text{OD sample (540 nm)} - \text{OD sample (630 nm)})}{(\text{OD control (540 nm)} - \text{OD control (630 nm)})} \times 100 \quad (2)$$

The half maximal inhibitory concentration (IC50) of NPs that cause death or inhibition of the growth of 50% of cells was calculated by using the Log (NP concentration) vs. normalized response - variable slope analysis for the non-linear fit using Prism 6.0 (GraphPad Software, San Diego, CA, USA).

Interference controls were performed to guarantee the validity of the assay with the samples as suggested by Rösslein et al. (2015). Therefore, NPs and polymers in cell culture media without cells were plated in 96-well plates and the absorbance was measured (540 and 630 nm).

Production of Reactive Oxygen Species

The production reactive oxygen species (ROS) was assessed using the dichlorofluorescein diacetate (DCFH-DA) probe (Molecular Probes®, Life Technologies, Eugene, OR, USA). RAW 264.7 cells

were incubated in black 96-well plates for 24 h at 37°C and 5% CO_2, at a density of 0.5×10^5 cells per well.

After that, serial dilutions of Chit NPs and Chit polymers (38 μg/mL to 156 μg/mL) were incubated with the cells in DMEM for 24 h at 37°C and 5% CO_2, to evaluate ROS stimulation. The NPs solvent (supernatant from the last washing centrifugation) and the polymer solvent (acetate buffer) were also tested in a dilution equivalent to the most concentrated samples. Lipopolysaccharide (LPS, 1 μg/mL, from Salmonella enterica serotype minnesota, Sigma-Aldrich, Saint Louis, MO, USA) was used as a positive control or in combination with the same NP and polymer concentrations to test if the NPs were able to inhibit LPS stimulated ROS production.

Then, the cell culture medium was replaced by DCFH-DA (50 μM) in serum-free DMEM and the cells were incubated for additional 2 h at 37°C and 5% CO_2. The resulting fluorescence was read at 485/20 (excitation) and 528/20 nm (emission) wavelengths.

To calculate the stimulation of ROS production (fluorescence fold increase) or the inhibition of ROS production (%) upon stimulation with LPS apply the following Equation (3) and (4), respectively.

$$\text{ROS production} = \frac{\text{Fluorescence}_{\text{SAMPLE}}}{\text{Fluorescence}_{\text{NEGATIVE CONTROL}}} \quad (3)$$

$$\text{ROS inhibition}(\%) = \frac{\text{Fluorescence}_{\text{SAMPLE}}}{\text{Fluorescence}_{\text{POSITIVE CONTROL}}} \times 100 \quad (4)$$

Interference controls were performed to guarantee the validity of the assay with the samples. Therefore, NPs and polymers in cell culture media without cells were plated in black 96-well plates and all procedures were followed as in the original assay described.

Nitric Oxide Production

Nitric oxide (NO) has a short half-life in oxygen-containing aqueous solutions, often attributed to a rapid oxidation to nitrite. Therefore, NO production by RAW 264.7 cells was estimated based on nitrite quantification using the Griess reagent [1% (w/v) sulphanilamide mixed with 0.1% (w/v) naphthylethylenediamine dihydrochloride (1:1), both solutions previously dissolved in 2.5% (v/v) phosphoric acid].

RAW 264.7 cells were incubated in 48-well plates at a density of 2.25×10^5 cells per well for 24 h at 37°C and 5% CO_2. After that, cell culture medium was replaced by serial dilutions of Chit NPs and Chit polymers (38–156 μg/mL), diluted in cell culture medium without phenol red, and cells incubated for 24 h at 37°C and 5% CO_2. The NPs solvent (supernatant from the last washing centrifugation) and the polymer solvent (acetate buffer) were also tested in a dilution equivalent to the most concentrated samples. LPS was used as a positive control (1 μg/mL). To test whether the NPs were able to inhibit LPS stimulated NO production, the same NP and polymer concentrations were incubated together with LPS (1 μg/mL).

After that, 100 μL of each cell supernatant were collected and plated in a 96-well plate and combined with an equal volume of the Griess Reagent. Several sodium nitrite solutions (0 μM to 80 μM) were also plated in duplicate to perform the calibration curve. The absorbance (Abs) of the samples was measured at 550 nm and the NO concentration (μM) was extrapolated from the calibration curve.

To calculate the inhibition of NO production upon stimulation with LPS, the Equation (5) was used.

$$\text{NO inhibition}(\%) = \frac{[\text{NO}]\ (\mu\text{M})_{\text{SAMPLE}}}{[\text{NO}]\ (\mu\text{M})_{\text{POSITIVE CONTROL}}} \times 100 \quad (5)$$

Interference control was performed to guarantee the validity of the assay with the samples containing the particles. Therefore, 100 μL of NPs and polymers in DMEM without phenol red and without cells were plated in 96-well plates. Additionally, the NO calibration curve was performed in the presence of NPs and polymers, by plating in 96-well plates 50 μL of the samples and 50 μL of the standards used in calibration curve. Then, an equal volume of the Griess Reagent was added to each well and the absorbance was read as described above. This interference control was made at least in duplicate.

In vitro Studies With Peripheral Blood Mononuclear Cells

PBMC Isolation

Peripheral blood (buffy coat) was kindly given by IPST, IP (Coimbra, PT) and was obtained from healthy donors in heparinized syringes followed by serum depletion. PMBCs were isolated on a density gradient with Lymphoprep (Axis-Shield, Dundee, SCT) according to the provider's guidance protocol, with minor modifications. Briefly, the blood dilution performed was 1:5 (v/v) in 0.9% sodium chloride, the centrifugation step was performed at 1,190 × g for 20 min (20°C) and the mononuclear cell dense ring was collected and washed with PBS (pH = 7.4 at 37°C) through consecutive centrifugations (487 × g, 10 min, 20°C) until the supernatant was clear. At the end, cells were suspended in Roswell Park Memorial Institute Medium (RPMI 1640) supplemented with 1% Penicillin/Streptomycin and 10% heat-inactivated FBS.

Cell Viability

Chit NP and polymer toxicity in PBMCs was assessed by MTT as described previously for RAW 264.7 cells, with some modifications. Briefly, cells were plated at a concentration of 7.5×10^6 cells/well, test samples ranged from 2.44 to 5,000 μg/mL and MTT incubation was prolonged for 4 h. To ensure the dissolution of the formazan crystals, cell culture plates were centrifuged (800 × g, 25 min, 20°C) and 180 μL/well of the culture medium were replaced by an equal volume of DMSO.

Cell viability results obtained with the MTT assay were confirmed with propidium iodide (PI) assay, using four different NP concentrations. Cells incubated with the NPs were centrifuged (800 × g, 25 min, 20°C), resuspended in PBS and collected for flow cytometry analysis (BD FACSCalibur, BD Biosciences, Bedford, MA, USA). A volume of 2 μL of PI solution was added immediately before the analysis to achieve a final concentration of 0.5 μg/mL.

Cytokine Secretion

To analyze the cytokine secretion induced by Chit NPs, cells were plated in 96-well plates at a density of 2.5×10^5 cells per well. Chit NPs and polymers (100 μg/mL) and positive controls (LPS 2 ng/mL, Con A 5 μg/mL) were incubated with the cells for 24 h, at 37°C and 5% CO_2. Then, cell culture plates were centrifuged (800 × g, 25 min, 20°C) and the supernatants were collected for Enzyme-Linked Immunosorbent Assay (ELISA) according to manufacturer's instructions (Human TNF-α and IL-6 Standard TMB ELISA Development Kit, Peprotech, NJ, USA).

Interference controls were performed to guarantee the validity of the assay with the samples. Therefore, NPs and polymers in RPMI were incubated for 24 h, at 37°C and 5% CO_2 without cells, in the presence of several concentrations of cytokine standards (TNF-α and IL-6), as used in the ELISA calibration curve. The same concentrations of each cytokine were also incubated in RPMI in the absence of the samples. After that time, supernatants were collected and analyzed by ELISA as described for the samples with cells, according to manufacturer's instructions.

In vitro Studies With Human Blood

Blood was collected from healthy volunteers at the Clinical Laboratory Analysis of Faculty of Pharmacy (University of Coimbra, Portugal). A written informed consent was obtained from all participants. Anonymous blood samples were used by the researchers for the hematological *in vitro* assays.

Hemolysis Assay

To perform hemolysis assay, plasma free hemoglobin (PFH) concentration was required to be below 1.0 mg/mL. Whole blood was collected in heparinized tubes and diluted in PBS to adjust total blood hemoglobin (TBH) concentration to 10 mg/mL ± 2 mg/mL (TBHd). A volume of 100 μL of cyanmethemoglobin (CMH, blank), Chit NP suspensions, Chit polymer suspensions, PBS (negative control), Triton-X-100 (positive control) or NPs solvent (interference control) were added to 700 μL of PBS in different tubes. Then, 100 μL of TBHd was added and incubated at 37°C for 3 h ± 15 min. NPs were also incubated with PBS without blood to evaluate the possible NP interference with the assay. Then, the mixture was centrifuged at 800 × g for 15 min. A volume of 100 μL of supernatant and 100 μL of CMH reagent were added to a 96-well plate. The CMH reagent was prepared by mixing 1,000 mL Drabkin's reagent and 0.5 mL of 30% Brij 35 solution (Sigma-Aldrich, Saint Louis, MO, USA). The absorbance (OD) was read at 540 nm. The percentage of hemolysis was calculated using the following equation:

$$\text{Hemolysis (\%)} = \frac{(\text{OD sample (540 nm)} - \text{OD negative control (540 nm)})}{(\text{OD TBHd (540 nm)} - \text{OD negative control (540 nm)})} \times 100 \quad (6)$$

Coagulation Assay

The two pathways of blood coagulation, the activated partial thromboplastin time (APTT) and the prothrombin time (PT) were separately tested. Blood was collected using sodium citrate tubes and the plasma was obtained by centrifugation of the blood at 2500 × g for 10 min. Plasma (450 μL) was incubated with a volume of 50 μL of Chit NPs and Chit polymer suspensions (two final concentrations: 0.1 and 1 mg/mL), for 30 min at 37°C. Then, samples were evaluated using Bio-TP LI (PT) and Bio-CK (APTT) kits (Biolabo S.A.S., Maizy, France) according to manufacturer's instructions, in an Option 4 plus coagulation analyzer (BioMérieux, Marcy-l'Étoile, France).

Platelet Aggregation Assay

Platelet-rich plasma (PRP) was obtained from blood collected in sodium citrate tubes, and centrifuged at 200 × g for 16 min. Platelet-free plasma (PFP) was obtained after blood centrifugation at 2,500 × g for 10 min, followed by plasma centrifugation at 18,000 × g for 5 min. A volume of 100 μL of PRP or 100 μL of PFP were added to 96-well plates and incubated for 5 min at 37°C. A volume of 25 μL of Chit NPs at 2 mg/mL, saline solution (negative control) and calcium chloride 0.25 M or collagen (positive controls) were added to the wells with PRP and incubated for 30 min at 37°C. Then, 4 μL of Giemsa dye was added to each well and incubated for 5 min. Finally, a 1:200 dilution with saline solution was applied for platelet counting (PC) using a light microscope. Chit NPs were also incubated with PFP to evaluate the NPs interference in plasma.

The percentage of platelet aggregation was calculated using the equation 7.

$$\text{Platelet aggregation (\%)} = \frac{(\text{PC negative control} - \text{PC sample})}{\text{PC negative control}} \times 100 \quad (7)$$

Statistical Analysis

Results were expressed as mean ± standard error of the mean (SEM). Prism 6.0 (GraphPad Software, San Diego, CA) was used for all statistical analysis. Statistical significance was assessed using one-way ANOVA.

RESULTS

Physicochemical Characterization of Polymers and Nanoparticles

Polymer Purification Reduces the Molecular Weight of the Lower Deacetylation Degree Chitosan

The characterization of the polymers used and the nanoparticulate delivery system developed is critical to prevent erroneous interpretations of resultant immunotoxicity findings. Different Chit characteristics can have different biological effects. Unfortunately, most studies addressing biological activity of Chit NPs lack the used polymer characterization, which also restricts comparisons among studies.

The two Chit polymers used in this study were purified under endotoxin-free conditions to eliminate possible contaminants. Since the purification process involves harsh conditions, namely heating the polymer suspension in NaOH 1 M, their DDA and MW were assessed before and after purification and the results presented in **Table 1A**. Chit deacetylation experienced no significant alterations, resulting in polymers with 80 and 93% DDA (Chit 80% and Chit 93%, respectively). In contrast, the MW before and after purification for the lower DDA Chit (Chit 80%) was altered. An important decrease from 168 to 49 kDa is compatible with the fact that lower DDA Chit has higher

TABLE 1 | Physicochemical characterization of Chit polymers and NPs. (A) Polymer molecular weight (MW), deacetylation degree (DDA), and size in acetate buffer and after resuspension in DMEM and RPMI at 37°C (Mean ± SEM). (B) Chit 80% and Chit 93% NPs size, polydispersity index and zeta potential (ζ), in water and after resuspension DMEM and RPMI at 37°C *(Mean ± SEM)*. (C) Endotoxin contamination evaluated with the Pyrochrome kit for Chit 80% NPs, Chit 93% NPs, Chit 80%, and Chit 93% and TPP solution. Endotoxin contamination of pyrogen-free water was also evaluated for comparison. Mean ± SEM; n = 3 (three different batches).

A

	MW (kDa) (n = 1–3)		DDA (%) (n = 1)		Size (μm) ($n \geq 3$)				
					Acetate buffer	DMEM		RPMI	
	Non-purified	Purified	Non-purified	Purified		1 h	24 h	1 h	24 h
Chit 80%	168	49	78	80	612 ± 40	529 ± 39	541 ± 49	628 ± 94	479 ± 58
Chit 93%	127	122	94	93	608 ± 23	590± 37	518 ± 57	555 ± 50	525 ± 53

B

		Water	DMEM		RPMI	
			1 h	24 h	1 h	24 h
Chit 80% NPs	**Size (nm)**	127 ± 5	109 ± 29	133 ± 22	116 ± 29	368 ± 141
($n \geq 3$)	**PDI**	0.28 ± 0.01	0.72 ± 0.03	0.62 ± 0.11	0.47 ± 0.08	0.52 ± 0.03
	ζ (mV)	+29.0 ± 1.0	−4.9 ± 0.2		−2.1 ± 0.4	
Chit 93% NPs	**Size (nm)**	292 ± 52	106 ± 20	147 ± 74	321 ± 48	327 ± 131
($n \geq 3$)	**PDI**	0.18 ± 0.03	0.49 ± 0.14	0.48 ± 0.21	0.91 ± 0.13	0.76 ± 0.16
	ζ (mV)	+20.0 ± 6.0	−3.9 ± 0.6		−4.4 ± 0.5	

C

	Endotoxin (EU/mL) (n = 3)			Endotoxin (EU/mL) (n = 3)	
	Mean	SEM		Mean	SEM
Pyrogen-free water	0.05861	0.00607	**TPP solution**	0.05492	0.00814
Chit 80%	0.06224	0.01815	**Chit 80% NPs**	0.07166	0.01246
Chit 93%	0.06820	0.03252	**Chit 93% NPs**	0.08844	0.03189

enzymatic and acid hydrolysis degradation rate (Kurita et al., 2000; Vårum, 2001; Szymanska and Winnicka, 2015).

Chit is soluble in acidic conditions, which is incompatible with cell culture as it leads to cell death. Therefore, *in vitro* studies with Chit polymers (purified raw material) were performed with Chit suspended in acetate buffer (pH = 5.0), further diluted in cell culture medium (156.25 μg/mL). Particle size in acetate buffer and cell culture media is illustrated in **Table 1A**. The mean average size of these particle suspensions was around 500 μm in all situations.

Chitosan With Higher Molecular Weight and Deacetylation Degree Leads to Larger-Sized NPs

Chit NPs were successfully produced by ionic gelation method, using TPP as the crosslink (Chit 80% NPs and Chit 93% NPs). These NPs were isolated and concentrated in water. Importantly, the analysis of the first supernatants revealed that more than 99% of the Chit used in the production was retained in the NPs. This result was important to calculate Chit NP concentration.

After isolation and concentration, NP mean particle size, polydispersity index (PDI), and zeta potential (ζ) were determined by DLS and ELS, respectively, and are summarized in **Table 1B**. Results illustrate the effect of the different Chit on the NP characteristics. In fact, the same methodology, when applied to Chit polymers with different DDA and MW, resulted in NPs with different sizes. Lowering the DDA from 93 to 80% caused the mean particle size to fall from 292 to 127 nm. These average particle sizes were illustrated by TEM and SEM analysis. The round shape of the NPs was the second conclusion inferred by observing the images (**Figures 1A,B**) of both techniques. Concerning zeta potential, both Chit 93% and Chit 80% NPs presented a positive charge when dispersed in deionized or pyrogen-free water, although slightly more positive for Chit 80% NPs (+20 and +29 mV, respectively).

Due to the complexity of cell culture media, and the variability of their supplementation, results from NP colloidal system characterization in water are not transposable to *in vitro* conditions (Moore et al., 2015). Chit NPs were therefore characterized in cell culture media to understand the changes that NPs experience during *in vitro* studies. Chit 80% and Chit 93% NPs were added to DMEM and RPMI (containing FBS) at 37°C at a concentration of 156.25 μg/mL for further size and PDI measurement after 1 and 24 h, and zeta potential measurement after 1 h (**Table 1B**). Even though the DLS methodology for size analysis in complex media (such as cell culture medium) has limitations, it can give us some insights about changes occurring to the different Chit NPs. Most notably, the suspension

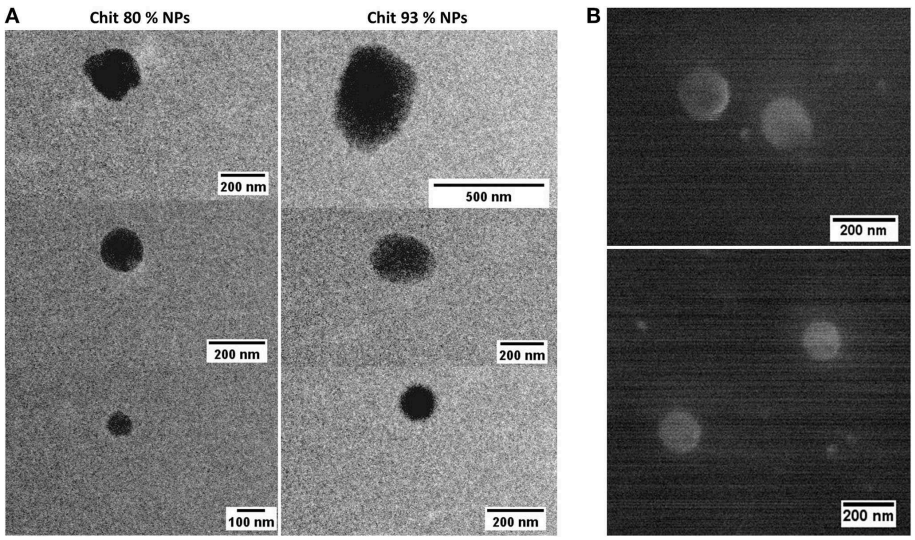

FIGURE 1 | Chit NP illustration by Electron Microscopy. **(A)** Transmission Electron Microscopy (TEM) of Chit 80% NPs, presented in the left side column and of Chit 93% NPs, presented in the right side column. **(B)** Scanning Electron Microscopy (SEM) of Chit 80% NPs.

of both Chit NPs in RPMI and DMEM resulted in increased PDI, meaning an increase of the size heterogeneity. The zeta potential of the NPs decreased when measured in both cell culture media (ranging from −2 to −5 mV) (**Table 1B**). This change induced by the adsorption of negatively charged proteins from the medium, to positively charged Chit residues, forms a protein corona, decreasing the suspension stability. Under these conditions, the appearance of aggregates is inevitable which is part of the explanation for the PDI increment. To further complement the information given by the PDI and intensity average size, graphics from size distribution illustrate the different size populations of Chit 80% NPs and Chit 93% NPs in the different media (**Figure 2**). In the water, the size of both NP was distributed over a single peak (**Figures 2A,D**), while in cell culture media, there were at least three independent peaks (**Figures 2B,C,E,F**). We can hypothesize that the alterations observed in cell culture media size dispersion, including smaller and bigger size populations simultaneously, were induced not only by the presence of proteins, but also by the high ion content in comparison to water (Moore et al., 2015). Furthermore, as the media composition is different between RPMI and DMEM, the observed changes in the NP size distribution were not similar. A comparable phenomenon was described by Yang et al. (2018) for silica and silica coated nanoparticles, whose great stability in buffered saline was not kept in cell culture media, where the authors verified the erosion of surface silica by DMEM ingredients.

Endotoxin-Free Conditions Guarantee the Production of LPS-Free Nanoparticles

The last step of characterization was related to endotoxin contamination. As previously mentioned, Chit polymers were purified by a method published by our group (Lebre et al., 2019). The method allows the obtainment of endotoxin-free chitosan, proved by two methods: Limulus Amebocyte Lysate (LAL) test and the absence of IL-6, secreted by dendritic cells (DCs), cultured in the presence of chitosan. The chitosan does not induce IL-6 secretion by DCs and endotoxins do that stimulation. Furthermore, for *in vitro* immunotoxicity studies, the NP production was performed under those conditions, to avoid endotoxin contamination, as the presence of these molecules can easily lead to false positive results. To assure that Chit purification and Chit NP production were successfully achieved, both Chit polymers and NPs as well as the pyrogen-free water and the TPP solution used for NP production, were submitted to LAL test. Importantly, before establishing the methodology for endotoxin quantification with Pyrochrome® testing kit, all recommended tests to evaluate sample interference with LAL test were done to guarantee the suitability of the LAL test for Chit NPs, as described in the manufacturer's instructions. The results were presented in **Table 1C**, and show that all tested samples were not significantly different from pyrogen-free water, the negative control, and all were far below 0.25 EU/mL, which is the limit for water for injection according to main health authorities (Ph. Eur. 9.0, 2019). Thus, it was demonstrated that the process and conditions used to minimize the contamination and remove existent endotoxins during Chit purification and NP production was effective, and that Chit polymers and NPs used in immunotoxicity tests were indeed LPS-free, supporting the reliability of the results.

In vitro Studies With RAW 264.7 Cell Line

The monocyte/macrophage-like RAW 264.7 cells have been widely used for 40 years, as a suitable *in vitro* model, since they present unique phenotype and functional characteristics of macrophages (Roberts et al., 2018). Nevertheless, these cells should be used carefully since their functional stability is not maintained at high passage number. Indeed, a recent article

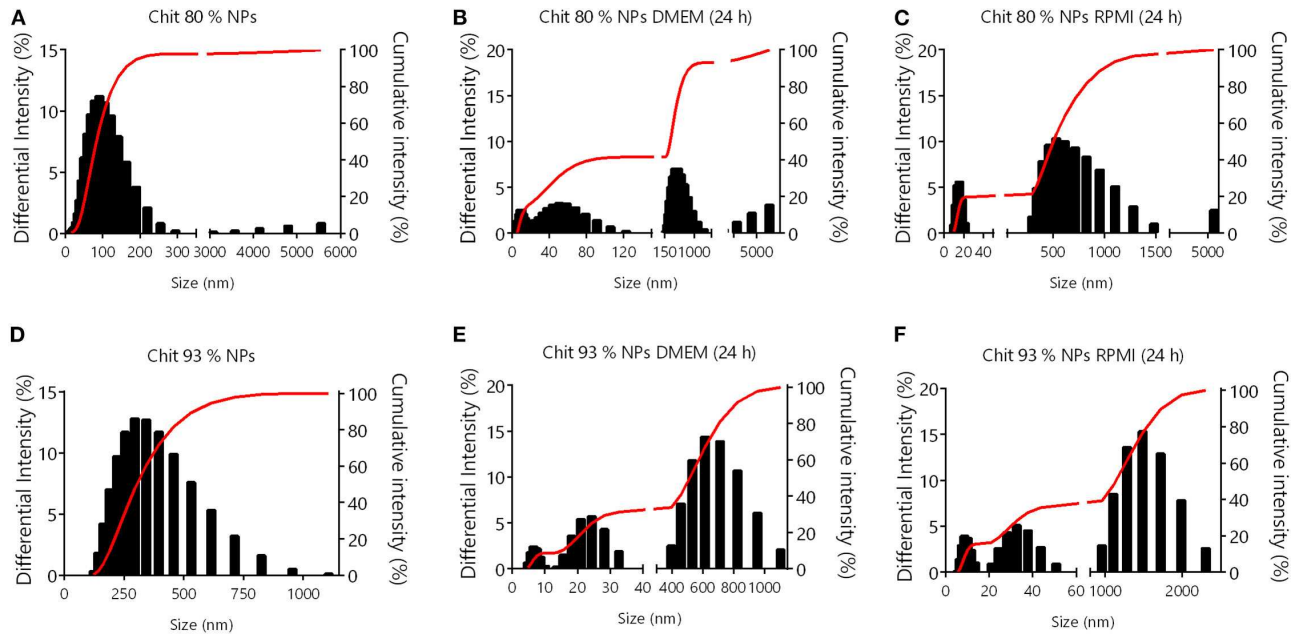

FIGURE 2 | NP size distribution by DLS. **(A)** Chit 80% NPs in water; **(B)** Chit 80% NPs after 24 h in DMEM medium; **(C)** Chit 80% NPs after 24 h in RPMI medium; **(D)** Chit 93% NPs in water; **(E)** Chit 93% NPs after 24 h in DMEM medium; **(F)** Chit 93% NPs after 24 h in RPMI medium.

mentions the phenotype and functional characteristics to remain stable from passage 10 to 30 (Roberts et al., 2018), and the American Type Culture Collection (ATTC) recommends to use them until passage 18.

Chitosan Nanoparticles Are More Cytotoxic for RAW 264.7 Cells Than Chitosan Polymers

The evaluation of the cytotoxic profile of Chit NPs and polymers was performed using the MTT metabolic activity assay, over a wide range of concentrations as illustrated in **Figure 3**. Results showed that Chit 80% and Chit 93% polymers were not cytotoxic in the concentration range tested (purple and orange lines, respectively), while Chit 80% and Chit 93% NPs induced significant decrease of cell viability above 2,500 and 3,000 μg/mL, respectively (**Figure 3A**). Based on the nonlinear regression analysis of the cell viability data of the Chit NPs, non-significant differences were found for the IC50 of Chit 80% NPs and Chit 93% NPs (**Figure 3B**).

The reduction of the reagent MTT by cells leads to the generation of insoluble crystals of formazan that once dissolved in DMSO generate a purple signal (van Meerloo et al., 2011). Since it is a colorimetric assay, and although the cell medium with the testing sample was aspirated before solubilizing the formazan crystals, NP interferences with the readout were tested to validate the assay (**Figure 3C**). As it is possible to observe, the measured absorbance (Abs) was not increased by the presence of the NPs or polymer suspension. Additionally, to guarantee that the cell viability results were only related with the NP and polymers, and not with the solvents, the supernatants collected from the NPs last washing step with water, as well as the acetate buffer used to disperse the polymers, were also tested using MTT assay (**Figure 3D**). Results showed that the solvents did not cause any decrease in cell viability.

Both Chitosan Polymers Hamper Nitric Oxide Release After LPS Stimulation and Only the Lower Deacetylation Degree Chitosan Induces Oxidative Stress

Reactive oxygen species (ROS) are unstable molecules that easily react with other molecules and may cause damage to DNA, RNA, proteins and ultimately lead to cell death, when accumulated (Schieber and Chandel, 2014).

To evaluate the effect of Chit polymers and Chit NPs on ROS production by RAW 264.7 cells, four different concentrations were used. As it is possible to see in **Figure 4A**, only Chit 80% NPs and the respective Chit polymer were able to induce ROS production, under non-cytotoxic concentrations. The increase in ROS production was concentration dependent, however, for the concentration range tested, the effect was not as high as LPS-induced ROS production. On the other hand, Chit 93% NPs and polymer had no effect on ROS production by RAW 264.7 cells. Importantly, all tested conditions did not induce cellular death as confirmed by the MTT assay performed at the end of each experiment (**Figure S1A**). In order to have a more complete picture, studies were conducted to evaluate that the polymers and NPs would not play an inhibitory role in the production of ROS by cells stimulated with LPS. Therefore, increasing concentrations of Chit polymer or Chit NPs were incubated together with cells and 1 μg/ml of LPS. Results in **Figure 4B** show that no inhibitory effect was observed for any of the tested samples. Consequently, it was possible to conclude that Chit 80%

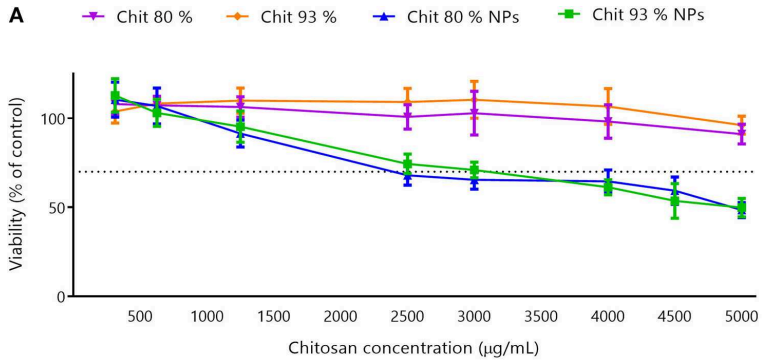

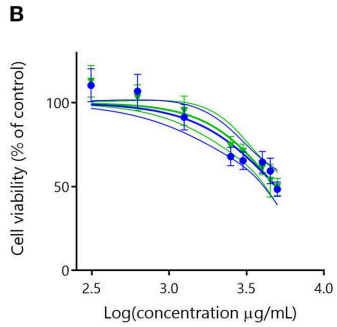

C

	Abs (no cells) (540/630 nm)
DMEM	0.076 ± 0.011
Chit 80 % NPs	0.061 ± 0.006
Chit 93 % NPs	0.047 ± 0.006
Chit 80 %	0.056 ± 0.002
Chit 93 %	0.053 ± 0.002

D

	RAW 264.7 viability (% of control)
Cell control	100 ± 0
Chit 80 % NPs solvent	110 ± 18
Chit 93 % NPs solvent	109 ± 15
Polymers solvent (acetate buffer)	98 ± 8

FIGURE 3 | Cell viability studies in RAW 264.7 cell line. **(A)** Cell viability decrease induced by different concentration of Chit 80% NPs, Chit 93% NPs, Chit 80%, and Chit 93% polymers evaluated by MTT assay after 24 h incubation. Dotted line represents the 70% of cell viability. **(B)** Nonlinear regression analysis of the cell viability data, allowing the extrapolation of IC50 values (4,949 µg/mL for Chit 80% NPs and 4,858 µg/mL for Chit 93% NPs). No statistical difference was found between Chit 80% NPs IC50 and Chit 93% NPs IC50 calculated using extra sum-of-squares F test. **(C)** Evaluation of possible NP and polymer interference with the wavelengths used to read MTT assay (540/630 nm) (Mean ± SEM, $n = 3$). **(D)** Evaluation of the cell viability resultant from the incubation of RAW 264.7 with the NPs solvent and polymers solvent (% of control). Results are expressed as mean ± SEM, obtained from a minimum of three independent experiments, each performed in triplicate ($n \geq 3$).

NPs, Chit 93% NPs and the respective polymers, when used in non-cytotoxic concentrations (cell viability results are on **Supplementary Figure S1B**), were not able to reduce the LPS-induced ROS production.

The possibility of having the nanoparticles interfering with the methods should not be ruled out, leading to false positives or false negatives. So, to evaluate the interference of Chit NPs and Chit polymers in the fluorescence readouts, the ROS production assay was performed without cells and at the highest polymer and NPs concentrations. The values obtained for test samples were similar to the medium alone (**Figure 4E**), meaning that they do not interfere with ROS measurement. Additionally, the possible interference of solvents was also assessed under the same testing conditions and as shown in **Figure 4F**, no stimulation of ROS production, as the fluorescence increase fold values were around 1.

NO is an important inflammatory mediator released by macrophages during inflammation, being one of the main cytostatic, cytotoxic, and pro-apoptotic mechanisms of the immune response (Bosca et al., 2005). NO production by RAW 264.7 cell line was measured using the Griess reaction method. Again, all test samples were sterile and endotoxin-free in order to prevent false positive results, and used in adequate concentrations that did not affect cell viability (Cell viability study in **Supplementary Figures 1C,D**).

With the aim to evaluate whether one of the polymers or Chit NPs would be able to induce cells to produce NO, samples were incubated with the RAW 264.7 cells for 24 h and the results were presented in **Figure 4C**. None of the Chit NPs or polymer concentrations tested induced NO production. Additionally, to evaluate whether the NPs and polymers had an inhibitory effect on NO production when cells were stimulated by LPS, increasing concentrations of the polymers and NPs were incubated with cells and with 1 µg/ml LPS. The results shown in **Figure 4D** indicate that there was a slight but significant inhibitory effect on LPS-induced NO production, at all concentrations tested when compared to the LPS control. Since the Chit and Chit NP concentrations tested did not induce significant reduction in cell viability (**Supplementary Figure 1D**) we can exclude the hypothesis that it was a consequence of cellular death.

For all NPs, the possible interference with optical detection methods is a hypothesis that should be tested before doing

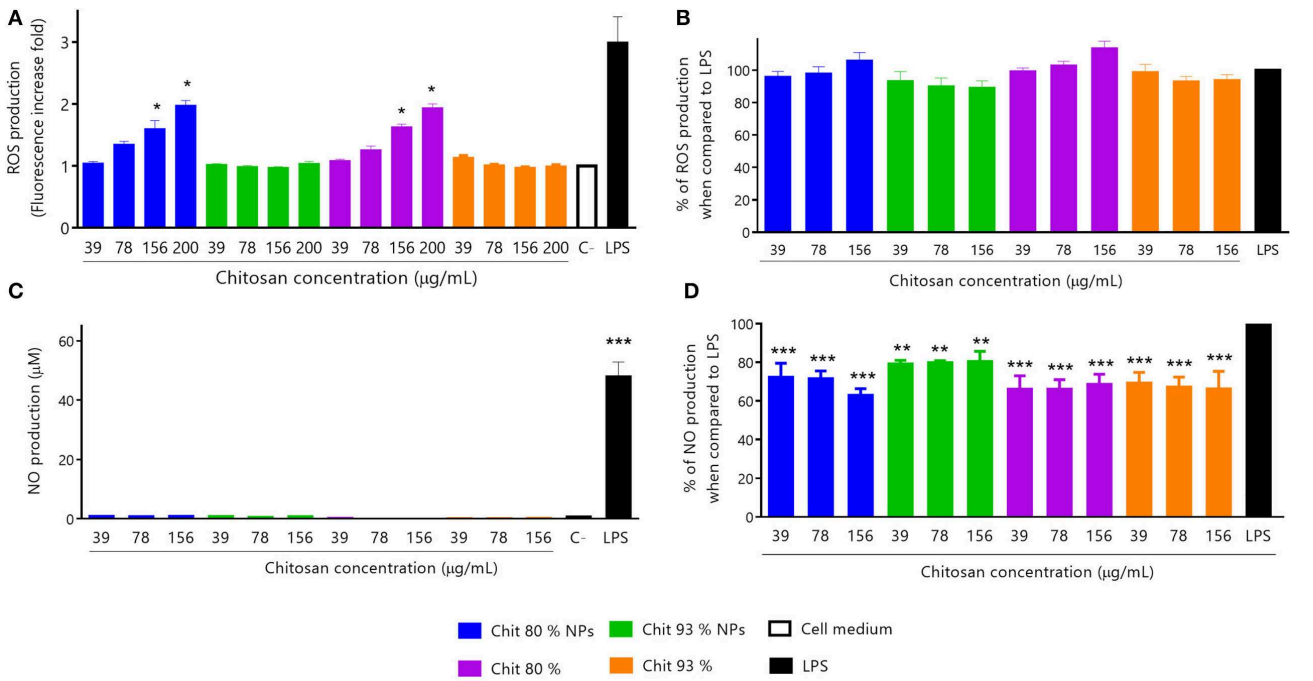

E

	Fluorescence (no cells) (485/20 – 528/20 nm)
DMEM	318 ± 4
Chit 80 % NPs	354 ± 4
Chit 93 % NPs	352 ± 8
Chit 80 %	353 8
Chit 93 %	367 ± 12

F

	ROS production (fluorescence fold increase)
Cell control	1 ± 0.00
Chit 80 % NPs solvent	0.95 ± 0.04
Chit 93 % NPs solvent	0.94 ± 0.05
Polymers solvent (acetate buffer)	1 ± 0.05

G

	Abs (no cells) (550 nm)
DMEM	0.047 ± 0.001
Chit 80 % NPs	0.051 ± 0.005
Chit 93 % NPs	0.047 ± 0.001
Chit 80 %	0.046 ± 0.001
Chit 93 %	0.047 ± 0.001

H

	NO production (μM)
Cell control	0.62 ± 0.37
Chit 80 % NPs solvent	0.43 ± 0.27
Chit 93 % NPs solvent	0.35 ± 0.58
Polymers solvent (acetate buffer)	- 1.5 ± 3.4

I

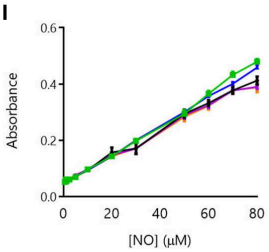

FIGURE 4 | Immunotoxicity assays in RAW 264.7 cell line. All assays were performed with non-cytotoxic concentrations of NPs, polymers and controls (evaluated by MTT assay after every experiment). **(A)** ROS production stimulated by Chit 80% NPs, Chit 93% NPs and the respective polymers prepared in endotoxin-free and sterile conditions. For the experiment, test samples were incubated with RAW 264.7 cell line for 24 h, as well as LPS, as a positive control. Mean ± SEM; obtained from four independent experiments, each performed in triplicate ($n = 4$), $^{*}p < 0.05$ compared to control. **(B)** Inhibition of ROS production by Chit 80% NPs, Chit 93% NPs and the respective Chit polymers prepared in endotoxin-free and sterile conditions. For the experiment, LPS and test samples were co-incubated with RAW 264.7 cell line for 24 h. Mean ± SEM, obtained from a minimum of seven independent experiments, each performed in triplicate ($n \geq 7$). **(C)** NO production stimulated by Chit 80% NPs, Chit 93% NPs and the respective polymers prepared in endotoxin-free and sterile conditions. For the experiment, test samples were incubated with RAW 264.7 cell line for 24 h, as well as LPS, as a positive control. Mean ± SEM, obtained from a minimum of three independent experiments, each performed in triplicate ($n \geq 3$), $^{***}p < 0.001$ compared to control. **(D)** Inhibition of NO production by Chit 80% NPs, Chit 93% NPs and the respective polymers prepared in endotoxin-free and sterile conditions. For the experiment, LPS and test samples were co-incubated with RAW 264.7 cell line for 24 h. Negative control (C–) was not co-incubated with LPS. Mean ± SEM, obtained from a minimum of three independent experiments, each performed in triplicate ($n \geq 3$), $^{**}p < 0.01$ and $^{***}p < 0.001$ compared to LPS control. **(E)** Evaluation of possible NP and polymer interference with the wavelength used to read ROS assay (Ex485/20 – Em528/20) (Mean ± SEM, $n = 3$). **(F)** Evaluation of the ROS production (fluorescence fold increase) induced by the NPs solvent and polymers solvent ($n = 3$). Data are presented as mean ± SEM. **(G)** Evaluation of possible NP and polymer interference with the wavelength used to read NO assay (550 nm) (Mean ± SEM, $n = 3$). **(H)** Evaluation of the NO production (%) induced by the NPs solvent and polymers solvent (% of control) ($n = 3$). Data are presented as mean ± SEM. **(I)** Control of interferences of **(A)** Chit NPs and **(B)** Chit polymers with known concentrations of NO without cells (Mean ± SEM, $n = 3$).

the test itself. So, similar to ROS assay, the NO assay was performed in the presence of the test samples, without cells and the results were presented on **Figure 4G**. The solvent of the Chit NPs suspension or the chitosan polymer suspension were evaluated to understand if they also had an effect on NO production (**Figure 4H**). No interferences were observed in the readout, and the solvents were not able to induce NO production. An additional control was performed for NO production assay, to evaluate whether Chit and Chit NPs, due to their cationic charge, could be adsorbing NO at their surface, reducing the amount of NO quantified. Such phenomenon would provide an explanation for the NO production inhibition observed. To evaluate this hypothesis, we performed the NO calibration curve in the presence and absence of Chit NPs and polymers (**Figure 4I**). As shown, the NO curves are all overlapping, meaning no interferences from Chit NPs and Chit polymers were observed.

In vitro Studies With Human Peripheral Blood Mononuclear Cells

PBMCs are a good model to study immune responses, since they secrete regulatory and pro-inflammatory cytokines and chemokines in the human body. *In vitro* cell viability experiments give an indication of a particle cytotoxic profile that may be observed *in vivo*.

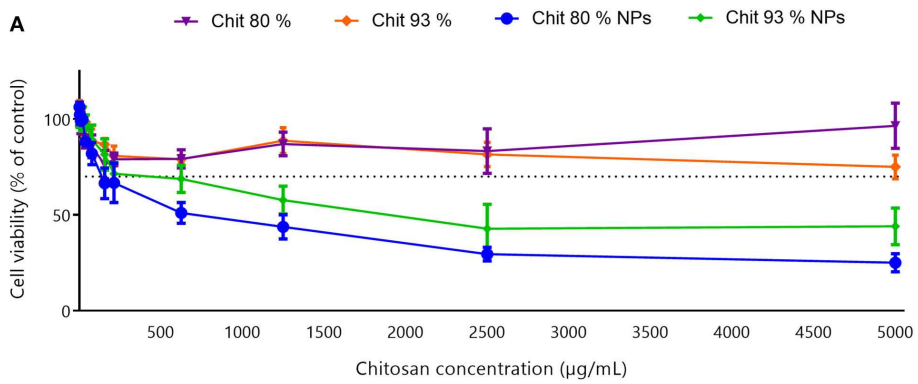

D

	Abs (no cells) (540/630 nm)
RPMI	0.064 ± 0.001
Chit 80 % NPs	0.060 ± 0.001
Chit 93 % NPs	0.077 ± 0.004
Chit 80 %	0.007 ± 0.001
Chit 93 %	0.012 ± 0.002

E

	PBMCs viability (% of control)
Cell control	100 ± 0
Chit 80 % NPs solvent	100 ± 2
Chit 93 % NPs solvent	100 ± 2
Polymers solvent (acetate buffer)	103 ± 6

FIGURE 5 | Cell viability studies in PBMCs and assay interference evaluation. **(A)** Cell viability decrease induced by different concentrations of Chit 80% NPs, Chit 93% NPs, Chit 80%, and Chit 93% in human PBMCs, evaluated by MTT assay following 24 h of incubation. Dotted line represents the 70% of cell viability. Results are expressed as mean ± SEM, obtained from four independent experiments, each performed in triplicate ($n = 4$). **(B)** Confirmation of MTT results by testing four different concentrations of Chit 80% NPs and Chit 93% NPs by flow cytometry using PI. Results are expressed as mean ± SEM, obtained from 1 to 4 independent experiments, each performed in duplicate ($n = 1$–4). **(C)** Nonlinear regression analysis of the cell viability data, allowing the extrapolation of IC50 values (720 µg/mL for Chit 80% NPs and 2104 µg/mL for Chit 93% NPs). Significant statistical difference between Chit 80% NPs IC50 and Chit 93% NPs IC50 calculated using extra sum-of-squares *F*-test. **(D)** Evaluation of possible NP and polymer interference with the wavelength used to read MTT assay (540/630 nm) (Mean ± SEM, $n = 3$). **(E)** Evaluation of the cell viability resultant from the incubation of PBMCs with the NPs solvent and polymers solvent (% of control) (Mean ± SEM, $n = 4$).

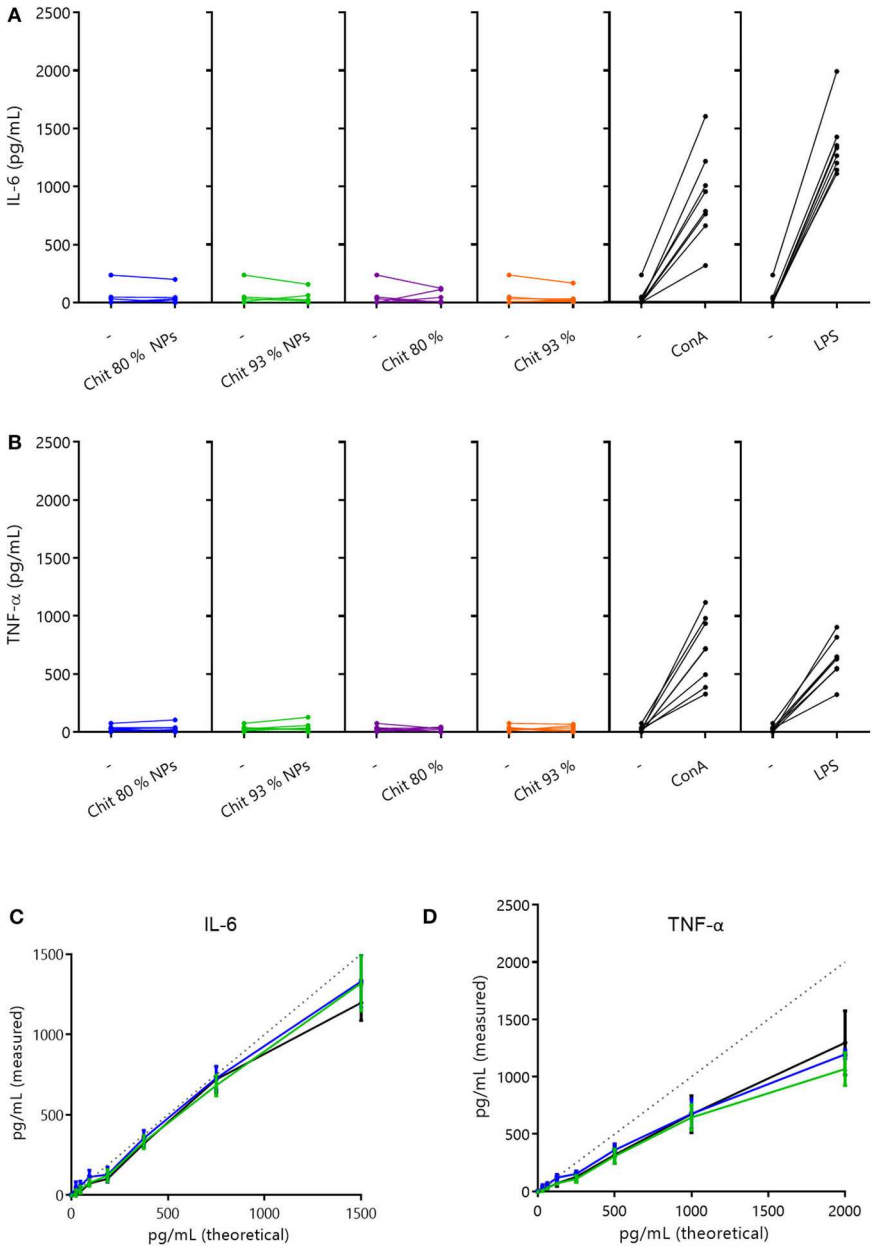

FIGURE 6 | Cytokine secretion in PBMCs and interference evaluation. **(A,B)** Cytokine secretion induced by 100 μg/mL of Chit 80% and Chit 93% polymers and NPs on human PBMCs, after 24 h incubation (A- IL-6 and B- TNF-α). Cytokine quantification was performed by ELISA. Results illustrate the increase in cytokine production (Chit 80% NPs, Chit 93% NPs, Chit 80%, Chit 93%, ConA, LPS), when compared to the basal level (–). The experiment was repeated with blood from eight different donors ($n = 8$). **(C,D)** Evaluation of the Chit 80% and Chit 93% NPs ability to interfere with cytokine quantification when compared to the cell culture media (experiment without cells). The results of the cytokine quantification for the calibration curve in the presence of Chit 80% NPs and Chit 93% NPs were compared to the cytokine quantification of the calibration curve in simple cell culture media (C- IL-6 and D- TNF-α). Dotted lines represent the original calibration curve in ELISA diluent. Data are represented as mean ± SEM ($n = 3$).

Lower Deacetylation Degree Chitosan NPs Are More Cytotoxic for PBMCs

Similar to RAW 264.7 cell line experiments, Chit NPs and polymers were incubated with cells, in this case human PBMCs, and the cell viability was evaluated using the MTT assay. The results depicted in **Figure 5A** showed that Chit NPs were more cytotoxic than the respective polymers.

Comparing the results achieved between the two NPs, Chit 80% NPs showed a tendency to be more cytotoxic than the Chit 93% NPs. This difference was further confirmed with the PI assay,

where the cell membrane integrity rather than the metabolic activity was evaluated (**Figure 5B**). A nonlinear regression of the MTT assay results clearly showed that Chit 80% NPs induced a more accentuated decrease in cell viability, with the 50% inhibitory concentration (IC50) calculated at ∼720 μg/mL (**Figure 5C**). Chit 93% NPs showed a statistically different IC50, calculated to be 2,104 μg/mL.

To note, Chit NP and polymer highest concentrations tested during cell viability assessment in both RAW 264.7 and PBMCs were very high and do not correlate with concentrations required for *in vivo* assays. Nevertheless, 5,000 μg/mL is recommended in OECD guidelines for genotoxicity testing of chemicals (test guideline 487) as the maximum concentration to be tested when no cytotoxicity or precipitates are observed. In our case, these concentrations were needed to correctly calculate the IC 50. For the Chit polymers, even though the highest sample concentration was very thick, it did not induce toxicity below 70%, confirming the great biocompatibility of the Chit polymers.

As explained for the RAW 264.7 cell line, experimental controls were performed and the results are presented in **Figures 5D,E**. The absorbance readout showed no interference for formulations (equal Abs values) and the resultant cell viability following solvent incubation with PBMCs during 24 h showed comparable cell viability to the control.

LPS-Free Chitosan Nanoparticles Do Not Stimulate IL-6 and TNF-α Release by PBMC's

Cytokines participate in many physiological processes, mostly in the regulation of immune and inflammatory responses (Ai et al., 2013). Interleukin-6 (IL-6) is a pleiotropic cytokine (inflammatory and anti-inflammatory properties) able to modulate the activity of immune cells (Wang et al., 2017). Tumor necrosis factor-α (TNF-α) is a pro-inflammatory cytokine released from macrophages or activated T cells which plays a crucial role in many immune and inflammatory processes, such as proliferation, apoptosis, and cell survival (Cai et al., 2017).

In order to understand if Chit NPs and polymers were able to stimulate the release of these cytokines by human PBMCs, the cells were incubated with 100 μg/mL Chit test samples for 24 h and the secreted cytokine results, measured by ELISA, were depicted in **Figures 6A,B**. Results showed that neither Chit NPs nor Chit polymers stimulated the production of IL-6 and TNF-α, as no differences were found before and after incubation with test samples. Importantly, the use of positive controls such as LPS and Con A, give us an indication of the cell function regarding the cytokine we are analyzing. Notably, both positive controls significantly increased the cytokine secretion in PBMCs.

Additionally, since chitosan's positive charge favors cytokine adsorption, the possible interference of Chit NPs in cytokine quantification was tested. For that, Chit NPs suspended in cell culture medium were incubated with known concentrations of each cytokine (calibration curve) for 24 h, then centrifuged and supernatant cytokine content similarly quantified by ELISA. The percentage of cytokine quantification in cell culture medium incubated with the nanoparticles in comparison to cell culture medium without nanoparticles, can reveal if the cytokines adsorbed to the NPs, preventing their quantification. Interestingly, **Figures 6C,D** suggest that Chit NPs did not adsorb IL-6 nor TNF-α, since cytokine quantification was equal or above 100%. Thus, we can assume that the absence of TNF-α and for IL-6 production upon stimulation with Chit NPs and polymers was indeed due to the lack of the samples' ability to stimulate the cells, which strengthens the conclusion that they do not induce a pro-inflammatory cytokine response, at least when produced under endotoxin-free conditions.

Hemocompatibility Assays

Chitosan Nanoparticles and Polymers Do Not Induce Hemolysis Even at High Concentrations

Hemolysis is characterized by the rupture of red blood cells (RBCs) and the release of their contents, ultimately leading to anemia, jaundice and renal failure (Dobrovolskaia et al., 2008). All materials entering the blood get in contact with RBCs and so the evaluation of the hemolytic ability of the biomaterials is of utmost importance.

Chit NPs and polymers hemolytic activity was evaluated following a 3 h incubation at 37°C with RBCs. Results showed that none of them induced a percentage of hemolysis superior to 5%, even in Chit concentrations of 2 mg/mL (**Figure 7A**). Triton X-100 was used as the hemolytic agent whose effect is possible to observe by the red color of the supernatant after centrifugation of the experiment tube 1 and 2 (**Figure 7B**). According to the ASTM E2524-08 standard, only hemolysis superior to 5% are considered significant. Although no hemolytic activity was induced by Chit NPs and polymers, solvents were tested as well as the NP interference with the assay readout. As depicted in **Figure 7C**, the NPs had no interference in the absorbance measurements and **Figure 7D** illustrates that no hemolysis was induced by the NPs or solvents of the suspensions of the NPs or polymers.

The Effect of Chitosan Nanoparticles in Coagulation and Platelet Aggregation Depends on the Nanoparticle Characteristics

The plasma coagulation cascade is responsible for blood clotting and consists of a series of protein interactions (Laloy et al., 2014). To evaluate the effect of Chit NPs and polymer samples on plasma coagulation time, two concentrations (0.1 and 1 mg/mL) of test samples were incubated with blood during 30 min. In this assay, both blood coagulation pathways, the activated partial thromboplastin time (APTT) and the prothrombin time (PT) were separately tested (**Figure 8A**).

The results showed that Chit NPs and polymers at 0.1 mg/mL concentration had no effect on plasma coagulation for both pathways. However, 1 mg/mL Chit 80% NPs prolonged APTT (intrinsic pathway), while no effect was observed with Chit 93% NPs and polymers 80% and 93% at the same concentration. NPs suspension solvent and polymer suspension solvent (acetate buffer) was also tested to discard any method interference and no effect was observed in plasma coagulation (**Figure 8B**).

Platelets play an important role not only in hemostasis but also in immune and inflammatory responses (Golebiewska and Poole, 2015). Homeostatic imbalance as a result of platelet

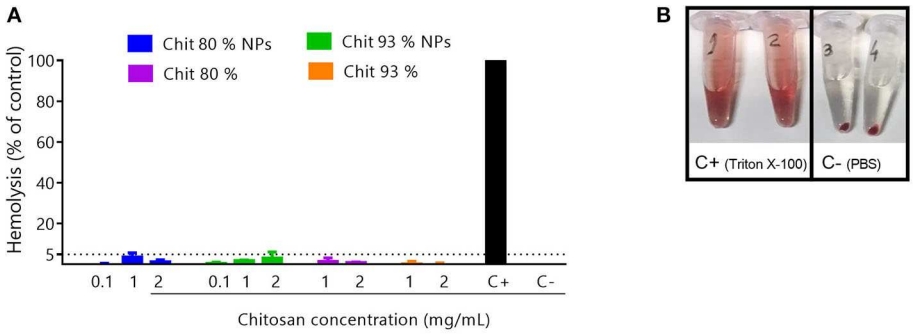

C

	Abs (no blood) (540 nm)
Chit 80 % NPs	0.036 ± 0.002
Chit 93 % NPs	0.034 ± 0.000
Chit 80 %	0.035 ± 0.001
Chit 93 %	0.035 ± 0.002

D

	Hemolysis (% of control)
Chit 80 % NPs solvent	0.67 ± 0.67
Chit 93 % NPs solvent	1.33 ± 0.88
Polymers solvent (acetate buffer)	1.31 ± 1.14

FIGURE 7 | Hemolysis assay. **(A)** Hemolytic activity of Chit polymers and NPs in human blood after 3 h incubation at 37°C. PBS and Triton-X-100 were respectively used as negative (C–) and positive control (C+). Results are expressed as mean ± SEM, obtained from at least three independent experiments, using blood from different donors, each performed in duplicate ($n \geq 3$). **(B)** Representation of 100% hemolysis generated by the positive control (tube 1 and 2) and the absence of hemolysis induced by the negative control (tube 3 and 4). **(C)** Evaluation of the Chit NP and Chit polymers interferences with the absorbance readout, without blood. Results are expressed as mean ± SEM, obtained from at least three independent experiments, using blood from different donors, each performed in duplicate ($n \geq 3$). **(D)** Evaluation of the hemolysis resultant from the incubation of NPs solvent and polymers solvent in human blood after 3 h incubation at 37°C.

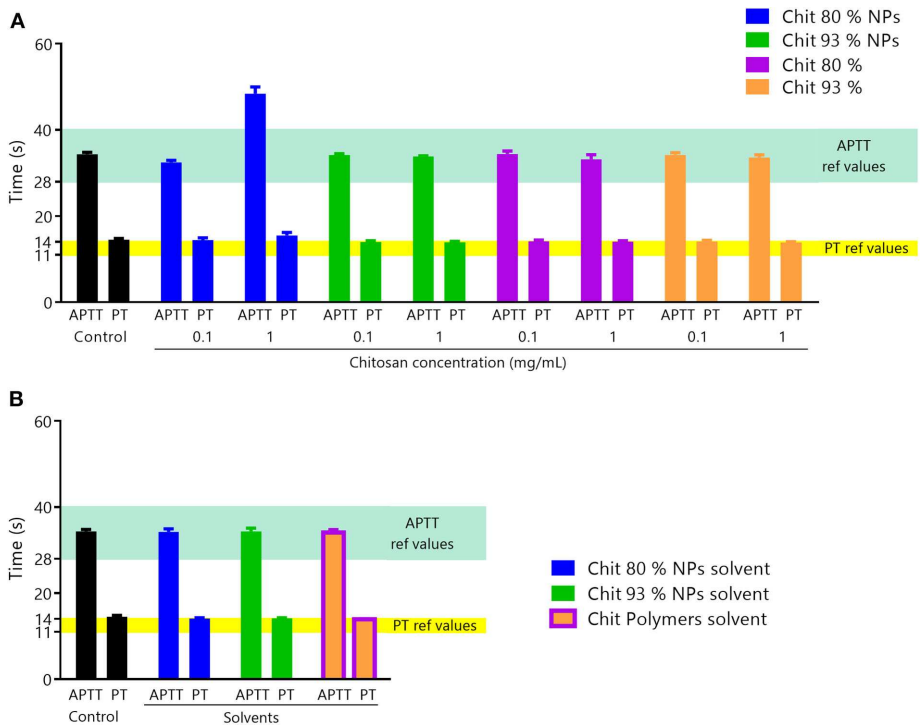

FIGURE 8 | Coagulation assay. **(A)** Effect of Chit NPs and polymers at 0.1 and 1 mg/mL on plasma coagulation time after incubation for 30 min. The two coagulation pathways, APTT and PT, were separately tested. APTT reference range of values is 20–40 s and for PT is 11–14 s. Results are expressed as mean ± SEM, obtained from three independent experiments, using blood from different donors, each performed in duplicate ($n \geq 3$). **(B)** Controls of interferences of NPs and polymers solvents with the coagulation times assay. Results are expressed as mean ± SEM, obtained from three independent experiments, using blood from different donors, each performed in duplicate ($n \geq 3$).

function alterations affect primary hemostasis and can result in thrombotic or hemorrhagic disorders (Golebiewska and Poole, 2015). Therefore, it is important to study Chit NPs interactions with platelet function.

To assess platelet aggregation, a cytometer is frequently used to count the platelets, however, by this method the interference of NPs, due to their size have to be taken into account. To evaluate the interference of Chit NPs with the platelet count, Chit NPs were incubated with platelet-free plasma (PFP) and visualized under the light microscope. Results showed that Chit NPs, most likely in the form of aggregates, were possibly counted as platelets, which invalidated the use of such method. To overcome this setback and assess platelet aggregation, the experiment was performed by counting platelets manually under a microscope, using a Neubauer chamber. Results from microscopy observation were summarized in **Figures 9A,B**.

The **Figure 9A**-1 clearly shows the absence of platelets typical from PFP, while plenty of platelets were observed in PRP, with no signs of aggregates (**Figure 9A**-2). When platelets were incubated with calcium chloride, we observed the formation of fibrins, a sign of platelet aggregation (**Figure 9A**-3). Similarly, collagen also induced platelet aggregation, but in this case no fibrins were observed (**Figure 9A**-4). When analyzing both types of Chit NPs incubated with PFP we can see their tendency to form NPs aggregates, which were hypothetically the cause of the observed interference in the cytometry technique (**Figures 9A**-5,7). Nevertheless, under microscopic observation, these aggregates were not misinterpreted as platelets. The Chit 80% NPs (**Figure 9A**-6) when incubated with PRP did not seem to induce platelet aggregation, as there was no evidence of platelet aggregates as found in the positive controls. On the other side, when Chit 93% NPs were incubated with PRP (**Figure 9A**-8) we observed that large NP agglomerates appear to have retained some platelets. Besides that, platelet aggregation was observed.

Using platelet count to calculate the percentage of platelet aggregation, positive controls induced an effect superior to 40%. The Chit 80% NPs did not induce platelet aggregation as only 4.9% of platelet aggregation was calculated for these samples. However, Chit 93% NPs resulted in 37.5% platelet aggregation similar to what was achieved with calcium chloride and collagen positive controls.

DISCUSSION

A hot topic in the nanomedicine field are polymeric NPs, which are engineered to either interact or not with the immune system. In the early stages of the development of a nanotechnology-based medicine, when the drug is to be encapsulated into NPs, the first question to be considered is, whether it is supposed that the new nanomedicine, in addition to its main pharmacological action, also acts on the immune system. This kind of approach is part of the SbD. Particularly, in the case of chitosan, as it is a set of polymers with different MW and DDA [quality attributes (QA)], it is important to understand if there are differences between them, regarding possible interactions with the immune system. For Chit NPs, in addition to polymer QA, NP characteristics, like size and zeta potential or shape can also be important. Therefore, physicochemical characteristics (PCC) of the polymers and NP might influence their immunological properties, and therefore a thorough characterization of both is very important to supplement the immunotoxicity studies and to draw meaningful conclusions (Crist et al., 2013). The lack of an exhaustive characterization may preclude the correct interpretation of results and may lead to misinterpretations hindering the establishment of trends regarding how Chit NP PCC influence the immune response. Additionally, one of the most important challenges encountered in *in vitro* immunotoxicity tests for NPs is related to their unique physicochemical properties. These can interfere with the established tests, originally developed for testing conventional chemicals (Dobrovolskaia and McNeil, 2016). Such interference depends both, on the NPs tested and the *in vitro* assay and can lead to false-positive or false-negative results (Dobrovolskaia and McNeil, 2016). Lastly, in order to achieve a correct result interpretation, it is important to identify the presence of biological contaminants in the NP preparation (Dobrovolskaia and McNeil, 2007). The main biological contamination in *in vitro* assays, even when working under sterile conditions, are endotoxins, which may lead to inflammatory responses (Dobrovolskaia and McNeil, 2007).

The present case study intends to provide a systematic analysis of the effects of Chit NPs and respective Chit polymers on different biological outcomes commonly tested under the immunotoxicity scope, considering, as most important the effect of DDA and MW, without neglecting possible interferences and contaminants.

In detail, as literature suggests, we found that Chit NPs appear to be more cytotoxic than the respective Chit polymers from which they were derived. In fact, for polymer concentrations up to the extraordinary concentration of 5,000 μg/mL, no cytotoxic effects were found neither in PBMCs, nor in RAW 264.7 cells. On the other hand, when the polymers were assembled into NPs, the same range of Chit concentrations induced a concentration dependent reduction in cell viability. Another important result we found was that PBMCs isolated from human blood were more sensitive to the NPs than RAW 264.7 cells, which is evident from the lower IC50 values extrapolated. Furthermore, this higher sensitivity of PBMCs exposed differences between the NPs produced with Chit 80% and Chit 93%. In fact, Chit 80% NPs induced a more accentuated decrease in cell viability. To discuss these results some aspects must be analyzed. To begin with, the cell culture media were different for PBMCs and RAW 264.7 cells (RPMI and DMEM, respectively). The physicochemical characterization of the NPs in water (stock suspension) is important, but their characterization when dispersed in the medium used for *in vitro* assays can provide further evidence. In fact, Chit 80% NPs presented a smaller size than Chit 93% NPs in water (127 nm vs. 292 nm), but these differences were not observed in cell culture media. Moreover, the NPs size analysis in cell culture media resulted in very high PDI. We realized that in RPMI (used for PBMCs) Chit 80% NPs presented an important size population around 500–1,000 nm, while Chit 93% showed a significant size population around 1,000–2,000 nm. On the other hand, Chit 80% NPs and Chit 93% NPs in DMEM (used for RAW 264.7) did not show such size distribution profile, with the most expressive populations around 300–700 nm and 400–800 nm, respectively. Therefore, the most noteworthy size

A

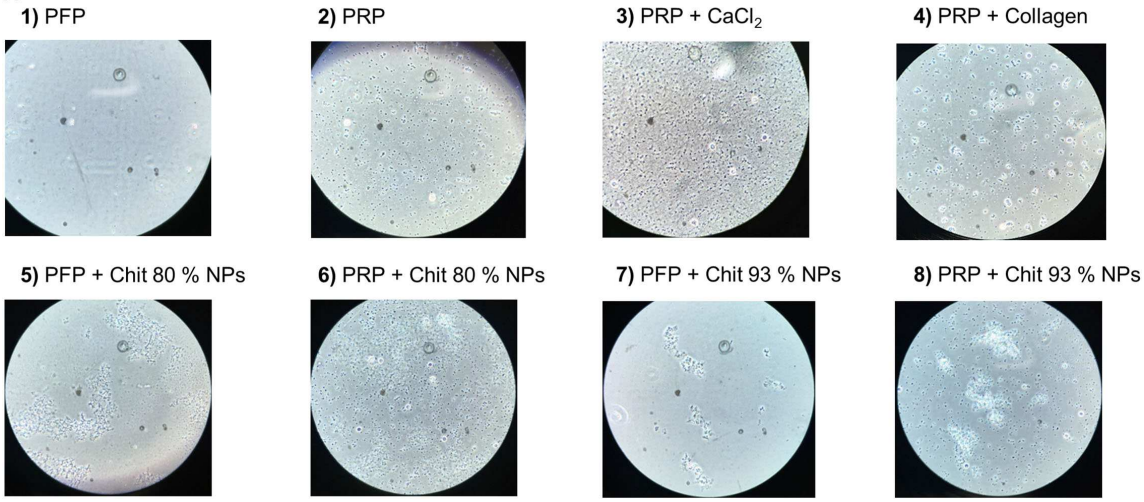

B

	Platelet count (x10^9/L) ± SEM, n=3-4	Platelet Aggregation (%) ± SEM, n=3-4
PRP + negative control (PBS)	210.5 ± 66.5	-
PRP + $CaCl_2$ (0.25 M)	105.3 ± 33.2	46.0 ± 2.4
PRP + Collagen (600 µg/mL)	113.7 ± 35.6	40.7 ± 9.8
PRP + Chit 80 % NPs (2 mg/mL)	196.5 ± 53.1	4.9 ± 4.4
PRP + Chit 93 % NPs (2 mg/mL)	135.1 ± 5.23	37.5 ± 4.5

FIGURE 9 | Effect of Chit 80% NPs and Chit 93% NPs in platelet aggregation. Platelet aggregation was detected by incubating PRP with 2 mg/mL of NPs for 15 min. PBS, collagen (200 and 600 µg/mL) and calcium chloride (CaCl2, 0.25 M) were used as negative and positive control, respectively. **(A)** Representative images of platelet aggregation assay stained with Giemsa dye. Untreated platelet free plasma (PFP) is represented in image 1 and untreated platelet rich plasma (PRP) is represented in image 2. For the experiment two different positive controls were used (CaCl2–3 and collagen−4). Chit 80% NPs and Chit 93% NPs were tested both with PFP (image 5 and 7) and PRP (image 6 and 8). **(B)** Quantification of the platelet aggregation effect. Platelet count is presented as the final average of a minimum of three donors ± SD. The percentage of aggregation was calculated using as reference the platelet count of the negative control, and is presented as the average of all assays ± SD ($n \geq 3$).

differences occurred in RPMI, which could explain the different cell viability profile between the NPs in PBMCs.

Literature review showed several contradictory results regarding Chit NPs effect on cellular ROS production. One study suggested that Chit NPs had an inhibitory activity (Bor et al., 2016), two studies reported no Chit NPs effect (Omar Zaki et al., 2015; Arora et al., 2016) and three reported a stimulating effect (Hu et al., 2011; Sarangapani et al., 2018; Wang et al., 2018) on basal ROS cellular production. Concerning the polymer, same conflicting results were also found (Arora et al., 2016; Salehi et al., 2017; Sarangapani et al., 2018). From our case study, we concluded that, despite no significant differences were found in the cytotoxic profile of both NPs in RAW 264.7 cells, in ROS assay these NPs had different effects when tested at non-cytotoxic concentrations. Only Chit 80% NPs induced ROS production in a concentration-dependent manner (starting at 156 µg/mL). Nevertheless, the 80% DDA polymer suspended in acetate buffer also induced ROS production. Thus, the effect was dependent on the type of Chit polymer: Chit with the lowest DDA induced ROS production. On the other hand, neither NPs nor polymers, irrespective of the DD were able to inhibit ROS production. While our results suggested an influence of the DDA of the polymer in cellular ROS stimulation, the above mentioned studies did not. In fact, all authors mentioned used similar DDA Chit (75–85%) and no pattern could be observed. Moreover, those results are also affected by other variables, such as the different cellular models and testing conditions, namely concentrations, used by each author, as previously reviewed elsewhere (Jesus et al., 2019). Furthermore, none of the studies mentioned used RAW 264.7 cells, which hinders the comparison with the results herein presented.

Concerning the ability to induce NO by cells, only one result was found in the literature that claim the ability of the chitosan NPs to induce cells to produce this inflammatory marker and it showed a concentration-dependent increase above 68.18 µg/mL, in PBMCs following 24 h incubation (Pattani et al., 2009). Our case study, however, did not allow us to confirm this trend. Our results showed that none of the Chit NP tested increased NO production, in the range 39 µg/mL to 156 µg/mL. To note, Pattani et al. used Chit NPs cross-linked with sodium carboxymethyl cellulose that possessed a much smaller average size (37 nm), which may have been one of the causes for the increased reactivity. For Chit polymer, two studies observed no effect in basal NO production (Jeong et al., 2000; Wu and Tsai,

2007) supporting our results (Chit polymers did not induce NO production), while two others reported an increase (Peluso et al., 1994; Wu et al., 2015). In the case of Peluso et al. (1994) we can hypothesize that the conflicting results can be due to the use of a different cellular model (rat peritoneal exudate macrophages) or a possible endotoxin contamination, which was not assessed. On the other hand, Wu et al. (2015) used RAW 264.7 cells and claimed the endotoxin level in the stock solution was <0.5 EU/mL, which is a much higher value than we have for the Chit polymers tested. In opposition, the ability of Chit NPs and polymers to inhibit LPS-induced NO production was verified for all testing samples. This effect was similar among them, suggesting no effect of the DDA or particle size. In this case, although we have excluded that Chit NPs or polymers were interacting with NO, hampering its quantification, we cannot rule out the ability of Chit to bind LPS, partially inhibiting its effect. These findings of NO inhibition are in agreement with most of the results found in the literature, where Chit NPs were reported to inhibit H_2O_2-stimulated NO production (Wen et al., 2013) and Chit was reported to inhibit LPS-induced NO production (Hwang et al., 2000; Wu and Tsai, 2007). In contrast, one study performed by Jeong et al. showed Chit had a synergistic effect with IFN-γ to induce NO production (Jeong et al., 2000). In this case, the polymer used had a higher MW (300 KDa) than the polymer used in this study.

Regarding the ability of the Chit polymer and NPs to stimulate cell to produce pro-inflammatory cytokines, for instance the induction of TNF-α has been reported in some studies. These studies, however, must be carefully discussed regarding endotoxin contamination. We realized that when the authors do not disclose the purity of the polymer used, namely whether it is an LPS-free chitosan or not, results are not consensual. In some of these studies, IL-6 and TNF-α were reported to be induced following Chit and Chit NPs stimulation (Feng et al., 2004; Koppolu and Zaharoff, 2013; Baram et al., 2014), while in others studies they were not (Villiers et al., 2009; Han et al., 2016). On the other hand, when authors used Chit-based samples prepared under endotoxin-free conditions (Pattani et al., 2009; Lieder et al., 2013; Stopinšek et al., 2016), they were unanimous proving that "pure/clean" non-cytotoxic Chit and particularly, Chit NPs, do not induce IL-6 or TNF-α secretion. In agreement with this, our endotoxin-free formulations confirmed that Chit NPs and polymers do not induce TNF-α or IL-6 secretion in PBMCs. Consistently, previous studies from our group using different endotoxin-free Chit-based particles (different DDA and MW polymer, cross-link compound and NPs size when compared with present NPs) also showed no ability to induce these cytokines in mice spleen cells (Soares et al., 2019) and mice bone marrow derived dendritic cells (BMDCs) (Lebre et al., 2019). However, the last study (Lebre et al., 2019) proved that Chit and Chit NPs were able to stimulate BMDCs, activating the NLRP3 inflammasome. As a consequence, it was observed an increase of the IL-1β (pro-inflammatory cytokine) secretion by cells.

Regarding hemocompatibility assessment, our studies also allowed to clarify some conflicting literature results. Considering the hemolytic activity, some original articles were found supporting the non-hemolytic activity of Chit NPs (Nadesh et al., 2013; Kumar et al., 2017) and also the Chit polymer (Nadesh et al., 2013). Nevertheless, two studies reported a slight hemolytic effect for Chit NPs (Shelma and Sharma, 2011; de Lima et al., 2015). The last study, however, suggested that the hemolytic activity was due to the NPs solvent, which was diluted acetic acid and neutralized diluted acetic acid (de Lima et al., 2015). Our studies enabled us to confirm that both Chit polymers and Chit NPs do not have hemolytic activity even at high concentrations (2 mg/mL) and that the washing procedure of the NPs eliminated the acetic acid traces of the NPs solvent, which could otherwise induce an erroneous hemolysis. Concerning coagulation studies, we found that only Chit 80% NPs caused a concentration dependent effect on coagulation. At similar concentrations, the Chit 93% NPs and both Chit polymers in acetate buffer had no effect, meaning the effect was dependent on the nanoscale dimension of the NPs and on the polymer characteristics (80% DDA and 49 kDa). We can hypothesize that Chit 80% NPs prolonged activated partial thromboplastin time due to the affinity of NPs for plasma clotting factors that are involved in the intrinsic pathway (XII, XI, IX, VIII), possibly adsorbing them (Palta et al., 2014). In previous studies, Shelma and Sharma (2011) showed that Chit NPs reduced the total normal coagulation time, while Nadesh et al. verified that Chit NPs did not alter coagulation time, when resuspended in saline (Nadesh et al., 2013). However, experimental conditions were significantly different. The first used 2 mg/mL which is a concentration similar to ours, but evaluated only the blood clotting time, and the second only used 0.05 mg/mL. Lastly, only Chit 93% NPs were able to induce platelet aggregation. We can hypothesize this effect was only observed with Chit 93% NPs due to the higher amount of NH_3^+ groups resulting from deacetylation, increasing the interaction with negatively charged groups of platelets. However, through microscope slide analysis we postulated that the effect may also be related to the formation of large NP aggregates when using a concentration of 2 mg/mL, that further leads to platelet aggregation at their surface. Accordingly, Shelma and Sharma (2011) also reported that platelet aggregation was induced by Chit NPs at a concentration of 2 mg/mL. However, since in the same Chit 80% NPs concentration we could not confirm this tendency, the influence of different physicochemical properties of NPs affecting the biological activity must be highlighted.

In addition to the specific immunotoxicity and hemocompatibility results presented here, this case study aims to raise awareness of the scientific community about the importance of adequate controls (experimental and sample controls). Indeed, some studies fail to report important experimental controls to validate whether a particular assay is appropriate for each NP formulation and to avoid false-positive and false-negative results. A simple control is the evaluation of NP interference in the assay readout (absorbance, luminescence or fluorescence) in the absence of the biological matrix. This is omitted most of the times even though it highly increases the reliability of the obtained results. For instance, in the platelet aggregation study, the cytometer counted NPs instead of platelets, which was the reason why we did not use this technique and we had to use a light microscope. Another desirable experimental control is the cellular viability at the end of each assay, to guarantee that the revealed effects are not only a side effect of cytotoxic concentrations. Regarding

sample controls, a parameter that is generally ignored is the solvent of the NP suspension. Usually, synthesized nanoparticles are in a solvent which is not designed to be biocompatible, but to stabilize the particles and prevent their aggregation in stock suspensions. The presence of such solvent in the culture medium may be enough to induce cell death, alter osmolality, pH, cause cellular damage, and decrease metabolic activity (Oostingh et al., 2011). Therefore, solvent control test is also useful to correctly interpret the results. Ultimately, we highlight the need to avoid endotoxin contamination of polymeric NPs, as it is frequently not considered and may be the source of false bioactivity or toxicity assumptions. In fact, endotoxins are a type of bacterial cell wall toxins, responsible for inducing a state of inflammation in organisms, resulting in fever, fibril reactions and organ damage (Dobrovolskaia et al., 2009). NPs are typically contaminated with endotoxins, mostly Chit NPs as their marked positive surface charge is especially susceptible to this kind of contamination. We believe that the increasing awareness of researchers about endotoxin contamination will contribute to reduce the disparity among NP immunotoxicity results.

Once more, we confirmed that our Chit NPs are more cytotoxic than Chit polymers, which justifies why we cannot rely on the Chit polymer attested safety to extrapolate to Chit NPs. More importantly, as we proposed, the presented results enabled us to shed light on some conflicting results found in literature. Notably, neither Chit NPs tested here demonstrated intrinsic pro-inflammatory ability. However, other assays showed that Chit DDA and MW influence Chit NPs immunotoxicity and hemocompatibility. Chit NPs with the lower DDA and lower MW (Chit 80% NPs) were more toxic in terms of reducing cell viability, ROS production and coagulation times. Nevertheless, all reported effects are concentration dependent and do not refrain Chit 80% NPs from being promising drug delivery systems or vaccine adjuvants.

To conclude, the present case-study together with further studies may contribute to the development of a knowledge-based guideline that enables NP product design based on the SbD approach. Nevertheless, we cannot overlook the current need to establish a set of methods for immunotoxicological assessments of NPs that need validation and standardization to allow the generation of a reliable database of results, essential to apply SbD more efficiently.

DATA AVAILABILITY STATEMENT

All datasets generated for this study are included in the article/**Supplementary Material**.

AUTHOR CONTRIBUTIONS

SJ, AM, and OB contributed conception and design of the study. AM, AD, ES, JC, and MC performed the experimental work. SJ wrote the first draft of the manuscript. SJ, AM, ES, MS, CS, GB, PW, and OB contributed to data analysis and manuscript revision. All authors read and approved the submitted version.

FUNDING

This work was financed by the European Regional Development Fund (ERDF), through the Centro 2020 Regional Operational Programme and through the COMPETE 2020 - Operational Programme for Competitiveness and Internationalization and Portuguese national funds via FCT – Fundação para a Ciência e Tecnologia, under project PROSAFE/0001/2016 and POCI-01-0145-FEDER-030331, and the strategic project UIDB/04539/2020. This work is part of the GoNanoBioMat project and has received funding from the Horizon 2020 framework program of the European Union, ProSafe Joint Transnational Call 2016 and from the CTI (1.1.2018 Innosuisse), under grant agreement Number 19267.1 PFNM-NM.

ACKNOWLEDGMENTS

The authors would like to thank Dra Ana Donato from the Faculty of Pharmacy Clinical Laboratory Analysis (University of Coimbra) for the hematological studies support, Dra Mónica Zuzarte from iLAB - Bioimaging Laboratory of the Faculty of Medicine of the University of Coimbra for TEM analysis, and Primex for supplying Chitoclear® chitosan polymers. NMR data was collected at the UC-NMR facility which is supported in part by FEDER – European Regional Development Fund through the COMPETE Programme (Operational Programme for Competitiveness) and by National Funds through FCT – Fundação para a Ciência e a Tecnologia (Portuguese Foundation for Science and Technology) through grants RECI/QEQ-QFI/0168/2012, CENTRO-07-CT62-FEDER-002012, and also through support to Rede Nacional de Ressonância Magnética Nuclear (RNRMN) and to Coimbra Chemistry Centre through grant UID/QUI/00313/2019.

SUPPLEMENTARY MATERIAL

The Supplementary Material for this article can be found online at: https://www.frontiersin.org/articles/10.3389/fbioe.2020.00100/full#supplementary-material

REFERENCES

Ai, W., Li, H., Song, N., Li, L., and Chen, H. (2013). Optimal method to stimulate cytokine production and its use in immunotoxicity assessment. *Int. J. Environ. Res. Public Health* 10, 3834–3842. doi: 10.3390/ijerph10093834

Al Rubeaan, K., Rafiullah, M., and Jayavanth, S. (2016). Oral insulin delivery systems using chitosan-based formulation: a review. *Expert Opin. Drug Deliv.* 13, 223–237. doi: 10.1517/17425247.2016.1107543

Ali, A., and Ahmed, S. (2018). A review on chitosan and its nanocomposites in drug delivery. *Int. J. Biol. Macromol.* 109, 273–286. doi: 10.1016/j.ijbiomac.2017.12.078

Arora, D., Dhanwal, V., Nayak, D., Saneja, A., Amin, H., Ur Rasool, R., et al. (2016). Preparation, characterization and toxicological investigation of copper loaded chitosan nanoparticles in human embryonic kidney HEK-293 cells. *Mater. Sci. Eng. C Mater. Biol. Appl.* 61, 227–234. doi: 10.1016/j.msec.2015.12.035

Baram, L., Cohen-Kedar, S., Spektor, L., Elad, H., Guzner-Gur, H., and Dotan, I. (2014). Differential stimulation of peripheral blood mononuclear cells in Crohn's disease by fungal glycans. *J. Gastroenterol. Hepatol.* 29, 1976–1984. doi: 10.1111/jgh.12701

Bento, D., Jesus, S., Lebre, F., Goncalves, T., and Borges, O. (2019). Chitosan plus compound 48/80: formulation and preliminary evaluation as a Hepatitis B vaccine adjuvant. *Pharmaceutics* 11:72. doi: 10.3390/pharmaceutics11020072

Bento, D., Staats, H. F., and Borges, O. (2015). Effect of particulate adjuvant on the anthrax protective antigen dose required for effective nasal vaccination. *Vaccine* 33, 3609–3613. doi: 10.1016/j.vaccine.2015.06.037

Bor, G., Mytych, J., Zebrowski, J., Wnuk, M., and Sanli-Mohamed, G. (2016). Cytotoxic and cytostatic side effects of chitosan nanoparticles as a non-viral gene carrier. *Int. J. Pharm.* 513, 431–437. doi: 10.1016/j.ijpharm.2016.09.058

Borges, O., Silva, M., de Sousa, A., Borchard, G., Junginger, H. E., and Cordeiro-da-Silva, A. (2008). Alginate coated chitosan nanoparticles are an effective subcutaneous adjuvant for Hepatitis B surface antigen. *Int. Immunopharmacol.* 8, 1773–1780. doi: 10.1016/j.intimp.2008.08.013

Bosca, L., Zeini, M., Traves, P. G., and Hortelano, S. (2005). Nitric oxide and cell viability in inflammatory cells: a role for NO in macrophage function and fate. *Toxicology* 208, 249–258. doi: 10.1016/j.tox.2004.11.035

Cai, X., Cao, C., Li, J., Chen, F., Zhang, S., Liu, B., et al. (2017). Inflammatory factor TNF-α promotes the growth of breast cancer via the positive feedback loop of TNFR1/NF-κB (and/or p38)/p-STAT3/HBXIP/TNFR1. *Oncotarget* 8, 58338–58352. doi: 10.18632/oncotarget.16873

Crist, R. M., Grossman, J. H., Patri, A. K., Stern, S. T., Dobrovolskaia, M. A., Adiseshaiah, P. P., et al. (2013). Common pitfalls in nanotechnology: lessons learned from NCI's Nanotechnology Characterization Laboratory. *Integr. Biol.* 5, 66–73. doi: 10.1039/c2ib20117h

de Lima, J. M., Sarmento, R. R., de Souza, J. R., Brayner, F. A., Feitosa, A. P., Padilha, R., et al. (2015). Evaluation of hemagglutination activity of chitosan nanoparticles using human erythrocytes. *Biomed Res. Int.* 2015:247965. doi: 10.1155/2015/247965

Dedloff, M. R., Effler, C. S., Holban, A. M., and Gestal, M. C. (2019). Use of biopolymers in mucosally-administered vaccinations for respiratory disease. *Materials* 12:2445. doi: 10.3390/ma12152445

Dobrovolskaia, M., and McNeil, S. (2016). "*In vitro* assays for monitoring nanoparticle interaction with components of the immune system," in *Handbook of Immunological Properties of Engineered Nanomaterials* (Singapore: World Scientific), 223–280.

Dobrovolskaia, M. A., Clogston, J. D., Neun, B. W., Hall, J. B., Patri, A. K., and McNeil, S. E. (2008). Method for analysis of nanoparticle hemolytic properties *in vitro*. *Nano Lett.* 8, 2180–2187. doi: 10.1021/nl0805615

Dobrovolskaia, M. A., Germolec, D. R., and Weaver, J. L. (2009). Evaluation of nanoparticle immunotoxicity. *Nat. Nanotechnol.* 4, 411–414. doi: 10.1038/nnano.2009.175

Dobrovolskaia, M. A., and McNeil, S. E. (2007). Immunological properties of engineered nanomaterials. *Nat. Nanotechnol.* 2, 469–478. doi: 10.1038/nnano.2007.223

EU-NCL (2019). *European Nanomedicine Characterisation Laboratory - Assay Cascade. Available online at: http://www.euncl.eu/about-us/assay-cascade/* (accessed October 25, 2019).

Feng, J., Zhao, L., and Yu, Q. (2004). Receptor-mediated stimulatory effect of oligochitosan in macrophages. *Biochem. Biophys. Res. Commun.* 317, 414–420. doi: 10.1016/j.bbrc.2004.03.048

Golebiewska, E. M., and Poole, A. W. (2015). Platelet secretion: from haemostasis to wound healing and beyond. *Blood Rev.* 29, 153–162. doi: 10.1016/j.blre.2014.10.003

Han, H. D., Byeon, Y., Jang, J.-H., Jeon, H. N., Kim, G. H., Kim, M. G., et al. (2016). *In vivo* stepwise immunomodulation using chitosan nanoparticles as a platform nanotechnology for cancer immunotherapy. *Sci. Rep.* 6:38348. doi: 10.1038/srep38348

Hu, Y. L., Qi, W., Han, F., Shao, J. Z., and Gao, J. Q. (2011). Toxicity evaluation of biodegradable chitosan nanoparticles using a zebrafish embryo model. *Int. J. Nanomed.* 6, 3351–3359. doi: 10.2147/IJN.S25853

Hwang, S. M., Chen, C. Y., Chen, S. S., and Chen, J. C. (2000). Chitinous materials inhibit nitric oxide production by activated RAW 264.7 macrophages. *Biochem. Biophys. Res. Commun.* 271, 229–233. doi: 10.1006/bbrc.2000.2602

Jeong, H. J., Koo, H. N., Oh, E. Y., Chae, H. J., Kim, H. R., Suh, S. B., et al. (2000). Nitric oxide production by high molecular weight water-soluble chitosan via nuclear factor-κB activation. *Int. J. Immunopharmacol.* 22, 923–933. doi: 10.1016/S0192-0561(00)00055-2

Jesus, S., Schmutz, M., Som, C., Borchard, G., Wick, P., and Borges, O. (2019). Hazard assessment of polymeric nanobiomaterials for drug delivery: what can we learn from literature so far. *Front. Bioeng. Biotechnol.* 7:261 doi: 10.3389/fbioe.2019.00261

Jesus, S., Soares, E., Borchard, G., and Borges, O. (2017). Poly-ϵ-caprolactone/chitosan nanoparticles provide strong adjuvant effect for Hepatitis B antigen. *Nanomedicine* 12, 2335–2348. doi: 10.2217/nnm-2017-0138

Jesus, S., Soares, E., Borchard, G., and Borges, O. (2018). Adjuvant activity of poly-epsilon-caprolactone/chitosan nanoparticles characterized by mast cell activation and IFN-γ and IL-17 production. *Mol. Pharm.* 15, 72–82. doi: 10.1021/acs.molpharmaceut.7b00730

Koppolu, B., and Zaharoff, D. A. (2013). The effect of antigen encapsulation in chitosan particles on uptake, activation and presentation by antigen presenting cells. *Biomaterials* 34, 2359–2369. doi: 10.1016/j.biomaterials.2012.11.066

Kumar, V., Leekha, A., Tyagi, A., Kaul, A., Mishra, A. K., and Verma, A. K. (2017). Preparation and evaluation of biopolymeric nanoparticles as drug delivery system in effective treatment of rheumatoid arthritis. *Pharm. Res.* 34, 654–667. doi: 10.1007/s11095-016-2094-y

Kurita, K., Kaji, Y., Mori, T., and Nishiyama, Y. (2000). Enzymatic degradation of β-chitin: susceptibility and the influence of deacetylation. *Carbohydr. Polym.* 42, 19–21. doi: 10.1016/S0144-8617(99)00127-7

Laloy, J., Minet, V., Alpan, L., Mullier, F., Beken, S., Toussaint, O., et al. (2014). Impact of silver nanoparticles on haemolysis, platelet function and coagulation. *Nanobiomedicine* 1:4. doi: 10.5772/59346

Lavertu, M., Xia, Z., Serreqi, A. N., Berrada, M., Rodrigues, A., Wang, D., et al. (2003). A validated 1H NMR method for the determination of the degree of deacetylation of chitosan. *J. Pharm. Biomed. Anal.* 32, 1149–1158. doi: 10.1016/S0731-7085(03)00155-9

Lebre, F., Borchard, G., Faneca, H., Pedroso de Lima, M. C., and Borges, O. (2016). Intranasal administration of novel chitosan nanoparticle/dna complexes induces antibody response to Hepatitis B surface antigen in mice. *Mol. Pharm.* 13, 472–482. doi: 10.1021/acs.molpharmaceut.5b00707

Lebre, F., Lavelle, E. C., and Borges, O. (2019). Easy and effective method to generate endotoxin-free chitosan particles for immunotoxicology and immunopharmacology studies. *J. Pharm. Pharmaco.* 71, 920–928. doi: 10.1111/jphp.13082

Lieder, R., Gaware, V. S., Thormodsson, F., Einarsson, J. M., Ng, C. H., Gislason, J., et al. (2013). Endotoxins affect bioactivity of chitosan derivatives in cultures of bone marrow-derived human mesenchymal stem cells. *Acta Biomater.* 9, 4771–4778. doi: 10.1016/j.actbio.2012.08.043

Moore, T. L., Rodriguez-Lorenzo, L., Hirsch, V., Balog, S., Urban, D., Jud, C., et al. (2015). Nanoparticle colloidal stability in cell culture media and impact on cellular interactions. *Chem. Soc. Rev.* 44, 6287–6305. doi: 10.1039/C4CS00487F

Muzzarelli, R. A. (1998). Colorimetric determination of chitosan. *Anal. Biochem.* 260, 255–257. doi: 10.1006/abio.1998.2705

Nadesh, R., Narayanan, D., Sreerekha, P. R., Vadakumpully, S., Mony, U., Koyakkutty, M., et al. (2013). Hematotoxicological analysis of surface-modified and -unmodified chitosan nanoparticles. *J. Biomed. Mater. Res. A* 101, 2957–2966. doi: 10.1002/jbm.a.34591

Oliveira, C. R., Rezende, C. M., Silva, M. R., Borges, O. M., Pego, A. P., and Goes, A. M. (2012). Oral vaccination based on DNA-chitosan nanoparticles against *Schistosoma mansoni* infection. *Sci. World J.* 2012:938457. doi: 10.1100/2012/938457

Omar Zaki, S. S., Katas, H., and Hamid, Z. A. (2015). Lineage-related and particle size-dependent cytotoxicity of chitosan nanoparticles on mouse bone marrow-derived hematopoietic stem and progenitor cells. *Food Chem. Toxicol.* 85, 31–44. doi: 10.1016/j.fct.2015.05.017

Oostingh, G. J., Casals, E., Italiani, P., Colognato, R., Stritzinger, R., Ponti, J., et al. (2011). Problems and challenges in the development and validation of human cell-based assays to determine nanoparticle-induced immunomodulatory effects. *Part. Fibre Toxicol.* 8:8. doi: 10.1186/1743-8977-8-8

Palta, S., Saroa, R., and Palta, A. (2014). Overview of the coagulation system. *Indian J. Anaesth.* 58, 515–523. doi: 10.4103/0019-5049.144643

Pattani, A., Patravale, V. B., Panicker, L., and Potdar, P. D. (2009). Immunological effects and membrane interactions of chitosan nanoparticles. *Mol. Pharm.* 6, 345–352. doi: 10.1021/mp900004b

Peluso, G., Petillo, O., Ranieri, M., Santin, M., Ambrosio, L., Calabro, D., et al. (1994). Chitosan-mediated stimulation of macrophage function. *Biomaterials* 15, 1215–1220. doi: 10.1016/0142-9612(94)90272-0

Ph. Eur. 9.0. (2019). "Monograph for water for injections (0.169)," in *European Pharmacopoeia*. Strasbourg: Council of Europe.

Roberts, D. D., Taciak, B., Białasek, M., Braniewska, A., Sas, Z., Sawicka, P., et al. (2018). Evaluation of phenotypic and functional stability of RAW 264.7 cell line through serial passages. *PLoS ONE* 13:e0198943. doi: 10.1371/journal.pone.0198943

Rösslein, M., Elliott, J. T., Salit, M., Petersen, E. J., Hirsch, C., Krug, H. F., et al. (2015). Use of cause-and-effect analysis to design a high-quality nanocytotoxicology assay. *Chem. Res. Toxicol.* 28, 21–30. doi: 10.1021/tx500327y

Salehi, F., Behboudi, H., Kavoosi, G., and Ardestani, S. K. (2017). Chitosan promotes ROS-mediated apoptosis and S phase cell cycle arrest in triple-negative breast cancer cells: evidence for intercalative interaction with genomic DNA. *RSC Adv.* 7, 43141–43150. doi: 10.1039/C7RA06793C

Sarangapani, S., Patil, A., Ngeow, Y. K., Elsa Mohan, R., Asundi, A., and Lang, M. J. (2018). Chitosan nanoparticles' functionality as redox active drugs through cytotoxicity, radical scavenging and cellular behaviour. *Integr. Biol.* 10, 313–324. doi: 10.1039/C8IB00038G

Schieber, M., and Chandel, N. S. (2014). ROS function in redox signaling and oxidative stress. *Curr. Biol.* 24, R453–R462. doi: 10.1016/j.cub.2014.03.034

Shelma, R., and Sharma, C. P. (2011). Development of lauroyl sulfated chitosan for enhancing hemocompatibility of chitosan. *Colloids Surf. B Biointerfaces* 84, 561–570. doi: 10.1016/j.colsurfb.2011.02.018

Soares, E., Groothuismink, Z. M. A., Boonstra, A., and Borges, O. (2019). Glucan particles are a powerful adjuvant for the HBsAg, favoring antiviral immunity. *Mol. Pharm.* 16, 1971–1981. doi: 10.1021/acs.molpharmaceut.8b01322

Soares, E., Jesus, S., and Borges, O. (2018a). Chitosan:beta-glucan particles as a new adjuvant for the Hepatitis B antigen. *Eur. J. Pharm. Biopharm.* 131, 33–43. doi: 10.1016/j.ejpb.2018.07.018

Soares, E., Jesus, S., and Borges, O. (2018b). Oral hepatitis B vaccine: chitosan or glucan based delivery systems for efficient HBsAg immunization following subcutaneous priming. *Int. J. Pharm.* 535, 261–271. doi: 10.1016/j.ijpharm.2017.11.009

Stopinšek, S., Ihan, A., Salobir, B., Terčelj, M., and Simčič, S. (2016). Fungal cell wall agents and bacterial lipopolysaccharide in organic dust as possible risk factors for pulmonary sarcoidosis. *J. Occup. Med. Toxicol.* 11:46. doi: 10.1186/s12995-016-0135-4

Szymanska, E., and Winnicka, K. (2015). Stability of chitosan—a challenge for pharmaceutical and biomedical applications. *Mar. Drugs* 13, 1819–1846. doi: 10.3390/md13041819

U.S. FDA (2019a). *United States Food and Drug Administration Generaly Regarded As Safe Notices Inventory*. Available online at: https://www.accessdata.fda.gov/scripts/fdcc/?set=GRASNotices&sort=GRN_No&order=DESC&startrow=1&type=basic&search=chitosan (accessed October 24, 2019).

U.S. FDA (2019b). *United States Food and Drug Admistration Medical Device Database*. Available online at: https://accessgudid.nlm.nih.gov/devices/search?page=1&query=%28%22chitosan%22%29 (accessed October 24, 2019).

Vårum, K. (2001). Acid hydrolysis of chitosans. *Carbohydr. Polym.* 46, 89–98. doi: 10.1016/S0144-8617(00)00288-5

van Meerloo, J., Kaspers, G. J. L., and Cloos, J. (2011). Cell sensitivity assays: the MTT *assay. Methods Mol. Biol.* 731, 237–245. doi: 10.1007/978-1-61779-080-5_20

Villiers, C., Chevallet, M., Diemer, H., Couderc, R., Freitas, H., van Dorsselaer, A., et al. (2009). From secretome analysis to immunology: chitosan induces major alterations in the activation of dendritic cells via a TLR4-dependent mechanism. *Mol. Cell Proteomics* 8, 1252–1264. doi: 10.1074/mcp.M800589-MCP200

Wang, H., Yu, X., Su, C., Shi, Y., and Zhao, L. (2018). Chitosan nanoparticles triggered the induction of ROS-mediated cytoprotective autophagy in cancer cells. *Artif. Cells Nanomed. Biotechnol.* 46 (suppl. 1), 293–301. doi: 10.1080/21691401.2017.1423494

Wang, L., Miyahira, A. K., Simons, D. L., Lu, X., Chang, A. Y., Wang, C., et al. (2017). IL6 signaling in peripheral blood T Cells predicts clinical outcome in breast cancer. *Cancer Res.* 77, 1119–1126. doi: 10.1158/0008-5472.CAN-16-1373

Wen, Z. S., Liu, L. J., Qu, Y. L., Ouyang, X. K., Yang, L. Y., and Xu, Z. R. (2013). Chitosan nanoparticles attenuate hydrogen peroxide-induced stress injury in mouse macrophage RAW264.7 cells. *Mar. Drugs* 11, 3582–3600. doi: 10.3390/md11103582

Wu, G. J., and Tsai, G. J. (2007). Chitooligosaccharides in combination with interferon-gamma increase nitric oxide production via nuclear factor-kappaB activation in murine RAW264.7 macrophages. *Food Chem. Toxicol.* 45, 250–258. doi: 10.1016/j.fct.2006.07.025

Wu, N., Wen, Z. S., Xiang, X. W., Huang, Y. N., Gao, Y., and Qu, Y. L. (2015). Immunostimulative activity of low molecular weight chitosans in RAW264.7 macrophages. *Mar. Drugs* 13, 6210–6225. doi: 10.3390/md13106210

Yang, S. A., Choi, S., Jeon, S. M., and Yu, J. (2018). Silica nanoparticle stability in biological media revisited. *Sci. Rep.* 8:185. doi: 10.1038/s41598-017-18502-8

Conflict of Interest: The authors declare that the research was conducted in the absence of any commercial or financial relationships that could be construed as a potential conflict of interest.

frontiers in Bioengineering and Biotechnology

REVIEW
published: 25 February 2020
doi: 10.3389/fbioe.2020.00127

Nanoscale Self-Assembly for Therapeutic Delivery

*Santosh Yadav, Ashwani Kumar Sharma and Pradeep Kumar**

Nucleic Acids Research Laboratory, CSIR Institute of Genomics and Integrative Biology, Delhi, India

Self-assembly is the process of association of individual units of a material into highly arranged/ordered structures/patterns. It imparts unique properties to both inorganic and organic structures, so generated, via non-covalent interactions. Currently, self-assembled nanomaterials are finding a wide variety of applications in the area of nanotechnology, imaging techniques, biosensors, biomedical sciences, etc., due to its simplicity, spontaneity, scalability, versatility, and inexpensiveness. Self-assembly of amphiphiles into nanostructures (micelles, vesicles, and hydrogels) happens due to various physical interactions. Recent advancements in the area of drug delivery have opened up newer avenues to develop novel drug delivery systems (DDSs) and self-assembled nanostructures have shown their tremendous potential to be used as facile and efficient materials for this purpose. The main objective of the projected review is to provide readers a concise and straightforward knowledge of basic concepts of supramolecular self-assembly process and how these highly functionalized and efficient nanomaterials can be useful in biomedical applications. Approaches for the self-assembly have been discussed for the fabrication of nanostructures. Advantages and limitations of these systems along with the parameters that are to be taken into consideration while designing a therapeutic delivery vehicle have also been outlined. In this review, various macro- and small-molecule-based systems have been elaborated. Besides, a section on DNA nanostructures as intelligent materials for future applications is also included.

Keywords: self-assembly, nanostructures, amphiphilicity, polymers, small molecules, drug delivery

OPEN ACCESS

Edited by:
Gianni Ciofani,
Italian Institute of Technology, Italy

Reviewed by:
Veikko Linko,
Aalto University, Finland
Stefano Leporatti,
Italian National Research Council, Italy

***Correspondence:**
Pradeep Kumar
pkumar@igib.res.in

Specialty section:
This article was submitted to Nanobiotechnology, a section of the journal Frontiers in Bioengineering and Biotechnology

Received: *27 September 2019*
Accepted: *10 February 2020*
Published: *25 February 2020*

Citation:
Yadav S, Sharma AK and Kumar P (2020) Nanoscale Self-Assembly for Therapeutic Delivery. Front. Bioeng. Biotechnol. 8:127. doi: 10.3389/fbioe.2020.00127

Abbreviations: Boc, t-butyloxy carbonyl; CDs, cyclodextrins; CMC, critical micellar concentration; DDSs, drug delivery systems; DEPC, dierucoylphosphatidylcholine; DMPC, dimyristoyl phosphatidylcholine; DMPG, dimyristoyl phosphatidylglycerol; DNA, deoxyribonucleic acid; DOPC, dioleoylphosphatidylcholine; DOPE, dioleoly-sn-glycero-phophoethanolamine; DOPS, dioleoylphosphatidylserine; DPPC, (1,2-dipalmitoyl-sn-glycero-3-phosphocholine); DPPG, dipalmitoylphosphatidylglycerol; DSPC, distearoylphosphatidylcholine; DSPE, distearoyl-sn-glycero-phosphoethanolamine; DSPE-MPEG-2000, (1,2-distearoyl-sn-glycero-3-phosphoethanolamine-*N*-methoxypolyethyleneglycol-2000); DSPG, distearoylphosphatidylglycerol; EPC, egg phosphatidylcholine; Fmoc, 9-fluorenylmethyloxy carbonyl; HA, hyaluronic acid; HSPC, hydrogenated soy phosphatidylcholine; MPEG, methoxy polyethylene glycol; MSPC, (1-stearoyl-2-hydroxy-sn-glycero-3-phosphocholine); PEG, polyethylene glycol; PGA, poly(glycolic acid); PISA, polymerization-induced self-assembly; POPC, palmitoyloleoylphosphatidylcholine; PLA, poly(D,L-lactic acid); PLGA, poly(D,L-lactic-co-glycolic acid); PTX, paclitaxel; RNA, ribonucleic acid; SM, sphingomyelin; Tm, transition temperature.

INTRODUCTION

Supramolecular self-assembly has recently attracted the attention of the researchers worldwide to generate nanostructures and nanomaterials bearing unique physical and chemical properties. The organization of molecules in these nanoassemblies has made it possible to design and develop new devices that can interact with the living cells and generate the response. These are not only being focused as important components in the emergence of cellular life, but also as materials that can be used in huge applications ranging from diagnostics and sensing to biomaterials, bioelectronics, energy generation, catalysis, drug delivery, and nanocomposites (Busseron et al., 2013; Du et al., 2015; Habibi et al., 2016; Xing and Zhao, 2016). Mainly, two strategies, viz., top-down and bottom-up, are being followed for the fabrication of nanostructures (**Figure 1**). The earlier one involves the carving out of the final nanostructure with a defined shape and size from a larger block of matter. As a result, the strategy does not require atomic level control. Alternatively, the later approach involves building up of the desired nanostructures from the basic components by the processes of molecular recognition and self-assembly, which is basically derived from the interactions of basic units to form well-organized structures. Therefore, the atomic or molecular level control is possible in the later approach over the formation of nanostructures by manipulating the structures of self-assembling molecular units.

SELF-ASSEMBLY

Self-assembly is the spontaneous molecular arrangement of the disordered entities of molecules into ordered structures resulting from specific local interactions among the components themselves (Mendes et al., 2013; Mattia and Otto, 2015; Stoffelen and Huskens, 2016). Formation of the most of the biological nanostructures is the outcome of the self-assembly such as construction of cell membranes by assembly of phospholipid bilayers, helical structure of DNA, folding of polypeptide chains, etc. The interaction of a ligand with its receptor is also attributed to self-assembly (Haburcak et al., 2016; Azevedo and da Silva, 2018). It also accounts for the development of molecular crystals, self-assembled monolayers, phase separated polymers, and colloids (Busseron et al., 2013; Mendes et al., 2013; Du et al., 2015; Mattia and Otto, 2015; Habibi et al., 2016; Haburcak et al., 2016; Stoffelen and Huskens, 2016; Sun et al., 2017; Azevedo and da Silva, 2018). In fact, molecular self-assembly is a natural process which is very essential in the emergence and maintenance of life. Synthetic molecules like amino acids, oligo- and polypeptides, polymers, dendrimers, and π-conjugated compounds have been considered as the primary focus used for building up nanostructures, such as nanotubes, nanofibers, micelles, and vesicles (Buerkle and Rowan, 2012; Correa et al., 2012). Moreover, self-assembly of small molecules as building units is a useful strategy for the formation of structure-controlled materials (Ariga et al., 2019). Likewise, DNA-based nanomaterials have shown their potential in diagnostics and therapeutic delivery.

The process of self-assembly plays a key role in the design, synthesis, and development of newer nanomaterials (Whitesides and Boncheva, 2002).

- Self-assembly is centrally important to living materials, e.g. a cell consists of a wide variety of complex structures, viz., lipid biomembranes, protein aggregates, folded proteins, structured nucleic acids, molecular machines, etc., which have shown the propensity of self-assembly.
- It helps in acquiring regular structures of materials, viz., molecular crystals, liquid crystals, and semicrystalline and phase-separated polymers.
- It also happens in large molecules, which has opened up newer avenues for their use in material sciences and delivery applications.
- It offers the most simple and versatile strategy for developing nanostructures.

Thus, self-assembly has exhibited a profound impact in a wide range of fields, viz., physical, chemical, and biological sciences, materials and biomedical sciences, and manufacturing. Besides, the concept has provided opportunities to develop new materials and components of life through the exchange of ideas and methodologies among these fields.

CLASSIFICATION OF SELF-ASSEMBLY

The term self-assembly was initially used by the researchers in different fields and subsequently, it was adopted by the chemists to describe the ordered arrangement of the molecules. Now, it has applied to materials of any size (from small molecules to galaxies) in the world around us (Xing and Zhao, 2016). Recently, the strategy has been shifted to synthesis of molecules which can be manipulated at the molecular level. This has become possible due to integration of chemistry, biology, and material science. Based on the size and nature of building blocks, self-assembly can be classified into three main categories, i.e. atomic, molecular, and colloidal self-assemblies (**Figure 2**). A variety of building blocks have been embraced in the term "self-assembly." The process of self-assembly not only covers bulk materials, but also it can apply to two-dimensional systems, i.e. surfaces and interfaces. Thus, on the basis of the systems and where it occurs, it can be classified as biological or interfacial. Further, based on its processing, it can be categorized as thermodynamic or kinetic self-assembly. Atomic, molecular, biological, and interfacial self-assemblies are covered under thermodynamic processes, while colloidal and some interfacial self-assemblies come under kinetic ones. Among these types of assemblies, atomic and biological self-assemblies are directional while others are random or non-directional such as colloidal, molecular, and interfacial self-assemblies. Self-assembly involving large building units can also be responsive to one or the other external stimuli, viz., gravity, magnetic field, flow, electric field, surrounding media, etc.

Thus, as a result of self-assembly, spontaneous association can lead to generation of ordered structures in a range from angstrom to centimeter of different sizes and shapes. Historically,

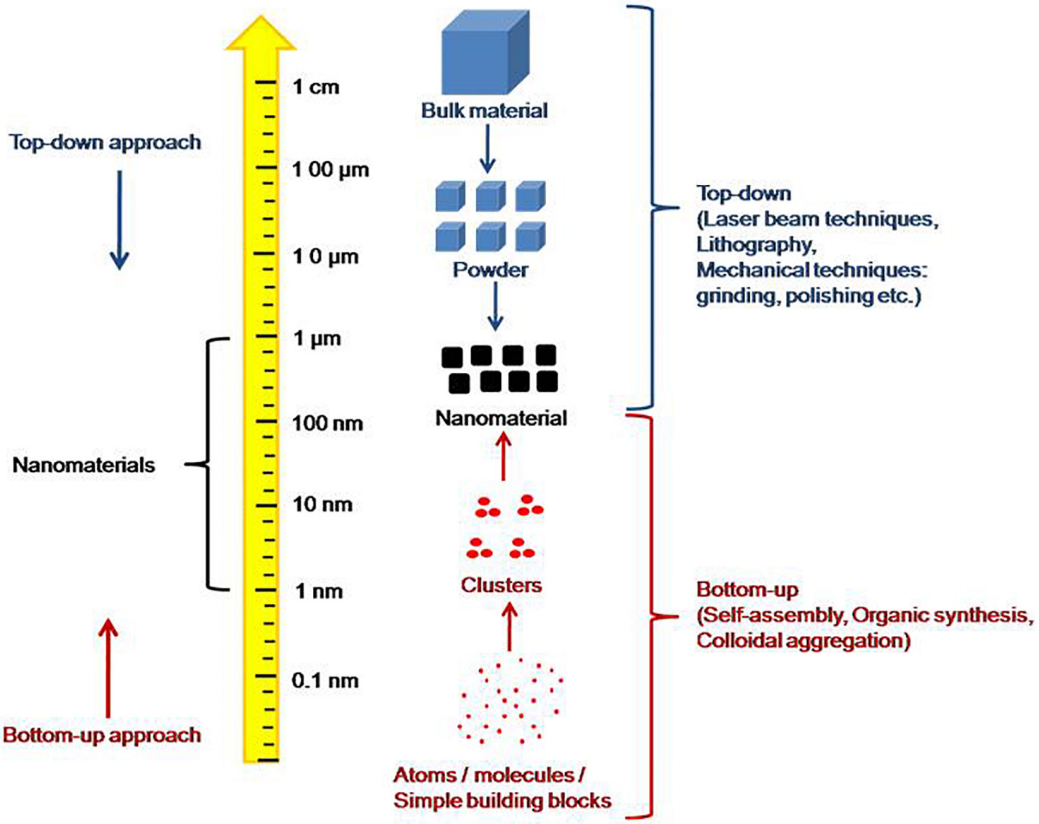

FIGURE 1 | "Top-down" and "bottom-up" approaches of self-assembly.

the concepts of self-assembly have come from the investigation of molecular/biological processes.

TYPES OF INTERACTIONS IN SELF-ASSEMBLY

Basically, the types of interactions that involved in the self-assembly processes occurring at colloidal, molecular, or atomic length scale are usually fragile and long range in contrast to chemical forces (Mendes et al., 2013). These are mainly non-covalently linked via van der Waals forces, hydrophobic, electrostatic, hydrogen bonding, π-π aromatic stacking, metal coordination, etc., which are normally weak (2–250 kJ/mol) individually in comparison to covalent linkages (100–400 kJ/mol) but together, if present in adequate numbers, they form very stable self-assembled structures and the shape, size, and functionality of the final assembly are administered by their fine balance (Mendes et al., 2013). Self-assembly between molecular units occurs when they interact with one another through a balance of usually weak and non-covalent intermolecular forces (Lee, 2008; Genix and Oberdisse, 2018). These interactions play a significant role in the alignment of molecular units in an ordered structure. These interactions are the main force that facilitates self-assembly of the units. Besides, the directionality and functionality of self-organized structures are determined by other functional interactions or forces (**Figure 3**). All these non-covalent interactions stabilize the self-assembled structures under different environmental conditions. Moreover, exhibition of completely new type of behavior as well as unique physical and chemical properties by self-assembled nanostructures have made them of special interest to researchers and scientists worldwide (Xing and Zhao, 2016). The distinctive intermolecular forces important in molecular self-assembly are given below (Mendes et al., 2013).

van der Waals Interactions

van der Waals interactions consist of attractive or repulsive forces between molecules which operate at moderate distances. These forces arise from dipole or induced dipole interactions at the atomic and molecular level (Lee, 2008). These are strong in vacuum or if there is no medium between two molecules. If a medium (such as water) comes between the two molecules, these forces are reduced because of dielectric screening from the medium. Obviously, this screening effect is particularly strong for water due to its high dielectric constant. The energy of the van der Waals interactions is around 1 $kJmol^{-1}$ whereas a covalent bond has a binding energy of around 150 $kJmol^{-1}$ or more (hydrogen bonds, for comparison, have typical energies of around 50 $kJmol^{-1}$). Overall, at atomic and molecular levels,

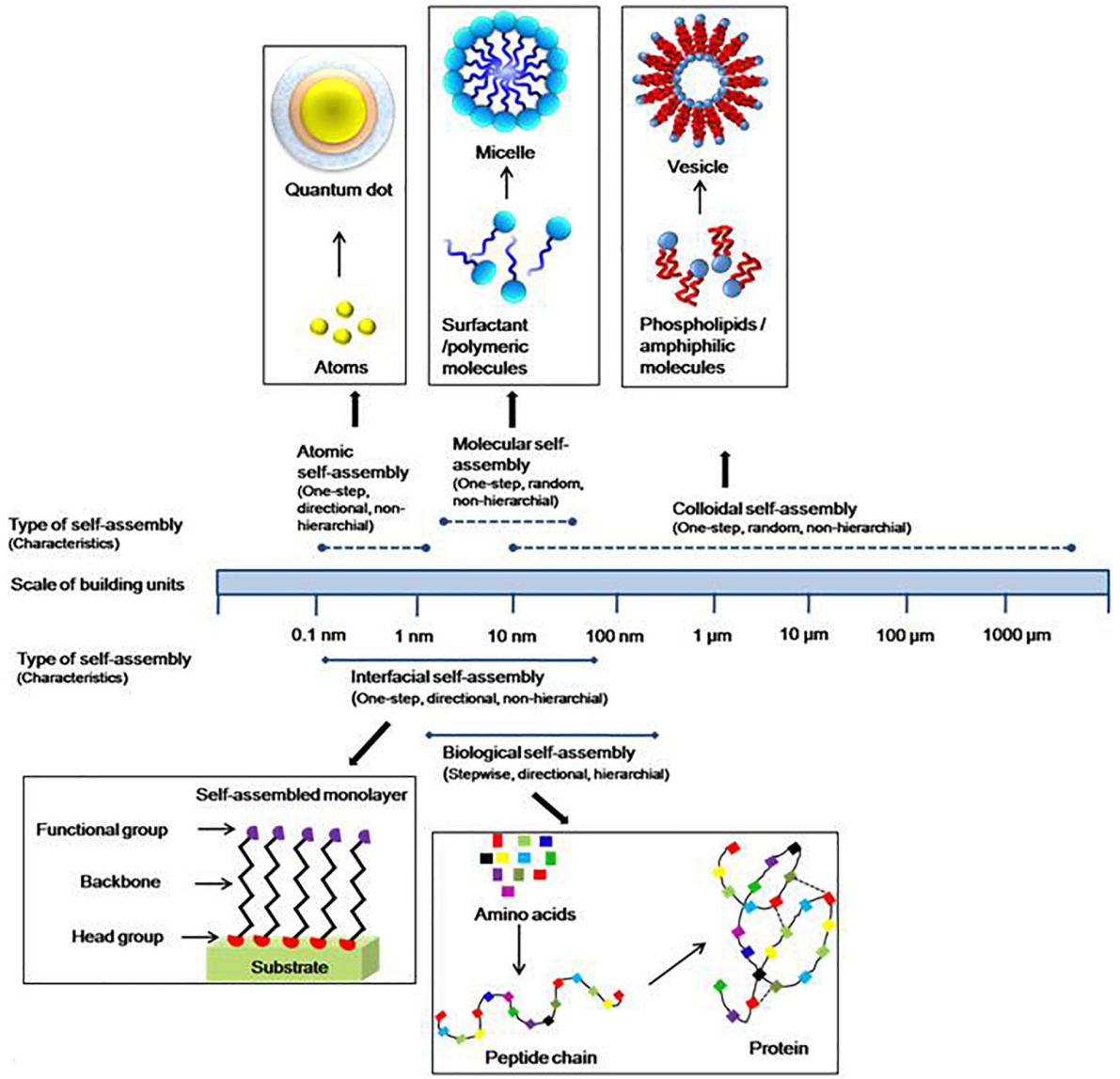

FIGURE 2 | Atomic, molecular, colloidal self-assemblies based on size or nature of building units, and biological, interfacial on the basis of system where the self-assembly occurs. The length range is of structural units.

van der Waals interactions are predominantly attractive, while, under certain conditions, these can also be repulsive (particularly, at short range).

Electrostatic Interactions and Electric Double Layer

Electrostatic interactions occur between two charged atoms, ions, or molecules, which can be either - attractive or repulsive forces, depending upon the sign of charges. These interactions are quite strong and act even at long range (upto ∼ 50 nm), however, decrease gradually with distance. Ionic self-assembly is straightforward and considered to be a reliable method for the organization of polyelectrolytes, charged surfactants, peptides, and lipids (Lee, 2008; Mendes et al., 2013). These forces originate from electrostatic interactions and impart a strong effect on many self-assembly processes. Further, these forces act as balancing interactions along with hydrophobic interactions, which result in the finite size and shape of self-aggregated structures. Sometimes these interactions get added onto during self-assembly process. Self-assembly processes at the atomic scale involve the electrostatic interactions in air as well as in vacuum, while in solution, molecular and colloidal/mesoscale self-assembly processes occur.

The interfacial double layers are generally quite evident in systems having large surface area to volume ratio, such as porous or colloidal bodies with pores or particles, respectively, in the range of micrometers to nanometers. Layer by layer or double

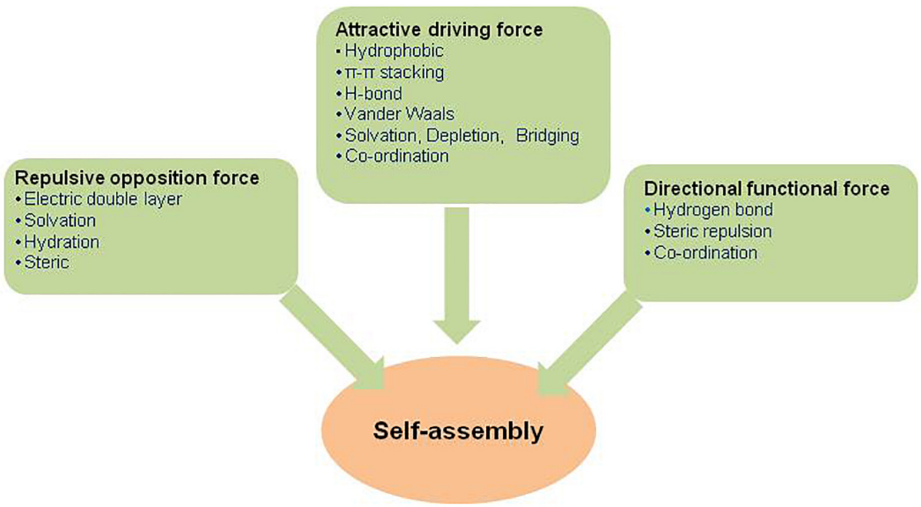

FIGURE 3 | Three classes of distinctive forces involved in self-assembly.

layer self-assembly plays an important part in several routinely employed materials, e.g. existence of homogenized milk, which is owing to coverage of fat droplets with a double layer that inhibits their agglomeration into butter.

Hydrophobic Interactions

Hydrophobic interactions play a big role in understanding the process of self-assembly. These interactions occur in water due to poor dispersibility of the hydrophobic moieties. Interaction of a hydrophobic moiety with water can be elucidated using thermodynamic effects which result in the change in free energy, entropy, enthalpy, and heat capacity. These changes can be studied by the thermodynamic principle, $\Delta G = \Delta H - T\Delta S$. When a hydrophobic substance interacts with water, the structure of water around that substance varies with the size and shape of the substance. This networking around the hydrophobic substance is called iceberg cluster or iceberg formation (Lee, 2008). The iceberg formation itself is not an entropic or enthalpic effect rather it depends upon the temperature and the geometry of the hydrophobic substance (Lee, 2008). Hydrophobic substances have been shown to exhibit extraordinary stronger interactions in aqueous phase as compared to the interactions in the gaseous state primarily because of van der Waals interactions. Therefore, due to poor dispersibility of hydrophobic moieties in water, they tend to form aggregates which ultimately result in self-assembly to generate micelles and lipid bilayers.

Hydrogen Bonding

Hydrogen bonding constitutes the most attractive type of bonding in controlling inter- or intramolecular orientations in self-assembly. It also helps in understanding the variety of events in biological systems (Lee, 2008; Mendes et al., 2013). The strength of H-bonding varies from 10–50 $kJmol^{-1}$, which indicates that this bonding has capability to provide sufficient stability to the self-assembled clusters. Basically, H-bonding occurs due to dipole-dipole attraction which takes place between a H-atom attached to an electronegative atom and an electronegative atom with lone pair of electrons present in the vicinity. Generally, it happens between H and O, F, and N. Strength of H-bonding is also affected by the surrounding medium, i.e. solvent. An additional feature of H-bonding is that it imparts stability as well as directionality to self-assembly. This property facilitates self-assembled structures to gain various morphologies useful for various biomedical applications.

Aromatic π-π Stacking

Aromatic π-π stacking refers to another type of non-covalent interactions which are quite attractive to researchers for cooperative binding during self-assembly. It occurs between aromatic residues as they contain pi bonds. These interactions have been found to be of considerable importance in DNA and RNA molecules (nucleic base stacking), folding of polypeptide/protein chains, template-directed synthesis, materials sciences, and molecular recognition (Bissantz et al., 2010). Large polarizabilities and a significant quadrupole moment, generated by a particular shape and electronic properties of the aromatic ring systems, result in a set of preferred interaction geometries. As demonstrated by various theoretical and practical investigations, it has been well established that aromatic ring systems have tendency to form ordered clusters of four different types, viz., parallel displaced, T-shaped, parallel staggered, or Herringbone (Gazit, 2002). These geometries might be possibly potential minimum configurations in the Lennard–Jones–Coulomb empirical potential calculations. For interactions between two π systems, the predominant arrangements are the T-shaped edge-to-face and the parallel-displaced stacking arrangement. In proteins, the parallel-displaced stacking arrangement is observed more frequently. Stacking is potentially more favored between electron deficient aromatic rings rather than electron rich rings. Moreover, the alignment of positive and negative partial charges and molecular dipoles significantly affects the preference among the orientation of heteroaromatic

rings. This becomes even more attractive when edge-to-face interactions are increased as a result of increased acidity of the interacting hydrogen atom. The effect is visible when a strongly electron withdrawing substituent in ortho or/and para position is introduced (Wheeler and Houk, 2009).

The steric constrains observed during the formation of the organized stacking structures have an essential role in the process of self-assembly that leads to the formation of supramolecular structures. Such π-π stacking interactions are responsible for stabilization of the tertiary structure of proteins, host–guest interactions, double-helix structure of DNA involved in core packing, and porphyrin aggregation in solution.

Gazit (2002) has also reported that π-π stacking interactions play a significant role in self-assembly of amyloid fibril formations. π-π stacking provides two important elements for the formation of these structures, (i) an energetic contribution that drives the self-assembly process thermodynamically and (ii) specific directionality and orientation that are driven by the set of stacking pattern (Gazit, 2002). This becomes more important because amyloid fibrils are well-defined supramolecular structures and a pre-determined pattern of stacking leads to formation of an organized structure. On analyzing a group of proteins with known structures having π-π stacking in them, it was noticed that a parallel displaced π-π stacking is the major organization of π-π interactions in proteins.

FABRICATION OF SELF-ASSEMBLED AGGREGATES

Self-assembly is a process that involves balancing between attractive driving force, repulsive opposition force, and directional force (Lee, 2008; Mendes et al., 2013; Genix and Oberdisse, 2018). Particularly, a sweet balance between attractive and repulsive forces initiates the formation of self-assembled aggregates, which is a random process and also shows non-hierarchical structures (**Figure 3**). Most of the colloidal and micellar systems fit in non-hierarchical type of self-assembly. Addition of directional force to the other forces, the self-assembly processes become directional. Moreover, the self-assembled aggregates in such cases usually show hierarchical structures that include biological and bio-mimetic systems.

Micelles

In case of micelle formation by surfactant molecules, the attractive and repulsive forces guide surfactant molecules to come close enough to acquire an ordered structure (Lee, 2008; Xing and Zhao, 2016). The driving force that allows the formation of micellar system is the hydrophobic attraction while ionic repulsion and/or solvation force acts as the opposition force. As a result of this arrangement, at a certain position, the attractive and repulsive forces balance each other, which results in the formation of micelles. Concentration of the surfactant is the concentration that is required to form the first micelle (CMC). Addition of more amounts of surfactant molecules in bulk solution will result in the formation of additional micelles following the same force balance scheme. During this process, the size of the micelles remains invariable.

Vesicles

Vesicles are sphere-shaped lamellar structures having a hollow aqueous core (Xing and Zhao, 2016). The formation of vesicles can be viewed as two-step self-assembly process in which amphiphiles first form a bilayer which then closes to form a vesicle. A number of amphiphilic organic compounds, varying from natural to synthetic, exhibit vesicle formation (Lombardo et al., 2015; Xing and Zhao, 2016). Natural phospholipids, amphiphilic polymers, and polypeptides capable of forming vesicles are called liposomes, polymerosomes, and peptosomes, respectively (Xing and Zhao, 2016). Among these classes of compounds, most of them are formed of a hydrophilic head and a lipophilic tail that induces formation of vesicles. During exposure to aqueous media, the hydrophilic head interacts with water while the hydrophobic tail contracts inside to minimize exposure to water. In this process, the lipophilic part of the amphiphile buries inside the bilayer and the hydrophilic part forms the interior and exterior positions exposed to aqueous environments. Differences in the arrangement of molecules lead to unilamellar or multilamellar vesicles with diameters in range from 20 nm to several micrometers according to the number of bilayers present in the newer structures formed.

In a self-assembly of amphiphiles into a vesicle or other types of structures, the volume ratio of the hydrophilic and lipophilic parts plays a significant role and it is a dominant factor which is now being applied for designing and development of vesicular structures.

In the equation, P = v/la,

"v" and "l" symbolize the volume and length of the lipophilic part, while "a" symbolizes the volume of the hydrophilic head. "P" values can help in speculating the morphology of the nanostructures and explaining the phase transitions.

If

$P < 1/3$, spherical micelles
$1/3 < P < 1/2$, worm-like micelles
$1/2 < P < 1$, vesicles
$P = 1$, planar bilayers
$P > 1$, inverted structures.

This theory was initially applied to surfactant systems but now it is being applied in studying self-assemblies of other kinds of amphiphiles that include amphiphilic block copolymers which follow the same principles as the small-molecule-based systems (Chu et al., 2013). Having both the hydrophilic interior and hydrophobic membrane, vesicles can be used to entrap both the hydrophobic as well as hydrophilic drugs at the same time. Liposomal vesicles have been well demonstrated to carry a wide range of therapeutic molecules and some of them are currently being used in clinical applications. Some recent papers focus on manipulating the size, shape, physical properties, and biodistribution of vesicles for drug delivery applications and emphasize the need of further control of these parameters of vesicles for therapeutic delivery applications (Zhao et al., 2017).

Fibrillar Networks or Hydrogels

Hydrogels are 3-D continuous interpenetrated network of phases, the solid and the liquid phase (Lee, 2008; Mendes et al., 2013; Shang et al., 2019). The liquid phase of a hydrogel comprises of water while the solid phase is network structure in which nanofibers are formed via molecular self-assembly (i.e. molecular gelators). Fibers can be formed from self-assembled proteins, peptides, lipids, and hybrid amphiphiles. However, their formation is significantly dependent on hydrophobic–hydrophilic balance as it is essential for self-assembly. These nanofibers act as the matrices of a hydrogel. It also prevents the undesirable precipitation or dissolution of the hydrogelators (Du et al., 2015). The hydrophilic part of the molecule locates itself as the exterior portion of the nanofibers, which gets involved in hydrogen bonding with the surrounded water molecules making it certain that hydrophilic biomolecules such as drug molecules (small peptides) can be translated into hydrogelators. Such supramolecular structures interact with the target molecules/sites more efficiently than the native biomolecules thereby increasing their bioactivity. As a hydrogel contains ∼97% of water, still it behaves like a solid and can flow only when a shear force is applied. Generally, hydrogels display response to an external stimulus and undergo a phase transition upon its application because these are formed via the self-assembly of small molecules through hydrogen bonding and hydrophobic interactions which are quite weak interactions. Apart from this, the supramolecular hydrogels offer an added advantage that these are biocompatible and biodegradable, as well as resemble to extracellular matrices which help in design and synthesis of novel supramolecular hydrogelators as materials for biomedical applications. Hydrogel materials have been intended to synthesize for encapsulation and delivery of water soluble therapeutic molecules. There are many reports in literature which demonstrate the encapsulation and release of small hydrophilic molecules, proteins, and cells from the hydrogels (Narayanaswamy and Torchilin, 2019). Drug molecules can be entrapped into the networked structure during initiation of self-assembly process. Hydrogels, formed mainly by the process of self-assembly, are joined together through non-covalent crosslinking (covalent or physical hydrogels), which also determines its actual mechanical strength. The classification of the hydrogels can be made on the basis of their source (natural or synthetic), nature (degradable or non-degradable), networking (covalent or physical), and the nature of network (homopolymeric, copolymeric, interpenetrating networks, and double networks).

APPLICATIONS OF SELF-ASSEMBLED MATERIALS

The term nanostructure generally refers to those materials/structures which have structured components with at least one dimension less than 100 nm. The properties (both physical and chemical) of nanostructures are markedly dissimilar from their monomeric unit or the bulk material having identical chemical composition. The main reason for this unique behavior at nano-scale is due to the appearance of new quantum effects as well as enhanced surface area to volume ratio (Dahman, 2017). As the nanostructures have higher surface area to volume ratio as compared to their conventional forms, they exhibit greater chemical reactivity and strength. These emergent properties exhibited at nano-scale have the potential for greater impacts in biomedical applications. Suitable modulation of the properties and response of nanostructures may result in the creation of new desired gadgets and technologies.

The area of nanobiotechnology for therapeutic delivery is flooded with new challenges as the demand for new medical therapies is increasing exponentially. Earlier, the nanomedicines were developed by reformulating the available drugs in nanostructures. With the development of nanomedicines, which have shown the potential to treat the diseases in a much better way, the demand for personalized medicines has grown up that requires the customization of the fabrication of the nanostructures with in-built desired properties (Cui et al., 2010). For this customization, an improved control over structure, composition, as well as function of the matter at molecular level is needed. To achieve this control at molecular level, self-assembly comes into picture which can play a very crucial role by adjusting various parameters such as size, shape, and surface chemistry mimicking the 3-D structure of biomacromolecules. Thus, novel nanomaterials can be produced with greater ease and economically by employing the tools of molecular self-assembly. Furthermore, diverse nanostructures with varied functionality can be produced by this process (Genix and Oberdisse, 2018). The great advantage of this scheme for the formation of nanosized structures is the structural control over the final self-assembled nanostructures which can be achieved by varying the monomer, its composition, and chemistry, by inducing environmental changes (solvents, temperature, pH, and co-assembling molecules), and changing the rate of self-assembly process (Dallin et al., 2019). The ultimate goal of these self-assembled nanostructures is to attain their required functions; whether these structures are thermodynamically stable or not. As discussed above, self-assembly easily provides the flexibility to develop newer materials with customized morphologies and preferred functionalities and thus provides better control over bulk properties of the resulting nanostructures. Hence, it is quite simple to presume the behavior of final assembly by controlling the structural changes in the constituent molecules. In recent past, a plethora of nanostructures have been produced using different biopolymers (proteins, carbohydrates, nucleic acids, etc.) which have further refined the concepts and knowledge of this process as well as enhanced the use of these self-assembled materials in diverse medical applications such as in fabrication of molecular devices, delivery systems, or scaffolds (Panda and Chauhan, 2014; Azevedo and da Silva, 2018; Lombardo et al., 2019). These systems have shown their promising potential, however, need more attention to address some limitations in terms of their *in vivo* stability which has hindered their safe use in human beings.

Self-assembled nanomaterials are being used for a very broad range of applications from fundamental to applied research, with striking implementations in biomedical sciences, information

technology, and environmental sciences. Here, in this article, self-assembled nanostructures useful for biomedical applications have been the main focus, specially, drug delivery and gene delivery, so the subsequent part deals with these aspects (Busseron et al., 2013; Xing and Zhao, 2016).

Drug Delivery

Therapeutic delivery is a very significant area to address concerns related to healthcare and medicine. Certain problems associated with the use of free drugs can be minimized by using the appropriate carriers for drugs such as stability issue of free drugs in biological system, short half-life, insolubility in aqueous environment, abnormality in biodistribution, and pharmacokinetics of the delivered drugs (Mohanraj and Chen, 2006). Controlled drug delivery has shown enhanced bioavailability of the therapeutic by avoiding their untimely degradation and improving their uptake, maintaining the therapeutic dose of the drug by controlling the kinetics of drug release, and reducing toxicity by targeting to desired sites/tissues. In this regard, nanoparticles have proved to be potential DDS due to their advantageous characteristics. Many positive aspects of nanoparticle-mediated delivery of therapeutics have been realized (Wang et al., 2018).

Nanoparticles as therapeutic delivery systems offer several advantages:

i. Particle size and surface properties of nanoparticles are amenable to manipulation to achieve drug targeting.
ii. Nanoparticles possess large surface to mass ratio; hence, they can bind, absorb, and carry large amounts of drug molecules.
iii. Nanoparticles can easily control the drug release during the process of uptake and internalization as well as at the intended site which helps in reducing side effects/toxicity of the drug.
iv. The rate of release of the drug as well as the degradation of a carrier can be manipulated by selecting appropriate matrix constituents. Moreover, the drug entrapment is quite high in nanoparticles and that too without any chemical reaction, rather these are retained via physical interactions which help in preserving the drug activity.
v. By attaching specific ligands onto the surface of the nanoparticles, site-specific targeting can be achieved.
vi. Nanoparticles can be delivered via different pathways such as parenteral, intra-ocular, intravenous, oral, nasal, etc.

Criteria for the Designing of New Delivery Vehicles

Criteria for the designing of a new delivery vehicle are highly dependent on the therapeutics to be delivered and intended applications. Some of the common points, that are kept in mind while designing these vectors, are given below (Yu et al., 2016; Knauer et al., 2019).

i. The delivery vehicles need to be non-toxic, biocompatible, and biodegradable, and get readily eliminated from the body.
ii. These must possess high therapeutic loading efficiency, which would reduce the number of cycles of drug administration.
iii. These should not damage or modify the therapeutic agent during entrapment process.
iv. These vectors should be able to deliver the drug in a controlled fashion to allow consistently defined release profiles.
v. When administered, the carriers should be capable of providing stability to the therapeutics from degradation and neutralization by antibodies.
vi. These should be amenable to modification so that ligands could be attached for site-specific delivery. In this case, accumulation of the carriers at the desired site of action would facilitate the release of the therapeutic at the desired rate.
vii. These should be easily administered with little discomfort.
viii. The preparation of delivery system should be easy, reasonably simple, reproductive and cost-effective, and should be amenable to scale-up.

Polymers

A wide range of self-assembled polymeric nanostructures have been used for drug delivery, but biodegradability is essential to overcome side effects and toxicity to healthy tissues (Sofi et al., 2018; George et al., 2019). The self-assembled nanostructures are formed from both natural and synthetic polymers. Numerous self-assembled DDSs have been developed which have successfully encapsulated drug molecules to improve bioavailability, bioactivity, and controlled delivery, with some achieving clinical testing (Felice et al., 2014) and some of them have been launched for commercial purposes (Felice et al., 2014) (**Table 1**).

Natural polymers

Natural polymers possess abundance of functional groups, amenable to modifications via chemical or biochemical routes that result in the generation of different types of biopolymer-based materials (Nitta and Numata, 2013; Abedini et al., 2018; Sofi et al., 2018). Among these natural polymers, polysaccharides constitute an important class of polymers which are being used more frequently for various biomedical applications. Polysaccharides are carbohydrate polymers of monosaccharide-based repeating units connected through glycosidic linkages. Their source of production is quite diverse; hence, these have different structures and properties, a wide variety of reactive functionalities, different chemical compositions, and molecular weights (Nitta and Numata, 2013). Based on their functional groups, these have been divided into two main categories, viz., non-ionic (dextrin, pullulan, dextran) and ionic polysaccharides (heparin, chitosan, alginate, etc.). Polysaccharides are considered to be highly stable, safe, non-toxic, biodegradable, hydrophilic, and biocompatible. By tethering lipophilic moieties on the polysaccharides, the resulting conjugates can readily self-assemble into micelles in aqueous solutions and can potentially be used for drug delivery applications. Some of the polysaccharides possess certain bioactive groups which can act as targeting

TABLE 1 | List of nanoengineered polymers for drug delivery applications (Felice et al., 2014; Bobo et al., 2016; Patra et al., 2018).

Product name	Carrier material	Drug/type of drug (Disease)	Approval year/phase
Livatag™	Poly(isohexyl-cyanoacrylate)	Doxorubicin/anthracycline (hepatocellular carcinoma)	Phase II
Lupron Depot™	PLA	Leuprolid/peptidic (Prostate and breast cancer)	1989
Estrasorb™	Lecithin	Estradiol/esteroide (Hot flushes during menopause)	2003
Risperdal consta™	PLGA	Risperidone/dopamine antagonist (bipolar disorder Schizophrenia)	2003
Abraxane™	Albumin	Paclitaxel/anthracycline (Breast cancer)	2005
Genexol-PM™	PEG–PLA	Paclitaxel/anthracycline (Breast cancer)	Phase II
Adagen™	PEG	Adenosine deaminase/peptidic (Severe combined immunodeficiency)	1990
Oncaspar™	PEG	Asparaginase/peptidic (Leukemia)	1994
PEG-intron™	PEG	Interferon α2b/proteic (Chronic hepatitis C)	2001
Cimzia™	PEG	Interferon α2b/proteic (Chron's disease)	2008
Omontys™	PEG	Peginesatide acetate/peptidic (Anemia)	2012
Xyotax™	Polyglumex	Paclitaxel/anthracycline (Lung cancer, ovarian cancer)	Phase III
Puricase™	PEG	Uricase/proteic (Hyperuricemia)	Phase III
Mylotarg™	Anti-CD33 monoclonal antibody	Ozogamicin/calicheamicins (Leukemia)	2000
Zevalin™	Anti-CD20 monoclonal antibody	Yttrium-90/radioactive material (Non-Hodgkin's lymphoma)	2002
Bexxar™	Anti-CD20 monoclonal antibody	Iodine-131/radioactive material (Non-Hodgkin's lymphoma)	2003
Kadcyla™	Anti-CD37 monoclonal antibody	Emtansine/maytansinoid (Breast cancer)	2013
Opaxio	Paclitaxel covalently linked to solid NPs of polyglutamate	Paclitaxel (Metastatic breast cancer)	2012
Cimzia	Pegylated antibody fragment	Certolizumab pegal (Crohn's disease, rheumatoid arthritis, psoriatic arthritis, spondylitis)	2008 2009 2013 2013
Plegridy	Pegylated IFN-B1 protein	Interferon B (Multiple sclerosis)	2015
Adynovate (Baxalta)	Pegylated factor VIII	FACTOR VIII (Hemophilia)	2015
Zilretta	Triamcinolone acetonide with a polylactic-co-glycolic acid matrix microsphere	Osteoarthritis of the knee	2017
Rebinyn	Coagulation factor IX GlycoPEGylated	Control and prevention of bleeding in perioperative setting for hemophilia B patients	2017

moieties. HA can act as ligand for targeting receptors present on the endothelial cells of liver and certain cancer cells. Self-assembled nanostructures of amphiphilic HAs have been highly investigated as active targeting agents in drug delivery (Cho et al., 2012). Self-assembled structures of modified cellulose, chitosan, and pullulan-based polysaccharides have also been used for colon targeting. These polymers promote drug absorption due to enhanced mucoadhesion in the small intestine. Similarly, amphiphilic heparin-based systems have also shown to reduce tumor size and blood vessel formation in tumor area (Niers et al., 2007). The most commonly and extensively used polysaccharides, namely, alginate, chitosan, and dextran, have been described here along with their therapeutic advantages.

Alginate. Alginate (sodium salt) is a water soluble polysaccharide which is made up of 1–4 linked α-L-glucuronic acid and α-D-mannuronic acid in alternating order. Modification of alginate produces diverse polymers which behave in different manners under physiological conditions. As biodegradability of polymer is improved by oxidation of hydroxyl group, sulfonation increases

blood compatibility (Kumar et al., 2004). Self-assembled PEG derivatives of alginate have shown significant improvement in hypocalcemia efficacy in rats by enhancing the oral delivery of calcitonin (Li et al., 2012). Recently, phenylalanine ethyl ester modified alginate self-assembled nanoparticles showed good *in vitro* cellular uptake efficiency and biocompatibility profile in human intestinal cell lines (Zhang P. et al., 2019). Ayub et al. (2019) synthesized cysteamine conjugated disulfide crosslinked sodium alginate nanoparticles by layer by layer self-assembly mechanism to get better delivery of an anticancer drug, PTX, for colon cancer. Further, the alginate nanoparticles have been used for antigen delivery also. Antigen-BSA encapsulated polylysine-sodium alginate nanoparticles were formed by process of self-assembly using electrostatic interactions between oppositely charged polyelectrolyte complexes. These particles showed sustained release behavior of vaccine and enhanced cellular uptake without imparting cytotoxicity *in vitro* (Yuan et al., 2018). The self-assembled alginate-based nanoparticles have been used in treatment of multidrug resistant tumors (Kumar et al., 2019) and in combinational chemotherapy (Zhang et al., 2017) as stimuli responsive (redox and light responsive) nanoparticles. Bazban-Shotorbani et al. (2016) synthesized alginate nanogels via microfluidics with tunable pore size and these nanogels were used for protein delivery.

Chitosan. Chitosan modifications and their use in delivery applications of various therapeutic molecules have been extensively reviewed in the literature (Coviello et al., 2007; Wasiak et al., 2016; Wang et al., 2017a; Quiñones et al., 2018). Chitosan, an unbranched linear polysaccharide, is made up of β-(1-4)-linked D-glucosamine (deacetylated unit) and *N*-acetyl-D-glucosamine (acetylated unit). It is produced from the skeleton of shellfish, including shrimp, lobster, and crab. It is used in various medicinal formulations such as filler in tablets, controlled-release drugs, and to improve the solubility of drugs. Self-assembly of the modified chitosans into micelles in aqueous solution with hydrophobic pockets has been used to entrap various anti-tumor therapeutics such as PTX, doxorubicin, and camptothecin (Quiñones et al., 2018). Recently, Trummer et al. (2018) synthesized *N*-benzyl-*N*,*O*-succinyl chitosan, *N*-naphthyl-*N*,*O*-succinyl chitosan, and *N*-octyl-*N*,*O*-succinyl chitosan-based self-assembled nanocarriers and successfully co-ordinated to antitumor drug cisplatin and evaluated the efficacy of these nanocarriers *in vitro* in human carcinoma cell line HN22 and HN29. The results showed high efficacy of *N*-benzyl-*N*,*O*-succinyl chitosan-mediated cisplatin delivery. They observed that the encapsulated formulation was less cytotoxic and caused lower cisplatin-induced renal cell death but it exhibited greater apoptosis in HN22 cells as compared to native cisplatin. Besides, the formulation provided long-lasting treatment with reduced nephrotoxicity. Chen et al. (2019) prepared polyelectrolyte complexes via self-assembly of opposite charged alginate-coated nanoparticles and chitosan nanoparticles and used this complex for pH sensitive controlled release of insulin.

Dextran. Dextran is a polymer formed from joining of glucose units through α-1,6-linkages with branch points at α-1,2, α-1,3, and α-1,4 linkages. It is non-toxic, highly biocompatible, and could be widely used in medicinal products including development of drug-delivery systems (Wasiak et al., 2016). It has been extensively used as a supplementary material to prevent the formation of blood clots by reducing blood viscosity and iron-dextran conjugates have been applied for fulfilling the iron deficiency. Derivatives of dextran have also been used as the source of biocompatible hydrogels for drug delivery applications to attain regulated and sustained drug release profile for longer time periods (Coviello et al., 2007). Wang et al. synthesized dextran nano-hydrogel by conjugating polyacrylic acid via disulfide crosslinking to dextran. The anticancer drug (doxorubicin) was conjugated to Dex-SS-PAA. The results showed that these nanohydrogels exhibited stimuli (pH and redox) responsive drug release behavior as well as greatly reduced the toxicity of free doxorubicin, and inhibited the growth of MDA-MB-231 tumors (Wang et al., 2017a). In another recent study, folic acid-dextran conjugates were synthesized which showed pH responsive self-assembly behavior. This conjugate self-assembled into nanoparticles at pH 7 and dissociated at pH > 9. The anticancer drug, doxorubicin, was efficiently entrapped in these particles and exhibited targeted drug delivery *in vitro* with enhanced antitumor activity in 4T1 subcutaneous tumor bearing mouse model (Tang et al., 2018). The modified soy-protein and dextran nanogels have been used for the delivery of riboflavin (Jin et al., 2016).

Cyclodextrins (CDs). Cyclodextrins are oligomers of glucose consisting of six, seven, and eight glucose units in α-, β-, and γ-CDs, respectively. The exterior of the cup-shaped molecule is hydrophilic while the internal part is hydrophobic, thus, they are readily soluble in aqueous environment and they can include small, hydrophobic "guest" molecules in their interior and thus forming inclusion complexes (Muankaew and Loftsson, 2018). Due to their inherent biocompatible nature, FDA approved their use in pharmaceutical formulations as solubilizing agents. CD derivatives are synthesized by replacing hydroxyl group on CDs with desired functional groups. The natural biocompatibility and self-assembling attributes of CDs have made them efficient nanocarriers for drug and gene delivery. These molecules can form diverse nanostructures such as nanoparticles, nanospheres, nanogels, nanomicelles, etc. The various modifications have been done on CDs to form amphiphilic derivatives that can self-assemble in aqueous environment and enhance interaction with cell membranes (Simoes et al., 2015). The modified CD amphiphiles can be cationic, anionic, or neutral depending on the groups attached to them. To form sustained drug release carriers, hydrophobic modifications have been done on CDs. He et al. (2013) synthesized acetalated α-CD material that showed pH modulated hydrolysis and pH triggered drug release behavior of encapsulated PTX drug *in vitro*. CDs have also been conjugated to various polymers to improve their physiochemical properties and enhance their drug delivery efficiency (Zhang and Ma, 2013; Zerkoune et al., 2014). Song et al. (2016) prepared β-CD conjugated poly[n-isopropylacrylamide] polymer as a temperature responsive drug carrier. This polymer self-assembled and formed inclusion complexes with PTX drug via host–guest interactions. The enhanced cellular uptake

and antitumor effect were observed in cancerous cell lines (Song et al., 2016).

Synthetic polymers

Among the commonly used synthetic polymers, block copolymers are a special class of polymers in which two or more blocks of polymers are attached in a regular arrangement. Block copolymers containing two, three, or more blocks are named as diblocks, triblocks, or multiblocks, respectively. PLA, PGA, and their copolymer PLGA, apart from being biodegradable and biocompatible, have been explored for therapeutic delivery and these are approved by the US Food and Drug Administration (Vilar et al., 2012).

Block copolymers are macromolecules which are formed by the linear and/or radial array of two or more dissimilar blocks having different monomer composition to impart amphiphilicity to molecule. The ever-increasing interest in block copolymers has recently arisen due to combinatorial qualities attained by the combination of two different polymers which leads to generation of micellar systems useful for carrying hydrophobic therapeutics.

A variety of amphiphilic copolymers, viz., di-block (A-B) and tri-block (A-B-A) grafted polymers, are being used to form self-assembled nanostructures for different biomedical applications. Among these nanostructures, the micelles are the most common structures formed from these copolymers or block polymers. On dissolving a block copolymer in a solvent, which can be an excellent solvent for dissolving one block and a poor solvent or precipitant for the second block, the copolymer molecules quickly align themselves to attain micellar structure and this phenomenon of micelle formation is reversible also. The most frequently used hydrophilic block is PEG. Other hydrophilic polymers which are commonly used are poly(*N*-vinylpyrrolidone) and poly(*N*-isopropylacrylamide). The core forming hydrophobic blocks which are most frequently used are poly(propyleneoxide), poly ε-caprolactone, polylactic acid (PLA), poly(lactide-co-glycolic acid) (PLGA), poly(L-aspartic acid), poly(L-histidine), poly(β-amino ester), etc. Among these polymers, PLA, PLGA, and PEG are the ones which have been approved or entered the clinical trial phases (Vilar et al., 2012; Felice et al., 2014) (**Table 1**).

In the last decade, for the fabrication of polymeric nanoparticles, the process of PISA has been used extensively in which polymerization as well as self-assembly occur simultaneously in one vessel to form polymeric nanoparticles. Drug can be encapsulated during the PISA process of nanoparticle formation as well as post-PISA process (Zhang W.J. et al., 2019).

Polylactic acid (PLA). Poly(D,L-lactic acid) is biodegradable polyester used in the fabrication of stents, implants, and various other medical devices (Hoffman, 2008). On hydrolysis, it degrades into monomeric lactic acid, which is also produced during anaerobic respiration in living beings. The polymer, characterized by its inherent viscosity, is dependent on its chain length/molecular weight. A controlled release of the entrapped therapeutic is also dependent on the PLA chain length. PLA is available commercially as Lupron Depot and Risperdal Consta in the form of microparticles. Among PLA matrices, the PLA-PEG micelles have extensively been used in drug delivery applications. For instance, Genexol PL^{TM} is PTX encapsulated PLA-PEG micelles. It is clinically approved in South Korea and Europe (Kim et al., 2004); however, in United States, it is still under phase II clinical trials. Amphotericin B was also encapsulated in PLA micelles and sustained drug release was observed. PLA-based micelles have been used in other drug delivery formulations also (Liu et al., 2008). Apart from these, PLA-based nanoparticles have also been used for entrapment of nucleic acid and their delivery (Munier et al., 2005). Several PLA-based nanostructures are under pre-clinical investigation.

Poly(lactic-co-glycolic acid) (PLGA). Poly(D,L-lactic-co-glycolic acid) is made up of two polymers, i.e. lactic acid and glycolic acid, which on hydrolysis yields biodegradable metabolite monomers, i.e. lactic acid and glycolic acid. These biodegradable metabolites are involved in several biochemical and physiological cycles in the living systems displaying minimal systemic toxicity. Degradation rate of PLGA highly depends on its molecular weight and monomer ratio (Danhier et al., 2012). Till now, PLGA-based therapeutic delivery systems have not been approved but certain PLGA-based systems are under pre-clinical and clinical trials. PLGA-based nanostructures are primarily used in the entrapment of lipophilic antitumor therapeutics, viz., PTX, vincristine sulfate, doxorubicin, curcumin, tetrandrine, etc. (Que et al., 2019). In one of the latest reviews, the industrial and scientific aspects of PLGA nanoparticles have been highlighted (Qi et al., 2019).

Polyethylene glycol (PEG). Polyethylene glycol is a polyether, a non-biodegradable hydrophilic polymer with a variety of applications in pharmaceutical and biomedical areas (Hutanu et al., 2014). PEG helps in increasing the dispersibility of the attached molecules. It has been used in the preparation of polymer-drug conjugates and provides stabilization as well as imparts stealth properties to the so formed DDS.

Polyethylene glycol polymers with reactive functionalities at their termini have been demonstrated to exhibit wide variety of applications. Bi-functional and mono-functional derivatives are also being used as crosslinkers and linkers or spacers. PEG-based carriers for drug delivery such as micelles, nanoparticles, dendrimers, and liposomes are better than PEG conjugates of the drugs (Hutanu et al., 2014).

Dendrimers. Dendrimers are the specialized macromolecules which offer regular and highly branched three-dimensional structures. Their unique structures show high density of functionalities at the periphery of the molecules. For instance, dendrimers with peripheral amines allow efficient condensation of negatively charged nucleic acids while the tertiary amines in the core remain available for playing an important role during endo/lysosomal acidification which enables more efficient endosomal release. Dendrimers consist of three major architectural components: a core, inner shell, and an outer shell. These can be synthesized in two ways to have different functionality in each of these components to modulate various properties such as solubility, thermal stability, and attachment of compounds for particular applications (Thota et al., 2015).

A dendrimer is typically symmetric around the core. Its structure provides relatively easy access to control their size, composition, and chemical reactivity very precisely. The degree of branching is expressed in the form of generation of the dendrimers. The size and surface charge on dendrimers vary with the number of "generations" during synthesis. Because of the presence of large number of tertiary amines, PAMAM dendrimers act not only as proton sponges in gene delivery applications but also along with carbon skeleton, they have been used as drug carriers simultaneously (Salzano et al., 2016; Abedi-Gaballu et al., 2018; Li et al., 2018). Haensler and Szoka (1993) reported for the first time the use of PAMAM dendrimers in gene delivery. They showed that the sixth-generation dendrimer was almost 10-folds better than lower generation ones. Based on this study, PAMAM dendrimers have recently been used in several *in vivo* and *in vitro* gene delivery applications and found to be biocompatible (Maruyama-Tabata et al., 2000; Yang et al., 2015; Araújo et al., 2018). PAMAM dendrimers have a well-defined size and shape but offer limited flexibility. Therefore, attempts have been made to hydrolytically cleave some of the amide bonds in the inner part. Breaking of some of the branches of dendrimers in the core enhances the flexibility and the resulting molecules are known as activated dendrimers. Although activated and inactivated dendrimers were found to form complexes with DNA by electrostatic interactions and mediated transfer of bound DNA into eukaryotic cells, the overall transfection efficiency of activated dendrimers was found to be two to three times higher than the inactivated (native) dendrimers. The fractured or activated dendrimers not only showed the greater flexibility to interact with plasmid DNA but their solubility also enhanced and presented less tendency to aggregate. This enhanced flexibility of activated dendrimers showed better endosomal release of the DNA and subsequently, the transfection efficiency. SuperFect (from QIAGEN, Hilden, Germany) is an example of commercially available efficient transfection reagents based on the fractured G-5 PAMAM dendrimer. In another attempt, the peripheral amines of PAMAM-G4 were converted into guanidinium (Gn) and tetramethylguanidinium (TMG) moieties. Although these modified dendrimers did not display cytotoxicity in various mammalian cells, higher transfection efficiency was observed only in case of guanidinium-PAMAM-G4 (Yadav et al., 2014b). Somani et al. have investigated the effect of pegylation (2 and 5 kDa) on G-3 and G-4 diaminobutyric polypropylenimine dendrimers. Cytotoxicity decreased significantly in these modified dendrimers without compromising DNA condensability; however, enhanced gene expression was found in G-3 and G-4 daminobutyric polypropylenimine dendrimers conjugated to 2 kDa PEG in cell specific manner (Somani et al., 2018). Further, Gao et al. studied structure activity relationship to design efficient gene delivery vectors. They demonstrated that both hydrophobic modification and density of amines modulate the gene transfer ability of synthetic vectors (Gao et al., 2018).

Subsequently, several hydrophobic modifications have also been incorporated in dendrimers to make them amphiphilic which can self-assemble and be used as delivery vectors (Bolu et al., 2018). Han et al. (2017) developed an amphiphilic conjugate of PAMAM dendrimer by conjugating hydrophobic PLA which on self-assembly formed core-shell nanostructures in which 5-FU and doxorubicin were entrapped efficiently for combinatorial anticancer therapy. This nanomicelle system showed synergistic antitumor effect on MDA-MB 231 tumor cell line and MDA-MB 231 xenograft mice model (Han et al., 2017). In another report, an amphiphilic block micelle was synthesized by conjugating hydrophobic block of linear poly e-caprolactone polymer with hydrophilic part of methoxy terminated PEG decorated G-3 polyester dendron (WooáBae, 2011). They further explored the effect of peripheral functional group such as amine, carboxylic, and acetyl using $-NH_2$, $-COOH$, $-COCH_3$ group terminated PEG chains instead of methoxy terminated PEG used in their earlier study (Pearson et al., 2012). The group used this amphiphilic micellar system to encapsulate and deliver anticancer drug, endoxifen. Dendron micelle system containing carboxy terminated PEG showed the highest potential to deliver the drug across skin layers among the tested systems (Yang et al., 2014). This research group further evaluated the effect of density of targeting moiety, folic acid, and PEG length on these dendritic micelles in terms of interaction with cells (Pearson et al., 2016). There are lots of preclinical studies on dendrimers-based drug delivery; however, the clinical ones are very few. A dendrimer drug formulation, DTXSPL8783, for advanced cancer treatment, is currently undergoing clinical phase 1 trial (Caster et al., 2017; Ventola, 2017), while another dendrimer-based antiviral product, Vivagel from Star Pharma, is in phase III trials for bacterial vaginosis (Ventola, 2017). Some of the nanoengineered polymeric systems either approved by FDA or in the advanced clinical phases are listed in **Table 1**.

Self-Assembling Small Molecules

The self-assembled nanostructures formed from the small peptides (Fleming and Ulijn, 2014; Panda and Chauhan, 2014), lipid-based systems (Li et al., 2015), and other small molecules (Xing and Zhao, 2016) can be used as carriers for different therapeutic molecules (Wang et al., 2017b; Liu et al., 2018; Yang et al., 2018). The small molecules can be produced easily as compared to the larger ones and act as efficient and economical alternatives to the large molecule-based systems. Moreover, different small peptides can be combined with diverse synthetic molecules thus producing tailored nanoscale engineered biomaterials that can be used as carriers of genetic materials, drug molecules, and antimicrobial agents. Now-a-days, carrier free and self-assembled small molecule-based nano-DDS are also being developed with the aim to eliminate the issue of undefined metabolism and clinical safety of the carriers (Guo et al., 2017; Jiang et al., 2017; Zheng et al., 2019). Recently, Guo et al. have demonstrated the efficacy of a carrier free system by developing a theranostic nanodrug delivery formulation for NIR imaging and chemotherapy. In this system, indocyanine green, ursolic acid, and PTX formed a self-assembled system via aromatic pi-pi and electrostatic interactions (Guo et al., 2017). Similarly, another carrier free nano-DDS was developed in which anticancer drug doxorubicin and ursolic

acid were co-assembled by pi-pi stacking, hydrophobic, and electrostatic interactions, and modified with HER-2 aptamer for targeting to HER-2 receptors overexpressing cancer cells (Jiang et al., 2017).

Lipids

This group of carrier materials comprise of cholesterol and phospholipids as the key constituents. Phospholipids, the constituent of all cell membranes as well as the major component of liposomes, are mainly one or two fatty acids linked to glycerol or sphingosin with a phosphate head group which impart amphiphilicity facilitating the formation of bilayered membranes in liposomes. It is reported in the literature that the ordinary amphiphiles have critical micellization concentrations in the range of 10^{-2}–10^{-4}M, whereas CMC of phospholipids is four to five times smaller, thus these materials have extremely low water solubility. As a consequence of this, they have high stability after administration in comparison to micelles (Felice et al., 2014). Among the natural and anionic phospholipids, the phosphatidylcholine, which is the most studied lipid, present in both plants and animals, consists of a phosphate and quaternary ammonium group. Among the natural anionic phospholipids, phosphatidic acid, phosphatidylglycerol, phosphatidylserine, and phosphatidyl ethanolamine are the most commonly used ones.

The natural cationic lipids such as the stearylamine are mainly used for encapsulation of nucleic acids. The synthetic phospholipids such as dimyristoyl-phosphatidylcholine, dipalmitoylphosphatidylcholine, and DSPC are also used. Natural phospholipids are preferred over synthetic ones as they show greater chemical biostability against phospholipases, esterases, bile salts, and serum proteins thus imparting the greater thermodynamic stability to the vesicles against alkaline pH, high temperature, and oxidative stress conditions. On the other hand, liposomes permeability can be controlled in a better way using synthetic lipids. In biological environment, the phospholipids are degraded by lipolysis and thus result in low toxicity. The fluidity of the liposomal membrane is influenced by the viscosity of the phospholipids which is regulated either by using phospholipids possessing elevated phase shift temperatures, or through insertion of cholesterol molecules. The second most commonly used lipid in nanoengineered DDSs is cholesterol, which is responsible for reducing the permeability of hydrophilic molecules by increasing the stability of liposomal membrane (Felice et al., 2014). Kirby et al. studied the effect of cholesterol on liposomal membranes prepared using natural phospholipids and found that cholesterol containing liposomal membranes were more stable in comparison to cholesterol deficient membranes (Felice et al., 2014) in blood. Deng et al. (2018) and Massiot et al. (2019) developed X-ray radiation triggered (Deng et al., 2018) and photo-triggered (Massiot et al., 2019) liposomal systems for sustained release of the drug molecules (Pattni et al., 2015; Deng et al., 2018; Massiot et al., 2019). A great development has been achieved on liposomal technology advancement; however, their full potential is yet to be explored, as successful bench to bedside applications are very few. So, there is still the need of further development of liposomal technology for advancement in therapeutic delivery systems (Pattni et al., 2015).

Most of the commercialized liposomes have been used to encapsulate anticancer drugs. Among them, Myocet^{TM} and Doxil^{TM}, which encapsulate doxorubicin, are the most efficacious formulations (Felice et al., 2014) (**Table 2**).

Doxil is the first liposomal formulation of anticancer drug, doxorubicin, permitted by the FDA (United States) in 1995 for AIDS associated with Kaposi's sarcoma (Northfelt et al., 1998). In this case, the stealth liposomal carrier consists of HSPC, cholesterol, and PEGylated phosphoethanolamine. By encapsulating doxorubicin into stealth liposome carriers, both the circulation half-life of drug and its accumulation in tumor environment were got enhanced. Doxorubicin, an anthracyclin, is currently being used against various carcinomas and exerts its effect by inhibiting DNA and RNA synthesis but it causes side effects such as severe myelo-suppression and cardiotoxicity (Felice et al., 2014). These side effects were reduced to an extent when doxorubicin was entrapped in liposomes (Fan and Zhang, 2013). Initially, doxorubicin, encapsulated in multilamellar liposomes by passive entrapment, was found to be unsuccessful because of fast release of the drug followed by rapid clearance by phagocytic system of the body. Then active drug loading technique was employed to enhance the drug encapsulation content and stability which resulted in two formulations, Myocet^{TM} and Doxil^{TM}. In Myocet^{TM}, doxorubicin was encapsulated by a pH gradient, while in Doxil^{TM}, potential gradient was used to load the drug molecules. Myocet^{TM} comprises cholesterol and EPC while Doxil^{TM} contains cholesterol and hydrogenated soya phosphatidylcholine. Of these two formulations, PEG coating in Doxil^{TM} improved its pharmaco-kinetic profile over Myocet^{TM}. Both Myocet^{TM} and Doxil^{TM} showed significant reduction in the toxic effects of doxorubicin (Hofheinz et al., 2005).

Other liposomal drugs clinically approved are Ambisome^{TM}, in which Amphotericin, an antifungal drug is loaded, Depodur^{TM}, in which morphine, an analgesic, is loaded and Visudyne^{TM}, in which verteporfin, a drug for treatment of macular disintegration, is loaded. Besides, there are a number of other liposomal systems which are under phase II and III clinical trials. Liposome-based formulations in clinical trials are more than other types of nanoengineered DDSs. Among these, ThermoDox^{TM} is a temperature-sensitive liposomal formulation encapsulating doxorubicin. ThermoDox^{TM} comprises DPPC, MSPC, and DSPE-MPEG-2000 (Poon and Borys, 2009), the synthetic phospholipids. ThermoDox^{TM} releases its doxorubicin content under the influence of temperature, i.e. above 39.5°C as this formulation has comparatively low Tm. Tm, phase Tm, is the temperature needed to induce change in the arrangement of lipid chains. At this temperature, the aligned gel phase structure changes into the non-aligned liquid crystalline phase structure. In the living system, this temperature (Tm) can be attained by heating the tumor with radio-frequency electromagnetic waves.

Small peptides

Liposomes are associated with some technological issues such as stability, reproducibility, poor drug loading, and insufficient

TABLE 2 | List of nanoengineered liposomal therapeutic delivery systems either approved by FDA or in advanced clinical trials (Felice et al., 2014; Bulbake et al., 2017; Patra et al., 2018).

Product name	Carrier material composition	Drug/type of drug (Disease)	Approval year/phase
Doxil™	HSPC:cholesterol:PEG 2000-DSPE (56:39:5 molar ratio)	Doxorubicin/anthracycline (Various types of cancers)	1995
DaunoXome™	DSPC and cholesterol (2:1 molar ratio)	Daunorubicin/anthracycline (HIV)	1996
Ambisome™	HSPC:DSPG:cholesterol:(2:0.8:1 molar ratio)	Amphotericin B/polyene (Fungal infections)	1997
Depocyt™	DOPC, DPPG, cholesterol, and triolein	Cytarabin/nucleoside (Lymphomatous meningitis)	1999
Visudyne™	Verteporphin:DMPC and EPG (1:8 molar ratio)	Verteporfin/benzoporphyrin (Macular degeneration)	2000
DepoDur™	DOPC, DPPG, cholesterol, and triolein	Morphine/opiate (Severe pain)	2004
Octocog™	Phospholipids	α Factor VIII/proteica (Hemophilia)	2009
Marqibo™	SM:cholesterol (60:40 molar ratio)	Vincristine/alkaloidsulfate (Hodgkin lymphoma)	2012
Myocet™	EPC:cholesterol (55:45 molar ratio)	Doxorubicin/anthracycline (Metastatic breast cancer)	Phase III/2000
Thermodox™	Low phase transition temperature phospholipids	Doxorubicin/anthracycline (Metastatic malignant melanoma, liver cancer)	Phase III
Onivyde™	DSPC:MPEG-2000:DSPE (3:2:0.015 molar ratio)	Irinotecan (Pancreatic cancer CRC, lung, glioma)	2015 (approved for pancreatic cancer), Phase II, III trials for other cancers
Mepact	DOPS:POPC (3:7 molar ratio)	Mifamurtide (Non-metastaic osteosarcoma)	2004
Abelcet	DMPC:DMPG (7:3 molar ratio)	Amphotericin B (Invasive several fungal infections)	1995
Amphotec	Cholesteryl sulfate	Amphotericin B (Severe fungal infections)	1996
Exparel	DEPC, DPPG, cholesterol, tricaprylin	Pain managment	2011
Epaxal	DOPC:DOPE (75:25 molar ratio)	Hepatitis A	1993
Inflexal	DOPC:DOPE (75:25 molar ratio)	Influenza	1997
Vyxeos (CPX-351)	DSPC:DSPG:cholesterol (7:2:1 molar ratio)	Acute myeloid leukemia	2017

control over drug release (Torchilin, 2005). The basic idea of fabricating nanostructures from peptide-based biomaterials came from the literature survey that showed that in certain diseases such as Parkinson's, Alzheimer's, and in Prion-related ones, the self-organized tubular shaped proteins were formed from otherwise soluble amphiphilic proteins in the cells (Gazit, 2004). These findings led the way to divert attention and focus researches on investigating self-assembly of peptides to form ordered structures. Peptides possess several inherent properties such as biocompatibility and biodegradability which make them very useful building blocks for forming self-assembled nanostructures for various biomedical applications (Panda and Chauhan, 2014). Furthermore, in case of peptides, the versatility of the chemical design and their capability to assume highly ordered organized structures offers chance of manipulating the final assembly by controlling structural features at the nanometric range. The properties of peptides such as sequence-based unique self-organization and recognition provide them a function of acting as a significant signaling molecule and key building component of living beings. A range of self-organized nanostructures with distinct shapes such as fibrous, tubular, rod, particles, and various other shapes are also formed through self-assembly of peptides (Gazit, 2004; Panda and Chauhan, 2014; Prakash Sharma et al., 2015). In the past few years, research on medium sized peptides, small peptides, ultra small peptides, and peptide-conjugates have opened up new avenues for designing and synthesis of peptide-based self-assembled nanostructures for different biological applications (Fan et al., 2017; Guyon et al., 2018; Ni and Zhuo, 2019; Tesauro et al., 2019). These self-assembled peptide-based nanomaterials can be designed with ease to act as new scaffolds to mimic various biomaterials, tissues, etc. The usefulness of di- or tri-peptide based self-assembled nanostructures has been reported by many research groups. A variety of peptides such as surfactant like peptides, amphiphilic peptides, bolaamphiphiles, peptides containing α-helix, β-sheets, and β-turns, as well as cyclic peptides have been nanotized and studied in detail the process involved in their conversion. Peptides are generally labile to enzymatic degradation which

limits their use as therapeutic delivery agents but this limitation has been circumvented, to an extent, by incorporation of non-coded residues in peptide sequences (Gupta et al., 2007).

The self-assembled peptide-based nanostructures, i.e. nanotubes were developed for the first time by Ghadiri et al. using cyclic polypeptides, cyclo-[-(L-Gln-D-Ala-L-Glu-D-Ala)$_2$-], containing even number of D- and L-amino acids alternatively (Hartgerink et al., 1996). These cyclic peptides self-assembled to form nanotubes via intermolecular hydrogen bonding in which side chains of the amino acids lied toward the exterior surface and formed a hollow tube type arrangement. The cyclic peptide-based nanotubes have been used as antimicrobial agents, biosensors, catalysts, etc. (Brea et al., 2010).

A large number of peptides self-organize via formation of β-sheeted secondary structures. β-Sheeted peptides self-assemble to form diverse supramolecular architectures such as nanoribbons, nanotubes, monolayers with nanoscale order, etc. (Reches and Gazit, 2003; Ashkenasy et al., 2006). The 16-amino acid residues containing peptides, RADA-16 I and RADA-16 II, formed β-sheeted structures that produced nanofibrous network followed by pH-responsive hydrogels (Holmes et al., 2000) via self-assembly. The stimuli responsive hydrogel network formation by these peptides can also be enhanced by increasing ionic strength or altering the pH of the assembling environment. These peptides are now available commercially with the name, PuraMatrix (3DM, Inc., Cambridge, MA, United States).

The surfactant-like peptides also self-assemble to form nanostructures (Vauthey et al., 2002). These seven to eight amino acids long surfactant-like peptides (A_6D_1, V_6D_1, V_6D_2, L_6D_2) have similar properties as observed in biological surfactant molecules. They also contain a negatively charged hydrophilic head group at C-terminus, i.e. aspartic acid, and the hydrophobic amino acids, i.e. alanine, valine, or leucine formed the part of lipophilic tail. The N-terminus of the peptides was acetylated to create a neutral moiety, which facilitated self-assembly via electrostatic and hydrophobic forces (Tsonchev et al., 2008).

Amphiphilic peptides are formed via hydrophilic peptide forming head group and hydrophobic alkyl tail. The hydrophobic alkyl end helps in arrangement of the hydrophilic part to self-assemble in different higher order structures. These amphiphilic peptides self organize to form diverse morphological structures with nanodimensions such as micelles, vesicles, or tubules (Panda and Chauhan, 2014).

Bolaamphiphiles (KA_6K, KA_4K, KA_8K) are amphiphilic molecules made up of two hydrophilic groups flanked by hydrocarbon chains. In these peptides, β-sheet H-bonding interactions result in formation of a variety of structures such as nanofibers, nanorods, nanotubes, nanoribbons, nanospheres, etc. (Panda and Chauhan, 2014). However, in case of nanostructure formation by these large linear peptides, cyclic and dendritic structures, the related expense and complexity of synthesis restrict the use of these peptides practically. In addition to this, these peptides are also not stable under enzymatic exposure which hampers the use of these peptides in biological applications.

Very short peptides such as di-, tri-, tetra-, and pentapeptides also self-assemble to form diverse nanostructures (Panda and Chauhan, 2014). These short peptide fragments were carefully studied in order to find out the minimum sequence required for amyloid formation. In amyloid fibrils polypeptide, a hexapeptide fragment NFGAIL (hIAPP22–27) of the islet amyloid polypeptide (IAPP) formed the well-organized amyloid fibrils which were alike to amyloid fibrils of complete polypeptide. Further, it was found that a pentapeptide fragment FGAIL (hIAPP23–27) of the IAPP also formed a fibrillar structure. Similarly, AILSS fragment was also discovered as strong amyloidogenic region of IAPP. Another peptide part, KLVFF of the amyloid β-peptide Ab-42, self-organized in saline buffer forming hydrogel. A pentapeptide sequence in human calcitonin, i.e. DFNKF, also formed the well-ordered amyloid fibrils similar to those observed in case of full length polypeptide. All these observations revealed that peptides which form amyloid fibers have a shorter sequence of amino acids which can also self-organize to form amyloid fibrils similar to those formed by complete peptide. Furthermore, these research studies recommended the significant role of aromatic amino acids in formation of amyloid fibrils. Further research on amyloid like fibrils suggested that α-amino isobutyric acid (U) containing small peptide, i.e. Boc-AUV-OMe, Boc-AUI-OMe, and Boc-AGV-OMe form β-sheet structures which self-organize in amyloid like fibrils (Panda and Chauhan, 2014).

Dipeptides also self-assemble to form nanostructures was demonstrated for the first time by Gazit et al. using dipeptides, FF (Reches and Gazit, 2003). This dipeptide self-assembled into different nanostructures, i.e. nanotubes/microtubes, nanowires, and nanoforests (Reches and Gazit, 2003; Marchesan et al., 2015). The nanotubes formed by FF dipeptide were thermally stable. They further demonstrated that an incorporation of –SH group in FF resulted in transition from tubular to spherical structures (Reches and Gazit, 2004). There are reports in literature that hydrophobic dipeptides, LL, LF, FL, and IL self-assemble to nanotubes via head to tail ($NH_3^{\pm}OOC$) H-bond formation (Panda and Chauhan, 2014). Further reports exist in the literature, which demonstrate that VA, LS, and FF can also form nanoporous structures. The amine and carboxyl terminal modified dipeptides also form self-assembled nanostructures. Fmoc-FF dipeptide form hydrogels with a nanofibrillar structure in aqueous conditions and physical attributes of these hydrogels were found to be better than the hydrogels formed by longer polypeptides. The same research group further evaluated the effect of modification of $–NH_2$ and –COOH terminals of FF dipeptides on self-assembly behavior and found that N and C terminal modified dipeptides also form self organized structures in nano-range. Furthermore, the hydrogels were formed from Fmoc protected dipeptides using a combination of glycine, alanine, leucine, and phenylalanine. The physical and structural features of these hydrogels were different, depending on the characteristic of amino acids used in dipeptide sequences. There are numerous reports in literature which suggest that aromatic moieties such as Fmoc and pyrene protected peptides form nanofibrillar hydrogel network due to π-π stacking and hydrophobic interactions. Unsaturated amino acids such as dehydrophenylalanine have also been used to form self-assembled nanostructures (Panda and Chauhan, 2014). The

introduction of dehydrophenylalanine provides conformational constrain and proteolytic stability to peptides. The extensive studies on dehydrophenylalanine (ΔF) containing dipeptides have been done by Chauhan et al. where the ΔF was used as C-terminal amino acid and N-terminal amino acid residue was varied with any one of the natural amino acids (Gupta et al., 2007). They found that dipeptides with aromatic amino acid at N-terminus formed nanotubes while the dipeptides having charged amino acid at N-terminus formed vesicles. They also revealed that these dipeptides having hydrophobic groups at their N-terminus give rise to self-assembled structures which can be seen from human eye while the structures formed with hydrophilic N-termini were invisible to naked human eye (Panda and Chauhan, 2014). The dipeptide, F-ΔF, assembled into hydrogels at pH 7.0. The hydrogel formed from F-ΔF dipeptides efficiently entrapped and released drugs, antibiotics, and vitamins. The kinetics of drug release was affected by change in pH and ion concentration (external stimuli). Thus, this system was used as a controlled self-regulated drug release system (Panda et al., 2008). Among the tested dipeptides having charged amino acids at N-termini, EΔF, KΔF, RΔF, and DΔF, the dipeptide, RΔF formed vesicular structures and was easily functionalized with folic acid to target folic acid receptors. These nanostructures showed enhanced cellular uptake in various cancer cell lines, like MDA-MB-231 and HeLa. These folic acid functionalized RΔF nanostructures also encapsulated doxorubicin efficiently. These doxorubicin-loaded nanostructures showed enhanced cytotoxicity toward cancer cells. These nanostructures further showed enhanced targeting and accumulation in tumor tissue in Ehrlich ascitic tumor bearing mice.

In yet another study, Mahato et al. (2012) prepared self-assembled nanostructures in aqueous environment from small glycolated dehydropeptides, Boc-F-ΔF-εAhx-GA and H-F-ΔF-εAhx-GA, wherein glucosamine was attached to peptides via 6-aminohexanoic acid linker. These peptides efficiently entrapped the hydrophobic dyes, eosin and *N*-fluoresceinyl-2-aminoethanol (FAE), in their core (TEM images in **Figures 4a,b**). At higher concentration, Boc-F-ΔF-εAhx-GA formed hydrogel also. Likewise, Yadav et al. synthesized Boc-F-ΔF-εAhx-Neomycin by conjugating Boc-F-ΔF-εAhx-OH with an aminoglycoside, neomycin, which on self-assembly in aqueous environment formed nanostructures having hydrophobic core and cationic hydrophilic shell. These cationic nanostructures efficiently interacted with pDNA and showed enhanced transfection efficiency in mammalian cells *in vitro*. Besides, these nanostructures efficiently entrapped hydrophobic molecules, eosin and curcumin, in the core of nanostructures which were characterized by electron microscopic imaging (TEM images, **Figures 4c,d**) (Yadav et al., 2014a). Later on, the same research group fabricated a tripeptide, Boc-P-F-G-OMe, which on self-assembly yielded nanostructures and acted as drug carrier by efficiently encapsulating hydrophobic drug molecules such as eosin, aspirin, and curcumin (**Figures 4e,f**) (Yadav et al., 2015). This group further synthesized a dehydropeptide, Boc-P-ΔF-G-OMe containing dehydrophenylalanine, an unnatural amino acid, to check the effect of dehydrophenylalanine on the formation of self-assembled nanostructures. The incorporation of dehydrophe instead of Phe improved the encapsulation efficiency of hydrophobic drug, curcumin, in these nanostructures (**Figures 4g,h**). These nanostructures were further stabilized with vitE-TPGS. These nanostructures showed that incorporation of constrained dehydro amino acid in peptides resulted in the construction of stable nanostructures for the development of nanomaterials with controlled drug release (Deka et al., 2017).

Stimuli-responsive peptide nanostructures have, recently, attracted the attention of the researchers as controlled drug delivery vehicles since these are capable of releasing the drug at the intended sites (Panda et al., 2008). The therapeutic molecule-encapsulated peptide nanostructures can be made to release the therapeutics on exposure to stimuli such as change in pH, temperature, and others. There is a report in the literature where anti-inflammatory prodrug, olsalazine, has been conjugated with a tripeptide derivative and this conjugate self-assembled in water to form supramolecular hydrogels (Li et al., 2010). Moreover, the release of 5-aminosalicylic acid from these hydrogels was made to occur in an organized way, attained by reducing the azo bond which resulted in disassembly of the hydrogels. Moreover, the nanovesicles developed from dipeptides using glutamic acid at C-terminus showed constant behavior over a range of pH. However, these vesicles were responsive to Ca^{2+} ions. In these nanovesicles, anticancer drugs, fluorescent dyes, and various biologically active molecules were entrapped and released in response to calcium ions (Naskar et al., 2011). The peptide nanostructures formed from peptide, Acp-YE (Acp, 3-amino caproic acid), showed stimuli responsive behavior to Ca^{2+} ions concentration and change in pH. The release of encapsulated anticancer drug (doxorubicin) from these vesicular structures was achieved on exposure to Ca^{2+} ions concentration.

Enormous literature exists on self-assembled peptide nanostructures useful for drug delivery applications; however, most of them are under *in vitro* studies. Only few *in vivo* studies have been undertaken and some of them have been listed in **Table 3** (Leite et al., 2015; Habibi et al., 2016; Lee et al., 2019).

DNA nanotechnology-based drug delivery

DNA nanotechnology involves assembly of synthetic DNA fragments into self-assembled nanostructures of different sizes, shapes, and morphology. The basic principle behind DNA nanotechnology is the complementary base pairing. Using this principle, a large number of simple DNA nanostructures have been produced (Hu et al., 2018; Madhanagopal et al., 2018; Kim et al., 2019). Initially, the research on DNA nanotechnology was initiated with the formation of simple topological morphologies which later on advanced to production of DNA tiles, periodic lattices, and 2D and 3D structures. Using this superamolecular DNA technology, wherein interactions such as van der Waals, pi-pi stacking, H-bonding, metal-coordination etc., are involved in DNA self-assembly, different molecules have been encapsulated (Sharma et al., 2018; Ariga et al., 2019). In the last decade, the advent of DNA origami in 2006 by Rothemund's group expanded the research on DNA nanotechnology from 2D to 3D confirmation forming complex 3D nanostructures of diverse shape and design. In DNA origami, a large natural single-stranded DNA is folded with the help of several chemically

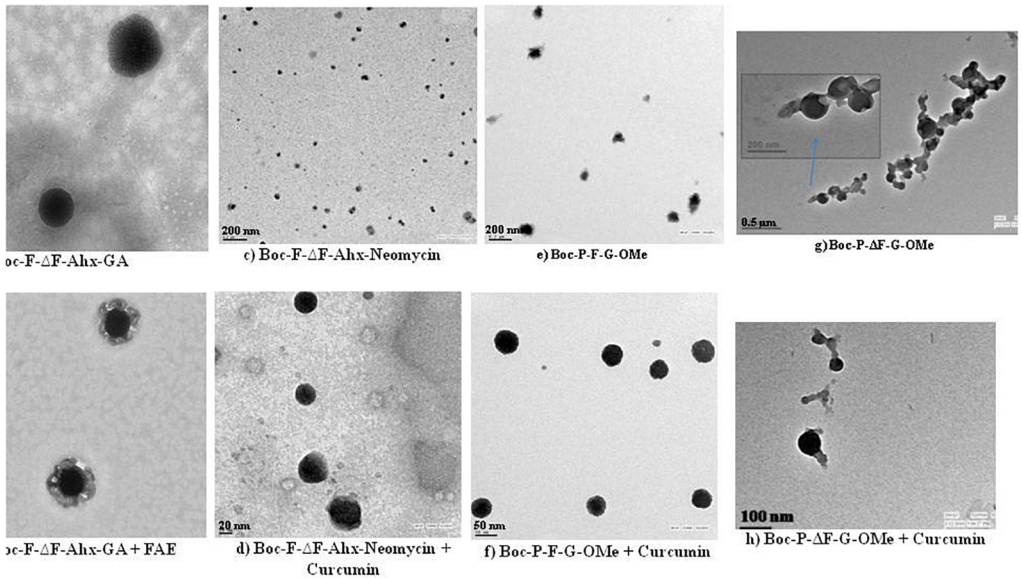

FIGURE 4 | TEM images of **(a)** Boc-F-ΔF-Ahx-GA dipeptide, **(b)** FAE-loaded Boc-F-ΔF-Ahx-GA dipeptide, **(c)** Boc-F-ΔF-Ahx-Neomycin dipeptide, **(d)** Curcumin-loaded Boc-F-ΔF-Ahx-Neomycin dipeptide, **(e)** Boc-P-F-G-OMe tripeptide and **(f)** Curcumin-loaded Boc-P-F-G-OMe tripeptide; **(g)** Boc-P-ΔF-G-OMe tripeptide and **(h)** Curcumin-loaded Boc-P-ΔF-G-OMe tripeptide. (**a** and **b:** Reproduced from Reference (Mahato et al., 2012) with permission from the Royal Society of Chemistry; **c** and **d:** Reproduced from reference (Yadav et al., 2014a) with permission from the Royal Society of Chemistry; **e** and **f:** Reproduced from reference (Yadav et al., 2015) with permission from Bentham Science Publishers; **g** and **h:** Reproduced from reference (Deka et al., 2017) with permission from Elsevier.

TABLE 3 | List of peptide-based self-assembled nanostructures for drug delivery applications.

Peptide nanostructure	Carrier material	Drug (Disease)	References
Nanofibers	RAD16-II AcN-(RARADADA)2-CNH2	IGF-1 (Myocardial infarction)	Davis et al., 2006
Nanofibers coated with chitosan	Leucine-enkephalin NH_2-Y(-O-palmitoyl)GGFL-OH	Enkephalin (Pain)	Lalatsa et al., 2015
Nanofibers coated with chitosan	NH_2-Y(-O-palmitoyl) GGFLR-OH	Dalargin (Pain)	Mazza et al., 2013
Nanofibers	Palmitoyl-A4G3E3	Camptothecin (Cancer)	Soukasene et al., 2011
Nanofibers	Palmitoyl-V2A2E2K	Dexamethasone (Inflammation)	Webber et al., 2012
Nanofibers	Palmitoyl-G3A4IKVAV	Spinal cord injury	Tysseling-Mattiace et al., 2008
Nanofibers	Palmitoyl-(K)-V3E3SGGGYPVH PST-NH_2	Bone morphogenetic protein-2 (Spinal arthrodesis)	Lee et al., 2015
Nanoparticles	Polylactide-V6K2(VVVVVKK)	Doxorubicin, Paclitaxel (Cancer)	Jabbari et al., 2013
Nanotubes	Lanreotide NH_2-(D)Naph-CY(D)WKVCT-$CONH_2$	Acromegaly	Freda et al., 2005; Theodoropoulou and Stalla, 2013

synthesized short DNA strands called staple strands to form well-defined 2D and 3D nanostructures. The different types of DNA nanostructures can be fabricated by varying the number and length of staple strands as well as by changing the relative sequence of nucleotides in individual strand. These small staple strands induce the folding of larger DNA strand by annealing with it. The complementary base pairing interaction of DNA scaffold with staple strands help in self-assembling in well defined nanoarchitectures (Hu et al., 2018; Madhanagopal et al., 2018; Sharma et al., 2018).

The self-assembled DNA nanostructures have been used in various biomedical applications such as drug delivery, gene delivery, biosensing, etc. (Ariga et al., 2019). The design and the strategy used to construct these DNA nanoarchitechtonics depend on the type of application these nanostructures are required. The DNA nanostructures, formed via self-assembly approach, are mostly based on sticky end cohesion of DNA strands. The sticky ends are unpaired nucleotide overhangs at the end of DNA molecules. These overhangs are mostly palindromic sequences. The sticky ends are used to combine DNA nanostructures via hybridization of their complementary single strands. Initially, the polyhedral DNA nanostructures were formed by this approach. Subsequently, periodic lattices were formed by tile-based self-assembly approach. With the

dawn of DNA origami approach, a lots of 2D and 3D objects were created. DNA origami approach is successfully used to create large nanostructures compared to tile-based approach, as in DNA origami, thousands of nucleotide long scaffold DNA strand is employed. Another strategy has also been used for DNA nanostructures in which single-stranded DNA tiles containing four domains are used to create DNA nanostructures and adjacent tiles bind with complementary parts forming DNA lattices composed of parallel DNA helix (Madhanagopal et al., 2018).

Construction of customized DNA nanostructures is driven by the type of therapy and therapeutic molecules to be delivered. Various types of therapeutic molecules can be delivered, e.g. drug molecules, fluorescent dyes, protein molecules, siRNA, miRNA, CpG sequences, mAB, etc. Fluorescent dyes, viz., fluorescein, cyanine, and rhodamine, have been tagged with self-assembled DNA nanostructures and delivered to cells for different cellular analysis (Hu et al., 2018; Lacroix et al., 2019). Ding et al. have used DNA origami to synthesize 2D DNA triangle and 3D DNA tubes to load anticancer drug, doxorubicin. These DNA origami nanostructures showed enhanced cellular uptake in adenocarcinoma cell lines, MCF-7 and Dox-resistant MCF-7 cells (Jiang et al., 2012; Zhao et al., 2012; Zhang et al., 2014; Mei et al., 2015; Li et al., 2017).

DNA nanostructures have also been used to deliver oligonucleotides, i.e. CpG dinucleotides as vaccine adjuvants for immunotherapy of infectious diseases (Zhang et al., 2015; Wang et al., 2016; Qu et al., 2017; Hu et al., 2018). The CpG motifs are present in bacterial genome and they are recognized as foreign molecules by vertebrate immune system. So these DNA motifs have been used to trigger host immune response as these are recognized by TLR-9 located on endosomes of host membrane of immune system which activates the innate immune pathway of host immune system. Similarly, siRNA and miRNA delivery have also been carried out using DNA nanostructures for gene silencing applications (Lee et al., 2012; Fakhoury et al., 2013; Bujold et al., 2016; Roh et al., 2016; Qian et al., 2017; Nahar et al., 2018). Various types of DNA nanostructures, that have been used as delivery vehicles, are listed in **Table 4** (Hu et al., 2018; Madhanagopal et al., 2018). Some of the recent reviews on DNA nanotechnology have described in detail the applications of DNA nanotechnology in drug delivery. Despite enormous advantages of DNA-based nanostructures, their stability *in vivo* is an issue as they are sensitive to cellular environment as well as salt concentration. Moreover, the high cost involved in the synthesis of DNA hampers their large-scale applications in biomedical field (Linko et al., 2015). In an attempt to address this concern, Praetorius et al. (2017) have presented a method to knock down the price of DNA nanostructure synthesis using biotechnological mass production. Although this method is not currently available in every lab, it is expected, in near future, that this cost-effective protocol would overcome this obstacle expanding the scope of DNA nanotechnology in other branches of science and technology.

CONCLUSION AND FUTURE PERSPECTIVES

In the last 20 years, tremendous developments have been made in the area of self-assembly of bioactive molecules. Post self-assembly, the nanostructure-based materials are potentially useful and have offered newer tools to revolutionize the area of biological and biomedical sciences. Nanotechnology has significantly contributed toward the realization of targeted and controlled delivery of therapeutics. For their delivery, different types of materials/systems have been developed. Barring a few, many of these materials have their own merits and demerits. Certain materials have been claimed to exhibit biocompatibility but the others that have been developed and are being used showing toxicity and hence proved inappropriate for *in vivo* applications. For example, cationic lipid-based nanostructures are found to activate the immune system. Besides, these are also associated with some technological issues such as stability, reproducibility, low drug loading, encapsulation, and uncontrolled drug leaching problems. Polymeric systems were then developed and evaluated but they were also associated with the similar types of limitations and hence surface functionalization was thought of to improve drug or gene-

TABLE 4 | Self-assembled DNA nanostructures as drug delivery vectors.

Type of DNA nanostructure	Drug (Disease)	*In vitro*	References
Tetrahedron	Doxorubicin (Cancer)	MDA-MB 468, MCF-7 cells	Setyawati et al., 2016
Icosahedron 30	Doxorubicin (Cancer)	Epithelial cancer cells	Chang et al., 2011
Pyramidal nanostructure	Doxorubicin (Cancer)	MDA-MB-231, HepG2, LoVo LoVo-R	Kumar et al., 2016
Triangular prisms	Doxorubicin (Cancer)	MCF-7 breast cancer cells	Chan et al., 2016
Crosslinked junctions	Doxorubicin (Cancer)	CCRF-CEM, Ramos, K562, K562/D	Wu et al., 2013
Concatamers	Doxorubicin (Cancer)	Ramos, CEM cells, mouse model	Zhu et al., 2013b
Nanoflowers	Doxorubicin (Cancer)	Ramos, CEM cells, mouse model, MCF-7, HeLa	Zhu et al., 2013a; Hu et al., 2014
Cocoon	Doxorubicin (Cancer)	MCF-7 cells	Sun et al., 2014
Triangular origami, Rectangular origami, Origami nanotubes	Doxorubicin (Cancer)	MCF-7, MDA-MB-231 cells	Jiang et al., 2012; Zhang et al., 2014
Origami nanorods	Daunorubicin (Cancer)	HL-60 cells	Halley et al., 2016
Origami nanoparticle superstructures	Doxorubicin (Cancer)	U87 cells	Yan et al., 2015

targeting, which is usually complicated. Similarly, natural polymers elicited unwanted immune reactions and also showed a batch to batch inconsistency, thus *in vivo* performance of these polymers became complex and questionable. Peptides and small molecule-based nanostructures can be good alternatives as carriers for therapeutic delivery as they possess certain characteristics such as good biocompatibility, ease of synthesis, and functionalization. Their self-assembled nanostructures present numerous prospective applications in biomedical field. Beside this, easy stimuli-responsiveness (internal/external stimuli) of self-assembled small molecules makes their role vital in the advancement of therapeutics delivery systems, where the therapeutic release behavior can be better controlled according to the requirements. Thus mild and rapid synthesis conditions, easy dispersibility in aqueous medium, simple functionalization, low production cost, and non-requirement of specialized equipments are some of the advantages which have advocated their promising potential to be used as future candidates for applications such as in drug/gene delivery, diagnosis, imaging, sensors, tissue engineering, bioelectronics, production of biomaterials, healthcare-related systems, etc. Various types of structures can be generated simply by varying the conditions. Thus, this area has emerged as a newer area of research which has shown promising potential. However, there exist several challenges which still need to be addressed in order to make them materials of choice for researchers. Although self-assembly results in the generation of various types of structures such as nanotubes, nanoparticles, nanospheres, nanotapes, nanofibers, nanogels, nanorods, etc., controlling the size of these structures during processing, their behavior under aqueous environment, degree of loading/entrapment of therapeutics and stability, as well as upscaling are still the gray areas where sincere attention of the researchers is required. Besides, studies to establish the biocompatibility and immunogenicity of these nanostructures are lacking.

Self-assembled DNA-origami nanostructure-based drug delivery offers a newer area which has shown tremendous potential in cancer treatment. These structures have been shown to possess stability in cell lysates upto 12 h, while, on prolonged exposures, degradation begins to occur. To improve their stability, several modifications have been suggested. Likewise, optimization in size and shape of these nanostructures reveals their effectiveness during drug release. Because of their multifunctional nature, easy amenability to modifications, biodegradability, as well as biocompatibility, these systems can be developed as safe and efficient drug delivery vectors. However, translation from bench to bedside applications, some crucial aspects are still required to examine in detail such as stability of these nanostructures under different conditions, their efficacy in different types of diseases, comparison of their performance with the commercially available formulations, systemic clearance, morphological parameters during their interactions with the different types of cells, effect of surface charge on their stability during circulation, etc. These investigations are required to ascertain that these systems will provide fascinating and promising solutions to improve the area of human healthcare.

AUTHOR CONTRIBUTIONS

SY wrote the manuscript with guidance from AS and PK. PK provided the critical feedback and helped in shaping the manuscript in current form. AS and PK supervised the manuscript.

FUNDING

SY is thankful to CSIR for providing Research Associateship (RA) vide reference File No. 31/43(349)/2017-EMR1 to carry out this work.

REFERENCES

Abedi-Gaballu, F., Dehghan, G., Ghaffari, M., Yekta, R., Abbaspour-Ravasjani, S., Baradaran, B., et al. (2018). PAMAM dendrimers as efficient drug and gene delivery nanosystems for cancer therapy. *Appl. Mater. Today* 12, 177–190. doi: 10.1016/j.apmt.2018.05.002

Abedini, F., Ebrahimi, M., Roozbehani, A. H., Domb, A. J., and Hosseinkhani, H. (2018). Overview on natural hydrophilic polysaccharide polymers in drug delivery. *Polym. Adv. Technol.* 29, 2564–2573. doi: 10.1002/pat.4375

Araújo, R. V. D., Santos, S. D. S., Igne Ferreira, E., and Giarolla, J. (2018). New advances in general biomedical applications of PAMAM dendrimers. *Molecules* 23:E2849. doi: 10.3390/molecules23112849

Ariga, K., Nishikawa, M., Mori, T., Takeya, J., Shrestha, L. K., and Hill, J. P. (2019). Self-assembly as a key player for materials nanoarchitectonics. *Sci. Technol. Adv. Mater.* 20, 51–95. doi: 10.1080/14686996.2018.1553108

Ashkenasy, N., Horne, W. S., and Ghadiri, M. R. (2006). Design of self-assembling peptide nanotubes with delocalized electronic states. *Small* 2, 99–102. doi: 10.1002/smll.200500252

Ayub, A. D., Chiu, H. I., Mat Yusuf, S. N. A., Abd Kadir, E., Ngalim, S. H., and Lim, V. (2019). Biocompatible disulphide cross-linked sodium alginate derivative nanoparticles for oral colon-targeted drug delivery. *Artif. Cells Nanomed. Biotechnol.* 47, 353–369. doi: 10.1080/21691401.2018.1557672

Azevedo, H. S., and da Silva, R. M. (2018). *Self-assembling Biomaterials: Molecular Design, Characterization and Application in Biology and Medicine*. Sawston: Woodhead Publishing.

Bazban-Shotorbani, S., Dashtimoghadam, E., Karkhaneh, A., Hasani-Sadrabadi, M. M., and Jacob, K. I. (2016). Microfluidic directed synthesis of alginate nanogels with tunable pore size for efficient protein delivery. *Langmuir* 32, 4996–5003. doi: 10.1021/acs.langmuir.5b04645

Bissantz, C., Kuhn, B., and Stahl, M. (2010). A medicinal chemist's guide to molecular interactions. *J. Med. Chem.* 53, 5061–5084. doi: 10.1021/jm100112j

Bobo, D., Robinson, K. J., Islam, J., Thurecht, K. J., and Corrie, S. R. (2016). Nanoparticle-based medicines: a review of FDA-approved materials and clinical trials to date. *Pharm. Res.* 33, 2373–2387. doi: 10.1007/s11095-016-1958-5

Bolu, B. S., Sanyal, R., and Sanyal, A. (2018). Drug delivery systems from self-assembly of dendron-polymer conjugates. *Molecules* 23:E1570. doi: 10.3390/molecules23071570

Brea, R. J., Reiriz, C., and Granja, J. R. (2010). Towards functional bionanomaterials based on self-assembling cyclic peptide nanotubes. *Chem. Soc. Rev.* 39, 1448–1456. doi: 10.1039/b805753m

Buerkle, L. E., and Rowan, S. J. (2012). Supramolecular gels formed from multi-component low molecular weight species. *Chem. Soc. Rev.* 41, 6089–6102. doi: 10.1039/c2cs35106d

Bujold, K. E., Hsu, J. C., and Sleiman, H. F. (2016). Optimized DNA "nanosuitcases" for encapsulation and conditional release of siRNA. *J. Am. Chem. Soc.* 138, 14030–14038. doi: 10.1021/jacs.6b08369

Bulbake, U., Doppalapudi, S., Kommineni, N., and Khan, W. (2017). Liposomal formulations in clinical use: an updated review. *Pharmaceutics* 9:E12.

Busseron, E., Ruff, Y., Moulin, E., and Giuseppone, N. (2013). Supramolecular self-assemblies as functional nanomaterials. *Nanoscale* 5, 7098–7140. doi: 10.1039/c3nr02176a

Caster, J. M., Patel, A. N., Zhang, T., and Wang, A. (2017). Investigational nanomedicines in 2016: a review of nanotherapeutics currently undergoing clinical trials. *Wiley Interdiscip. Rev. Nanomed. Nanobiotechnol.* 9:e1416. doi: 10.1002/wnan.1416

Chan, M. S., Tam, D. Y., Dai, Z., Liu, L. S., Ho, J. W. T., Chan, M. L., et al. (2016). Mitochondrial delivery of therapeutic agents by amphiphilic DNA nanocarriers. *Small* 12, 770–781. doi: 10.1002/smll.201503051

Chang, M., Yang, C.-S., and Huang, D.-M. (2011). Aptamer-conjugated DNA icosahedral nanoparticles as a carrier of doxorubicin for cancer therapy. *ACS Nano* 5, 6156–6163. doi: 10.1021/nn200693a

Chen, T., Li, S., Zhu, W., Liang, Z., and Zeng, Q. (2019). Self-assembly pH-sensitive chitosan/alginate coated polyelectrolyte complexes for oral delivery of insulin. *J. Microencapsul.* 36, 96–107. doi: 10.1080/02652048.2019.1604846

Cho, H.-J., Yoon, I.-S., Yoon, H. Y., Koo, H., Jin, Y.-J., Ko, S.-H., et al. (2012). Polyethylene glycol-conjugated hyaluronic acid-ceramide self-assembled nanoparticles for targeted delivery of doxorubicin. *Biomaterials* 33, 1190–1200. doi: 10.1016/j.biomaterials.2011.10.064

Chu, Z., Dreiss, C. A., and Feng, Y. (2013). Smart wormlike micelles. *Chem. Soc. Rev.* 42, 7174–7203. doi: 10.1039/c3cs35490c

Correa, N. M., Silber, J. J., Riter, R. E., and Levinger, N. E. (2012). Nonaqueous polar solvents in reverse micelle systems. *Chem. Rev.* 112, 4569–4602. doi: 10.1021/cr200254q

Coviello, T., Matricardi, P., Marianecci, C., and Alhaique, F. (2007). Polysaccharide hydrogels for modified release formulations. *J. Control. Release* 119, 5–24. doi: 10.1016/j.jconrel.2007.01.004

Cui, H., Webber, M. J., and Stupp, S. I. (2010). Self-assembly of peptide amphiphiles: from molecules to nanostructures to biomaterials. *Biopolymers* 94, 1–18. doi: 10.1002/bip.21328

Dahman, Y. (2017). *Nanotechnology and Functional Materials for Engineers*. Amsterdam: Elsevier.

Dallin, B. C., Yeon, H., Ostwalt, A. R., Abbott, N. L., and Van Lehn, R. C. (2019). Molecular order affects interfacial water structure and temperature-dependent hydrophobic interactions between nonpolar self-assembled monolayers. *Langmuir* 35, 2078–2088. doi: 10.1021/acs.langmuir.8b03287

Danhier, F., Ansorena, E., Silva, J. M., Coco, R., Le Breton, A., and Préat, V. (2012). PLGA-based nanoparticles: an overview of biomedical applications. *J. Control. Release* 161, 505–522. doi: 10.1016/j.jconrel.2012.01.043

Davis, M. E., Hsieh, P. C., Takahashi, T., Song, Q., Zhang, S., Kamm, R. D., et al. (2006). Local myocardial insulin-like growth factor 1 (IGF-1) delivery with biotinylated peptide nanofibers improves cell therapy for myocardial infarction. *Proc. Natl. Acad. Sci. U.S.A.* 103, 8155–8160. doi: 10.1073/pnas.0602877103

Deka, S. R., Yadav, S., Kumar, D., Garg, S., Mahato, M., and Sharma, A. K. (2017). Self-assembled dehydropeptide nano carriers for delivery of ornidazole and curcumin. *Colloids Surf. B Biointerfaces* 155, 332–340. doi: 10.1016/j.colsurfb.2017.04.036

Deng, W., Chen, W., Clement, S., Guller, A., Zhao, Z., Engel, A., et al. (2018). Controlled gene and drug release from a liposomal delivery platform triggered by X-ray radiation. *Nat. Commun.* 9:2713. doi: 10.1038/s41467-018-05118-3

Du, X., Zhou, J., Shi, J., and Xu, B. (2015). Supramolecular hydrogelators and hydrogels: from soft matter to molecular biomaterials. *Chem. Rev.* 115, 13165–13307. doi: 10.1021/acs.chemrev.5b00299

Fakhoury, J. J., McLaughlin, C. K., Edwardson, T. W., Conway, J. W., and Sleiman, H. F. (2013). Development and characterization of gene silencing DNA cages. *Biomacromolecules* 15, 276–282. doi: 10.1021/bm401532n

Fan, T., Yu, X., Shen, B., and Sun, L. (2017). Peptide self-assembled nanostructures for drug delivery applications. *J. Nanomater.* 2017:4562474.

Fan, Y., and Zhang, Q. (2013). Development of liposomal formulations: from concept to clinical investigations. *Asian J. Pharm. Sci.* 8, 81–87. doi: 10.1016/j.ajps.2013.07.010

Felice, B., Prabhakaran, M. P., Rodriguez, A. P., and Ramakrishna, S. (2014). Drug delivery vehicles on a nano-engineering perspective. *Mater. Sci. Eng. C* 41, 178–195. doi: 10.1016/j.msec.2014.04.049

Fleming, S., and Ulijn, R. V. (2014). Design of nanostructures based on aromatic peptide amphiphiles. *Chem. Soc. Rev.* 43, 8150–8177. doi: 10.1039/c4cs00247d

Freda, P. U., Katznelson, L., Van Der Lely, A. J., Reyes, C. M., Zhao, S., and Rabinowitz, D. (2005). Long-acting somatostatin analog therapy of acromegaly: a meta-analysis. *J. Clin. Endocrinol. Metab.* 90, 4465–4473. doi: 10.1210/jc.2005-0260

Gao, Y.-G., Lin, X., Dang, K., Jiang, S.-F., Tian, Y., Liu, F.-L., et al. (2018). Structure–activity relationship of novel low-generation dendrimers for gene delivery. *Org. Biomol. Chem.* 16, 7833–7842. doi: 10.1039/c8ob01767k

Gazit, E. (2002). A possible role for π-stacking in the self-assembly of amyloid fibrils. *FASEB J.* 16, 77–83. doi: 10.1096/fj.01-0442hyp

Gazit, E. (2004). The role of prefibrillar assemblies in the pathogenesis of amyloid diseases. *Drugs Future* 29:613. doi: 10.1358/dof.2004.029.06.853453

Genix, A.-C., and Oberdisse, J. (2018). Nanoparticle self-assembly: from interactions in suspension to polymer nanocomposites. *Soft Matter* 14, 5161–5179. doi: 10.1039/c8sm00430g

George, A., Shah, P. A., and Shrivastav, P. S. (2019). Natural biodegradable polymers based nano-formulations for drug delivery: a review. *Int. J. Pharm.* 561, 244–264. doi: 10.1016/j.ijpharm.2019.03.011

Guo, Y., Jiang, K., Shen, Z., Zheng, G., Fan, L., Zhao, R., et al. (2017). A small molecule nanodrug by self-assembly of dual anticancer drugs and photosensitizer for synergistic near-infrared cancer theranostics. *ACS Appl. Mater. Interfaces* 9, 43508–43519. doi: 10.1021/acsami.7b14755

Gupta, M., Bagaria, A., Mishra, A., Mathur, P., Basu, A., Ramakumar, S., et al. (2007). Self-assembly of a dipeptide-containing conformationally restricted dehydrophenylalanine residue to form ordered nanotubes. *Adv. Mater.* 19, 858–861. doi: 10.1002/adma.200601774

Guyon, L., Lepeltier, E., and Passirani, C. (2018). Self-assembly of peptide-based nanostructures: synthesis and biological activity. *Nano Res.* 11, 2315–2335. doi: 10.1007/s12274-017-1892-9

Habibi, N., Kamaly, N., Memic, A., and Shafiee, H. (2016). Self-assembled peptide-based nanostructures: smart nanomaterials toward targeted drug delivery. *Nano Today* 11, 41–60. doi: 10.1016/j.nantod.2016.02.004

Haburcak, R., Shi, J., Du, X., Yuan, D., and Xu, B. (2016). Ligand–receptor interaction modulates the energy landscape of enzyme-instructed self-assembly of small molecules. *J. Am. Chem. Soc.* 138, 15397–15404. doi: 10.1021/jacs.6b07677

Haensler, J., and Szoka, F. C. Jr. (1993). Polyamidoamine cascade polymers mediate efficient transfection of cells in culture. *Bioconjug. Chem.* 4, 372–379. doi: 10.1021/bc00023a012

Halley, P. D., Lucas, C. R., McWilliams, E. M., Webber, M. J., Patton, R. A., Kural, C., et al. (2016). Daunorubicin-loaded DNA origami nanostructures circumvent drug-resistance mechanisms in a leukemia model. *Small* 12, 308–320. doi: 10.1002/smll.201502118

Han, R., Sun, Y., Kang, C., Sun, H., and Wei, W. (2017). Amphiphilic dendritic nanomicelle-mediated co-delivery of 5-fluorouracil and doxorubicin for enhanced therapeutic efficacy. *J. Drug Target.* 25, 140–148. doi: 10.1080/1061186X.2016.1207649

Hartgerink, J. D., Granja, J. R., Milligan, R. A., and Ghadiri, M. R. (1996). Self-assembling peptide nanotubes. *J. Am. Chem. Soc.* 118, 43–50.

He, H., Chen, S., Zhou, J., Dou, Y., Song, L., Che, L., et al. (2013). Cyclodextrin-derived pH-responsive nanoparticles for delivery of paclitaxel. *Biomaterials* 34, 5344–5358. doi: 10.1016/j.biomaterials.2013.03.068

Hoffman, A. S. (2008). The origins and evolution of "controlled" drug delivery systems. *J. Control. Release* 132, 153–163. doi: 10.1016/j.jconrel.2008.08.012

Hofheinz, R.-D., Gnad-Vogt, S. U., Beyer, U., and Hochhaus, A. (2005). Liposomal encapsulated anti-cancer drugs. *Anticancer Drugs* 16, 691–707. doi: 10.1097/01.cad.0000167902.53039.5a

Holmes, T. C., de Lacalle, S., Su, X., Liu, G., Rich, A., and Zhang, S. (2000). Extensive neurite outgrowth and active synapse formation on self-assembling

peptide scaffolds. *Proc. Natl. Acad. Sci. U.S.A.* 97, 6728–6733. doi: 10.1073/pnas.97.12.6728

Hu, Q., Li, H., Wang, L., Gu, H., and Fan, C. (2018). DNA nanotechnology-enabled drug delivery systems. *Chem. Rev.* 119, 6459–6506. doi: 10.1021/acs.chemrev.7b00663

Hu, R., Zhang, X., Zhao, Z., Zhu, G., Chen, T., Fu, T., et al. (2014). DNA nanoflowers for multiplexed cellular imaging and traceable targeted drug delivery. *Angew. Chem. Int. Ed.* 53, 5821–5826. doi: 10.1002/anie.201400323

Hutanu, D., Frishberg, M. D., Guo, L., and Darie, C. C. (2014). Recent applications of polyethylene glycols (PEGs) and PEG derivatives. *Mod. Chem. Appl.* 2:132.

Jabbari, E., Yang, X., Moeinzadeh, S., and He, X. (2013). Drug release kinetics, cell uptake, and tumor toxicity of hybrid VVVVVVKK peptide-assembled polylactide nanoparticles. *Eur. J. Pharm. Biopharm.* 84, 49–62. doi: 10.1016/j.ejpb.2012.12.012

Jiang, K., Han, L., Guo, Y., Zheng, G., Fan, L., Shen, Z., et al. (2017). A carrier-free dual-drug nanodelivery system functionalized with aptamer specific targeting HER2-overexpressing cancer cells. *J. Mater. Chem. B* 5, 9121–9129. doi: 10.1039/c7tb02562a

Jiang, Q., Song, C., Nangreave, J., Liu, X., Lin, L., Qiu, D., et al. (2012). DNA origami as a carrier for circumvention of drug resistance. *J. Am. Chem. Soc.* 134, 13396–13403. doi: 10.1021/ja304263n

Jin, B., Zhou, X., Li, X., Lin, W., Chen, G., and Qiu, R. (2016). Self-assembled modified soy protein/dextran nanogel induced by ultrasonication as a delivery vehicle for riboflavin. *Molecules* 21:282. doi: 10.3390/molecules21030282

Kim, J., Narayana, A., Patel, S., and Sahay, G. (2019). Advances in intracellular delivery through supramolecular self-assembly of oligonucleotides and peptides. *Theranostics* 9, 3191–3212. doi: 10.7150/thno.33921

Kim, T.-Y., Kim, D.-W., Chung, J.-Y., Shin, S. G., Kim, S.-C., Heo, D. S., et al. (2004). Phase I and pharmacokinetic study of Genexol-PM, a cremophor-free, polymeric micelle-formulated paclitaxel, in patients with advanced malignancies. *Clin. Cancer Res.* 10, 3708–3716. doi: 10.1158/1078-0432.ccr-03-0655

Knauer, N., Pashkina, E., and Apartsin, E. (2019). Topological aspects of the design of nanocarriers for therapeutic peptides and proteins. *Pharmaceutics* 11:E91. doi: 10.3390/pharmaceutics11020091

Kumar, J. N., Wu, Y.-L., Loh, X. J., Ho, N. Y., Aik, S. X., and Pang, V. Y. (2019). The effective treatment of multi-drug resistant tumors with self-assembling alginate copolymers. *Polym. Chem.* 10, 278–286. doi: 10.1039/c8py01255e

Kumar, M. R., Muzzarelli, R. A., Muzzarelli, C., Sashiwa, H., and Domb, A. (2004). Chitosan chemistry and pharmaceutical perspectives. *Chem. Rev.* 104, 6017–6084. doi: 10.1021/cr030441b

Kumar, V., Bayda, S., Hadla, M., Caligiuri, I., Russo Spena, C., Palazzolo, S., et al. (2016). Enhanced chemotherapeutic behavior of open-Caged DNA@doxorubicin nanostructures for cancer cells. *J. Cell. Physiol.* 231, 106–110. doi: 10.1002/jcp.25057

Lacroix, A. L., Vengut-Climent, E., de Rochambeau, D., and Sleiman, H. F. (2019). Uptake and fate of fluorescently labeled DNA nanostructures in cellular environments: a cautionary tale. *ACS Cent. Sci.* 5, 882–891.

Lalatsa, A., Schätzlein, A. G., Garrett, N. L., Moger, J., Briggs, M., Godfrey, L., et al. (2015). Chitosan amphiphile coating of peptide nanofibres reduces liver uptake and delivers the peptide to the brain on intravenous administration. *J. Control. Release* 197, 87–96. doi: 10.1016/j.jconrel.2014.10.028

Lee, H., Lytton-Jean, A. K., Chen, Y., Love, K. T., Park, A. I., Karagiannis, E. D., et al. (2012). Molecularly self-assembled nucleic acid nanoparticles for targeted in vivo siRNA delivery. *Nat. Nanotechnol.* 7, 389–393. doi: 10.1038/nnano.2012.73

Lee, S., Trinh, T. H., Yoo, M., Shin, J., Lee, H., Kim, J., et al. (2019). Self-assembling peptides and their application in the treatment of diseases. *Int. J. Mol. Sci.* 20:5850. doi: 10.3390/ijms20235850

Lee, S. S., Hsu, E. L., Mendoza, M., Ghodasra, J., Nickoli, M. S., Ashtekar, A., et al. (2015). Gel scaffolds of BMP-2-binding peptide amphiphile nanofibers for spinal arthrodesis. *Adv. Healthc. Mater.* 4, 131–141. doi: 10.1002/adhm.201400129

Lee, Y. S. (2008). *Self-Assembly and Nanotechnology: A Force Balance Approach*. Hoboken, NJ: John Wiley & Sons.

Leite, D. M., Barbu, E., Pilkington, G. J., and Lalatsa, A. (2015). Peptide self-assemblies for drug delivery. *Curr. Top. Med. Chem.* 15, 2277–2289. doi: 10.2174/1568026615666150605120456

Li, B. L., Setyawati, M. I., Chen, L., Xie, J., Ariga, K., Lim, C.-T., et al. (2017). Directing assembly and disassembly of 2D MoS2 nanosheets with DNA for drug delivery. *ACS Appl. Mater. Interfaces* 9, 15286–15296. doi: 10.1021/acsami.7b02529

Li, J., Liang, H., Liu, J., and Wang, Z. (2018). Poly (amidoamine)(PAMAM) dendrimer mediated delivery of drug and pDNA/siRNA for cancer therapy. *Int. J. Pharm.* 546, 215–225. doi: 10.1016/j.ijpharm.2018.05.045

Li, J., Wang, X., Zhang, T., Wang, C., Huang, Z., Luo, X., et al. (2015). A review on phospholipids and their main applications in drug delivery systems. *Asian J. Pharm. Sci.* 10, 81–98. doi: 10.1016/j.ajps.2014.09.004

Li, N., Li, X.-R., Zhou, Y.-X., Li, W.-J., Zhao, Y., Ma, S.-J., et al. (2012). The use of polyion complex micelles to enhance the oral delivery of salmon calcitonin and transport mechanism across the intestinal epithelial barrier. *Biomaterials* 33, 8881–8892. doi: 10.1016/j.biomaterials.2012.08.047

Li, X., Li, J., Gao, Y., Kuang, Y., Shi, J., and Xu, B. (2010). Molecular nanofibers of olsalazine form supramolecular hydrogels for reductive release of an anti-inflammatory agent. *J. Am. Chem. Soc.* 132, 17707–17709. doi: 10.1021/ja109269v

Linko, V., Ora, A., and Kostiainen, M. A. (2015). DNA nanostructures as smart drug-delivery vehicles and molecular devices. *Trends Biotechnol.* 33, 586–594. doi: 10.1016/j.tibtech.2015.08.001

Liu, S., Fukushima, K., Venkataraman, S., Hedrick, J. L., and Yang, Y. Y. (2018). Supramolecular nanofibers self-assembled from cationic small molecules derived from repurposed poly (ethylene teraphthalate) for antibiotic delivery. *Nanomedicine* 14, 165–172. doi: 10.1016/j.nano.2017.09.007

Liu, Z., Chen, K., Davis, C., Sherlock, S., Cao, Q., Chen, X., et al. (2008). Drug delivery with carbon nanotubes for in vivo cancer treatment. *Cancer Res.* 68, 6652–6660. doi: 10.1158/0008-5472.CAN-08-1468

Lombardo, D., Kiselev, M. A., and Caccamo, M. T. (2019). Smart nanoparticles for drug delivery application: development of versatile nanocarrier platforms in biotechnology and nanomedicine. *J. Nanomater.* 2019:3702518.

Lombardo, D., Kiselev, M. A., Magazù, S., and Calandra, P. (2015). Amphiphiles self-assembly: basic concepts and future perspectives of supramolecular approaches. *Adv. Condens. Matter Phys.* 2015:151683.

Madhanagopal, B. R., Zhang, S., Demirel, E., Wady, H., and Chandrasekaran, A. R. (2018). DNA nanocarriers: programmed to deliver. *Trends Biochem. Sci.* 43, 997–1013. doi: 10.1016/j.tibs.2018.09.010

Mahato, M., Arora, V., Pathak, R., Gautam, H. K., and Sharma, A. K. (2012). Fabrication of nanostructures through molecular self-assembly of small amphiphilic glyco-dehydropeptides. *Mol. Biosyst.* 8, 1742–1749. doi: 10.1039/c2mb25023c

Marchesan, S., Vargiu, A., and Styan, K. (2015). The Phe-Phe motif for peptide self-assembly in nanomedicine. *Molecules* 20, 19775–19788. doi: 10.3390/molecules201119658

Maruyama-Tabata, H., Harada, Y., Matsumura, T., Satoh, E., Cui, F., Iwai, M., et al. (2000). Effective suicide gene therapy in vivo by EBV-based plasmid vector coupled with polyamidoamine dendrimer. *Gene Ther.* 7, 53–60. doi: 10.1038/sj.gt.3301044

Massiot, J., Rosilio, V., and Makky, A. (2019). Photo-triggerable liposomal drug delivery systems: from simple porphyrin insertion in the lipid bilayer towards supramolecular assemblies of lipid–porphyrin conjugates. *J. Mater. Chem. B* 7, 1805–1823. doi: 10.1039/c9tb00015a

Mattia, E., and Otto, S. (2015). Supramolecular systems chemistry. *Nat. Nanotechnol.* 10:111. doi: 10.1038/nnano.2014.337

Mazza, M., Notman, R., Anwar, J., Rodger, A., Hicks, M., Parkinson, G., et al. (2013). Nanofiber-based delivery of therapeutic peptides to the brain. *ACS Nano* 7, 1016–1026. doi: 10.1021/nn305193d

Mei, L., Zhu, G., Qiu, L., Wu, C., Chen, H., Liang, H., et al. (2015). Self-assembled multifunctional DNA nanoflowers for the circumvention of

multidrug resistance in targeted anticancer drug delivery. *Nano Res.* 8, 3447–3460. doi: 10.1007/s12274-015-0841-8

Mendes, A. C., Baran, E. T., Reis, R. L., and Azevedo, H. S. (2013). Self-assembly in nature: using the principles of nature to create complex nanobiomaterials. *Wiley Interdiscip. Rev. Nanomed. Nanobiotechnol.* 5, 582–612. doi: 10.1002/wnan.1238

Mohanraj, V., and Chen, Y. (2006). Nanoparticles-a review. *Trop. J. Pharm. Res.* 5, 561–573.

Muankaew, C., and Loftsson, T. (2018). Cyclodextrin-based formulations: a non-invasive platform for targeted drug delivery. *Basic Clin. Pharm. Toxicol.* 122, 46–55. doi: 10.1111/bcpt.12917

Munier, S., Messai, I., Delair, T., Verrier, B., and Ataman-Önal, Y. (2005). Cationic PLA nanoparticles for DNA delivery: comparison of three surface polycations for DNA binding, protection and transfection properties. *Colloids Surf. B Biointerfaces* 43, 163–173. doi: 10.1016/j.colsurfb.2005.05.001

Nahar, S., Nayak, A., Ghosh, A., Subudhi, U., and Maiti, S. (2018). Enhanced and synergistic downregulation of oncogenic miRNAs by self-assembled branched DNA. *Nanoscale* 10, 195–202. doi: 10.1039/c7nr06601e

Narayanaswamy, R., and Torchilin, V. P. (2019). Hydrogels and their applications in targeted drug delivery. *Molecules* 24:603. doi: 10.3390/molecules24030603

Naskar, J., Roy, S., Joardar, A., Das, S., and Banerjee, A. (2011). Self-assembling dipeptide-based nontoxic vesicles as carriers for drugs and other biologically important molecules. *Org. Biomol. Chem.* 9, 6610–6615. doi: 10.1039/c1ob05757j

Ni, M., and Zhuo, S. (2019). Applications of self-assembling ultrashort peptides in bionanotechnology. *RSC Adv.* 9, 844–852. doi: 10.1039/c8ra07533f

Niers, T., Klerk, C., DiNisio, M., Van Noorden, C., Büller, H., Reitsma, P., et al. (2007). Mechanisms of heparin induced anti-cancer activity in experimental cancer models. *Crit. Rev. Oncol. Hematol.* 61, 195–207. doi: 10.1016/j.critrevonc.2006.07.007

Nitta, S., and Numata, K. (2013). Biopolymer-based nanoparticles for drug/gene delivery and tissue engineering. *Int. J. Mol. Sci.* 14, 1629–1654. doi: 10.3390/ijms14011629

Northfelt, D. W., Dezube, B. J., Thommes, J. A., Miller, B. J., Fischl, M. A., Friedman-Kien, A., et al. (1998). Pegylated-liposomal doxorubicin versus doxorubicin, bleomycin, and vincristine in the treatment of AIDS-related Kaposi's sarcoma: results of a randomized phase III clinical trial. *J. Clin. Oncol.* 16, 2445–2451. doi: 10.1200/jco.1998.16.7.2445

Panda, J. J., and Chauhan, V. S. (2014). Short peptide based self-assembled nanostructures: implications in drug delivery and tissue engineering. *Polym. Chem.* 5, 4418–4436.

Panda, J. J., Mishra, A., Basu, A., and Chauhan, V. S. (2008). Stimuli responsive self-assembled hydrogel of a low molecular weight free dipeptide with potential for tunable drug delivery. *Biomacromolecules* 9, 2244–2250. doi: 10.1021/bm800404z

Patra, J. K., Das, G., Fraceto, L. F., Campos, E. V. R., del Pilar, Rodriguez-Torres, M., et al. (2018). Nano based drug delivery systems: recent developments and future prospects. *J. Nanobiotechnol.* 16:71. doi: 10.1186/s12951-018-0392-8

Pattni, B. S., Chupin, V. V., and Torchilin, V. P. (2015). New developments in liposomal drug delivery. *Chem. Rev.* 115, 10938–10966. doi: 10.1021/acs.chemrev.5b00046

Pearson, R. M., Patra, N., Hsu, H.-J., Uddin, S., Král, P., and Hong, S. (2012). Positively charged dendron micelles display negligible cellular interactions. *ACS Macro Lett.* 2, 77–81. doi: 10.1021/mz300533w

Pearson, R. M., Sen, S., Hsu, H.-J., Pasko, M., Gaske, M., Krail, P., et al. (2016). Tuning the selectivity of dendron micelles through variations of the poly (ethylene glycol) corona. *ACS Nano* 10, 6905–6914. doi: 10.1021/acsnano.6b02708

Poon, R. T., and Borys, N. (2009). Lyso-thermosensitive liposomal doxorubicin: a novel approach to enhance efficacy of thermal ablation of liver cancer. *Expert Opin. Pharmacothera.* 10, 333–343. doi: 10.1517/14656560802677874

Praetorius, F., Kick, B., Behler, K. L., Honemann, M. N., Weuster-Botz, D., and Dietz, H. (2017). Biotechnological mass production of DNA origami. *Nature* 552, 84–87. doi: 10.1038/nature24650

Prakash Sharma, P., Rathi, B., and Rodrigues, J. (2015). Self-assembled peptide nanoarchitectures: applications and future aspects. *Curr. Top. Med. Chem.* 15, 1268–1289. doi: 10.2174/1568026615666150408105711

Qi, F., Wu, J., Li, H., and Ma, G. (2019). Recent research and development of PLGA/PLA microspheres/nanoparticles: a review in scientific and industrial aspects. *Front. Chem. Sci. Eng.* 13, 14–27. doi: 10.1007/s11705-018-1729-4

Qian, H., Tay, C. Y., Setyawati, M., Chia, S., Lee, D., and Leong, D. (2017). Protecting microRNAs from RNase degradation with steric DNA nanostructures. *Chem. Sci.* 8, 1062–1067. doi: 10.1039/c6sc01829g

Qu, Y., Yang, J., Zhan, P., Liu, S., Zhang, K., Jiang, Q., et al. (2017). Self-assembled DNA dendrimer nanoparticle for efficient delivery of immunostimulatory CpG motifs. *ACS Appl. Mater. Interfaces* 9, 20324–20329. doi: 10.1021/acsami.7b05890

Que, X., Su, J., Guo, P., Kamal, Z., Xu, E., Liu, S., et al. (2019). Study on preparation, characterization and multidrug resistance reversal of red blood cell membrane-camouflaged tetrandrine-loaded PLGA nanoparticles. *Drug Deliv.* 26, 199–207. doi: 10.1080/10717544.2019.1573861

Quiñones, J. P., Peniche, H., and Peniche, C. (2018). Chitosan based self-assembled nanoparticles in drug delivery. *Polymers* 10:235. doi: 10.3390/polym10030235

Reches, M., and Gazit, E. (2003). Casting metal nanowires within discrete self-assembled peptide nanotubes. *Science* 300, 625–627. doi: 10.1126/science.1082387

Reches, M., and Gazit, E. (2004). Formation of closed-cage nanostructures by self-assembly of aromatic dipeptides. *Nano Lett.* 4, 581–585. doi: 10.1021/nl035159z

Roh, Y. H., Deng, J. Z., Dreaden, E. C., Park, J. H., Yun, D. S., Shopsowitz, K. E., et al. (2016). A multi-RNAi microsponge platform for simultaneous controlled delivery of multiple small interfering RNAs. *Angew. Chem. Int. Ed.* 55, 3347–3351. doi: 10.1002/anie.201508978

Salzano, G., Costa, D. F., Sarisozen, C., Luther, E., Mattheolabakis, G., Dhargalkar, P. P., et al. (2016). Mixed nanosized polymeric micelles as promoter of doxorubicin and miRNA-34a Co-delivery triggered by dual stimuli in tumor tissue. *Small* 12, 4837–4848. doi: 10.1002/smll.201600925

Setyawati, M. I., Kutty, R. V., and Leong, D. T. (2016). DNA nanostructures carrying stoichiometrically definable antibodies. *Small* 12, 5601–5611. doi: 10.1002/smll.201601669

Shang, J., Le, X., Zhang, J., Chen, T., and Theato, P. (2019). Trends in polymeric shape memory hydrogels and hydrogel actuators. *Polym. Chem.* 10, 1036–1055. doi: 10.1039/c8py01286e

Sharma, A., Vaghasiya, K., Verma, R. K., and Yadav, A. B. (2018). "DNA nanostructures: chemistry, self-assembly, and applications," in *Emerging Applications of Nanoparticles and Architecture Nanostructures*, eds A. Sharma, K. Vaghasiya, R. K. Verma, and A. B. Yadav (Amsterdam: Elsevier), 71–94. doi: 10.1016/b978-0-323-51254-1.00003-8

Simoes, S. M., Rey-Rico, A., Concheiro, A., and Alvarez-Lorenzo, C. (2015). Supramolecular cyclodextrin-based drug nanocarriers. *Chem. Commun.* 51, 6275–6289. doi: 10.1039/c4cc10388b

Sofi, H. S., Ashraf, R., Khan, A. H., Beigh, M. A., Majeed, S., and Sheikh, F. A. (2018). Reconstructing nanofibers from natural polymers using surface functionalization approaches for applications in tissue engineering, drug delivery and biosensing devices. *Mater. Sci. Eng. C. Mater Biol Appl.* 94, 1102–1124. doi: 10.1016/j.msec.2018.10.069

Somani, S., Laskar, P., Altwaijry, N., Kewcharoenvong, P., Irving, C., Robb, G., et al. (2018). PEGylation of polypropylenimine dendrimers: effects on cytotoxicity, DNA condensation, gene delivery and expression in cancer cells. *Sci. Rep.* 8:9410. doi: 10.1038/s41598-018-27400-6

Song, X., Wen, Y., Zhu, J.-L., Zhao, F., Zhang, Z.-X., and Li, J. (2016). Thermoresponsive delivery of paclitaxel by β-cyclodextrin-based poly(N-isopropylacrylamide) star polymer via inclusion complexation. *Biomacromolecules* 17, 3957–3963. doi: 10.1021/acs.biomac.6b01344

Soukasene, S., Toft, D. J., Moyer, T. J., Lu, H., Lee, H.-K., Standley, S. M., et al. (2011). Antitumor activity of peptide amphiphile nanofiber-encapsulated camptothecin. *ACS Nano* 5, 9113–9121. doi: 10.1021/nn203343z

Stoffelen, C., and Huskens, J. (2016). Soft supramolecular nanoparticles by noncovalent and host–guest interactions. *Small* 12, 96–119. doi: 10.1002/smll.201501348

Sun, L., Zheng, C., and Webster, T. J. (2017). Self-assembled peptide nanomaterials for biomedical applications: promises and pitfalls. *Int. J. Nanomed.* 12, 73–86. doi: 10.2147/IJN.S117501

Sun, W., Jiang, T., Lu, Y., Reiff, M., Mo, R., and Gu, Z. (2014). Cocoon-like self-degradable DNA nanoclew for anticancer drug delivery. *J. Am. Chem. Soc.* 136, 14722–14725. doi: 10.1021/ja5088024

Tang, Y., Li, Y., Xu, R., Li, S., Hu, H., Xiao, C., et al. (2018). Self-assembly of folic acid dextran conjugates for cancer chemotherapy. *Nanoscale* 10, 17265–17274. doi: 10.1039/c8nr04657c

Tesauro, D., Accardo, A., Diaferia, C., Milano, V., Guillon, J., Ronga, L., et al. (2019). Peptide-based drug-delivery systems in biotechnological applications: recent advances and perspectives. *Molecules* 24:351. doi: 10.3390/molecules24020351

Theodoropoulou, M., and Stalla, G. K. (2013). Somatostatin receptors: from signaling to clinical practice. *Front. Neuroendocrinol.* 34:228–252. doi: 10.1016/j.yfrne.2013.07.005

Thota, B. N., Urner, L. H., and Haag, R. (2015). Supramolecular architectures of dendritic amphiphiles in water. *Chem. Rev.* 116, 2079–2102. doi: 10.1021/acs.chemrev.5b00417

Torchilin, V. P. (2005). Block copolymer micelles as a solution for drug delivery problems. *Expert Opin. Ther. Pat.* 15, 63–75. doi: 10.1517/17425247.2014.945417

Trummer, R., Rangsimawong, W., Sajomsang, W., Kumpugdee-Vollrath, M., Opanasopit, P., and Tonglairoum, P. (2018). Chitosan-based self-assembled nanocarriers coordinated to cisplatin for cancer treatment. *RSC Adv.* 8, 22967–22973. doi: 10.1039/c8ra03069c

Tsonchev, S., Niece, K. L., Schatz, G. C., Ratner, M. A., and Stupp, S. I. (2008). Phase diagram for assembly of biologically-active peptide amphiphiles. *J. Phys. Chem. B* 112, 441–447. doi: 10.1021/jp076273z

Tysseling-Mattiace, V. M., Sahni, V., Niece, K. L., Birch, D., Czeisler, C., Fehlings, M. G., et al. (2008). Self-assembling nanofibers inhibit glial scar formation and promote axon elongation after spinal cord injury. *J. Neurosci.* 28, 3814–3823. doi: 10.1523/JNEUROSCI.0143-08.2008

Vauthey, S., Santoso, S., Gong, H., Watson, N., and Zhang, S. (2002). Molecular self-assembly of surfactant-like peptides to form nanotubes and nanovesicles. *Proc. Natl. Acad. Sci. U.S.A.* 99, 5355–5360. doi: 10.1073/pnas.072089599

Ventola, C. L. (2017). Progress in nanomedicine: approved and investigational nanodrugs. *Pharm. Ther.* 42, 742–755.

Vilar, G., Tulla-Puche, J., and Albericio, F. (2012). Polymers and drug delivery systems. *Curr. Drug Deliv.* 9, 367–394.

Wang, C., Sun, W., Wright, G., Wang, A. Z., and Gu, Z. (2016). Inflammation-triggered cancer immunotherapy by programmed delivery of CpG and anti-PD1 antibody. *Adv. Mater.* 28, 8912–8920. doi: 10.1002/adma.201506312

Wang, H., Dai, T., Zhou, S., Huang, X., Li, S., Sun, K., et al. (2017a). Self-assembly assisted fabrication of dextran-based nanohydrogels with reduction-cleavable junctions for applications as efficient drug delivery systems. *Sci. Rep.* 7:40011. doi: 10.1038/srep40011

Wang, J., Hu, X., and Xiang, D. (2018). Nanoparticle drug delivery systems: an excellent carrier for tumor peptide vaccines. *Drug Deliv.* 25, 1319–1327. doi: 10.1080/10717544.2018.1477857

Wang, H., Lu, Z., Wang, L., Guo, T., Wu, J., Wan, J., et al. (2017b). New generation nanomedicines constructed from self-assembling small-molecule prodrugs alleviate cancer drug toxicity. *Cancer Res.* 77, 6963–6974. doi: 10.1158/0008-5472.CAN-17-0984

Wasiak, I., Kulikowska, A., Janczewska, M., Michalak, M., Cymerman, I. A., Nagalski, A., et al. (2016). Dextran nanoparticle synthesis and properties. *PLoS One* 11:e0146237. doi: 10.1371/journal.pone.0146237

Webber, M. J., Matson, J. B., Tamboli, V. K., and Stupp, S. I. (2012). Controlled release of dexamethasone from peptide nanofiber gels to modulate inflammatory response. *Biomaterials* 33, 6823–6832. doi: 10.1016/j.biomaterials.2012.06.003

Wheeler, S. E., and Houk, K. (2009). Through-space effects of substituents dominate molecular electrostatic potentials of substituted arenes. *J. Chem. Theory Comput.* 5, 2301–2312. doi: 10.1021/ct900344g

Whitesides, G. M., and Boncheva, M. (2002). Beyond molecules: self-assembly of mesoscopic and macroscopic components. *Proc. Natl. Acad. Sci. U.S.A.* 99, 4769–4774. doi: 10.1073/pnas.082065899

WooáBae, J. (2011). Dendron-mediated self-assembly of highly PEGylated block copolymers: a modular nanocarrier platform. *Chem. Commun.* 47, 10302–10304. doi: 10.1039/c1cc14331j

Wu, C., Han, D., Chen, T., Peng, L., Zhu, G., You, M., et al. (2013). Building a multifunctional aptamer-based DNA nanoassembly for targeted cancer therapy. *J. Am. Chem. Soc.* 135, 18644–18650. doi: 10.1021/ja4094617

Xing, P., and Zhao, Y. (2016). Multifunctional nanoparticles self-assembled from small organic building blocks for biomedicine. *Adv. Mater.* 28, 7304–7339. doi: 10.1002/adma.201600906

Yadav, S., Mahato, M., Pathak, R., Jha, D., Kumar, B., Deka, S. R., et al. (2014a). Multifunctional self-assembled cationic peptide nanostructures efficiently carry plasmid DNA in vitro and exhibit antimicrobial activity with minimal toxicity. *J. Mater. Chem. B* 2, 4848–4861. doi: 10.1039/c4tb00657g

Yadav, S., Priyam, A., Mahato, M., Deka, S. R., and Sharma, A. K. (2014b). Ligands with delocalized charge density and hydrophobicity significantly affect the transfection efficacy of the PAMAM dendrimer. *Pharm. Nanotechnol.* 2, 196–207. doi: 10.2174/2211738503666150421234612

Yadav, S., Rai, V., Mahato, M., Singh, M., Rekha Deka, S., and Kumar Sharma, A. (2015). Vitamin E–TPGS stabilized self-assembled tripeptide nanostructures for drug delivery. *Curr. Top. Med. Chem.* 15, 1227–1235. doi: 10.2174/1568026615666150330111348

Yan, J., Hu, C., Wang, P., Zhao, B., Ouyang, X., Zhou, J., et al. (2015). Growth and origami folding of DNA on nanoparticles for high-efficiency molecular transport in cellular imaging and drug delivery. *Angew. Chem. Int. Ed.* 54, 2431–2435. doi: 10.1002/anie.201408247

Yang, D., Gao, S., Fang, Y., Lin, X., Jin, X., Wang, X., et al. (2018). The π–π stacking-guided supramolecular self-assembly of nanomedicine for effective delivery of antineoplastic therapies. *Nanomedicine* 13, 3159–3177. doi: 10.2217/nnm-2018-0288

Yang, J., Zhang, Q., Chang, H., and Cheng, Y. (2015). Surface-engineered dendrimers in gene delivery. *Chem. Rev.* 115, 5274–5300. doi: 10.1021/cr500542t

Yang, Y., Pearson, R. M., Lee, O., Lee, C. W., Chatterton, R. T. Jr., Khan, S. A., et al. (2014). Dendron-based micelles for topical delivery of endoxifen: a potential chemo-preventive medicine for breast cancer. *Adv. Funct. Mater.* 24, 2442–2449. doi: 10.1002/adfm.201303253

Yu, X., Trase, I., Ren, M., Duval, K., Guo, X., and Chen, Z. (2016). Design of nanoparticle-based carriers for targeted drug delivery. *J. Nanomater.* 2016:1087250.

Yuan, J., Guo, L., Wang, S., Liu, D., Qin, X., Zheng, L., et al. (2018). Preparation of self-assembled nanoparticles of ε-polylysine-sodium alginate: a sustained-release carrier for antigen delivery. *Colloids Surf. B Biointerfaces* 171, 406–412. doi: 10.1016/j.colsurfb.2018.07.058

Zerkoune, L., Angelova, A., and Lesieur, S. (2014). Nano-assemblies of modified cyclodextrins and their complexes with guest molecules: incorporation in nanostructured membranes and amphiphile nanoarchitectonics design. *Nanomaterials* 4, 741–765. doi: 10.3390/nano4030741

Zhang, C., Shi, G., Zhang, J., Niu, J., Huang, P., Wang, Z., et al. (2017). Redox-and light-responsive alginate nanoparticles as effective drug carriers for combinational anticancer therapy. *Nanoscale* 9, 3304–3314. doi: 10.1039/c7nr00005g

Zhang, J., and Ma, P. X. (2013). Cyclodextrin-based supramolecular systems for drug delivery: recent progress and future perspective. *Adv. Drug Deliv. Rev.* 65, 1215–1233. doi: 10.1016/j.addr.2013.05.001

Zhang, L., Zhu, G., Mei, L., Wu, C., Qiu, L., Cui, C., et al. (2015). Self-assembled DNA immunonanoflowers as multivalent CpG nanoagents. *ACS Appl. Mater. Interfaces* 7, 24069–24074. doi: 10.1021/acsami.5b06987

Zhang, P., Zhao, S., Yu, Y., Wang, H., Yang, Y., and Liu, C. (2019). Biocompatibility profile and in vitro cellular uptake of self-assembled alginate nanoparticles. *Molecules* 24:E555. doi: 10.3390/molecules24030555

Zhang, W. J., Hong, C. Y., and Pan, C. Y. (2019). Polymerization-induced self-assembly of functionalized block copolymer nanoparticles and their application in drug delivery. *Macromol. Rapid Commun.* 40:1800279. doi: 10.1002/marc.201800279

Zhang, Q., Jiang, Q., Li, N., Dai, L., Liu, Q., Song, L., et al. (2014). DNA origami as an in vivo drug delivery vehicle for cancer therapy. *ACS Nano* 8, 6633–6643. doi: 10.1021/nn502058j

Zhao, Y., Li, X., Zhao, X., Yang, Y., Li, H., Zhou, X., et al. (2017). Asymmetrical polymer vesicles for drug delivery and other applications. *Front. Pharmacol.* 8:374. doi: 10.3389/fphar.2017.00374

Zhao, Y.-X., Shaw, A., Zeng, X., Benson, E., Nyström, A. M., and Högberg, B. R. (2012). DNA origami delivery system for cancer therapy with tunable release properties. *ACS Nano* 6, 8684–8691. doi: 10.1021/nn3022662

Zheng, J., Fan, R., Wu, H., Yao, H., Yan, Y., Liu, J., et al. (2019). Directed self-assembly of herbal small molecules into sustained release hydrogels for treating neural inflammation. *Nat. Commun.* 10:1604. doi: 10.1038/s41467-019-09601-3

Zhu, G., Hu, R., Zhao, Z., Chen, Z., Zhang, X., and Tan, W. (2013a). Noncanonical self-assembly of multifunctional DNA nanoflowers for biomedical applications. *J. Am. Chem. Soc.* 135, 16438–16445. doi: 10.1021/ja406115e

Zhu, G., Zheng, J., Song, E., Donovan, M., Zhang, K., Liu, C., et al. (2013b). Self-assembled, aptamer-tethered DNA nanotrains for targeted transport of molecular drugs in cancer theranostics. *Proc. Natl. Acad. Sci. U.S.A.* 110, 7998–8003. doi: 10.1073/pnas.1220817110

Conflict of Interest: The authors declare that the research was conducted in the absence of any commercial or financial relationships that could be construed as a potential conflict of interest.

frontiers in Bioengineering and Biotechnology

REVIEW
published: 10 March 2020
doi: 10.3389/fbioe.2020.00165

How the Lack of Chitosan Characterization Precludes Implementation of the Safe-by-Design Concept

*Cíntia Marques[1,2], Claudia Som[3], Mélanie Schmutz[3], Olga Borges[2,4] and Gerrit Borchard[1]**

[1] Institute of Pharmaceutical Sciences of Western Switzerland, University of Geneva, Geneva, Switzerland, [2] Faculty of Pharmacy, University of Coimbra, Coimbra, Portugal, [3] Empa, Swiss Federal Laboratories for Materials Science and Technology, Technology and Society Laboratory, St. Gallen, Switzerland, [4] Center for Neuroscience and Cell Biology, University of Coimbra, Coimbra, Portugal

OPEN ACCESS

Edited by:
Qingxin Mu,
University of Washington,
United States

Reviewed by:
Giulia Suarato,
Italian Institute of Technology, Italy
Gaoxing Su,
Nantong University, China

****Correspondence:***
Gerrit Borchard
gerrit.borchard@unige.ch

Specialty section:
This article was submitted to Nanobiotechnology, a section of the journal Frontiers in Bioengineering and Biotechnology

Received: *03 October 2019*
Accepted: *18 February 2020*
Published: *10 March 2020*

Citation:
Marques C, Som C, Schmutz M, Borges O and Borchard G (2020) How the Lack of Chitosan Characterization Precludes Implementation of the Safe-by-Design Concept. Front. Bioeng. Biotechnol. 8:165. doi: 10.3389/fbioe.2020.00165

Efficacy and safety of nanomedicines based on polymeric (bio)materials will benefit from a rational implementation of a Safe-by-Design (SbD) approach throughout their development. In order to achieve this goal, however, a standardization of preparation and characterization methods and their accurate reporting is needed. Focusing on the example of chitosan, a biopolymer derived from chitin and frequently used in drug and vaccine delivery vector preparation, this review discusses the challenges still to be met and overcome prior to a successful implementation of the SbD approach to the preparation of chitosan-based protein drug delivery systems.

Keywords: safe by design, polymeric drug carriers, chitosan, insulin, protein drug delivery

INTRODUCTION

Nanoparticles (NPs) have been extensively investigated as delivery systems for targeted drug delivery, controlled drug release, *in vivo* imaging, diagnostics, and medical devices. These systems may offer more convenient routes of administration, decrease drug toxicity, and potentially reduce healthcare costs (Vasile, 2019). However, despite numerous publications on nanoparticulate drug carrier systems ("nanomedicines"), the extent of their translation into clinical application has been unsatisfactory (Hua et al., 2018; Rosenblum et al., 2018). The first generation of these nanomedicines passed regulatory approval by meeting standards in place for "conventional" drugs of low molecular weight. However, with regard to the complexity of nanomedicines, these standards were reviewed and partially replaced by nano-specific critical quality attributes (CQAs) that need to be reported in order to confirm quality, safety, and efficacy of NPs (Gaspar, 2007; U. S. Food and Drug Administration, 2017). Quality control assays for nanomaterial characterization, the need of establishing specialized toxicology studies for nanomedicines, and the lack of suitable standards and dedicated regulatory guidelines are a few examples of the challenges to their development and effective clinical translation (Hua et al., 2018).

The research community is working to establish protocols for nanomaterial characterization (Brown et al., 2010). The Nanotechnology Regulatory Science Research Plan, established by the Food and Drug Administration (FDA), addresses five major criteria, namely, physicochemical characterization, pre-clinical models, risk characterization, risk assessment, and risk communication (Rosenblum et al., 2018). In this regard, the Nanotechnology Characterization Laboratory (US NCL) was founded, focusing on the characterization of nanomedicines for cancer therapy. In Europe, the European Nanomedicine Characterization Laboratory (EU-NCL) was created as a multi-national organization within the H2020 framework. EU-NCL focuses on the pre-clinical characterization of nanomaterials in order to accelerate their development toward the approval by the regulatory agencies (European Nanomedicine Characterization Laboratory, 2019a). Moreover, in the European Union, other projects such as NANoREG, NANoREG II, ProSafe, and NanoDefine have also explored the standardization of nanomaterial characterization, and the development of better prediction models, such as the application of the Safe-by-Design (SbD) approach to nanosystems (Kraegeloh et al., 2018).

The principle behind SbD includes the safety assessment of nanomedicines as early as possible in their innovation process and throughout their lifecycle by designing out the physicochemical properties with an adverse effect on human health and the environment (Bottero et al., 2017; Soeteman-Hernandez et al., 2019). Several concepts of SbD have arisen from the European projects mentioned above. For example, the NANoREG project describes three pillars: safe product by design, safe use of products and safe industrial production. In addition, according to NANoREG II, the SbD concept aims at the development of functional and safer nanomaterials, safer processes as well as safer products. In general, the application of this concept requires the examination of which physicochemical properties render a nanomaterial safe, means to implement this knowledge into industrial innovation processes, and information exchange between stakeholders. The SbD concept can be implemented to design nanomaterials with an optimal balance between functionality and risk, based on relevant physicochemical parameters (Kraegeloh et al., 2018).

The European project GoNanoBioMat created a SbD approach to support industries, particularly small and medium-size enterprises (SMEs) to identify risks and uncertainties early in the research and development phase, support safe production and handling, and deliver safe products. The SbD approach is applied to polymeric nanobiomaterials for drug delivery and it focuses on safe nanobiomaterials, safe production and safe storage and transport (Som et al., 2019).

Particularly, one goal of GoNanoBioMat was to establish the characteristics of different types of chitosan nanoparticles (Chit NPs), to establish a correlation between the physicochemical properties of this biopolymer and its immunostimulatory activity and, finally, to establish a guideline to select the most suitable chitosan polymer according to its purpose, allowing an SbD approach. To address these points, an extensive literature search was initiated and will be presented in this report.

Chitosan, the deacetylated form of chitin, is a biopolymer investigated for the preparation of particles as vectors for drug delivery. Chitosan nanoparticles are under investigation for a wide variety of biomedical applications, due to the polysaccharide's exceptional versatility (Koppolu et al., 2014). One of the major applications of chitosan is the preparation of medical micro- and nano-particles. Nanoparticles of natural polymers are a promising approach for drug delivery due to their biocompatibility and biodegradability, as well as for their ability to provide a controlled drug release profile (Erel et al., 2016). Even though chitosan is one of the most studied biopolymers, there is no standardization as far as its properties and the resulting biological activity are concerned.

The goal of this review was to understand whether it is possible to identify physicochemical properties of chitosan that are correlated to its biological effects. To this end, supportive information on protocols used to prepare chitosan NPs encapsulating insulin (Chit-Ins NPs) as a model protein drug were collected. Protocol details and Chit-Ins NPs characterization data were compared. Literature was also examined for available information on the immunotoxicological response to Chit-Ins NPs administration. Finally, the report summarizes the current state of the art, identifies the challenges in applying the SbD concept to the bionanomaterial chitosan and establishes future perspectives on Chit NPs characterization.

METHODS

A literature search was performed through PubMed and Science Direct using as Medical Subject Headings (MeSH) keywords chitosan, immune activity, gelation, insulin, encapsulation, and adjuvant. We focused on ionotropic gelation, using tripolyphosphate (TPP) as crosslinker because it is the most used process to prepare Chit NPs. Insulin was chosen as a model for protein encapsulation into these nanoparticles.

CHITOSAN: POTENTIAL AND VERSATILITY

Chitosan is the partially deacetylated form of chitin – a poly (D-glucosamine) – and comprises a wide range of linear polymers differing in polymer length and deacetylation degree. The polymer is composed of randomly distributed β-(1→4)-linked D-glucosamine (deacetylated unit) and N-acetyl-D-glucosamine (acetylated unit) (**Figure 1**) and it appears in the market with different purity degrees (Primex, 2019). Chitin is a natural biopolymer extracted from the exoskeleton of crustaceans (shrimp, crabs, lobsters, etc.) and from the cell walls of fungi or yeast (Illum, 1998; Mukhopadhyay et al., 2013; Vasiliev, 2015; Bugnicourt and Ladavière, 2016; Jafary Omid et al., 2018; Primex, 2019).

In fact, chitosan is one of the most studied biopolymers. This polysaccharide is exceptionally versatile as it can be used in solutions, suspensions, hydrogels and/or micro- and

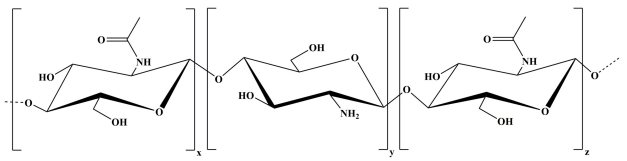

FIGURE 1 | Chitosan composed of randomly distributed deacetylated unit (y, z) and acetylated unit (x).

nanoparticles. Moreover, it is possible to proceed to its chemical functionalization through its amino and hydroxyl groups, and/or by conjugation of peptides and other molecules to the polymer backbone. This allows for the modification of physicochemical properties and/or the introduction of desirable characteristics, further broadening chitosan potential applications (Sreekumar et al., 2018).

Chitosan is well known for its inherent biological properties, namely biocompatibility (Hirano et al., 1990), non-toxicity (Hu et al., 2011; Pradines et al., 2015), antimicrobial activity (Zheng and Zhu, 2003; Qin et al., 2006; Cerchiara et al., 2015), plant strengthening (Choudhary et al., 2017), hydrating ability (Cerchiara et al., 2015), gel and film forming (Shan et al., 2010; Nie et al., 2016), mucoadhesive properties (Cerchiara et al., 2015; Patel et al., 2015), immunostimulant activity (Nishimura et al., 1985; Scherliess et al., 2013), hemocompatibility (Malette et al., 1983; Lee et al., 1995; Zhao et al., 2011), and biodegradability (Lee et al., 1995; Patel et al., 2015).

This polymer is one of the most widely used for biomedical applications. Actually, chitosan has been under investigation for drug and vaccine delivery (Borges et al., 2008; Esmaeili et al., 2010; Jafary Omid et al., 2018; Soares et al., 2018; Bento et al., 2019), gene delivery (Thanou et al., 2002), surgical sutures (Muzzarelli et al., 1993; Altinel et al., 2018), rebuilding of bone (Lee et al., 2009), corneal contact lenses (Silva et al., 2016), dental implants (Yokoyama et al., 2002), wound healing (Mizuno et al., 2003), antimicrobial applications (Dai et al., 2009), and tissue engineering (Madihally and Matthew, 1999; Kanimozhi et al., 2016). Moreover, chitosan has been used as a dietary supplement in preparations for treatment of obesity and hypercholesterolemia (Bokura and Kobayashi, 2003; Zhang et al., 2008) and also in medical devices for the treatment and control of bleeding (Millner et al., 2009). The polysaccharide is classified by FDA as Generally Recognized As Safe (GRAS) for food (Nutrition Center for Food Safety Applied, 2019a,b). The polymer description was first introduced into the European Pharmacopeia 6.0 and the 29th edition of the United States Pharmacopeia (USP) 34-NF. Monographs contain the assays and establish limits to be observed when the polymer is used as a pharmaceutical excipient (Council of Europe, 2019). Currently the efficacy of chitosan nanoparticles in the treatment of postoperative pain and antibacterial activity against *Enterococcus faecalis* in infected root canals is being studied in a phase 2 clinical trial (U. S National Library of Medicine, 2018).

CHALLENGES FOR SAFE-BY-DESIGN OF CHIT-NPs

Characterization of Chitosan Is Not Standardized

Despite the large number of papers about chitosan, reproducibility of the reported results is often an issue (Nasti et al., 2009). As mentioned above, chitosan is a family of polymers, which differ in their degree of deacetylation (DD), molecular weight (MW) and purity. The different characteristics can be correlated with the diversity of physicochemical properties and diverse biological activities of the polysaccharide. As a matter of fact, these structural characteristics are dependent on the source of chitin, its extraction, and the deacetylation method (Bellich et al., 2016), whose correlations with chitosan biological properties has been reviewed elsewhere (Younes and Rinaudo, 2015).

As illustrated in **Table 1**, chitosan basic characterization is neglected in many papers making it difficult to critically comment on conflicting experimental results (Vasiliev, 2015; Bellich et al., 2016). Even when the MW is provided, there is often an ambiguous classification. For example, Mehrabi et al. (2018) classify chitosan into high molecular weight (HMW) at the range of 700–1,000 kDa, low molecular weight (LMW) when less than 150 kDa, and medium molecular weight (MMW) between low and high molecular weight. On the other hand, Vila et al. (2004) mention chitosan of 23 and 38 kDa as LMW and chitosan of 70 kDa as HMW.

Moreover, Vasiliev (2015) pointed out the importance of method harmonization and validation to chitosan analysis, such as size exclusion chromatography (SEC) to determine MW, capillary viscosimetry to check for viscosity, nuclear magnetic resonance (NMR) to define the degree of deacetylation (DD), and *Limulus amebocyte* lysate (LAL) test to verify endotoxin content.

Other authors go even deeper with respect to chitosan characterization. Even knowing that patterns of acetylation (P_A) – random, alternating or blockwise – are linked to different polymer functionalities, such as polymer-solvent interactions (Bellich et al., 2016; Wattjes et al., 2019) and biological activity (enzyme recognition) (Weinhold et al., 2009), it is not usually taken into consideration in papers on chitosan characterization. In fact, studies have shown that chitosan with the same DD can have different solubility properties due to different patterns of distribution of its monomers *N*-glucosamine and *N*-acetyl-glucosamine (Bellich et al., 2016). Because commercially available chitosan is produced by chemical deacetylation of chitin under heterogeneous conditions (Wattjes et al., 2019), it usually results in heterogeneous products with random patterns of acetylation (Varum et al., 1991; Weinhold et al., 2009). Enzymatic deacetylation is an interesting alternative to chitosan preparation as the application of chitin deacetylases allows for a controlled process, resulting in a polysaccharide with well-defined patterns of acetylation (Tsigos et al., 2000).

Despite different opinions, the accurate determination of chitosan properties should be unavoidable (Bellich et al., 2016). MW, DD, viscosity and purity should be presented as

TABLE 1 | Summary of Chit-Ins NPs production protocols by ionotropic-gelation method.

			Preparation method					NP characterization					
System	**Insulin, source**	**Chitosan, source**	**Chitosan solution**	**Insulin solution**		**TPP solution**	**Final pH**	**Size**	**Zeta Potential**	**Insulin AE%**	**Toxicity assay**	**Anti-insulin IgG**	**References**
Chit NPs	Porcine pancreas insulin, Sigma	186 kDa; 85% DDA Aldrich Chemicals	8 mL chitosan 2 mg/mL	Insulin 31.65 μg/mL to 235.25	1 mL premixed with TPP or	4 mL TPP 1 mg/mL	pH 2.8 to 6.1	237 nm ±53 nm to 325 nm ±45 nm	–	2–85%	–	–	Ma et al., 2002
Chit NPs	Insulin 27.6 I.U/mg, Xuzhou biochemical plant	? kDa 88.9% DDA; viscosity 45 mPa.s Shenyang	4 mL chitosan 2.6 mg/mL	Concen-tration? mins/mChit = 0.1	Solution Premixed with TPP solution	? mL TPP 0.45 mg/mL	–	265.3 nm ±34.1 nm	+40.71 mV ±0.69 mV	88.6% ± 2.4%	–	–	Pan et al., 2002
Chit NPs	Porcine pancreas insulin 27.8 USP/mg, Sigma Chemicals	186 kDa; 85% DDA Aldrich Chemical, Milwaukee	8 mL chitosan 2 mg/mL	Insulin 2 mg/mL in 0.01 M HCl	1 mL premixed with TPP solution	4 mL TPP 1 mg/mL in 0.05 M NaOH	pH 5.3	269 nm ± 7 nm	+34.9 mV ± 0.9 mV	38.5% ± 1.5%	–	–	Ma et al., 2005
						4 mL TPP 1 mg/mL in 0.075 M NaOH	pH 6.1	339 nm ± 8 nm	+21.8 mV ± 0.6 mV	78.5% ± 2.3%	–	–	
Chit NPs	Human insulin Novolin R®, 100 IU/mL	Low viscosity chitosan ? kDa; DDA ?	5 mL chitosan 4 mg/mL	Insulin solution 4.6 mg/Ml	Premixed with TPP solution	2 ml TPP 1 mg/mL	pH 6.1	312.8 nm PDI 0.48	+23 mV ± 2 mV	69.37% ± 4.71%	–	–	Azevedo et al., 2011
Chit NPs	Bovine pancreas insulin (27 USP/mg) Sigma-Aldrich, United States	200 kDa DDA ? Sigma-Aldrich, United States	? mL chitosan 2 mg/mL	Insulin solution 0.5 mg/ml	Premixed with TPP solution	? ml TPP 0.5 mg/mL	pH 5.5	215 nm PDI 0.16	+20.7 mV ± 0.7 mV	49.43% ± 0.44%	–	–	Makhlof et al., 2011
Chit NPs	Crystalline recombinant human insulin Novo Nordisk, Denmark	LMWC; 98% DDA; viscosity 22 cP	10 mL chitosan 1 mg/mL or 3 mg/mL	Insulin 0.5 mg/mL and 1 mg/mL (concentration in TPP)	Premixe d with TPP solution	? ml TPP solution 1 mg/mL and 3 mg/mL	–	261 nm PDI 0.4 or 419 nm PDI 0.45	+27.2 mV or +48.4 mV	61.61% ± 4.52% or 61.88% ± 5.59%	–	–	Kouchak et al., 2012

(Continued)

TABLE 1 | Continued

System	Insulin, source	Chitosan, source	Preparation method					NP characterization					References
			Chitosan solution	Insulin solution		TPP solution	Final pH	Size	Zeta Potential	Insulin AE%	Toxicity assay	Anti-insulin IgG	
		MMWC; 92% DDA; viscosity 715 cP Primex, Iceland	10 mL; chitosan 0.5 mg/mL or 1 mg/mL					132 nm PDI 0.28 or 343 nm PDI 0.49	+25.1 mV or +39.3 mV	70.89% ± 3.32% or 70.59% ± 1.70%	–	–	
		HMWC; 96% DDA; viscosity 1234 cP Primex, Iceland	10 mL; chitosan 0.5 mg/mL or 1 mg/mL					112 nm PDI 0.27 or 160 nm PDI 0.28	+27.5 mV or +29.0 mV	53.50% ± 2.61% or 53.73% ± 2.29%	–	–	
Chit NPs	Zinc-free human insulin	150 kDa; 87% DDA; viscosity 2.37 dL/g Sigma-Aldrich, Missouri	? mL chitosan 2.5 mg/mL (in acetic acid)	4 mg/mL insulin solution	Premixed with TPP solution	? mL TPP 0.25 mg/mL	pH 5.5	330 nm ± 36 nm	+30 mV ± 4 mV	55% ± 8%	No death or inflammatory response (CAM assay in fertilized chicken eggs)	–	Rampino et al., 2013
Chit NPs	Insulin 27.5 IU/mg Jiangsu Wangbang Bio-Technology	400 kDa; DDA? Haixin Biological Product	? mL chitosan 50 mg (in acetic acid)	4 mg insulin solution in NaOH	Premixed with chitosan solution	3 mL TPP solution 0.5 mg/mL	pH 3	91.28 nm ± 7.9 nm to 220.2 nm ± 9.5 nm	+14.4 mV ± 2.9 mV	93.1%	–	–	Zhao et al., 2014
Chit NPs into transdermal patch	Pure insulin powder Sigma-Aldrich	LMWC; DDA? Sigma-Aldrich	? mL chitosan 1.5 mg/mL or 2 mg/mL (in acetic acid)	1 mL of insulin 20 mg/mL	Premixed with chitosan solution	? mL TPP 2.5 mg/mL	pH 5	465 nm or 661 nm	–	77.3% ± 0.5% to 78.9% ± 0.25%	–	–	Sadhasivam et al., 2015
Chit-TPP-micro emulsion	Recombinant human insulin (Humulin R 100 IU/mL) Eli Lilly and Company,	MMWC; 75% to 85% DDA Sigma-Aldrich, United States	? mL chitosan 3 mg/mL (in acetic acid)	–	Insulin added to solution after NPs formation	? mL TPP solution 1 mg/mL	–	80.8 nm ± 7.0 nm to 401.8 nm ± 41.7 nm	+38.1 mV to +47.0 mV	–	Viability depend on concentration (XTT assay)	–	Erel et al., 2016

Cs NPs, chitosan nanoparticles; TPP, tripolyphosphate; AE, association efficiency; CAM assay, Chick Chorioallantoic Membrane assay; XTT assay, Cell Viability Assay. Units were converted to standardization, so they can differ from the ones at the original paper. ? refers to data that could not be confirmed in the respective publication and thus remain unknown.

chitosan characterization parameters. Moreover, it is known that the properties discussed above will influence Chit NP physicochemical properties such as size and zeta potential, but also determine its biological activity. It is therefore essential to define the properties of chitosan in order to assure the reproducibility of Chit NP preparation (Hua et al., 2018) and to obtain the desired biological response. Moreover, in order to follow a SbD approach, as mentioned before, it is important to classify with accuracy the physicochemical properties that determine the safety of the nanomaterial.

Drug Encapsulation Into Chitosan/Tripolyphosphate Nanoparticles (Chit-TPP NPs): Insulin as Case-Study

Chit NPs can be prepared through numerous methods. Among them, ionotropic gelation is based on the electrostatic interactions between charged polymers and non-toxic anionic cross-linking agent species, such as citrate, sulfate, or TPP. Ionotropic gelation is performed in aqueous media, avoiding organic solvents, high temperatures, and high shear rates. Because of that, it is a safe preparation method resulting in low-toxicity NPs (Dash et al., 2011; Bugnicourt and Ladavière, 2016). In the case of Chit NPs preparation, the convenient characteristics of ionotropic gelation along with the cationic sites available all along the polymer chain of chitosan allow the interaction and encapsulation of fragile poly-anionic molecules, such as proteins and deoxyribonucleic acids (DNA), producing stable colloidal complexes (Xu and Du, 2003; Bugnicourt and Ladavière, 2016).

Chit NP production, particularly by using TPP as a crosslinker, is a generally established method and it is by far the most mentioned in the literature. Usually, the preparation of Chit-Ins NPs by ionotropic gelation consists in dissolving the polysaccharide in an aqueous acetic acid solution, while TPP is dissolved in deionized water. Then, TPP solution is added dropwise to the chitosan solution under stirring (magnetic stirring or using a high-speed homogenizer), leading to the spontaneous formation of Chit NPs (Calvo et al., 1997).

There are many different protocols for insulin encapsulation into Chit NPs (**Figure 2**). Insulin can be pre-dissolved in diluted hydrogen chloride (HCl) solution (Abbad et al., 2015), the pH of this final solution can be adjusted with sodium hydroxide (NaOH) (Hecq et al., 2015; Li et al., 2017), or insulin can even be directly solubilized into diluted NaOH, or directly into TPP solution (Zhao et al., 2014). Then, the insulin solution is added to the chitosan solution right before or during TPP addition (Ma et al., 2005; Azevedo et al., 2011; Makhlof et al., 2011) or added after TPP addition to chitosan (Ma et al., 2002; Erel et al., 2016). Nanoparticles form spontaneously, the system stays under stirring for a while in order to stabilize the nanoparticles.

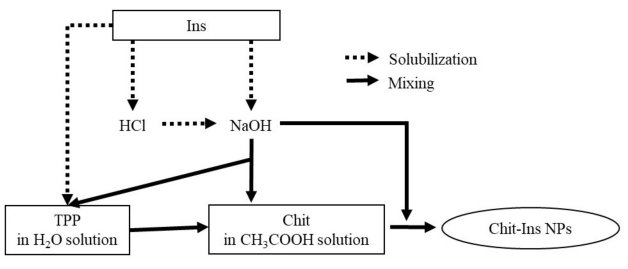

FIGURE 2 | Differences on Chit-ins NPs production protocols.

Despite similar formulation and preparation procedures, different properties of the resulting insulin-loaded chitosan nanoparticles (Chit-Ins NPs) have been reported (Ma et al., 2002), as shown in **Table 1**. Factors such as chitosan and TPP concentrations, pH, chitosan origin and its characteristics, rotation speed, insulin concentration, among others, greatly influence the final nanoparticle properties, thus having a serious impact on batch reproducibility and bioactivity (Ma et al., 2002; Sreekumar et al., 2018).

Note that the systems listed in **Table 1** were developed mainly for the oral administration of insulin. This protein is highly susceptible to enzymatic degradation in the gastrointestinal (GI) tract, thus nanoparticles may aid to protect it from the acidic environment and enzymatic degradation, and to promote insulin absorption by using mucoadhesive polymers, such as chitosan (Makhlof et al., 2011; Al Rubeaan et al., 2016). Despite their well-known potential, Chit-TPP NPs are not stable under acidic conditions, as the protonation of the amino groups of chitosan at low pH values promotes their dissolution and successive insulin degradation, decreasing its bioavailability (Al Rubeaan et al., 2016).

In order to increase nanocarrier stability in the gastric environment recent delivery systems have been developed based on modified chitosan through conjugation, quaternization, thiolation, substitution, and grafting (Chaudhury and Das, 2011; Al Rubeaan et al., 2016). For example, permanently positively charged *N*-(2-hydroxy)propyl-3-trimethyl ammonium chitosan chloride (HTCC), increases Chit-Ins NPs stability (Hecq et al., 2015). Another derivative, thiomalyl chitosan, produces negatively charged NPs that, curiously, seem to enhance mucoadhesion and permeation, when compared to Chit NPs. This system is also suggested to inhibit insulin degradation due to its protease inhibitory effect (Rekha and Sharma, 2015).

Moreover, hydroxypropyl methylcellulose phthalate used as crosslinker (instead of TPP) in Chit-Ins NPs preparation also proved to increase NP stability and, additionally, to improve intestinal mucoadhesion and penetration (Makhlof et al., 2011). Finally, another interesting approach is an emulsion-based delivery system, where Chit-Ins NPs were suspended in a microemulsion, successfully protecting insulin under gastric conditions and reducing blood glucose levels for 8 h after oral administration (Erel et al., 2016).

As can be extracted from **Table 1**, depending on the preparation method, reported NP size may range between 112 and more than 400 nm. Zeta potential, when measured, was also highly variable with values ranging between 20 and 40 mV. Even more variable was the encapsulation efficiency for insulin reported, with values ranging from as little as 2% to almost 90%. Overall it can be said that generally not all relevant data

on the materials and methods used were reported, rendering the selection of the optimal preparation method from the literature difficult.

Chitosan as an Immunostimulant: An Additional Source of Disagreement

As mentioned before, chitosan is known for its immunostimulatory activity. Because of that, the polysaccharide has been extensively studied and reviewed as an adjuvant and/or as a delivery system for vaccines (Van der Lubben et al., 2001a; Ghendon et al., 2009; Esmaeili et al., 2010; Mehrabi et al., 2018).

Establishing the physicochemical properties that are correlated with chitosan immune stimulation is important to define Chit NPs activity in view of a SbD approach. However, as for other data available for chitosan, reports on its immunomodulation activity are contradictory. Some publications claim that chitosan is not able to stimulate antibody production (de Geus et al., 2011), while other studies confirm that chitosan can only induce immunostimulation due to the synergic effect between the components of the chitosan formulation and the antigen (Seferian and Martinez, 2000; Bivas-Benita et al., 2004). In addition, many articles claim the obvious adjuvant potential of the polysaccharide (Nishimura et al., 1985; Zaharoff et al., 2007; Ghendon et al., 2009; Esmaeili et al., 2010; Dzung et al., 2011; Vasiliev, 2015; El Temsahy et al., 2016).

The adjuvant activity of chitosan was first attributed to its mucoadhesive properties, which prolong the residence time of the loaded antigen at mucosal sites. This, in turn, increases antigenic uptake (Illum, 1998; Alpar et al., 2005) and improves immunological response via transmucosal routes (Illum, 1998): nasal (Van der Lubben et al., 2001b; Esmaeili et al., 2010), pulmonary (Esmaeili et al., 2010), and oral (Van der Lubben et al., 2001b; Borges et al., 2006, 2007; Esmaeili et al., 2010). Furthermore, the physical association of chitosan with an antigen (Calvo et al., 1997; Seferian and Martinez, 2000) and its slow release are very important to the overall adjuvant activity of the biopolymer (Calvo et al., 1997).

Other authors explored the potential of chitosan immune stimulation through the parenteral route (Borges et al., 2008), based on preliminary data that attributed adjuvant activity to chitin derivatives, including chitosan. These biopolymers increased immune response in guinea pigs after immunization applied to their footpads (Nishimura et al., 1985). Zaharoff et al. (2007) vaccinated mice with β-galactosidase dissolved in a viscous chitosan solution. The adjuvant activity was attributed to the combination of an antigen depot with the stimulation of both humoral and cell-mediated immune responses (Zaharoff et al., 2007). Correspondingly, Ghendon et al. (2009) explored the properties of chitosan as an adjuvant for inactivated influenza vaccines, showing that the polysaccharide induced the production of high titers of antibodies against the antigen and increased cytotoxic activity of NK-cells. Furthermore, Chit NPs are known to induce mixed Th1/Th2 responses with a great variability of antigens. An increase of interferon-ɣ (IFN-ɣ) and IgG2a is characteristic for a Th1 response, while the Th2 pathway is elicited by IL-4 and IgG1 production (Zaharoff et al., 2007; Borges et al., 2008). Additionally, Chit NPs interact with antigen-presenting cells (APCs), such as macrophages, and induce $CD4^+$ T cell proliferation (Zaharoff et al., 2007). In case of mucosal administration, an increased production of sIgA has been shown (Vila et al., 2004; Borges et al., 2007).

Recently, Chit NPs prepared by ionotropic gelation have been tested as an adjuvant in several vaccine systems (Vila et al., 2004; Danesh-Bahreini et al., 2011; Dzung et al., 2011; El Temsahy et al., 2016). For example, El Temsahy et al. (2016) produced *Toxoplasma* lysate vaccines by encapsulating virulent RH and avirulent Me49 *Toxoplasma* strains into Chit NPs, while Danesh-Bahreini et al. (2011) applied the Chit-TPP system to develop a leishmaniasis vaccine. In the first example, the *Toxoplasma* lysate vaccines were injected by the intraperitoneal route into mice, stimulating both humoral and cellular immune responses (El Temsahy et al., 2016). Furthermore, the Chit-TPP-antigen system was shown to be as effective as Freund's incomplete adjuvant (FIA) in enhancing the efficacy of *Toxoplasma* vaccine (El Temsahy et al., 2016). The reported data are in agreement with other studies comparing the polysaccharide with commonly used adjuvants, FIA and aluminum hydroxide, demonstrating the biopolymer to be equipotent to those adjuvants (Zaharoff et al., 2007; Dzung et al., 2011). Chit NPs where also loaded with *Leishmania* superoxide dismutase (SODB1), and injected into BALB/c mice, eliciting both IgG2a1 and IgG1 production (Danesh-Bahreini et al., 2011). Therefore, chitosan is an alternative to traditional adjuvants applied in vaccine development (Zaharoff et al., 2007; El Temsahy et al., 2016).

In general, immune responses depend on the system's physicochemical characteristics, properties and dose of antigen (Amidi et al., 2010). Furthermore, polysaccharide features appear to influence the elicited response. Chitosan from different sources and suppliers, of different DD (Nishimura et al., 1985; Scherliess et al., 2013) and MW (Ghendon et al., 2009; Dzung et al., 2011; Scherliess et al., 2013) have been used to explore its immunostimulant activity. Nishimura et al. (1985) observed a correlation between the immunological activity and chitosan DD, in which 70% DD was the optimal value, whereas 30% DD resulted in lower adjuvanticity. This appears to be in agreement with data showing that positively charged particles are associated with increased immunogenicity (Foged et al., 2005). However, recent reports also showed that chitosan with 76% DD elicited higher immune responses than 81% DD chitosan (Scherliess et al., 2013).

Data is also contradictory with respect to the influence of MW on chitosan immunostimulant activity. While some authors claim that LMW chitosan (10 kDa) is more effective in immune system stimulation than HMW chitosan (300 kDa) (Ghendon et al., 2009), others show that MW around 300 kDa has a greater effect than LMW chitosan (Dzung et al., 2011). Moreover, another paper stated that MW had no significant impact on Chit NPs stimulated immune response (Vila et al., 2004). Note that the last classification of LMW and HMW was based on Ghendon et al. (2009).

The contradictory information suggests that the chitosan formulation can also affect its adjuvant action (Scherliess et al., 2013). In case of chitosan particulate systems, the preparation

technique has a direct influence on the particle size, which also influences the triggered immune pathway (Bueter et al., 2011; Scherliess et al., 2013; Soares and Borges, 2018). Note that the particle size also depends on chitosan MW and DD (Scherliess et al., 2013). Moreover, the antigen release pattern from the chitosan system and the injection site seem to affect the immune response, as well (Vila et al., 2004; Scherliess et al., 2013).

Furthermore, there is a lack of information on the biopolymer purity, such as the presence of endotoxins, LPS, proteins, nucleic acids and heavy metals, which can have an important influence on the immune response elicited. As a consequence, it has been proposed that the adjuvant activity attributed to chitosan can be related to its impurities and not to the polymer itself (Vasiliev, 2015).

In the end, it is not clear which factor is responsible for the differences in immune responses elicited by the biopolymer. There is most probably an interaction between all the properties mentioned before affecting chitosan adjuvanticity (Scherliess et al., 2013).

Undesired Adjuvanticity of Chit: Potential Immunotoxicity of Chit-Ins NPs

The adjuvant activity of chitosan has been studied for the purpose of vaccine formulation. That means that the active pharmaceutical ingredient (API) encapsulated is already known to have immunogenic properties, whether the antigen is highly or poorly immunogenic. The great majority of Chit-TPP systems loaded with insulin are studied as an alternative to the subcutaneous administration of insulin. Thus, immunogenic studies are not usually a concern as shown in **Table 1**, which illustrates the lack of information on the immunotoxicological and immunopharmacological profile of Chit-Ins NPs.

Note that mucosal delivery routes—oral, nasal, etc.—studied for insulin administration generally imply absorption through a mucosal surface, where chitosan has also been widely applied as a vaccine adjuvant (Illum, 1998; Van der Lubben et al., 2001b). Insulin is indeed poorly immunogenic (Fineberg et al., 2007). Its formulations for subcutaneous administration have been developed and improved, indicating rare severe immunological complications. Actually, less than 0.1% of recipients experience insulin resistance due to immune reactions (Fineberg et al., 2007). However, insulin resistance due to Chit-Ins NPs administration cannot be totally excluded in the absence of in-depth studies.

Chit NPs adhere to the mucosa and transiently open intercellular tight junctions. Due to the pH variation, these NPs become less stable and disintegrate releasing the insulin, which is absorbed through the paracellular pathway into the systemic circulation (Borchard et al., 1996; Sung et al., 2012). In reality, other transport pathways can be involved after oral administration of Chit-Ins NPs (Abbad et al., 2015), such as transcytosis through enterocytes, receptor-mediated transcytosis, and transcellular absorption by M cells in the Peyer's patches. As part of the gut associated lymphoid tissue (GALT), Peyer's patches have an important role in eliciting immune responses against oral antigens, as reviewed elsewhere (Soares and Borges, 2018). However, since absorption studies do not use models that include enterocytes, goblet, and M cells simultaneously, the insulin absorption pathway is still unknown (Abbad et al., 2015). Furthermore, these studies showed NP uptake by epithelial cells, but did not prove their transport across those cells. Thus, there is a risk of intercellular degradation of the NPs (Amidi et al., 2010; Hu and Luo, 2018).

Depending on the route of administration, Chit-Ins NPs can be taken up and processed by APCs, or transported into lymphatic tissues, triggering a local and/or systemic immune response against the protein (Amidi et al., 2010; Soares and Borges, 2018). Furthermore, it should be kept in mind that the repeated administration of the formulation increases the potential risk of antibody formation against insulin (Jiskoot et al., 2009).

The Hurdles of Protein Delivery by Chit-NPs

Even though there is plenty of information on chitosan in the literature, there is also a huge gap with regard to chitosan standardization, making it difficult to relate its characteristics with the outcomes reported (Vasiliev, 2015) and to establish guidelines for SbD implementation. Note that polymer composition is a requirement of the assay cascade for nanomedicines elaborated by both US NCL and EU-NCL (European Nanomedicine Characterization Laboratory, 2019b; Nanotechnology Characterization Lab, 2019), thus the complete characterization of chitosan is revealed to be the greatest need and challenge of all.

The FDA Department Guidance for Industry "Drug Products, Including Biological Products that Contain Nanomaterials" requires the full description of nanomaterial composition, based on their functionality and intended use (U. S. Food and Drug Administration, 2017). Furthermore, the FDA guidance states that the nanomaterial critical quality attributes (CQAs) should be determined as early as possible, considering their functions and potential impact on the final product performance (quality, safety, and efficacy). Moreover, risk assessment should be applied linking the structure-function relationship of the nanomaterial to attributes that need to be examined and controlled in case of manufacturing changes – for example, the source and supplier of chitosan for NP production (U. S. Food and Drug Administration, 2017). Scarce good laboratory practice (GLP) conditions and questions regarding the validity and reproducibility of the scientific results are obstacles to collaboration with pharmaceutical industry and approval by regulatory authorities (Rosenblum et al., 2018). For example, clinical translation relies on a consistent and reproducible product (Anselmo and Mitragotri, 2016). As far as chitosan is concerned, contradictory information available in the literature on chitosan-biological activity correlation may be a potential source of problems during the drug approval process.

The risk assessment approach should also be applied to evaluate possible adverse immune responses that may be associated with nanomaterial administration, affecting both safety and efficacy. Biological products with a nanomaterial component may have a different immunogenic profile compared

to the biological substance alone, which may apply to Chit-Ins NPs (U. S. Food and Drug Administration, 2017).

As reviewed elsewhere (Jiskoot et al., 2009), the particulate character of drug delivery systems makes them predisposed to be recognized as foreign by immune cells and the complement system. In general, the elicited immune response depends on the route and frequency of administration. Moreover, in case of Chit-Ins NPs the potential immune response will also depend on chitosan characteristics and its source, on the properties of the nanocarrier (size, surface charge, polydispersity, etc.), and on the insulin employed. Often recombinant human insulin is applied, which usually does not stimulate immune responses. However, the immunogenicity risk of frequent administration of Chit-Ins NPs is unknown, as chitosan is known to have adjuvant properties, and recombinant human therapeutic proteins are also known to trigger antibody production after chronic treatment (Hermeling et al., 2004). Chitosan systems stimulate both cellular and humoral responses. Therefore, studies should be carried out to detect anti-insulin IgG1 and IgG2a production after Chit-Ins NPs administration. Screening of cytokine production, such as IL-4 and IFN-ɣ, and detection of IgA, in the case of mucosal administration, would also be of interest.

In the end, the potential problems regarding Chit-Ins NP administration can be analyzed from a larger scope. The application of Chit NPs to protein delivery, in general, should take into account chitosan characteristics and the potential triggering of an immune response. These must be taken into consideration when examining the human health risks of a formulation in the framework of a SbD approach, especially when it is not desirable to stimulate the immune system.

CONCLUSION

This review shows that the characterization of chitosan is frequently missing in scientific reports, which complicates the translation into a SbD driven approach. Since the term chitosan is applied to a large group of polymers, the biological effects can be different and dependent on the degree of deacetylation and molecular weight of the polymer used on the study. This fact may explain, at least in part, the contradictory biological effects of chitosan reported in literature. Moreover, the purity of the polymers is not always mentioned, and the observed effects may be influenced by the presence of contaminants and impurities. Additionally, a similar situation can be observed with Chit NPs. Several protocols can be found in literature for insulin encapsulation into Chit NPs, however, in view of the lack of complete information given, it is difficult to reproduce them. Protocols also differ, which is an additional problem for data analysis and its comparison.

Furthermore, even though the immunostimulatory effect of chitosan systems has been well reported in the vaccine delivery field, the undesirable potential immune stimulation of those nanocarriers has been given less attention.

The data presented in this report illustrate the challenges encountered when implementing the SbD concept to polymeric drugs based on chitosan. The SbD approach defined by GoNanoBioMat establishes an early risk identification through material design and characterization. However, as it is shown in this report, the correlation between chitosan's physicochemical properties and its activity is far from being established. Consequently, it is also difficult to correlate Chit NP characteristics with the efficacy of the final drug product. Moreover, the potential hazard, namely, the eliciting of an unwanted immune activity, is also difficult to predict.

The full understanding of the composition of the nanoformulation is a critical point, thus a lack of knowledge in this field may explain why the number of approved drugs with chitosan as excipient is limited. Harmonization and validation of chitosan analysis will enable comparison between future studies. By developing these studies, it will be possible to establish the characteristics of different types of chitosan nanoparticles, establish a correlation between chitosan properties and its immunostimulant activity and, finally, to establish a guideline to select the most appropriate chitosan according to its purpose, allowing a safe-by-design approach.

AUTHOR CONTRIBUTIONS

CM drafted the manuscript, was responsible for the acquisition, analysis, and interpretation of the data for the work. CS, MS, and OB provided critical revision and redrafted the manuscript. GB provided critical revision, redrafted the manuscript, and gave approval for publication of the content.

FUNDING

This study was part of the GoNanoBioMat project and has received funding from the Horizon 2020 framework program of the European Union, ProSafe Joint Transnational Call 2016; from the CTI (1.1.2018 Innosuisse), under grant agreement Number 19267.1 PFNM-NM; and from FCT Foundation for Science and Technology under the project PROSAFE/0001/2016.

REFERENCES

Abbad, S., Zhang, Z., Waddad, A. Y., Munyendo, W. L., Lv, H., and Zhou, J. (2015). Chitosan-modified cationic amino acid nanoparticles as a novel oral delivery system for insulin. *J. Biomed. Nanotechnol.* 11, 486–499. doi: 10.1166/jbn.2015.1924

Al Rubeaan, K., Rafiullah, M., and Jayavanth, S. (2016). Oral insulin delivery systems using chitosan-based formulation: a review. *Expert Opin. Drug Deliv.* 13, 223–237. doi: 10.1517/17425247.2016.1107543

Alpar, H. O., Somavarapu, S., Atuah, K. N., and Bramwell, V. W. (2005). Biodegradable mucoadhesive particulates for nasal and pulmonary antigen and DNA delivery. *Adv. Drug Deliv. Rev.* 57, 411–430. doi: 10.1016/j.addr.2004.09.004

Altinel, Y., Chung, S. S., Okay, G., Ugras, N., Isik, A. F., Ozturk, E., et al. (2018). Effect of chitosan coating on surgical sutures to strengthen the colonic

anastomosis. *Ulus. Travma Acil Cerrahi Derg.* 24, 405–411. doi: 10.5505/tjtes.2018.59280

Amidi, M., Mastrobattista, E., Jiskoot, W., and Hennink, W. E. (2010). Chitosan-based delivery systems for protein therapeutics and antigens. *Adv. Drug Deliv. Rev.* 62, 59–82. doi: 10.1016/j.addr.2009.11.009

Anselmo, A. C., and Mitragotri, S. (2016). Nanoparticles in the clinic. *Bioeng. Transl. Med.* 1, 10–29. doi: 10.1002/btm2.10003

Azevedo, J., Sizilio, R., Brito, M., Costa, A., Serafini, M., Araújo, A., et al. (2011). Physical and chemical characterization insulin-loaded chitosan-TPP nanoparticles. *J. Therm. Anal. Calorim.* 106, 685–689. doi: 10.1007/s10973-011-1429-5

Bellich, B., D'Agostino, I., Semeraro, S., Gamini, A., and Cesaro, A. (2016). "The Good, the Bad and the Ugly" of chitosans. *Mar. Drugs* 14:E99. doi: 10.3390/md14050099

Bento, D., Jesus, S., Lebre, F., Goncalves, T., and Borges, O. (2019). Chitosan plus compound 48/80: formulation and preliminary evaluation as a hepatitis B vaccine adjuvant. *Pharmaceutics* 11:E72. doi: 10.3390/pharmaceutics11020072

Bivas-Benita, M., van Meijgaarden, K. E., Franken, K. L., Junginger, H. E., Borchard, G., Ottenhoff, T. H., et al. (2004). Pulmonary delivery of chitosan-DNA nanoparticles enhances the immunogenicity of a DNA vaccine encoding HLA-A*0201-restricted T-cell epitopes of Mycobacterium tuberculosis. *Vaccine* 22, 1609–1615. doi: 10.1016/j.vaccine.2003.09.044

Bokura, H., and Kobayashi, S. (2003). Chitosan decreases total cholesterol in women: a randomized, double-blind, placebo-controlled trial. *Eur. J. Clin. Nutr.* 57, 721–725. doi: 10.1038/sj.ejcn.1601603

Borchard, G., Lueβen, H. L., de Boer, A. G., Verhoef, J. C., Lehr, C.-M., and Junginger, H. E. (1996). The potential of mucoadhesive polymers in enhancing intestinal peptide drug absorption. III: effects of chitosan-glutamate and carbomer on epithelial tight junctions *in vitro*. *J. Control. Release* 39, 131–138. doi: 10.1016/0168-3659(95)00146-8

Borges, O., Cordeiro-da-Silva, A., Romeijn, S. G., Amidi, M., de Sousa, A., Borchard, G., et al. (2006). Uptake studies in rat Peyer's patches, cytotoxicity and release studies of alginate coated chitosan nanoparticles for mucosal vaccination. *J. Control. Release* 114, 348–358. doi: 10.1016/j.jconrel.2006.06.011

Borges, O., Silva, M., de Sousa, A., Borchard, G., Junginger, H. E., and Cordeiro-da-Silva, A. (2008). Alginate coated chitosan nanoparticles are an effective subcutaneous adjuvant for hepatitis B surface antigen. *Int. Immunopharmacol.* 8, 1773–1780. doi: 10.1016/j.intimp.2008.08.013

Borges, O., Tavares, J., de Sousa, A., Borchard, G., Junginger, H. E., and Cordeiro-da-Silva, A. (2007). Evaluation of the immune response following a short oral vaccination schedule with hepatitis B antigen encapsulated into alginate-coated chitosan nanoparticles. *Eur. J. Pharm. Sci.* 32, 278–290. doi: 10.1016/j.ejps.2007.08.005

Bottero, J. Y., Rose, J., de Garidel, C., Masion, A., Deutsch, T., Brochard, G., et al. (2017). SERENADE: safer and ecodesign research and education applied to nanomaterial development, the new generation of materials safer by design. *Environ. Sci. Nano* 4, 526–538. doi: 10.1039/C6EN00282J

Brown, S. C., Palazuelos, M., Sharma, P., Powers, K. W., Roberts, S. M., Grobmyer, S. R., et al. (2010). Nanoparticle characterization for cancer nanotechnology and other biological applications. *Methods Mol. Biol.* 624, 39–65. doi: 10.1007/978-1-60761-609-2_4

Bueter, C. L., Lee, C. K., Rathinam, V. A., Healy, G. J., Taron, C. H., Specht, C. A., et al. (2011). Chitosan but not chitin activates the inflammasome by a mechanism dependent upon phagocytosis. *J. Biol. Chem.* 286, 35447–35455. doi: 10.1074/jbc.M111.274936

Bugnicourt, L., and Ladavière, C. (2016). Interests of chitosan nanoparticles ionically cross-linked with tripolyphosphate for biomedical applications. *Prog. Polym. Sci.* 60, 1–17. doi: 10.1016/j.progpolymsci.2016.06.002

Calvo, P., Remunan-Lopez, C., Vila-Jato, J. L., and Alonso, M. J. (1997). Chitosan and chitosan/ethylene oxide-propylene oxide block copolymer nanoparticles as novel carriers for proteins and vaccines. *Pharm. Res.* 14, 1431–1436.

Cerchiara, T., Abruzzo, A., di Cagno, M., Bigucci, F., Bauer-Brandl, A., Parolin, C., et al. (2015). Chitosan based micro- and nanoparticles for colon-targeted delivery of vancomycin prepared by alternative processing methods. *Eur. J. Pharm. Biopharm.* 92, 112–119. doi: 10.1016/j.ejpb.2015.03.004

Chaudhury, A., and Das, S. (2011). Recent advancement of chitosan-based nanoparticles for oral controlled delivery of insulin and other therapeutic agents. *AAPS Pharm. Sci. Tech.* 12, 10–20. doi: 10.1208/s12249-010-9561-2

Choudhary, R. C., Kumaraswamy, R. V., Kumari, S., Sharma, S. S., Pal, A., Raliya, R., et al. (2017). Cu-chitosan nanoparticle boost defense responses and plant growth in maize (*Zea mays* L.). *Sci. Rep.* 7, 9754. doi: 10.1038/s41598-017-08571-0

Council of Europe (2019). *European Pharmacopoeia 9.8*. Strasbourg: Council of Europe, 2028–2029.

Dai, T., Tegos, G. P., Burkatovskaya, M., Castano, A. P., and Hamblin, M. R. (2009). Chitosan acetate bandage as a topical antimicrobial dressing for infected burns. *Antimicrob. Agents Chemother.* 53, 393–400. doi: 10.1128/aac.00760-08

Danesh-Bahreini, M. A., Shokri, J., Samiei, A., Kamali-Sarvestani, E., Barzegar-Jalali, M., and Mohammadi-Samani, S. (2011). Nanovaccine for leishmaniasis: preparation of chitosan nanoparticles containing Leishmania superoxide dismutase and evaluation of its immunogenicity in BALB/c mice. *Int. J. Nanomed.* 6, 835–842. doi: 10.2147/IJN.S16805

Dash, M., Chiellini, F., Ottenbrite, R. M., and Chiellini, E. (2011). Chitosan—A versatile semi-synthetic polymer in biomedical applications. *Prog. Polym. Sci.* 36, 981–1014. doi: 10.1016/j.progpolymsci.2011.02.001

de Geus, E. D., van Haarlem, D. A., Poetri, O. N., de Wit, J. J., and Vervelde, L. (2011). A lack of antibody formation against inactivated influenza virus after aerosol vaccination in presence or absence of adjuvantia. *Vet. Immunol. Immunopathol.* 143, 143–147. doi: 10.1016/j.vetimm.2011.05.023

Dzung, N. A., Hà, N. T. N., Van, D. T. H., Phuong, N. T. L., Quynh, N. T. N., Hiep, D. M., et al. (2011). Chitosan nanoparticles as a novel delivery system for H1N1 influenza vaccine: safe properties and immunogenicity in mice. *World Acad. Sci. Eng. Technol.* 60, 1839–1846.

El Temsahy, M. M., El Kerdany, E. D., Eissa, M. M., Shalaby, T. I., Talaat, I. M., and Mogahed, N. M. (2016). The effect of chitosan nanospheres on the immunogenicity of Toxoplasma lysate vaccine in mice. *J. Parasit. Dis.* 40, 611–626. doi: 10.1007/s12639-014-0546-z

Erel, G., Kotmakç, M., Akbaba, H., Sözer Karadağlı, S., and Gülten Kantarc, A. (2016). Nanoencapsulated chitosan nanoparticles in emulsion-based oral delivery system: *in vitro* and *in vivo* evaluation of insulin loaded formulation. *J. Drug Deliv. Sci. Technol.* 36, 161–167. doi: 10.1016/j.jddst.2016.10.010

Esmaeili, F., Heuking, S., Junginger, H. E., and Borchard, G. (2010). Progress in chitosan-based vaccine delivery systems. *J. Drug Deliv. Sci. Technol.* 20, 53–61. doi: 10.1016/S1773-2247(10)50006-6

European Nanomedicine Characterization Laboratory (2019a). *About Us*. Available online at: http://www.euncl.eu/about-us/overview/ (accessed February 7, 2020).

European Nanomedicine Characterization Laboratory (2019b). *Assay Cascade*. Available online at: http://www.euncl.eu/about-us/assay-cascade/ (accessed February 7, 2020).

Fineberg, S. E., Kawabata, T. T., Finco-Kent, D., Fountaine, R. J., Finch, G. L., and Krasner, A. S. (2007). Immunological responses to exogenous insulin. *Endocr. Rev.* 28, 625–652. doi: 10.1210/er.2007-0002

Foged, C., Brodin, B., Frokjaer, S., and Sundblad, A. (2005). Particle size and surface charge affect particle uptake by human dendritic cells in an *in vitro* model. *Int. J. Pharm.* 298, 315–322. doi: 10.1016/j.ijpharm.2005.03.035

Gaspar, R. (2007). Regulatory issues surrounding nanomedicines: setting the scene for the next generation of nanopharmaceuticals. *Nanomedicine* 2, 143–147. doi: 10.2217/17435889.2.2.143

Ghendon, Y., Markushin, S., Vasiliev, Y., Akopova, I., Koptiaeva, I., Krivtsov, G., et al. (2009). Evaluation of properties of chitosan as an adjuvant for inactivated influenza vaccines administered parenterally. *J. Med. Virol.* 81, 494–506. doi: 10.1002/jmv.21415

Hecq, J., Siepmann, F., Siepmann, J., Amighi, K., and Goole, J. (2015). Development and evaluation of chitosan and chitosan derivative nanoparticles containing insulin for oral administration. *Drug Dev. Ind. Pharm.* 41, 2037–2044. doi: 10.3109/03639045.2015.1044904

Hermeling, S., Crommelin, D. J. A., Schellekens, H., and Jiskoot, W. (2004). Structure-immunogenicity relationships of therapeutic proteins. *Pharm. Res.* 21, 897–903. doi: 10.1023/B:PHAM.0000029275.41323.a6

Hirano, S., Seino, H., Akiyama, Y., and Nonaka, I. (1990). "Chitosan: a biocompatible material for oral and intravenous administrations," in *Progress in Biomedical Polymers*, eds C. G. Gebelein and R. L. Dunn (Boston, MA: Springer), 283–290. doi: 10.1007/978-1-4899-0768-4_28

Hu, Q., and Luo, Y. (2018). Recent advances of polysaccharide-based nanoparticles for oral insulin delivery. *Int. J. Biol. Macromol.* 120, 775–782. doi: 10.1016/j.ijbiomac.2018.08.152

Hu, Y.-L., Qi, W., Han, F., Shao, J.-Z., and Gao, J.-Q. (2011). Toxicity evaluation of biodegradable chitosan nanoparticles using a zebrafish embryo model. *Int. J. Nanomed.* 6, 3351–3359. doi: 10.2147/IJN.S25853

Hua, S., de Matos, M. B. C., Metselaar, J. M., and Storm, G. (2018). Current trends and challenges in the clinical translation of nanoparticulate nanomedicines: pathways for translational development and commercialization. *Front. Pharmacol.* 9:790. doi: 10.3389/fphar.2018.00790

Illum, L. (1998). Chitosan and its use as a pharmaceutical excipient. *Pharm. Res.* 15, 1326–1331.

Jafary Omid, N., Bahari Javan, N., Dehpour, A. R., Partoazar, A., Rafiee Tehrani, M., and Dorkoosh, F. (2018). In-vitro and in-vivo cytotoxicity and efficacy evaluation of novel glycyl-glycine and alanyl-alanine conjugates of chitosan and trimethyl chitosan nano-particles as carriers for oral insulin delivery. *Int. J. Pharm.* 535, 293–307. doi: 10.1016/j.ijpharm.2017.11.020

Jiskoot, W., van Schie, R. M. F., Carstens, M. G., and Schellekens, H. (2009). Immunological risk of injectable drug delivery systems. *Pharm. Res.* 26, 1303–1314. doi: 10.1007/s11095-009-9855-9

Kanimozhi, K., Khaleel Basha, S., and Sugantha Kumari, V. (2016). Processing and characterization of chitosan/PVA and methylcellulose porous scaffolds for tissue engineering. *Mater. Sci. Eng. C* 61, 484–491. doi: 10.1016/j.msec.2015.12.084

Koppolu, B. P., Smith, S. G., Ravindranathan, S., Jayanthi, S., Suresh Kumar, T. K., and Zaharoff, D. A. (2014). Controlling chitosan-based encapsulation for protein and vaccine delivery. *Biomaterials* 35, 4382–4389. doi: 10.1016/j.biomaterials.2014.01.078

Kouchak, M., Avadi, M., Abbaspour, M., Jahangiri, A., and Boldaji, S. K. (2012). Effect of different molecular weights of chitosan on preparation and characterization of insulin loaded nanoparticles by ion gelation method. *Int. J. Drug Dev. Res.* 4, 271–277.

Kraegeloh, A., Suarez-Merino, B., Sluijters, T., and Micheletti, C. (2018). Implementation of safe-by-design for nanomaterial development and safe innovation: why we need a comprehensive approach. *Nanomaterials* 8:239. doi: 10.3390/nano8040239

Lee, E.-J., Shin, D.-S., Kim, H.-E., Kim, H.-W., Koh, Y.-H., and Jang, J.-H. (2009). Membrane of hybrid chitosan–silica xerogel for guided bone regeneration. *Biomaterials* 30, 743–750. doi: 10.1016/j.biomaterials.2008.10.025

Lee, K. Y., Ha, W. S., and Park, W. H. (1995). Blood compatibility and biodegradability of partially N-acylated chitosan derivatives. *Biomaterials* 16, 1211–1216. doi: 10.1016/0142-9612(95)98126-y

Li, L., Jiang, G., Yu, W., Liu, D., Chen, H., Liu, Y., et al. (2017). Preparation of chitosan-based multifunctional nanocarriers overcoming multiple barriers for oral delivery of insulin. *Mater. Sci. Eng. C Mater. Biol. Appl.* 70(Pt 1), 278–286. doi: 10.1016/j.msec.2016.08.083

Ma, Z., Lim, T. M., and Lim, L. Y. (2005). Pharmacological activity of peroral chitosan-insulin nanoparticles in diabetic rats. *Int. J. Pharm.* 293, 271–280. doi: 10.1016/j.ijpharm.2004.12.025

Ma, Z., Yeoh, H. H., and Lim, L. Y. (2002). Formulation pH modulates the interaction of insulin with chitosan nanoparticles. *J. Pharm. Sci.* 91, 1396–1404. doi: 10.1002/jps.10149

Madihally, S. V., and Matthew, H. W. T. (1999). Porous chitosan scaffolds for tissue engineering. *Biomaterials* 20, 1133–1142. doi: 10.1016/S0142-9612(99)00011-3

Makhlof, A., Tozuka, Y., and Takeuchi, H. (2011). Design and evaluation of novel pH-sensitive chitosan nanoparticles for oral insulin delivery. *Eur. J. Pharm. Sci.* 42, 445–451. doi: 10.1016/j.ejps.2010.12.007

Malette, W. G., Quigley, H. J., Gaines, R. D., Johnson, N. D., and Rainer, W. G. (1983). Chitosan: a new hemostatic. *Ann. Thorac. Surg.* 36, 55–58. doi: 10.1016/S0003-4975(10)60649-2

Mehrabi, M., Montazeri, H., Mohamadpour Dounighi, N., Rashti, A., and Vakili-Ghartavol, R. (2018). Chitosan-based nanoparticles in mucosal vaccine delivery. *Arch. Razi Inst.* 73, 165–176. doi: 10.22092/ari.2017.109235.1101

Millner, R. W., Lockhart, A. S., Bird, H., and Alexiou, C. (2009). A new hemostatic agent: initial life-saving experience with Celox (chitosan) in cardiothoracic surgery. *Ann. Thorac. Surg.* 87, e13–e14. doi: 10.1016/j.athoracsur.2008.09.046

Mizuno, K., Yamamura, K., Yano, K., Osada, T., Saeki, S., Takimoto, N., et al. (2003). Effect of chitosan film containing basic fibroblast growth factor on wound healing in genetically diabetic mice. *J. Biomed. Mater. Res. A* 64, 177–181. doi: 10.1002/jbm.a.10396

Mukhopadhyay, P., Sarkar, K., Chakraborty, M., Bhattacharya, S., Mishra, R., and Kundu, P. P. (2013). Oral insulin delivery by self-assembled chitosan nanoparticles: *in vitro* and *in vivo* studies in diabetic animal model. *Mater. Sci. Eng. C* 33, 376–382. doi: 10.1016/j.msec.2012.09.001

Muzzarelli, R. A. A., Biagini, G., Bellardini, M., Simonelli, L., Castaldini, C., and Fratto, G. (1993). Osteoconduction exerted by methylpyrrolidinone chitosan used in dental surgery. *Biomaterials* 14, 39–43. doi: 10.1016/0142-9612(93)90073-B

Nanotechnology Characterization Lab (2019). *Assay Cascade Protocols*. Available online at: https://ncl.cancer.gov/resources/assay-cascade-protocols (accessed February 7, 2020).

Nasti, A., Zaki, N. M., de Leonardis, P., Ungphaiboon, S., Sansongsak, P., Rimoli, M. G., et al. (2009). Chitosan/TPP and chitosan/TPP-hyaluronic acid nanoparticles: systematic optimisation of the preparative process and preliminary biological evaluation. *Pharm. Res.* 26, 1918–1930. doi: 10.1007/s11095-009-9908-0

Nie, J., Wang, Z., and Hu, Q. (2016). Difference between chitosan hydrogels via alkaline and acidic solvent systems. *Sci. Rep.* 6:36053. doi: 10.1038/srep36053

Nishimura, K., Nishimura, S., Nishi, N., Numata, F., Tone, Y., Tokura, S., et al. (1985). Adjuvant activity of chitin derivatives in mice and guinea-pigs. *Vaccine* 3, 379–384. doi: 10.1016/0264-410x(85)90127-6

Nutrition Center for Food Safety Applied (2019a). *GRAS Notice Inventory - Agency Response Letter GRAS Notice No. GRN 000397*. Available online at: https://wayback.archive-it.org/7993/20171031010838/https://www.fda.gov/Food/IngredientsPackagingLabeling/GRAS/NoticeInventory/ucm287638.htm (accessed February 7, 2020).

Nutrition Center for Food Safety Applied (2019b). *GRAS Notice Inventory - Agency Response Letter GRAS Notice No. GRN 000443*. Available online at: https://wayback.archive-it.org/7993/20171031005742/https://www.fda.gov/Food/IngredientsPackagingLabeling/GRAS/NoticeInventory/ucm347791.htm (accessed February 7, 2020).

Pan, Y., Li, Y. J., Zhao, H. Y., Zheng, J. M., Xu, H., Wei, G., et al. (2002). Bioadhesive polysaccharide in protein delivery system: chitosan nanoparticles improve the intestinal absorption of insulin *in vivo*. *Int. J. Pharm.* 249, 139–147. doi: 10.1016/s0378-5173(02)00486-6

Patel, N., Baldaniya, M., Raval, M., and Sheth, N. (2015). Formulation and development of *in situ* nasal gelling systems for quetiapine fumarate-loaded mucoadhesive microemulsion. *J. Pharm. Innov.* 10, 357–373. doi: 10.1007/s12247-015-9232-7

Pradines, B., Bories, C., Vauthier, C., Ponchel, G., Loiseau, P. M., and Bouchemal, K. (2015). Drug-free chitosan coated poly(isobutylcyanoacrylate) nanoparticles are active against trichomonas vaginalis and non-toxic towards pig vaginal mucosa. *Pharm. Res.* 32, 1229–1236. doi: 10.1007/s11095-014-1528-7

Primex (2019). *History of Chitin*. Available online at: http://www.primex.is/quality-and-environment/history-of-chitin/# (accessed February 7, 2020).

Qin, C., Li, H., Xiao, Q., Liu, Y., Zhu, J., and Du, Y. (2006). Water-solubility of chitosan and its antimicrobial activity. *Carbohydr. Polym.* 63, 367–374. doi: 10.1016/j.carbpol.2005.09.023

Rampino, A., Borgogna, M., Blasi, P., Bellich, B., and Cesàro, A. (2013). Chitosan nanoparticles: preparation, size evolution and stability. *Int. J. Pharm.* 455, 219–228. doi: 10.1016/j.ijpharm.2013.07.034

Rekha, M. R., and Sharma, C. P. (2015). Simultaneous effect of thiolation and carboxylation of chitosan particles towards mucoadhesive oral insulin delivery applications: an *in vitro* and *in vivo* evaluation. *J. Biomed. Nanotechnol.* 11, 165–176. doi: 10.1166/jbn.2015.1904

Rosenblum, D., Joshi, N., Tao, W., Karp, J. M., and Peer, D. (2018). Progress and challenges towards targeted delivery of cancer therapeutics. *Nat. Commun.* 9:1410. doi: 10.1038/s41467-018-03705-y

Sadhasivam, L., Dey, N., Francis, A. P., and Devasena, T. (2015). Transdermal patches of chitosan nanoparticles for insulin delivery. *Int. J. Pharm. Pharm. Sci.* 7, 84–88.

Scherliess, R., Buske, S., Young, K., Weber, B., Rades, T., and Hook, S. (2013). *In vivo* evaluation of chitosan as an adjuvant in subcutaneous vaccine formulations. *Vaccine* 31, 4812–4819. doi: 10.1016/j.vaccine.2013.07.081

Seferian, P. G., and Martinez, M. L. (2000). Immune stimulating activity of two new chitosan containing adjuvant formulations. *Vaccine* 19, 661–668. doi: 10.1016/s0264-410x(00)00248-6

Shan, C., Yang, H., Han, D., Zhang, Q., Ivaska, A., and Niu, L. (2010). Graphene/AuNPs/chitosan nanocomposites film for glucose biosensing. *Biosens. Bioelectron.* 25, 1070–1074. doi: 10.1016/j.bios.2009.09.024

Silva, D., Pinto, L. F. V., Bozukova, D., Santos, L. F., Serro, A. P., and Saramago, B. (2016). Chitosan/alginate based multilayers to control drug release from ophthalmic lens. *Colloids Surf. B Biointerfaces* 147, 81–89. doi: 10.1016/j.colsurfb.2016.07.047

Soares, E., and Borges, O. (2018). Oral vaccination through peyers patches: update on particle uptake. *Curr. Drug Del.* 15, 321–330. doi: 10.2174/1567201814666170825153955

Soares, E., Jesus, S., and Borges, O. (2018). Chitosan:β-glucan particles as a new adjuvant for the hepatitis B antigen. *Eur. J. Pharm. Biopharm.* 131, 33–43. doi: 10.1016/j.ejpb.2018.07.018

Soeteman-Hernandez, L. G., Apostolova, M. D., Bekker, C., Dekkers, S., Grafström, R. C., Groenewold, M., et al. (2019). Safe innovation approach: towards an agile system for dealing with innovations. *Mater. Today Commun.* 20:100548. doi: 10.1016/j.mtcomm.2019.100548

Som, C., Schmutz, M., Borges, O., Jesus, S., Borchard, G., Nguyen, V., et al. (2019). *Guidelines for Implementing a Safe-by-Design Approach for Medicinal Polymeric Nanocarriers*. Available online at: https://www.empa.ch/web/s403/gonanobiomat

Sreekumar, S., Goycoolea, F. M., Moerschbacher, B. M., and Rivera-Rodriguez, G. R. (2018). Parameters influencing the size of chitosan-TPP nano- and microparticles. *Sci. Rep.* 8:4695. doi: 10.1038/s41598-018-23064-4

Sung, H. W., Sonaje, K., Liao, Z. X., Hsu, L. W., and Chuang, E. Y. (2012). pH-responsive nanoparticles shelled with chitosan for oral delivery of insulin: from mechanism to therapeutic applications. *Acc. Chem. Res.* 45, 619–629. doi: 10.1021/ar200234q

Thanou, M., Florea, B. I., Geldof, M., Junginger, H. E., and Borchard, G. (2002). Quaternized chitosan oligomers as novel gene delivery vectors in epithelial cell lines. *Biomaterials* 23, 153–159. doi: 10.1016/s0142-9612(01)00090-4

Tsigos, I., Martinou, A., Kafetzopoulos, D., and Bouriotis, V. (2000). Chitin deacetylases: new, versatile tools in biotechnology. *Trends Biotechnol.* 18, 305–312.

U. S. Food, and Drug Administration, Department of Health and Human Services, Center for Drug Evaluation and Research, and Center for Biologics Evaluation and Research (2017). *Drug Products, Including Biological Products, that Contain Nanomaterials - Guidance for Industry - Draft Guidance*. Available online at: https://www.fda.gov/regulatory-information/search-fda-guidance-documents/drug-products-including-biological-products-contain-nanomaterials-guidance-industry (accessed February 7, 2020).

U. S National Library of Medicine (2018). *Assessment of Pain and Antibacterial Activity of Chitosan Versus Sodium Hypochlorite as Irrigant in Infected Canal*. Bethesda, MD: National Library of Medicine.

Van der Lubben, I. M., Verhoef, J. C., Borchard, G., and Junginger, H. E. (2001a). Chitosan and its derivatives in mucosal drug and vaccine delivery. *Eur. J. Pharm. Sci.* 14, 201–207. doi: 10.1016/s0928-0987(01)00172-5

Van der Lubben, I. M., Verhoef, J. C., Borchard, G., and Junginger, H. E. (2001b). Chitosan for mucosal vaccination. *Adv. Drug Del. Rev.* 52, 139–144. doi: 10.1016/S0169-409X(01)00197-1

Varum, K. M., Anthonsen, M. W., Grasdalen, H., and Smidsrod, O. (1991). Determination of the degree of N-acetylation and the distribution of N-acetyl groups in partially N-deacetylated chitins (chitosans) by high-field n.m.r. spectroscopy. *Carbohydr. Res.* 211, 17–23. doi: 10.1016/0008-6215(91)84142-2

Vasile, C. (2019). "Chapter 1 - polymeric nanomaterials: recent developments, properties and medical applications," in *Polymeric Nanomaterials in Nanotherapeutics*, ed. C. Vasile (Amsterdam: Elsevier), 1–66.

Vasiliev, Y. M. (2015). Chitosan-based vaccine adjuvants: incomplete characterization complicates preclinical and clinical evaluation. *Expert Rev. Vaccines* 14, 37–53. doi: 10.1586/14760584.2015.956729

Vila, A., Sanchez, A., Janes, K., Behrens, I., Kissel, T., Vila Jato, J. L., et al. (2004). Low molecular weight chitosan nanoparticles as new carriers for nasal vaccine delivery in mice. *Eur. J. Pharm. Biopharm.* 57, 123–131. doi: 10.1016/j.ejpb.2003.09.006

Wattjes, J., Niehues, A., Cord-Landwehr, S., Hoßbach, J., David, L., Delair, T., et al. (2019). Enzymatic production and enzymatic-mass spectrometric fingerprinting analysis of chitosan polymers with different nonrandom patterns of acetylation. *J. Am. Chem. Soc.* 141, 3137–3145. doi: 10.1021/jacs.8b12561

Weinhold, M. X., Sauvageau, J. C. M., Kumirska, J., and Thöming, J. (2009). Studies on acetylation patterns of different chitosan preparations. *Carbohydr. Polym.* 78, 678–684. doi: 10.1016/j.carbpol.2009.06.001

Xu, Y., and Du, Y. (2003). Effect of molecular structure of chitosan on protein delivery properties of chitosan nanoparticles. *Int. J. Pharm.* 250, 215–226. doi: 10.1016/S0378-5173(02)00548-3

Yokoyama, A., Yamamoto, S., Kawasaki, T., Kohgo, T., and Nakasu, M. (2002). Development of calcium phosphate cement using chitosan and citric acid for bone substitute materials. *Biomaterials* 23, 1091–1101. doi: 10.1016/S0142-9612(01)00221-6

Younes, I., and Rinaudo, M. (2015). Chitin and chitosan preparation from marine sources. Structure, properties and applications. *Mar. Drugs* 13, 1133–1174. doi: 10.3390/md13031133

Zaharoff, D. A., Rogers, C. J., Hance, K. W., Schlom, J., and Greiner, J. W. (2007). Chitosan solution enhances both humoral and cell-mediated immune responses to subcutaneous vaccination. *Vaccine* 25, 2085–2094. doi: 10.1016/j.vaccine.2006.11.034

Zhang, J., Liu, J., Li, L., and Xia, W. (2008). Dietary chitosan improves hypercholesterolemia in rats fed high-fat diets. *Nutr. Res.* 28, 383–390. doi: 10.1016/j.nutres.2007.12.013

Zhao, A., Wang, T., Yao, M., and Li, H. (2011). Effects of chitosan-TPP nanoparticles on hepatic tissue after severe bleeding. *J. Med. Coll. PLA* 26, 283–292. doi: 10.1016/S1000-1948(11)60054-3

Zhao, L., Su, C., Zhu, B., and Jia, Y. (2014). Development and optimization of insulin-chitosan nanoparticles. *Trop. J. Pharm. Res.* 13, 3–8. doi: 10.4314/tjpr.v13i1.1

Zheng, L.-Y., and Zhu, J.-F. (2003). Study on antimicrobial activity of chitosan with different molecular weights. *Carbohydr. Polym.* 54, 527–530. doi: 10.1016/j.carbpol.2003.07.009

Conflict of Interest: The authors declare that the research was conducted in the absence of any commercial or financial relationships that could be construed as a potential conflict of interest.

frontiers in Bioengineering and Biotechnology

REVIEW
published: 20 March 2020
doi: 10.3389/fbioe.2020.00228

Hydrogel Biomaterials for Application in Ocular Drug Delivery

*Courtney R. Lynch[1], Pierre P. D. Kondiah[1], Yahya E. Choonara[1], Lisa C. du Toit[1], Naseer Ally[2] and Viness Pillay[1]**

[1] Wits Advanced Drug Delivery Platform Research Unit, Department of Pharmacy and Pharmacology, School of Therapeutics Sciences, Faculty of Health Sciences, University of the Witwatersrand, Johannesburg, South Africa, [2] Division of Ophthalmology, Department of Neurosciences, School of Clinical Medicine, Faculty of Health Sciences, University of the Witwatersrand, Johannesburg, South Africa

There are many challenges involved in ocular drug delivery. These are a result of the many tissue barriers and defense mechanisms that are present with the eye; such as the cornea, conjunctiva, the blinking reflex, and nasolacrimal drainage system. This leads to many of the conventional ophthalmic preparations, such as eye drops, having low bioavailability profiles, rapid removal from the administration site, and thus ineffective delivery of drugs. Hydrogels have been investigated as a delivery system which is able to overcome some of these challenges. These have been formulated as standalone systems or with the incorporation of other technologies such as nanoparticles. Hydrogels are able to be formulated in such a way that they are able to change from a liquid to gel as a response to a stimulus; known as "smart" or stimuli-responsive biotechnology platforms. Various different stimuli-responsive hydrogel systems are discussed in this article. Hydrogel drug delivery systems are able to be formulated from both synthetic and natural polymers, known as biopolymers. This review focuses on the formulations which incorporate biopolymers. These polymers have a number of benefits such as the fact that they are biodegradable, biocompatible, and non-cytotoxic. The biocompatibility of the polymers is essential for ocular drug delivery systems because the eye is an extremely sensitive organ which is known as an immune privileged site.

Keywords: biopolymers, ocular drug delivery, hydrogel, nanotechnology, biomaterials, safety by design

OPEN ACCESS

Edited by:
Gerrit Borchard, Université de Genève, Switzerland

Reviewed by:
Mark William Tibbitt, ETH Zürich, Switzerland
Jianxun Ding, Changchun Institute of Applied Chemistry, Chinese Academy of Sciences, China

****Correspondence:***
Viness Pillay
viness.pillay@wits.ac.za

Specialty section:
This article was submitted to Biomaterials, a section of the journal Frontiers in Bioengineering and Biotechnology

Received: *21 October 2019*
Accepted: *05 March 2020*
Published: *20 March 2020*

Citation:
Lynch CR, Kondiah PPD, Choonara YE, du Toit LC, Ally N and Pillay V (2020) Hydrogel Biomaterials for Application in Ocular Drug Delivery. Front. Bioeng. Biotechnol. 8:228. doi: 10.3389/fbioe.2020.00228

INTRODUCTION

There have been many recent advancements made in the delivery of drugs to the eye, a site that is challenging to treat. The eye is a relatively isolated organ within the body, with many barriers and mechanisms that limit the entry of foreign substances into the eye. These include, among others, the cornea, blinking reflex, blood-aqueous barrier, blood–retina barrier, and the nasolacrimal drainage system. Collectively, these systems make the delivery of drugs to both the anterior and posterior segment of the eye more difficult (Patel et al., 2013). Novel drug delivery systems are constantly being developed to overcome the low bioavailability observed in many conventional ophthalmic formulations; these novel systems include the development of hydrogels.

Hydrogels have been largely investigated within the medical industry for a number of purposes; including drug delivery and tissue engineering. These systems are composed of cross-linked polymers which are capable of swelling when placed in water or an aqueous environment. Hydrogels have been researched in terms of drug delivery because they are able to hold, within the cross-linked matrix, a number of different substances. These range from hydrophobic and

hydrophilic molecules to both micro- and macromolecules (Kang Derwent and Mieler, 2008). An example of the effectiveness of hydrogels in drug delivery is shown in the article by Li et al. (2018) where the delivery of antibiotics by hydrogel systems was discussed. It was highlighted how hydrogels are able to deliver antibiotics to a local site (overcoming the severity of side effects often seen with systemic administration), offer controlled release of the active ingredient, and have better biocompatibility than conventional drug delivery systems (Li et al., 2018). These benefits can be translated into the development of hydrogel systems for the delivery of drugs to the eye.

Due to the fact that hydrogels are so versatile and are able to be modified to exploit the environment and function they are being designed for; these systems are highly advantageous in the effective delivery of drugs to the eye (Kang Derwent and Mieler, 2008). **Figure 1** indicates the various potential applications for hydrogels in ocular drug delivery.

Hydrogels have been shown to alter the drug release profiles of a formulation (to a sustained drug release profile), largely due to the swelling rate and water adsorption properties of the biotechnology platform. This swelling rate of the hydrogel can be induced as a response to a change in the environment into which the hydrogel is placed; these are known as "smart" or stimuli-responsive hydrogels. The stimulus can be chemical or physical and allows for the development of drug delivery systems which are regulated by the body. In addition, these "smart" hydrogels are able to respond to external stimuli such as in the process of iontophoresis (Fathi et al., 2015).

Through the development of stimuli-responsive hydrogel systems, not only are researchers able to overcome the issues of low bioavailability and rapid removal from administration site which is currently seen with conventional formulations, they are also able to do so without comprising on patient comfort. These delivery systems are able to be administered as a liquid and then form a gel once in contact with the eye (Hamcerencu et al., 2020). This is an important factor to consider in terms of patient compliance as patients are less likely to make use of an ophthalmic formulation if it is difficult to administer which is often the case with formulations that are highly viscous such as ointments (Singh et al., 2019).

Polymers have received much attention for use in drug delivery, and more specifically ocular drug delivery, over recent years. Although there are countless polymers available, this review article focuses on those which occur naturally, also known as biopolymers. These specific polymers offer the beneficial properties of being biodegradable, biocompatible, and non-cytotoxic. They also have the advantages of being readily available, renewable, and less expensive in comparison to synthetic polymers (Oh et al., 2009).

PHYSIOLOGICAL OCULAR BARRIERS AND DEFENSE SYSTEMS WHICH IMPACT DRUG DELIVERY

There are many challenges when it comes to effective delivery of drugs to the eye. Many of these are as a result of the barriers and mechanisms present within the eye which are designed to protect it from foreign particles and substances. A brief overview of the major ocular defense mechanisms is discussed below.

The first defense mechanism found in the eye is pre-corneal factors which result in the low bioavailability of topically applied ocular formulations. These include the blinking reflex, high tear turnover rate, and the lacrimal drainage of the solution. The cul-de-sac of the eye can hold approximately 30 μl of an administered eye drop. However, majority of this is removed within 15–30 s after the drops have been administered (Gaudana et al., 2010). Considering these factors, drug delivery systems need to be developed that are able to improve the retention of the formulation at the administration site. Consequently, this will improve the penetration of the active ingredient into the eye. Both hydrogel systems and mucoadhesive biopolymers could furnish formulations with these much-needed advantages (Biro and Aigner, 2019).

One of the major barriers to foreign substance entry into the eye is the multiple layers through which substances must pass through in order to penetrate into the target tissues. These layers include the cornea and the conjunctiva, among others. The cornea is located in the anterior segment of the eye and it made up of six layers: the epithelium, Bowman's membrane, stroma, Dua's layer, Descemet's membrane, and the endothelium (Ludwig, 2005; Dua et al., 2013). It is one of the main penetration-limiting layers in terms of drug delivery. This layer is highly lipophilic which largely prevents the entry of hydrophilic molecules into the eye (Moiseev et al., 2019).

The conjunctiva is a highly vascularized membrane that covers most of the anterior aspect of the eye. This high vascularity means that, although it can be used for the delivery of hydrophilic and large molecules, a large portion of the administered drug will be removed via the conjunctiva and enter systemic circulation before penetrating into the eye. This is also one of the main reasons why topically administered drugs are not able to reach the posterior segment of the eye in effective concentrations (Willoughby et al., 2010).

The eye is composed of two segments; the anterior segment (composed of the aqueous humor, conjunctiva, cornea, iris, ciliary body, and lens) and the posterior segment (composed of the choroid, optic nerve, retina, sclera, choroid, and vitreous humor). Each segment is susceptible to a range of conditions and each poses its own challenges when it comes to drug delivery (Souto et al., 2019). There are two blood-ocular barriers; the blood-aqueous barrier and the blood-retinal barrier. These largely prevent the entry of substances into the eye from systemic circulation. Although systemic administration has been considered as a route for drugs needed in the posterior segment of the eye, the dose needed is often high which leads to unwanted side effects (Nettey et al., 2016). **Figure 2** highlights the blood-ocular barriers in addition to the tissues which comprise these barriers.

When a formulation is applied to the surface of the eye (i.e., topical administration), it is rapidly removed through the blinking reflex and nasolacrimal drainage. This drainage system removes the drug from the eye via the nasolacrimal duct. It then enters the nose and is absorbed by the nasal mucosa where it

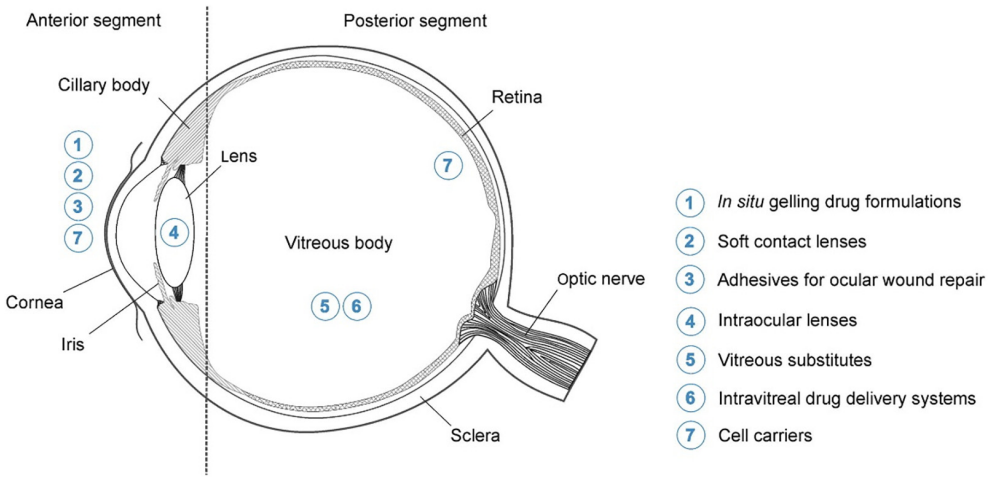

FIGURE 1 | Highlighting the potential application for hydrogels in ocular drug delivery. These include the delivery of drugs to both the anterior and posterior segments of the eye which will aid in overcoming the physiological barriers. Possible topical formulations for delivery to the anterior segment include systems which gel upon application (*in situ* gelling formulations) and contact lenses. Posterior segment formulations include intravitreal injections, which are made more effective by hydrogel technology, and cell carrier systems (adapted with permission from Kirchhof et al., 2015).

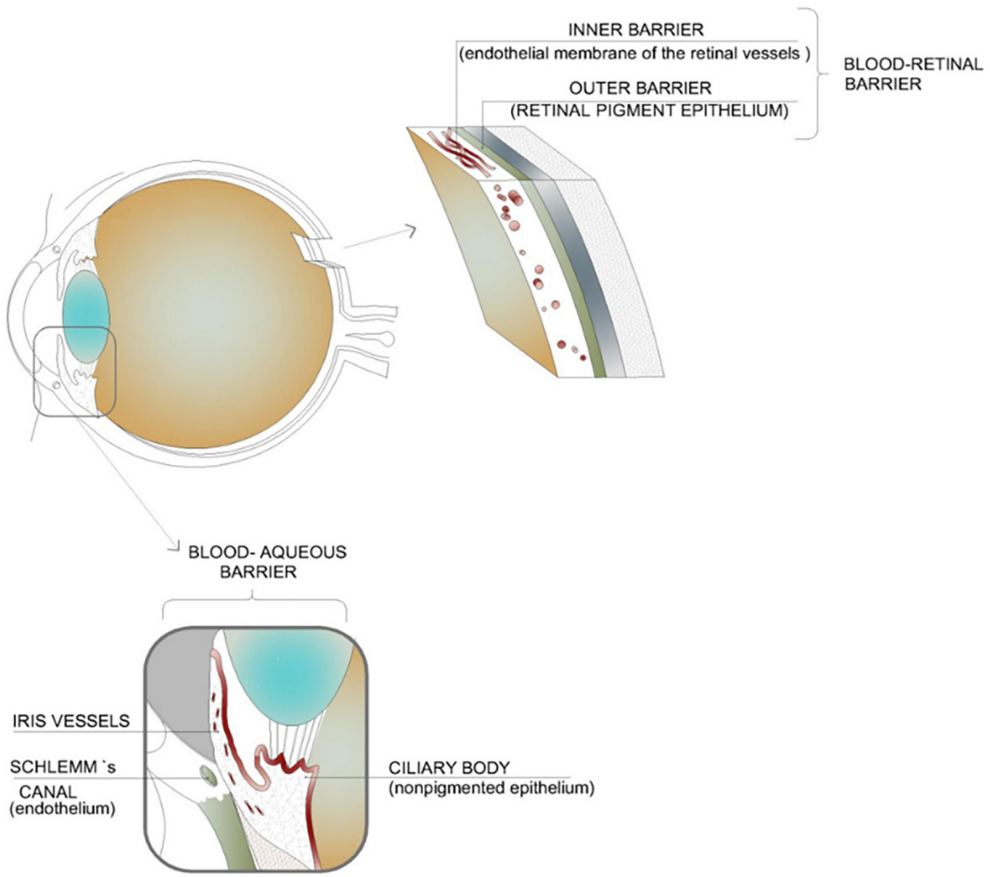

FIGURE 2 | Illustration of the blood–ocular barriers which inhibit the movement of active ingredients into the eye from systemic circulation; namely, the blood–aqueous barrier and the blood–retinal barrier. These barriers result in the need for high systemic dosages of drugs in order to achieve an adequate concentration within the intended tissues. This high dosage can lead to unwanted side effects (adapted with permission from Occhiutto et al., 2012).

enters into systemic circulation. This is another factor which furthers the low bioavailability of topical applied ophthalmic preparations (Rajasekaran et al., 2010).

Hydrogels have been shown to increase the residence time of an active ingredient, allowing more time for it to diffuse through the layers of the eye. This plays a major role by increasing the bioavailability of topically administered ophthalmic formulations (Vashist et al., 2014). Due to the increased viscosity of a hydrogel system, it is also better able to withstand the clearance of the formulation due to blinking, further improving the bioavailability (Li Z. et al., 2013).

Biopolymers have also been shown to help overcome these barriers to drug delivery. Some, such as chitosan, have inherent mucoadhesive properties which allow the formulation to remain at the administered site for a longer period of time (Fulgencio et al., 2012). Cellulose derivatives have also been used to enhance the viscosity of a formulation, thereby preventing it from being washed away from the ocular surface too rapidly (Rajasekaran et al., 2010).

CURRENT COMMERCIAL FORMULATIONS UTILIZED FOR THE DELIVERY OF DRUGS TO THE EYE

There are many formulations currently on the market which are designed to treat ophthalmic conditions. These range from anterior segment conditions such glaucoma, bacterial conjunctivitis, and post-operative inflammation to posterior segment conditions such as neovascular age-related macular degeneration, uveitis, and macular edema (Sultana et al., 2006b; Bao et al., 2017; Kaji et al., 2018). Each of the drug delivery systems discussed below has distinctive disadvantages when it comes to the effective delivery of drugs to the eye. It has been shown that the inclusion of hydrogels into the drug delivery system has been able to overcome some of these challenges, as is highlighted by the various studies included below.

Currently, the most common dosage form used to treat ocular conditions is eye drops. These formulations can be solutions or suspensions. However, although they are the first line treatment, there are many limitations to their use. These range from low bioavailability and rapid clearance from the administration site, to poor patient compliance (Yellepeddi and Palakurthi, 2016). Active ingredients in eye drops are not able to penetrate through to the posterior segment of the eye and thus are mainly used to treat anterior segment conditions (Urtti, 2006).

Conventional, commercially available eye drops often have frequent dosing schedules (ranging from daily to multiple times a day) and, in the case of chronic conditions such as glaucoma, require the patient to use them on a long-term basis. This can lead to unwanted side effects, which, for example, has been seen with latanoprost eye drops (daily administered dose of one drop). These side effects can cause patients to stop using their medications as prescribed, or to not use them at all. This is another reason why novel drug delivery systems such as hydrogels are needed; to reduce the frequency of dosing, reduce side effects and be patient-friendly enough so that patients will use them for an extended period of time if need be (Cheng et al., 2016).

In a recent article written by Yadav et al. (2019), it was highlighted how pre-corneal factors lead to the low absorption of ocular active ingredients used to treat glaucoma, administered as eye drops. These factors, such as tear turnover rate and the drainage of the formulation from the administration site, result in a 70–80% loss of the amount of drug which is administered. It was also highlighted how the frequent dosing schedules of eye drops can cause damage of to the eye. The consideration of ointments has been made, as these formulations have a higher viscosity and are not as rapidly drained from the eye as a liquid formulation. However, ointments are known to cause blurred vision when administered which leads to poor patient compliance (Yadav et al., 2019).

Posterior segment conditions are generally treated using sub-tenon, intravitreal, or systemic administration. However, each of these routes also comes with challenges of its own. One of the main objectives in the development of new drug delivery systems for the posterior segment is to reduce the invasiveness of the formulations which are currently used. For example, anti-vascular endothelial growth factors (anti-VEGFs) are used to treat a number of posterior segment conditions, namely those affecting the retina such as myopic choroidal neovascularization and diabetic macular edema. However, anti-VEGF is currently only able to be administered via intravitreal injections as the molecules are large and hydrophilic which prevent them from penetrating through the various barriers. This highlights the need for new technologies and drug delivery systems which are able to deliver molecules such as anti-VEGF without frequent, invasive injections (Wong and Wong, 2019).

Intravitreal injections are able to deliver a high concentration of the drug directly into the vitreous of the eye but are invasive and pose risks such as retinal detachment, vitreous hemorrhage, and endophthalmitis. The chances of these happening increase with the frequency of administration (Urtti, 2006; Gaudana et al., 2009). The use of hydrogels as intravitreal injections, with their extended drug release profiles, can delay the frequency of intravitreal injections, thus lowering the chances of the aforementioned risks occurring. **Table 1** highlights the formulations which are currently used to treat ophthalmic conditions, both in the anterior and posterior segment of the eye. A brief breakdown of the disadvantages of each of the formulations is also given.

CHARACTERIZATION BETWEEN PHYSICALLY AND CHEMICALLY CROSS-LINKED BIOTECHNOLOGY HYDROGEL SYSTEMS

As previously mentioned, hydrogels are formed from polymers through a process known as cross-linking. Cross-linking occurs when one polymer chain is linked to another chain via a bond, either through a chemical or physical process. It is these

TABLE 1 | Current ophthalmic formulations which are used to treat anterior and posterior segment conditions.

Administration	Preparations	Conditions	Disadvantages	References
Topical preparations	Eye drops (solutions and suspensions)	Glaucoma, dry eye, infectious keratitis, conjunctivitis anterior uveitis, post-operative inflammation.	Low bioavailability, frequent dosing regimen, preservatives often used in formulation.	Sultana et al., 2006b; Gupta et al., 2013
	Ointments and gels	Open-angle glaucoma, dry eye, blepharitis bacterial conjunctivitis.	Poor content uniformity, Known to cause blurred vision when applied, inaccurate dosing, eyelid matting.	Li J. et al., 2013; Bao et al., 2017; Shen et al., 2018
	Contact lenses	Post-operative barrier for protection of cornea, pain relief, protection of cornea following injury.	Lack of controlled release mechanism, drug is released from the system very quickly.	Lim et al., 2001; Tieppo et al., 2012
Intraocular preparations	Intravitreal injections	Neovascular age-related macular degeneration, diabetic macular edema, proliferative diabetic retinopathy choroidal neovascularization.	Invasive procedure for the patient, possible complications (retinal detachment, endophthalmitis, subconjunctival hemorrhage, and cataract formation)	Kaji et al., 2018
	Subtenon injections	Macular edema, intermediate uveitis.	Active ingredient must cross multiple barriers before reaching the retina, occasionally less effective than intravitreal injections	Bonfioli et al., 2005; Ozdek et al., 2006; Thomas et al., 2006
	Intraocular implants	Uveitis, cytomegalovirus retinitis, diabetic macular edema.	Invasive surgical insertion and removal (if the implant is not biodegradable), predetermined drug release rates	Wang et al., 2013; Yasin, 2014

These formulations, both topical and intraocular, each have a number of disadvantages or challenges in terms of drug delivery which can be overcome by hydrogel systems.

bonds which give hydrogels their stability and multidimensional network structure. The process of cross-linking a hydrogel can have an impact on its physical properties such as elasticity, viscosity, and solubility (Maitra and Shulka, 2014).

Although chemical and physical cross-linking methods each have their own advantages and disadvantages, it is worth noting that physically cross-linked hydrogels do not employ agents containing reactive functional groups which may cause inflammatory responses *in vivo.* However, these hydrogels also result in limited control over how the hydrogel is degraded within the body and, if the physical bonds are not strong enough, the inevitable dilution within the body can negatively impact the mechanical integrity of the hydrogel (Patenaude et al., 2014).

Hydrogels Which Are Cross-Linked Through Physical Bonds

Physical bonding occurs through interactions between the polymer chains such as ionic bonding, Van der Waals forces, hydrogen bonding, or hydrophobic forces. Due to these types of bonds, the hydrogels formed through physical bonds are known to be reversible and have a degree of instability (Trombino et al., 2019). The hydrogels formed through physical interactions are generally less stable than those formed through chemical interaction as these bonds are susceptible to formation and breakage when there are changes in pH, temperature, and ionic strength. However, this can be a favorable characteristic if the desired outcome is a reversible hydrogel (Kirchhof et al., 2015).

Hydrogels Which Are Cross-Linked Through Chemical Bonds

Chemically formed hydrogels are known as "permanent" hydrogels due to the covalent bonds which form between polymer chains. These systems allow more stability and maintain their structure better than the physical hydrogels (Trombino et al., 2019). However, it is important that the cross-linking agent can be removed completely from the hydrogel or a non-toxic agent is used so as to prevent adverse tissue reactions when the hydrogel is placed into the eye (Hoare and Kohane, 2008).

The stability of a chemically cross-linked hydrogel was demonstrated by Yu et al. (2015). In this study a hydrogel comprised of hyaluronic acid and dextran was evaluated for the delivery of bevacizumab, a monoclonal antibody which is used to treat neovascular diseases (Grisanti and Ziemssen, 2007). The hydrogel system was designed so that once it had been injected intravitreally, the polymers would form a solid gel. While this delivery system design has the benefits of a chemically cross-linked hydrogel, it also does not contain any cross-linking agent (the polymers cross-link with each other in response to physiological conditions) thereby improving its biocompatibility. The hydrogel system was able to release the active ingredient via a controlled release mechanism and maintain a therapeutically relevant concentration within the vitreous over a period of 6 months during *in vivo* studies. This would eliminate the current monthly schedule needed for bevacizumab administration, the risks of which have been discussed above (Yu et al., 2015).

STIMULI-RESPONSIVE AND *IN SITU* HYDROGEL SYSTEMS AND THEIR APPLICATIONS IN OCULAR DRUG DELIVERY

In situ forming gel preparations offer an interesting advancement in sustained drug release profiles. This can be particularly useful

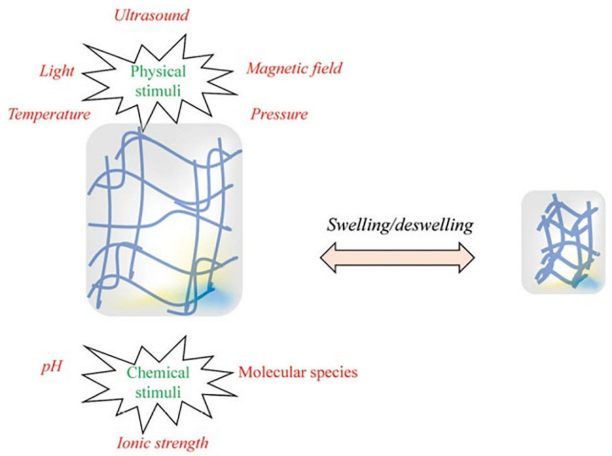

FIGURE 3 | Illustration of the chemical and physical stimuli to which a hydrogel can respond. These stimuli are able to be provided by the body (for example, temperature and/or pH changes between conditions under which the hydrogels are stored and the conditions of the site into which it is administered) or externally (for example, ultrasound waves or a magnetic field). These stimuli can cause or a hydrogel to swell or de-swell, depending on how the formulation is designed. Reversible hydrogels are able to return to their original state when the stimulus is removed (adapted with permission from Fathi et al., 2015).

in terms of the delivery of drugs to the eye as these systems provide an increased retention time at the cornea as well as prevent the rapid removal of the formulation via the nasolacrimal drainage system (Cheng et al., 2016). Both of these factors play a role in overcoming the current challenge of low bioavailability seen in many ocular drug delivery preparations.

These *in situ* gelling systems are a type of stimuli-responsive hydrogels that are able to be administered to the eye as a liquid drop and subsequently form a gel after administration; known as a sol–gel transition. Gelation can be brought about as a response to a change in pH, ionic content, or temperature; although not all hydrogel systems are designed as stimuli-responsive systems and are simply administered as a gel (Al Khateb et al., 2016). Along with the ease of administration and prolonged retention time, *in situ* gelling systems have other advantages such as accurate dosing, simple formulation processes, and easy sterilization (Agrawal et al., 2010). **Figure 3** depicts the various stimuli which can cause a hydrogel to swell or de-swell.

In situ gelling systems have also been shown to exhibit sustained drug release profiles, another beneficial factor in ophthalmic drug delivery. This has been observed in many of the studies which are discussed below.

Temperature-Sensitive Hydrogel Systems

Temperature-sensitive, also known as thermosensitive, hydrogels undergo swelling or de-swelling in response to a change in temperature. There are three classifications of thermosensitive hydrogels; negatively thermosensitive (these contract in response to an increase in temperature), positively thermosensitive (these contract in response to a decrease in temperature), and thermally reversible gels (Masteikova et al., 2003).

Thermosensitive *in situ* hydrogels, which are commonly utilized for drug delivery purposes are liquid at room temperature (20–25°C) and form viscous gels at body temperature (34–37°C). The polymers used in these systems have a lower critical solvent temperature; the temperature at which the sol–gel transition occurs. It is important that this critical temperature is close to bodily temperatures so that the systems do not require an external heat source to form a gel (Kumar et al., 2013). The thermosensitive properties of these hydrogels have also be proven to be beneficial in recent cartilage tissue engineering research as they allow for minimally invasive administration yet form a scaffold with suitable mechanical strength. These systems are also able to mold into the irregular shaped area into which they are administered (Wang et al., 2019).

An *in situ* thermosensitive hydrogel was developed by Chen et al. (2012) for the delivery of a model drug, levocetirizine dihydrochloride. The hydrogel system was comprised of chitosan and disodium α-D-glucose-1-phosphate (DGP) and showed many favorable results. The formulation was a low viscosity liquid at room temperature and a gel at physiological temperature. It showed an initial rapid release of the drug, followed by a sustained drug profile. When in a gel form, the system showed that it had a prolonged residency time, in comparison to that of an aqueous solution, as well as improved cornea penetration of the drug (Chen et al., 2012). This shows that a thermosensitive hydrogel system is able to overcome some of the challenges seen in conventional ophthalmic treatments.

pH-Sensitive Hydrogel Systems

These *in situ* gelling systems either swell or de-swell as a response to a change in the pH within the environment into which it is placed. The polymers used in pH-sensitive hydrogels have ionic groups which give them their responsive ability. For example, cellulose acetate phthalate latex (formulation pH of 4.4) has been shown to form a viscous gel when placed into the cul-de-sac of the eye. However, the development of pH-sensitive gels must take into account the delicate environment of the eye. The formulation must have a buffer capacity that can form a gel when placed into the eye but not cause damage to the eye (Kushwaha et al., 2012).

Although many of the polymers used in pH-sensitive hydrogels are synthetic polymers, such as carbopol [polyacrylic acid (PAA)] and polyethylene glycol, natural biopolymers are also used in the formulations to give them more favorable characteristics (Kushwaha et al., 2012; Wu et al., 2013). For example, in a study performed by Kumar and Himmelstein (1995), it was shown that, although PAA is able to change from a low viscosity liquid when in an acidic solution to a gel at a higher pH, the amount of PAA needed for this to occur was too high. This means that the solution could not be neutralized by the tear fluid which acts as a buffer in the eye. To overcome this, hydroxymethylcellulose, a natural polymer also able to act as a viscosity modifier was added. Both the PAA and the hydroxymethylcellulose were low viscosity liquids at pH 4.0 and transformed

into viscous gels at a pH of 7.4. This meant that the concentration of PAA could be reduced to a safe level, without compromising the gelling and rheological behavior of the system (Kumar and Himmelstein, 1995).

The ability of methylcellulose, as hydroxypropylmethylcelullose, to act as a viscosity modifier in a pH-sensitive gelling system was further demonstrated by Srividya et al. (2001). The researchers developed a pH-triggered *in situ* gelling system comprised of PAA and hydroxypropylmethylcellulose which was shown to be a viable system in the topical delivery of ofloxacin.

Ion-Sensitive Hydrogel Systems

An ion-sensitive gel transforms from a liquid to a gel as a result of a change in ion concentration within the environment it is exposed to. An example of such a gel is shown in a study by Liu et al. (2006). The researchers formulated an alginate hydrogel for the delivery of gatifloxacin, a broad-spectrum antibiotic, which underwent a sol–gel transition when exposed to divalent cations. Methylcellulose was incorporated in order to decrease the amount of alginate needed for gelation. This formulation was able to release the active ingredient over an 8-h period *in vitro* and formed a gel within the cul-de-sac of the eye when administered as a drop. This renders an ion-sensitive hydrogel a suitable alternative to conventional eye drops as it increased the residence time and sustained drug release profile will lead to an improved bioavailability (Liu et al., 2006).

Ultrasound-Responsive Hydrogel Systems

Ultrasound responsive systems are able to deliver drugs to a specific site which prevents the side effects which can be seen with systemic administration of certain drugs. These systems can incorporate nanotechnology. Polymeric hydrogels or nanocarriers such as nanobubbles are loaded with the drug and, once administered, exposed to ultrasound waves. This then leads to cavitation and high temperatures at the site, causing the rupture of the polymeric chains of the nanobubble (Mura et al., 2013; Mahlumba et al., 2016).

Ultrasound-responsive systems are able to deliver a drug at a rate which is controlled from an external source which make them particularly useful in the investigation of cancer treatment. An example is the use of oxygen nanobubbles used for the delivery of mitomycin-C. The nanobubbles system was capable of lower tumor progression rates with a 50% lower drug concentration (Bhandari et al., 2018).

The application of ultrasound waves has been shown to be beneficial in the penetration of drugs through the various barriers of the eye, including the cornea. This was shown to be true in a study performed using dexamethasone where a significant increase in the permeability of the cornea was observed (Nabili et al., 2013). However, there is some concern over the increase in temperature which is induced as it may cause damage to the sensitive structures within the eye. A study was completed by Nabili et al. (2015), which showed that the ultrasound frequency which had previously been shown to increase penetration was safe for the ocular tissues tested.

Iontophoresis: An External Stimulus for More Effective Ocular Drug Delivery

Iontophoresis is a physical force-based response technique which is used to enhance the penetration of an ocular active ingredient through the various tissue layers found in the eye. This is done by applying an electric current between two electrodes; one which is used to deliver the drug and another which is placed on the body. The ionized drug is then able to travel through the tissue as a conductor of the current. Iontophoresis has been illustrated extensively in transdermal applications but has also been investigated for use in ocular drug delivery (Eljarrat-Binstock and Domb, 2006).

There are many challenges, which have highlighted throughout this article, associated with the delivery of drugs to the anterior chamber of the eye but there are even more challenges in the delivery to the posterior segment. Most active ingredients aren't able to penetrate through to the posterior segment when they are applied topically. This has led to the investigation of alternative routes of delivery such as intravitreal, subconjunctival, or transscleral. Iontophoresis has also been considered to aid in delivering drugs to the posterior segment. This allows for the treatment of conditions such as retinitis, uveitis, diabetic retinopathy, and age-related macular degeneration (Myles et al., 2005).

There are various device designs which can be utilized for iontophoresis; one such design includes a hydrogel. A hydrogel pad is saturated with a drug and acts as the delivery probe. This system has been shown to have promising results when tested with various drug entities such as dexamethasone. Transscleral hydrogel-based iontophoresis devices have been tested in both *in vivo* studies and clinical trials in healthy subjects and have shown good safety profiles as well as successful delivery of drug to the retina and choroid (Huang et al., 2018).

Although there are some iontophoresis devices which have been designed for transscleral drug delivery, the process does have some disadvantages. As with any medical procedure, there are risks involved; these include epithelial edema, inflammation, and burns (depending on the current density and duration of treatment). Iontophoresis has been demonstrated to be effective in improving the penetration of steroids, antibiotics, and antivirals. However, it has been reported that it is not able to deliver macromolecules to the vitreous in rabbits at a significant concentration (Thrimawithana et al., 2011).

In a study by Eljarrat-Binstock et al. (2008), hydrogel iontophoresis was employed to deliver nanoparticles to the eyes in an *in vivo* rabbit model. This study also investigated whether positively or negatively charged fluorescence nanoparticles penetrated through the tissues better. The researchers noted that, while iontophoresis is effective in improving the penetration of drugs into the eye, each active ingredient needs to be evaluated separately due to the fact that the physicochemical properties of the molecule will influence its behavior during the procedure. In this study, the, respectively, charged nanoparticles

were loaded into a hydrogel sponge and were administered via an iontophoretic device at the central cornea and at the sclera. After a specified amount of time the eyes of the rabbits were enucleated and tissue samples collected. The negatively charged particles showed penetration into the inner ocular tissues after 4 h, which increased after 12 h. However, the positively charged nanoparticles showed extensive penetration into the inner tissues at just 4 h after administration, illustrating the effect of the physicochemical properties of the particles on their behavior. Both of these indicate that iontophoresis is an effective way of ensuring the penetration of nanoparticles (which are able to be loaded with an active ingredient) through the eye (Eljarrat-Binstock et al., 2008).

Iontophoresis has also been used for the delivery of drugs through the suprachoroidal space (SCS). In a study performed by Jung et al. (2018), a micro-needle device was tested for the delivery of nanoparticles in an *ex vivo* rabbit model. The results showed that with an injection into the SCS without iontophoresis the nanoparticles that were localized around the site of injection (less than 15% delivered to the posterior region of the SCS). However, in the eyes on which iontophoresis was performed, over 30% of the nanoparticles were found in the posterior region of the SCS; this was also found in the *in vivo* study. These studies show how iontophoresis is able to improve the delivery of drugs to the eye and is able to be used in place of other delivery systems such as intravitreal injections (Jung et al., 2018).

BIOPOLYMERS EMPLOYED IN THE FORMULATION OF OCULAR HYDROGEL SYSTEMS

Natural polymers have been widely investigated in a number of medical fields, including tissue engineering and drug delivery. This is largely due to the fact that they are biodegradable within the body and do not induce an inflammatory reaction (Singh, 2011). In terms of tissue engineering, they have also been shown to be conducive to cell growth and have a structure similar to the tissue matrix (Zhang et al., 2019). This section will focus on how natural polymers are employed in drug delivery systems.

These polymers, also known as biopolymers, have long been viewed as a crucial aspect in the developments that are achieved in the field of drug delivery. Highlighted below are biopolymers commonly used in ocular drug delivery systems. Their chemical structures are shown in **Figure 4**.

Chitosan Polymeric Bio-Platforms

Chitosan is one of the most widely used polymers in polymeric drug delivery systems due to its biocompatibility, biodegradability, and low toxicity profiles (Bhattarai et al., 2010). It is a cationic polysaccharide which is derived from chitin. One of chitosan's most beneficial qualities is its mucoadhesive properties. The mucoadhesion is due to the fact that the positively charged chitosan is able to interact with the negative charges found in mucin (Fulgencio et al., 2012). This quality allows for improved permeation of drugs through ocular tissues as well as their controlled release from the formulation; both of which are vital in improving the delivery of drugs to the eye (Duttagupta et al., 2015).

Although chitosan is a very useful biopolymer for drug delivery, it is only soluble in acidic solutions. This is not desirable, especially when it is being formulated in ophthalmic formulations. For this reason, chitosan is often modified, for example through PEGylation and carboxymethylation (Xu et al., 2013).

A thermosensitive chitosan-based hydrogel was formulated by Cheng et al. (2016). This system was designed to overcome some of the challenges seen with latanoprost eye drops such as unwanted side effects after long-term use and low bioavailability. The hydrogel was characterized using both *in vitro* and *in vivo* tests for drug release and biocompatibility. The system was shown to be well tolerated and non-cytotoxic. During the *in vivo* studies, using a rabbit model, latanoprost was found in the aqueous humor 7 days after a single topical administration of the system, suggesting that this system could be administered on a weekly base instead of a daily basis as the commercial product is currently (Cheng et al., 2016).

Chitosan is often used in combination with other natural or synthetic polymers. For example, a study was performed by Cao et al. (2007) where a poly(*N*-isopropylacrylamide)-chitosan (PNIPAAm-CS) polymer was formulated into a thermosensitive *in situ* gelling system for the topical delivery of timolol, an active ingredient used for the treatment of glaucoma. The PNIPAAm-CS delivery system showed a higher Cmax and area under the curve (AUC) of blood concentration against time than that of a convention eye drop containing timolol. The gel system was also able to lower the intraocular pressure more than the eye drop over a 12-h period (Cao et al., 2007).

Another example is a hydrogel system was developed by Yu et al. (2017) containing carboxymethyl chitosan and a poloxamer composed of poly (ethylene oxide)/poly (propylene oxide)/poly (ethylene oxide) (PEO–PPO–PEO). The hydrogel was chemically crosslinked using glutaraldehyde and was able to undergo a reversible sol–gel transition in response to a change in pH and/or temperature. Preliminary studies, including cell studies performed with human cornea epithelial cells, showed that the hydrogel was not cytotoxic and has sustained drug release profiles (in comparison to a sample drug solution systems). This shows that this system could be further developed for ocular drug delivery (Yu et al., 2017).

Hyaluronic Acid Polymeric Platforms

Hyaluronic acid is an anionic biopolymer which is found naturally within the human body. It is biodegradable and does not cause an immune response when used in medical systems. Due to this, hyaluronic acid has been a major interest in the design of drug delivery systems. It is particularly useful in respect to ocular drug delivery because it is a component within the vitreous humor of the eye and also has ligands for receptors found in many types of retinal cells, such as CD-44 (Martens et al., 2015).

Hyaluronic acid is endogenous to the body, making it highly biocompatible and non-immunogenic. However, it is not able to form a gel on its own and thus hydrogels made from hyaluronic acid rely on chemical modifications

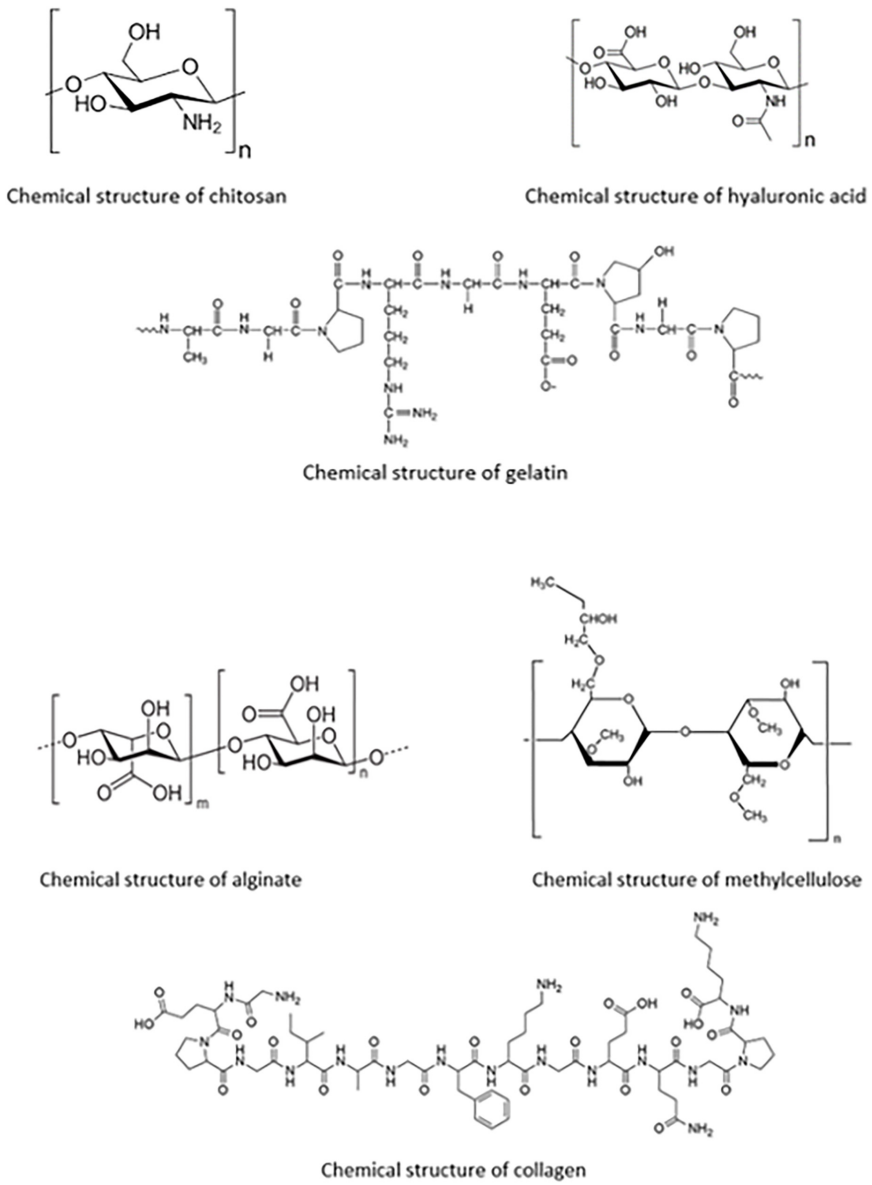

FIGURE 4 | Chemical structures of each of the biopolymers; chitosan, hyaluronic acid, gelatin, alginate, methylcellulose, and collagen, for ocular polymeric drug delivery.

and cross-linking or gelling agents. Hyaluronic acid hydrogels have been investigated as a drug delivery system because they are able to be formulated as both static and stimuli-response (Trombino et al., 2019).

Hydrogels are able to be utilized in conjunction with other technologies in order to improve ocular drug delivery. This can be seen in a study by Widjaja et al. (2015), where a hyaluronic acid-nanocomposite hydrogel was formulated with a sample drug, latanoprost. This system, in which the modified hyaluronic acid was combined with liposomes which contained the drug before crosslinking occurred, showed longer drug release profiles than the hydrogel and liposomes each did on their own. The composite system also improved the stability of the liposomes and the viscosity of the formulation. The hyaluronic acid was modified in two ways, using either adipic dihydrazide (ADH) or methacrylic anhydride (MA). Both modifications were tested throughout the study. The drug release mechanism is shown in **Figure 5**; it was found that both liposomes with entrapped drug and free drug were released from the hydrogel matrix which is what is believed to be the reason behind the sustained drug delivery profile which was observed. Although only preliminary studies were conducted; with further research, these nanocomposite systems are a potential candidate for the delivery of drugs to the eye after a single administration (Widjaja et al., 2015). **Figure 5** shows how the drug is released from the system.

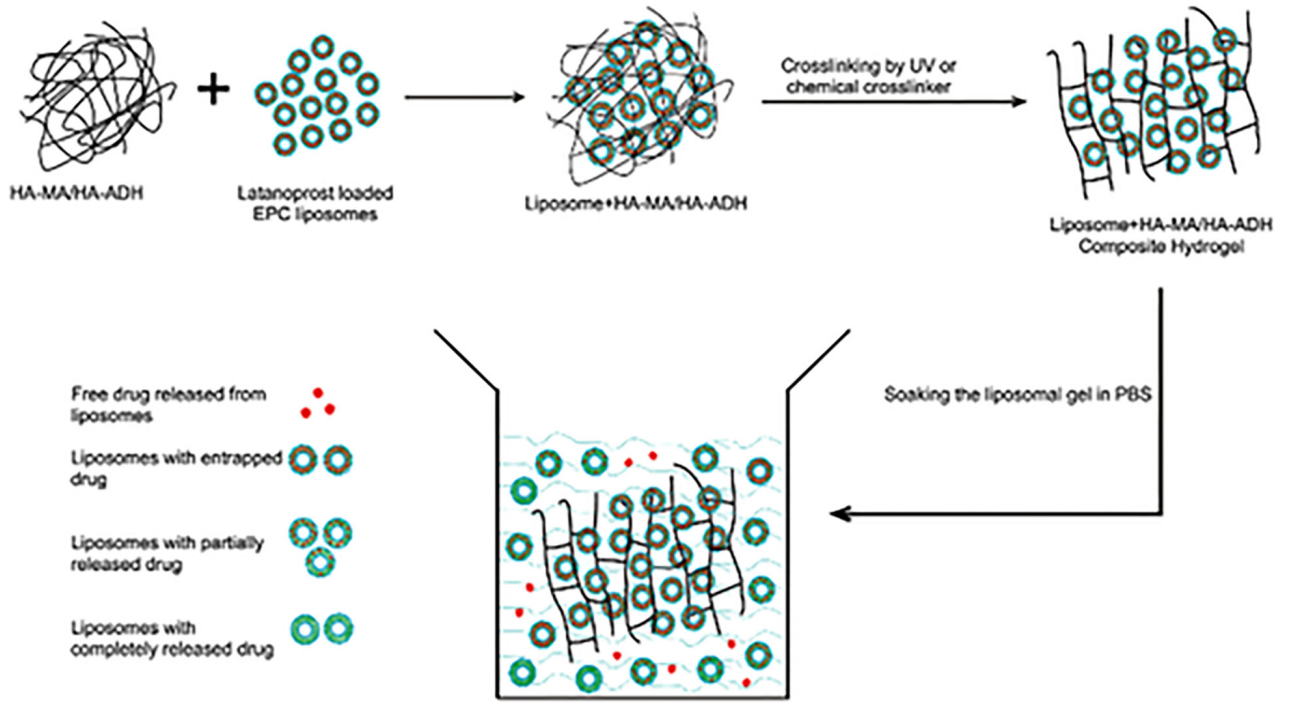

FIGURE 5 | Drug release mechanism from hyaluronic acid-based nanocomposite hydrogel system. The active ingredient is loaded within the liposomes which are in turn loaded into the hydrogel. The drug is then released from the liposomes and diffuses through the hydrogel. It was also found that liposomes themselves were able to be released from the hydrogel. Both of these release mechanisms resulted in the sustained drug release seen in the formulation. This figure also highlights how the liposomes were incorporated into the hydrogel before it was cross-linked (adapted with permission from Widjaja et al., 2015).

Another hyaluronic acid-based hydrogel system was developed by Wu et al. (2013). This system was designed to be a thermoresponsive microgel for the topical delivery of drugs to the eye. Hyaluronic acid was coupled with g-poly(*N*-isopropylacrylamide) to form HA-g-PNIPAAm which was shown to have high drug loading capabilities. The gel was tested for biocompatibility in rabbit eyes with the results showing that is was safe and did not cause any irritation. The formulated system, with a sample drug cyclosporine A (CyA), was tested against a castor oil solution of CyA and a commercial product also containing CyA. There was a significantly higher concentration of CyA in the corneas of rabbits who received the HA-g-PNIPAAm system than in those who received the other two solutions. This shows that *in situ* thermoresponsive gels are able to improve the bioavailability of ocular active ingredients (Wu et al., 2013).

Hyaluronic acid hydrogels have been investigated not only as a drug delivery system but also as an artificial vitreous substitute. Schramm et al. (2012) completed a study whereby hyaluronic acid hydrogels were formulated using two different cross-linking methods; the first through the use of dihydrides as a cross-linking agent and the second through photocrosslinking. Both methods resulted in three-dimensional hydrogels which had suitable optical transparency and rubber-like consistency. The results of this study showed that these hydrogels are able to replace the conventionally used silicone oils, which have disadvantages such as the formation of cataracts and a need for surgical removal of the oil, as a vitreous replacement on a long-term basis (Schramm et al., 2012).

Gelatin Polymeric Platforms

Gelatin is a natural polymer which is biocompatible and biodegradable. It is derived from collagen, a substance which is found naturally within the stroma of the cornea and sclera. It has been investigated for a number of ocular drug delivery systems; including nanoparticles (Vandervoort and Ludwig, 2004). Natu et al. (2007) performed a study where gelatin hydrogels were investigated as a drug delivery system for pilocarpine, an ocular active used in the treatment of glaucoma. The hydrogels were formulated through chemical crosslinking with *N*-hydroxysuccinimide (NHS) and *N*, *N*-(3-dimethylaminopropyl)-*N*′-ethylcarbodiimide hydrochloride (EDC). These crosslinkers were used in a variety of concentrations which altered the degree of crosslinking and subsequently the release of the drug from the hydrogel. The release of pilocarpine from the various hydrogels ranged from 29.2 to 99.2% over an 8-h period. The hydrogels also displayed good adhesion and non-cytotoxicity profiles. This shows hydrogels comprised of gelatin to be a viable option for the delivery of drugs to the eye (Natu et al., 2007).

In a study by Song et al. (2018), chitosan and gelatin were used to form a hydrogel aimed at improving the sustained delivery of drugs to the eye. The hydrogel was formed using a double crosslinking method; using both genipin and β-glycerophosphate

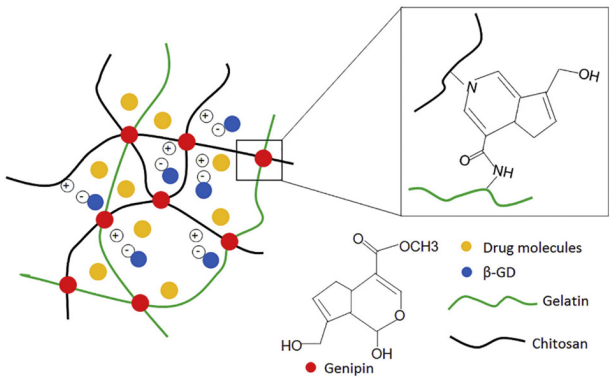

FIGURE 6 | Illustration of the double crosslinking method using β-glycerophosphate disodium and genipin. The β-glycerophosphate disodium negatively charged phosphate groups underwent electrostatic attraction to the positively charged chitosan which gave this formulation the ability to transition between a solution and a gel (adapted with permission from Song et al., 2018).

disodium salt hydrate as crosslinking agents. The resulting hydrogel had *in situ* gelling properties; showing rapid gelation at 37°C. Timolol maleate was used as a sample drug as a comparison could be made against a commercially available product. The hydrogel delivery system was non-toxic and showed a sustained release drug release profile. During *in vivo* studies, in comparison to the commercial product, the hydrogel delivery system was able to show a longer lasting and more effective reduction (due to a twofold increase in duration) in the intraocular pressure. The *in situ* gelling property also prevented the system from being rapidly removed from the lower conjunctival sac by tears following administration (Song et al., 2018). **Figure 6** shows the double crosslinking-method which is used in this formulation.

Alginate Polymeric Platforms

Alginate is another highly biocompatible polysaccharide that is able to undergo ion-responsive gelation (Liu et al., 2008). It is classified as a polyanionic copolymer and is extracted from brown sea algae. Alginate forms a hydrogel when it is exposed to divalent cations such as Ca^{2+} (Lin et al., 2004). It has been used in ocular hydrogel preparations because it is non-cytotoxic and biodegradable. It was used in a formulation by Lin et al. (2004) which is discussed below under "ion-sensitive hydrogels."

The utilization of alginate can also be seen in the study reported by Mandal et al. (2012) where an *in situ* forming gel was prepared using sodium alginate for the sustained delivery of moxifloxacin hydrochloride, a broad spectrum antibiotic. In this formulation, although sodium alginate was used as the primary gelling polymer, hydroxypropyl methylcellulose (HPMC) was also added as a viscosity enhancer. The resultant formulation was able to lengthen the precorneal residence time of the drug (also due to sodium alginate's mucoadhesive properties) and improve its bioavailability. The polymer was able to undergo a sol–gel transition in response to an ion exchange when administered to the eye. *In vivo* studies were performed for biocompatibility using healthy male albino rabbits. The rabbits showed no signs of irritation after the formulation was administered to the eye and no ophthalmic damage was noted. This makes this formulation a viable alternative to conventional eye drops for the delivery of moxifloxacin with a less frequent dosage schedule (Mandal et al., 2012).

Sodium alginate hydrogels have also been used in the delivery of anti-inflammatory drugs to the eye. One such formulation is that prepared by Pandit et al. (2007). They highlighted the preference for hydrogel systems over implants as novel ocular drug delivery systems due to the fact that hydrogels are more cost effective and comfortable to the patient while still overcoming the bioavailability issues that are seen with convention drug delivery systems. The hydrogel which was produced supported these sentiments; sodium alginate was formulated into an *in situ* gelling system which would increase the residency time of the drug as well as exhibit sustained drug release profiles; both of which are vital in improving the bioavailability of ocular drugs (Pandit et al., 2007).

Methylcellulose Polymeric Platforms

Methylcellulose is natural polymer which is often used as a viscosity enhancer in ocular formulations. It is capable of undergoing a reversible sol–gel transition when it is heated. This makes it useful in the development of *in situ* gelling hydrogel systems (Sultana et al., 2006a).

In a study by Silva et al. (2017), a HPMC hydrogel was used to aid in the delivery of chitosan-hyaluronic acid nanoparticles to the eye, giving another example in how a hydrogel can be employed in a drug delivery system. Methylcellulose was used because it is safe to sterilize within an autoclave, it has a suitable pH for the eye and has been shown to be used successfully in other ophthalmic preparations (Silva et al., 2017). This study highlights one of the derivatives of methylcellulose, among others, which are often used in preparations. This is due to the fact that these derivatives influence the temperature at which the methylcellulose is able to undergo a sol–gel transition. For example, by lowering the molar substitution of hydroxyl propyl groups, the transition temperature is reduced from between 75 and 90 to 40°C (Gambhire et al., 2013).

Methylcellulose can also be added to a formulation to adjust its gelation behavior. This was investigated by Dewan et al. (2015) in a study where methylcellulose of varying molecular weights were added to Poloxamer 407 (PM), a polymer previously investigated for the delivery of various drugs to the eye. However, when used in these formulations, PM is diluted by the lacrimal fluid of the eye and loses its ability to form a gel. Increasing the concentration of PM is not a viable solution as it causes the gelation temperature to drop; resulting in the formulation turning into a gel at room temperature. It was found that the addition of methylcellulose resulted in a decrease in the gelation temperature of the PM formulations and facilitated extended drug release profiles of the sample drug; making it a viable option for sustained drug delivery to the eye (Dewan et al., 2015).

A further study which illustrates that methylcellulose can be utilized in ophthalmic drug delivery preparations is that

performed by Bain et al. (2009). Agents such as fructose and sodium citrate tribasic dehydrate were added to the formulation to reduce the gelation temperature. These additives have an impact on the gelation temperature by affecting the interactions between the polymer and the water molecules. The sample drug used was ketorolac tromethamine (KT). The resulting formulation was able to extend the release of the drug from 5 to 9 h, largely due to the presence of fructose which further enhances the viscosity of the formulation. Although further testing and *in vivo* studies are needed, the resulting formulation is a viable option for the delivery of drug to the eye in the place of conventional eye drops (Bain et al., 2009).

Collagen Polymeric Platforms

Collagen is a natural polymer which is also available to be used in ocular drug delivery systems. Type 1 collagen is one of the primary components of the cornea and has been used in scaffolds for tissue engineering (Chen et al., 2005). Collagen shields have been formulated and are able to deliver drugs to the eye for a maximum of 72 h. This is more beneficial than soft contact lenses, which have been shown to only delivery the drug for the first 1–2 h after insertion. These shields are generally used following ophthalmic surgery for the delivery of anti-inflammatory or immunosuppressive active ingredients, among others. However, these shields are non-transparent and have to be applied by a surgeon (Liu et al., 2008).

However, there are some collagen shields available which have the potential to be self-administered. As reported by Khan and Khan (2013), these bandage contact lenses are able to facilitate the healing of the cornea following surgery or injury by protecting it from abrasion caused by blinking. They are also able to be laden with active ingredients; as the tears dissolve the contact lens, the drug is released along with a layer of collagen which is able to lubricate the eye. This provides a system which is able to increase the residency time of the drug at the cornea, allowing for increased permeability and bioavailability (Khan and Khan, 2013).

An example of a formulation where collagen, along with hydrogel technology, has been developed is that reported by Liu et al. (2006) where composite collagen hydrogels were formulated which contained alginate microspheres for the delivery of drugs to the eye. The composite hydrogels were characterized and shown to be suitable for use in ocular inserts or contact lens formulations as they were biocompatible and showed sustained drug release profiles as well as supported the attachment and growth of corneal epithelial cells (Liu et al., 2006).

Collagen has also been used in hydrogels that are intended for tissue engineering purposes. They have been investigated as an alternative to amniotic membrane which is used for clinical ocular surface reconstruction. This is due to the fact that they biodegrade at a suitable rate and offer very low immunogenicity. In a study by Mi et al. (2010), these collagen-based scaffolds were investigated. It was found that collagen gels are difficult to manipulate because of their weak structure. This was overcome through controlled unconfined plastic compression which, depending on the collage concentration and time for which the gel was compressed, produced a scaffold which closely mimiced the structure of the cornea. These hydrogel scaffolds were able to adequately support cell attachments and epithelial cell growth (Mi et al., 2010).

SAFETY BY DESIGN OF POLYMERIC HYDROGELS THROUGH OCULAR BIOCOMPATIBILITY AND BIODEGRADATION

The eye is an organ of immune privilege, which protects its visual capability from the potentially sight-threatening sequelae of intraocular inflammation (Keino et al., 2018). Consequently, any potential formulations used in the eye, whether it be for drug delivery, tissue engineering, or any other medical procedure need to be vigorously tested for biocompatibility.

Biocompatibility

Many studies in which new ophthalmic formulations are being investigated include biocompatibility studies. Typically, the first step in determining biocompatibility is to determine the cytocompatibility of the formulation. This is done through cytotoxicity or cell proliferation tests which are performed *in vitro*. The cell line most commonly used for these tests is human corneal epithelial cells (HCECs). These *in vitro* tests are useful in determining biocompatibility as they provide a controlled environment whereby researchers can observe the impact of the polymers used in their formulation on cell characteristics such as adhesion, proliferation, and viability. It has been noted that cell studies which are performed with multiple, different cell lines provide a more accurate representation of the cells found within tissues than studies where only a single cell line is used (Huhtala et al., 2007).

The second process in determining biocompatibility is through *in vivo* testing. This is usually performed using animal models. The New Zealand white rabbit model is most commonly used in ophthalmic bioavailability studies. This is because the eye of an adult rabbit is big enough to ensure the procedure is performed accurately (for example, rat eyes are sometimes used but are often too small for formulations designed for use in human eyes) and there is no pigment epithelium in the eye (Short, 2008).

Although the majority of the studies that are detailed in this review include biocompatibility studies in addition to other characterizations, either through *in vitro* or *in vivo* testing, there are those available which focus primarily on biocompatibility. One such study is that performed by Lai (2010). The authors investigated the effect of different cross-linkers [namely glutaraldehyde (GTA) and 1-ethyl-3-(3-dimethyl aminopropyl) carbodiimide (EDC)] on the ocular biocompatibility of gelatin hydrogels. Gelatin has been shown to have a rapid dissolution when it has not been cross-linked and is placed within an aqueous environment, which would limit its potential application in the delivery of drugs to the eye. The biocompatibility was tested using both cell culture

techniques and *in vivo* animal testing. The cell line selected was primary rat iris pigment epithelial cells; these were cultured and observed for cell proliferation, viability, and presence of pro-inflammatory genes.

The results showed that the EDC cross-linked gels were better tolerated than the GTA hydrogels. This was then corroborated in the *in vivo* tests whereby the gelatin hydrogels were inserted into the anterior chamber of the eye of New Zealand white rabbits and observed for 12 weeks. The rabbits who were given the GTA cross-linked hydrogels showed a significant inflammation reaction whereas the EDC cross-linked hydrogels were well tolerated, concluding that EDC is more suitable as a cross-linking agent for the formulation of ophthalmic gelatin hydrogels. This study highlights that, although gelatin itself is biocompatible, the cross-linking agents which are used in the formulation of hydrogels have the ability to change the biocompatibility of a formulation (Lai, 2010).

The results mentioned in the study above were further corroborated in another study; also focusing on the biocompatibility of GTA and EDC cross-linked hydrogels, with the exception of using hyaluronic acid as the polymer. The results of the *in vivo* tests, performed using rabbits, showed that the EDC crosslinked hydrogel elicited no inflammatory response whereas the GTA cross-linked hydrogels produced a severe tissue response. This further highlights the importance of biocompatibility testing, not only for the polymer, but also for the other reactants used within a formulation (Lai et al., 2010).

Other *in vitro* methods for testing biocompatibility have been developed. An example of this is the development of a three-dimensional, curved epithelium model which is able to mimic the cornea. This model was designed and created by Postnikoff et al. (2014) in the hopes of removing the need for the use of animal testing in the development of some ophthalmic preparations. This particular model was shown to be multi-layered and responsive to cytotoxic compounds, as a cornea would which makes it a viable option in the biocompatibility assessment of contact lenses (Postnikoff et al., 2014).

Biodegradability

Biodegradability is one of the aspects which makes the polymers discussed in this review beneficial for use in ocular drug delivery. This allows sustained drug release systems to be able to breakdown and be absorbed by the body, eradicating the necessity for surgical removal. The most common form of biodegradable system is that where a drug is embedded within a polymeric system and is released as the polymer degrades. The advantage of biodegradable over non-biodegradable ocular systems has been seen in implants developed for sustained drug release. Majority of ocular implants currently available on the market are non-biodegradable but research is being done into the development of biodegradable formulations (Lee et al., 2010).

The biodegradable nature of polymers, while advantageous, can sometimes hinder their ability to maintain their integrity for an extended time within the environment into which they are placed. For example, hyaluronic acid, which is broken down by hyaluronidase, does not have a sufficient residence time for long-term delivery. Hyaluronic acid is often modified to overcome this issue (du Toit et al., 2013).

INCORPORATION OF HYDROGELS AND NANOTECHNOLOGY FOR OCULAR DRUG DELIVERY

Hydrogels can form a vital role in the development of nanotechnologies for the delivery of drugs to the eye. An example of this is the formulation of hydrogel nanoparticles. This drug delivery system combines the benefits of a hydrogel (hydrophilic and high-water content) with the minute size of a nanoparticle. These have been developed using both synthetic and natural polymers but, in this article, only those employing natural polymers are discussed (Hamidi et al., 2008).

Although hydrogels themselves offer many advantages to overcome these challenges, by combining hydrogels in colloidal drug delivery systems the effective delivery of drugs to the eye is further improved. Nanotechnology, such as nanoparticles and nanoliposomes, has been given a lot of focus in recent years for use in ocular drug delivery. These nanocarriers are able to offer advantages such as the more targeted delivery of drugs and controlled release as well as reduced toxicity and improved efficacy of formulations. These carriers, which range from 1 to 1000 nm in size, are also able to deliver drugs which are poorly water soluble (a problem that in the past has seen ocular active drugs not being made into effective preparations) as well as provide improved penetration into tissues. Colloidal drug delivery systems are also able to increase the retention time at the surface of the cornea, resulting in improved bioavailability (Ameeduzzafar et al., 2016).

In terms of ocular drug delivery, nanoparticles are useful due to their small size which allows for targeted drug delivery and improved bioavailability. The drugs in these delivery systems can be incorporated into the nanoparticle either through entrapment, encapsulation, or attachment to the surface. Nanoparticles with intrinsic hydrogel structure are able to be formulated using either physical or chemical cross-linking methods and have been prepared using a number of synthetic and natural polymers. Nanoparticles are able to be combined with hydrogel technology either in the way that they are synthesized or in the way that they are administered where the hydrogel acts as a suspending agent (Hamidi et al., 2008).

A further example of the combination of hydrogels and nanotechnology is nanogels. These nanoparticle carriers have many beneficial properties in terms of ocular drug delivery. These include sustained drug delivery profiles and improved stability of the drug in water (Jamard et al., 2016).

In a study by Jamard et al. (2016), it was noted that many nanogels require harsh conditions for formulation, such as high temperatures and the use of organic solvents. However, it was noted that by using biopolymers (such as methylcellulose) which have been modified with hydrophobic moieties [such as poly(*N*-tert-butylacrylamide)], self-assembling nanogels could be formulated through hydrophobic interaction within an

aqueous environment. This renders the resultant, non-cytotoxic nanogel suitable for the delivery of biological compounds with a prolonged release profile (Jamard et al., 2016).

A further study, focusing on the delivery of fluconazole to the cornea, was performed by Nishil et al. (2013) where fluconazole loaded chitin nanogels were synthesized. The system was shown to have sustained drug release drug profiles while also being cytocompatible. It was also noted that the system allowed for penetration through the cornea in *ex vivo* studies. The nanogel can be considered for improved bioavailability for the fluconazole in the treatment of corneal fungal infections (Nishil et al., 2013).

Solid lipid nanocarriers (SLN) are another form of nanotechnology which have been researched for the replacement of conventional ocular drug delivery systems. These SLNs are advantageous as they have low toxicity due to the fact that they are prepared from lipids natural to the body, are able to undergo autoclave sterilization, and are able to be loaded with both hydrophilic and hydrophobic drugs (Farid et al., 2017). SLNs fall under a larger group of lipid-based nanocarriers which also includes lipid-drug conjugates (Puglia et al., 2015).

Nanoparticles offer a particular benefit in that, due to the large surface area-to-volume ratio, they are able to support a vast number of surface functional groups (Jacob et al., 2018). These surface modifications are able to improve some of the disadvantages which are seen in certain nanotechnologies. An example of this can be seen in a study by Attama et al. (2008) where a phospholipid was used as a surface modifier on SLNs. The results showed that the drug release from the SLNs which were formulated without the phospholipid happened in a burst release fashion due to the fact that there was more drug present in the periphery of the nanoparticles. In addition, a large amount of drug was found in the bulk aqueous medium. Those that were formulated with the phospholipid had a sustained drug release profile. This illustrates how surface modifications are able to have an effect on not only the drug release profiles but also the encapsulation efficacy of SLNs (Attama et al., 2008).

The concept of colloidal nanoparticulate-based systems has been investigated for therapeutic contact lenses. The incorporation of nanoparticles allows for improved drug release from the contact lens as well as prevents the interaction of the drug with the polymers of which the lens is composed. An example of such system was formulated by Jung et al. (2013). Nanoparticles which contained timolol, a drug used to treat glaucoma, were loaded onto commercial contact lenses. The contact lenses were tested in preliminary drug release and *in vivo* studies which showed that, in addition of being biocompatible, they were able to release timolol over an extended period (5 days) resulting in a lowering of the intraocular pressure. These are promising results as an alternative to conventional timolol eye drops which must be administered multiple times a day; however, there is still further research which needs to be conducted (Jung et al., 2013). This research would include the impact of colloidal systems on the contact lens' transparency and ion and oxygen permeability (Maulvi et al., 2016).

FUTURE PERSPECTIVES

The primary focus of the research that is being done, and that has been commented on in this article is to improve the shortfalls seen in current ophthalmic treatments. Whether that be the low bioavailability and rapid clearance from the administration site found with eye drop formulations or the frequency of invasive procedures seen with intravitreal injections, future developments made in ocular drug delivery are vital (Sapino et al., 2019).

Many of the advancements being made in this area of drug delivery include harnessing the benefits highlighted for both biopolymers and hydrogel systems. One of the main focuses of the future perspectives is the further testing of the systems that have been discussed in this paper. This testing includes *in vivo* animal testing of systems that have undergone cell testing, and clinical trials for the systems that have undergone animal pilot studies. It has been noted that not many of the newly developed systems have been made commercially available and these studies would further this process (Barbu et al., 2006).

Natural, biodegradable polymers have uses in other future prospects for ocular drug delivery outside of their use in hydrogel systems, both on their own and in conjunction with synthetic polymers. These include the development of polymeric ocular inserts [as an example, an insert was developed by Jain et al. (2010) with sodium carboxymethylcellulose and polyvinyl alcohol for the topical delivery of ciprofloxacin]. Majority of the ocular inserts which are commercially available are composed of synthetic polymers so the development and commercialization of biopolymer-based inserts is a definite avenue for the future prospects of biopolymer technology.

Hydrogel systems have been demonstrated in many studies to be highly beneficial in their role as ophthalmic drug delivery systems. The advances that have been made in recent years, particularly in terms of "smart" or stimuli-responsive hydrogels, have made a large impact. However, many of these formulations have not been made commercially available, mainly because many of them have yet to undergo clinical trials. This would be a vital step in improving the quality of life of patients; especially those who require eye drop administration on a daily basis. According to the research that has been done, hydrogels provide an option for far less frequent dosing schedules (in some cases weeks or months) (Chang et al., 2019).

CONCLUSION

Although hydrogels are not as extensively investigated as some of the other developments that are being made in ocular drug delivery, they are making an impact. These systems provide two vital benefits to drug delivery; sustained drug release and increased retention time. They are able to be formulated in such a way that they are able to respond to stimuli, which has been shown to be very beneficial. This stimuli-response ability allows for ease of administration, making these formulations more favorable for patients. This takes the ease of administration of eye drops and combines it with the increased viscosity of ointments, resulting in effective topical drug delivery without

frequent dosing schedules (seen with eye drops) and blurred vision (seen with ointments).

Biopolymers are at the forefront of many studies undertaken in ocular drug delivery. These polymers, with their non-cytotoxic, biodegradable profiles enable researchers to develop technologies without the risk of causing inflammation and the need for surgical removal. They also lend themselves to safety-by-design aspects for new formulations as there are many studies which illustrate their low toxicity profiles. Biopolymers provide an easily available and relatively cheaper option to some synthetic polymers.

Both hydrogels and biopolymers lend themselves to use in nanotechnology for ocular drug delivery. Whether it be in the form of the intrinsic make-up of the nanoparticles, nanoliposomes, or nanowires, or as a suspending agent, hydrogels can greatly impact the developments which are being made in this field of drug delivery. Although there are still developments to be made, both hydrogel and biopolymer technology play a vital role in the improvements being investigated for the effective delivery of drugs to the eye.

AUTHOR CONTRIBUTIONS

All authors listed have made a substantial, direct and intellectual contribution to the work, and approved it for publication.

FUNDING

This work was financially supported by the National Research Foundation (NRF) of South Africa.

REFERENCES

Agrawal, A. K., Das, M., and Jain, S. (2010). *In situ* systems as "smart" carriers for sustained ocular drug delivery. *Exp. Opin. Drug Deliv.* 9, 383–402. doi: 10.1517/17425247.2012.665367

Al Khateb, K., Ozhmukhametova, E. K., Mussin, M. N., Seilkhanov, S. K., Rakhypbekov, T. K., Lau, W. M., et al. (2016). *In situ* gelling systems based on Pluronic F127/Pluronic F68 formulations for ocular drug delivery. *Int. J. Pharm.* 502, 70–79. doi: 10.1016/j.ijpharm.2016.02.027

Ameeduzzafar, J. A., Ali, J., Fazil, M., Qumbar, M., Khan, N., and Ali, A. (2016). Colloidal drug delivery system: amplify the ocular delivery. *Drug Deliv.* 23, 700–716. doi: 10.3109/10717544.2014.923065

Attama, A., Reichi, S., and Muller-Goymann, C. C. (2008). Diclofenac sodium delivery to the eye: *In vitro* evaluation of novel solid lipid nanoparticle formulation using human cornea construct. *Int. J. Pharm.* 355, 307–313. doi: 10.1016/j.ijpharm.2007.12.007

Bain, M. K., Bhowmik, M., Ghosh, S. H., and Chattopadhyay, D. (2009). *In situ* fast gelling formulation of methyl cellulose for *in vitro* ophthalmic controlled delivery of ketorolac tromethamine. *J. Appl. Polymer Sci.* 113, 1241–1246. doi: 10.1002/app.30040

Bao, Q., Jog, R., Shen, J., Newman, B., Wang, Y., and Choi, S. (2017). Physicochemical attributes and dissolution testing of ophthalmic ointments. *Int. J. Pharm.* 523, 310–319. doi: 10.1016/j.ijpharm.2017.03.039

Barbu, E., Verestiuc, L., Nevell, T. G., and Tsibouklis, J. (2006). Polymeric materials for ophthalmic drug delivery: trends and perspectives. *J. Mater. Chem.* 16, 3439–3443. doi: 10.1039/B605640G

Bhandari, P., Novikova, G., Goergen, C. J., and Irudayaraj, J. (2018). Ultrasound beam steering of oxygen nanobubbles for enhanced bladder cancer therapy. *Sci. Rep.* 8:3112. doi: 10.1038/s41598-018-20363-8

Bhattarai, N., Gunn, J., and Zhang, M. (2010). Chitosan-based hydrogels for controlled, localized drug delivery. *Adv. Drug Deliv. Rev.* 62, 83–99. doi: 10.1016/j.addr.2009.07.019

Biro, T., and Aigner, Z. (2019). Current approaches to use cyclodextrins and mucoadhesive polymers in ocular drug delivery – a mini review. *Sci. Phar.* 87:15. doi: 10.3390/scipharm87030015

Bonfioli, A. A., Damico, F. M., Curi, A. L., and Orefice, F. (2005). Intermediate uveitis. *Semin. Ophthalmol.* 20, 147–154. doi: 10.1080/08820530500232035

Cao, Y., Zhang, C., Shen, W., Cheng, Z., Yu, L. L., and Ping, Q. (2007). Poly(N-isopropylacrylamide)-chitosan thermosensitive *in situ* gel-forming system for ocular drug delivery. *J. Contr. Release* 120, 186–194. doi: 10.1016/j.jconrel.2007.05.009

Chang, D., Park, K., and Famili, A. (2019). Hydrogels for sustained delivery of biologics to the back of the eye. *Drug Discov. Today* 24, 1470–1482. doi: 10.1016/j.drudis.2019.05.037

Chen, J., Li, Q., Huang, Y., Ding, Y., Deng, H., and Zhao, S. (2005). Study on biocampatibility of complexes of collagen-chitosan-sodium hyaluronate and cornea. *Artif. Organs* 29, 104–113. doi: 10.1111/j.1525-1594.2005.29021.x

Chen, X., Li, X., Zhou, Y., Wang, X., Zhang, Y., and Fan, Y. (2012). Chitosan-based thermosensitive hydrogel as a promising ocular drug delivery system: Preparation, characterization and *in vivo* evaluation. *J. Biomater. Appl.* 27, 391–402. doi: 10.1177/0885328211406563

Cheng, Y., Tsai, T. H., Jhan, Y. Y., Chiu, A. W., Tsai, K. L., Chien, C. S., et al. (2016). Thermosensitive chitosan-based hydrogel as a topical ocular drug delivery system of latanaprost for glaucoma treatment. *Carbohydr. Polym.* 144, 390–399. doi: 10.1016/j.carbpol.2016.02.080

Dewan, M., Bhowmick, B., Sarkar, G., Rana, D., Bain, M. K., and Bhowmick, M. (2015). Effect of methyl cellulose on gelation behavior and drug release from poloxamer based ophthalmic formulations. *Int. J. Biol. Macromol.* 72, 706–710. doi: 10.1016/j.ijbiomac.2014.09.021

du Toit, C., Carmichael, T., Govender, T., Kumar, P., Choonara, Y. E., and Pillay, V. (2013). *In vitro*, *in vivo*, and *in silico* evaluation of the bioresponsive behavior of an intelligent intraocular implant. *Phar. Res.* 31, 607–634. doi: 10.1007/s11095-013-1184-3

Dua, H. S., Faraj, L. A., Said, D. G., Gray, T., and Lowe, J. (2013). Human corneal anatomy redefined: a novel pre-Descemet's layer (Dua's layer). *Ophthalmology* 120, 1778–1785. doi: 10.1016/j.ophtha.2013.01.018

Duttagupta, S., Jadhav, V. M., and Kadam, V. J. (2015). Chitosan: a propitious biopolymer of drug delivery. *Curr. Drug Deliv.* 12, 369–381. doi: 10.2174/1567201812666150310151657

Eljarrat-Binstock, E., and Domb, A. J. (2006). Iontophoresis: a non-invasive ocular drug delivery. *J. Control. Release* 110, 479–489. doi: 10.1016/j.jconrel.2005.09.049

Eljarrat-Binstock, E., Orucov, F., Aldouby, Y., Frucht-Pery, J., and Domb, A. J. (2008). Charged nanoparticles delivery to the eye using hydrogel iontophoresis. *J. Control. Release* 126, 156–161. doi: 10.1016/j.jconrel.2007.11.016

Farid, R. M., El-Salamouni, N. S., El-Kamel, A. H., and El-Gamal, S. S. (2017). Lipid-based nanocarriers for ocular drug delivery. *Nanostructures for Drug Delivery* eds E., Andronescu and A. M., Grumezescu (Elsevier: Amsterdam)

Fathi, M., Barar, J., Aghanejad, A., and Omidi, Y. (2015). Hydrogels for ocular drug delivery and tissue engineering. *Bioimpacts* 5, 159–164. doi: 10.15171/bi.2015.31

Fulgencio, G. O., Viana, F. A., Ribeiro, R. R., Yoshida, M. I., Faraco, A. G., and Cunha-Junior Ada, S. (2012). New mucoadhesive chitosan film for ophthalmic drug delivery of timolol maleate: *In vivo* evaluation. *J. Ocul. Pharmacol. Ther.* 28, 350–358. doi: 10.1089/jop.2011.0174

Gambhire, S., Bhalerao, K., and Singh, S. (2013). *In situ* hydrogel: different approached to ocular drug delivery. *Int. J. Phar. Pharma. Sci.* 5, 27–36.

Gaudana, R., Ananthula, H. K., Parenky, A., and Mitra, A. K. (2010). Ocular drug delivery. *AAPS J.* 12, 348–360. doi: 10.1208/s12248-010-9183-9183

Gaudana, R., Jwala, J., Boddu, S. H., and Mitra, A. K. (2009). Recent perspectives in ocular drug delivery. *Pharm. Res.* 26, 1197–1216. doi: 10.1007/s11095-008-9694-0

Grisanti, S., and Ziemssen, F. (2007). Bevacizumab: off-label use in ophthalmology. *Ind. J. Ophthalmol.* 55, 417–420. doi: 10.4103/0301-4738.36474

Gupta, H., Aqil, M., Khar, R. K., Ali, A., Bhatnagar, A., and Mittal, G. (2013). Nanoparticles laden *in situ* gel for sustained ocular drug delivery. *J. Pharm. Bioallied Sci.* 5, 162–165. doi: 10.4103/0975-7406.111824

Hamcerencu, M., Desbrieres, J., and Popa, M. (2020). Thermo-sensitive gellan maleate/N-isopropylacrylamide hydrogels: initial "*in vitro*" and "*in vivo*" evaluation as ocular inserts. *Polym. Bull.* 77, 741–755. doi: 10.1007/s00289-019-02772-5

Hamidi, M., Azadi, A., and Rafiei, P. (2008). Hydrogel nanoparticles in drug delivery. *Adv. Drug Deliv. Rev.* 60, 1638–1649. doi: 10.1016/j.addr.2008.08.002

Hoare, T. R., and Kohane, D. S. (2008). Hydrogels in drug delivery: progress and challenges. *Polymer* 49, 1993–2007. doi: 10.1016/j.polymer.2008.01.027

Huang, D., Chen, Y. S., and Rupenthal, I. D. (2018). Overcoming ocular drug delivery barriers through the use of physical forces. *Adv. Drug Deliv. Rev.* 126, 96–112. doi: 10.1016/j.addr.2017.09.008

Huhtala, A., Pohjonen, T., Salminen, L., Salminen, A., Kaarniranta, K., and Uusitalo, H. (2007). *In vitro* biocompatibility of degradable biopolymers in cell line cultures from various ocular tissues: direct contact studies. *J. Biomed. Mater. Res. A* 83A, 407–413. doi: 10.1002/jbm.a.31319

Jacob, J., Haponiuk, J. T., Thomas, S., and Gopi, S. (2018). Biopolymer based nanomaterials in drug delivery systems: a review. *Mat. Today Chem.* 9, 43–55. doi: 10.1016/j.mtchem.2018.05.002

Jain, D., Csarvalho, E., and Banerjee, R. (2010). Biodegradable hybrid polymeric membranes for ocular drug delivery. *Acta Biomater.* 6, 1370–1379. doi: 10.1016/j.actbio.2009.11.001

Jamard, M., Hoare, T., and Sheardown, H. (2016). Nanogels of methylcellulose hydrophobized with N-tert-butylacrylamide for ocular drug delivery. *Drug Deliv. Transl. Res.* 6, 648–659. doi: 10.1007/s13346-016-0337-4

Jung, H. J., Abou-Jaoude, M., Carbia, B. E., Plummer, C., and Chauhan, A. (2013). Glaucoma therapy by extended release of timolol from nanoparticle loaded silicone-hydrogel contact lenses. *J. Control. Release* 165, 82–89. doi: 10.1016/j.jconrel.2012.10.010

Jung, J. H., Chiang, B., Grossniklaus, H. E., and Prausnitz, M. R. (2018). Ocular drug delivery targeted by iontophoresis in the suprachoroidal space using a microneedle. *J. Control. Release* 277, 14–22. doi: 10.1016/j.jconrel.2018.03.001

Kaji, H., Nagai, N., Nishizawa, M., and Abe, T. (2018). Drug delivery devices for retinal diseases. *Adv. Drug Deliv. Rev.* 128, 148–157. doi: 10.1016/j.addr.2017.07.002

Kang Derwent, J. J., and Mieler, W. F. (2008). Thermoresponsive hydrogels as a new ocular drug delivery platform to the posterior segment of the eye. *Trans. Am. Ophthalmo. Soc.* 106, 206–214.

Keino, H., Horie, S., and Sugita, S. (2018). Immune privilege and eye-derived T-regulatory cells. *J. Immunol. Res.* 2018, 1679197. doi: 10.1155/2018/1679197

Khan, R., and Khan, M. H. (2013). Use of collagen as a biomaterial: an update. *J. Indian Soc. Periodontol.* 17, 539–542. doi: 10.4103/0972-124X.118333

Kirchhof, S., Goepferich, A. M., and Brandl, F. P. (2015). Hydrogels in ophthalmic applications. *Eur. J. Pharm. Biopharm.* 95, 227–238. doi: 10.1016/j.ejpb.2015.05.016

Kumar, D., Jain, N., Gulati, N., and Nagaich, U. (2013). Nanoparticles laden *in situ* gelling system for ocular drug targeting. *J. Adv. Pharm. Technol. Res.* 4, 9–17. doi: 10.4103/2231-4040.107495

Kumar, S., and Himmelstein, K. J. (1995). Modification of *in situ* gelling behavior of carbopol solutions by hydroxypropyl methylcellulose. *J. Pharm. Sci.* 84, 344–348. doi: 10.1002/jps.2600840315

Kushwaha, S. K. S., Sexena, P., and Rai, A. K. (2012). Stimuli sensitive hydrogels for ophthalmic drug delivery: a review. *Int. J. Pharma. Investig.* 2, 54–60. doi: 10.4103/2230-973X.100036

Lai, J. Y. (2010). Biocompatibility of chemically cross-linked gelatin hydrogels for ophthalmic use. *J. Mater. Sci. Mater. Med.* 21, 1899–1911. doi: 10.1007/s10856-010-4035-3

Lai, J.-Y., Ma, D. H., Cheng, H. Y., Sun, C. C., Huang, S. J., and Li, Y. T. (2010). Ocular biocompatibility of carbodiimide cross-linked hyaluronic acid hydrogels for cell sheet delivery carriers. *J. Biomater. Sci. Polym. Ed.* 21, 359–376. doi: 10.1163/156856209X416980

Lee, S. S., Hughes, P., Ross, A. D., and Robinson, M. R. (2010). Biodegradable implants for sustained drug release in the eye. *Pharma. Res.* 27, 2043–2053. doi: 10.1007/s11095-010-0159-x

Li, J., Wu, L., Wu, W., Wang, B., Wang, Z., and Xin, H. (2013). A potential carrier based on liquid crystal nanoparticles for ophthalmic delivery of pilocarpine nitrate. *Int. J. Pharm.* 455, 75–84. doi: 10.1016/j.ijpharm.2013.07.057

Li, S., Dong, S., Xu, W., Tu, S., Yan, L., Zhao, C., et al. (2018). Antibacterial hydrogels. *Adv. Sci.* 5:1700527. doi: 10.1002/advs.553

Li, Z., Zhang, Z., and Chen, H. (2013). Development and evaluation of fast forming nano-composite hydrogel for ocular delivery of diclofenac. *Int. J. Pharm.* 448, 96–100. doi: 10.1016/j.ijpharm.2013.03.024

Lim, L., Tan, D. T., and Chan, W. K. (2001). Therapeutic use of bausch and lomb purevision contact lenses. *CLAO J.* 27, 179–185.

Lin, H. R., Sung, K. C., and Vong, W. J. (2004). *In situ* gelling of alginate/pluronic solutions for ophthalmic delivery of pilocarpine. *Biomacromolecules* 5, 2358–2365. doi: 10.1021/bm0496965

Liu, W., Griffith, M., and Li, F. (2008). Alginate microsphere-collagen composite hydrogel for ocular drug delivery and implantation. *J. Mater. Sci. Mater. Med.* 19, 3365–3371. doi: 10.1007/s10856-008-3486-2

Liu, Z., Li, J., Nie, S., Liu, H., Ding, P., and Pan, W. (2006). Study of am alginate/HPMC-based system for gatifloxacin. *Int. J. Pharm.* 315, 12–17. doi: 10.1016/j.ijpharm.2006.01.029

Ludwig, A. (2005). The use of mucoadhesive polymers in ocular drug delivery. *Adv. Drug Deliv. Rev.* 57, 1595–1639. doi: 10.1016/j.addr.2005.07.005

Mahlumba, P., Choonara, Y. E., Kumar, P., du Toit, L. C., and Pillay, V. (2016). Stimuli-responsive polymeric systems for controlled protein and peptide delivery: future implications for ocular delivery. *Molecules* 21:1002. doi: 10.3390/molecules21081002

Maitra, J., and Shulka, V. K. (2014). Cross-linking in hydrogel – a review. *Am. J. Poly. Sci.* 4, 25–31. doi: 10.5923/j.ajps.20140402.01

Mandal, S., Thimmasetty, M. K., Prabhushankar, G., and Geetha, M. (2012). Formulation and evaluation of an *in situ* gel-forming ophthalmic formulation of moxifloxacin hydrochloride. *Int. J. Pharm. Investig.* 2, 78–82. doi: 10.4103/2230-973X.100042

Martens, T. F., Remaut, K., Deschout, H., Engbersen, J. F., Hennink, W. E., van Steenbergen, M. J., et al. (2015). Coating nanocarriers with hyaluronic acid facilitates intravitreal drug delivery for retinal gene therapy. *J. Control. Release* 202, 83–92. doi: 10.1016/j.jconrel.2015.01.030

Masteikova, R., Chalupova, Z., and Sklubalova, Z. (2003). Stimuli-sensitive hydrogels in controlled and sustained drug delivery. *Medicina* 39, 19–24.

Maulvi, F. A., Soni, T. G., and Shah, D. O. (2016). A review on therapeutic contact lenses for ocular drug delivery. *Drug Deliv.* 23, 3017–3026. doi: 10.3109/10717544.2016.1138342

Mi, S., Chen, B., Wright, B., and Connon, C. J. (2010). Plastic compression of a collagen gel forms a much improved scaffold for ocular surface tissue engineering over conventional collagen gels. *J. Biomed. Mater. Res. A* 95, 447–453. doi: 10.1002/jbm.a.32861

Moiseev, R. V., Morrison, P. W. J., Steele, F., and Khutoryanskiy, V. V. (2019). Penetration enhancers in ocular drug delivery. *Pharmaceutics* 11:321. doi: 10.3390/pharmaceutics11070321

Mura, S., Nicolas, J., and Couvreur, P. (2013). Stimuli-responsive nanocarriers for drug delivery. *Nat. Mater.* 12, 991–1003. doi: 10.1038/nmat3776

Myles, M. E., Neumann, D. M., and Hill, J. M. (2005). Recent progress in ocular drug delivery for posterior segment disease: Emphasis on transscleral iontophoresis. *Adv. Drug Deliv. Rev.* 57, 2063–2079. doi: 10.1016/j.addr.2005.08.006

Nabili, M., Geist, C., and Zderic, V. (2015). Thermal safety of ultrasound−enhanced ocular drug delivery: A modeling study. *Med. Phys.* 42, 5604–5615. doi: 10.1118/1.4929553

Nabili, M., Patel, H., Mahesh, S. P., Liu, J., Geist, C., and Zderic, V. (2013). Ultrasound-enhanced delivery of antibiotics and anti-inflammatory drugs into the eye. *Ultra. Med. Biol.* 39, 638–646. doi: 10.1016/j.ultrasmedbio.2012.11.010

Natu, M. V., Sardinha, J. P., Correia, I. J., and Gil, M. H. (2007). Controlled release gelatin hydrogels and lyophilisates with potential application as ocular inserts. *Biomed. Mater.* 2, 241–249. doi: 10.1088/1748-6041/2/4/006

Nettey, H., Darko, Y., Bamiro, A., and Addo, R. T. (2016). "Ocular barriers," in *Ocular Drug Delivery: Advances, Challenges and Applications*, ed. R. T. Addo (Berlin: Springer), 27–36. doi: 10.1007/978-3-319-47691-9_3

Nishil, M., Rejinold, N. S., Mangalathillam, S., Biswas, R., Nair, S. V., and Jayakumar, R. (2013). Fluconazole loaded chitin nanogels as a topical ocular drug delivery agent for corneal fungal infections. *J. Biomed. Nanotechnol.* 9, 1521–1531. doi: 10.1166/jbn.2013.1647

Occhiutto, M. L., Freitas, F. R., Maranhao, R. C., and Costa, V. P. (2012). Breakdown of the blood-ocular barriers as a strategy for the systemic use of nanosystems. *Pharmaceutics* 4, 252–275. doi: 10.3390/pharmaceutics4020252

Oh, J. K., Lee, D. I., and Park, J. M. (2009). Biopolymer-based microgels/ nanogels for drug delivery applications. *Prog. Poly. Sci.* 34, 1261–1282. doi: 10.1016/j.progpolymsci.2009.08.001

Ozdek, S., Bahceci, U. A., Gurelik, G., and Hasanreisoglu, B. (2006). Posterior subtenon and intravitreal triamcinolone acetonide for diabetic macular edema. *J. Diab. Comp.* 20, 246–251. doi: 10.1016/j.jdiacomp.2005.06.015

Pandit, J. K., Bharathi, D., Srinathga, A., Ridhurkar, N., and Singh, S. (2007). Long acting ophthalmic formulation of indomethacin: evaluation of alginate gel systems. *Ind. J. Pharm. Sci.* 69, 37–40. doi: 10.4103/0250-474X.32105

Patel, A., Cholkar, K., Agrahari, V., and Mitra, A. K. (2013). Ocular drug delivery systems: an overview. *World J. Pharmacol.* 2, 47–64. doi: 10.5497/wjp.v2.i2.47

Patenaude, M., Smeets, N. M. B., and Hoare, T. (2014). Designing injectable, covalently cross−linked hydrogels for biomedical applications. *Macromol. Rapid Commun.* 35, 598–617. doi: 10.1002/marc.201300818

Postnikoff, C. K., Pintwala, R., Williams, S., Wright, A. M., Hileeto, D., and Gorbet, M. B. (2014). Development of a curved, stratified, *in vitro* model to assess ocular biocompatibility. *PLoS One* 9:e96448. doi: 10.1371/journal.pone.0096448

Puglia, C., Offerta, A., Carbone, C., Bonina, F., Pignatello, R., and Puglisi, G. (2015). Lipid nanocarriers (LNC) and their applications in ocular drug delivery. *Curr. Med. Chem.* 22, 1589–1602. doi: 10.2174/0929867322666150209152259

Rajasekaran, A., Kumaran, K. S. G., Preetha, J. P., and Karthika, K. (2010). A comparative review on conventional and advanced drug delivery formulation. *Int. J. PharmTech. Res.* 2, 668–674. doi: 10.1517/17425247.2011.548801

Sapino, S., Chirio, D., Peira, E., Rubio, E. A., Brunella, V., and Jadhav, S. A. (2019). Ocular drug delivery: a special focus on the thermosensitive approach. *Nanomaterials* 9:884. doi: 10.3390/nano9060884

Schramm, C., Spitzer, M. S., Henke-Fahle, S., Steinmetz, G., Januschowski, K., Heiduschka, P., et al. (2012). The cross-linked biopolymer hyaluronic acid as an artificial vitreous substitute. *Invest. Ophthalmol. Vis. Sci.* 53, 613–621. doi: 10.1167/iovs.11-7322

Shen, A. Y., Haddad, E. J., Hunter-Smith, D. J., and Rozen, W. M. (2018). Efficacy and adverse effects of topical chloramphenicol ointment use for surgical wounds: a systematic review. *ANZ J. Surg.* 88, 1243–1246. doi: 10.1111/ans.14465

Short, B. G. (2008). Safety evaluation of ocular drug delivery formulations: techniques, and practical considerations. *Toxicol. Pathol.* 36, 49–62. doi: 10.1177/0192623307310955

Silva, M. M., Calado, R., Marto, J., Bettencourt, A., Almeida, A. J., and Goncalves, L. M. D. (2017). Chitosan nanoparticles as a mucoadhesive drug delivery system for ocular administration. *Mar. Drugs* 15:370. doi: 10.3390/md15120370

Singh, A., Dogra, T. S., Mandal, U. K., and Narang, R. K. (2019). Novel approaches for ocular drug delivery: a review. *Int. J. Bio-Pharm. Res.* 8, 2722–2732.

Singh, A. V. (2011). Biopolymers in drug delivery: a review. *Pharmacology* 1, 666–674.

Song, Y., Nagai, N., Saijo, S., Kaji, H., Nishizawa, M., and Abe, T. (2018). *In situ* formation of injectable chitosan-gelatin hydrogels through double crosslinking for sustained intraocular drug delivery. *Mater. Sci. Eng. C Mater. Biol. Appl.* 88, 1–12. doi: 10.1016/j.msec.2018.02.022

Souto, E. B., Dias-Ferreira, J., Lopez-Machado, A., Ettcheto, M., Cano, A., and Camins, E. A. (2019). Advanced formulation approaches for ocular drug delivery: state-of-the-art and recent patents. *Pharmaceutics* 11:460. doi: 10.3390/pharmaceutics11090460

Srividya, B., Cardoza, R. M., and Amin, P. D. (2001). Sustained ophthalmic delivery of ofloxacin from a pH triggered *in situ* gelling system. *J. Control. Release* 73, 205–211. doi: 10.1016/s0168-3659(01)00279-6

Sultana, Y., Agil, M., Ali, A., and Zafar, S. (2006a). Evaluation of Carbopol-methylcellulose based sustained-release ocular delivery system for pefloxacin mesylate using rabbit eye model. *Pharm. Dev. Technol.* 11, 313–319. doi: 10.1080/10837450600767698

Sultana, Y., Jain, R., Agil, M., and Ali, A. (2006b). Review of ocular drug delivery. *Curr. Drug Deliv.* 3, 207–217. doi: 10.2174/156720106776359186

Thomas, E. R., Wang, J., Ege, E., Madsen, R., and Hainsworth, D. P. (2006). Intravitreal triamcinolone acetonide concentration after subtenon injection. *Am. J. Ophthalmol.* 142, 860–861. doi: 10.1016/j.ajo.2006.05.023

Thrimawithana, T. R., Young, S., Bunt, C. R., Green, C., and Alany, R. G. (2011). Drug delivery to the posterior segment of the eye. *Drug Discov. Today* 16, 270–277. doi: 10.1016/j.drudis.2010.12.004

Tieppo, A., White, C. J., Paine, A. C., Voyles, M. L., McBride, M. K., and Byrne, M. E. (2012). Sustained *in vivo* release from imprinted therapeutic contact lenses. *J. Control. Release* 157, 391–397. doi: 10.1016/j.jconrel.2011.09.087

Trombino, S., Servido, C., Curcio, F., and Cassano, R. (2019). strategies for hyaluronic acid-based hydrogel design in drug delivery. *Pharmaceutics* 11:407. doi: 10.3390/pharmaceutics11080407

Urtti, A. (2006). Challenges and obstacles of ocular pharmacokinetics and drug delivery. *Adv. Drug Deliv. Rev.* 58, 1131–1135. doi: 10.1016/j.addr.2006.07.027

Vandervoort, J., and Ludwig, A. (2004). Preparation and evaluation of drug-loaded gelatin nanoparticles for topical ophthalmic use. *Eur. J. Pharm. Biopharm.* 57, 251–261. doi: 10.1016/s0939-6411(03)00187-5

Vashist, A., Vashist, A., Gupta, Y. K., and Ahmad, S. (2014). Recent advances in hydrogel based drug delivery systems for the human body. *J. Mater. Chem. B.* 2, 147–166. doi: 10.1039/C3TB21016B

Wang, C., Feng, N., Chang, F., Wang, J., Yuan, B., Chneg, Y., et al. (2019). Injectable cholesterol−enhanced stereocomplex polylactide thermogel loading chondrocytes for optimized cartilage regeneration. *Adv Healthcare Mat.* 8:1900312. doi: 10.1002/adhm.201900312

Wang, J., Jiang, A., Joshi, M., and Christoforidis, J. (2013). Drug delivery implants in the treatment of vitreous inflammation. *Med. Inflamm.* 2013:780634. doi: 10.1155/2013/780634

Widjaja, L. K., Bora, M., Chan, P. N., Lipik, V., Wong, T. T., and Venkatraman, S. S. (2015). Hyaluronic acid−based nanocomposite hydrogels for ocular drug delivery applications. *J. Biomed. Mater. Res. A* 102, 3056–3065. doi: 10.1002/jbm.a.34976

Willoughby, C. E., Diego, P., Ferrari, S., Aires, L., Landua, K., Yadollah, O., et al. (2010). Anatomy and physiology of the human eye: effects of mucopolysaccharidoses disease on structure and function–a review. *Clin. Experiment. Ophthalmol.* 38, 2–11. doi: 10.1111/j.1442-9071.2010.02363.x

Wong, C. W., and Wong, T. T. (2019). Posterior segment drug delivery for the treatment of exudative age-related macular degeneration and diabetic macular oedema. *Brit. J. Ophthal.* 103, 1356–1360. doi: 10.1136/bjophthalmol-2018-313462

Wu, Y., Yao, J., Zhou, J., and Dahmani, F. Z. (2013). Enhanced and sustained topical ocular delivery of cyclosporine A in thermosensitive hyaluronic acid-based *in situ* forming microgels. *Int. J. Nanomed.* 8, 3587–3601. doi: 10.2147/IJN.S47665

Xu, X., Weng, Y., Xu, L., and Chen, H. (2013). Sustained release of Avastin§from polysaccharides cross-linked hydrogels for ocular drug delivery. *Int. J. Biol. Macromol.* 60, 272–276. doi: 10.1016/j.ijbiomac.2013.05.034

Yadav, K. S., Rajpurohit, R., and Sharma, S. (2019). Glaucoma: current treatment and impact of advanced drug delivery systems. *Life Sci.* 221, 362–376. doi: 10.1016/j.lfs.2019.02.029

Yasin, M. N. (2014). Implants for drug delivery to the posterior segment of the eye: a focus on stimuli-responsive and tunable release systems. *J. Control. Release* 196, 208–221. doi: 10.1016/j.jconrel.2014.09.030

Yellepeddi, V. K., and Palakurthi, S. (2016). Recent advances in topical ocular drug delivery. *J. Ocul. Pharmacol. Ther.* 32, 67–82. doi: 10.1089/jop.2015.0047

Yu, S., Zhang, X., Tan, G., Tian, L., Liu, D., and Liu, Y. (2017). A novel pH-induced thermosensitive hydrogel composed of carboxymethyl chitosan and poloxamer cross-linked by glutaraldehyde for ophthalmic drug delivery. *Carbohydr. Polym.* 155, 208–217. doi: 10.1016/j.carbpol.2016.08.073

Yu, Y., Lau, L. C. M., Lo, A. C., and Chau, Y. (2015). Injectable chemically crosslinked hydrogel for the controlled release of bevacizumab in vitreous: A 6-Month *in vivo* study. *Transl. Vis. Sci. Technol.* 4:5. doi: 10.1167/tvst.4.2.5

Zhang, Y., Yu, J., Ren, K., Zuo, J., Ding, J., and Chen, X. (2019). Thermosensitive hydrogels as scaffolds for cartilage tissue engineering. *Biomacromolecules* 20, 1478–1492. doi: 10.1021/acs.biomac.9b00043

Conflict of Interest: The authors declare that the research was conducted in the absence of any commercial or financial relationships that could be construed as a potential conflict of interest.

frontiers in Bioengineering and Biotechnology

PERSPECTIVE
published: 02 April 2020
doi: 10.3389/fbioe.2020.00258

A Methodological Safe-by-Design Approach for the Development of Nanomedicines

*Mélanie Schmutz[1], Olga Borges[2], Sandra Jesus[2], Gerrit Borchard[3], Giuseppe Perale[4], Manfred Zinn[5], Ädrienne A. J. A. M Sips[6], Lya G. Soeteman-Hernandez[6], Peter Wick[7] and Claudia Som[1]**

[1] Technology and Society Laboratory, Empa – Swiss Federal Laboratories for Materials Science and Technology, St. Gallen, Switzerland, [2] Center for Neuroscience and Cell Biology, Faculty of Pharmacy, University of Coimbra, Coimbra, Portugal, [3] School of Pharmaceutical Sciences Geneva-Lausanne, Geneva, Switzerland, [4] Polymer Engineering Laboratory, Department of Innovative Technologies, Mechanical Engineering and Materials Technology Institute, University of Applied Sciences and Arts of Southern Switzerland, Manno, Switzerland, [5] Institute of Life Technologies, University of Applied Sciences and Arts Western Switzerland (HES-SO Valais-Wallis), Sion, Switzerland, [6] National Institute for Public Health and the Environment, Bilthoven, Netherlands, [7] Particles-Biology Interactions Lab, Empa – Swiss Federal Laboratories for Materials Science and Technology, St. Gallen, Switzerland

OPEN ACCESS

Edited by:
Michele Iafisco, Italian National Research Council, Italy

Reviewed by:
Diana Boraschi, Istituto di Biochimica delle Proteine (IBP), Italy
Ivana Fenoglio, University of Turin, Italy
Henriqueta Louro, Instituto Nacional de Saúde Doutor Ricardo Jorge, Portugal

***Correspondence:**
Claudia Som
claudia.som@empa.ch

Specialty section:
This article was submitted to Nanobiotechnology, a section of the journal Frontiers in Bioengineering and Biotechnology

Received: *31 October 2019*
Accepted: *12 March 2020*
Published: *02 April 2020*

Citation:
Schmutz M, Borges O, Jesus S, Borchard G, Perale G, Zinn M, Sips ÄAJAM, Soeteman-Hernandez LG, Wick P and Som C (2020) A Methodological Safe-by-Design Approach for the Development of Nanomedicines. Front. Bioeng. Biotechnol. 8:258. doi: 10.3389/fbioe.2020.00258

Safe-by-Design (SbD) concepts foresee the risk identification and reduction as well as uncertainties regarding human health and environmental safety in early stages of product development. The EU's NANoREG project and further on the H2020 ProSafe initiative, NanoReg2, and CALIBRATE projects have developed a general SbD approach for nanotechnologies (e.g., paints, textiles, etc.). Based on it, the GoNanoBioMat project elaborated a methodological SbD approach (GoNanoBioMat SbD approach) for nanomedicines with a focus on polymeric nanobiomaterials (NBMs) used for drug delivery. NBMs have various advantages such as the potential to increase drug efficacy and bioavailability. However, the nanoscale brings new challenges to product design, manufacturing, and handling. Nanomedicines are costly and require the combination of knowledge from several fields. In this paper, we present the GoNanoBioMat SbD approach, which allows identifying and addressing the relevant safety aspects to address when developing polymeric NBMs during design, characterization, assessment of human health and environmental risk, manufacturing and handling, and combines the nanoscale and medicine field under one approach. Furthermore, regulatory requirements are integrated into the innovation process.

Keywords: Safe-by-Design, polymeric nanobiomaterials, nanocarriers, drug delivery, nanomedicine

INTRODUCTION

The concept of Safe-by-Design (SbD) was addressed in the field of nanotechnology because of the continuous uncertainty about the potentially harmful effects of nanomaterials on humans and the environment. Its implementation started with the Dutch NanoNextNL program[1] and the European NANoREG project and was further developed by the H2020 ProSafe initiative and

[1] www.nanonextnl.nl

H2020 NanoReg2 project (Soeteman-Hernandez et al., 2019). Since then, an increasing number of European Union projects focused on SbD for nanomaterials (Lynch, 2017). Even though various concepts of SbD coexist, they share the purpose of assessing safety as early as possible in the innovation process of a nanomaterial or nanoproducts. They aim at reducing adverse effects on human health and the environment by altering nanoproduct design (Soeteman-Hernandez et al., 2019) and by ensuring safety along its lifecycle (Bottero et al., 2017; Kraegeloh et al., 2018). The SbD concept is therefore different from conventional risk assessment approaches, which only consider safety when the product is already fully developed (Schwarz-Plaschg et al., 2017).

Despite being a rather novel concept in the context of nanotechnology, the principle behind SbD is not new and already applied by other industries (Kraegeloh et al., 2018). The medicine field has also long expertise in ensuring safety throughout the drug discovery and development process (Hjorth et al., 2017). However, how to handle safety issues effectively at the very beginning of drug development, to allow the selection of drug candidates, and mitigate toxicity is still being investigated (Kramer et al., 2007; Loiodice et al., 2019). The concept of Quality-by-Design (QbD) is widely used by pharmaceutical industry and its implementation is foreseen by the pharmaceutical development guidelines. The SbD is a new concept for the Pharmaceutical industry and it is not yet included in ICH, EMA, or FDA guidelines. This means that even if safety is considered during the pharmaceutical development, there is no systematic SbD approach yet in place. The concept of QbD presupposes the definition of the critical quality attributes (CQA) that will lead to the achievement of a product with proven effectiveness and the SbD would establish CQA that will lead to a product with high safety.

The application of nanotechnology in the medicine field (nanomedicine) brought new barriers precluding the prediction of potential adverse effects to human health and the environment because of the complexity of nanobiomaterials (NBMs). The unpredictability of nanomedicines' interaction with biological systems makes it difficult to bring these to the market (Resnik and Tinkle, 2007; Accomasso et al., 2018) and consequently, their potential benefits in medicine are still underexploited (Tinkle et al., 2014; Troiano et al., 2016). The lack of guidelines, standards and tools adapted to nanomedicines for assessing their risks represents one of the causes for this situation (Accomasso et al., 2018).

The development of such products remains therefore challenging. In addition, nanomedicines are costly and based on an interdisciplinary approach. They are at the junction of pharma, medtech, biotech and nanotech companies, and academia, which are important economic and social players in Switzerland and Europe. These companies may have different roles in the value chain of nanomedicines' development and as they have different backgrounds, they may have various needs to overcome the complexity of nanotechnology for medical applications.

As there is no systematic SbD approach in place for nanomedicines and that not all actors (coming from different fields) are experienced in considering safety to reduce risks on human health and the environment, there is a need for a methodological approach enabling to consider all necessary aspects to evaluate the safety of nanomedicines early during product development. This would ultimately improve the efficiency of the innovation process and the collaboration of all involved interdisciplinary actors and thus ensure the development of a safe product from the beginning of the process.

In order to fill this gap, within the GoNanoBioMat project,[2] we aimed at elaborating a methodological SbD approach by taking up the principles of the SbD approach developed for nanotechnologies in general and by adapting it to the field of nanomedicines. The developed methodological approach has a focus on polymeric nanocarriers for drug delivery (Som et al., 2019) as they are valuable materials, widely used to prepare nanoparticles and microparticles for the purpose of encapsulating drugs (Etheridge et al., 2013), can be biodegradable, biocompatible, and can be tailored to have targeting abilities (Bennet and Kim, 2014; Moritz and Geszke-Moritz, 2015). Therefore, these materials are expected to increase drug efficacy and safety (Ariën and Stoffels, 2016).

The aim of this paper is (1) to present what we adapted from the SbD concept developed within the EU projects NANoREG and NanoReg2, and the ProSafe initiative (hereafter general SbD approach) for the field of nanomedicines and (2) present the methodological SbD approach (hereafter the GoNanoBioMat SbD approach).

ADAPTATION OF THE GENERAL SbD APPROACH TO NANOMEDICINES

The general SbD approach can be applied in many different fields (e.g., paints, textiles, etc.), is addressed to industries, and can be used by regulators as a reference tool (Kraegeloh et al., 2018). Its goal is to "*reduce uncertainties and risks of human and environmental safety of nanotechnology, starting as early as possible during the innovation process, on the basis of mandatory and voluntary safety and efficacy compliance requirements*" (Soeteman-Hernandez et al., 2019). The main elements of the general SbD approach are: (1) it uses a stage-gate innovation approach, (2) it is based on three pillars, which are *Safe materials and products*, *Safe production,* and *Safe use and end-of-life*; (3) it includes SbD action for maximizing safety while maintaining functionality, and (4) it is integrated into a *Safe Innovation Approach* (see extensive description in Kraegeloh et al., 2018; Soeteman-Hernandez et al., 2019). Below we show how we changed or adapted these elements of the general SbD approach to nanomedicines (the comparison can be seen in **Table 1**).

As can be seen in **Table 1**, the GoNanoBioMat SbD approach is not based on a stage-gate innovation approach. Instead, it is an iterative approach. This decision was made in order to better represent the reality of "drug discovery and development" field, which also uses an iterative approach (Hjorth et al., 2017). In addition, the iterations are necessary to build up knowledge, as

[2]The GoNanoBioMat project was initiated by the ProSafe initiative

TABLE 1 | Comparison of the general SbD approach developed by NANoREG, NanoReg2, and the ProSafe initiative with the GoNanoBioMat SbD approach.

Comparison of the general and GoNanoBioMat SbD approaches	
General SbD approach	***GoNanoBioMat SbD approach***
Built on the stage-gate innovation approach	Built on an iterative approach
Based on three design pillars: (1) Safe materials and products for human health and the environment (2) Safe production for occupational health (3) Safe use and end-of-life for preventing exposure during use and having adapted recycling and disposal routes	Based on three design pillars: (1) Safe Nanobiomaterials: designing low-hazard NBMs for specific drug delivery applications by assessing human health and environmental risks (2) Safe Production: manufacturing and control of NBMs to ensure their safety and quality (3) Safe Storage and Transport: ensuring the safety and quality of NBMs
It includes Safe-by-Design actions for maximizing safety while maintaining functionality	It includes Safe-by-Design actions for maximizing safety while optimizing efficacy and costs
It is integrated into a Safe Innovation Approach (SIA), which combines the SbD concept and the Regulatory Preparedness (RP) concept. It provides a Trusted Environment (TE), which is a space for enabling a dialogue among stakeholders and regulators for sharing and exchanging knowledge on nanomaterials	It is embedded into and frames the guidelines, which provides the state of scientific knowledge by meta-analysis, specific methods for production of nanocarriers, relevant endpoints to test, and safety aspects to consider

it will be shown in the section "GoNanoBioMat SbD Approach," on physico-chemical properties and their biological effects. This is because currently, it is not possible to predict these effects only based on literature and modeling.

The GoNanoBioMat SbD approach is also based on three pillars (**Table 1**), but these were modified to match the scope of the topic at hand. The pillar *Safe Nanobiomaterials* corresponds to the first pillar of the general SbD approach and has the same aim. In the general and GoNanoBioMat SbD approaches, the second pillar is *Safe Production*. However, the focus in the GoNanoBioMat SbD approach is not only on the safety of workers but also on ensuring safety and quality of the NBMs and on applying good manufacturing practices (GMP), which are a prerequisite to produce medicines and consequently nanomedicines. On the one hand, the third pillar of the general SbD approach is about *Safe use and end-of-life*. Its main goal is to prevent exposure during use and to have adapted recycling and disposal routes. On the other hand, the third pillar of the GoNanoBioMat SbD approach is about *Safe Storage and Transport* in order to ensure the safety and quality of NBMs because they may experience transformations (Cobaleda-Siles et al., 2017), which may affect their safety and quality (USP36–NF31, 2012; European Commission, 2013). Storage, and more particularly shelf-life, is an aspect being highly connected to the logistics and costs of the final nanomedicine and therefore its viability on the market (Diven et al., 2015). As can be seen, here the pillar is a bit narrower than in the general approach. This is to better represent the needs for developing nanomedicines.

Both approaches include SbD actions (**Table 1**). The difference between the two is that the functionality is specified into efficacy in the GoNanoBioMat SbD approach. It was changed into efficacy because efficacy is a measurement of the successful pharmacological effect of a drug and therefore more representative for developing nanomedicines. The goal of these SbD actions is to maximize safety while optimizing efficacy and costs by comparing different forms of NBMs. However, it should be pointed out that sometimes it is not feasible to maximize both efficacy and safety at the same time (Soeteman-Hernandez et al., 2019). Optimization will always require iterations in order to be able to balance efficacy and safety (Hjorth et al., 2017).

Finally, in **Table 1** it is possible to see that the general SbD approach is integrated into a *Safe Innovation Approach* and provides a *Trusted Environment* (Soeteman-Hernandez et al., 2019). The *Safe Innovation Approach* combines the SbD concept and the *Regulatory Preparedness* concept. The *Regulatory Preparedness* concept being the improvement of anticipation of regulators to keep up with the fast growing knowledge on nanomaterials and thus facilitate the development of adaptable regulations. The *Trusted Environment* is a space for enabling a dialogue among stakeholders and regulators for sharing and exchanging knowledge on nanomaterials. The GoNanoBioMat SbD approach, however, is embedded into and sets the frame for a document whose title is "Guidelines for implementing a SbD approach for medicinal polymeric nanocarriers" written and published by the GoNanoBioMat project consortium (Som et al., 2019). The guidelines provide the state of scientific knowledge with meta-analyses, decision trees, methods for producing NBMs, relevant endpoints to test, and safety aspects to consider early and throughout the development of polymeric NBMs for drug delivery. The guidelines can be downloaded under this link: www.empa.ch/gonanobiomat.

GoNanoBioMat SbD APPROACH

As mentioned, the GoNanoBioMat SbD approach is a methodological approach for developing nanomedicines with a focus on polymeric NBMs for drug delivery and is presented in **Figure 1**. It contains the following steps: *Material Design*, *Characterization*, *Human Health* and *Environmental Risks* (first pillar), *Manufacturing and Control* (second pillar), and *Storage and Transport* (third pillar). The regulatory framework for developing nanomedicines is also included within the approach starting at the end of the *Material Design* step. The bullet points inside the boxes correspond to methods and tools that can be used or endpoints that should be considered and tested in each step. The blue arrows represent the flow of polymeric NBMs from their design until their storage and transport. The red arrows are feedback loops (iterations) going back to the *Material Design* step.

It is important to note, that most of these steps also apply to other NBMs and other type of nanomedicine applications. For example, the *Human Health* and *Environmental Risks* steps

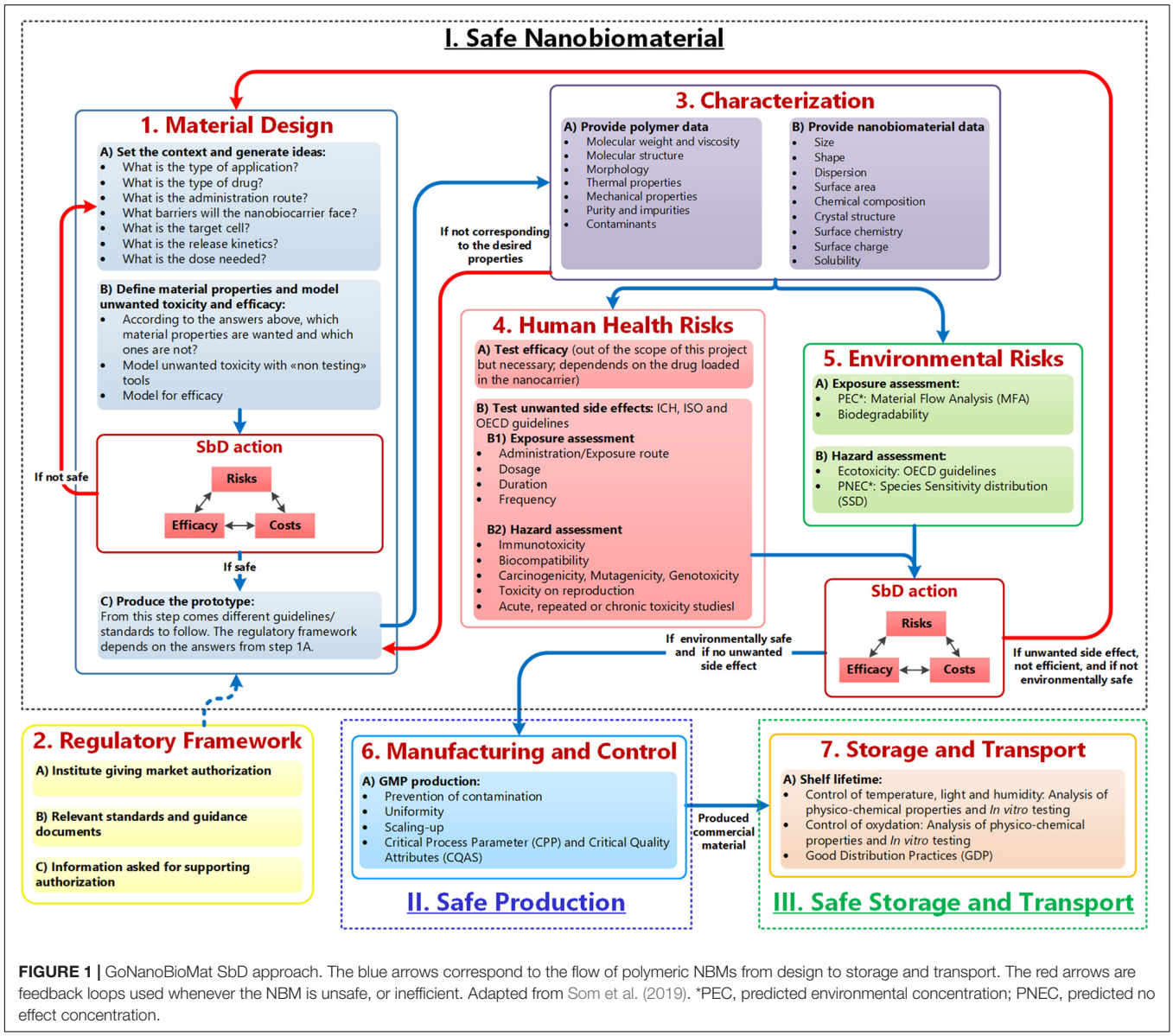

FIGURE 1 | GoNanoBioMat SbD approach. The blue arrows correspond to the flow of polymeric NBMs from design to storage and transport. The red arrows are feedback loops used whenever the NBM is unsafe, or inefficient. Adapted from Som et al. (2019). *PEC, predicted environmental concentration; PNEC, predicted no effect concentration.

could be applied to any type of NBMs. However, in the *Material Design* step and in the *Characterization* step, specific questions (e.g., what is the type of drug and what is the release kinetics) for drug delivery and specific parameters to characterize polymers are provided, respectively. Therefore, the total of questions only applies to polymeric NBMs for drug delivery, even if many questions also apply to other NBMs or other applications.

As can be seen in **Figure 1**, the GoNanoBioMat SbD approach starts with the *Material Design* step. This step is divided into three sub-steps, which are (a) set the context and generate ideas, (b) define material properties and screen for unwanted toxicity and efficacy, and (c) produce the prototype.

In the first sub-step, a set of questions can be used to guide the conceptual process for developing NBMs for drug delivery, and searching for the relevant literature. The questions include the type of application, type of drug (possibility of chemical interaction between drug and polymer), administration route, the biological barriers, target cells, release kinetics, and dose needed. All these aspects influence the design of nanocarriers (Elsabahy and Wooley, 2012), in other words, its physicochemical properties to be efficient as a drug delivery system and lining up for safe application. An important consideration to bear in mind is that the properties of the polymer (particles larger than 1 micron) may not be equal to the properties of the polymer when the size of its particles is reduced to the nanoscale. Once the data from literature are collected, the data can be used to screen for efficacy but also toxicity and to define the wished material properties of the nanocarriers (second sub-step) by using modeling tools (i.e., non-testing tools), such as quantitative structure–activity relationship tools (OECD, 2007). These tools have for aim to find a correlation between NBMs properties and their corresponding

effect (e.g., cell internalization, cytotoxicity) and may enable to assess whether a material is safe for medical purposes. However, it has to be noted that such methods still need to be further developed.

As aspects of safety and functionality should be taken into account at the very beginning of the project's conception (Cobaleda-Siles et al., 2017), these two sub-steps based on literature and modeling are facilitating their consideration. However, assessing the human health risks in an early stage of innovation only based on data found in the literature is currently not adequate. This may be a result of the lack of standardized assays, which lead to a high variation in reported studies (Hofmann-Amtenbrink et al., 2015). Also some studies have no proper characterization and lack appropriate controls specific to the nanoscale (Jesus et al., 2019), which makes comparisons between toxicity outcomes difficult. Therefore, experimental studies are still needed.

After these two sub-steps, comes the first SbD action. Its goal is to compare different possible NBMs for the intended use/application, which was defined in the beginning of the *Material Design* step, and to select the NBMs having a good balance between, safety, efficacy, and costs. After this, the selected NBMs should be produced as prototypes.

These prototypes should be then characterized in order to be able to find relationships between physicochemical properties of NBMs and their biological effects, and thus apply the concept of SbD. As can be seen in **Figure 1**, the properties attributed to the polymer itself (e.g., molecular weight) and the properties attributed to the nanosize (e.g., size) should be characterized. If the desired properties of the prototypes do not correspond to the measured properties, the prototypes should go back to the prototype production sub-step in order to optimize the production process. One criterion in SbD requires understanding the variables contributing to undesired side effects (Lin et al., 2018). Therefore, to have a thorough characterization of polymeric NBMs, the *Characterization* step includes specific parameter to be tested for polymers NMBs, such as molecular weight, size and surface area. This step is also essential to determine later the CQAs, which are defined as "physical, chemical, biological, or microbiological properties or characteristics that should be within an appropriate limit, range, or distribution to ensure the desired product quality" (ICH Q8 (R2), 2009).

The next two steps are experimental steps to evaluate the human health and the environmental risks of the selected NBMs. For both, the exposure and the hazard should be evaluated. For the *Human Health Risks* step, the route of administration/exposure, the dosage, the duration and frequency should be determined as safety of NBMs depends on the route of administration/exposure and the resulting respective pharmacokinetic profiles (Jesus et al., 2019). For the hazard, the following endpoints should be tested: immunotoxicity, biocompatibility, carcinogenicity, mutagenicity, genotoxicity, toxicity on reproduction, acute, repeated, or chronic toxicity studies. All tested endpoints should as well include appropriate controls for the nanoscale. The proposed endpoints are in line with current regulation (Jesus et al., 2019).

In parallel, the assessment of the environmental risks should be performed. To do so, the predicted environmental concentration and the predicted no effect concentration have to be calculated (Hauser et al., 2019). The former can be assessed via a material flow analysis and the latter via performing a (probabilistic) species sensitivity distribution. For this, ecotoxicity data are needed, which can be obtained either via literature or experimentally by following OECD guidelines.

After the *Human Health* and *Environmental risks* steps comes the second SbD action. As for the first one, the goal is to compare the selected NBMs and choose the one maximizing safety, while optimizing efficacy and costs. At this point, either one NBM is selected as the final candidate or if no NBMs have a good balance between benefits and risks, the developer should go back to the *Material Design* step. The results of these two steps can help to build up a useful database. In other words, with iterations, a database with the experimental results could be established and these data could be used for modeling. Ultimately, it would enable better predictions of NMBs' efficacy and toxicity.

If one final candidate has been selected, the developer of NBMs should go to the *Manufacturing and Control* step. The goal of this step is to scale-up the production by applying GMP, preventing contamination and ensuring uniformity between the batches. In this step, CQAs of NBMs must be identified as well as Critical Process Parameters. These are defined as the "process parameters that influence CQAs and therefore should be monitored or controlled to ensure the process produces the desired quality" (ICH Q8 (R2), 2009). It can be noted that this step is typically valid for any type of NBMs.

After scale-up, usually the nanocarrier and their encapsulated drug system would go to clinical trials. However, as we did not include clinical trials in the approach because it was out of the scope of the project, the next step is *Storage and Transport*. The (nano)medicine stability studies have to be performed (SME Office, 2016; MDR, 2017), because nanocarriers and encapsulated drug, both, or just one of them, might experience degradation process during their life cycle, which might affect the quality and safety of the nanomedicine (Cobaleda-Siles et al., 2017).

Finally, the Swiss and European regulatory frameworks for the marketing authorization of nanomedicine is embedded within the GoNanoBioMat SbD approach. More information on this aspect can be directly found in the GoNanoBioMat guidelines.[3]

DISCUSSION

In case of nanomedicines, SbD approaches should be included in the International Council for Harmonisation of Technical Requirements for Pharmaceuticals for Human Use (ICH) guidelines and relevant OECD guidance and guidelines. ICH is unique in bringing together the regulatory authorities and pharmaceutical industry to discuss scientific and technical aspects of drug registration and thus to discuss what should be included within guidelines concerning the safety of the NBMs and nanomedicines.

[3]www.empa.ch/gonanobiomat

The GoNanoBioMat SbD approach is methodological, contains all important elements to consider in order to integrate safety early and throughout the development of polymeric NBMs for drug delivery. It can as well to a certain extent be applied to other types of NBMS and nanomedicine applications. Including safety in the design of NBMs is an important aspect, especially for nanomedicines, which are highly regulated, cost and time consuming, and complex. However, the approach should not be seen as a warranty of complete safety, because absolute safety is unreachable (Cobaleda-Siles et al., 2017; Hjorth et al., 2017; van de Poel and Robaey, 2017), and should therefore be considered as a design strategy (van de Poel and Robaey, 2017) since the past showed that each nanomedicine has to be taken as case-by-case (McNeil, 2009). As for the general SbD concept, it has no legal binding and does not replace regulatory requirements (Soeteman-Hernandez et al., 2019).

The GoNanoBioMat SbD approach was focusing only on the safety of nanocarriers (polymeric NBMs) and not on the nanocarriers and its encapsulated drug. For regulatory purpose, it is necessary to test the safety of the nanocarrier alone in addition to the nanocarrier/drug system. Therefore, this GoNanoBioMat SbD approach is a first step toward the integration of safety early in the development of such products. Efficacy, which is closely related to the drug used, could not be included in the approach and therefore must be evaluated case-by-case. In a future development of the GoNanoBioMat SbD approach adding steps for clinical trials and use will be developed.

Finally, we believe that the GoNanoBioMat SbD approach as presented here may facilitate the implementation of the general SbD concept and to find a balance between benefits and risks by comparing different nanocarrier candidates in terms of their respective safety, efficacy, and costs. For instance, the GoNanoBioMat SbD approach provides all relevant steps for developing polymeric NBMs; provides methodology and endpoints to test human health and environmental risks, which are in line with current regulations; is an iterative process; and combines the nanoscale and medicine field under one methodological approach. In addition, the approach may bring the different actors of the value chain on a common ground. Ultimately, the approach may enable to move toward safe and efficient NBMs, safe production, and safe storage and transport.

AUTHOR CONTRIBUTIONS

MS created the GoNanoBioMat SbD approach in collaboration with CS, OB, SJ, PW, GB, GP, ÄS, and LS-H. MS wrote the manuscript. CS wrote some part of the manuscript. OB, SJ, PW, GB, GP, ÄS, and LH read and reviewed the manuscript. All authors approved the submitted version.

FUNDING

This study is part of the GoNanoBioMat project and has received funding from the Horizon 2020 framework program of the European Union, ProSafe Joint Transnational Call 2016; CTI (1.1.2018 Innosuisse), under grant agreement Number 19267.1 PFNM-NM; and FCT Foundation for Science and Technology under the project PROSAFE/0001/2016.

REFERENCES

Accomasso, L., Cristallini, C., and Giachino, C. (2018). Risk assessment and risk minimization in nanomedicine: a need for predictive, alternative, and 3Rs Strategies. *Front. Pharmacol.* 9:228. doi: 10.3389/fphar.2018.00228

Ariën, A., and Stoffels, P. (2016). "History: potential, challenges, and future development in nanopharmaceutical research and industry," in *Pharmaceutical Nanotechnology: Innovation and Production*, eds J. Cornier, A. Owen, A. Kwade, and M. H. Vander Voorde (Hoboken, NJ: Wiley), 3–12.

Bennet, D., and Kim, S. (2014). "Polymer nanoparticles for smart drug delivery," in *Application of Nanotechnology in Drug Delivery*, ed. A. D. Sezer (London: IntechOpen), 257–310.

Bottero, J. Y., Rose, J., Garidel, C., De, Masion, A., Deutsch, T., et al. (2017). Serenade: safer and ecodesign research and eductaion applied to nanomaterial development, the new generation of materials safer by design. *Environ. Sci. Nano* 4, 526–538. doi: 10.1039/c6en00282j

Cobaleda-Siles, M., Guillamon, A. P., Delpivo, C., Vázquez-Campos, S., and Puntes, V. F. (2017). Safer by design strategies. *J. Phys. Conf. Ser.* 838:012016. doi: 10.1088/1742-6596/838/1/012016

Diven, D. G., Bartenstein, D. W., and Carroll, D. R. (2015). Extending shelf life just makes sense. *Mayo Clin. Proc.* 90, 1471–1474. doi: 10.1016/j.mayocp.2015.08.007

Elsabahy, M., and Wooley, K. L. (2012). Design of polymeric nanoparticles for biomedical delivery applications. *Chem. Soc. Rev.* 41, 2545–2561. doi: 10.1039/c2cs15327k

Etheridge, M. L., Campbell, S. A., Erdman, A. G., Haynes, C. L., Wolf, S. M., and McCullough, J. (2013). The big picture on nanomedicine: the state of investigational and approved nanomedicine products. *Nanomed. Nanotechnol. Biol. Med.* 9, 1–14. doi: 10.1016/j.nano.2012.05.013

European Commission. (2013). Information from European Union institutions, bodies, offices and agencies, european commission guidelines of 5 november 2013 on good distribution practice of medicinal products for human use (Text with EEA relevance) (2013/C 343/01). *Offi. J. Eur. Union* 2013, C343/1–14.

Hauser, M., Li, G., and Nowack, B. (2019). Environmental hazard assessment for polymeric and inorganic nanobiomaterials used in drug delivery. *J. Nanobiotechnol.* 17, 1–10.

Hjorth, R., Hove, L., Van, and Wickson, F. (2017). What can nanosafety learn from drug development? The feasibility of "safety by design". *Nanotoxicology* 11, 305–312. doi: 10.1080/17435390.2017.1299891

Hofmann-Amtenbrink, M., Grainger, D. W., and Hofmann, H. (2015). Nanoparticles in medicine: current challenges facing inorganic nanoparticle toxicity assessments and standardizations. *Nanomedicine Nanotechnology Biol. Med.* 11, 1689–1694. doi: 10.1016/j.nano.2015.05.005

ICH Q8 (R2) (2009). *Requirements for Registration of Pharmaceuticals for Human Use - Guidlines for Elemental Impurities*. Guidel: ICH Harmon.

Jesus, S., Schmutz, M., Som, C., Borchard, G., Wick, P., and Borges, O. (2019). Hazard assessment of polymeric nanobiomaterials for drug delivery: what can we learn from literature so far. *Front. Bioeng. Biotechnol.* 7:261. doi: 10.3389/fbioe.2019.00261

Kraegeloh, A., Suarez-merino, B., Sluijters, T., and Micheletti, C. (2018). Implementation of Safe-by-Design for nanomaterial development and safe innovation: why we need a comprehensive approach. *Nanomaterials* 8:239. doi: 10.3390/nano8040239

Kramer, J. A., Sagartz, J. E., and Morris, D. L. (2007). The application of discovery toxicology and pathology towards the design of safer pharmaceutical lead candidates. *Nat. Rev. Drug Discov.* 6, 636–649. doi: 10.1038/nrd2378

Lin, S., Yu, T., Yu, Z., Hu, X., and Yin, D. (2018). Nanomaterials safer-by-design: an environmental safety perspective. *Adv. Mater.* 30:1705691. doi: 10.1002/adma.201705691

Loiodice, S., Nogueira, da Costa, A., and Atienzar, F. (2019). Current trends in silico, in vitro toxicology, and safety biomarkers in early drug development. *Drug Chem. Toxicol.* 42, 113–121. doi: 10.1080/01480545.2017.1400044

Lynch, I. (2017). *Compendium of Projects in the European NanoSafety Cluster*. Birmingham: University of Birmingham, 259.

McNeil, S. E. (2009). Nanoparticle therapeutics: a personal perspective. *Wiley Interdiscip. Rev. Nanomed. Nanobiotechnol.* 1, 264–271. doi: 10.1002/wnan.6

MDR (2017). *Regulation (EU) 2017/745 of the European Parliament and of the Council of 5 April 2017 on Medical Devices, Amending Directive 2001/83/EC, Regulation (EC) No 178/2002 and Regulation (EC) No 11223/2009 and Repealing Council Directives 90/385/EEC and 93/42/EEC*. Available online at: https://eur-lex.europa.eu/legal-content/EN/ALL/?uri (accessed October 29, 2019).

Moritz, M., and Geszke-Moritz, M. (2015). Recent developments – In the application of polymeric nanoparticles as drug carriers. *Adv. Clin. Exp. Med.* 24, 749–758. doi: 10.17219/acem/31802

OECD (2007). *Guidance Document on the Validation of (quantitative) Structure-Activity Relationship [(Q)SAR] models. OECD Environment, Health and Safety Publications. Series on Testing and Assessment No.* 69. ENV/JM/MONO (2007) 2. Paris: Organisation for Economic Co-operation and Development.

Resnik, D. B., and Tinkle, S. S. (2007). Ethics in nanomedicine. *Nanomedicine* 2, 345–350. doi: 10.2217/17435889.2.3.345

Schwarz-Plaschg, C., Kallhoff, A., and Eisenberger, I. (2017). Making nanomaterials safer by design? *Nanoethics* 11, 277–281. doi: 10.1007/s11569-017-0307-4

SME Office (2016). *User Guide for Micro, Small and Medium-Sized Enterprises (SMEs)*. Amsterdam: European Medicines Agency, 44.

Soeteman-Hernandez, L. G., Apostolova, M. D., Bekker, C., Dekkers, S., Grafström, R. C., Groenewold, M., et al. (2019). Safe innovation approach: towards an agile system for dealing with innovations. *Mater. Today Commun.* 20:100548. doi: 10.1016/j.mtcomm.2019.100548

Som, C., Schmutz, M., Borges, O., Jesus, S., Borchard, G., Nguyen, V., et al. (2019). *Guidelines for Implementing a Safe-by-Design Approach for Medicinal Polymeric Nanocarriers*. Available online at: www.empa.ch/gonanobiomat.

Tinkle, S., Mcneil, S. E., Mühlebach, S., Bawa, R., Borchard, G., Barenholz, Y. C., et al. (2014). Nanomedicines: addressing the scientific and regulatory gap. *Ann. N. Y. Acad. Sci.* 1313, 35–56. doi: 10.1111/nyas.12403

Troiano, G., Nolan, J., Parsons, D., Van Geen Hoven, C., and Zale, S. (2016). A quality by design approach to developing and manufacturing polymeric nanoparticle drug products. *AAPS J.* 18, 1354–1365. doi: 10.1208/s12248-016-9969-z

USP36–NF31 (2012). *USP36–NF31, G. C* 1079 Good Storage and Distribution Practices for Drug Products. Rockville, MD: The United States Pharmacopeial Convention.

van de Poel, I., and Robaey, Z. (2017). Safe-by-design: from safety to responsibility. *Nanoethics* 11, 297–306. doi: 10.1007/s11569-017-0301-x

Conflict of Interest: The authors declare that the research was conducted in the absence of any commercial or financial relationships that could be construed as a potential conflict of interest.

frontiers in Bioengineering and Biotechnology

BRIEF RESEARCH REPORT
published: 30 June 2020
doi: 10.3389/fbioe.2020.00718

Permeation of Biopolymers Across the Cell Membrane: A Computational Comparative Study on Polylactic Acid and Polyhydroxyalkanoate

Tommaso Casalini[1], Amanda Rosolen[1], Carolina Yumi Hosoda Henriques[1] and Giuseppe Perale[1,2]*

[1] Polymer Engineering Laboratory, Department of Innovative Technologies, Institute for Mechanical Engineering and Materials Technology, University of Applied Sciences and Arts of Southern Switzerland, Manno, Switzerland, [2] Ludwig Boltzmann Institute for Experimental and Clinical Traumatology, Vienna, Austria

Polymeric nanoparticles, which by virtue of their size (1–1000 nm) are able to penetrate even into cells, are attracting increasing interest in the emerging field of nanomedicine, as devices for, e.g., drugs or vaccines delivery. Because of the involved dimensional scale in the nanoparticle/cell membrane interactions, modeling approaches at molecular level are the natural choice in order to understand the impact of nanoparticle formulation on cellular uptake mechanisms. In this work, the passive permeation across cell membrane of oligomers made of two employed polymers in the biomedical field [poly-D,L-lactic acid (PDLA) and poly(3-hydroxydecanoate) (P3HD)] is investigated at fundamental atomic scale through molecular dynamics simulations. The free energy profile related to membrane crossing is computed adopting umbrella sampling. Passive permeation is also investigated using a coarse-grained model with MARTINI force field, adopting well-tempered metadynamics. Simulation results showed that P3HD permeation is favored with respect to PDLA by virtue of its higher hydrophobicity. The free energy profiles obtained at full atomistic and coarse-grained scale are in good agreement each for P3HD, while only a qualitative agreement was obtained for PDLA. Results suggest that a reparameterization of non-bonded interactions of the adopted MARTINI beads for the oligomer is needed in order to obtain a better agreement with more accurate simulations at atomic scale.

Keywords: molecular dynamics, lipid bilayer, permeation, molecular modeling, biopolymers

OPEN ACCESS

Edited by:
Emilio Isaac Alarcon, University of Ottawa, Canada

Reviewed by:
Jeffrey Robert Comer, Kansas State University, United States
Ariela Vergara, University of Talca, Chile

****Correspondence:***
Tommaso Casalini
tommaso.casalini@supsi.ch

Specialty section:
This article was submitted to Biomaterials, a section of the journal Frontiers in Bioengineering and Biotechnology

Received: *01 December 2019*
Accepted: *08 June 2020*
Published: *30 June 2020*

Citation:
Casalini T, Rosolen A, Henriques CYH and Perale G (2020) Permeation of Biopolymers Across the Cell Membrane: A Computational Comparative Study on Polylactic Acid and Polyhydroxyalkanoate. Front. Bioeng. Biotechnol. 8:718. doi: 10.3389/fbioe.2020.00718

INTRODUCTION

The detailed knowledge of drug/membrane interactions plays a key role for the determination of the ADME (adsorption, distribution, metabolism and excretion) profile of active compounds. The efficacy of an administered drug also depends on its ability to cross cellular membranes or barriers of biological interest, such as the blood–brain barrier, to reach the desired target. Membrane permeation can occur through different mechanisms; passive diffusion (i.e., membrane crossing due to the concentration gradient) plays a key role when small uncharged molecules are involved (Smith et al., 2014) and its detailed understanding is essential for drug design. There are established experimental techniques and protocols for investigating drug permeation in model membranes, but their limited spatial resolution does not allow shedding light behind the specific interactions. Simulations at fundamental molecular level emerged as the ideal tool

to improve our knowledge, thanks to the detail at atomic scale that allows highlighting the most relevant interactions behind the observed or expected permeation rate (Di Meo et al., 2016; Shinoda, 2016). A lipid bilayer is a heterogeneous environment because of the presence of polar head groups and hydrophobic chains (Nagle and Tristram-Nagle, 2000). These aspects can be accounted for, in detail, by means of simulations at molecular level, which allow developing mechanistic interpretations and models for lipophilic compounds permeation, as widely discussed by Dickson and coworkers (Dickson et al., 2017). In this regard, the growing use of computational techniques such as molecular dynamics (MD) simulations is the result of several aspects: First, the increasing availability of computational resources, coupled with software optimization, which lead to affordable and meaningful simulations. Second, the continuous development and improvement of accurate force fields tailored for lipid bilayers; indeed, the reliability of MD simulations outcomes is strongly dependent on the robustness of the chosen force field, whose importance cannot be underestimated. Third, it should be mentioned that membrane permeation usually involves an energy barrier much higher than the thermal energy k_BT (where k_B is Boltzmann constant and T is absolute temperature) available to molecule in standard simulation at temperature T. This implies that a membrane crossing event would rarely be observed in a standard MD simulation, while multiple events should occur in a simulation in order to obtain statistically meaningful results. In other words, the characteristic time scale of molecule diffusion is larger than the time scale accessible to MD simulations. This issue can be overcome by means of enhanced sampling methods, which enhance the transition between metastable states separated by free energy barriers higher than k_BT. The most popular method for drug/membrane interactions is umbrella sampling (US) (Torrie and Valleau, 1977), which allows obtaining the potential of mean force (PMF) as a function of a relevant reaction coordinate, usually taken as the distance between the center of the membrane and the center of mass of the molecule of interest. Position-dependent diffusion coefficients and permeation coefficients can be also obtained through the inhomogeneous solubility-diffusion model (ISDM) (Marrink and Berendsen, 1994). Such protocol is still widely employed nowadays for different systems of interest (Bochicchio et al., 2015; Dickson et al., 2017, 2019; Teixeira and Arantes, 2019). Another useful technique is constituted by well-tempered metadynamics (WTMD) (Barducci et al., 2008); briefly, WTMD allows recovering the free energy landscape of the system of interest as a function of few relevant degrees of freedom [commonly referred as collective variables (CV)] by adding a time-dependent bias. WTMD attracted some interest for the study of the permeation of small molecules, because of its increased computational efficiency with respect to US and to the possibility to add easily a bias potential to other CV that can play a role in membrane permeation, such as permanent orientation or intramolecular hydrogen bonds (Minozzi et al., 2011; Jambeck and Lyubartsev, 2013; Loverde, 2014; Saeedi et al., 2017). Simulations usually consider the interaction of a single drug molecule with a model membrane, usually made of dioleoylphosphatidylcholine (DOPC) or dipalmitoylphosphatidylcholine (DPPC), thanks to the availability of validated force fields (Dickson et al., 2014; Ingolfsson et al., 2016; Frederix et al., 2018). The use of a model membrane is an accepted approximation; adopting more realistic models still suffers from the lack of experimental data needed to validate force field parameters (Poger et al., 2016) but there is an increasing number of examples of heterogeneous membranes in literature. A common solution is the addition of cholesterol or other molecules in the model membrane (Murzyn et al., 2005; Hoopes et al., 2011; Tse et al., 2018). Recently, Tse et al. (2019) proposed a full atomistic model of a mammalian cell membrane, which contains 26 different components. The same considerations can be in principle extended also to biomaterials/membrane interactions, whose simulations are attracting an increasing interest because of the new paradigms introduced by nanomedicine. Indeed, simulations at fundamental molecular level, due to the involved time and length scales, are the natural modeling tool for improve our understanding of the interactions between nanocarriers (whose size is between 1 and 1000 nm) and biological components (proteins, carbohydrates, membranes, *et cetera*). Focusing on biomaterials/membrane interactions, on the one side, nanocarriers such as nanoparticles can cross the cellular membrane also through passive permeation. On the other side, when bioresorbable polymers are employed, degradation products can permeate through cellular membranes and accumulate into the cells, thus leading to adverse effects. Overall, this approach matches the requirements of the "safety by design" paradigm too. Because of the involved time and length scales, MD simulations with enhanced sampling methods are not always suitable to investigate nanoparticles/membrane interactions (Schulz et al., 2012; Casalini et al., 2019a) and coarse-grained (CG) models should be employed. As recently discussed (Ingolfsson et al., 2014; Lunnoo et al., 2019), CG models also allow including heterogeneous lipid bilayers, moving toward a more realistic description of the cellular membranes. Despite the loss of the atomic detail, they provide interesting insights if accurately parameterized against experimental data or full atomistic simulations (Marrink and Tieleman, 2013). Parameterization can be performed, e.g., by reproducing with a CG model the PMF of interested obtained with MD simulations (de Jong et al., 2013). In this work, we study by means of molecular dynamics simulations the diffusion across a DOPC model membrane of small oligomers made of poly-D,L-lactic acid (PDLA) and poly(3-hydroxydecanoate) (P3HD) chosen as representative compound of the family of polyhydroxyalkanoates (PHA). PDLA and PHA gained a wide interest in the biomedical field since they merge several interesting peculiarities, such as biocompatibility, good mechanical properties and an *in situ* degradation due to hydrolysis mechanism (Bassas-Galia et al., 2017; Butt et al., 2018; Casalini et al., 2019b). This led to the development of a wide range of biomedical devices, from bone fixation screws to nanoparticles for targeted drug delivery. On the one side, the excessive accumulation of degradation products inside cells may lead to adverse effects (Ramot et al., 2016); on the other side, a deeper understanding of the endocytic pathway for nanoparticle uptake can support the experimental design of new and more effective formulations. This constitutes the starting

point of this work, which is structured as follows. First, the free energy landscape related to the permeation of small PDLA and P3HD oligomers (representative of degradation products from polymer hydrolysis) is obtained adopting umbrella sampling. Membrane crossing is subsequently simulated adopting a coarse-grained model and the free energy landscape is computed by means of WTMD. The assessment of the suitability of a coarse-grained model, parameterized on more accurate simulations at atomic scale, is fundamental to investigate the permeation of entire nanoparticles in model membranes, which would not be feasible with full atomistic simulations due to the involved time and length scales.

METHODS

Force Field Parameterization

The second-generation general amber force field (GAFF2) (Wang et al., 2004) was employed for PDLA and P3HD. Atomic charges were computed by means of restrained electrostatic potential (RESP) method (Bayly et al., 1993; Cornell et al., 1993), consistently with force field parameterization procedure. Oligomers composed of 6 monomer units were optimized *in vacuo* through density functional theory (DFT) calculations at B3LYP/6-31G(d,p) level of theory. The obtained conformations were subsequently employed to compute electrostatic potentials *in vacuo* at HF/6-31G* level of theory. Calculations were performed my means of Gaussian09 software (Frisch et al., 2016). Atomic charges were then fitted by means of RESP procedure, adopting a two-step protocol. First, partial atomic charges were calculated starting from the previously obtain electrostatic potential values, imposing an overall charge value equal to zero. In the second step, charge equivalence is imposed for chemically equivalent atoms. This procedure allowed obtaining a library of building blocks that can be used to build polymer chains of different length. Lipid17 force field (Dickson et al., 2014) was adopted for DOPC lipid bilayer because of its validated parameters. TIP3P water model (Jorgensen et al., 1983) was employed for explicit solvent molecules, consistently with force field parameterization. Parameters for monovalent ions, optimized for TIP3P model, were taken from Joung and Cheatham (2008, 2009). Details are reported in **Supplementary Material**.

Creation of the Molecular Models

Polymer chains were built using *tLeap* module included in *AmberTools*; chain ends were saturated with methyl groups. The same tool was used to solvate with TIP3P water molecules and add ions to assure electroneutrality, where needed. A DOPC lipid bilayer composed of 128 DOPC molecules was assembled and solvated by means of CHARMM-GUI web server (Wu et al., 2014; Lee et al., 2019). The membrane lies on *xy*-plane and water molecules were placed only along *z* direction, so that an infinite surface can be obtained by applying periodic boundary conditions. A suitable number of Na^+ and Cl^- was added to reach 0.15 M salt concentration, which mimics physiological conditions. The bilayer/polymer system was assembled starting from equilibrated configurations of the single components by means of *AddToBox* module included in *AmberTools*; ions were added in order to mimic physiological conditions. A coarse-grained model was built adopting MARTINI force field (Marrink et al., 2007), chosen for its validated results and its straightforward parameterization procedure. A bilayer composed of 128 DOPC molecules was built by means of CHARMM-GUI web server, similarly to the full atomistic model, with explicit water and ions beads. Parameters for bonded and non-bonded interactions of DOPC molecules are already available in MARTINI library. PDLA was coarse-grained by adopting 7 C5 beads, while P3HD was modeled using 7 Na beads for the backbone and one C1 bead and one C3 bead for each side chain. Structures are depicted in **Figures 4A,B**.

Parameters for bonded interactions were computed to best reproduce the bond, angle dihedral distributions obtained with MD simulations at full atomistic level. Parameters for non-bonded interactions were taken from MARTINI library. Details are reported in **Supplementary Material**.

Molecular Dynamics Simulations

Molecular dynamics simulations were performed according to the following protocol. First, energy minimization step procedure was carried out by fixing the solute with a harmonic restraint (force constant equal to 500 kcal mol^{-1} $Å^{-2}$), in order to remove bad solvent/solvent and solute/solvent contacts due to the random placement of water molecules. Energy minimization was subsequently repeated removing the restraint on solute molecules. Temperature was raised from 0 to 310 K by means of 20 ps in NVT ensemble (constant number of particles *N*, volume *V*, and temperature *T*). When the lipid bilayer was present in the simulation box, temperature was slowly increased from 0 to 310 K through 10 ns in NVT ensemble adopting a linear ramp. Solute was kept fixed through a weak harmonic restraint (force constant equal to 10 kcal mol^{-1} $Å^{-2}$); temperature was maintained to the desired production value by means of Langevin thermostat, adopting a collision frequency equal to 1 ps^{-1}. Finally, system equilibration was achieved by means of molecular dynamics simulations in NPT ensemble (i.e., at constant number of particles *N*, pressure *P*, and temperature *T*) at 310 K and 1 atm. Pressure was controlled by means of isotropic (for polymer/water systems) and anisotropic (for systems containing lipid bilayer) Berendsen barostat. Simulations were performed adopting periodic boundary conditions; the chosen cutoff value for long-range interactions was set equal to 1 nm. Particle Mesh Ewald (PME) was chosen for treating electrostatic interactions. SHAKE algorithm was employed to constrain all covalent bonds involving hydrogen atoms; this allowed propagating system dynamics through Leap-Frog algorithm using a time step equal to 2 fs. Simulations were carried out with GPU cards using the *pmemd.cuda* module implemented in AMBER 16 (Salomon-Ferrer et al., 2013; Case et al., 2016). A summary of performed MD simulations is reported in **Supplementary Material**.

Umbrella Sampling

Umbrella sampling was performed by choosing the distance between the center of mass (COM) of oligomer chain and the

center of the lipid bilayer as the relevant reaction coordinate (Di Meo et al., 2016; Shinoda, 2016). Simulations were carried out using 41 windows, covering a distance range from 0 to 40 Å with a spacing value equal to 1 Å.

Oligomers were restrained to the reference distance of each window by means of a harmonic potential with a force constant equal to 2.5 kcal mol^{-1} $Å^{-2}$, chosen so that a good overlap between distance distributions among adjacent windows could be obtained. Only the *z* component of the distance was subjected to the restraint, while oligomers were free to move along *x* and *y* directions.

First, the oligomer was placed in the center of the membrane by applying a harmonic potential and 40 ns MD simulation in NPT ensemble were carried out to reach equilibration. Then, Umbrella Sampling simulations were performed so that the oligomer was pulled out from membrane center to the external environment; indeed, it has been shown in scientific literature that this procedure (rather than gradually placing a molecule in the bilayer) improves the convergence of the results (Filipe et al., 2014); 80 ns MD simulations in NPT ensemble at 1 atm and 310 K were carried out for each window, leading to 3.2 μs of total sampling time for each system.

Free energy as a function of the chosen reaction coordinate was obtained by means of weighted histogram analysis method (WHAM) (Kumar et al., 1992; Roux, 1995), using a 0–40 Å distance grid with a grid spacing equal to 0.025 Å; a further decrease of grid spacing did not lead to appreciable variations of the obtained results.

For each window, the first 50 ns were used for system equilibration and discarded; free energy was computed using the last 30 ns, using three blocks of 10 ns each. Results are expressed as average ± standard deviation. Details are reported in **Supplementary Material**.

A position-dependent diffusion coefficient can be computed by means of inhomogeneous solubility-diffusion model (Marrink and Berendsen, 1994), which was applied in literature to small solutes (water, methanol, etc.) (Bemporad et al., 2004; Orsi et al., 2009; Lee et al., 2016) as well as to drug-like molecules (Dickson et al., 2017). Diffusivity as a function of z coordinate *D(z)* can be computed as follows (Hummer, 2005):

$$D(z) = \frac{var(z)^2}{\int_0^\infty C_{zz}(t)\,dt} \tag{1}$$

where $var(z)$ is the variance of the *z*-component of the distance in a US window and C_{zz} is the position autocorrelation function, defined as follows:

$$C_{zz}(t) = \delta z(0)\delta z(t) \tag{2}$$

$$\delta z(t) = z(t) - z \tag{3}$$

where $<z>$ is the average value of the distance in the US window.

Autocorrelation function was numerically integrated by means of *trapz* algorithm implemented in MATLAB (which takes advantage of the trapezoidal rule) until it decayed to $\mathrm{var}(z)\cdot 10^{-2}$, in order to exclude from the integration the noise around $C_{zz}(t) = 0$ (Dickson et al., 2017). The position-dependent resistance can be also computed:

$$R(z) = \frac{\exp(\beta \Delta G(z))}{D(z)} \tag{4}$$

where β is equal to $(k_B T)^{-1}$, k_B is Boltzmann constant, *T* is the absolute temperature, and $\Delta G(z)$ is the free energy profile. While $D(z)$ is evaluated for every window (41 values), $\Delta G(z)$ is obtained for every grid point. Therefore, in order to compute $R(z)$, the diffusion coefficient is evaluated along the distance grid using a shape-preserving interpolant by means of *mpich* algorithm implemented in MATLAB. An overall permeation coefficient can be obtained by integrating the resistance profile:

$$P_{eff} = \frac{1}{R_{eff}} = \frac{1}{\int_{-z_B}^{z_B} R(z)\,dz} \tag{5}$$

where the integration boundaries are referred to water phase at either side of the lipid bilayer (i.e., z_B = 40 Å and $-z_B$ = -40 Å). Binding free energy $\Delta G^0_{\mathrm{Bind}}$ and membrane partitioning constant K_{lip} can be also obtained:

$$\Delta G^0_{\mathrm{Bind}} = -k_B T\, ln\left(\frac{1}{z_B}\int_0^{z_B} \exp(-\beta \Delta G(z))\,dz\right) \tag{6}$$

$$K_{lip} = \exp(-\beta \Delta G^0_{\mathrm{Bind}}) \tag{7}$$

Coarse-Grained Simulations

Simulations were performed with GROMACS 2018.3 (Pall et al., 2015). Focusing on DOPC bilayer, after energy minimization the system was progressively equilibrated by running five simulations of 10 ns each in NPT ensemble at 310 K and 1 atm. A harmonic restraint was applied to lipid molecules, reducing the value of the force constant in each simulation; force constant values equal to 200, 100, 50, 20 and 10 kJ nm^{-2} mol^{-1} were chosen for this purpose. Temperature and pressure were controlled by means of velocity rescaling algorithm (Bussi et al., 2007) and semiisotropic Berendsen barostat, respectively, with coupling time constants equal to 1 and 12 ps. Finally, 600 ns in NPT ensemble at 310 K and 1 atm was performed, adopting velocity rescaling algorithm and semiisotropic Parrinello-Rahman barostat (Parrinello and Rahman, 1981) for temperature and pressure control, respectively. Coupling time constants were not modified. A cutoff value equal to 1.1 nm was chosen for long-range electrostatic and Van der Waals interactions, which were computed adopting a reaction field (with a dielectric constant beyond the cutoff equal to 15) and a straight cutoff. A potential modifier was applied to VdW interactions to better perform with the Verlet cutoff scheme. Periodic boundary conditions were applied along *x*, *y*, and *z* directions; dynamics were propagated using Leap-Frog algorithm using a time step equal to 20 fs.

WTMD simulations were carried out with GROMACS 2018.3 patched with PLUMED 2.5 (Tribello et al., 2014). PDLA and P3HD were added in the water phase in the simulation box of the equilibrated DOPC bilayer, replacing water beads if necessary, with the *insert-molecule* tool implemented in GROMACS. After energy minimization and a brief equilibration (20 ns) in NPT

ensemble at 310 K and 1 atm, WTMD simulations were carried out, considering the component along z direction of the distance between oligomer and bilayer centers of mass. The initial Gaussian height, sigma, and bias factor values were set equal to 0.8 kJ mol^{-1}, 0.05 Å, and 30, respectively. Bias potential was added every 5000 steps (100 ps). Harmonic potentials were applied by means of *upper_walls* and *lower_walls* algorithms implemented in PLUMED (force constant equal to 50 kJ mol^{-1} nm^{-2}) in order to promote membrane crossing events and to limit the CV exploration in a range of values of interest, i.e., between -45 and 45 Å.

The convergence of the free energy landscape was evaluated with two different methods, that is, checking the free energy difference as a function of simulation time and computing the error according to Bonomi et al. (2009):

$$\varepsilon^2(t) = \frac{1}{vol(\Omega)} \int ds \left[V(s,t) - F(s)\right]^2 \quad (8)$$

where ε is the error, t is time, s represents the chosen collective variables, Ω is the explored CV region, $V(s,t)$ is the external bias added to the system, and $F(s)$ is the reference free energy profile, i.e., the one obtained at the end of the simulation. Plots are reported in **Supplementary Material**.

Free energy profiles as well as binding free energies were computed as an average of the last 2000 ns.

RESULTS AND DISCUSSION

Oligomers and Lipid Bilayer Equilibration

First, MD simulations were carried out in order to obtain equilibrated structures of both oligomers and the DOPC lipid bilayer, which mimics a cellular membrane. Each oligomer was equilibrated with 50 ns MD simulations in NPT ensemble at 1 atm and 310 K (**Figures 1A,B**). The attainment of reasonable equilibrated structures was checked by computing the root

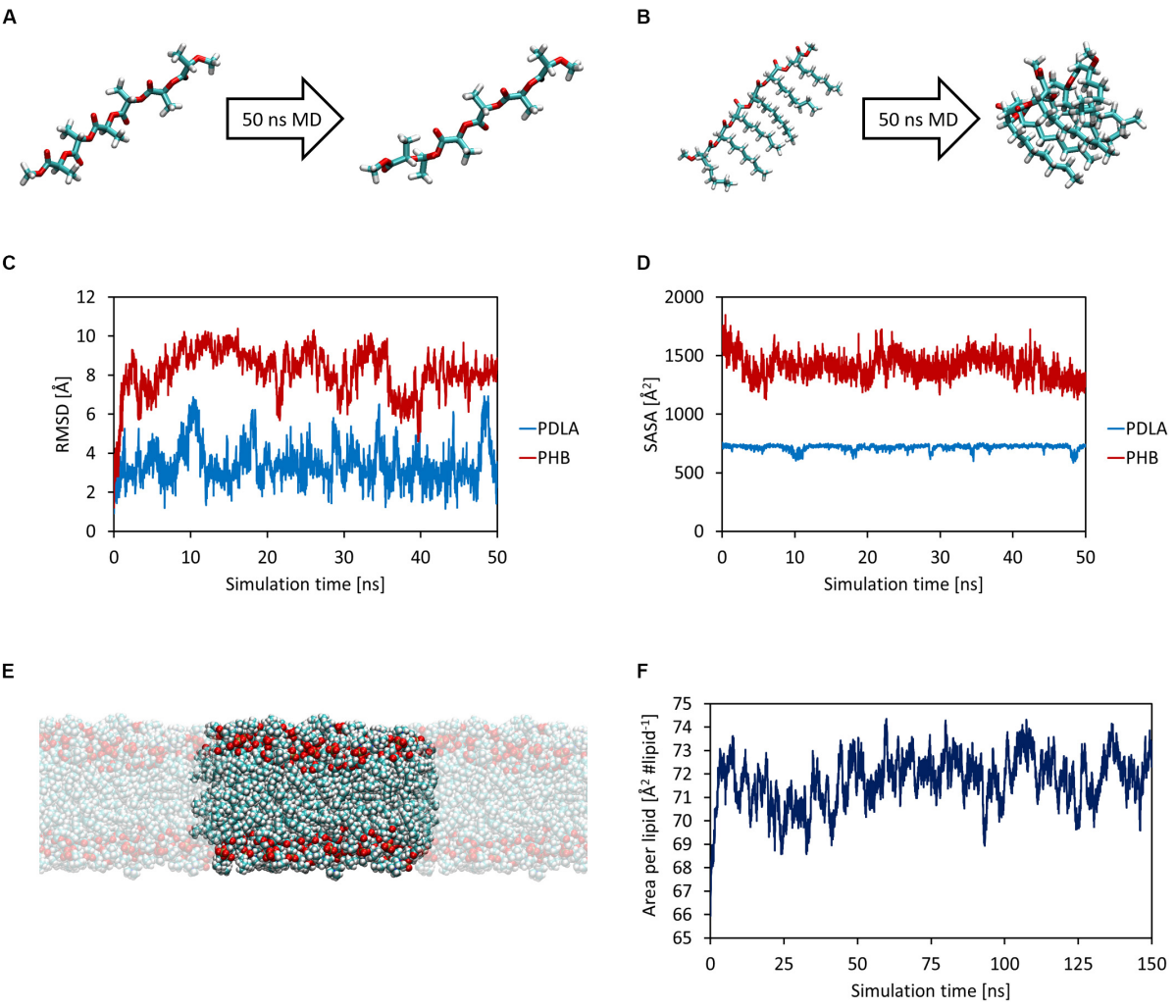

FIGURE 1 | Equilibrated structures of PDLA **(A)** and P3HD **(B)** oligomers. RMSD **(C)** and SASA **(D)** as a function of simulation time. Equilibrated bilayer structure along with its periodic images that result in an infinite surface that lies on xy-plane **(E)**. Area per lipid as a function of simulation time **(F)**.

mean square displacement (RMSD) and the solvent accessible surface area (SASA) as a function of simulation time, as shown in **Figures 1C,D**. While PDLA oligomer did not experience substantial structural variations, P3HD oligomer folded due to its increased hydrophobicity related to aliphatic side chains. Focusing on DOPC bilayer, 150 ns MD simulations were performed for equilibration and the attainment of an equilibrated structure (**Figure 1E**) was verified by computing the area per lipid (**Figure 1F**) and membrane thickness (computed from the peak-to-peak distance of electron density profiles) as a function of simulation time. Equilibration led to an area per lipid and membrane thickness values equal to 72.04 ± 0.88 Å^2 lipid^{-1} and 35.75 ± 0.45 Å, respectively; values are expressed as average ± standard deviation. The obtained values are consistent with the reported computational and experimental data provided by Dickson et al. (2014).

The equilibrated structures were thus employed for the study of oligomers permeation in the lipid bilayer.

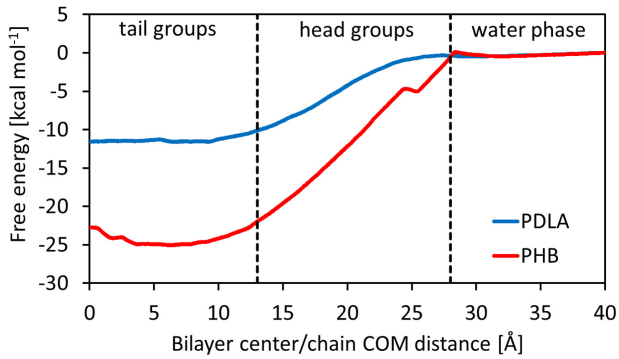

FIGURE 2 | Free energy as a function of the distance between oligomer COM and bilayer center.

Oligomers Permeation

The main outcome from Umbrella Simulations is the free energy landscape as a function of the z-component of the distance between the center of mass of the oligomer and the center of the membrane. In this regard, it is possible to identify three different zones, related to the heterogeneous environment of the bilayer: tail groups ($0 < z < 13$ Å), head groups ($13 < z < 27$ Å) and water phase ($27 < z < 40$ Å). Results are shown in **Figure 2**. PDLA and P3HD free energy landscapes are consistent with the results shown in literature for hydrophobic molecules (Bemporad et al., 2004; Orsi et al., 2009; Bochicchio et al., 2015), since such oligomers preferably partition inside the membrane. Indeed, ΔG^0_{Bind} computed through equation 6 is equal to -11.49 ± 0.69 and -23.85 ± 0.99 kcal mol^{-1} for PDLA and P3HD, respectively. The more favorable value related to P3HD is due to the relevant interactions between polymer/bilayer aliphatic chains. The minimum of the free energy lies in the region with the tail groups, by virtue of hydrophobic effects. Free energy increases

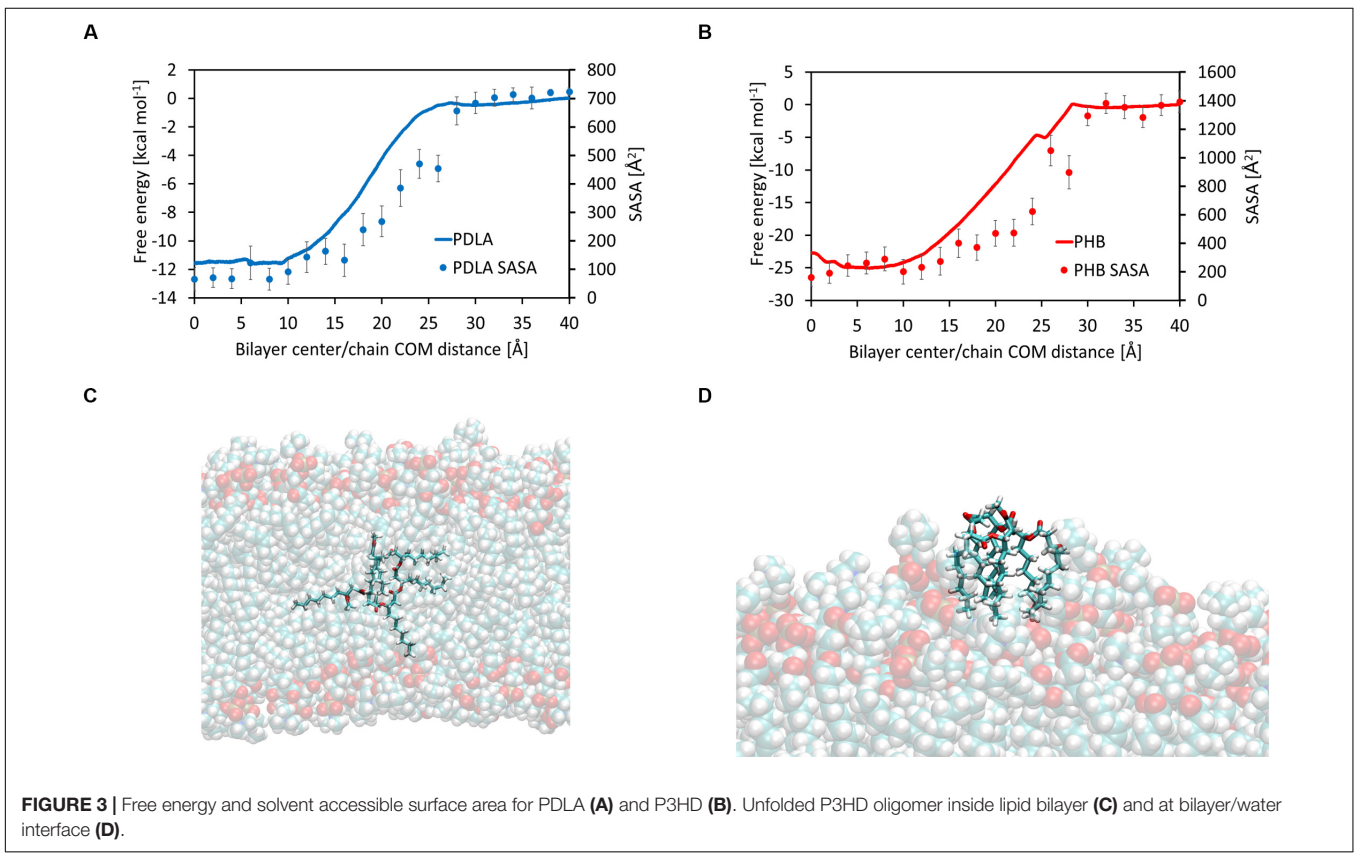

FIGURE 3 | Free energy and solvent accessible surface area for PDLA **(A)** and P3HD **(B)**. Unfolded P3HD oligomer inside lipid bilayer **(C)** and at bilayer/water interface **(D)**.

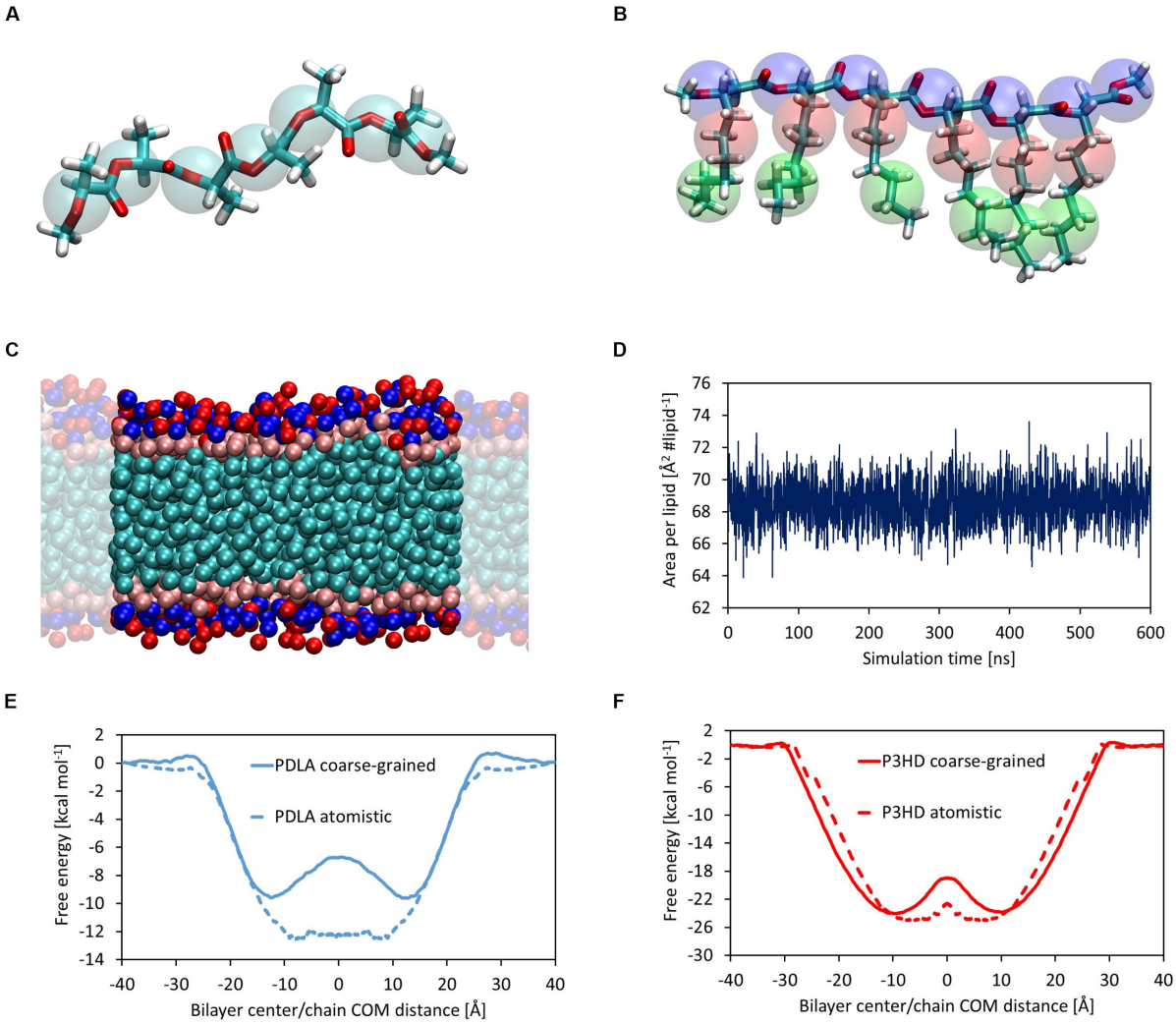

FIGURE 4 | Coarse-grained representation of PDLA oligomer; C5 MARTINI beads are represented as transparent cyan spheres **(A)**. Coarse-grained representation of P3HD oligomer; Na, C3, and C1 MARTINI beads are represented as transparent blue, red, and green spheres, respectively **(B)**. Equilibrated structure of DOPC CG model **(C)**. Area per lipid as a function of simulation time for DOPC bilayer CG model **(D)**. Comparison of free energy profiles obtained from full atomistic and coarse-grained simulations for PDLA **(E)** and P3HD **(F)**. Profile from full atomistic simulations was mirrored for the sake of clarity.

moving toward the hydrophilic head groups, where no favorable interactions take place since no hydrogen bonds can be formed.

Hydrophobic effects behind the free energy landscape can be highlighted through SASA values, computed using the last 10 ns of each window, as shown in **Figures 3A,B**; indeed, free energy profiles for PDLA and P3HD exhibit the same trend of SASA decrease due to permeation. Notably, P3HD oligomer also experiences unfolding inside the bilayer (**Figure 3C**), when it is surrounded by the hydrophobic tails. In addition, P3HD is still unfolded at the bilayer/water interface (**Figure 3D**); aliphatic chains point toward the lipid bilayer, while the backbone is exposed to the solvent. Up to authors' best knowledge, experimental diffusion coefficients are not available, while computational studies are usually focused on smaller molecules. Comparison with literature data reveals that P3HD and PDLA diffusion coefficients are about two orders of magnitude lower if compared to low molecular weight compounds (ranging from water to benzene) or small drugs (Orsi et al., 2009; Dickson et al., 2017) and can be considered acceptable. The resistance as a function of collective coordinate reaches it minimum value in the center of the bilayer (by virtue of the favorable interactions) and it is maximum at water/bilayer interface. Indeed, polar head groups are the major obstacle to permeation, due to the not favorable interactions with the oligomers. All computed values are reported in **Supplementary Material**.

Coarse-Grained Simulations

The first step was evaluating the attainment of an equilibrated bilayer structure at CG level (**Figure 4C**) and its agreement with the outcomes from atomistic simulations. The average values of area per lipid and membrane thickness are equal to 68.57 ± 1.25 $Å^2$ $lipid^{-1}$ and 36.67 ± 0.57 Å, respectively, in

good agreement with the results obtained at full atomistic level. It should also point out that in this case membrane, thickness was computed from the distance between the beads representative of the phosphate groups. Moreover, an equilibrated structure is rapidly obtained, as shown by the time evolution of the area per lipid (**Figure 4D**).

Free energy landscapes were obtained by means of WTMD; thanks to the higher accessible time scales provided by the intrinsic computational efficiency of CG simulations with respect to full atomistic ones, the sampling was performed considering the full CV range from -40 to 40 Å, in order to observe multiple membrane crossing events. The comparison between free energy profiles from full atomistic and coarse-grained simulations is shown in **Figures 4E,F** for PDLA and P3HB, respectively.

While the agreement for P3HD is good from both a qualitative and a quantitative point of view, only a fair qualitative agreement was obtained for PDLA. This is evident also focusing on ΔG_{Bind} values, which were computed also from CG simulations using the last 2000 ns. The value obtained for P3HD, equal to -22.69 $\pm$ 0.23 kcal mol^{-1} is in good agreement with the estimation from US, equal to -23.85 $\pm$ 0.99 kcal mol^{-1}. On the other hand, the analogous comparison for PDLA oligomer showed an expected poor agreement, by virtue of ΔG_{Bind} values equal to -8.33 $\pm$ 0.11 and -11.49 $\pm$ 0.69 kcal mol^{-1} obtained from coarse-grained and full atomistic simulations, respectively.

The observed disagreement for PDLA results can be explained by taking into account the parameterization of non-bonded interactions of MARTINI beads. Indeed, PDLA has a backbone composed of ester bonds, which act as polar groups, and hydrophobic side chains constituted by methyl groups. The parameterization of the non-bonded interactions of the chosen MARTINI bead is thus not able to account for this balance, since the hydrophobicity in underestimated. Modeling PDLA polymer with Na MARTINI beads, representative of ester bonds only, leads to physically not consistent results: preliminary explorative simulations showed that the oligomer would preferably partition in water phase. On the other hand, more hydrophobic beads essentially take into account aliphatic backbones and would provide an overestimation of the affinity for the lipid phase.

Summarizing, while C5 MARTINI beads for PDLA polymer represent the best compromise, they do not provide a description of the polymer at CG level with an acceptable accuracy level. Therefore, while the CG model for P3HD presented here could be readily used to simulate an entire nanoparticle, a reparameterization of non-bonded interactions for PDLA oligomer is needed to improve the agreement with more accurate atomistic simulations.

CONCLUSION

In this study, the passive permeation of small oligomers of polymer of interest in the biomedical field was studied by means of molecular dynamics simulations, at both full atomistic and coarse-grained level.

Simulations at atomic scale allowed obtaining the free energy landscape as a function of the distance between the center of the membrane and the center of mass of PDLA and P3HD, chosen as collective coordinate. Results showed that both oligomers preferably partition into the membrane; this trend could be explained in terms of hydrophobic effects by computing the solvent accessible surface area as a function of the collective coordinate.

The obtained free energy landscape can be in principle employed to tune a coarse-grained model, which can be used to simulate the permeation of an entire nanoparticle into a lipid bilayer, by virtue of the higher accessible time and length scales. For this reason, coarse-grained simulations were performed using MARTINI force field, to check whether the free energy landscape from atomistic simulations could be reproduced without further reparameterization.

Results showed a good quantitative agreement for P3HD oligomer and only a fair qualitative agreement for PDLA, highlighting the need of a further reparameterization of non-bonded interactions in order to better account for the hydrophobicity due to the methyl side groups.

DATA AVAILABILITY STATEMENT

All datasets generated for this study are included in the article/**Supplementary Material**.

AUTHOR CONTRIBUTIONS

TC, AR, and CH performed simulations and post processing. TC wrote the first draft of the manuscript. GP contributed to supervision of the work. All authors discussed and approved the contents of the manuscript and contributed to its final version by reading and editing.

FUNDING

This study is part of the GoNanoBioMat project and has received funding from the Horizon 2020 framework program of the European Union, ProSafe Joint Transnational Call 2016, from the Swiss KTI (from 1.1.2018 Swiss Innosuisse) under Grant Number 19267.1 PFNM-NM and from EU FCT Foundation for Science and Technology under the project PROSAFE/0001/2016.

ACKNOWLEDGMENTS

TC acknowledges the contribution of Michela Castelnuovo, B. Des., for image editing.

SUPPLEMENTARY MATERIAL

The Supplementary Material for this article can be found online at: https://www.frontiersin.org/articles/10.3389/fbioe.2020.00718/full#supplementary-material

REFERENCES

Barducci, A., Bussi, G., and Parrinello, M. (2008). Well-tempered metadynamics: a smoothly converging and tunable free-energy method. *Phys. Rev. Lett.* 100:020603.

Bassas-Galia, M., Follonier, S., Pusnik, M., and Zinn, M. (2017). Natural polymers: a source of inspiration. *Bioresorb. Poly. Biomed. Appl.* 120, 31–64.

Bayly, C. I., Cieplak, P., Cornell, W. D., and Kollman, P. A. (1993). A well-behaved electrostatic potential based method using charge restraints for deriving atomic charges - the resp model. *J. Phys. Chem.* 97, 10269–10280. doi: 10.1021/j100142a004

Bemporad, D., Essex, J. W., and Luttmann, C. (2004). Permeation of small molecules through a lipid bilayer: a computer simulation study. *J. Phys. Chem. B* 108, 4875–4884. doi: 10.1021/jp035260s

Bochicchio, D., Panizon, E., Ferrando, R., Monticelli, L., and Rossi, G. (2015). Calculating the free energy of transfer of small solutes into a model lipid membrane: comparison between metadynamics and umbrella sampling. *J. Chem. Phys.* 143:144108. doi: 10.1063/1.4932159

Bonomi, M., Barducci, A., and Parrinello, M. (2009). Reconstructing the equilibrium boltzmann distribution from well-tempered metadynamics. *J. Comput. Chem.* 30, 1615–1621. doi: 10.1002/jcc.21305

Bussi, G., Donadio, D., and Parrinello, M. (2007). Canonical sampling through velocity rescaling. *J. Chem. Phys.* 126:014101. doi: 10.1063/1.2408420

Butt, F. I., Muhammad, N., Hamid, A., Moniruzzaman, M., and Sharif, F. (2018). Recent progress in the utilization of biosynthesized polyhydroxyalkanoates for biomedical applications - review. *Intern. J. Biol. Macromol.* 120, 1294–1305. doi: 10.1016/j.ijbiomac.2018.09.002

Casalini, T., Limongelli, V., Schmutz, M., Som, C., Jordan, O., Wick, P., et al. (2019a). Molecular modeling for nanomaterial-biology interactions: opportunities, challenges, and perspectives. *Front. Bioeng. Biotechnol.* 7:268. doi: 10.3389/fbioe.2019.00268

Casalini, T., Rossi, F., Castrovinci, A., and Perale, G. (2019b). A perspective on polylactic acid-based polymers use for nanoparticles synthesis and applications. *Front. Bioeng. Biotechnol.* 7:259. doi: 10.3389/fbioe.2019.00259

Case, D. A., Betz, R. M., Cerutti, D. S., Cheatham, T. E., Darden, T., Duke, R. E., et al. (2016). *AMBER 2016*. San Francisco: University of California.

Cornell, W. D., Cieplak, P., Bayly, C. I., and Kollman, P. A. (1993). Application of resp charges to calculate conformational energies, hydrogen-bond energies, and free-energies of solvation. *J. Am. Chem. Soc.* 115, 9620–9631. doi: 10.1021/ja00074a030

de Jong, D. H., Singh, G., Bennett, W. F., Arnarez, C., Wassenaar, T. A., Schafer, L. V., et al. (2013). Improved parameters for the martini coarse-grained protein force field. *J. Chem. Theory Comput.* 9, 687–697.

Di Meo, F., Fabre, G., Berka, K., Ossman, T., Chantemargue, B., Paloncyova, M., et al. (2016). In silico pharmacology: drug membrane partitioning and crossing. *Pharmacol. Res.* 111, 471–486. doi: 10.1016/j.phrs.2016.06.030

Dickson, C. J., Hornak, V., Bednarczyk, D., and Duca, J. S. (2019). Using membrane partitioning simulations to predict permeability of forty-nine drug-like molecules. *J. Chem. Inform. Model.* 59, 236–244. doi: 10.1021/acs.jcim.8b00744

Dickson, C. J., Hornak, V., Pearlstein, R. A., and Duca, J. S. (2017). Structure-kinetic relationships of passive membrane permeation from multiscale modeling. *J. Am. Chem. Soc.* 139, 442–452. doi: 10.1021/jacs.6b11215

Dickson, C. J., Madej, B. D., Skjevik, A. A., Betz, R. M., Teigen, K., Gould, I. R., et al. (2014). Lipid14: the amber lipid force field. *J. Chem. Theory Comput.* 10, 865–879. doi: 10.1021/ct4010307

Filipe, H. A. L., Moreno, M. J., Rog, T., Vattulainen, I., and Loura, L. M. S. (2014). How to tackle the issues in free energy simulations of long amphiphiles interacting with lipid membranes: convergence and local membrane deformations. *J. Phys. Chem. B* 118, 3572–3581. doi: 10.1021/jp501622d

Frederix, P. W. J. M., Patmanidis, I., and Marrink, S. J. (2018). Molecular simulations of self-assembling bio-inspired supramolecular systems and their connection to experiments. *Chem. Soc. Rev.* 47, 3470–3489. doi: 10.1039/c8cs00040a

Frisch, M. J., Trucks, G. W., Schlegel, H. B., Scuseria, G. E., Robb, M. A., Cheeseman, J. R., et al. (2016). *Gaussian 09 Rev. D.01*. Wallingford, CT: Gaussian Inc.

Hoopes, M. I., Noro, M. G., Longo, M. L., and Faller, R. (2011). Bilayer structure and lipid dynamics in a model stratum corneum with oleic acid. *J. Phys. Chem. B* 115, 3164–3171. doi: 10.1021/jp109563s

Hummer, G. (2005). Position-dependent diffusion coefficients and free energies from bayesian analysis of equilibrium and replica molecular dynamics simulations. *New J. Phys.* 7:34. doi: 10.1088/1367-2630/7/1/034

Ingolfsson, H. I., Arnarez, C., Periole, X., and Marrink, S. J. (2016). Computational 'microscopy' of cellular membranes. *J. Cell Sci.* 129, 257–268. doi: 10.1242/jcs.176040

Ingolfsson, H. I., Melo, M. N., Van Eerden, F. J., Arnarez, C., Lopez, C. A., Wassenaar, T. A., et al. (2014). Lipid organization of the plasma membrane. *J. Am. Che. Soc.* 136, 14554–14559.

Jambeck, J. P. M., and Lyubartsev, A. P. (2013). Exploring the free energy landscape of solutes embedded in lipid bilayers. *J. Phys. Chem. Lett.* 4, 1781–1787. doi: 10.1021/jz4007993

Jorgensen, W. L., Chandrasekhar, J., Madura, J. D., Impey, R. W., and Klein, M. L. (1983). Comparison of simple potential functions for simulating liquid water. *J. Chem. Phys.* 79, 926–935. doi: 10.1063/1.445869

Joung, I. S., and Cheatham, T. E. (2008). Determination of alkali and halide monovalent ion parameters for use in explicitly solvated biomolecular simulations. *J. Phys. Chem. B* 112, 9020–9041. doi: 10.1021/jp8001614

Joung, I. S., and Cheatham, T. E. (2009). Molecular dynamics simulations of the dynamic and energetic properties of alkali and halide ions using water-model-specific ion parameters. *J. Phys. Chem. B* 113, 13279–13290. doi: 10.1021/jp902584c

Kumar, S., Bouzida, D., Swendsen, R. H., Kollman, P. A., and Rosenberg, J. M. (1992). The weighted histogram analysis method for free-energy calculations on biomolecules .1 the Method. *J. Comput. Chem.* 13, 1011–1021. doi: 10.1002/jcc.540130812

Lee, C. T., Comer, J., Herndon, C., Leung, N., Pavlova, A., Swift, R. V., et al. (2016). Simulation-based approaches for determining membrane permeability of small compounds. *J. Chem. Informat. Model.* 56, 721–733. doi: 10.1021/acs.jcim.6b00022

Lee, J., Patel, D. S., Stahle, J., Park, S. J., Kern, N. R., Kim, S., et al. (2019). CHARMM-GUI membrane builder for complex biological membrane simulations with glycolipids and lipoglycans. *J. Chem. Theory Comput.* 15, 775–786. doi: 10.1021/acs.jctc.8b01066

Loverde, S. M. (2014). Molecular simulation of the transport of drugs across model membranes. *J. Phys. Chem. Lett.* 5, 1659–1665. doi: 10.1021/jz500321d

Lunnoo, T., Assaeakhajornsak, J., and Puangmali, T. (2019). In silico study of gold nanoparticle uptake into a mammalian cell: interplay of size, shape, surface charge and aggregation. *J. Phys. Chem. C* 123, 3801–3810. doi: 10.1021/acs.jpcc.8b07616

Marrink, S. J., and Berendsen, H. J. C. (1994). Simulation of water transport through a lipid-membrane. *J. Phys. Chem.* 98, 4155–4168. doi: 10.1021/j100066a040

Marrink, S. J., Risselada, H. J., Yefimov, S., Tieleman, D. P., and De Vries, A. H. (2007). The MARTINI force field: coarse grained model for biomolecular simulations. *J. Phys. Chem. B* 111, 7812–7824.

Marrink, S. J., and Tieleman, D. P. (2013). Perspective on the martini model. *Chem. Soc. Rev.* 42, 6801–6822.

Minozzi, M., Lattanzi, G., Benz, R., Costi, M. P., Venturelli, A., and Carloni, P. (2011). Permeation through the cell membrane of a boron-based beta-lactamase inhibitor. *PLoS One* 6:23187. doi: 10.1371/journal.pone.0023187

Murzyn, K., Rog, T., and Pasenkiewicz-Gierula, M. (2005). Phosphatidylethanolamine-phosphatidylglycerol bilayer as a model of the inner bacterial membrane. *Biophys. J.* 88, 1091–1103. doi: 10.1529/biophysj.104.048835

Nagle, J. F., and Tristram-Nagle, S. (2000). Structure of lipid bilayers. *Biochim. Biophys. Acta Rev. Biomemb.* 1469, 159–195.

Orsi, M., Sanderson, W. E., and Essex, J. W. (2009). Permeability of small molecules through a lipid bilayer: a multiscale simulation study. *J. Phys. Chem. B* 113, 12019–12029. doi: 10.1021/jp903248s

Pall, S., Abraham, M. J., Kutzner, C., Hess, B., and Lindahl, E. (2015). Tackling exascale software challenges in molecular dynamics simulations with GROMACS. *Solv. Softw. Challeng. Exasc.* 8759, 3–27. doi: 10.1007/978-3-319-15976-8_1

Parrinello, M., and Rahman, A. (1981). Polymorphic transitions in single-crystals - a new molecular-dynamics method. *J. Appl. Phys.* 52, 7182–7190. doi: 10.1063/1.328693

Poger, D., Caron, B., and Mark, A. E. (2016). Validating lipid force fields against experimental data: progress, challenges and perspectives. *Biochim. Biophys. Acta Biomemb.* 1858, 1556–1565. doi: 10.1016/j.bbamem.2016.01.029

Ramot, Y., Haim-Zada, M., Domb, A. J., and Nyska, A. (2016). Biocompatibility and safety of PLA and its copolymers. *Adv. Drug Deliv. Rev.* 107, 153–162. doi: 10.1016/j.addr.2016.03.012

Roux, B. (1995). The calculation of the potential of mean force using computer-simulations. *Comput. Phys. Commun.* 91, 275–282. doi: 10.1016/0010-4655(95)00053-i

Saeedi, M., Lyubartsev, A. P., and Jalili, S. (2017). Anesthetics mechanism on a DMPC lipid membrane model: insights from molecular dynamics simulations. *Biophys. Chem.* 226, 1–13. doi: 10.1016/j.bpc.2017.03.006

Salomon-Ferrer, R., Gotz, A. W., Poole, D., Le Grand, S., and Walker, R. C. (2013). Routine microsecond molecular dynamics simulations with AMBER on GPUs. 2. explicit solvent particle mesh ewald. *J. Chem. Theory Comput.* 9, 3878–3888. doi: 10.1021/ct400314y

Schulz, M., Olubummo, A., and Binder, W. H. (2012). Beyond the lipid-bilayer: interaction of polymers and nanoparticles with membranes. *Soft. Matter.* 8, 4849–4864.

Shinoda, W. (2016). Permeability across lipid membranes. *Biochim. Biophys. Acta Biomemb.* 1858, 2254–2265. doi: 10.1016/j.bbamem.2016.03.032

Smith, D., Artursson, P., Avdeef, A., Di, L., Ecker, G. F., Faller, B., et al. (2014). Passive lipoidal diffusion and carrier-mediated cell uptake are both important mechanisms of membrane permeation in drug disposition. *Mol. Pharm.* 11, 1727–1738. doi: 10.1021/mp400713v

Teixeira, M. H., and Arantes, G. M. (2019). Effects of lipid composition on membrane distribution and permeability of natural quinones. *RSC Adv.* 9, 16892–16899. doi: 10.1039/c9ra01681c

Torrie, G. M., and Valleau, J. P. (1977). Nonphysical sampling distributions in monte carlo free-energy estimation: umbrella sampling. *J. Computat. Phys.* 23, 187–199. doi: 10.1016/0021-9991(77)90121-8

Tribello, G. A., Bonomi, M., Branduardi, D., Camilloni, C., and Bussi, G. (2014). PLUMED 2: new feathers for an old bird. *Comput. Phys. Commun.* 185, 604–613. doi: 10.1016/j.cpc.2013.09.018

Tse, C. H., Comer, J., Chu, S. K. S., Wang, Y., and Chipot, C. (2019). Affordable membrane permeability calculations: permeation of short-chain alcohols through pure-lipid bilayers and a mammalian cell membrane. *J. Chem. Theory Comput.* 15, 2913–2924. doi: 10.1021/acs.jctc.9b00022

Tse, C. H., Comer, J., Wang, Y., and Chipot, C. (2018). Link between membrane composition and permeability to drugs. *J. Chem. Theory Comput.* 14, 2895–2909. doi: 10.1021/acs.jctc.8b00272

Wang, J. M., Wolf, R. M., Caldwell, J. W., Kollman, P. A., and Case, D. A. (2004). Development and testing of a general amber force field. *J. Comput. Chem.* 25, 1157–1174. doi: 10.1002/jcc.20035

Wu, E. L., Cheng, X., Jo, S., Rui, H., Song, K. C., Davila-Contreras, E. M., et al. (2014). CHARMM-GUI membrane builder toward realistic biological membrane simulations. *J. Computat. Chem.* 35, 1997–2004.

Conflict of Interest: The authors declare that the research was conducted in the absence of any commercial or financial relationships that could be construed as a potential conflict of interest.

Advantages of publishing in Frontiers

OPEN ACCESS
Articles are free to read for greatest visibility and readership

FAST PUBLICATION
Around 90 days from submission to decision

HIGH QUALITY PEER-REVIEW
Rigorous, collaborative, and constructive peer-review

TRANSPARENT PEER-REVIEW
Editors and reviewers acknowledged by name on published articles

Frontiers
Avenue du Tribunal-Fédéral 34
1005 Lausanne | Switzerland

Visit us: www.frontiersin.org
Contact us: info@frontiersin.org | +41 21 510 17 00

REPRODUCIBILITY OF RESEARCH
Support open data and methods to enhance research reproducibility

DIGITAL PUBLISHING
Articles designed for optimal readership across devices

FOLLOW US
@frontiersin

IMPACT METRICS
Advanced article metrics track visibility across digital media

EXTENSIVE PROMOTION
Marketing and promotion of impactful research

LOOP RESEARCH NETWORK
Our network increases your article's readership